PB81-176067

Proceedings of a Fourth Workshop on Catalytic Combustion Held at Cincinnati, Ohio on May 14-15, 1980

Acurex Corp.
Mountain View, CA

Prepared for

Industrial Environmental Research Lab.
Research Triangle Park, NC

Aug 80

U.S. Department of Commerce
National Technical Information Service
NTIS

IERL-RTP-1077

TECHNICAL REPORT DATA
(Please read Instructions on the reverse before completing)

1. REPORT NO. EPA-600/9-80- 035	2.	3. RECIPIENT'S ACCESSION NO. PB81 176067
4. TITLE AND SUBTITLE Proceedings: Fourth Workshop on Catalytic Combustion (Cincinnati, OH, May 1980)		5. REPORT DATE August 1980 Issuing date. 6. PERFORMING ORGANIZATION CODE
7. AUTHOR(S) John P. Kesselring, Compiler		8. PERFORMING ORGANIZATION REPORT NO.
9. PERFORMING ORGANIZATION NAME AND ADDRESS Acurex Corporation 485 Clyde Avenue Mountain View, California 94042		10. PROGRAM ELEMENT NO. EHE624A 11. CONTRACT/GRANT NO. 68-02-3122
12. SPONSORING AGENCY NAME AND ADDRESS EPA, Office of Research and Development Industrial Environmental Research Laboratory Research Triangle Park, NC 27711		13. TYPE OF REPORT AND PERIOD COVERED Proceedings; 9/78-5/80 14. SPONSORING AGENCY CODE EPA/600/13

15. SUPPLEMENTARY NOTES IERL-RTP project officer is G. Blair Martin, Mail Drop 65, 919/541-2235. EPA-600/7-79-038 documents the Third Workshop and contains summaries of the First and Second Workshops.

16. ABSTRACT

The proceedings document the major presentations at the Fourth Workshop on Catalytic Combustion, held in Concinnati, OH, May 14-15, 1980. Sponsored by the Combustion Research Branch of EPA's Industrial Environmental Research Laboratory (Research Triangle Park), the workshop served as a forum for the presentation of results of recent research in the areas of catalyst performance, components and applications of catalytic combustion systems, and the use of alternative fuels in catalytic combustors. The workshop provided industrial, university, and government representatives with the current state of the art in the application of catalyst systems for pollution control and performance improvement. Applications include fire tube and water tube boilers, and gas turbines for utility, industrial, automotive, and aircraft systems.

17. KEY WORDS AND DOCUMENT ANALYSIS

a. DESCRIPTORS	b. IDENTIFIERS/OPEN ENDED TERMS	c. COSATI Field/Group
Pollution	Pollution Control	13B
Combustion	Stationary Sources	21B
Catalysts	Catalytic Combustion	07D
Boilers		13A
Gas Turbines		13G

18. DISTRIBUTION STATEMENT Release to Public	19. SECURITY CLASS *(This Report)* Unclassified	21. NO. OF PAGES
	20. SECURITY CLASS *(This page)* Unclassified	22. PRICE

EPA Form 2220-1 (9-73)

i

☆ U.S. GOVERNMENT PRINTING OFFICE: 1980--657-165/0161

United States
Environmental Protection
Agency

Industrial Environmental Research
Laboratory
Research Triangle Park NC 27711

EPA-600/9-80-035
August 1980

PB81-176067

Research and Development

EPA

Proceedings Fourth Workshop on Catalytic Combustion (Cincinnati, OH, May 1980)

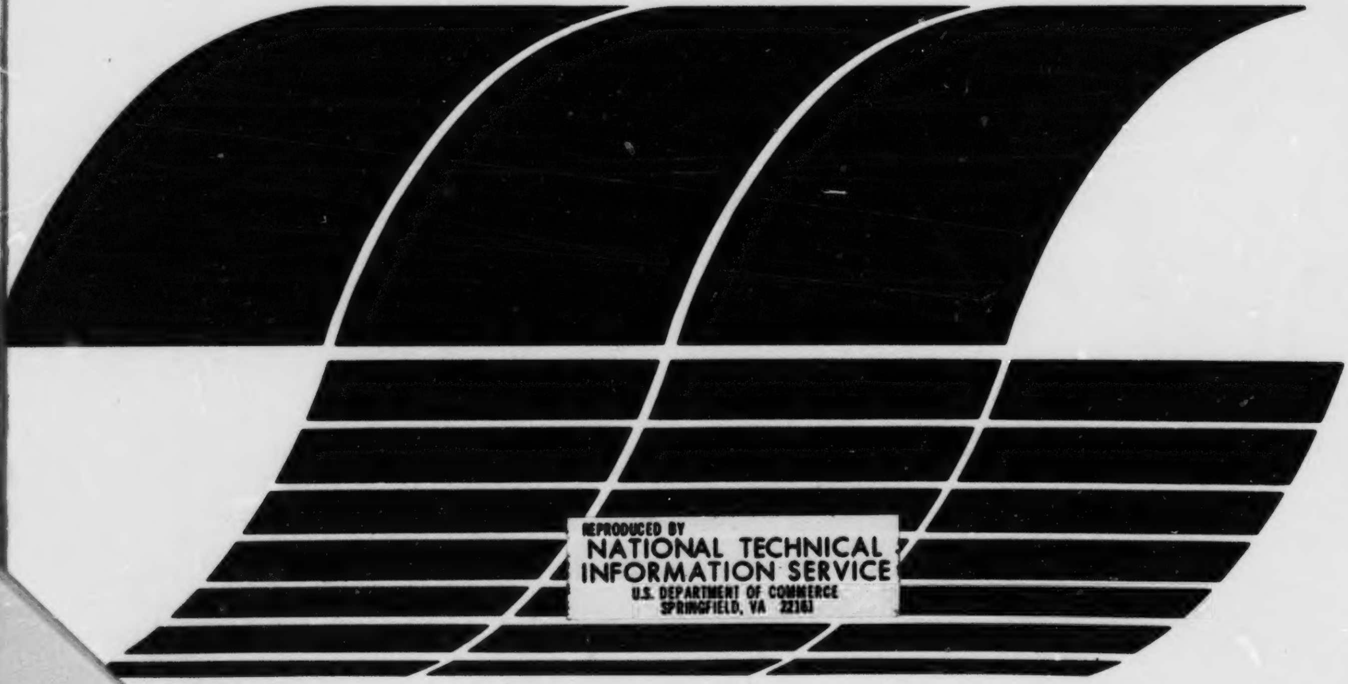

REPRODUCED BY
NATIONAL TECHNICAL
INFORMATION SERVICE
U.S. DEPARTMENT OF COMMERCE
SPRINGFIELD, VA 22161

RESEARCH REPORTING SERIES

Research reports of the Office of Research and Development, U.S. Environmental Protection Agency, have been grouped into nine series. These nine broad categories were established to facilitate further development and application of environmental technology. Elimination of traditional grouping was consciously planned to foster technology transfer and a maximum interface in related fields. The nine series are:

1. Environmental Health Effects Research
2. Environmental Protection Technology
3. Ecological Research
4. Environmental Monitoring
5. Socioeconomic Environmental Studies
6. Scientific and Technical Assessment Reports (STAR)
7. Interagency Energy-Environment Research and Development
8. "Special" Reports
9. Miscellaneous Reports

This document is available to the public through the National Technical Information Service, Springfield, Virginia 22161.

EPA 600/9-80-035
August 1980

PROCEEDINGS: FOURTH WORKSHOP ON CATALYTIC COMBUSTION (CINCINNATI, OH, MAY 1980)

John P. Kesselring, Compiler

Acurex Corporation
Energy and Environmental Division
485 Clyde Avenue
Mountain View, California 94042

Contract No. 68-02-3122

Project Officer:
G. Blair Martin

Office of Energy, Minerals, and Industry
Industrial Environmental Research Laboratory
Research Triangle Park, NC 27711

Prepared for

U.S. ENVIRONMENTAL PROTECTION AGENCY
Office of Research and Development
Washington, DC 20460

INDUSTRIAL ENVIRONMENTAL RESEARCH LABORATORY
OFFICE OF RESEARCH AND DEVELOPMENT
U.S. ENVIRONMENTAL PROTECTION AGENCY
RESEARCH TRIANGLE PARK, NC 27711

DISCLAIMER

This report has been reviewed by the Industrial Environmental Research Laboratory - Research Triangle Park, N.C., U.S. Environmental Protection Agency, and approved for publication. Approval does not signify that the contents necessarily reflect the views and policies of the U.S. Environmental Protection Agency, nor does mention of trade names or commercial products constitute endorsement or recommendation for use.

PREFACE

This proceedings document covers the presentations of the Fourth Workshop on Catalytic Combustion, held May 14-15, 1980 at the Netherland Hilton Hotel in Cincinnati, Ohio. Sponsored by the Combustion Research Branch of the EPA's Industrial Environmental Research Laboratory — Research Triangle Park, the workshop served as a forum for the presentation of results of recent research in the areas of catalytic combustion system components and applications, catalyst performance, and alternative fuels use in catalytic combustors. The First and Second Workshops on Catalytic Combustion were held at the Plantation Inn in Raleigh, North Carolina on May 25-26, 1976 and June 21-22, 1977, respectively. The Third Workshop on Catalytic Combustion was held at the Grove Park Inn in Asheville, North Carolina on October 3-4, 1978. Summaries of the First and Second Workshops and the Proceedings of the Third Workshop appear in EPA-600/7-79-038, "Proceedings: Third Workshop on Catalytic Combustion."

Dr. John P. Kesselring, Acurex Corporation, acted as Workshop Coordinator, and G. Blair Martin, Combustion Research Branch, Environmental Protection Agency, was the Project Officer.

PROCEEDINGS: FOURTH WORKSHOP ON CATALYTIC COMBUSTION
(Cincinnati, Ohio, May 1980)

ABSTRACT

The proceedings document the major presentations at the Fourth Workshop on Catalytic Combustion, held in Cincinnati, Ohio, May 14-15, 1980. Sponsored by the Combustion Research Branch of EPA's Industrial Environmental Research Laboratory — Research Triangle Park, the workshop served as a forum for the presentation of results of recent research in the areas of catalyst performance, components and applications of catalytic combustion systems, and the use of alternative fuels in catalytic combustors. The workshop provided industrial, university, and government representatives with the current state of the art in the application of catalyst systems for pollution control and performance improvement. Applications include firetube and watertube boilers and gas turbines for utility, industrial, automotive, and aircraft systems.

TABLE OF CONTENTS

Page

Session I — Components of the Catalytic Combustion System 1

"Autoignition in a Premixing-Prevaporizing Duct at Inlet Air Temperatures up to 1000K," Robert R. Tacina 2

"Fuel Injector, Ignition, and Temperature Measurement Techniques for Catalytic Combustors," S. J. Anderson, W. V. Krill, and J. P. Kesselring 3

"Preliminary Design of Catalytic Combustors," William B. Retallick . . . 35

"Catalytic Flame Stabiliization," Moshe Lavid and A. E. Cerkanowicz . . . 44

"Thermal Shock Resistant Catalytic Monoliths Using Foam Ceramics Technology," William C. Pfefferle 64

Session II — Catalyst Performance 73

"Computed and Measured Emissions from the Catalytic Combustion of Propane/Air Mixtures," F. V. Bracco, C. Bruno, Y. Yaw, P. M. Walsh. . . . 74

"Modeling of Transient Operation of Catalytic Combustor," James S. T'ien. 117

"The Effect of Catalyst Length and Downstream Reaction Distance on Catalytic Combustor Performance," David N. Anderson 147

"CATCOM Catalyst 5 atm 1000 Hour Aging Study Using #2 Fuel Oil," I. T. Osgerby, B. A. Olson, H. C. Lee 172

"Fuel-Nitrogen Conversion and Combustion Efficiency in a Catalytic Combustor," Ronald D. Matthews, Mark L. Graham, Jeryl L. Lederman 216

"CATCOM Catalyst Axial Temperature Profile Measurements," I. T. Osgerby, B. A. Olson, H. Lew, A. Cohn 244

"Development of Improved Catalyst Systems," J. P. Kesselring, W. V. Krill, M. J. Angwin, and H. L. Atkins 246

"Catalyzed Combustion of Lean Fuel/Air Mixtures," R. W. Schefer, F. Robben 277

"Examination of the Nickel Catalyst Role in Rich Combustion," Gerald E. Voecks 297

Session III — Applications of Catalytic Combustion 313

"Prototype Catalytic Systems," W. V. Krill, J. P. Kesselring, S. J. Anderson 314

"EPRI Stationary Gas Turbine Catalytic Combustor Development Program," Leonard C. Angello 335

"Catalytic Combustion for Gas Turbines," Hisashi Fukuzawa, Yoshimi Ishihara 363

"Soot Reduction in Diesel Engines by Catalytic Effects," R. Sapienza, T. Butcher, C. Krishna, J. Gaffney 380

"High Pressure Test Results," D. E. Carl, M. C. Krepinevich, I. T. Osgerby 400

"Combustion Catalyst Study for Simulated Aircraft Idle Mode Operation," I. T. Osgerby, R. M. Heck, R. V. Carrubba, C. C. Gleason, E. J. Mularz . 415

"Experimental Evaluation of Catalytic Combustion With Heat Removal at Near Stoichiometric Conditions," Daniel Bulzan 446

Session IV — Alternate Fuels and the Catalytic Combustor 449

"Fuel Nitrogen Conversion — The Impact of Catalyst Type," B. A. Folsom, W. D. Clark, C. W. Courtney, M. P. Heap, W. R. Seeker. 450

"Catalytic Combustion Characteristics of Low and Medium Btu Gas Fuels," H. C. Lee, I. T. Osgerby 475

"Catalytic Combustion of Alternative Fuels," Henry Tong, Edward K. Chu, Gerry C. Snow 509

"Gasification of a Heavy and a Distillate Fuel," E. J. Szetela, R. A. Sederquist, J. A. TeVelde 536

"Catalytic Combustion of Heavy Partially-Vaporized Fuels," T. J. Rosfjord 548

"Evaluation of a Novel Lean Burn Low NO_x Catalytic Combustion Concept," E. K. Chu, R. Chang, H. Tong 560

SESSION I

COMPONENTS OF THE CATALYTIC COMBUSTION SYSTEM

AUTOIGNITION IN A PREMIXING-PREVAPORIZING DUCT AT INLET AIR TEMPERATURES UP TO 1000K

By:

Robert R. Tacina
National Aeronautics and Space Administration
Lewis Research Center
Cleveland, Ohio 44135

Conditions were determined in a premixing-prevaporizing fuel preparation duct at which autoignition (upstream burning) occurred. An air blast type fuel injector with nineteen fuel injection points was used that provided a uniform fuel-air mixture. The range of inlet conditions were: inlet air temperatures of 600 to 1000K, air pressures of 180-660 kPa, fuel-air ratios from 0.009 to 0.070, and velocities from 3.5 to 30 m/s. The duct was insulated and the diameter was 12 cm. Mixing lengths were varied from 16.5 to 47.6 cm. and residence times ranged from 4.6 to 107 ms. The fuel used was diesel #2. Results showed a strong effect of fuel-air ratio and pressure on the conditions where autoignition occurs. The effect of length or residence time on autoignition was not apparent in these tests. A correlation of the conditions where autoignition would occur which apply to this fuel injector over the conditions tested is $p \phi^{0.7} = 73 e^{\frac{1100}{T}}$, where p is the pressure in kPa, ϕ the equivalence ratio, and T the temperature in K.

FUEL INJECTOR, IGNITION, AND TEMPERATURE MEASUREMENT TECHNIQUES FOR CATALYTIC COMBUSTORS

By:

S. J. Anderson, W. V. Krill, and J. P. Kesselring
Acurex Corporation/Energy & Environmental Division
485 Clyde Avenue
Mountain View, California 94042

ABSTRACT

As catalytic combustion systems approach the demonstration phase of of development, special auxiliary components are required for fuel injection, ignition, and catalyst temperature measurement. Following preliminary screening of potential concepts, several auxiliary systems were designed and tested. Design details and test results are reported.

Liquid and gaseous fuel aerodynamic injectors and liquid fuel atomizing nozzles were tested in both large and small duct sizes. Aerodynamic injectors provided rapid and uniform gas mixing. However, they did not adequately vaporize liquid fuels, which require spray nozzles for injection. To maintain short mixing lengths in large ducts, multiple point injection was employed.

Among many catalyst lightoff concepts that were reviewed, the opposed jet igniter and the aft-end torch were selected for detailed testing. The opposed jet demonstrated excellent catalyst lightoff capabilities over a wide range of mainstream stoichiometries and flowrates. It delivered preheated gas temperatures as high as 1366K (2000^{o}F) with both natural gas and diesel fuels. In contrast, aft-end torch lightoff was possible only with gaseous fuels at low gas velocities. This restriction considerably limits its application to catalytic combustors.

Thermocouple probes and pyrometers were evaluated as alternative temperature measurement techniques to thermocouples attached directly to catalyst surfaces. Probes located immediately downstream of the catalyst were found to be unreliable because temperature measurement depended in a complicated manner on system geometry and exhaust gas velocities. Although inserting a probe into the catalyst bed improved measurement accuracy, further testing is required at gas velocities greater than 7 m/s. Testing showed that a single wavelength optical pyrometer can accurately measure surface temperature within 10K (15^{o}F) of actual bed temperature if surface emissivity is known as a function of temperature. However, interference in the sitepath (e.g., soot) adversely affected measurement accuracy. To maintain accuracy when interference was a problem, dual wavelength pyrometers were employed.

INTRODUCTION

Catalytic combustion is an innovative technology capable of significantly reducing NO_x formation while maintaining high combustion efficiency. However, catalytic combustors require special ignition techniques and premixed fuel and air. For catalyst lightoff, an ignitor must heat the catalyst to over 700K in a controlled manner. Once lightoff is achieved, the ignitor must be easily shut off. To effectively utilize all catalyst material and prevent excessive temperatures due to locally enriched reactant mixtures, air and fuel should be evenly distributed prior to entering the catalyst. Fuel injectors must provide thorough and rapid mixing to minimize mixing length, prevent recirculation which may lead to flameholding, and promote rapid prevaporization of liquid fuels. Finally, catalyst temperature must be carefully monitored during startup and steady state operation to maintain catalyst material within allowable operating limits. Correspondingly, a reliable system must be developed to continuously measure catalyst surface temperature.

As part of the EPA's catalytic prototype system development program, Acurex is investigating auxiliary system components capable of providing acceptable fuel/air mixing, controlled-temperature ignition, and reliable monitoring of catalyst surface temperature. This paper will describe the development of gaseous and liquid fuel injectors, catalytic combustor ignition systems, and catalyst temperature measurement techniques.

FUEL INJECTION CONCEPTS

Optimum catalyst performance requires uniform reactor inlet profiles of temperature, fuel/air ratio, and velocity. This assures effective use of the entire catalyst area and prevents substrate damage caused by high temperatures due to locally enriched fuel/air mixtures. The primary function of the fuel injector is to introduce the fuel to the air stream in such a manner as to provide complete mixing before entry into the catalyst. For liquid fuels, the fuel must also be at least partially prevaporized. Both mixing and vaporization occur in a flow region between the injector and the catalyst, and proper fuel injection can greatly facilitate these processes.

Rapid mixing results from intimate fuel/air contact. This can be accomplished by placing multiple injectors across an incoming air duct or maintaining strong recirculation in the mixing zone. The latter technique is often intolerable in catalytic systems, since flashback from the hot catalyst surface can cause flameholding in the areas of recirculation. Therefore, in systems with large sectional areas, multiple fuel injection points are preferred.

For systems operating on liquid fuels, the injector must also promote rapid vaporization. It has been estimated in one study (Reference 1) that 90 to 95 percent of the fuel must be vaporized for stable catalyst operation. However, tests at Acurex have shown that 70 percent vaporization may be acceptable in some system applications. The rate of droplet vaporization is controlled by the initial size of the droplet and the heat transfer to the drop by convection from the surrounding air and radiation from the catalyst bed. Total prevaporization can be achieved by allowing long mixing times to transfer sufficient energy to vaporize the drop before entrance to the catalyst. However, the allowable mixing length is limited by autoignition delay times which are particularly short in high pressure, high temperature systems. Therefore, the alternative to long residence time is to produce a fine, uniform droplet distribution over the cross-sectional area of the combustor mixing section at the fuel injector.

Several fuel injection techniques exist which can provide rapid fuel/air mixing and fine liquid fuel atomization. Aerodynamic fuel injectors for both gaseous and liquid fuels and atomizing spray nozzles for liquid fuels were selected as candidate injectors. Design details and test results as they apply to both small and large scale combustors are dicussed below.

AERODYNAMIC FUEL INJECTION

Aerodynamic fuel injectors promote fuel-air mixing by injecting fuel into a relatively high velocity air stream. High velocities are achieved by constricting the flow in a narrow duct, then gradually expanding the fuel-air mixture to the catalyst front face. For larger systems with high air flow requirements, an array of multiple ducts may be necessary to provide uniform fuel-air distribution to the catalyst while maintaining high gas velocity. In general, liquid fuels are injected at velocities below the air velocity to increase atomization of the liquid fuel by droplet shear. In contrast, gaseous fuels are injected at velocities comparable to the duct air velocity to minimize recirculation regions in the mixture stream which could support flameholding.

Two types of aerodynamic fuel injectors, one for a small area duct and one for a large area duct, were constructed and tested at Acurex. A layout of the fuel injector for a small duct is shown in Figure 1. A total of six tubes were oriented concurrent with the air stream: three small diameter tubes for distillate oil and three larger tubes for gaseous (natural gas and propane) fuels. Each of the fuel tubes supplies an equal area segment of the duct cross-section. The tubes were sized such that the fuel injection velocity is near the air stream velocity under most operating conditions, and several inches of length in the flow direction allow flow recovery from upstream disturbances prior to the injection point. Therefore, intimate fuel-air contact is achieved without the formation of recirculation regions. The three tubes for each fuel type are manifolded exterior to the test apparatus, and the injector plate is bolted between flanges in the facility mixing section. Expansion of the mixture occurs in a refractory-lined section with a total cone angle of 0.087 radians (5 degrees).

Performance of the injector with gaseous fuels has been excellent. Fuel-air mixing appears to be complete at the catalyst face (as indicated by catalyst temperature variations) for a mixing length of 1.07 m (3.5 ft). Even at conditions where incoming fuel and air are at greatly dissimilar velocities, mixing appears complete and no flashback or flameholding problems have been encountered.

Operation on distillate oil with the same mixing length provides varying results. At lower air velocities, the fuel appears to be more heavily concentrated at the lower half of the catalyst, even at preheats of 700K (800°F) (well above the upper distillation point of the oils tested). This phenomenon is attributed to rather large droplets coming off of the injector and gravitating to the lower half of the duct during mixing. Since shear force induced by the air flowing over the tips of the injector ports is the only mechanism of droplet atomization, the maldistributions experienced are consistent with poor atomization at low flow velocities. At higher air velocities (usually in excess of the incoming fuel velocity as well), the distribution again appears uniform. It therefore appears that finer atomization is required to meet the wide range of flow conditions anticipated in systems applications.

For a large area duct, a multiple venturi fuel injector based on a concept of Tacina (Reference 2) was fabricated for a model gas turbine combustor. The fuel injector, capable of operation with both gaseous and distillate fuels, is shown in Figure 2. This concept produces a number of high velocity air streams, injects fuels into the high velocity regions, and expands the fuel-air mixture into a large duct.

During testing of the injector assembly, flameholding resulted within the expansion cones. Several features of the design may account for this difficulty. The downstream end of the injector cones is a close-packed hexagonal array of seven tubes. The tested design did not attempt to eliminate the base region between cones, and recirculation certainly existed in these regions. The potential for flameholding in these regions is compounded by the introduction of fuel at the upstream end of the assembly in that a partially premixed, partially prevaporized mixture can occur at the outlet of the cones.

Other features of the design may also result in operational problems. A relatively long venturi cone is required to provide high velocities at the fuel injection port, and a small cone angle is required to prevent boundary layer separation on the internal walls. In addition, atomization of the distillate fuel results only from shear of the air over the fuel ports and may produce relatively large droplets. Finally, great care is required to insure uniform injection in all cones under varying fuel flowrates. Tacina and others have revised their initial designs to address some of these problems. As a result of these problems, atomizing spray nozzle injectors were developed for liquid fuels.

ATOMIZING SPRAY NOZZLE INJECTORS

To improve mixing and vaporization of liquid fuels, atomizing spray nozzles were developed for small bench scale tests and for larger catalytic system tests. Each application used an air-atomizing type of nozzle that produces a mean drop size of approximately 60 to 100 µm.

The single injector is currently used for catalyst screening tests in an atmospheric test facility. Details of the fuel injector assembly are shown in Figure 3. The system is oriented vertically and operates with both gaseous and liquid fuels. Gaseous fuel and air are premixed and introduced through four ports concentric about the spray nozzle. For liquid fuel injection, air enters the same four ports with fuel sprayed axially into a conical venturi. Further mixing occurs in a 6.35 cm diameter section below the venturi prior to entering the catalyst. The nozzle assembly also includes a pneumatic on/off valve and a coolant housing through which air is passed to prevent heatup of the assembly by preheated air or radiation from the catalyst.

Operation of the fuel introduction system with gaseous fuels has been totally acceptable for over 40 catalyst tests performed to date. Similarly with diesel fuel, the fine atomization promotes rapid mixing and vaporization over a wide range of velocities (1.5 to 7.6 m/sec, 5 to 25 ft/sec) through the premixing section. Flashbacks occurred only when operating at low velocities approaching the mixture flamespeed. The overall success of the injector in achieving uniform mixing has made it possible to operate catalysts with partially vaporized fuel in the air stream.

For systems that cannot accommodate long mixing lengths or pressure losses associated with small ducts, a more sophisticated multiple point injection scheme is required. The concept, with the model gas turbine combustor can, is shown in Figure 4. The injector is a three nozzle arrangement for distillate fuel injection in a 12.7 cm duct. The spray nozzles are mounted on extensions approximately 5 cm away from the injector plate. The injector plate is mounted between flanges of the test facility. Vaporization or mixing are nearly complete in the allowed mixing length without autoignition difficulties.

During initial testing of the multiple injectors, the nozzles' wide spray angle caused fuel to impinge directly on the wall of the combustor can. Some thermal NO_x was produced, apparently as a result of upstream burning of the distillate fuel on the wall. This was confirmed by cold water model tests using a clear acrylic combustor can. Fuel contact with the wall was suppressed by reducing the nozzle spray angle from 77 to 15 degrees. Subsequent combustion testing with a low spray angle was quite successful. The injection system provided a uniform fuel mixture without upstream burning.

In summary, aerodynamic fuel injectors provide rapid and complete fuel-air mixing of gaseous fuels over a wide range of flowrates. If system pressure drop is not important, a single injector is sufficient. To minimize pressure drop, multiple point injection may be necessary. Aerodynamic injectors do not adequately atomize liquid fuels, however. Consequently, spray nozzles are recommended for these applications. In addition, for large systems, multiple point injection should be employed to reduce mixing length while maintaining uniform fuel-air distribution.

COMBUSTOR IGNITION CONCEPTS

Catalyst lightoff occurs when a minimum catalyst temperature is achieved. The lightoff temperature varies primarily with catalyst and fuel type and secondarily with stoichiometry and mass throughput. In general, temperatures in excess of 700K (800°F) are necessary for lightoff. For example, noble metal catalysts such as platinum and palladium require 617K to 784K (650°F to 950°F) lightoff temperatures, while metal oxide catalysts such as nickel and cobalt require 866K to 1367K (1100°F to 2000°F) temperatures. In early EPA testing, lightoff temperature was achieved using electric air preheaters. However, air preheat temperatures at this level are not available in boiler and gas turbine systems. Consequently, alternate techniques for lightoff were investigated. Table I lists advantages and disadvantages of possible catalyst ignition systems. Each system has potential application to utility and industrial boilers, and stationary gas turbines. Two systems were chosen for test evaluation: the opposed jet igniter and the aft-end torch. The opposed jet was selected due to its simple operation, variable temperature control, and wide mixture ratio and flowrate blowout limits. The aft-end torch technique was chosen for its simplicity.

OPPOSED JET IGNITER

During operation, a jet of premixed fuel and air (approximately 1 percent of the total mainstream mass flow) is injected counterflow to the main stream of reactants, producing a stagnation point flow condition. An upstream spark plug ignites the jet and a bow flame front stabilizes in the jet region. By consuming the mainstream reactants, the opposed jet acts as an aerodynamic flameholder, providing a preheated fuel-air mixture to the catalyst located downstream. When the desired ignition temperature is achieved, the jet fuel and air are turned off, thereby extinguishing the flame. The jet is shown in Figure 5 during operation. The opposed jet igniter was evaluated using both gaseous and prevaporized liquid fuel in the mainstream. Test results are discussed below.

Operation with Gaseous Fuel

Optimum performance of the jet was identified initially without a catalyst by varying mainstream and jet stoichiometry. Catalyst lightoff capability was then evaluated with a catalyst. Although tests were conducted mainly with natural gas in the jet and mainstream, similar results are achievable for other gases with similar heating values (e.g., propane). Opposed jet stability depended primarily on the relative magnitude of gas momentum in the mainstream duct and the jet. Based on visual observation, the most stable jet operating condition occurred at a jet-to-mainstream velocity ratio of 7.4 and a jet-to-mainstream mass flowrate ratio of 0.01 to 0.02. Preheat temperatures delivered by the opposed jet show small variations with jet stoichiometry and large variations with mainstream stoichiometry. At a nominal 105 MJ/hr (100,000 Btu/hr) heat release rate with natural gas under lean mainstream conditions, the jet operated at stoichiometries between 5.6 and 17.0 percent theoretical air. Exit temperature varied from 28K to 56K (50 to 100°F) with changes in jet stoichiometry. Smaller temperature variations occurred at decreasing mainstream stoichiometries.

The jet operated effectively over a wide range of mainstream stoichiometries; specifically, 180 to 270 percent theoretical air. This yielded exit temperatures of 1089K to 617K (1500 to 650°F). This temperature range appears suitable for ignition of both noble metal and metal oxide catalysts. Figure 6 plots exit temperature as a function of mainstream stoichiometry for 10.9 percent theoretical air in the jet. The opposed jet demonstrated excellent catalyst lightoff capability under lean conditions with natural gas. A comparison of an opposed jet lightoff sequence with a typical lightoff using preheated air and fuel is given in Figure 7. As shown, the preheated air technique with a noble metal catalyst required a bed temperature near 750K (900°F) for startup under typical flowrate conditions with the lightoff rate controlled by the stoichiometry of the reactant stream (two are shown). In contrast, the opposed jet can operate with a reactant stream at ambient temperature while the heating rate is controlled by jet and mainstream stoichiometry and the thermal mass of the particular combustion system. For a specific application, the desired heating rate is dictated by both catalyst material and other system startup constraints.

Additional tests were run on the opposed jet using natural gas with the mainstream under fuel-rich conditions. Although the flammability limit of natural gas under rich conditions is approximately 57 percent theoretical air, the jet igniter will not start between 57 and 80 percent. Above 80 percent, violent explosions can occur. It appears that for safe operation, the opposed jet igniter is not appropriate for ignition under rich conditions. For staged combustors, where the first stage operates fuel rich, ignition can be done under lean conditions followed by shutdown of the igniter and a switch to rich operation.

Operation with Liquid Fuel

Based on successful experience with gaseous fuels, the opposed jet igniter was further tested with liquid fuels. The igniter was added to the primary components of the model gas turbine; namely, the multiple spray fuel injector and combustor can. The opposed jet was located approximately equidistance within the 0.46 m (18-inch) distance between the fuel injector and the catalyst front face. A spark plug mounted on the combustor can wall

12.7 cm (5 inches) upstream of the jet serves to ignite the jet. After the catalyst has attained necessary bed temperature (lightoff), the jet injection tube can be withdrawn from the fuel-air stream to avoid interferences in the mixing region.

To simplify manifolding of gas to the jet, the jet was redesigned to operate solely on natural gas, rather than a fuel-air mixture as was used previously for gaseous fuels. Although this approach did not restrict performance of the jet, a much higher jet to mainstream velocity ratio (20 to 25) was required to maintain jet stability.

Tests were conducted using No. 2 diesel fuel at a nominal 210 MJ/hr (200,000 Btu/hr) heat release rate. This corresponds to a duct velocity of approximately 0.38 m/sec (15 ft/sec). Fuel was prevaporized using air preheated to 561K (550°F). The jet operated over a wide range of mainstream stoichiometries; namely, 150 percent theoretical air to no fuel in the mainstream. Below 150 percent theoretical air, flameholding developed on the fuel injectors upstream of the jet. As shown in Figure 8, exhaust temperature from the jet increased linearly from 1005 to 1422K (1350 to 2100°F) with decreasing mainstream stoichiometry. Similar to jet performance with natural gas, this temperature range is suitable for ignition of both noble metal and metal oxide catalysts.

Previously, catalytic combustion with liquid fuels was accomplished by igniting the catalyst first with gaseous fuel followed by a switch to liquid fuel. The opposed jet igniter allows lightoff directly with liquid fuel. During testing of the model gas turbine, lightoff with diesel fuel was successfully performed 15 times using an Acurex chromium oxide catalyst on a Corning MCB-1 substrate. The lightoff sequence, from jet ignition to catalyst stabilization, can be tailored to meet system requirements.

Despite difficulties under rich conditions, the opposed jet demonstrated excellent lightoff capability under lean conditions with both natural gas and diesel fuels. Following successful preliminary testing, the jet was incorporated into both the atmospheric and high pressure test facilities at Acurex. During 1 year of operation, the opposed jet has become a routine ignition technique for both catalyst screening and system component development.

AFT-END TORCH LIGHTOFF

In addition to the opposed jet, aft-end torch lightoff was evaluated as a catalyst ignition technique for gaseous fuels. This approach is very simple and only requires a small port in the exhasut downstream of the bed for insertion of the torch. In operation, the air/fuel mixture passing through the catalyst bed is ignited downstream using a propane torch. The torch is then withdrawn. Gas velocities are set relatively low to allow stabilization of the flame on the catalyst aft-end. As the catalyst is preheated, the flame propagates upstream into the catalyst. After the bed is fully active, fuel and air flow can be increased to the desired heat release rate.

The aft-end torch was tested in the atmospheric pressure facility at Acurex using natural gas. Lightoff was easily accomplished but complete activation of the bed required a lengthy 2 to 3 minutes.

Although simple in concept, aft-end lightoff has a very limited range of applicability. During lightoff, the gas velocity must be low to allow flame propagation back into the bed. Thus, a particular combustion system must be capable of low flowrates to facilitate lightoff.

Among the possible techniques for catalyst lightoff, the opposed jet is the preferred ignition system. It can operate over wide stoichiometric blowout limits using both gaseous and liquid fuels and has performed many successful catalyst lightoffs in duct sizes ranging from 3.8 to 12.7 cm (1.5 to 5 inches).

CATALYST TEMPERATURE MEASUREMENT TECHNIQUES

To maintain efficient, stable combustion and not exceed its material temperature limitations, a catalyst must be operated within a relatively narrow range of steady state temperatures. Thus, measurement of the catalyst surface temperature is a key parameter in system control. The instrument used for temperature measurement must be accurate within 28 to 56K (50 to 100°F), maintain adequate life at low cost, and respond quickly to temperature transients. Furthermore, it should be simple to install and readily accessible for easy maintenance.

Currently, in-depth thermocouples attached directly to the substrate are used to provide direct measurement of the catalyst wall temperature. However, this technique is expensive (thermocouples are not reusable), relatively unreliable for extended use, and requires complex installation. Consequently, thermocouple probes (which measure gas phase temperature) and optical pyrometers were investigated as alternate techniques for catalyst temperature measurement. Both approaches use instruments external to the catalyst, thereby facilitating installation and maintenance. However, using these techniques may result in a loss of accuracy. Each approach is discussed below.

THERMOCOUPLE PROBE

The first thermocouple probe configuration tested was a platinum/rhodium (Type R) thermocouple located 0.64 cm downstream of a graded cell catalyst bed with the junction on the central axis of the bed. The ratio of thermocouple probe measurement (gas phase temperature) to in-bed thermocouples (catalyst wall temperature) is plotted as a function of inlet gas velocity in Figure 9. At all velocities, the downstream probe indicated a lower temperature than the bed surface temperature (which runs near the adiabatic flame temperature). The closest agreement between the downstream and bed thermocouple measurements occurred at an inlet bed velocity of approximately 6.1 m/sec (20 ft/sec). This velocity corresponds to the baseline heat release rate of 105.5×10^6 J/hr (100,000 Btu/hr).

The probe is heated by radiation from the catalyst surfaces and convection with combustion exhaust gases. It's cooled by radiation to cold walls downstream of the combustor. A balance of these heat transfer mechanisms determines the temperature measured by the probe. At low reference velocities, radiative cooling dominates convective heating and results in a large difference between catalyst wall temperature and gas temperature measured at the probe. As convective heat transfer increases with velocity, this temperature difference decreases (see Figure 9).

At high reference velocities, however, temperature differences between the bed and probe increase with increasing velocity despite high convective heat transfer to the probe. It appears that combustion is incomplete in the bed, and additional fuel conversion occurs downstream of the probe. Therefore, the gas temperature at the probe is again suppressed below the near-adiabatic flame temperature at the catalyst wall.

Although a curve can be constructed for the data, certain system dependencies make it difficult to infer bed temperature from downstream measurements. The correlation presented is expected to depend on such parameters as:

- Catalyst type and geometry -- controlling in-bed and downstream combustion efficiencies which determine exhaust gas temperature
- System geometries -- controlling radiative and convective gains and losses from the probe

Due to the complexity of this correlation, an aft-end temperature probe is not a preferred technique for temperature measurement.

To minimize the differences in temperature measurement. the probe was inserted between the medium and small cell segments of a catalyst bed. The ratio of probe to bed temperature as a function of velocity is shown as the upper curve in Figure 9. As indicated, the correlation between gas temperature measured by the probe and the actual surface temperature was excellent. A negligible difference in probe and bed temperature was measured at all gas velocities tested. For the interbed configuration, it appears that radiation from the catalyst surfaces in the front and rear segments dominates heat transfer to the probe. However, additional testing of the probe at higher velocities is required.

Although thermocouple probes are easy to fabricate and install, their reliability is uncertain (as with in-depth thermocouples) due to direct exposure to high combustion temperatures. For this reason, thermocouple probes are not a preferred technique for long-term catalyst temperature measurement.

PYROMETRY

Although an interbed probe may be an accurate technique for catalyst temperature measurement, it may lack reliability for continuous use since it depends on instrumentation in a high temperature region. In contrast, a pyrometer can be isolated from the combustion zone, enabling longer life without loss of instrument reliability. However, a pyrometer requires a clear visual path to the target and knowledge of the surface emissivity as a function of temperature.

Typically, the front (inlet) or back (exhaust) face of the catalyst bed is accessible to sensing by a pyrometer. In order to avoid significant infrared absorption by various hydrocarbon fuels, viewing the catalyst exit face may be preferred, since combustion byproducts only weakly absorb infrared radiation in the operating range of most pyrometers. Furthermore, the higher temperatures at the aft end of the catalyst produce shorter wavelengths which are capable of more accurate temperature measurement.

Two types of pyrometers are commercially available for test evaluation: (1) single color instruments which determine temperature based on absolute intensity of emitted radiation, and (2) dual color instruments which determine temperature based on the ratio of radiation intensity at two wavelengths. The accuracy of each instrument was evaluated by comparing the temperature measured by the pyrometers with in-depth thermocouples (R-type) over a 1200 to 1866K (1700 to 2900°F) temperature range. Tests were conducted using a Corning proprietary monolith (MCB-11) at high temperatures (greater than 1590K) and a platinum catalyst on DuPont alumina Torvex at lower temperatures. Test results are discussed below.

For the single wavelength pyrometer (Thermodot Model TD-73), temperature measurement was accurate within 27K (50°F) at an apparent surface emissivity of 0.7. However, with a dirty viewing window and the same catalyst, apparent emissivity dropped to 0.45 and measured temperature was 139 to 194K (250 to 350°F) below actual bed temperature. Test data are illustrated in Figure 10. It appears that the accuracy of single color pyrometers depends strongly on apparent surface emissivity. As shown above, emissivity depends upon the integrity of the sight path (affected by infrared absorption by the quartz viewing window and by obstructions such as dirt and soot).

In addition, depending upon the material, surface emissivity may change with temperature. For example, although surface emissivity of the Corning substrate remained constant (0.70) with temperature, emissivity of the DuPont

Torvex substrate decreased from 0.48 to 0.40 with decreasing temperature. Test data for the DuPont model are shown in Figure 11. The marked drop of apparent emissivity at 1255K (1800°F) is probably due to nonuniform surface temperature (cold spots) resulting from unstable combustion at low temperatures.

Despite emissivity variations with temperature, true catalyst temperature can be calculated from pyrometer readings based on a known emissivity-temperature profile (Figure 11 for example). The relationship is given by the following expression:

$$T_T = T_p \left[1 + \frac{\lambda_p T_p}{C} \ln(\varepsilon_\lambda) \right]^{-1}$$

where T_T = true surface temperature (K)

T_p = temperature indicated by the pyrometer (K)

λ_p = pyrometer wavelength (cm)

C = conversion constant = 1.44 (cm-K)

ε_λ = surface emissivity at pyrometer wavelength λ and surface temperature T_T

Using test data, bed temperature was predicted within 10K of actual bed temperature with this formula.

By measuring the ratio of radiation signals at two adjacent wavelengths, two-color pyrometers are designed to accurately measure temperature regardless of obstructions in the view path or changes in emissivity with temperature. A dual wavelength instrument was used with the Corning substrate at high temperature. Data are given in Figure 10. In this case, temperatures measured with the pyrometer were 55K less than actual bed temperatures. Closer agreement may be possible if the unit is calibrated for the specific material. Over the range investigated, measurement accuracy was independent of temperature, but further testing is required at lower temperatures.

Although single wavelength pyrometers can be adversely affected by obstructions in the sight path (soot, dirty window, etc.), temperature measurement depends in a simple and predictable manner on surface emissivity.

In contrast, two-color pyrometers are not affected by obstructions, but depend in a complicated manner on the ratio of surface emissivity at the two operating wavelengths. In addition, a single color instrument grade pyrometer typically costs $1500 compared with $2500 for a two-color pyrometer. Choosing the preferred type of pyrometer depends on the particular application. For systems with a clear sight path, a single color pyrometer is adequate. However, for combustors which produce some soot or must operate unattended for long periods, a two-color pyrometer may be justified. In either case, pyrometers appear to be the preferred method of catalyst temperature measurement. They are easy to maintain, accurate, and should provide reliable, long term operation.

CONCLUSIONS

Aerodynamic fuel injectors, characterized by fuel injection into a high velocity duct, provide rapid and complete mixing of gaseous fuels. However, because aerodyanmic injectors rely strictly on droplet shear forces for atomization, they do not adequately atomize liquid fuels for the variety of conditions encountered in catalytic combustors. Atomizing spray nozzles, in contrast, do provide rapid and complete fuel mixing. For large systems with short mixing lengths, multiple injection points are necessary for even distribution of fuel and air.

The opposed jet igniter is the recommended technique for catalyst lightoff. It is a versatile system capable of operating over a wide range of mainstream gas velocities and stoichiometries. The jet has been tested successfully using both natural gas and No. 2 fuel diesel fuel and is capable of delivering controlled, high temperature exhaust products to the catalyst for lightoff.

Pyrometers can accurately measure catalyst temperature (within 30K) if surface emissivity is known as a function of temperature. Because the sensor is external to the combustion zone, it does not suffer reliability problems due to direct exposure to high temperatures (as do thermocouple probes). Temperature measurement by thermocouple probes located downstream of the catalyst bed depend in a complicated manner on gas velocity and system geometry. Consequently, they are not an accurate method of temperature measurement. In contrast, at the gas velocities investigated, interbed thermocouple probes do accurately measure catalyst temperature. Their performance in system applications requires further development, however.

Prototype combustion systems are currently being developed to demonstrate the feasibility of catalytic combustion. Due to the uniquesness of these combustors, special techniques are required for fuel injection, catalyst lightoff, and temperature control. Substantial progress has been made in the development of these systems. They will be further integrated with catalytic combustor concepts as they are scaled up to the prototype demonstration phase.

REFERENCES

1. Rosfjord, T. J. Catalytic Combustors for Gas Turbine Engines." AIAA paper 76-46, Washington, D.C., January 1976.

2. Tacina, Robert R. Experimental Evaluation of Fuel Preparation Systems for an Automative Gas Turbine Catalytic Combustors. DOE/NASA/1011-78/23, June 1977.

TABLE I. CATALYST IGNITION CONCEPTS

Igniter	Description	Advantages	Disadvantages
Packaged burner	-- Off-the-shelf burner system -- Gas/No. 2 oil -- Flame safeguard and fuel train -- Maximum 100 percent excess air on gas yields 1370K (adiabatic) -- Maximum 300 percent excess air on oil yields 950K (adiabatic) -- Installed in separate firebox, with exhaust ducted upstream of catalyst	-- Readily available complete burner system -- Very reliable -- No engineering required on burner hardware -- Rich lightoff may be possible due to separation of mainstream and igniter stream	-- Possible control problem during transition between burner throttle-down and catalyst lightoff -- Can't leave on after catalyst is ignited (to increase catalyst performance)
Opposed jet	-- Aerodynamic flameholder -- Jet directed axially upstream with premixed reactants -- Jet/mainstream velocity ratio ≈10 -- Stable combustion possible between 60 percent and 200 percent theoretical air mainstream with a stoichiometric jet -- At 200 percent theoretical air mainstream and with a stoichiometric jet, maximum exhaust temperature is 980K	-- Long history of use as experimental tool -- Wide stoichiometry blowout limits -- No control problems during catalyst lightoff; reactants immediately exposed to catalyst after jet is turned off	-- Rich lightoff probably not possible -- Jet may have to be water-cooled -- Flameholding may occur behind jet upstream of catalyst

TABLE I. CONCLUDED

Igniter	Description	Advantages	Disadvantages
Electrical resistance preheated air	-- Preheat combustion air by electric heater -- Max temp = 810K	-- Simple operation -- Continuously preheated air increases catalyst performance	-- Limited operating temperature -- Long startup time -- Large size -- Expensive to operate
Hydrogen injection	-- H_2 gas is injected upstream of catalyst -- H_2 ignites catalyst at room temperature	-- Simple concept and operation	-- Dangerous, difficult to handle -- Unattractive to potential users
Hydride device	-- H_2-impregnated structure (i.e., gauze) upstream of catalyst -- Electrical current releases H_2, acts like H_2 igniter	-- Fairly simple concept and operation -- Safer than H_2 injection	-- Experimental stage only
Metal monolith	-- Metal monolith heated when electrical current is applied	-- Simple concept and operation -- Safe; no flame or ancillary ignition equipment needed	-- Experimental stage only -- Catalyst-specific -- Required high temperature electrical connectors
Aft-end torch	-- Gas torch ignites reactants downstream of bed -- Flame propagates upstream into the bed, igniting the catalyst	-- Simple concept and operation -- Inexpensive	-- No preheat capability -- Difficult to achieve at high velocity

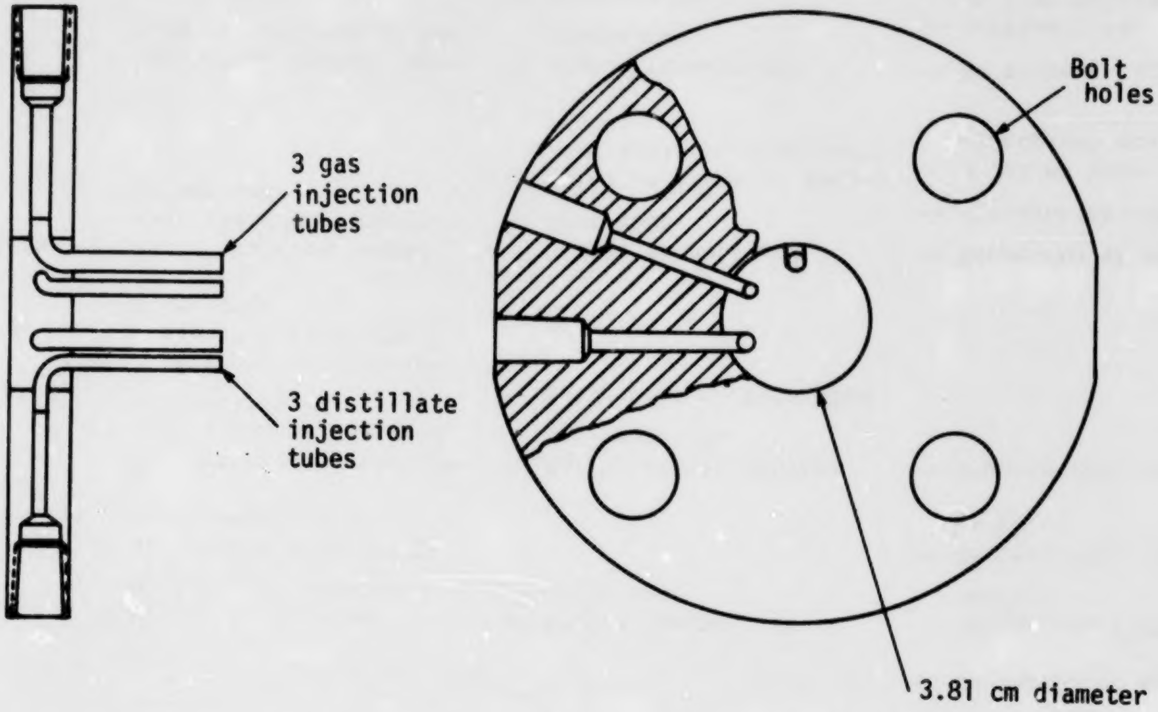
3 gas
injection
tubes
3 distillate
injection
tubes
Bolt
holes
3.81 cm diameter

Figure 1. Aerodynamic fuel injector.

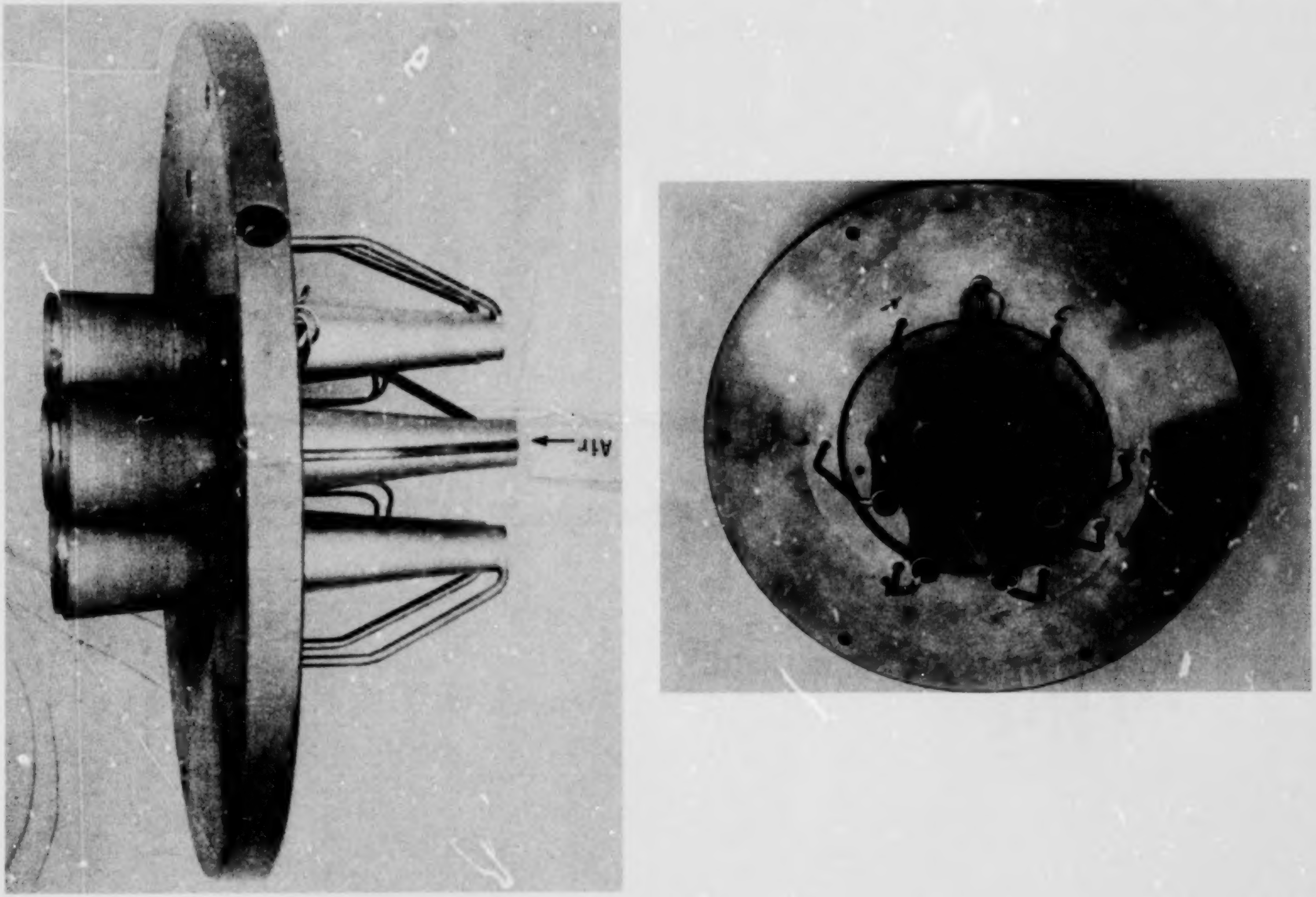

Figure 2. Multiple venturi fuel injector assembly.

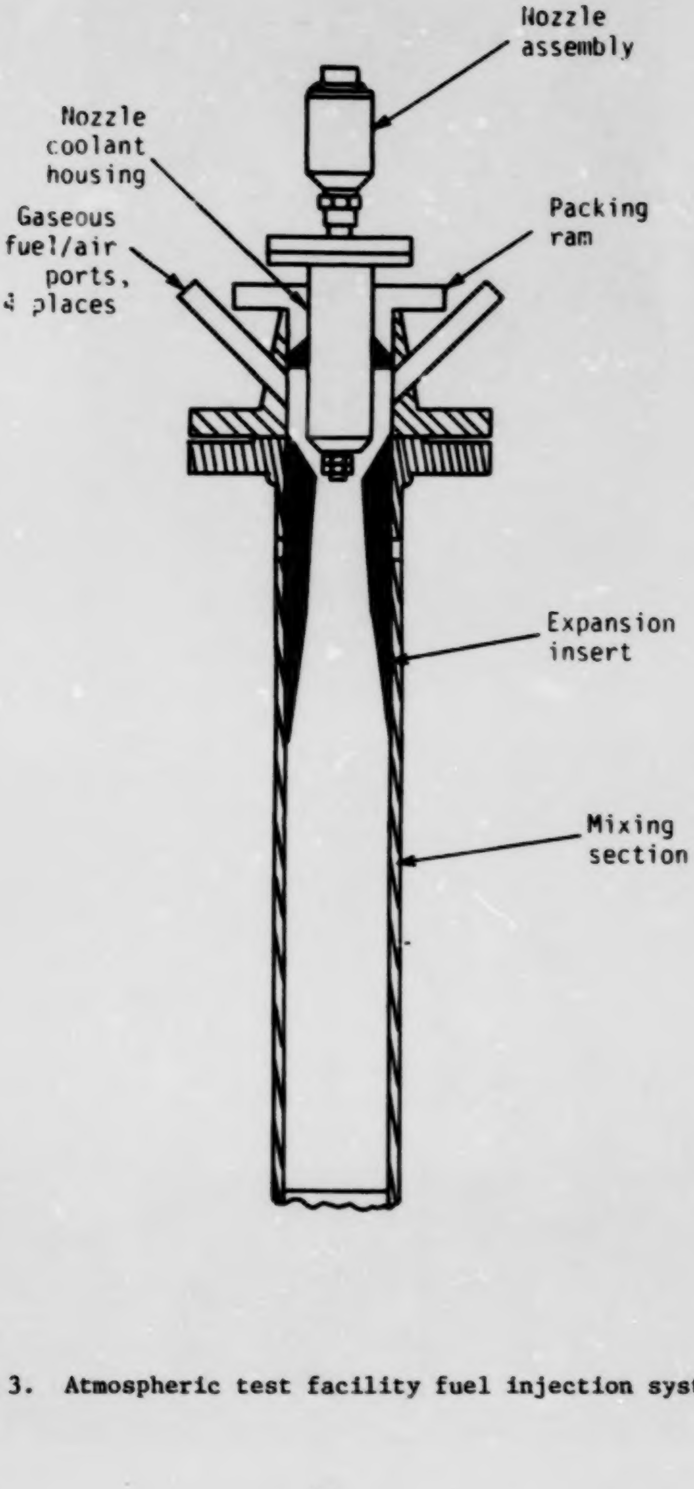
Nozzle assembly
Nozzle coolant housing
Gaseous fuel/air ports, 4 places
Packing ram
Expansion insert
Mixing section

Figure 3. Atmospheric test facility fuel injection system.

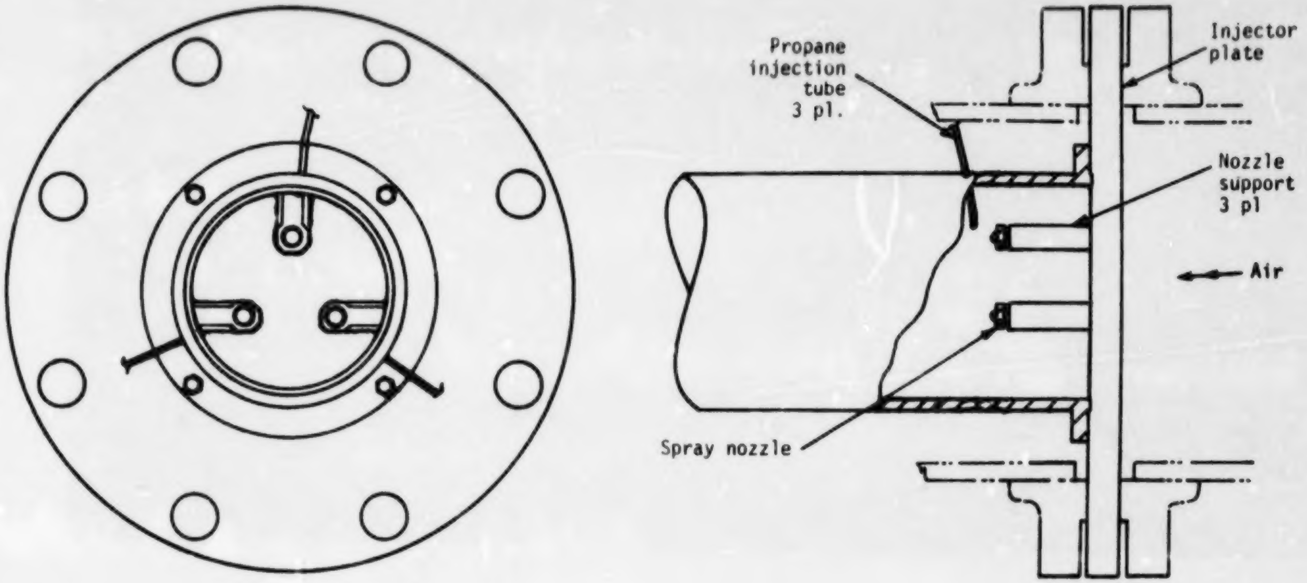
Propane
injection
tube
3 pl.
Injector
plate
Nozzle
support
3 pl
Air
Spray nozzle

Figure 4. Multiple spray fuel injector.

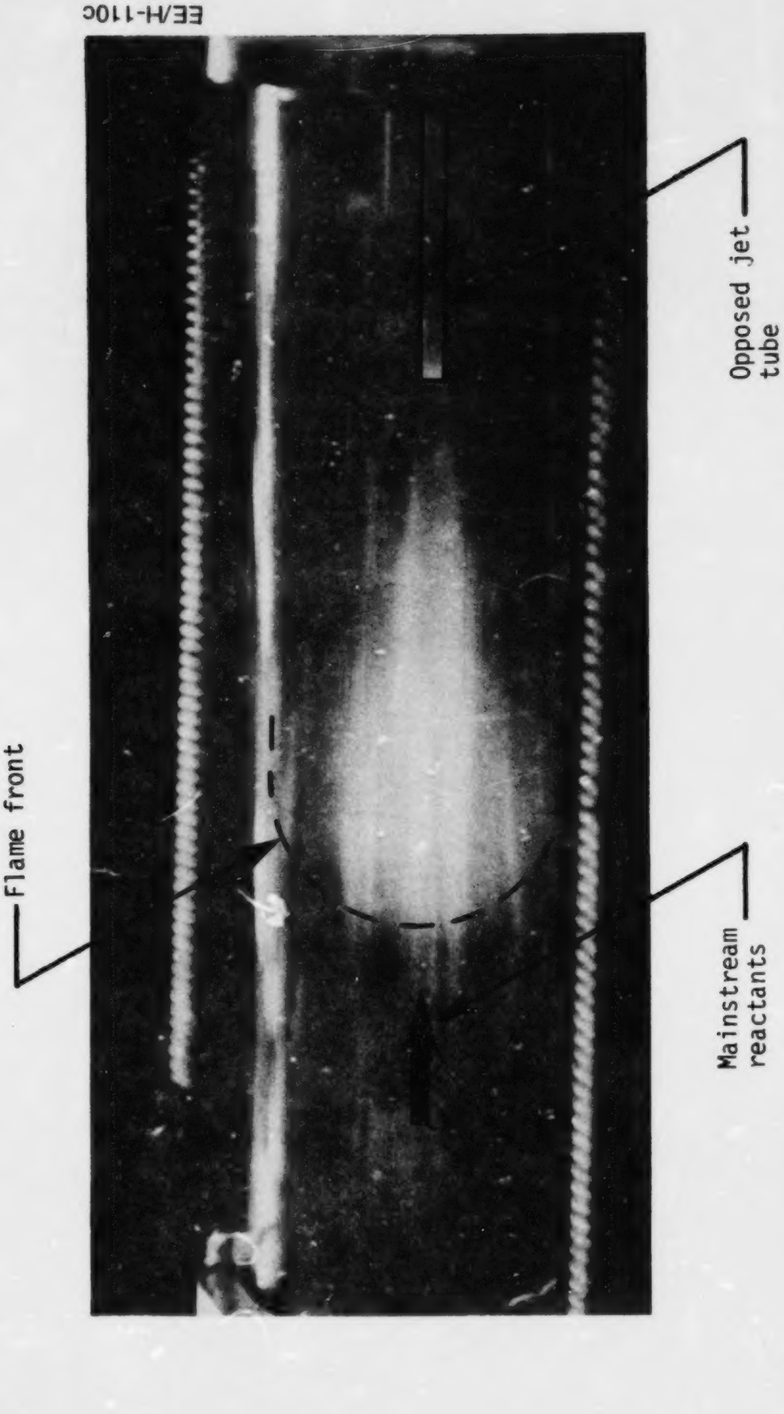
EE/H-110c
Opposed jet tube
Flame front
Mainstream reactants

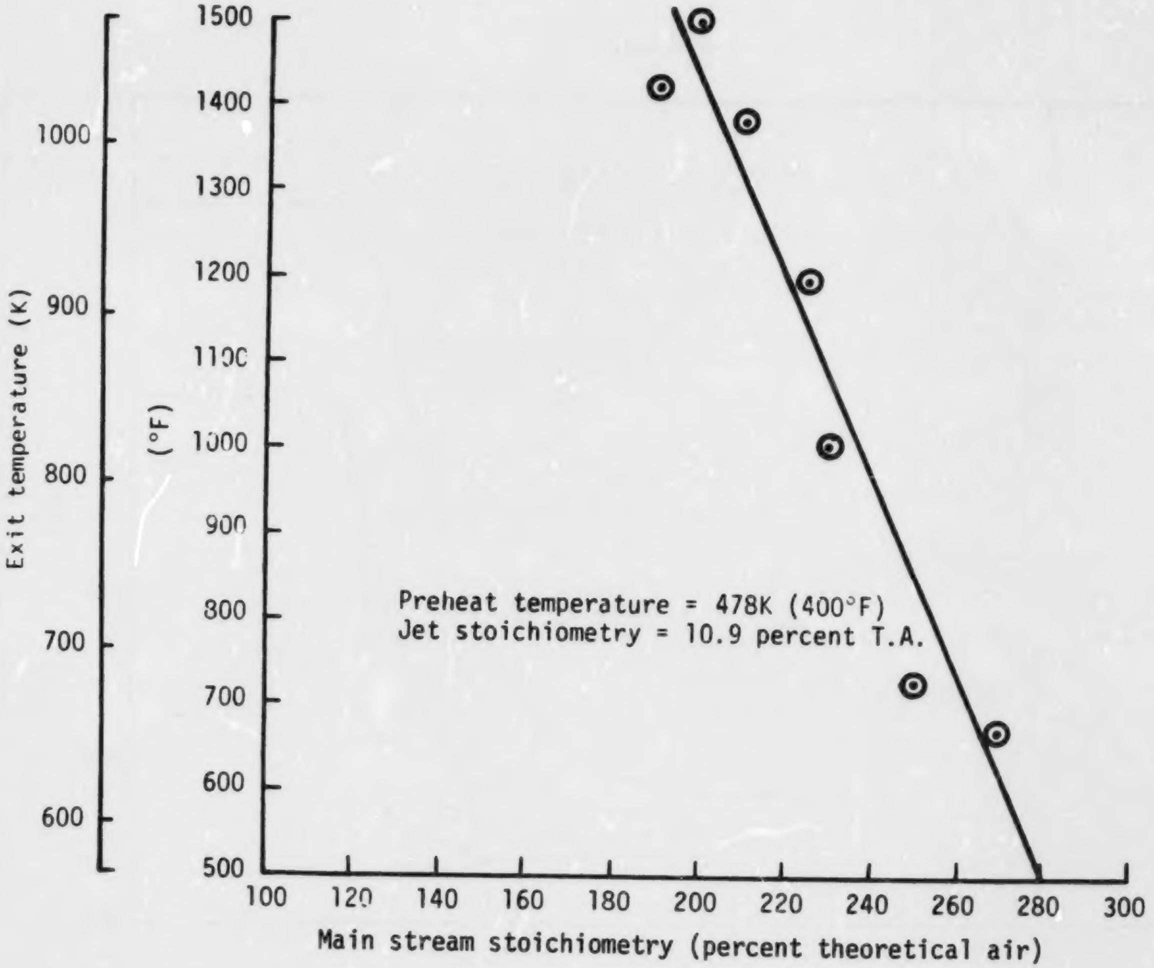

Figure 6. Opposed jet igniter -- exit temperature versus mainstream stoichiometry.

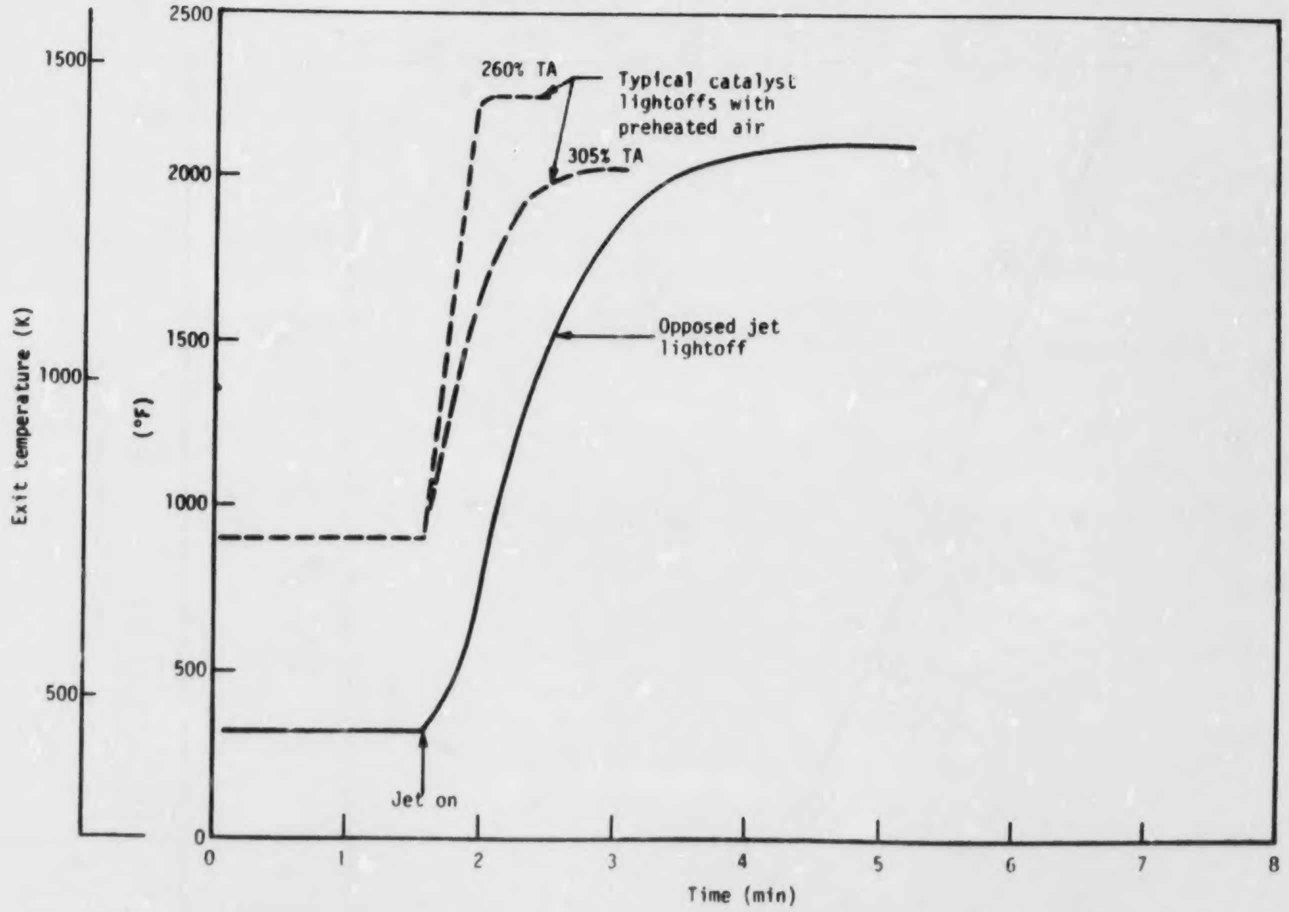

Figure 7. Lightoff time comparison.

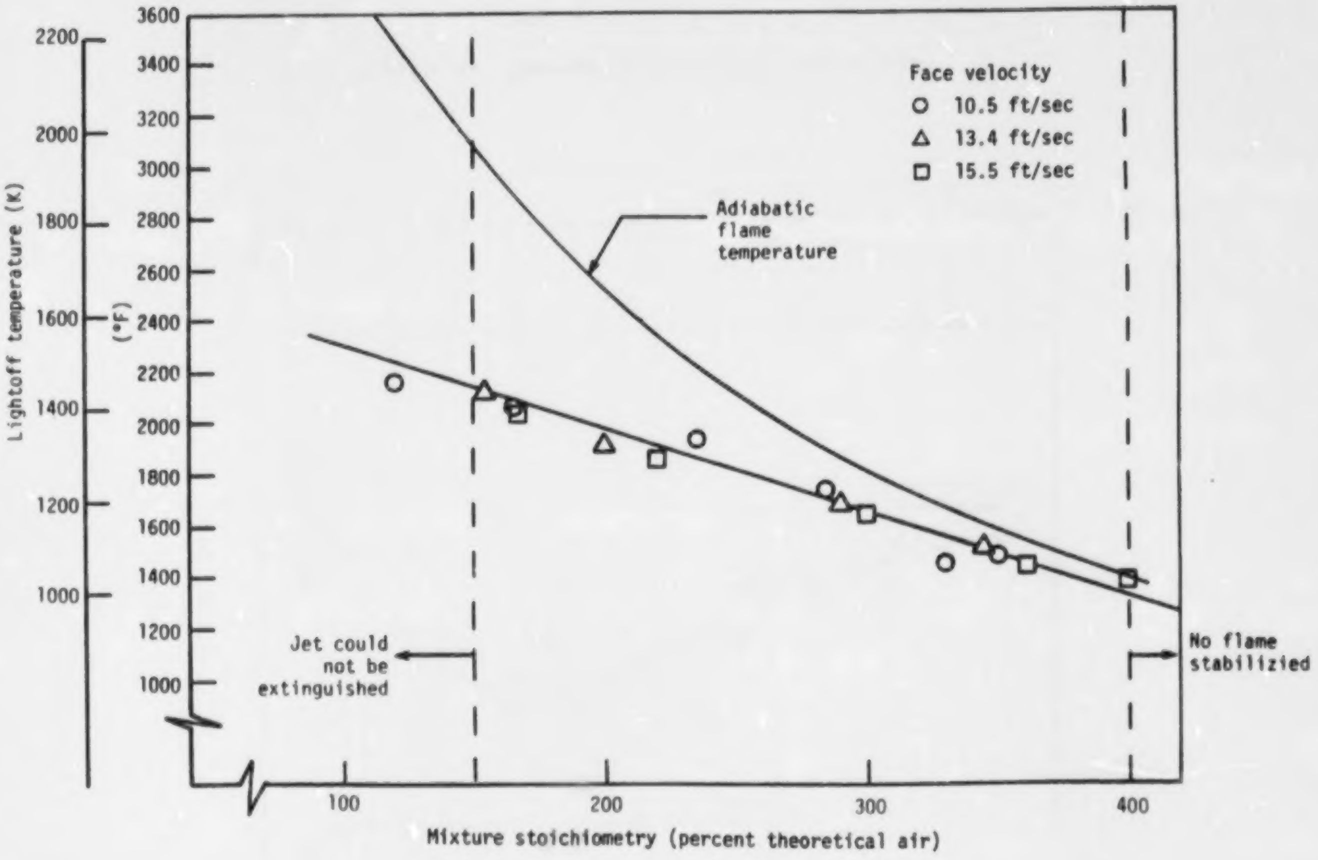

Figure 8. Gas turbine opposed jet results.

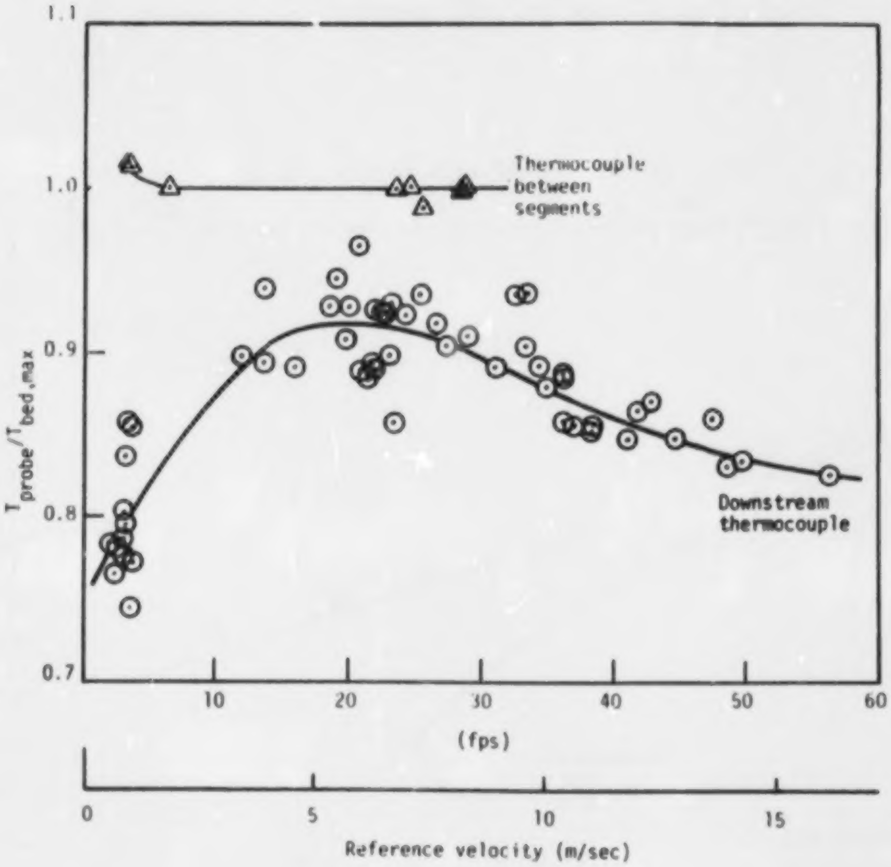

Figure 9. Thermocouple probe comparison.

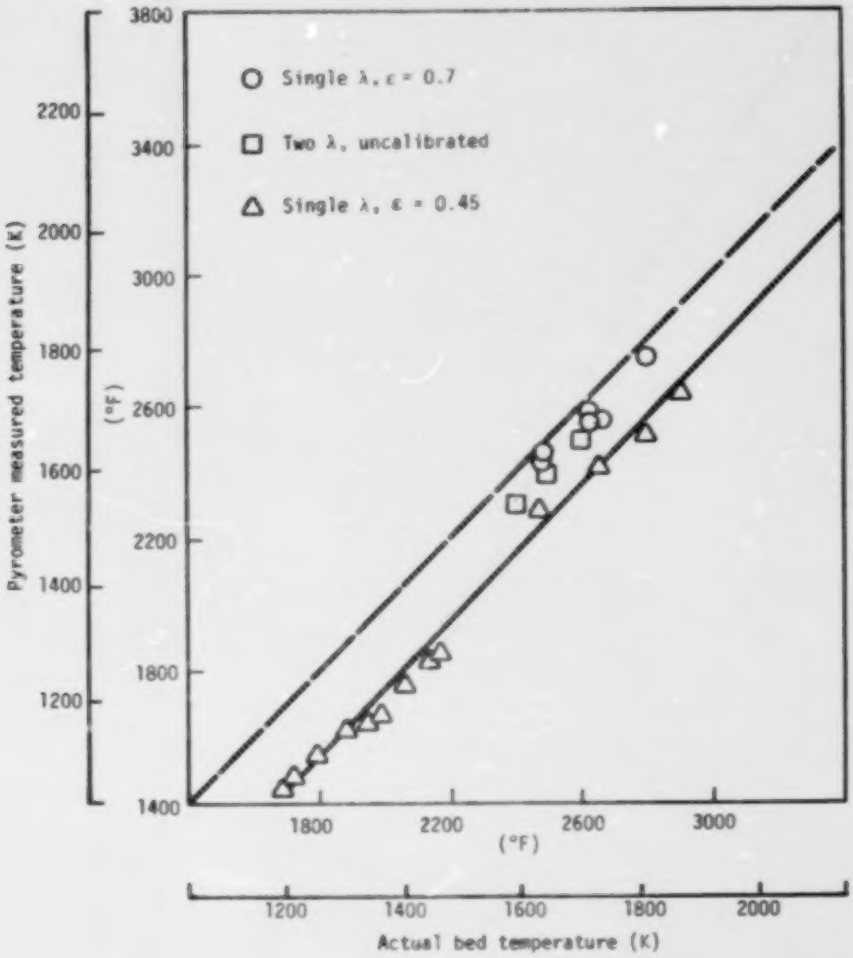

Figure 10. Pyrometer temperature measurement comparison.

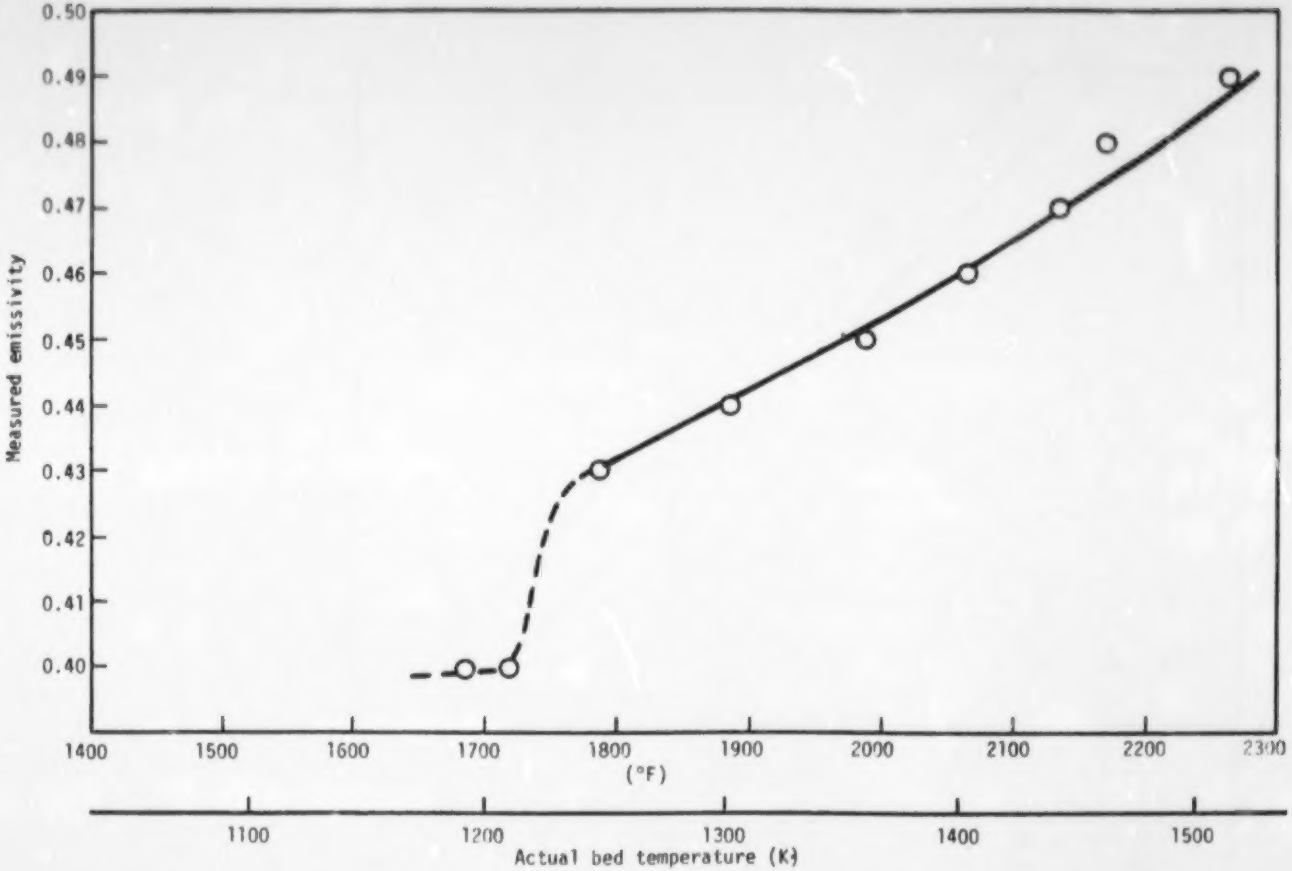

Figure 11. Torvex emissivity changes with temperature (Pt catalyst).

PRELIMINARY DESIGN OF CATALYTIC COMBUSTORS

By:

William B. Retallick
Consultant
West Chester, PA 19380

ABSTRACT

At high temperatures the rate of surface combustion can be so fast that the observed rate is simply the rate of mass transfer to the surface. When the flow is turbulent, mass transfer is analogous to momentum transfer, and the rate of momentum transfer is proportional to the pressure drop. We can measure the pressure drop per length of honeycomb, and use this measurement to calculate the length of honeycomb to give any desired conversion.

In laminar flow, mass transfer occurs by diffusion alone, and the diffusional process is not coupled to the pressure drop. Here, however, we can calculate the length of honeycomb for the desired conversion directly from the velocity, the diameter of the channel, and the properties of the fluid.

These calculations are quick and simple, but are accurate enough for preliminary design.

SYMBOLS

Re	Reynolds number
Pr	Prandtl number
Sc	Schmidt number
f	Friction factor
K	Mass transfer coefficient, $\frac{\text{Length}}{\text{Time}}$
h	Heat transfer coefficient, $\frac{\text{Heat}}{(\text{Area})(\text{Time})(\text{Temperature})}$
K_H	Heat conductivity, $\frac{\text{Heat}}{(\text{Length})(\text{Time})(\text{Temperature})}$
ρ	Density, $\frac{\text{Mass}}{\text{Volume}}$
C_p	Heat capacity, $\frac{\text{Heat}}{(\text{Mass})(\text{Temperature})}$
d	Effective diameter of a channel, $\frac{4\ (\text{Sectional Area})}{\text{Wetted Perimeter}} = \frac{4}{a}$
v	Velocity, $\frac{\text{Length}}{\text{Time}}$
ΔP_f	Pressure drop from fluid friction, $\frac{\text{Force}}{\text{Area}}$
g_c	Gravitational constant, $\frac{(\text{Mass})(\text{Length})}{(\text{Force})(\text{Time})^2}$
T	Temperature
D	Diffusion coefficient $\frac{(\text{Length})^2}{\text{Time}}$

THE TRANSFER UNIT

For both turbulent and laminar flow, the measure of the rate of transfer is the length of the transfer unit. We will derive the length of the transfer unit from the differential equation that describes the transfer process. For mass transfer, this is:

$$\frac{dC}{dL} = -\frac{aKC}{v}$$

which leads to $\ln \frac{C_L}{C_{inlet}} = -\frac{aKL}{v}$

when the length of reactor equals $\frac{v}{Ka}$, $\frac{C_L}{C_{inlet}} = e^{-1}$

This shows what one transfer unit does, and thereby defines the length of one transfer unit. We can write similar equations for heat transfer, and then summarize the results for both mass and heat transfer as:

$$L_{mass} = \frac{v}{Ka}$$

$$L_{heat} = \frac{v\rho C_p}{ha}$$

These definitions are general, and hold for both turbulent and laminar flow. It is not convenient to use these equations directly, because that would require us to calculate the transfer coefficients h and K. For turbulent flow, we will bypass the coefficients by using instead the friction factor, which we can measure experimentally. For laminar flow, the coefficients are buried in the Nusselt number, which we calculate from a mathematical model.

TURBULENT FLOW

In fast turbulent flow, when all of the transfer results from turbulent motion, and diffusional resistance is suppressed, the Reynolds analogy applies.

In words, what the Reynolds analogy says is:

$$\frac{\text{rate at which mass is transferred to the solid surface}}{\text{total rate at which the component, in excess of the interfacial concentration, flows past the surface}} =$$

$$\frac{\text{rate of heat transfer to the solid surface}}{\text{total rate at which heat, measured above the temperature of the surface, flows past the surface}} =$$

$$\frac{\text{rate of momentum transfer due to friction}}{\text{total momentum of the stream which flows past the surface}}$$

Translated into symbols, the analogy becomes:

$$\frac{dC}{\Delta C} = \frac{dT}{\Delta T} = -\frac{\Delta P_f}{\rho}\frac{2g_c}{v^2}$$

Introducing the transfer coefficients for mass and heat converts the last equation into

$$\frac{v}{Ka} = \frac{\rho v C_p}{ha} = \frac{2}{fa}$$

$$L_{mass} = L_{heat}$$

which shows that the two transfer units have equal lengths when (and only when) the Reynolds analogy applies. In the usual case where there is some diffusional resistance, this resistance is accounted for by Colburn's modification of the Reynolds analogy, which leads to

$$\frac{v}{Ka}(Pr)^{-2/3} = \frac{\rho v C_p}{ha}(Sc)^{-2/3} = \frac{2}{fa}$$

or

$$L_{mass} = \frac{2}{fa}(Sc)^{2/3}$$

$$L_{heat} = \frac{2}{fa}(Pr)^{2/3}$$

Now we will use our pressure drop data to obtain the friction factor f and then L_{mass} and L_{heat}. The most convenient way to get the data would be to blow ambient air through the honeycomb, and to plot the pressure drop per length against the velocity. For our present purpose, these data are converted to a plot of friction factor vs the Reynolds number in the channels of the honeycomb. For channels having an irregular cross section, the effective diameter d is

$$d = \frac{4\ (\text{Sectional Area})}{\text{Wetted Perimeter}} = \frac{4}{a}$$

Calculate the Reynolds number at the velocity and temperature expected in the combustor, enter the plot with this Reynolds number, and pick off the friction factor. Use this value of f to calculate L_{mass} and L_{heat} in the combustor. Now we can calculate the length of honeycomb needed to give any desired conversion, since $\frac{C_{in}}{C_{out}} = e^{-N}$ where N is the number of transfer units.

Another quantity that is useful for preliminary design is the number of velocity heads lost to friction in the length of one transfer unit. The velocity head is defined as $\frac{v^2}{2g_c}$ and it has the dimensions of energy per unit mass of fluid. Rearranging the friction factor equation gives the number of velocity heads used up in any length L

$$-\frac{\Delta P_f}{\rho}\frac{2g_c}{v^2} = \frac{4fL}{d} = afL$$

substituting for L the values we just calculated for L_{mass} and L_{heat} gives

number of velocity heads per mass transfer unit = $2\ (Sc)^{2/3}$

number of velocity heads per heat transfer unit = $2\ (Pr)^{2/3}$

What makes these numbers so useful is that they are independent of the velocity and of the diameter of the channel. We can estimate the number of velocity heads needed to give any desired conversion, without measuring the pressure drop.

LAMINAR FLOW

In laminar flow it is possible to calculate the lengths of the transfer units directly from the velocity, the diameter of the channel, and the properties of the fluid, without measuring the pressure drop. This is so because the transfer occurs by diffusion alone, and the diffusional process is not coupled to the pressure drop.

As a model for the calculations, assume laminar flow of a fluid in a circular channel with heat transfer to or from the wall. We define the heat transfer coefficient from the relationship

$$\frac{h}{K_H} = \frac{\frac{\partial T}{\partial r} \text{ at the wall}}{T_{wall} - T_{bulk}}$$

From the model we can show that the Nusselt number = $\frac{hd}{K_H}$ = 4.4. Likewise, for mass transfer, $\frac{Kd}{D}$ = 4.4. The derivation is given by Holman, "Heat Transfer," McGraw-Hill, 1976.

Now we have sufficient information to calculate L_{mass} and L_{heat}. For circular channels, $a = \frac{4}{d}$, so that

$$L_{mass} = \frac{v}{Ka} = \frac{vd}{4K} \sim \frac{1}{18}\,\frac{vd^2}{D}$$

and

$$L_{heat} = \frac{v\rho C_p}{ha} = \frac{v\rho C_p d}{4h} \sim \frac{1}{18}\,\frac{v\rho C_p d^2}{K_H}$$

These values of L_{mass} and L_{heat} were derived for circular channels, and we need to estimate the error from applying them to channels of other shapes. The Nusselt number is not very sensitive to the shape of the cross section; it is 4.4 for a circle of diameter d and 4.1 for parallel plates at spacing d. The difference is small, considering the great difference in shape.

We calculate the number of velocity heads lost to friction in the length of one transfer unit, just as we did for turbulent flow:

$$\begin{aligned} &\text{number of velocity heads per mass transfer unit} = \frac{4f}{18}\,\frac{vd}{D} \\ &= \frac{4f}{18}\,(Re)\,(Sc) \\ &\text{number of velocity heads per heat transfer unit} = \frac{4f}{18}\,\frac{v\rho C_p d}{K_H} \\ &= \frac{4f}{18}\,(Re)\,(Pr) \end{aligned}$$

Note that these expressions can be written so that they contain the product of the friction factor and the Reynolds number. For laminar flow in circular channels, this product is equal to 16, and the constant 16 comes from the Poiseulle equation. For parallel plates the product is 24, when the effective diameter for calculating both f and Re is the same as for the circle:

$$\frac{4\ (\text{Sectional Area})}{\text{Wetted Perimeter}} = d$$

The constants for other shapes should fall between 16 and 24.

The results of all of these calculations are summarized in Table I.

TABLE I. SUMMARY OF THE CALCULATIONS

WHAT IS BEING TRANSFERRED	CONCENTRATION PER VOLUME OF FLUID	TRANSFER COEFFICIENT	DIMENSIONS OF THE COEFFICIENT	LAMINAR OR TURBULENT FLOW	LENGTH OF ONE TRANSFER UNIT	VELOCITY HEADS USED UP IN ONE TRANSFER UNIT
Mass	$\frac{\text{Weight or Mols}}{\text{Volume}}$	K	$\frac{\text{Length}}{\text{Time}}$	Turbulent	$\frac{d}{2f}$[1] $Sc^{2/3}$	$2\ Sc^{2/3}$
Heat	$\rho C_p T$	h	$\frac{\text{Heat}}{(\text{Area})(\text{Time})(\text{Temp})}$	Turbulent	$\frac{d}{2f}\ Pr^{2/3}$	$2\ Pr^{2/3}$
Mass	Above	K	Above	Laminar	$\frac{1}{18}\ \frac{vd^2}{D}$	$\frac{4f}{18}\ Re\ Sc$
Heat	Above	h	Above	Laminar	$\frac{1}{18}\ \frac{v\rho C_p d^2}{K_H}$	$\frac{4f}{18}\ Re\ Pr$

[1] Effective diameter d is $4\ \left(\frac{\text{Cross Sectional Area}}{\text{Wetted Perimeter}}\right) = \frac{4}{a}$

CATALYTIC FLAME STABILIZATION

By:

Moshe Lavid and A. E. Cerkanowicz
Exxon Research and Engineering Company
Corporate Research-Technology Feasibility Center
P. O. Box 45
Linden, New Jersey 07036

ABSTRACT

The Catalytic Flame Stabilization process is applied to aeropropulsion afterburners combustion. For this application, a portion of the inlet fuel-air stream passes through the porous flameholder wherein heterogeneous reactions are promoted by catalytically coated surfaces. The partially reacted mixture having higher temperatures, then passes into the aft region. The other portion of the approaching fuel-air mixture flows around the porous flameholder merging downstream with the previous stream. As a result of the supplemental heat release due to the catalytic reactions, higher wake temperature and improved combustion stability are obtained with concurrent reduction in pressure drop.

In this concept the key role of the catalyst is to "bootstrap" the conditions of temperature and concentration of partially reacted species to levels favorable to stable efficient gas phase combustion. Consequently, the catalytic unit need only process a portion of the reactant mixture and need only provide for the initial stimulus.

This paper outlines the catalytic flame stabilization program undertaken by Exxon. It is a comprehensive experimental research directed and guided by a complementary analytical modeling effort.

ACKNOWLEDGMENT

This work is supported in part by the Air Force Office of Scientific Research, under Contract No. F49620-77-C-0085. Dr. B. T. Wolfson is the Contract Monitor.

INTRODUCTION

Combustion systems are limited by combustion associated phenomena such as flammability, flame propagation, ignition and stable combustion, and by the formation of combustion-related pollutants. Recent research has identified catalytic combustion as a potentially promising technique for rectifying these limitations. The technique involves the utilization of heterogeneous catalysis to enhance combustion processes and to broaden normally encountered stability limits, particularly at fuel lean and low temperature conditions.

In general, catalytic combustion is a concept wherein chemical reactions initiated by a heterogeneous catalyst play an important role in the energy release processes of a reacting fuel-air system. The effect of the solid catalyst is predominant only during the early phases of the overall combustion process. As fuel is oxidized and energy is released, the importance of homogeneous reactions increases and eventually they become controlling, and the balance of energy release is achieved through them.

A number of general potential applications have been considered. Catalytic gas-turbine combustors can achieve stable combustion at lower temperatures than that required to insure stable combustion in conventional combustors. The lower temperatures will result in a substantial reduction in NO_x emissions (1) from the unacceptable levels produced in the primary zone of the conventional combustors due to the high temperatures. Fuel-air mixture that cannot be combusted efficiently and stably by ordinary homogeneous means such as various types of low heating value fuels, can be utilized by catalytically augmenting the combustion, (2). Catalytic converters represent another commonly used application in the automotive industry. In this application, the heterogeneous reactions dominate while the gas phase reactions are of little importance (3,4). In some other application, catalytic combustion is used as a means for flame stabilization.

Catalytic flame stabilization differs from catalytic combustion in that the heterogeneous reactions are only needed to promote the combustion process to a point where normal gas phase reactions take over and become dominant. This catalytic flame stabilization concept is particularly important to aeropropulsion combustion; turbopropulsion mainburners, afterburners, duct burners, and ramjet dump combustors.

This paper outlines the catalytic flame stabilization program currently underway at the Corporate Laboratories of Exxon Research and Engineering Company in Linden, New Jersey.

PROGRAM OBJECTIVES

The objectives of the program are to develop a fundamental understanding of the aerothermochemistry of catalytic flame stabilization and to establish design aids to be used in subsequent exploratory development efforts. Fundamental information includes: (1) characterization of the flow field around a catalytic stabilizer, (2) determination of the role of the catalyst in stabilizing the combustion process, (3) establishment of catalyst and monolith material choices, (4) characterization of downstream combustion zone processes including wake circulation, turbulent shear layer combustion and flame propagation, (5) quantification of stability limits, and (6) development of an analytical model of the catalytic flame stabilization process. Design aids include correlations and models of the catalytic flame stabilization process as well as guidelines for application related to fuel types, fuel impingement, and gradients of fuel-air ratio and temperatures in the approach flow.

The catalytic flame stabilizer is conceptually illustrated in Figure 1. The conventional solid bluff-body flameholder, which stabilizes the flame by producing a wake region behind it, is replaced by a porous device with catalytically coated surfaces along its passages. The porous design permits flow through, as well as around, the device resulting in less pressure drop than a solid flameholder of equal cross-section area. However, the flow through the porous catalytic unit has some adverse effect on the flame stability. It tends to wash out the recirculating region which is needed to provide flow residence times of the same order as the characteristic chemical reaction times, and thus reduces flame stability. This difficulty is alleviated by coating the surface of the passages with solid catalysts. The key role of the catalyst is to "bootstrap" the conditions of temperature and species concentration to levels favorable to stable, efficient gas phase combustion. Thus, the catalyst offsets the problem associated with the reduction in flow residence time, due to the flow stream through the catalytic porous unit.

PROGRAM APPROACH

The catalytic flame stabilization program encompasses experimental work as well as analytical modeling effort.

The experimental portion of the program involves a detailed study of the region about various flame stabilization devices. Figure 2 depicts some representative samples of the devices to be investigated. Initially, a standard bluff-body flameholder (V-gutter) and a non-catalytic monolith will be tested to establish an experimental baseline (A and B in Figure 2). Subsequent test will employ catalytic monoliths or specially fabricated flameholders which simulate catalytic stabilizing device operation (C and D in Figure 2). In this latter case, a flameholder with its downstream side sealed with a sintered metal plate will be used. It is a simulated unit which has the bluff-body appearance of a catalytic unit but also one in which we can vary the type of species and its concentrations. In other words, it is a diagnostic device capable of simulating different modes of catalytic stabilization operation, by introducing into the wake region various gas compositions at different temperatures, representative of initial as well as partially oxidized fuels. This simulated catalytic flameholder provides us with the capability of evaluating the important combustion mechanisms in the catalytic flameholder under well monitored and reproducible conditions independent of actual heterogeneous reactions. The experimental variables include fuel type, inlet temperature and velocity.

The experimental work is also aimed at the examination of broad variations in catalyst and monolith types. Catalysts will include from various noble metals (especially platinum and palladium) either singly or in combination with transition metal oxides (oxides of nickel, chromium, etc). Substrates of different blockage ratios, configuration (triangle, rectangular, circular, etc), material composition (ceramic or metal), and overall shape (triangular, disc, etc) are considered for evaluation.

Experimental direction and guidance will be provided by a complementary analytical modeling effort described later in this paper.

EXPERIMENTAL APPARATUS

A combustion tunnel is currently under construction in Exxon Corporate Laboratories. It is a very versatile apparatus designed to conduct combustion experiments under continuous flow conditions. A diagram of the combustion tunnel is shown in Figure 3. Essentially, it comprises of a horizontal test section; 5" square and/or 6" cylindrical, equipped with transparent side windows to allow visual observations and optical diagnostics. Regulated and metered air is provided by a blower with a capacity of up to 2000 SCFM. The air flows through a precombustor where it can be vitiated up to 1200°K, and enters a settling chamber, housing a number of flow smoothing grids. Then, through a transition piece, it flows into a mixing chamber where it mixes with gaseous or liquid fuels. Before entering the test section, it passes through turbulence grids. The test section is designed to conduct catalytic as well as radiative combustion augmented experiments. The catalytic flame stabilization experiment is depicted in the first blow out. The premixed fuel/air mixture is split into two streams, one stream bypasses the catalytic flameholder while the other one flows through it. The former stream provides the stabilizing wake region, and the latter one improves combustor stabilization due to the catalytically induced heat release, which increases the heat content of the wake region. Concurrently, this flow configuration reduces the pressure drop in the combustor.

The following diagnostics will be emphasized in the combustion tunnel:

LDV - upstream and downstream point velocity measurements
Schlieren - nonreactive/reactive flow patterns
Sampling probes/Gas analyzer - species concentrations
Thermocouples - temperatures
Pitot probes - pressure

In summary, the capabilities of the test facility are as follows:

- Continuous flow (not blow down)

- Cross section: 12.5 cm square, 15.0 cm round
- Velocity: 0-200 m/s
- Temperature: 300-1000°K (vitiated)
- Pressure: 101 kPa
- Fuel: liquid (Jet A, JP4) or gaseous (propane)
- Diagnostics: LDV, Schlieren, species, temperature, and pressure

CATALYTIC FLAMEHOLDER MODELING

The catalytic stabilization process can be analytically analyzed by incorporating Exxon catalytic combustion model (5) with a bluff body flame stabilization theory.

The flow pattern of the porous catalytic flameholder is depicted in Figure 4. It is a simple engineering model aimed to elucidate the fundamental physical and chemical processes, and it is similar to the model proposal by Mullins (6) for solid bluff body. In the model, the inlet reactant stream mixes behind the bluff body with a partially combusted gas stream at higher temperature, resulting in an increase in temperature of the mixture. Part of this mixture enters into the recirculation region, which causes an increase in residence time. During this period of time, more fuel is combusted resulting in additional increase in temperature until self-sustained combustion prevails. However, the catalytic porous flameholder has an additional flow through the catalytic passages which represents a variation from the solid bluff body model. This flow experiences a temperature increase due to the catalytically induced reactions before merging with the gas recirculation stream. As a result of this supplemental heat input, higher wake temperatures and improved combustion stability are achieved, with concurrent reduction in pressure drop. Alternatively, an increase in area of the porous flameholder at constant pressure drop would result in shorter overall combustor lengths.

The catalytic portion of the model utilizes Exxon catalytic combustion model. The assumptions underlying the model are discussed in Reference 5. It essentially employs one dimensional, steady-state, plug flow with global reaction rates in each phase; heterogeneous and homogeneous. Some of the basic physical and chemical processes which are accounted for by the model are illustrated in Figure 5. They include: (1) mass transport of fuel and oxidant from the main stream to the surface as the flow proceeds through the channel, (2) heat release on the surface caused by a global heterogeneous reaction, (3) heat transport by forced convection into the gas phase, (4) axial heat conduction in the substrate, and (5) global homogeneous reaction in the channel.

The model was used to simulate experimental results obtained by Pfefferle et al (7). Figure 6 shows the effects of varying inlet gas temperature on fuel conversion for operating conditions given in the legend. The experimental data points are indicated by solid circles, while the solid and dashed curves were obtained from computer solutions of the analytical model.

Examining the results exhibited in Figure 6 three main features can be identified:

1. Three operating regions of the catalytic system exist. Prior to "light-off" (temperature less than 500 K) the system is limited by the slow surface reaction rate. At intermediate temperatures (500-800 K) surface reaction is fast but fuel conversion levels off at about 70% due to diffusion limitations. The third zone (temperature greater than 800 K) involves complete fuel conversion due to the contribution of gas phase reactions which are initiated ("bootstrapped") by the surface reactions.
2. If no catalyst was present the inlet temperature would have to be increased to 1050 K before appreciable fuel conversion occurs. With the catalyst present, appreciable fuel conversion occurs at temperatures as low as 500 K.
3. Our capability of modeling the complex behavior of the catalytic device is illustrated by the good agreement between experiment and modeling.

Figure 7 illustrates the fraction of fuel conversion attributed to catalytic and gas phase reactions as a function of reactor length or the reaction temperature. It clearly demonstrates that the primary function of the heterogeneous reactions is to "bootstrap" the mixture to conditions such that homogeneous reactions become predominant. For this particular system, the catalytic reactor could probably be shortened by as much as 30%, allowing the gas phase reactions to continue independent of any catalytic surface.

Typical results for catalytic performance at conditions similar to that encountered in afterburners are presented in Figure 8. Increased fuel conversion is observed at lower combustor velocities due to increased gas residence time. As the velocity increases larger catalytic units are required in order to obtain full conversion. The initial conversions observed at short catalytic length are due entirely to surface reactions. At approximately 25% conversion, there is an inflection point in the curve, indicating rapid increase in conversion due to simultaneous occurrence of gas phase reactions within the catalytic unit.

The analytical model of the catalytic flameholder will provide experimental direction and guidance. It will assist in understanding the interaction of the various encountered processes. It will provide a more detailed understanding of the experimental data, and will help predict trends in combustor performances as a function of operating characteristics.

SUMMARY

To summarize, the major advantages of catalytic flameholder are:

1) it can perhaps act as a passive autoignition device
2) it can extend the stability range of an afterburner by allowing for operation at inlet velocities and temperatures where conventional flameholders begin to fail
3) it has the potential of reducing the length required to spread the flame throughout the afterburner cross section by utilizing a porous bluff body larger than a solid one for the same pressure drop
4) alternatively, it has the potential to reduce the pressure drop for the same flame spreading rate.

REFERENCES

1. Blazowski, W. S., and Walsh, D. E., "Catalytic Combustion: An Important Consideration for Future Applications"; Combustion Science and Technology, Vol. 10, pp. 233-244, 1975.

2. Pfefferle, W. C., "The Catalytic Combustor: An Approach to Cleaner Combustion," Journal of Energy, Vol. 2, No. 3, pp. 142-146, 1978.

3. Young, L. C., and Finlayson, B. A. "Mathematical Models of the Monolith Catalytic Converter: Part II. Application to Automobile Exhaust," AIChE Journal, Vol. 22, No. 2, pp. 343-353, Mar., 1976.

4. Hawthorne, R. D., "Afterburner Catalysts - Effects of Heat and Mass Transfer Between Gas and Catalyst Surface," AIChE Symposium Series, No. 137, Vol 70, pp. 428-438, 1974.

5. Cerkanowicz, A. E., and Stevens, J. G., "Case Studies in Simulation of Novel Combustion Techniques", proceedings of the 1979 Summer Simulation Conference, July 10-18, Toronto, Canada.

6. Mullins, B. P., "A Spontaneous Ignition Theory of Combustion Intensity and Combustion Stability Behind a Baffle", Combustion Researches and Reviews, pp. 58-71, Butterworths, 1955.

7. Pfefferle, W. C., et.al., "Catathermal Combustion: A New Process for Low-Emissions Fuel Conversion," ASME Paper No. 75-WA/Fu-1.

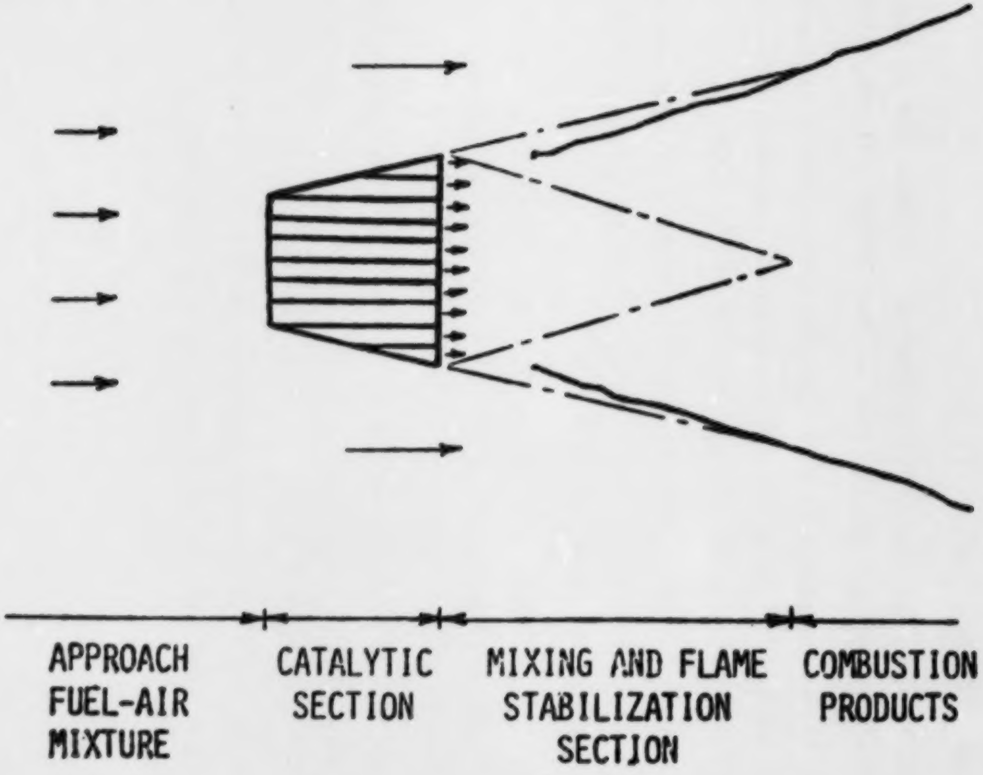
APPROACH FUEL-AIR MIXTURE
CATALYTIC SECTION
MIXING AND FLAME STABILIZATION SECTION
COMBUSTION PRODUCTS

Figure 1. Catalytic flame-stabilization concept.

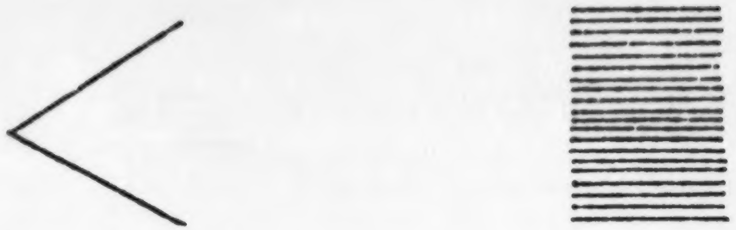

A. Standard V-Gutter

B. Non-Catalytic Monolith

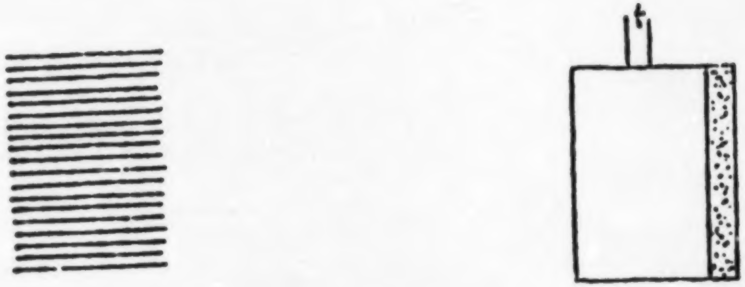

C. Catalytic Monolith

D. Simulated Catalytic Stabilizer

Figure 2. Flame Stabilizing Devices.

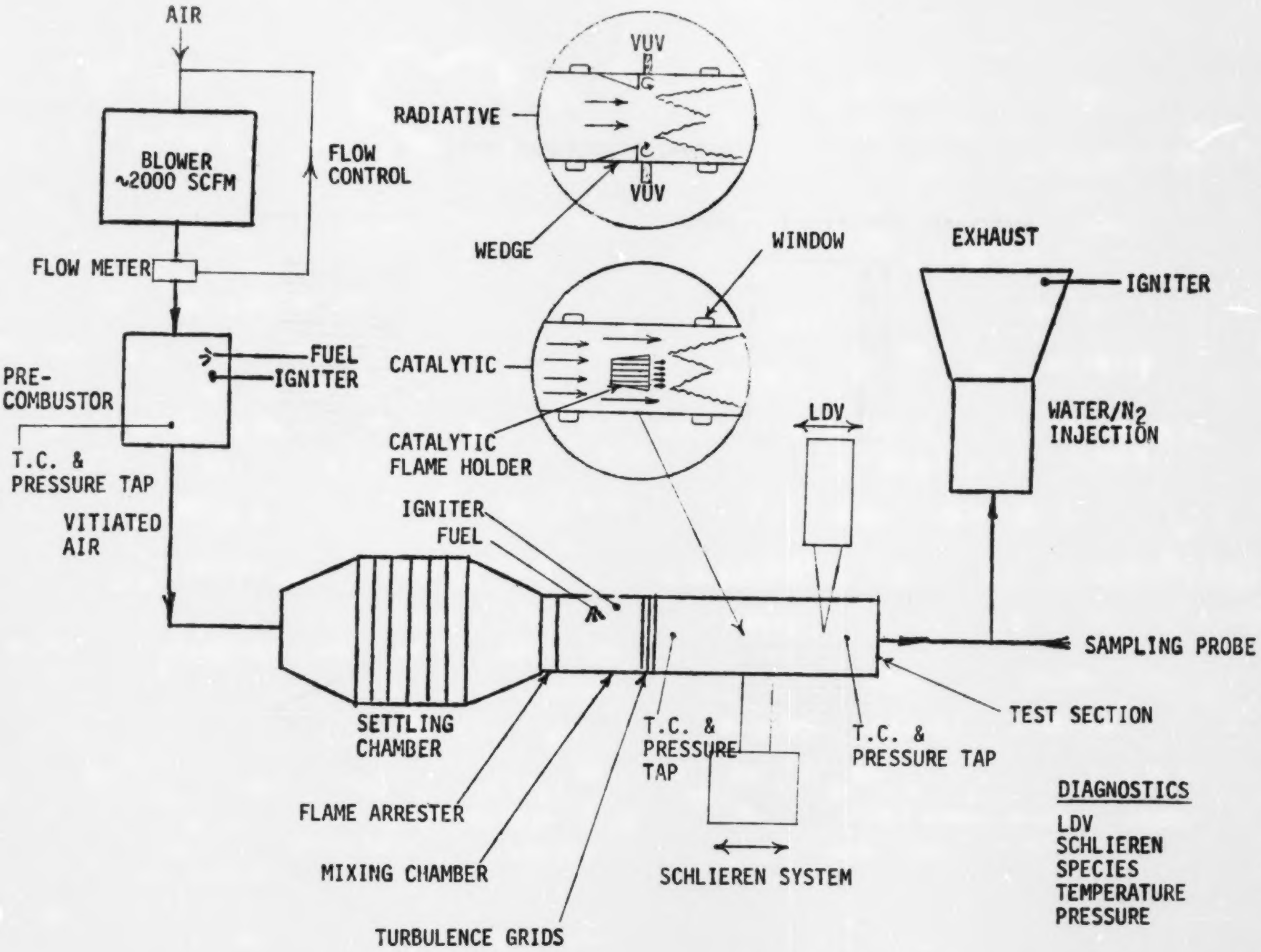

AIR
BLOWER ~2000 SCFM
FLOW CONTROL
FLOW METER
FUEL
IGNITER
PRE-COMBUSTOR
T.C. & PRESSURE TAP
VITIATED AIR
RADIATIVE
VUV
VUV
WEDGE
WINDOW
CATALYTIC
CATALYTIC FLAME HOLDER
EXHAUST
IGNITER
WATER/N2 INJECTION
LDV
IGNITER
FUEL
SAMPLING PROBE
TEST SECTION
SETTLING CHAMBER
T.C. & PRESSURE TAP
T.C. & PRESSURE TAP
FLAME ARRESTER
MIXING CHAMBER
SCHLIEREN SYSTEM
TURBULENCE GRIDS
DIAGNOSTICS
LDV
SCHLIEREN
SPECIES
TEMPERATURE
PRESSURE

Figure 3. Combustion tunnel diagram.

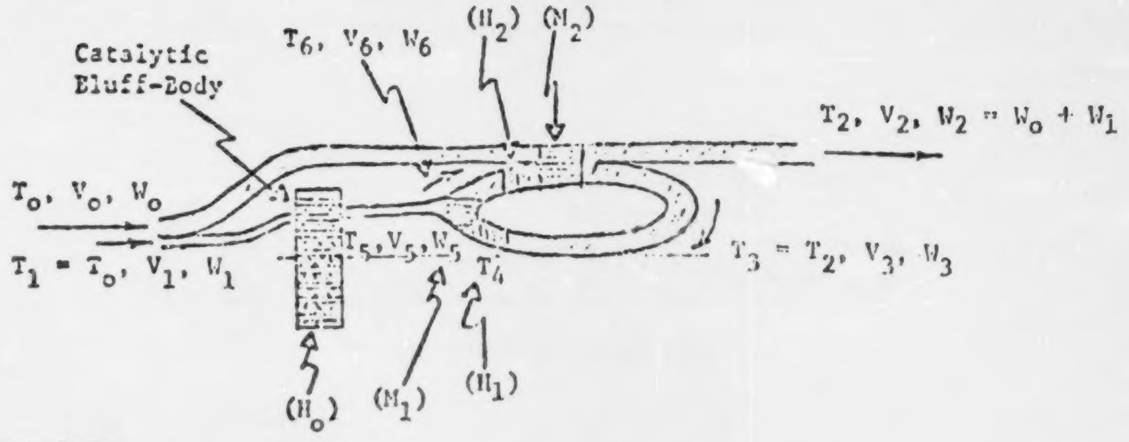
Catalytic Bluff-Body
T_6, V_6, W_6
(H_2)
(M_2)
T_2, V_2, W_2 = W_o + W_1
T_o, V_o, W_o
T_1 = T_o, V_1, W_1
T_5, V_5, W_5
T_4
T_3 = T_2, V_3, W_3
(H_o)
(M_1)
(H_1)

T = temperature
V = velocity
W = mass flow rate
(M) = mixing zone
(H) = heat release zone

Figure 4. Model for catalytic stabilization theory.

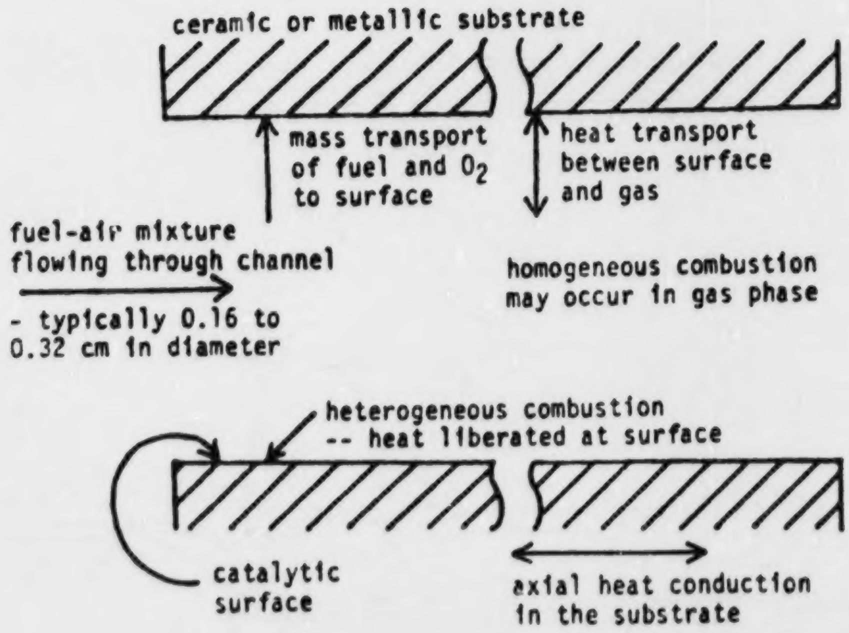
ceramic or metallic substrate
mass transport of fuel and O_2 to surface
heat transport between surface and gas
fuel-air mixture flowing through channel
- typically 0.16 to 0.32 cm in diameter
homogeneous combustion may occur in gas phase
heterogeneous combustion -- heat liberated at surface
catalytic surface
axial heat conduction in the substrate

Figure 5. Chemical and physical processes modeled in catalytic combustion.

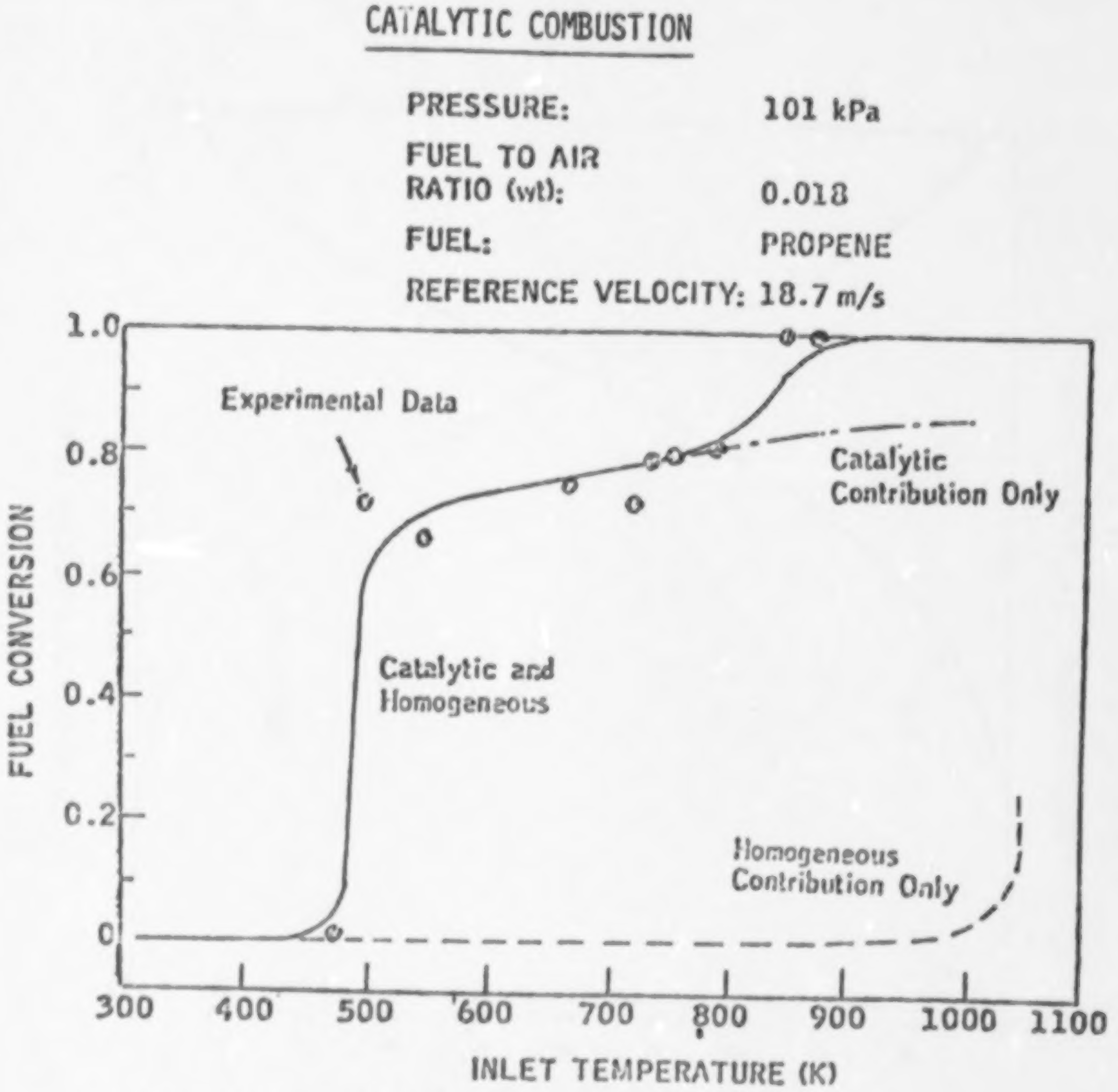

Figure 6. Experimental data (o) and model-generated curves showing the effect of inlet temperature on fuel conversion.

PRESSURE: 101 kPa
INLET TEMPERATURE: 662 K
FUEL: PROPENE
REFERENCE VELOCITY: 18.3 m/s
FUEL/AIR RATIO: 0.0258 kg/kg

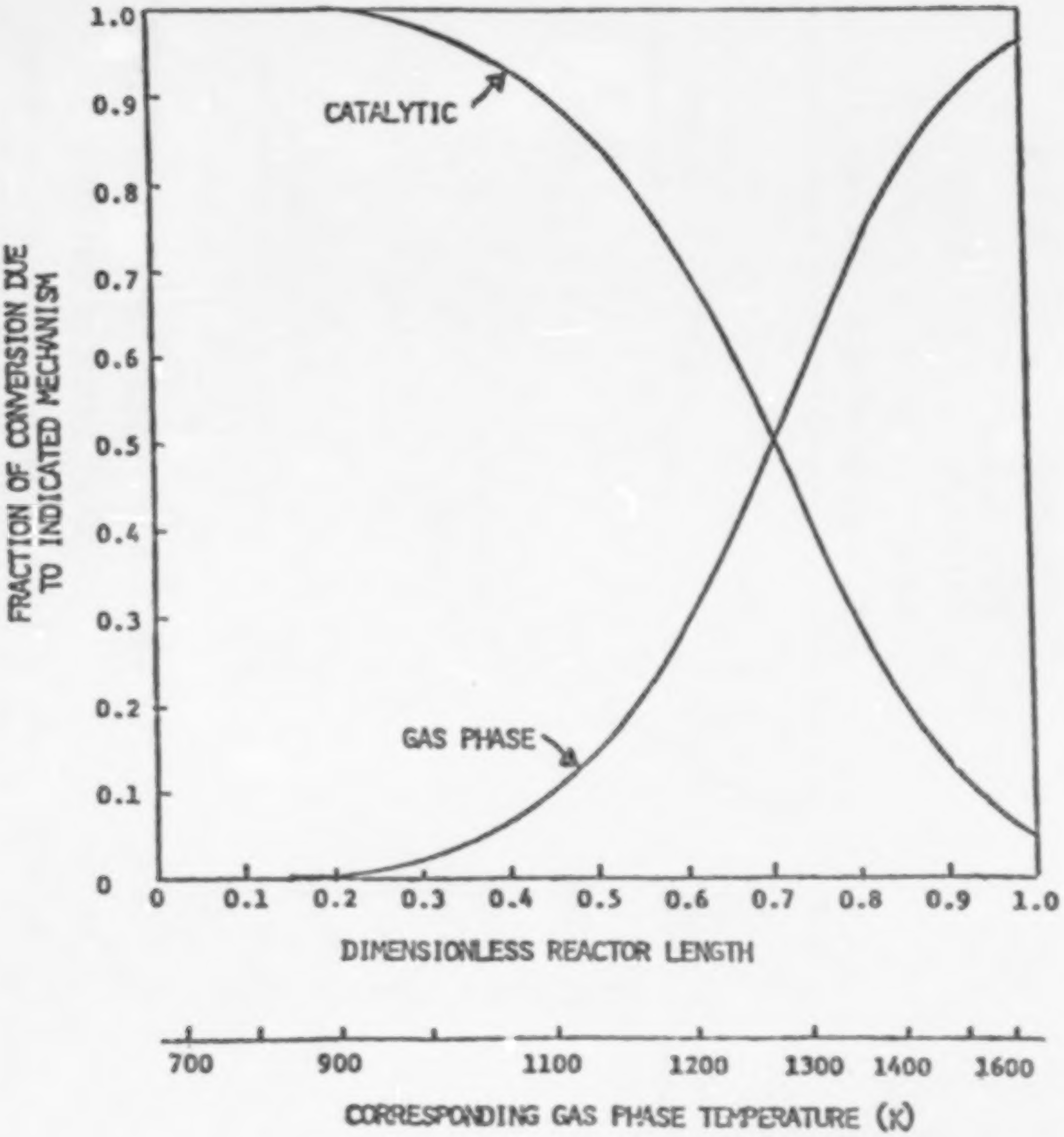

Figure 7. Change in mechanism of fuel conversion during catalytic combustion.

Fuel: C_3H_6 at T_{inlet} = 978 K, P_{inlet} = 101.3 kPa

Catalyst: Platinum

Substrate: Channel Diameter = 0.32 cm, Open Area = 0.93,
Thermal Conductivity = 16.76 W/mK

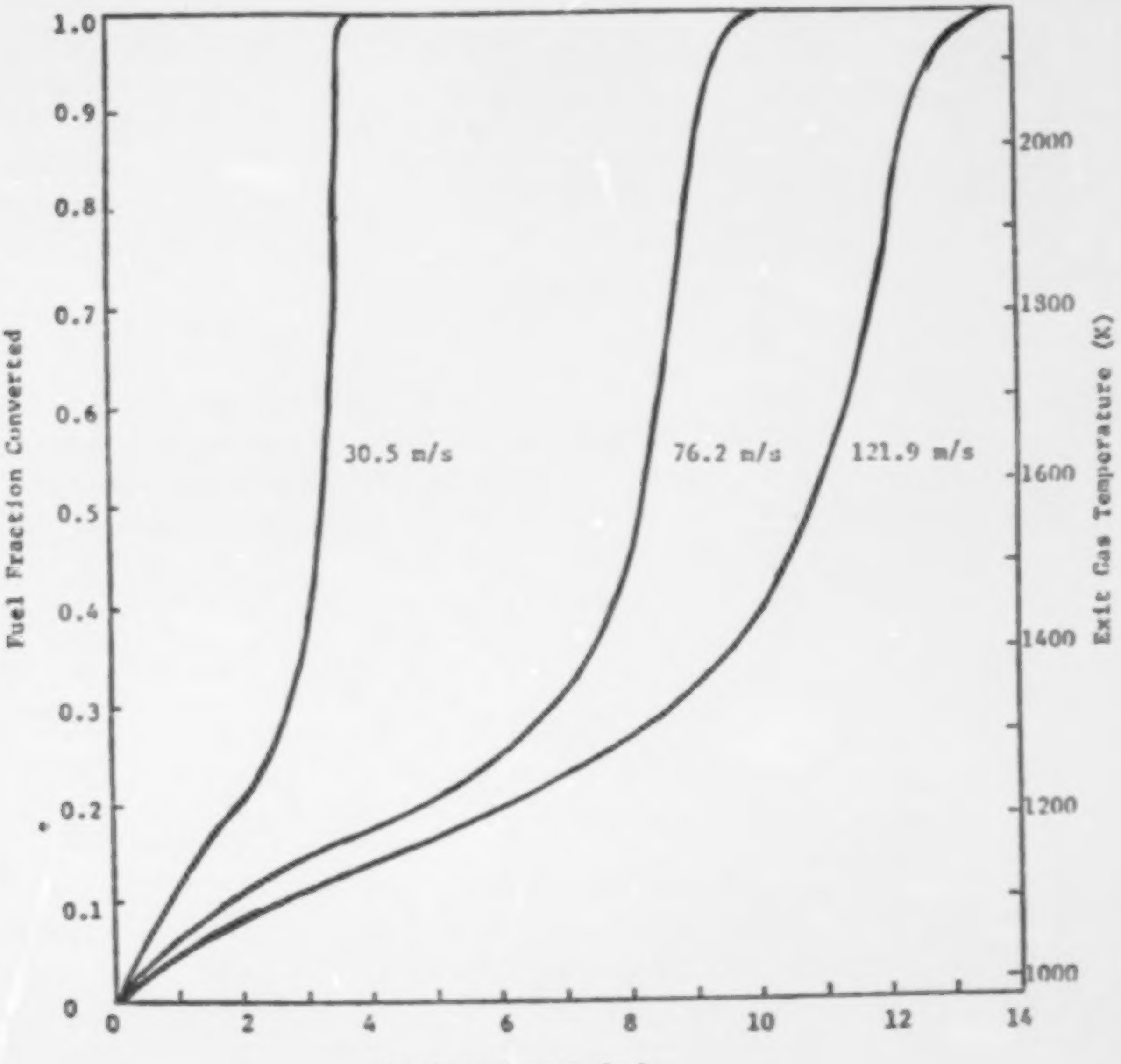

Figure 8. Typical catalytic reactor performance at afterburner conditions.

THERMAL SHOCK RESISTANT CATALYTIC MONOLITHS USING FOAM CERAMICS TECHNOLOGY

BY

William C. Pfefferle
Consultant
51 Woodland Drive
Middletown, New Jersey 07748

ABSTRACT

A review of the design considerations for the use of ceramic materials has shown that thermal shock tolerant catalytic combustor designs are feasible. Several such designs are proposed. Foam ceramics technology is most useful in producing thermal shock resistant monolith catalysts based on such designs.

INTRODUCTION

As is well documented, the high efficiency of a catalytic combustor as compared to catalytic converters is the result of gas phase homogeneous reactions induced by the catalyst. Thus, for efficient combustor performance, monolith combustor catalysts must be able to operate at a temperature high enough to promote thermal reactions, i.e. a temperature above 1800-2000F. To achieve a reasonable turn-down ratio, operable catalyst temperature must be even higher, for example 2500F or higher. For such high use temperatures, ceramics are obvious materials of choice. Although certain metals can be used in this temperature range, the high cost of the exotic materials required is a serious drawback. The use of ceramics, on the other hand, imposes stringent limitations on combustor design, and thus on catalyst configuration, because of the need to limit thermal tensile stresses to relatively low values. There would be no problem of course if stable zero expansion ceramics were available. With available ceramics, the configurations required to minimize thermal shock stresses are difficult or impossible to make using conventional monolith manufacturing processes. Fortunately, ceramic sponge technology makes possible catalytic monoliths of almost any desired configuration.

CERAMIC MONOLITH DESIGN CONSIDERATIONS

Before discussing the advantages of sponge ceramics, it is well to review the pertinent design considerations governing the use of ceramic materials. As is well known, thermal shock failure is a major factor limiting the usefulness of ceramic materials. For high temperature applications such as catalytic combustor catalysts, it is often relatively easy to find materials which possess satisfactory structural properties at relatively high use temperatures. Nevertheless, failures can occur at much lower temperatures during heating or cooling. The explosive shattering of hot ceramic ovenware placed on a cold surface is a common experience. A primary reason for this is that unlike metals, ceramics possess almost no ductility except at very high temperatures and typically are low in thermal conductivity and tensile strength. Only beryllia and silicon carbide are comparable to metals in thermal conductivity. No polycrystalline ceramic comes closer than about 25% of the tensile strength of readily available metal alloys at temperatures below 2000F. Cermets, although far better in thermal shock resistance than most ceramics, are subject to oxidation of the metallic component and thus limited to lower use temperatures than available high temperature ceramics.

The key to the successful use of ceramics, as with any material, is proper design. Although ceramics are more susceptible to thermal shock damage than most metals, even a metal structure can be readily destroyed by thermal shock. Thus, care must be exercised in bringing large metal wheel gas turbines and metal tube furnaces up to operating temperature. For ceramic combustor catalysts, good design can permit rapid thermal cycling of even high expansion ceramics.

It should first be noted that if a structure is homogeneous, isotropic and free of restraints against movement, then no stresses result from thermal expansion. However, very large stresses can develop if the structure is kept from expanding (or contracting) by internal or external restraints. Thus, a solid, homogeneous ceramic rod will not suffer damage no matter how great the axial temperature gradient if it is held at one end and heated or cooled only at the opposite end. On the other hand, the same rod uniformly cooled at the sides will rupture with rather modest radial gradients. If the surface is chilled rapidly so that temperature equilibrium with the interior is not maintained, then the surface will be prevented from contracting by the hotter interior substrate. Compressive stress in the interior balances tensile stress in the surface layer. For elastic materials such as ceramics, the surface stress can be calculated using the following equation:

$$\sigma = E \cdot a \cdot \Delta T/(1 - \mu) \qquad \text{Eq. 1}$$

where,

E = modulus of elasticity,

a = coefficient of linear expansion,

T = Difference between surface temperature and the mean temperature of the rod,

μ = Poisson's Ratio,

σ = Tensile stress at surface

For a typical polycrystalline alumina, $E = 55 \times 10^6$ psi, $a = 7 \times 10^{-6}/^\circ C$, and $\mu = 0.25$. Thus, if $\Delta T = 100^\circ C$, $\sigma = 51000$psi compared to a tensile strength of only about 35,000psi at 300°C. With surface flaws, the effective tensile strength could be lower than 10,000psi with failure resulting from a temperature difference of as little as 10 or 20°C.

For many honeycomb catalysts, cell walls are thin enough so that temperature differences between the surface and the interior are much less than 10°C under most flow conditions. Thus, an alumina honeycomb with 10 mil walls would suffer temperature differnces of no more than about 3°C within the cell walls for a step change in air temperature of 500°C at a flow rate of twenty pounds per second per square foot (i.e. at an air to surface heat transfer coefficient of 0.01 cal/sec/cm^2/ and an alumina thermal conductivity of 0.02 cal/sec/cm/°C). The maximum temperature difference would be less at lower flow rates or with thinner cell walls. For a low thermal conductivity material such as zirconia, the temperature gradient could be as high as 20°C. With sufficiently low gas flow rates, temperature differences can be maintained within safe limits for any monolith substrate. A graded cell catalyst system reduces temperature differences for a given flow rate.

Just as solid ceramic rods or monolith cell walls can be subjected to damaging tensile stresses from temperature differences between the surface and the interior, so honeycomb catalyst structures can be similarly damaged. If the fuel air flow distribution is such that the interior flow channels are hotter or colder than those at the perphery, tensile stresses will result, even under steady state flows. The maximum stress developed for a given temperature difference increases linearly with catalyst diameter. Such stresses can be reduced somewhat by use of a flexible cell structure such as Corning's flex-cell honeycomb. However, the flex-walls of a flexible cell structure must be free of cracks or other stress concentration features. The requirement for crack-free walls is particularly hard to achieve with extrusion processes for any but the smallest diameter extrusions.

In the axial or flow direction, a honeycomb catalyst structure can, in principle, be designed so that there are no tensile stresses resulting from axial temperature gradients. Avoidance of external restraints on movement in the axial direction is quite simple. However, with a slip coated catalyst stresses arise as a result of differences in expansion coefficients of the structure ceramic and the slip coating. These stresses will cause loss of the catalyst coating unless the coefficient of expansion of the catalyst layer is closely matched to that of the substrate material. Note that an alumina catalyst would be a poor choice for a coating on cordierite. However, any coating differing in composition from the support material will have a mismatch problem. Active monoliths eliminate the need for a surface coating.

Differences in temperature profile between channels, such as from flow differences or catalytically inactive areas, could also lead to destructive tensile stresses. However, this should not be a major problem since the resulting temperature differences would normally be small between adjacent channels.

Inasmuch as ceramics are brittle materials as compared to metals, it is vital that honeycomb combustion catalysts be free of pre-existing strains, cracks or other points of stress concentration. Thus, catalysts should be formed to the correct size and shape rather than cut since cutting introduces cracks. Similarly, a monolith is likely to be weakened if coated with any material which can interact with the support structure at operating temperatures.

From the foregoing it can be seen that careful design is required if maximum performance is to be obtained from monolith combusotr catalysts. As will now be shown, foam ceramics can play an important role in such designs.

A DESIGN BASIS

From the foregoing discussion, it is evident that a ceramic monolithic structure, such as a combustor catalyst, can withstand extreme variations in temperature provided only that design of the structure, and that of the system in which it is used, are such that there are essentially no restraints to movement. It will now be shown that it is both possible and feasible to design such structures and systems.

In the first place, it should be noted that external restraint should not be a problem in view of the extensive art on the restraint-free mounting of ceramics. However, internal restraints can be a problem without proper design. Accordingly, the discussion will be limited to the control of internal restraint. The appropriate restraint-free mounting is assumed.

The simplest form of a restraint-free design would be a combustor made up of thin walled catalyst tubes placed perpendicular to the direction of flow. If the walls are no thicker than about 10 mils there are no significant internal restraints even for gas flow rates encountered in gas turbine combustors. Thus, such a combustor could withstand thermal cycling without damage at least as well as any conventional combustor. Even a thermal shock sensitive ceramic such as stabilized zirconia could be used. Moreover, if the tubes were made of an electrically conductive metal oxide, such as lanthanum chrome, the catalyst could, in principle, be electrically heated to full operating temperature in milliseconds without damage. This is because uniform heating does not lead to temperature gradients. The only stresses are from inertial forces. Note that a conductive coated tube would shatter under the same conditions.

A similar design is a combustor with vertically suspended U-tubes. Although inferior, it is a good approximation to a restraint-free design. U-tube designs are used in heat exchangers because the tube ends can be firmly secured. A derivative of the U-tube design is the hemispherical or dished plate. Although not completely restraint-free, a dished plate honeycomb exhibits far better thermal shock resistance than flat honeycomb plates or cylinders. Another U-tube design is the split cylinder annular flow combustor. This type design is almost restraint-free. Such dished shapes are readily fabricated only using foam ceramic technology.

FOAM CERAMICS

In any given structural configuration, foam ceramics have superior thermal shock resistance. Accordingly, foam ceramics have long been used in applications where this property is important. It should be noted that the thin walled spherical cells of a foam can expand or contract more or less freely just as is the case for a U-tube or dished plate. As a result, many foams can withstand direct flame impingement without cracking and thus make excellent high temperature insulating materials. Made from catalytic oxide, such foams represent almost the ideal form for a combustor catalyst.

A major advantage of foam ceramics technology is the capability to produce complex shapes. Although a number of companies have long had foam ceramics processes, the process recently developed by Merano and Marcaccioli of Montedison (1) is most interesting. In the Merano process, a polyurethane sponge may be converted, by plasma spraying with an appropriate material, into a sponge of metal, cermet, or ceramic. Cermet sponges of chrome, nickel and alumina were made as were sponges of pure alumina, of zirconia, and of catalytic substrates. It is claimed that a zirconia sponge will withstand an oxyacetylene flame. Insley et al (2) of Champion Spark Plug Company also have invented a method for converting urethane aponges to ceramic sponges. The group at Alfred University under W. Crandall have also developed urethane to ceramics foam technology. These processes appear admirably suited to producing thermal shock resistant catalytic monoliths based on restraint-free designs.

CONCLUSIONS

It has been shown that restraint-free designs for combustor catalyst monoliths are possible. Such designs are in principle immune to thermal shock damage. Monoliths based on such designs can be readily manufactured using existing foam ceramics technology. Inasmuch as foam ceramics are inherently resistant to thermal shock, it should be possible to produce monolith catalysts which can safely be thermally cycled over wide temperature ranges at least as rapidly as can conventional combustors.

---

(1) U.S. Patent 4,083,905 (April 1978)
(2) U.S. Patent 4,076,888 (February 1978)

SESSION II

CATALYST PERFORMANCE

COMPUTED AND MEASURED EMISSIONS FROM THE CATALYTIC COMBUSTION OF PROPANE/AIR MIXTURES

By

F. V. Bracco, C. Bruno, Y. Yaw, P. M. Walsh
Department of Mechanical and Aerospace Engineering
Princeton University
Princeton, NJ 08544

ABSTRACT

The objective of this program is to collect detailed data within a honeycomb catalyst for the development and testing of a two-dimensional model, and to further current understanding of the fundamental subprocesses which control catalytic combustion. Results are presented on the combustion of propane/air mixtures in a Pt/γ-Al_2O_3/Cordierite honeycomb catalyst. The test conditions were: inlet temperature, 650 K to 800 K; inlet pressure, 110 kPa; inlet velocity, 10 to 40 m/s; C_3H_8/air equivalence ratio, .19 to .32; and H_2O concentration, 1.2 to 1.7 mol%.

Efforts were made to obtain uniform profiles of temperature, velocity, and C_3H_8 concentration across the inlet gas stream. Temperature and concentration are uniform within ±1%, but velocity only within ±8%. The philosophy of the program is that a detailed model of the catalytic combustor is necessary to be able to draw consistent conclusions from the experimental data. The model developed during the present investigation solves the 2-D, steady-state, reactive flow in a cylindrical pipe with catalytic walls. When the experimental wall temperature is used as boundary condition for the gas-phase equations, the emission predictions are in reasonably good agreement with the measured ones. The indications obtained from the model are that propane is oxidized via a multi-step kinetic mechanism, and that, in the range of temperatures and equivalence ratios explored, most of the fuel is burnt at the catalytic wall rather than in the gas phase.

CONTENTS

List of Figures

List of Tables

Symbols

Acknowledgments

Introduction

Equipment and Procedure

Data and Discussion

Theoretical Model and Results

Conclusion

References

LIST OF FIGURES

1. Schematic diagram of the flow reactor.

2. Details of the catalyst test section.

3. Catalyst inlet uniformity measurements.

4. Exhaust gas composition downstream of the catalyst.

5. Exhaust gas composition downstream of the catalyst.

6. Exhaust gas composition downstream of the catalyst.

7. Exhaust gas composition downstream of the catalyst.

8. Temperature and composition as a function of T_{inlet}.

9. Temperature and composition as a function of Φ.

10a. Temperature as a function of inlet velocity u_1.

10b. Exhaust gas composition as a function of inlet velocity u_1.

11. Physical and chemical processes in a channel of a catalyst.

12. Coordinate system and variables in the model of a catalyst channel.

13. Theoretical profiles of unburned HC vs. r and x for 3-step (overall) catalytic oxidation of C_3H_8.

14. Theoretical profiles of unburned HC vs. r and x for 3-step (overall) catalytic oxidation of C_3H_8.

15. Theoretical profiles of CO vs. r and x for 3-step (overall) catalytic oxidation of C_3H_8.

16. Theoretical profiles of CO vs. r and x for 3-step (overall) catalytic oxidation of C_3H_8.

17. Pressure drop.

18. Unburned hydrocarbons.

19. Unburned CO.

20. CO_2 product.

21. Relative importance of gas-phase vs. surface reaction rates.

LIST OF TABLES

1. Catalyst Properties.

2. Dimensional Governing Equations for Reacting Flow in a Circular Tube with Catalytic Wall.

3. Chemical Reaction Rate Data Used in the Modeling of 3-Step Kinetics of Propane Oxidation on Pt/γ-Al_2O_3/Cordierite Catalyst.

SYMBOLS

C_p	specific heat at constant pressure (J/kg·K)
D	diffusion coefficient (m^2/s)
E	activation energy (J/mol)
h	enthalpy (J/Kg)
k	rate constant (cm^3/mol·s); Thermal conductivity (W/m·k)
Le	Lewis number = $\lambda/\rho DC_p$
P	pressure (Pa)
q	heat flux (J/m·s)
Q	heat of reaction (J/kg)
r	radial coordinate (m)
R	gas constant = 8.31 J/K·mol; pipe radius (m)
s	pipe thickness (m)
t	time (s)
T	temperature (K)
u	axial gas velocity (m/s)
v	radial gas velocity (m/s)
W	molecular weight
Y	mass fraction
z	axial coordinate (m)
ν', ν''	stoichiometric coefficients
ρ	density (kg/m^3)
σ	stress component (Pa)
ϕ	equivalence ratio
[ ]	concentration (mol/cm^3)

Subscripts

ad	adiabatic (reaction temperature)
b	backward reaction
f	forward reaction
in	condition at catalyst inlet
k	species k
ℓ	reaction ℓ
out	condition at catalyst outlet
r	radial
ref	reference condition (velocity)
w	wall
z	axial

ACKNOWLEDGMENTS

This project is supported by the Air Force Office of Scientific Research under Grant No. AFOSR-76-3052, Dr. B. T. Wolfson, Grant Monitor; and by the Department of Energy under Contract No. DE-AC21-80MC14036, Mr. T. O'Brien, Technical Project Officer.

The authors are indebted to Dr. W. C. Pfefferle for his many valuable suggestions.

INTRODUCTION

Although many important features of catalytic combustion have been investigated and identified, the relative importance of the relevant fundamental physico-chemical processes still needs to be assessed. Especially interesting is to find out the interaction between mass transport and heterogeneous and homogeneous chemical kinetics. The design of large scale practical devices for heat and power generation could therefore make use of a model which accurately describes the system in terms of basic chemical and physical phenomena and which relates performance to all the relevant design parameters. The goal of our program is to develop a useful model for combustion in monolithic catalysts and to obtain experimental data for testing the model and the predictions of other investigators. The present work describes experimental results from a preliminary study of C_3H_8 combustion in $Pt/\gamma\text{-}Al_2O_3$/Cordierite.

EQUIPMENT AND PROCEDURE

INLET CONDITIONS

A sketch of the experimental apparatus is shown in Figure 1. Preheated air at a measured flowrate is supplied to a 690 mm long test section with 25.4 mm square channel. A catalyst is placed with its downstream end 90 mm from the test section outlet, and insulated from the wall by Fiberfrax paper. Details of the catalyst section are shown in Figure 2. A fuel injector consisting of five 1.6 mm diameter tubes, each containing five 0.3 mm diameter holes, is located 440 mm from the catalyst inlet. A combination pitot tube and thermocouple is mounted 200 mm from the catalyst inlet. In addition to measuring gas velocity and temperature, the pitot tube is used to extract gas samples which are analyzed to determine equivalence ratio. Pressure is regulated by a valve in the exhaust pipe, and taps placed up and downstream of the catalyst are used to measure inlet pressure and pressure drop. A mass flowmeter (Hastings Model AHL-100P with H-3M/L-100 Transducer) measured the air flowrate. The water content of the inlet air was measured using a semiconductor sensor (Thunder Model 2000 with BR-101B probe) mounted in the airstream between the receiving tank and the heaters. The inlet conditions used in the experiments are summarized below.

Inlet temperature (T_{in}) = 650 ± 13 K to 800 ± 16 K
Inlet pressure (P_{in}) = 110 ± 5 kPa
Inlet Velocity (u_{in}) = 10 ± 4 to 40 ± 7 m/s
C_3H_8/air equivalence ratio (ϕ) = .19 ± .03 to .32 ± .04
H_2O = 1.2 ± .6 to 1.7 ± .6 mol%

A continuous effort has been made to minimize crosswise gradients in temperature, velocity, and fuel concentration of the inlet stream. The entire test section is insulated so that uniform temperature across the width of the test section is obtained when sufficient time (∿ 1 hr) has elapsed after startup of the air preheat system. Figure 3 shows velocity, temperature and propane concentration profiles obtained by traversing the width of the test section with the pitot/thermocouple probe. The uniformity is independent of air flowrate over the range of velocities used. Sufficient fuel/air mixing was obtained only by placing baffles downstream of the fuel injector, and these affect the velocity profile. By trying various configurations, the velocity uniformity was improved while maintaining an even distribution of fuel. The arrangement used in the present experiments consisted of two screens, each containing four 9 mm diameter holes, placed 30 and 110 mm downstream of the fuel injector. Another screen perforated with 1.6 mm diameter holes was 190 mm from the injector and 50 mm upstream of the pitot tube. The resulting fuel distribution shows good uniformity over the measured range. Velocity profiles are less satisfactory (range ± 6% over 50% of the channel width). Average reference velocities were determined using the C_3H_8 and air flowrates, inlet temperature and pressure, and the cross section area of the catalyst. The catalyst inlet velocity, taking into account the fraction of open monolith area, is $u_{in} = (1.67 \pm .06)u_{ref}$.

SUBSTRATE AND EXHAUST MEASUREMENTS

Substrate temperatures are measured by a method similar to that described by Kesselring, Krill, and Kendall (1). Ni-Cr/Ni-Al thermocouples are fed through the test section wall and into the ends of catalyst channels. The lengths of wire inside the catalyst are covered by mullite insulator and both ends of the channel sealed with ceramic adhesive. The lifetime of these thermocouples under test conditions is short (5 - 20 hr). Exhaust gas samples were taken through an expansion quenched, water cooled, stainless steel probe mounted in an elbow downstream of the test section. Exhaust gas temperature was measured with a thermocouple mounted on the probe. CO and CO_2 were determined by infrared absorption (Horiba Model AIA-21), O_2 by magnetic susceptibility (Scott Model 250), and total hydrocarbon (HC, reported here as C_3) by a flame ionization detector (Scott Model 415). Pressure was measured inside the catalyst at 3 locations.

CATALYST AND FUEL

The catalyst was platinum supported on split cell corrugated Cordierite with γ-alumina washcoat. The overall dimensions of the monolith were 24 x 24 x 76 mm, the open area was 64%, the channel cross-section area was 1.9 mm^2, and the platinum loading was 4.2 kg/m^3. The physical properties of the catalyst are listed in Table 1. The sample was pretreated by burning propane for two hours with the maximum substrate temperature at 1480 K. The fuel was natural propane, 96 mole%, nominal.

DATA AND DISCUSSION

The combustor was operated over a range of equivalence ratios, inlet temperatures and reference velocities at fixed inlet pressure. No attempt was made to minimize unburned fuel, since the objective was to understand the relationship between operating conditions and physico-chemical phenomena. Typical exhaust gas composition results are shown in Fig. 4, 5, 6 and 7. Fig. 4 shows CO formed by the C_3H_8 breakdown, being oxidized to CO_2 in the exhaust gas downstream of the catalyst.

A primary objective was the measurement of gas temperature and composition as functions of axial position inside a catalyst. This was accomplished by drilling an 8 mm diameter hole partway through the catalyst along its axis. The hole is lined with a ceramic sleeve to minimize the activity of the wall. A combination gas sampling and thermocouple probe is moved along the catalyst axis from downstream toward the bottom of the hole. If conditions are properly adjusted, the measured gas temperature and composition at the bottom of the hole are equal to their values at the same axial position in a catalyst with no hole. The condition which is most affected by the presence of the hole and probe is the gas velocity in the catalyst channels opening into the hole. The problem of establishing the correct velocity has been solved by feeding pressure taps through the side of the catalyst to measure the pressure at the bottom of the probe hole.

The velocity is adjusted until the pressure is equal to its value at the same axial position in a catalyst without a hole. Measured pressures show a linear decrease with increasing distance from the inlet during propane combustion in the Pt/Al_2O_3/Cordierite catalyst. Another requirement for reliable gas measurement inside a catalyst is that the substrate temperature be unaffected. This condition can also be satisfied despite the changed gas velocity because substrate temperature does not have a strong dependence on velocity. It is the constraint of fixed substrate temperature which distinguishes this experiment from one in which the overall length of catalyst is varied. In a catalyst of given length, the substrate temperature profile is different from the profile in an equivalent section of a longer catalyst. Direct measurements of fuel, oxygen, and product concentrations and gas temperature as functions of axial position inside a catalyst provide data for a rigorous test of a model for combustor operation. Calculations of species concentrations inside monolithic catalytic combustors have been presented by Kelly, Kendall, Chu, and Kesselring (2) and by Cerkanowicz, Cole, and Stevens (3), but an experiment with which to compare these predictions had, to our knowledge, not yet been performed. Fig. 5 refers to results obtained from a catalyst with a hole depth equal to half the length of the catalyst. For the conditions of this experiment, fuel breaks down monotonically while at the same time the CO formed oxidizes to CO_2 and decreases as HC decreases.

Fig. 6 is interesting in the fact that while the UHC at the outlet keep decreasing with X, CO has a relative maximum. This is an indication that CO may be produced inside the catalyst at a rate larger than its rate of oxidation to CO_2.

This suspicion is confirmed by the results of Fig. 7, in which probing inside the hole reveals that not all the CO produced by propane pyrolysis is immediately oxidized to CO_2, and that a maximum exists inside the catalyst channels. More definite trends appear when temperatures and compositions are plotted versus inlet parameters. Fig. 8 has as parameter the inlet temperature. This has a strong effect on catalyst temperature and unburned HC at the outlet, which decreases rapidly as T_{in} is raised. However CO behaves non-monotonically: as T_{in} is raised, CO emissions at the outlet at first increase and then decrease.

The larger the UHC at the outlet, the higher the CO peak corresponding to HC breakdown to CO. From the figure it can be seen that the maxima of the rates of HC disappearance and CO production occur at approximately the same axial location.

The effect of varying equivalence ratio is shown in Fig. 9. Φ has a very strong influence on catalyst temperature, since it affects directly the adiabatic flame temperature, to which the wall temperature is close. For low Φ the UHC are relatively large at the outlet, and the low exhaust temperature results into low rates of HC breakdown into CO and CO oxidation. As Φ is increased both HC breakdown and CO oxidation proceed faster and faster: this seems to indicate that the CO axial peak tends to move inside the catalyst channels as Φ is raised.

Figs. 10a and 10b show the effect of varying inlet velocity and therefore residence time inside the channels. The wall temperature is only weakly affected by changing u_1, since it is always close to the adiabatic flame temperature corresponding to given T_{inlet} and Φ, which is independent of velocity. Emissions, instead, are strongly affected, and both UHC and CO become progressively larger as u_1 is increased. A maximum of CO at the outlet can be seen when u_1 is sufficiently high. This brief discussion of the experimental results points out the complexity of the interaction between physics and chemistry inside of the catalyst channels. The physical size of the probe used precludes a direct investigation inside an individual catalyst channel. What the probe can measure are quantities averaged over several channels cross sections, and no indication of radial diffusion effects can be obtained. A detailed description of these and other effects may be supplied only by the mathematical model.

THEORETICAL MODEL AND RESULTS

A sketch of the fundamental phsyico-chemical and fluid dynamics processes in a catalyst channel is shown in Fig. 11. The purpose of the model is to predict the effect of these processes on the exhaust products and the substrate. After reaching good agreement between predictions and experimental data, the model was used to investigate the relationship between the different processes.

For simplicity the catalyst channels are approximated by cylindrical channels. Preliminary results indicated that radiative heat transfer may be important at the two ends of the channel and for about 6% of the channel length. Therefore radiation is neglected in the model. With this simplification the equations describing catalytic combustion and the coordinate system are shown in Fig. 12 and Table 2.

These equations describe a two-dimensional, axisymmetrical, compressible, fluid flow with arbitrary chemical reactions in the gas phase, and with heat transfer and conduction in the substrate modeled assuming constant temperature across the substrate thickness s.

The reaction rates used in this study are shown in Table 3. The 3-step mechanism for propane oxidation in the gas phase was essential for a good agreement with the experimental data. (No reasonable results could be obtained by simply assuming C_3H_8 to break down into CO and then oxidizing CO to CO_2). This mechanism was obtained by Hautman et al. (4)(7) at Princeton and some slight adjustments were made to the activation energies and preexponential factors of reactions 1. and 2. These adjustments did not change the corresponding rates at the average temperature of the gas inside the pipe.

To test the validity of the model and separate gas phase effects from substrate effects, the gas phase equations were solved by uncoupling them from the substrate energy equation. In this case the only extra variable unknown is T_w, which was taken from the experiments and imposed as boundary condition at the wall. This procedure has as advantage the implicit inclusion of radiative effects in the model (provided the gas is optically thin), since the experimental wall temperature does include the effects of radiation.

The basic structure of the computer program used to solve the set of equations, "CATEACH", was based on the TEACH hydrodynamic code designed by A. D. Gosman and coworkers at The Imperial College. Details of CATEACH can be found in (5) and (6).

Some of the theoretical results are shown in Figs. 13 through 16 [see (6) for a detailed discussion]. Fig. 13 shows the monotonical decrease in HC concentration along the axis and from the axis to the catalytic wall. The rate of HC breakdown and oxidation is a function of the radial mass transfer and of the CO oxidation rate. Increasing the inlet velocity, as in Fig. 14, results in a correspondent decrease in residence time and a slower HC disappearance. Consistently, CO is still being formed at the outlet for this higher velocity case (see Fig. 15), and would presumable peak in the exhaust as in Fig. 10a. For the lower velocity case of Fig. 16, the residence time is sufficiently large for CO to begin to be oxidized inside the channel. Thus a relative CO maximum must occur, as in Fig. 5.

Overall comparison between theory and experiments is shown in Figs. 17 through 20. The pressure drop between catalyst inlet and outlet is important for gas turbine applications. There is a certain amount of disagreement between predictions and data; this is likely to be the effect of having approximated the [roughly] trapezoidal shape of the channel cross section by a circular one. The trends, however, are reproduced (see Fig. 17). Fig. 18 shows good agreement in the UHC comparison. Less satisfactory (but consistent as far as the trends) is the comparison for CO and CO_2 (see Figs. 19 and 20). It should be noted that the outlet emissions predictions are averages over the cross section, while data were taken with a probe hole slightly smaller than the channel size; part of the disagreement may be also due to radial gradients effects on the probe. A second cause may be a gradual loss of catalyst activity observed with increasing total run time (aging).

Once the computer code has proved itself in predicting reasonable trends over the range of experimental measurement, some conclusions can be drawn. Fig. 21 shows the relative magnitude of gas phase vs. catalytic reaction rates. Most of the HC is oxidized at the catalytic wall, but this tends to change as the inlet temperature or the equivalence ratio is increased. The effect of velocity is opposite to the effect of inlet temperature but not as strong.

CONCLUSION

The agreement between mathematical model and experimental data for C_3H_8 combustion in Pt/γ-Al_2O_3/cordierite monoliths is reasonably satisfactory. Preliminary results exhibit several interesting features.

1. Substrate temperature is only weakly dependent on gas velocity.
2. Emissions depend strongly on all three parameters investigated.
3. Propane oxidation takes place via a multi-step mechanism involving at least three overall steps.
4. While unburned hydrocarbon varies monotonically with the three parameters investigated, CO emissions do not.
5. Most of the fuel is burned at the wall by catalyzed reactions rather than in the gas phase.

Future work will include mathematical coupling of gas and substrate to make the code independent of experimentally measured inputs.

REFERENCES

1. Kesselring, J. P., W. V. Krill, and R. M. Kendall. Design Criteria for Stationary Source Catalytic Combustors. Presented at the Second EPA Workshop on Catalytic Combustion, Raleigh, NC, June 21-22, 1977.

2. Kelly, J. T., R. M. Kendall, E. Chu, and J. P. Kesselring. Development and Application of the PROF-HET Catalytic Combustor Code. Paper 77-33, Presented at the Fall 1977 Meeting, Western States Section, The Combustion Institute, Stanford, CA, October 17-18, 1977.

3. Cerkanowicz, A. E., R. B. Cole, and J. G. Stevens. Catalytic Combustion Modeling: Comparisons with Experimental Data. Presented at the ASME Gas Turbine Conference and Products Show, Philadelphia, PA, March 27-31, 1977.

4. Hautman, D. J., Hydrocarbon Oxidation Analysis. Paper presented at the Combustion Phenomena Contractors Review Meeting, U.S. Department of Energy, Pittsburgh Energy Technology Center, Pittsburgh, PA, Sept. 19, 1979.

5. Gosman, A. D., and F. J. K. Ideriah, "TEACH" - A General Computer Program for Two-Dimensional, Turbulent, Recirculating Flows. Dept. of Mech. Eng. Report, The Imperial College, London, SW7, 1976.

6. Yaw, Y., MSc Thesis, Princeton University, to be published.

7. Hautman, D. J., Pyrolysis and Oxidation Kinetic Mechanism for Propane, Ph.D. Thesis, Princeton University, 1980.

Table 1. Catalyst Properties

SUBSTRATE: Cordierite, American Lava Corp., AlSiMag 795, split cell

length 0.0760 ± 0.0003 m
wall thickness 0.25×10^{-3} m
open area 64%
channels per unit area $0.34 \times 10^{6}\ \mathrm{m}^{-2}$
open area per channel $1.9 \times 10^{-6}\ \mathrm{m}^2$
ratio surface area to total volume 2100 $\mathrm{m}^2/\mathrm{m}^3$
ratio surface area to gas volume 3260 $\mathrm{m}^2/\mathrm{m}^3$
channel hydraulic diameter (4/3260) 0.00123 m
bulk density 610 $\mathrm{kg/m}^3$
solid density 1700 $\mathrm{kg/m}^3$
safe operating temperature 1473 K
specific heat 800 J/kg•K
coefficient of thermal expansion (linear, 294 - 1033 K) $3.8 \times 10^{-6}\ \mathrm{K}^{-1}$
thermal conductivity of solid (572 K) 1.4 J/m•s•K

approximate channel cross-section is a trapezoid with base lengths .0011 m and .0023 m, and height .0012 m

WASHCOAT: γ-alumina

loading 115-125 $\mathrm{kg/m}^3$
surface area (BET) $(29.2 - 33.0) \times 10^{6}\ \mathrm{m}^2/\mathrm{m}^3$

CATALYST: platinum

loading 4.2 $\mathrm{kg/m}^3$
surface area (CO chemisorption) $6 \times 10^{4}\ \mathrm{m}^2/\mathrm{m}^3$
The γ-alumina and platinum were applied by Matthey Bishop, Inc., Malvern, PA.

Table 2. Dimensional Governing Equations for Reacting Flow in a Circular Tube with Catalytic Wall.

$$\frac{\partial \rho}{\partial t} + \frac{1}{r}\frac{\partial \rho v r}{\partial r} + \frac{\partial \rho u}{\partial z} = 0 \qquad \text{continuity}$$

$$\frac{D\rho v}{Dt} = - \frac{\partial p}{\partial r} + \frac{1}{r}\frac{\partial \sigma_{rr} \cdot r}{\partial r} + \frac{\partial \sigma_{rz}}{\partial z} - \frac{\sigma_{\phi\phi}}{r} \qquad \text{radial momentum}$$

$$\frac{D\rho u}{Dt} = - \frac{\partial p}{\partial z} + \frac{1}{r}\frac{\partial \sigma_{rz}}{\partial r} + \frac{\partial \sigma_{zz}}{\partial z} \qquad \text{axial momentum}$$

$$\begin{aligned} \frac{D\rho h}{Dt} = {} & \frac{\partial p}{\partial t} + \frac{1}{r}\frac{\partial}{\partial r}(\sigma_{rr} vr + \sigma_{rz} ur) \\ & + \frac{\partial}{\partial z}(\sigma_{rz} v + \sigma_{zz} u) - \frac{1}{r}\frac{\partial r q_r}{\partial r} - \frac{\partial q_z}{\partial z} \\ & + \sum_{\ell} Q_\ell \left[k_{f\ell} \prod_k \left(\frac{\rho_k}{W_k}\right)^{\nu'_{k\ell}} - k_{b\ell} \prod_k \left(\frac{\rho_k}{W_k}\right)^{\nu''_{k\ell}} \right] \qquad \text{energy} \end{aligned}$$

$$\begin{aligned} \frac{D\rho k}{Dt} = {} & \frac{1}{r}\frac{\partial}{\partial r}\left[\rho D_k r \frac{\partial(\rho_k/\rho)}{\partial r}\right] + \frac{\partial}{\partial z}\left[\rho D_k \frac{\partial(\rho_k/\rho)}{\partial z}\right] + \\ & \sum_{\ell} W_k \, (\nu''_{k\ell} - \nu'_{k\ell}) \left[k_{f\ell} \prod_k \left(\frac{\rho_k}{W_k}\right)^{\nu''_{k\ell}} - k_{b\ell} \prod_k \left(\frac{\rho_k}{W_k}\right)^{\nu''_{k\ell}} \right] \qquad \text{species} \end{aligned}$$

$$p = \rho T R \Sigma (Y_k/W_k) \qquad \text{state}$$

$$\frac{\partial T_w}{\partial t} = \frac{\partial^2 T_w}{\partial z^2} - \frac{2}{s}\frac{k}{k_w}\left[\frac{\partial T}{\partial r}\right]_{R^-} + \frac{2}{s k_w} \sum_{\ell} Q_\ell k_{f\ell} \prod_k \left(\frac{\rho_k}{W_k}\right)^{\nu_{k\ell}} \qquad \text{substrate energy}$$

TABLE 3. CHEMICAL REACTION RATE DATA USED IN THE MODELING OF 3-STEP KINETICS OF PROPANE OXIDATION ON $Pt/\gamma\text{-}Al_2O_3$/CORDIERITE CATALYST

REACTIONS

GAS	WALL
1. $C_3H_8 + \frac{1}{2} O_2 \rightarrow \frac{3}{2} C_2H_4 + H_2O$	1. $C_3H_8 + 5O_2 \rightarrow 3CO_2 + 4H_2O$
2. $C_2H_4 + 2O_2 \rightarrow 2CO + 2H_2O$	2. $C_2H_4 + 3O_2 \rightarrow 2CO_2 + 2H_2O$
3. $CO + \frac{1}{2} O_2 \rightarrow CO_2$	3. $CO + \frac{1}{2} O_2 \rightarrow CO_2$

RATES

GAS ($mol/cm^3 \cdot s$)	WALL ($mol/cm^2 Pt \cdot s$)
1. $1.4 \times 10^8 \exp(-40608/RT)$ $\cdot ([C_3H_8]/[C_3H_8]_{in})^{.25} [O_2]^{1.04}$	1. $1.09 \times 10^9 \exp(-17600/RT)[C_3H_8]$
2. $4.8 \times 10^{14} \exp(-70000/RT)$ $\cdot ([C_2H_4]/[C_3H_8]_{in})^{.96} [O_2]^{1.18}$	2. $10^{7.04} \exp(-12000/RT)[C_2H_4]$
3. $1.0 \times 10^{10} \exp(-30000/RT)$ $\cdot [CO][O_2]^{.25} [H_2O]^{.5}$	3. $3.83 \times 10^3 \exp(-24900/RT)[CO]$

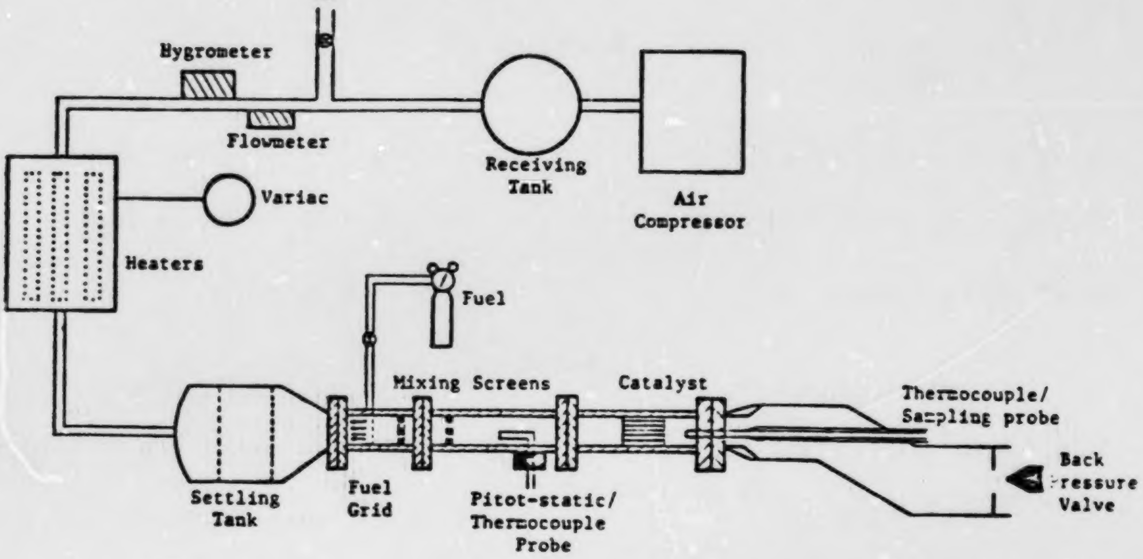
Bypass Air
Hygrometer
Flowmeter
Receiving Tank
Air Compressor
Variac
Heaters
Fuel
Mixing Screens
Catalyst
Thermocouple/ Sampling probe
Back Pressure Valve
Settling Tank
Fuel Grid
Pitot-static/ Thermocouple Probe

Figure 1. Schematic diagram of the flow reactor with catalytic combustion test section.

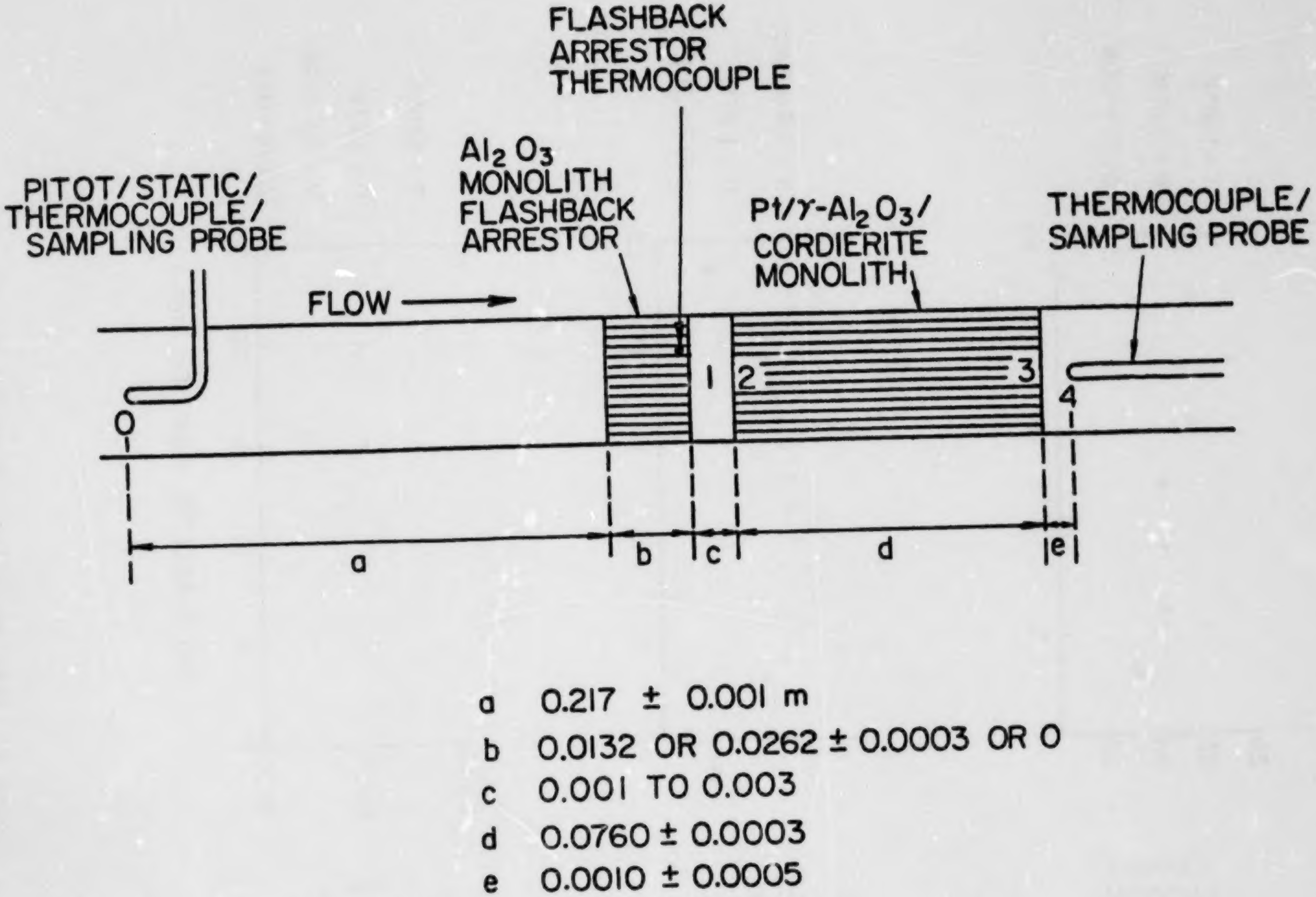
FLASHBACK ARRESTOR THERMOCOUPLE
Al_2O_3 MONOLITH FLASHBACK ARRESTOR
PITOT/STATIC/ THERMOCOUPLE/ SAMPLING PROBE
Pt/γ-Al_2O_3/ CORDIERITE MONOLITH
THERMOCOUPLE/ SAMPLING PROBE
FLOW
0
1
2
3
4
a
b
c
d
e
a 0.217 ± 0.001 m
b 0.0132 OR 0.0262 ± 0.0003 OR 0
c 0.001 TO 0.003
d 0.0760 ± 0.0003
e 0.0010 ± 0.0005

Figure 2. Details of the catalyst test section.

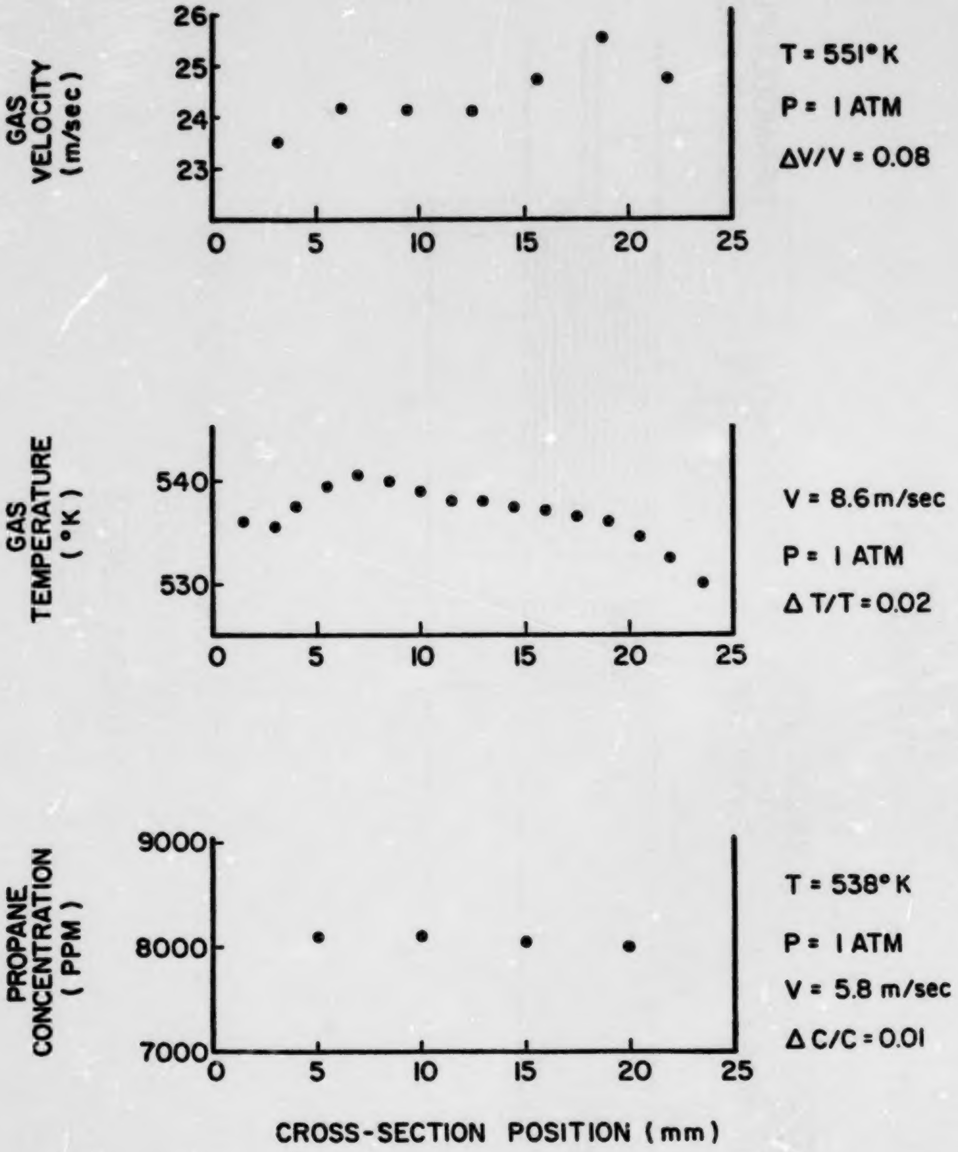

Figure 3. Catalyst inlet uniformity measurements.

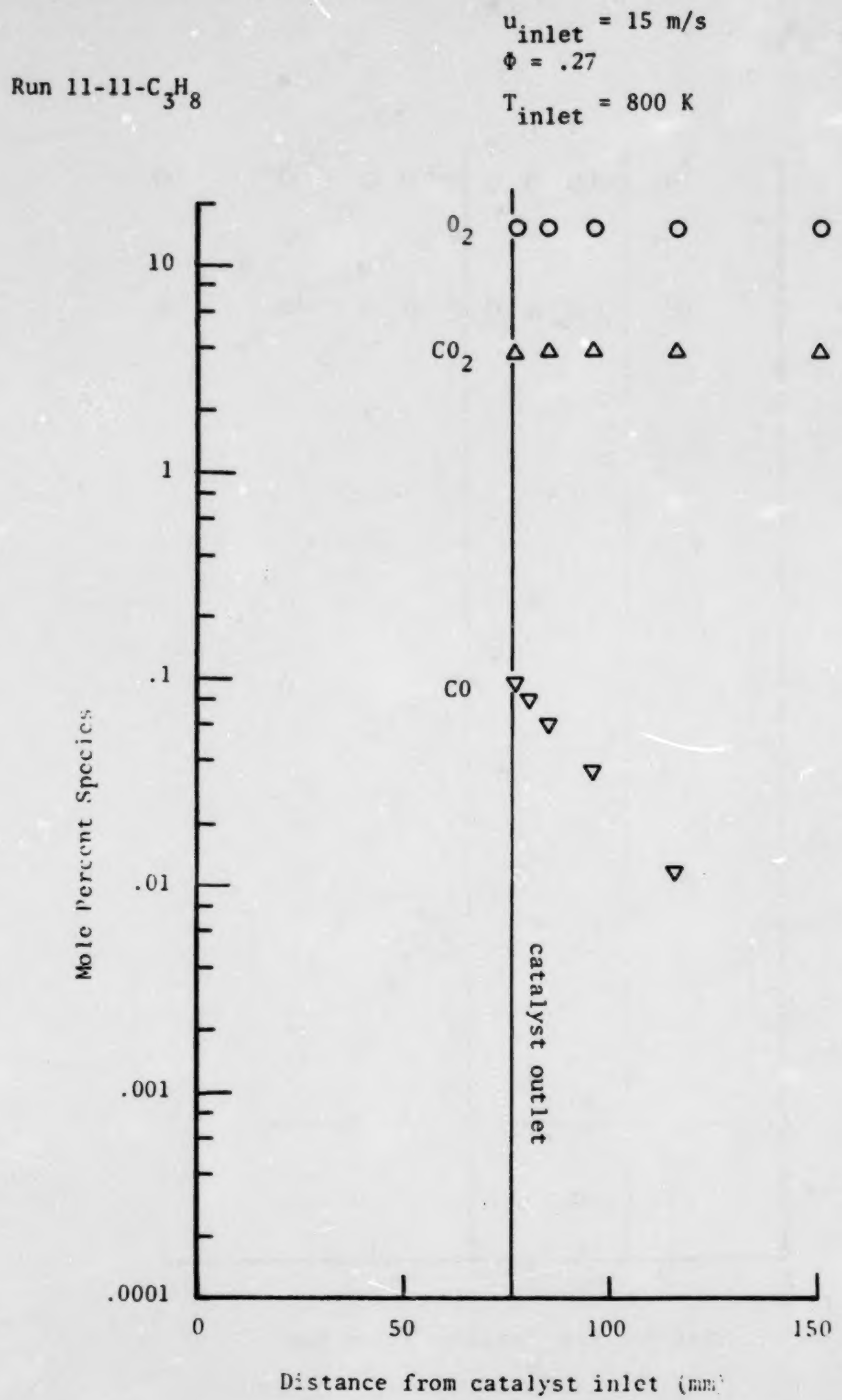

Figure 4. Exhaust gas composition downstream of the catalyst.

Run 11-13-C_3H_8

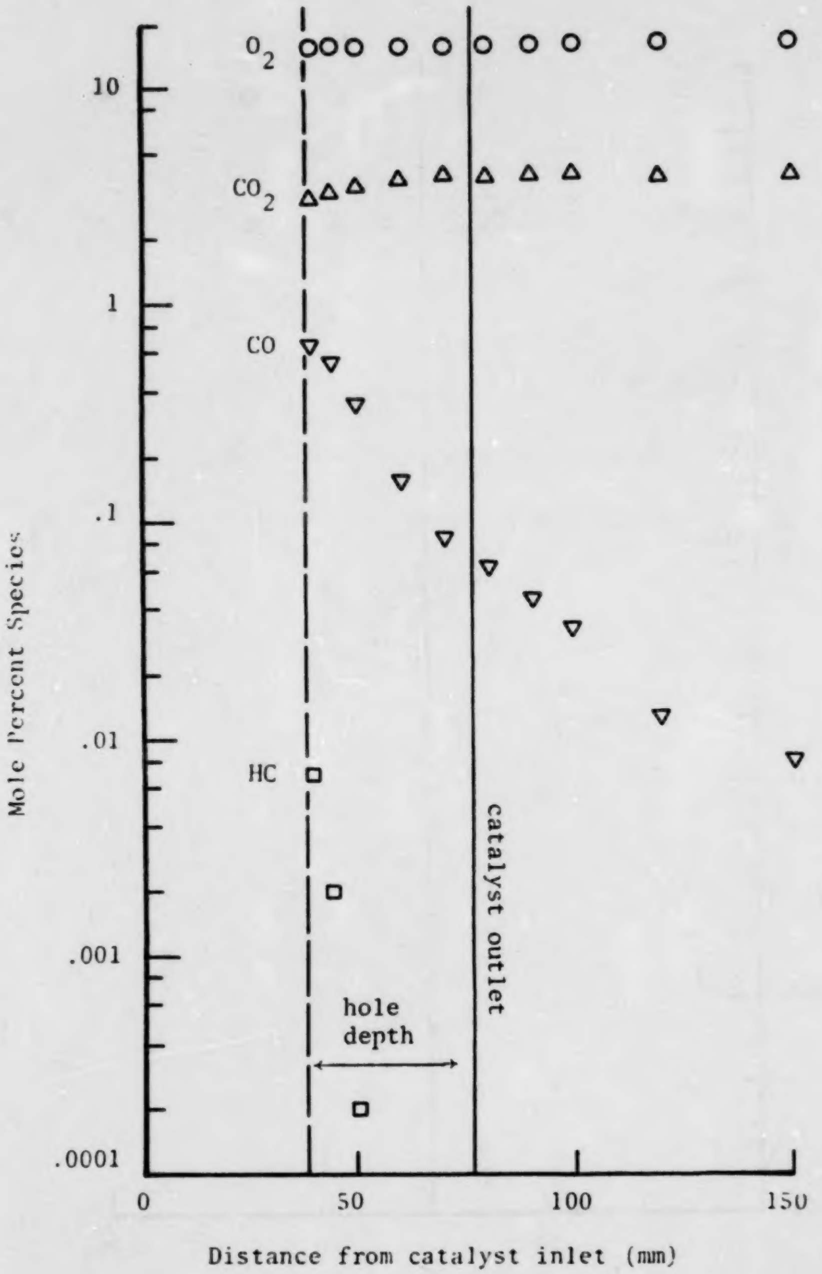

Figure 5. Exhaust gas composition inside and downstream of the catalyst.

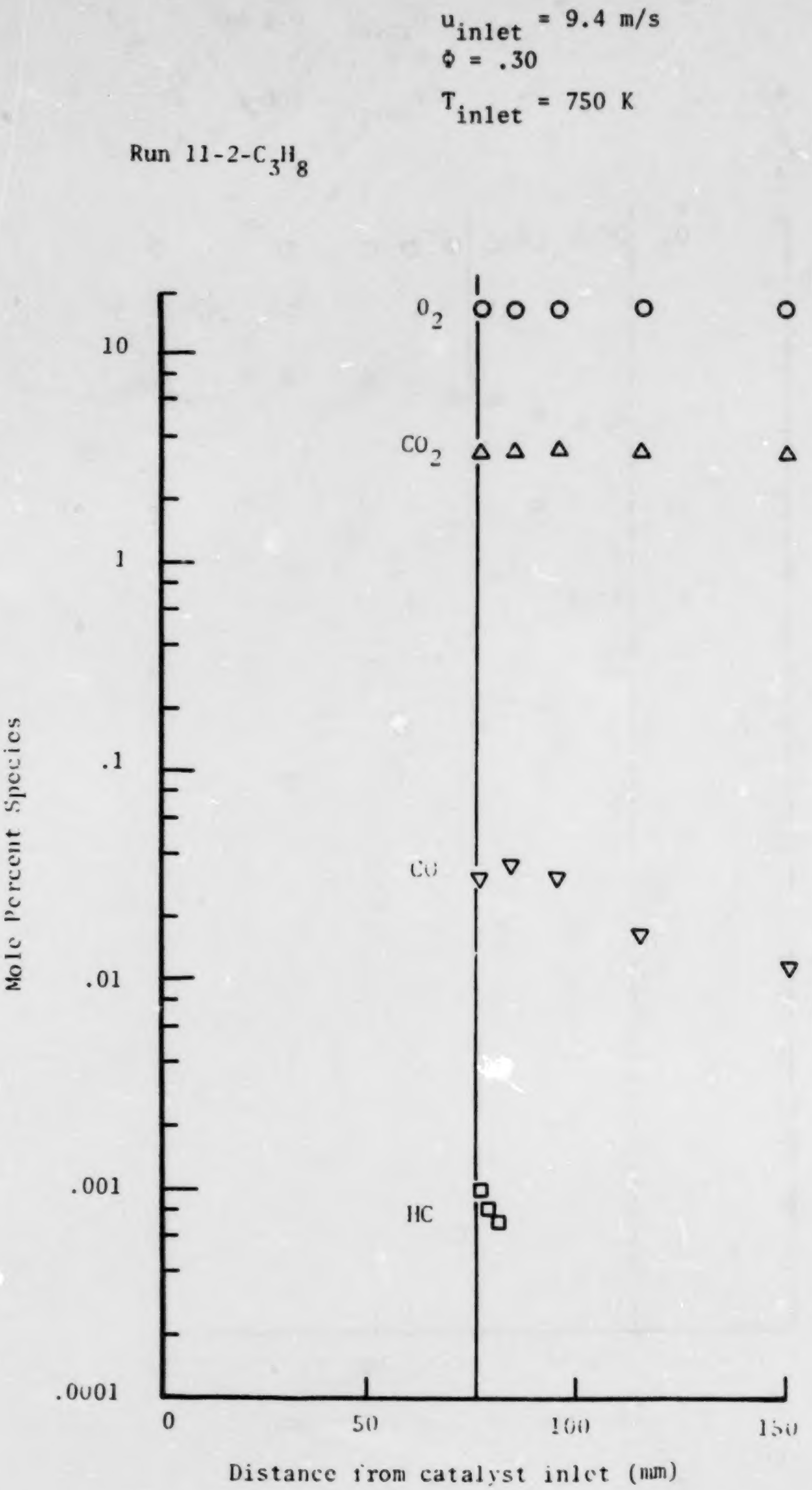

Figure 6. Exhaust gas composition downstream of the catalyst.

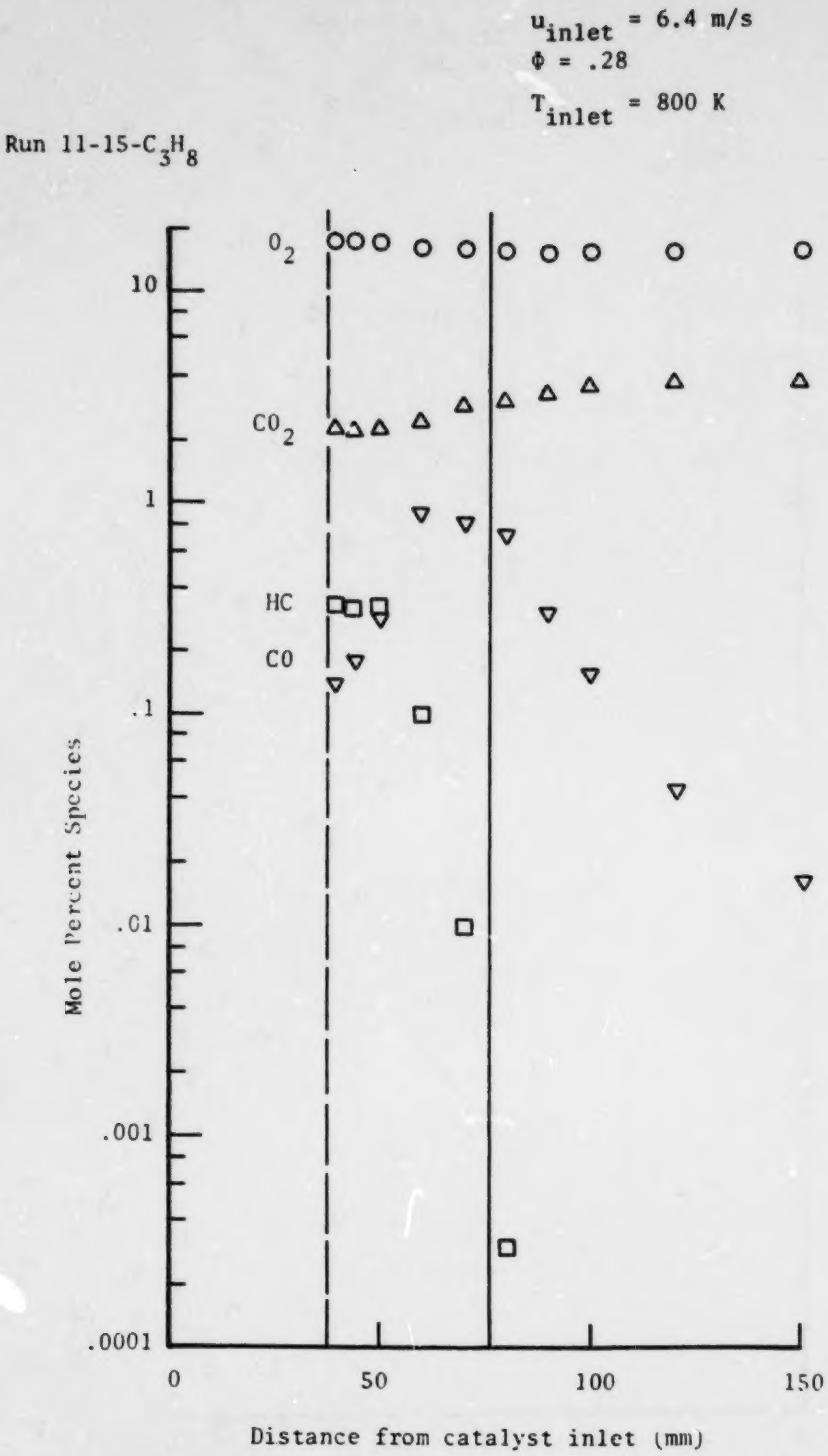

Figure 7. Exhaust gas composition inside and downstream of the catalyst.

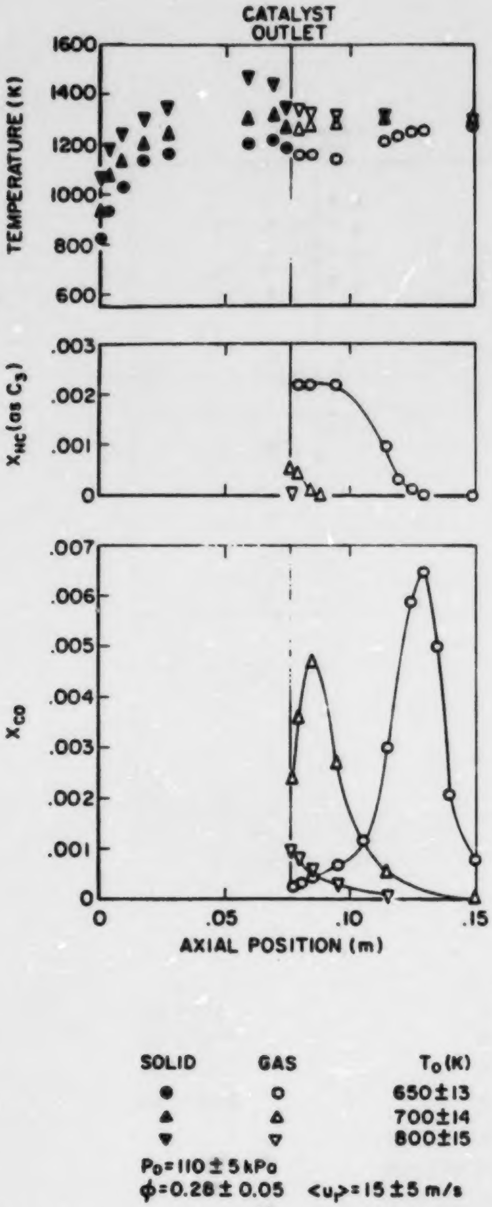

Figure 8. Temperature and composition as a function of T_{inlet}.

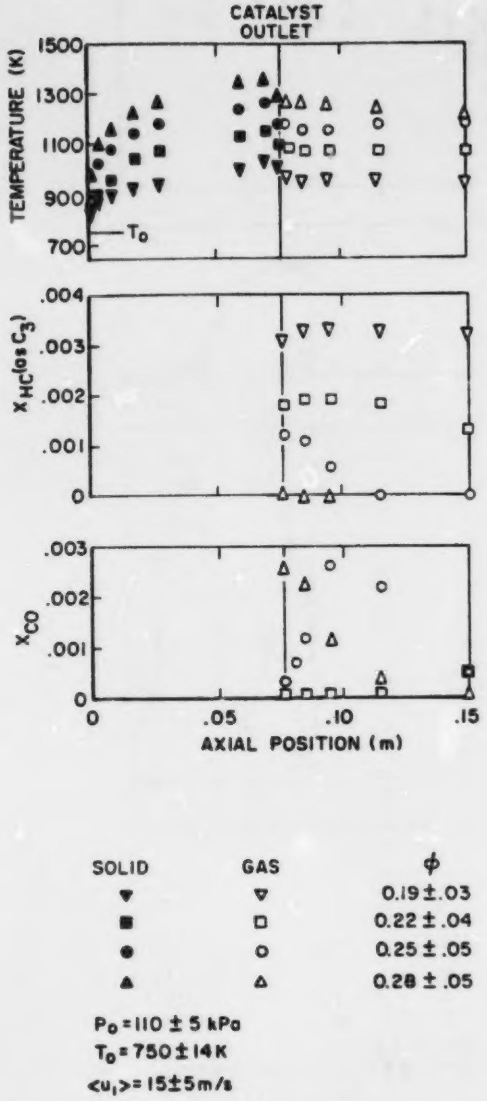

Figure 9. Temperature and composition as a function of ϕ.

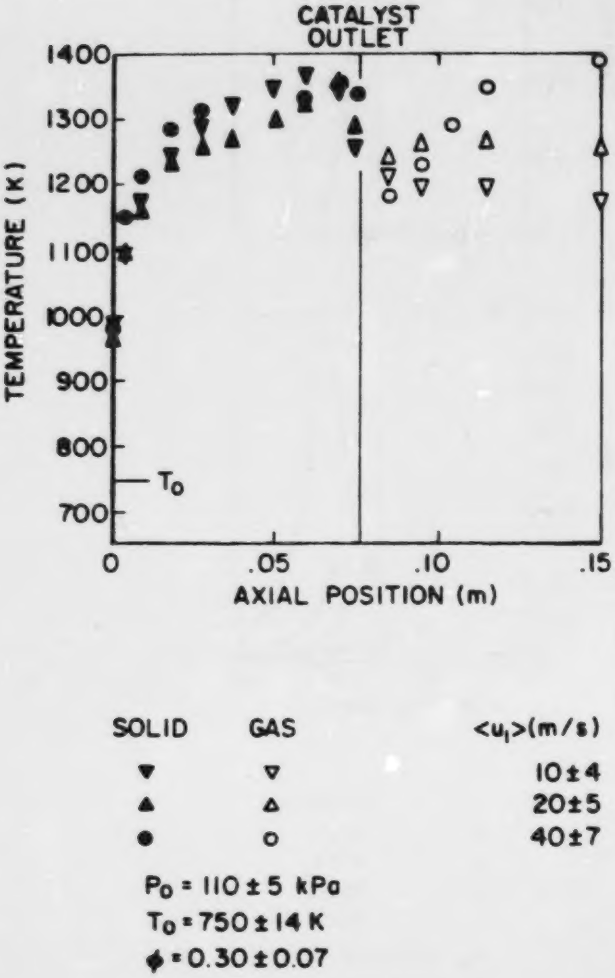

Figure 10a. Temperature as a function of inlet velocity u_1.

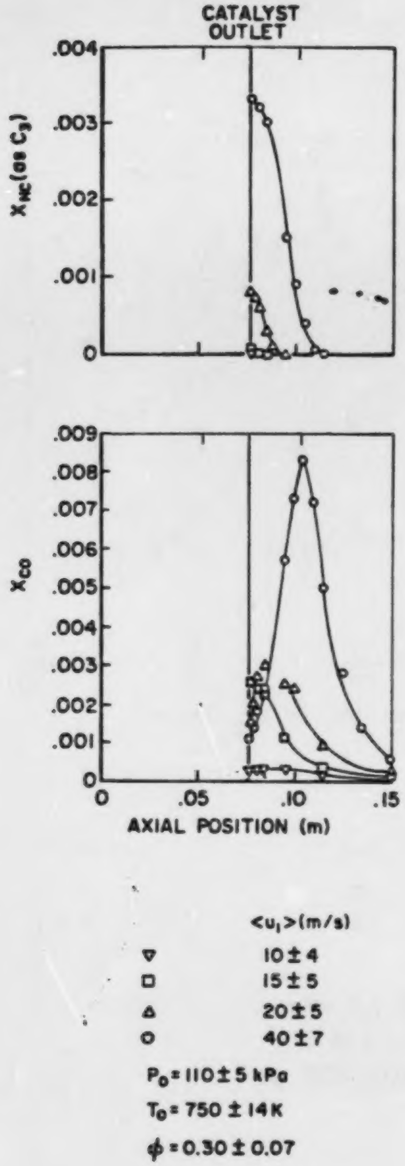

Figure 10b. Composition as a function of inlet velocity u_1.

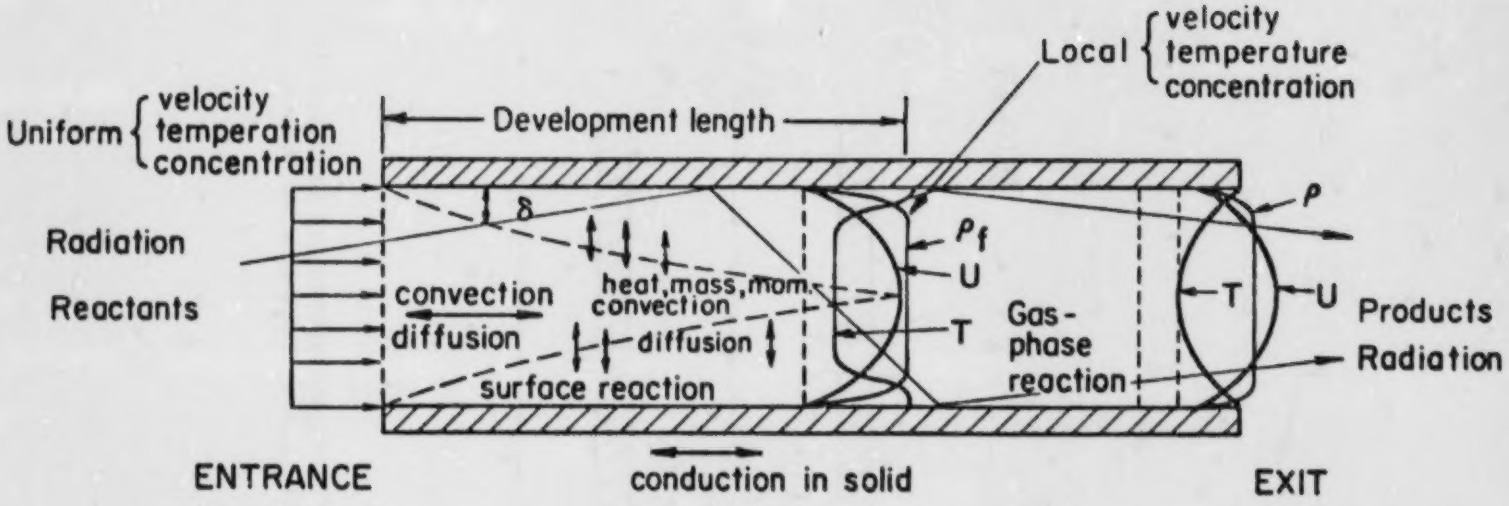
Uniform { velocity
temperation
concentration
Development length
Local { velocity
temperature
concentration
Radiation
Reactants
δ
convection
diffusion
heat, mass, mom.
convection
diffusion
surface reaction
ρ_f
U
T
Gas-
phase
reaction
ρ
T
U
Products
Radiation
ENTRANCE
conduction in solid
EXIT

Figure 11. Physical and chemical processes in a channel of catalyst.

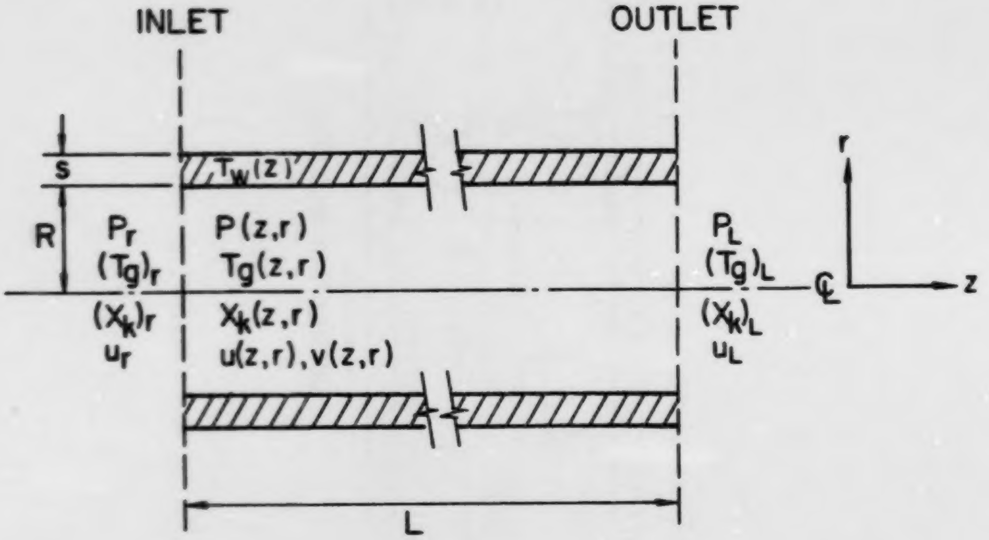
INLET
OUTLET
s
$T_w(z)$
R
P_r
$(T_g)_r$
$(X_k)_r$
u_r
$P(z,r)$
$T_g(z,r)$
$X_k(z,r)$
$u(z,r), v(z,r)$
P_L
$(T_g)_L$
$(X_k)_L$
u_L
r
z
℄
L

Figure 12. Coordinate system and variables in the model of a catalyst channel.

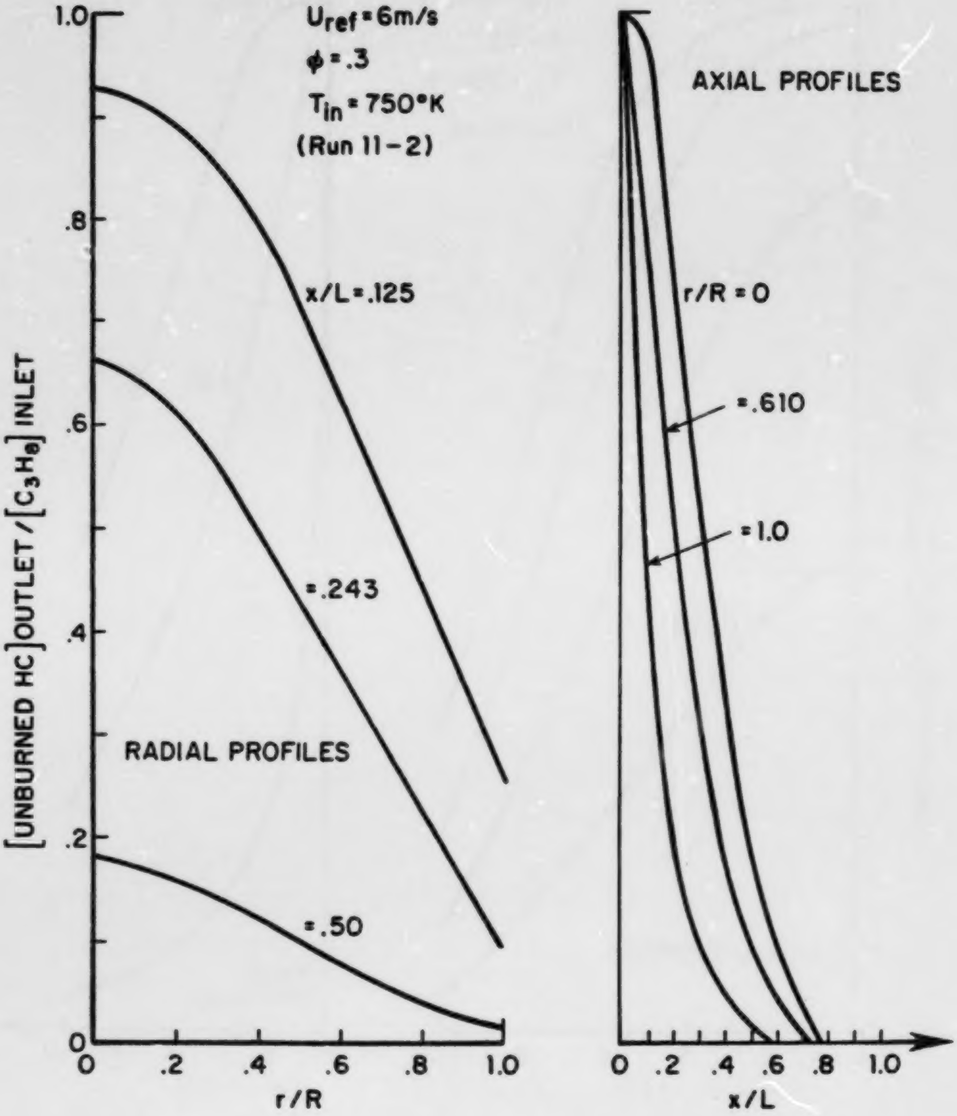

Figure 13. Theoretical profiles of unburned HC versus r and x for 3-step (overall) catalytic oxidation of C_3H_8.

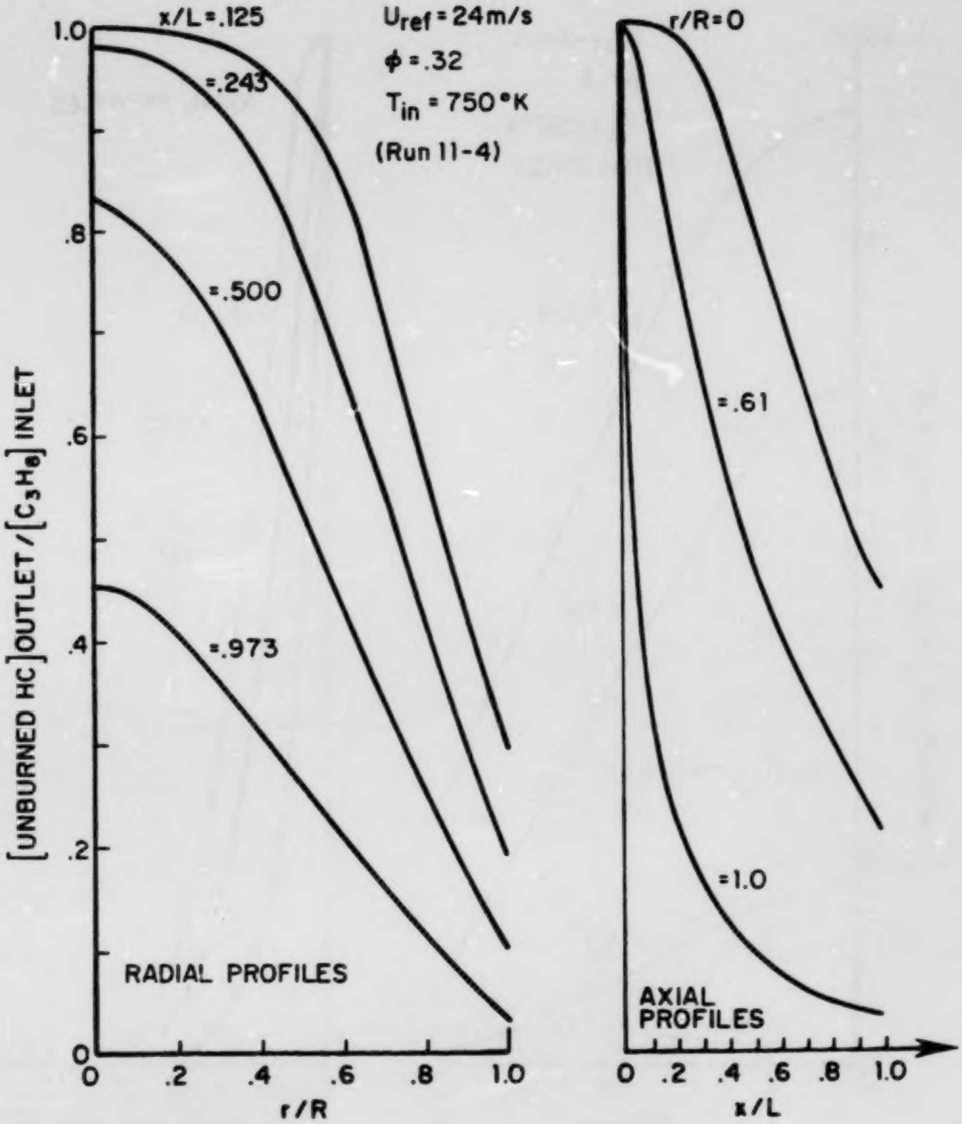

Figure 14. Theoretical profiles of unburned HC vs. r and x for 3-step (overall) catalytic oxidation of C_3H_8.

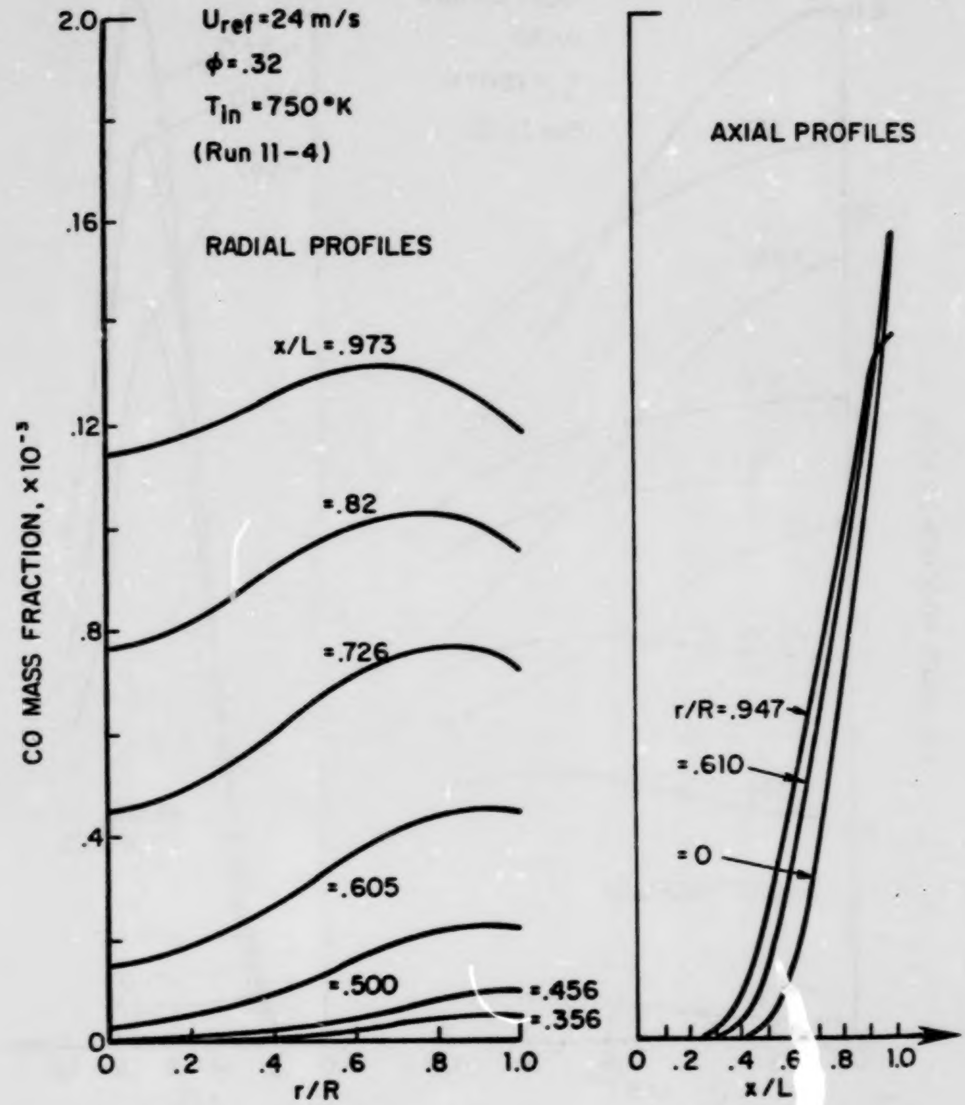

Figure 15. Theoretical profiles of CO vs. r and x for 3-step (overall) catalytic oxidation of C_3H_8.

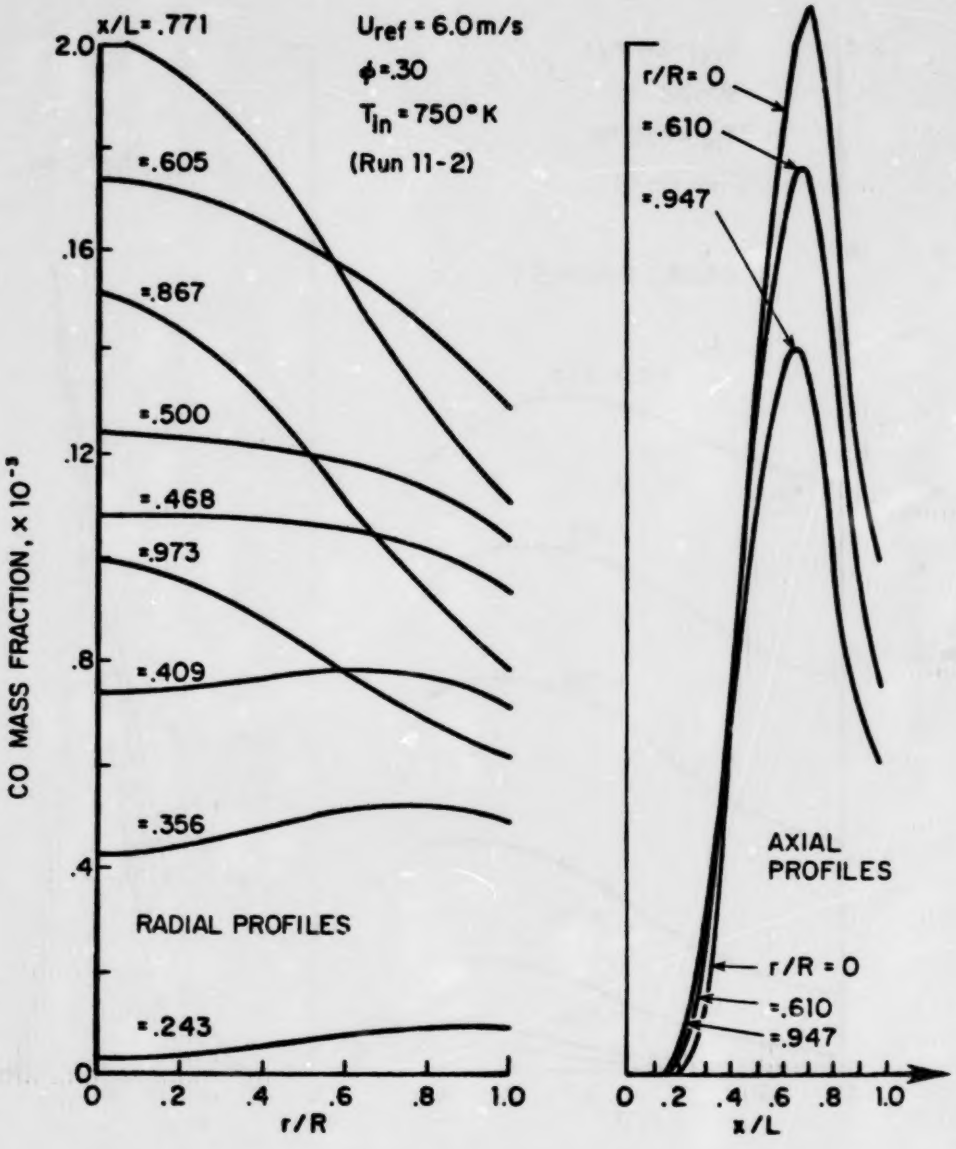

Figure 16. Theoretical profiles of CO vs. r and x for 3-step (overall) catalytic oxidation of C_3H_8.

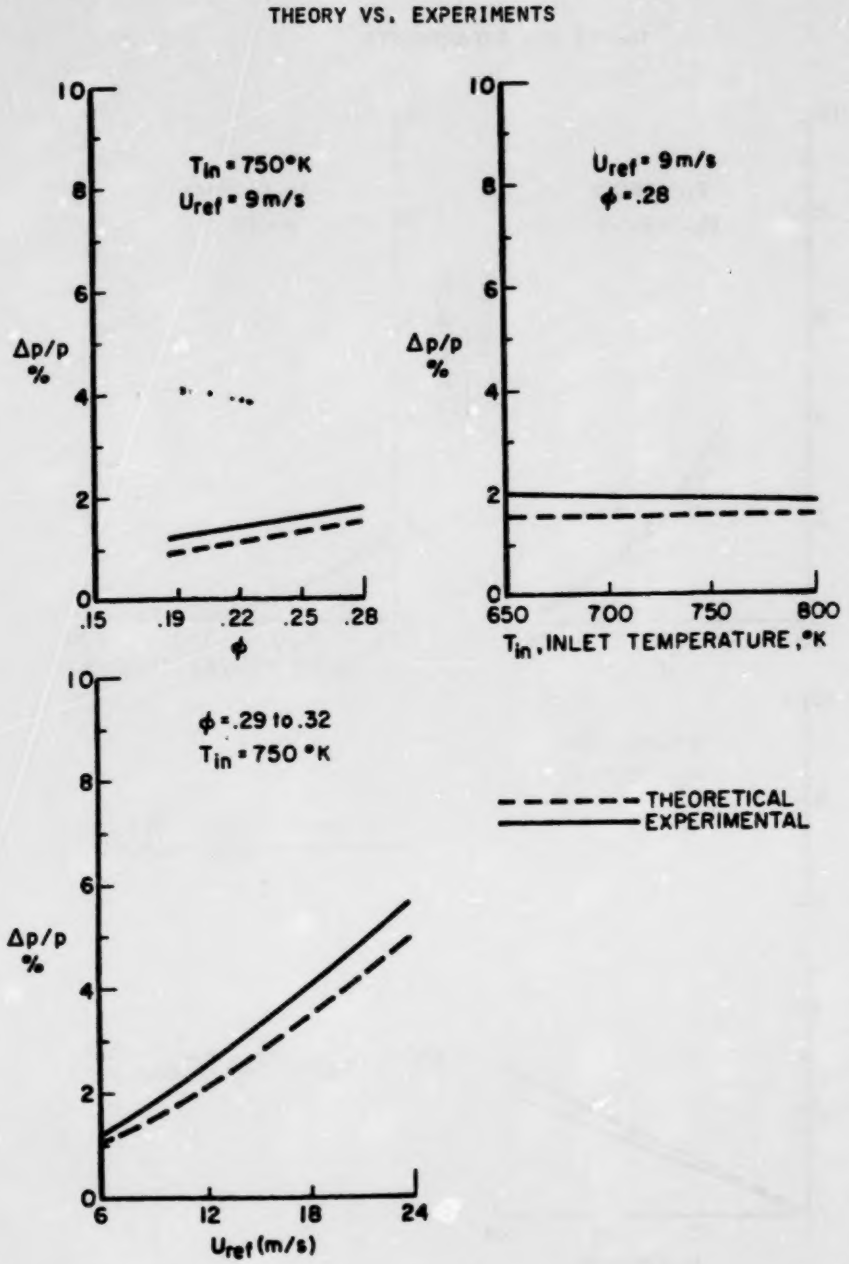

Figure 17. Pressure drop.

THEORY VS. EXPERIMENTS

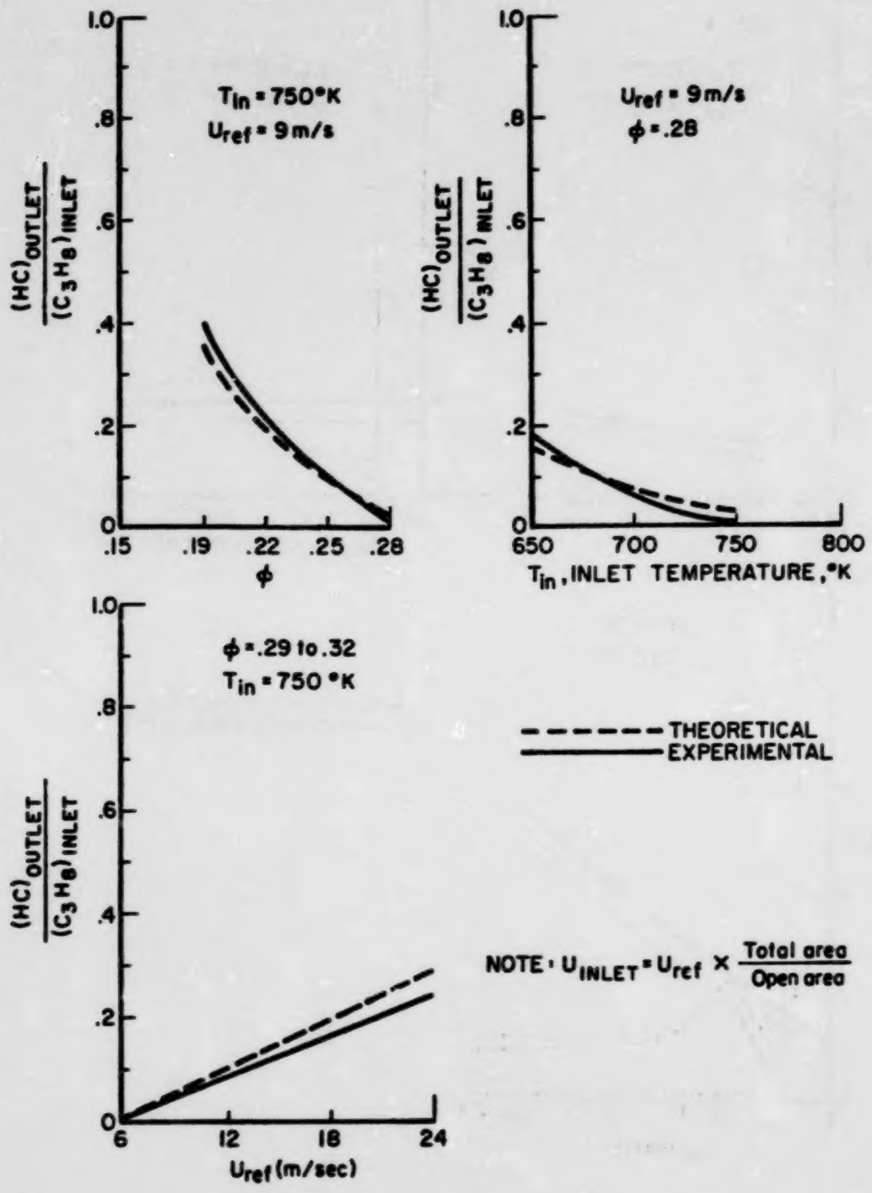

Figure 18. Unburned hydrocarbons.

THEORY VS. EXPERIMENTS

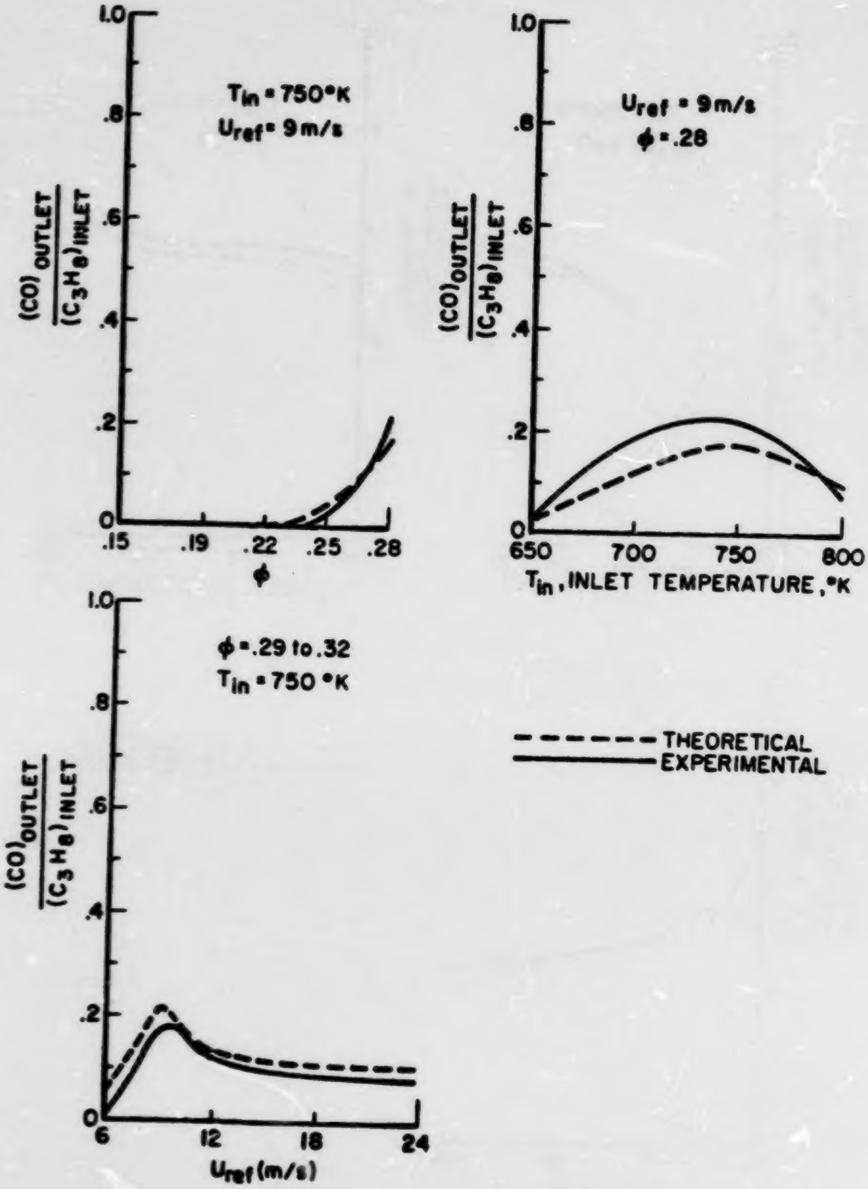

Figure 19. Unburned CO.

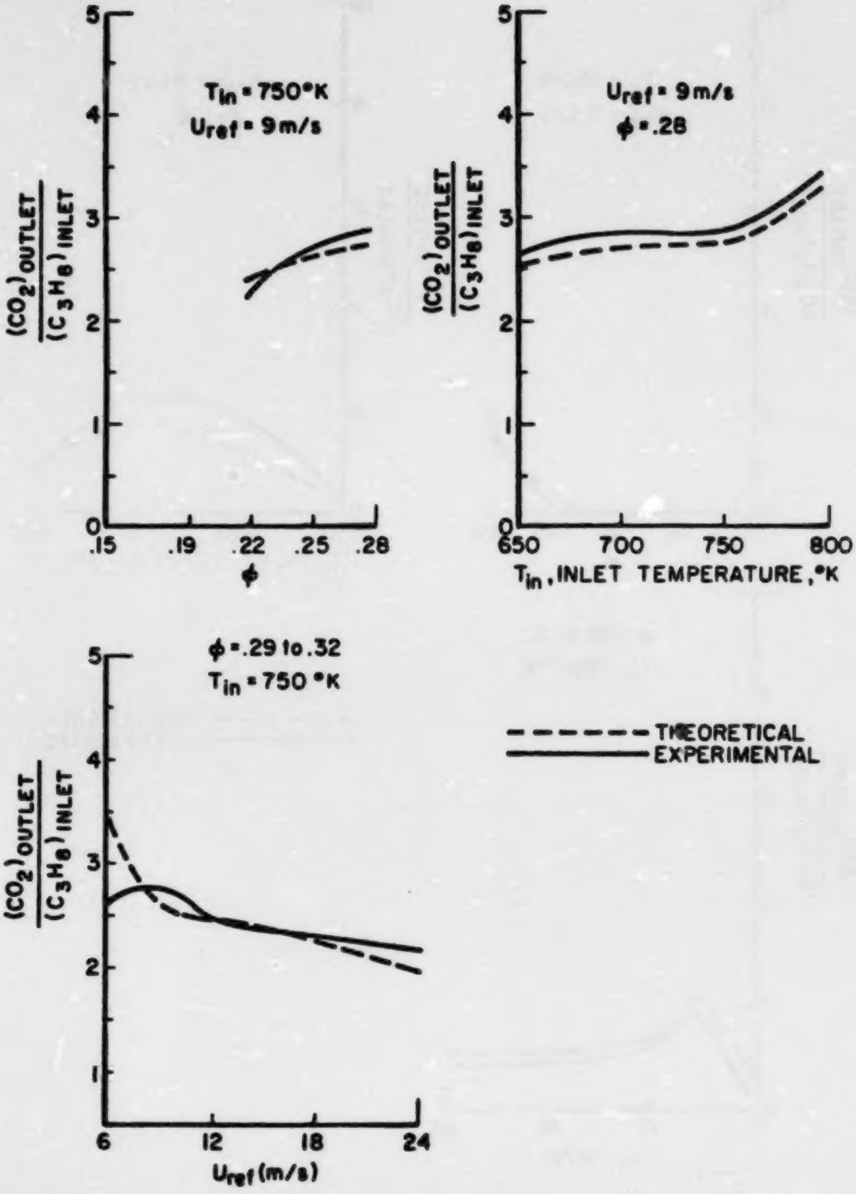

THEORY VS. EXPERIMENTS

Figure 20. CO_2 product.

THEORY VS. EXPERIMENTS

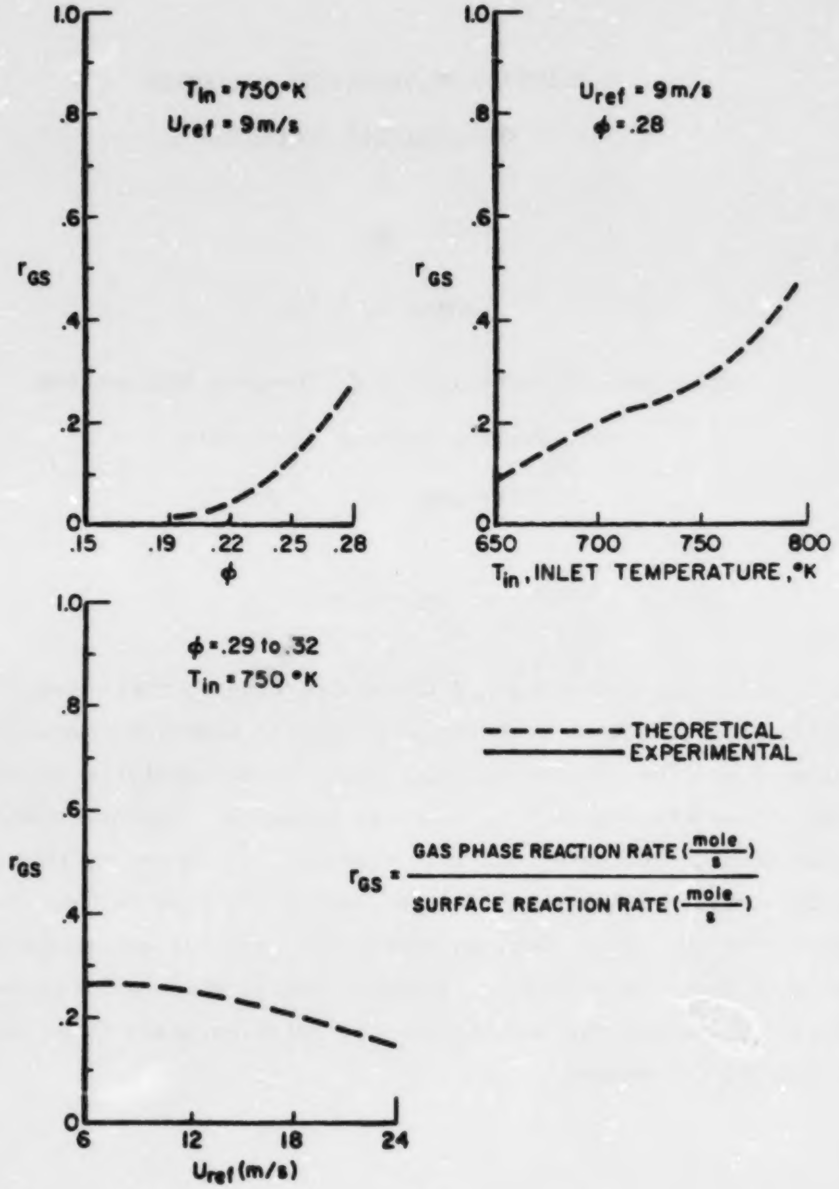

$$r_{GS} = \frac{\text{GAS PHASE REACTION RATE } \left(\frac{\text{mole}}{\text{s}}\right)}{\text{SURFACE REACTION RATE } \left(\frac{\text{mole}}{\text{s}}\right)}$$

Figure 21. Relative importance of gas phase vs. surface reaction rates.

MODELING OF TRANSIENT OPERATION OF CATALYTIC COMBUSTOR

by

James S. T'ien

Department of Mechanical and Aerospace Engineering
Case Western Reserve University
Cleveland, Ohio 44106

ABSTRACT

A quasisteady-gas-phase and thermally-thin-substrate model is used to analyze the transient behavior of catalytic monolith combustors in fuel-lean operation. One particular concern for catalytic combustors used in transportation engines is their transient response time. The computed results indicate that fast response is favored by thin substrate, short catalytic bed length and large channel diameter in high inlet-temperature operation. From combined steady and unsteady considerations, it is possible to choose a catalytic combustor design which has reasonably fast response (~1 second) and can satisfy the emission goals in an acceptable total combustor length.

ACKNOWLEDGEMENT

This project is supported by the Department of Energy under NASA Grant NSG-3230 administered by NASA Lewis Research Center.

The author wishes to express his sincere thanks to Dr. David N. Anderson, without whose advice and suggestions this paper would not be possible.

Nomenclature

A^* crossectional area of one gas channel

A_s^* substrate cross-sectional area associated with one gas channel, see Fig. 1

$$B_1 = \frac{L^*}{u^*(0,0)} \frac{1}{\rho^*(0,0)} \frac{1}{Y_{HC}(0,0)} C_1^* p^*(0,0)^{\alpha_1} \rho^*(0,0)^{(\alpha_2+\alpha_3)} T^*(0,0)^{\alpha_4} Y_{HC}(0,0)^{\alpha_2} Y_{O_2}(0,0)^{\alpha_3} \times W_{HC}^{(1-\alpha_2)} W_{O_2}^{-\alpha_3}$$

$$B_2 = \frac{L^*}{u^*(0,0)} \frac{1}{\rho^*(0,0)} \frac{1}{Y_{HC}(0,0)} C_2^* p^*(0,0)^{\beta_1} \rho^*(0,0)^{(\beta_2+\beta_3+\beta_5)} T^*(0,0)^{\beta_4} Y_{HC}(0,0)^{\beta_2} \times Y_{O_2}^{\beta_3}(0,0) W_{CO}^{(1-\beta_2)} W_{O_2}^{-\beta_3} W_{H_2O}^{-\beta_5}$$

$B_3 = C_3^* d^* / \alpha^* W_{HC} Nu_\infty$

$B_4 = C_4^* d^* / \alpha^* W_{CO} Nu_\infty$

$C_n = n W_{CO} / W_{HC}$

C_s^* specific heat of substrate

C_p^* gas specific heat

d^* catalytic monolith combustor channel equivalent diameter

d_s^* half thickness of the substrate

E^* activation energy

J_3^* mass consumption rate of hydrocarbons per unit surface area through reaction (C)

J_4^* mass consumption rate of CO per unit surface area through reaction (D)

$J_{Di} = J_H (Le_i)^{2/3}$

$J_H = 4\, Nu_x(\alpha^*(0,0)/d^{*2})(L^*/u^*(0,0))(k^*/k^*(0,0))$

k^* heat conductivity of the gas

L^* catalytic bed length

L^*_{EG}		total combustor length (catalytic bed plus after-bed space) required to meet emission goals
Le_1		Lewis number for hydrocarbon gas in air
Le_2		Lewis number for CO in air
m		number of hydrogen atom in C_nH_m
n		number of carbon atom in C_nH_m
Nu_x		Nusselt number at x
Nu_∞		Nusselt number for fully developed flow
p	=	$p^*/p^*(0,0)$, nondimensional pressure
q_1	=	$q^*_1/C^*_pT^*(0,0)$, nondimensional heat of combustion per unit mass of C_nH_m in reaction A
q_2	=	$q^*_2/C^*_pT^*(0,0)$, nondimensional heat of combustion per unit mass of CO in reaction B
q_3	=	$q^*_3/C^*_pT^*(0,0)$, nondimensional heat of combustion per unit mass of C_nH_m in reaction C
q_4	=	$q^*_4/C^*_pT^*(0,0)$, nondimensional heat of combustion per unit mass of CO in reaction D, same as q_2
r_{nk}		see Eq. (17)
S^*		circumferential length of one channel crossection ($= \pi d^*$)
T	=	$T^*/T^*(0,0)$, nondimensional gas temperature
T_s	=	$T^*_s/T^*(0,0)$, nondimensional substrate temperature
T^*_{af}		adiabatic flame temperature
T^*_{in}		combustor inlet temperature
t	=	t^*/τ^*, nondimensional time
u	=	$u^*/u^*(0,0)$, nondimensional flow velocity
W_i		molecular weight of specie i
x	=	x^*/L^*, nondimensional axial distance measured from catalytic bed entrance to downstream

u^*_{ref}	reference gas velocity, measured at upstream of catalytic bed
Y_i	mass fraction of specie i
α^*	thermal diffusivity of gas
β	rate constant, see Eq. (22)
ρ^*	gas density
ρ^*_s	substrate density
τ^*	characteristic substrate heat-up time, see Eq. (16)
η_{CB}	carbon-balanced efficiency
η_T	combustion efficiency based on temperature difference
$[\quad]$	concentration, g-mole/c.c.

I. Introduction

Due to the large thermal inertia of the substrate, the transient behavior of catalytic combustors is expected to be different from that of a conventional gas turbine burner. Non-steady operations are obviously important to transportation engines since their power levels have to be changed frequently. Transient may also be a concern with stationary gas turbine applications, since the ignition/shutdown operation can produce excessive thermal stress or thermal shock if the combustor is not designed or operated properly and substrate can fail as a result [1].

Typical questions concerning transient operations include the combustor response time, the type of response, the unsteady substrate temperature history and the resultant thermal stress distribution. At the present time, both experiment and theory on transient catalytic combustion are lacking. A model is presented here attempting to analyze the problem theoretically. This paper will proceed first to discuss the time scales associated with the unsteady processes in a monolith catalytic combustor. Then a lean combustion model will be presented for the limiting case of "quasisteady gas phase and thermally thin substrate." The computed results will then follow.

II. Nonsteady Combustion Model

II.1 Consideration of Time Scales

For a monolith catalytic combustor with uniform cell distribution in the plane normal to the approaching flow direction, if the combustor wall is well insulated, then the study of whole reactor can be reduced to the consideration of a single cell unit. Referring to Fig. 1, each cell unit. consists of an open gas channel and the associated substrate volume.

Considering first the steady-state combustion, the relevant time scales are the gas residence time in the reactor, the heat and mass transfer time between the gas and the solid surface inside the channel and the gas-phase and surface reaction times. When a transient is caused by an upstream parameter variation, then the new time scales involved include the input characteristic time, the time for the temperature wave to reach the central plane of the substrate and the time for heating-up (or cooling-down) the substrate.

Table 1 defines these characteristic times and their estimated magnitudes. It should be noted that some of the time scales vary along the channel of the reactor bed. For example, the heat/mass transfer time and the substrate heat-up time are shorter at the flow entrance region than those for far downstream, and the ones used in Table 1 are those based on fully-developed flow profiles. However, the estimation from Table 1 does serve the purpose of order-of-magnitude comparison. From this table we see that the longest time is the solid heat-up time, being of the order of seconds. If the time scale we are interested in is much greater than the gas residence time (~15 msec), then the gas phase processes (including heat/mass transfer and chemical reactions) can be regarded as in a quasi-steady state. If furthermore the substrate half-thickness is smaller than about .2 mm, then the substrate temperature distribution in the direction normal to the channel axis can be regarded as uniform at any given time. In this limiting case then, a "quasi-steady-gas-phase and thermally-thin-substrate" model is applicable with the only transient process being the substrate heating-up or cooling-down. In the following section, this model will be described in mathematical form.

II.2 Quasisteady Gas Phase

Quasisteady gas phase implies that the differential equations for the gas-phase processes are the same as those for the steady state. Only the boundary conditions on the solid surface are different. There are several steady-state catalytic combustor models in existence [2-5] and they show a high degree of success in describing the events occurring in the combustor. In particular, the model by Kelly et al [3] containing detailed chemistry for methane/air reactions can predict pollutant emissions. Detailed kinetics, unfortunately, are not yet available for most other practical fuels. Since emission characteristics are important considerations for catalytic combustor design, in the absence of more detailed information, a model consisting of several key semi-global chemical steps is proposed.

For fuel-lean catalytic combustion using nitrogen-free hydrocarbon fuels, the NO_x emission is negligible because of low flame temperatures. The only pollutants needed to be considered are unburnt hydrocarbons (UHC) and carbon monoxide (CO). For this reason, the two semi-global chemical reactions used in the gas phase are:

(A) $$C_nH_m + \frac{1}{2}\left(n+\frac{m}{2}\right) O_2 \longrightarrow n\,CO + \frac{m}{2} H_2O$$

$$\frac{d[C_nH_m]}{dt^*} = -C_1^* p^{*\alpha_1} [C_nH_m]^{\alpha_2} [O_2]^{\alpha_3} T^{*\alpha_4} e^{-E_1^*/RT^*} \quad (1)$$

(B) $$CO + \frac{1}{2} O_2 \longrightarrow CO_2$$

$$\frac{d[CO]}{dt} = -C_2^* p^{*\beta_1} [CO]^{\beta_2} [O_2]^{\beta_3} [H_2O]^{\beta_5} T^{*\beta_4} \times \exp(-E_2^*/RT^*) \quad (2)$$

In describing the flow in the reactor channel, we follow previous investigators to use the plug flow approximation. For transient, in general, the fluid properties are functions of x, the distance along the channel axis and t, the time. For example, density of the gas will be expressed as $\rho(x,t)$. More detailed derivation of the gas-phase conservation equations can be found in Ref. 9. The nondimensional forms of these equations are summarized in the following (subscript * denotes dimensional quantity and without * denotes nondimensional quantities).

Continuity: $\rho u = \rho(o,t)\, u(o,t)$ (3)

Momentum: $p = p(o,t)$ (4)

Energy: $$\rho u \frac{\partial T}{\partial x} + J_H (T - T_s) = q_1 Y_{HC}(0,0)\, w_1 + q_2 Y_{HC}(0,0)\, w_2 \quad (5)$$

Species:

Hydrocarbon:

$$\rho u \frac{\partial y_{HC}}{\partial x} + J_{D1} (y_{HC} - y_{HC,s}) = -w_1 \quad (6)$$

Carbon monoxide:

$$\rho u \frac{\partial y_{CO}}{\partial x} + J_{D2} (y_{CO} - y_{CO,s}) = w_1 c_n - w_2 \quad (7)$$

Oxygen:

$$y_{O_2} = 1 - \phi(1 - y_{HC}) + \frac{1}{2} y_{CO}\left(\frac{Y_{HC}(0,0)}{Y_{O_2}(0,0)}\,\frac{W_{O_2}}{W_{CO}}\right) \tag{8}$$

Equation of state: $p = \rho T$ (9)

The reaction rates are given by

$$w_1 = B_1 p^{\alpha_1} \rho^{(\alpha_2+\alpha_3)} T^{\alpha_4} y_{HC}^{\alpha_2} y_{O_2}^{\alpha_3} e^{-(E_1/T)} \tag{10}$$

$$w_2 = B_2 p^{\beta_1} \rho^{(\beta_2+\beta_3+\beta_5)} T^{\beta_4} y_{CO}^{\beta_2} y_{O_2}^{\beta_3} Y_{H_2O}^{\beta_5} e^{-(E_2/T)} \tag{11}$$

and $$Y_{H_2O}(x,t) = \frac{m}{2}\,\frac{W_{H_2O}}{W_{HC}}\,Y_{HC}(0,0)\left[y_{HC}(0,t) - y_{HC}(x,t)\right] \tag{12}$$

The definition of B_1 and B_2 can be found in the nomenclature.

In deriving Eqns (5-8), heat conduction and mass diffusion in the axial direction are neglected because the Peclet number based on typical gas velocity (>10 M/sec) is much greater than unity [5]. The dimensionless lateral heat and mass transfer coefficients J_H and J_{Di}, in Eqns (5-7) are derived from Nusselt number calculation in entrance flow in tube of constant surface temperature [10]. Following Ref. 3, a modification is made at the entrance point based on local stagnation flow estimation. The use of entrance flow transport properties, rather than fully-developed constant value, make a great difference in the temperature and species distributions in the flow entrance region. More detailed discussion can be found in Ref. 9.

The above system of equations can also be applied to the after-bed space where only gas-phase reactions occur. This is done by putting J_H and J_{Di} equal to zero in Eqns (5-7) and by properly changing the mass flux per unit area in Eq (3) due to area change.

II.3 Unsteady Solid with Thin-Wall Substrate

When the substrate wall is thermally thin, the solid temperature can be regarded as a function of axial distance and time only, i.e., $T_s(x,t)$. The energy balance of the solid, including the solid surface, results in the following equation:

$$A_s^* \rho_s^* C_s^* \frac{\partial T_s^*}{\partial t^*} - h_T^* S^* (T^* - T_s^*) = S^* \left[q_3^* J_3^* + q_4^* J_4^* \right] \tag{13}$$

In Eq (13) the heat conduction in axial direction in the solid is neglected in comparison with the heat transfer rate across the gas channel. A more detailed discussion of this approximation can be found in Ref. 9.

Two semi-global catalytic surface reactions are assumed. They are

$$\text{(C)} \qquad C_n H_m + \left(n + \frac{m}{4}\right) O_2 \longrightarrow n\, CO_2 + \frac{m}{2} H_2O \tag{14}$$

with the corresponding surface reaction rate J_3^* given by

$$J_3^* = C_3^* \, [C_n H_m]_s \, e^{-E_3^*/RT_s^*}$$

and

$$\text{(D)} \qquad CO + \frac{1}{2} O_2 \longrightarrow CO_2 \tag{15}$$

with

$$J_4^* = C_4^* \, [CO]_s \, e^{-E_4^*/RT_s^*}$$

In surface reaction (C), the hydrocarbon is oxidized to form CO_2 and H_2O, not CO such as in gas-phase reaction (A). This is based on the present available experimental evidence that in oxygen-rich system, only CO_2, not CO, is found on or close to the catalytic surface [6-8].

Eq (13) is nondimensionalized by first defining a proper reference time scale τ^*.

$$\tau^* \equiv \frac{1}{Nu_\infty} \frac{1}{\pi} \frac{A_s^* \rho_s^* C_s^*}{k^*(0,0)} \tag{16}$$

and

$$t \equiv t^*/\tau^*$$

$$r_{nk} \equiv \frac{Nu_x}{Nu_\infty} \frac{k^*}{k^*(0,0)} \tag{17}$$

Eq (13) becomes

$$\frac{\partial T_s}{\partial t} - r_{nk}(T - T_s) = B_3\, Y_{HC}(0,0)\, \overset{q}{\gamma}_3\, \rho\, y_{HC,s}\, \exp(-E_3/T_s)$$

$$+ B_4\, Y_{HC}(0,0)\, \overset{q}{\gamma}_4\, \rho\, y_{CO,s}\, \exp(-E_4/T_s) \qquad (18)$$

Neglecting transient accumulation on the surface, the surface hydrocarbon and carbon monoxide are given by

$$r_{nk}(y_{HC} - y_{HC,s}) = \frac{1}{(Le_1)^{2/3}} B_3\, \rho\, y_{HC,s}\, \exp(-E_3/T_s) \qquad (19)$$

$$r_{nk}(y_{CO} - y_{CO,s}) = \frac{1}{(Le_2)^{2/3}} B_4\, \rho\, y_{CO,s}\, \exp(-E_4/T_s) \qquad (20)$$

II.4 Initial and Boundary Conditions

The system of equations (3-12, 18-20) needs initial and boundary conditions. Initial conditions (at t = 0) are required for T_s, $(y_{HC})_s$ $(y_{CO})_s$ as a function of x and upstream boundary conditions (at x = 0) should be specified for y_{HC}, y_{CO}, y_{O2}, T, p and u as a function of time. These conditions depend on the types of transient input which can vary with engine designs and mode of operations. In the present paper, two simple types of transient are investigated. They are catalytic combustor ignition and exponential change of fuel flow rate.

1. Ignition

Catalytic combustor ignition is modeled by specifying the substrate temperature at time t = 0. This temperature can be the result of external heating of the substrate, say, by a torch. The fuel and air are then supplied at upstream. The model is intended to describe the events from t = 0 to the final steady state. Mathematically, the conditions used are

$$
\begin{aligned}
T_s(x,0) &= \text{constant (specified)} \\
y_{HC,s}(x,0) &= 0 \\
y_{CO,s}(x,0) &= 0 \\
T(0,t) &= 1 \\
y_{HC}(0,t) &= 1 \\
y_{CO}(0,t) &= 0 \\
y_{O2}(0,t) &= 1 \\
p(0,t) &= 1 \\
u(0,t) &= 1
\end{aligned}
\qquad (21)
$$

2. Exponential Variation of Fuel-Flow Rate

In this category, we start with a given steady state, the upstream fuel-flow rate (or equivalence ratio) is then changed to another level in an exponential fashion. We are interested in the transient combustor response due to this unsteady upstream variation. Mathematically, the surface distribution of $T_s(x,0)$, $y_{HC,s}(x,0)$ and $y_{CO,s}(x,0)$ are given by the initial steady-state computation. The upstream fuel/air equivalence ratio is described by

$$\phi(0,t) = \phi_2 + (\phi_1 - \phi_2) \exp(-\beta t) \qquad (22)$$

where ϕ_1 = initial upstream equivalence ratio
ϕ_2 = final upstream equivalence ratio
β = rate constant

The corresponding upstream fuel variation, $y_{HC}(0,t)$, can be obtained directly from Eq (22). The conditions for $T(0,t)$, $y_{CO}(0,t)$, $y_{O2}(0,t)$, $p(0,t)$ and $u(0,t)$ are held constant as specified in Eq (21).

II.5 Numerical Solution Procedure

Although most dependent variables in this problem are function of both x and t which, in general, results in partial differential equations, the assumption of quasisteady gas phase and thermally thin substrate greatly simplifies the mathematical property of the system and results in simpler solution procedure.

The gas-phase differential equations (5-7) have only first derivative in x with t as a parameter, the solid equation (18) has only derivative in t with x as a parameter; therefore, they can be integrated at each time (t) or position (x) as ordinary differential equations using Runge-Kutta method. The procedure is started by first integrating Eqns (5-7) forward in x from upstream to the end of combustor for $T, \mathcal{Y}_{HC}, \mathcal{Y}_{CO}$ using the solid surface quantities specified by the initial conditions, then Eq (18) is integrated for one time step (Δt) to find $T_s(x, \Delta t)$ and Eqns (19,20) are solved algebraically to find $\mathcal{Y}_{HC,s}(x,\Delta t)$ and $\mathcal{Y}_{CO,s}(x, \Delta t)$. These surface quantity are substituted back to Eqns (5-7) to start another cycle of integration.

III. Computed Results

III.1 Steady State

Although the main objective of this paper is for transient response, the unsteady calculation has to be based on a realistic steady combustion model. Detailed steady-state predictions and their comparison with experiment can be found in Ref. 9. Here several key features of the steady model will be mentioned as they are important to the discussion of nonsteady results.

Table II lists the values of chemical kinetic constants for reactions A to D used in this paper. The hydrocarbon fuel chosen is propane. Its semi-global kinetics are from Edelman with the pre-exponential factor adjusted to match Dryer's data at 1000°K [12]. The CO oxidation data are from Ref. 11. The activation energies for reactions C and D are obtained from Refs. 8 and 13 respectively with adjusted pre-exponential factors. It should be noted that the surface reaction rates contain information on catalyst type and loading density as well as the washcoat properties; therefore, they can vary from one combustor to the other. The purpose of this computation is not to match a particular set of experimental combustor data, but, rather, after choosing a reasonable set of kinetic constants, to study the effects of other combustor design and operating parameters.

The design parameters considered are d^*, channel hydraulic diameter, A^*/A^*_s, the ratio of open-to-close areas, L^*, the catalytic bed length and L^*_{EG}, the total catalytic combustor length (catalytic bed length plus afterbed length) required to reach the emission goal in steady-state operations. The emission goal is chosen to be 1.64 g/kg of fuel for UHC and 13.6 g/kg of fuel for CO [14]. The operating parameters include ϕ, fuel/air equivalence ratio, p^*, pressure, T^*_{in}, combustor inlet temperature and u^*_{ref}, the reference velocity of the approaching gas.

Figure 2 gives the profiles for one sample calculation. In this case, the propane fuel is oxidized quickly on the catalyst surface upon entering into the reactor channel and resulting in a high surface temperature, the gas temperature is raised by heat transfer from the substrate, gas-phase oxidation of propane is accelerated to form CO, and CO, in turn, is oxidized by both gas-phase and surface reactions to CO_2. Actually, two cases are shown in Fig. 2. In one case, the reactor bed length is 4 cm, in the other, 8 cm. When the bed length is cut short at 4 cm, the surface reactions for hydrocarbon fuel and CO stop there. This results in a higher CO concentration as shown by the dotted curve. The hydrocarbon curve also shows a difference after 4 cm but the difference is too small to be shown clearly in this figure. The gas temperature is also lower in a portion of the combustor for the 4-cm case.

Figure 3 gives the combustor length required to reach the emission goal vs. catalytic bed length for three inlet temperatures. The three curves have different fuel/air equivalence ratio so that their adiabatic flame temperatures are approximately the same ($1370°K < T^*_{af} < 1392°K$).

The effect of the approaching flow reference velocity is shown in Fig. 4. When L^*_{EG} and L^* are divided by the reference velocities, the three velocity cases approximately collapse into one curve. Therefore the residence time should be a good correlation parameter for catalytic combustors.

III.2 Ignition Transient

One of the major concerns of the catalytic combustor application to transportation gas turbine engines is that the response time might be long. The computed ignition transient results to be presented are combustor responses to a stepwise increase of fuel flow rate (zero to a fixed value). Therefore, they can be used as a guidance in our search for "fast-response" catalytic combustor designs.

Some indication of the order of magnitude of the response time can be obtained from the definition of the characteristic time τ^* as defined in eq. (16). Small τ^* requires small thermal inertia, $A^*_s \rho^*_s C^*_s$. If the substrate density and heat capacity are fixed, small τ^* can be achieved with small solid crossectional area A_s^*, see Fig. 1 for definition of A_s^*. Table III lists the values of τ^* for a range of cell diameter, d^*, and open-to-close area ratio, A^*/A_s^*. It should be noted that there are other parameters such as catalytic bed length and channel diameter which will influence the response time and they are not contained in τ^*. This will be discussed later as we see the computed results.

The combustion efficiency at the end of the combustor will be used to characterize the combustor response time. There are two ways to define the combustion efficiency. One is the so-called "carbon-balanced" efficiency, η_{CB} [15], where the combustion inefficiency is measured by the emission levels of CO and UHC and the energy carried away by them. The other efficiency is the ordinary one defined by the enthalpy rise across the combustor divided by the chemical energy available. If the gas specific heat is approximated as a constant, this efficiency, η_T, is given by $(T - T_{in})/(T_{af} - T_{in})$ where T is measured at the same location as the efficiency. For a perfectly insulated catalytic combustor in steady state, η_{CB} and η_T are the same. However, the two are different in transient operations when there is a thermal lag in the substrate.

For the following transient ignition calculation, the initial surface temperature condition is given by $T_s(x,0) = 1$, see Eq. (21). Also, the combustor length has to be specified. From Fig. 3, we see that the required combustor length is a function of catalytic bed length. For 1000°K inlet temperature, two bed lengths, 4 cm and 8 cm, are chosen for transient ignition calculation. Fig. 5 shows the combustion efficiencies as a function of non-dimensional time. Looking at the curves for η_T (efficiency based on temperatures), the shorter bed (4 cm) combustor has a faster response than that of the longer bed (8 cm). If we take the time for η_T to reach 70% as an indication of characteristic response time, for the 4-cm bed, $t_{Ch} = 1.1$ and for the 8-cm bed, $t_{ch} = 2$; namely, the response time of 4-cm bed combustor is only half of that of the 8-cm bed combustor. From the consideration of steady-state operation alone, one would choose the 8-cm catalytic bed since according to Fig. 3, this produces the shortest required combustor length (12 cm). However, combining transient and steady-state considerations, the 4-cm bed combustor may be a better choice as its response time is 50% of that of the 8-cm bed, with the total combustor length only slightly longer (7.5%).

To understand why longer reactor bed results in a longer response time, surface and gas temperature distributions are plotted in Fig. 6 as a function of time. From the substrate temperature distribution we see that during ignition transient, the solid temperature is higher in the flow entrance region as a result of higher mass transport and surface reaction rates. Comparing the solid and gas temperature histories for the case when catalytic bed length is 8 cm, we see that at $t = 0.5$, the solid is transfering heat to the gas in the upstream region in the bed. This raises the gas temperature and accelerates the gas phase reaction so that at $x^* = 3.5$ cm, the gas temperature becomes higher than the substrate temperature. Heat is then transferred from the gas to the solid in the downstream portion of the reactor channel. If the heat loss rate is greater than heat generation rate due to gas phase reactions, then the gas temperature will drop as shown in Fig. 6. If we cut the reactor bed short at 4 cm, portion of this heat loss can be eliminated and the downstream gas temperature ($x^* > 4$ cm) will be higher as indicated by the dotted curves in Fig. 6. This explains why a shorter reactor bed can have a faster response.

The effect of catalytic channel diameter has also been studied. In varying the diameter, the substrate cross-sectional area, A_s^*, is kept constant so that the characteristic time τ^* is constant. The lower graph of Fig. 7 shows the variations of A^*/A_s^* and the minimum combustor length required to reach emission goal. The increase of L_{EG}^* with d^* is small over the range of diameters studied. This is partly because A^*/A_s^* is larger for larger d^* which leads to a lower gas channel velocity and a greater gas residence time in the catalytic bed. The upper graph in Fig. 7 gives the combustor response time as a function of channel diameter. The decrease of response time with increasing diameter is quite drastic. Take 3.6 mm channel, for example, the time to reach 70% efficiency is only one third of that for the 1.8 mm channel. Translated into dimensional time using the numbers in Table III, the response time for the 3.6 mm diameter channel combustor is about 1.5 seconds.

For the cases studied so far, the combustor inlet temperature is 1000°K. The computed results show that faster combustor response is favored by thin substrate, short catalytic bed and large channel diameter. Shorter bed and larger channel, however, tend to increase the required total combustor length. Therefore, a combined steady and unsteady consideration is needed for a realistic design. In the calculations just presented, it is possible to reduce the response time significantly with only slight increase of the combustor length. However, we have not had enough time to perform more computation in the low inlet temperature cases so it is not certain at this time that all the trends we mentioned above will be the same for low combustor inlet temperatures. In particular, the effect of channel diameter is uncertain.

The response time has been found to be invariant with reference velocity if the gas residence times in the reactor bed and in the after-bed space are unchanged.

III.3 Response to Exponential Decrease of Fuel Flow Rate

Here we study the combustor response from one steady combustion state to the other due to an exponentially decreasing upstream fuel/air equivalence ratio, ϕ. Mathematically, ϕ as a function of time is given by Eq. (22). In the computation performed, ϕ_1 is chosen to be 0.24 and ϕ_2 is 0.20 with rate constant β as a variable. The combustor length is 25 cm long with a 10 cm bed and bed channel diameter of 1.8 mm. The reference velocity is fixed at 10 M/S and the combustor inlet temperature is 800°K.

The ordinate in Fig. 8 is a temperature difference ratio, $\left\{T - T_{in}\right\} / \left\{T_{af}(t) - T_{in}\right\}$, where $T_{af}(t)$ is the adiabatic flame temperature corresponding to the instantaneous upstream equivalence ratio $\phi(t)$ and T is the gas temperature at the combustor exit. When the transient is very slow so that the whole combustor is in a quasisteady state (including the substrate), this temperature difference ratio is the combustion efficiency. For ϕ equal to 0.2 and 0.24, combustion efficiencies are nearly 100%. In transient due to fuel flow rate reduction, this temperature difference ratio exceeds one as shown in Fig. 8. This means that the gas in the bed channel is receiving heat from the substrate in excess of the quasisteady value. This of course is reasonable for the fuel reduction case because of the thermal lag in the substrate. The departure of the temperature difference ratio from the steady-state combustion efficiency (one in Fig. 8) is a good measure of the extent of unsteadiness in the combustor.

Referring to Fig. 8, the curve with $\beta = 100$ peaks very early and is a good approximation of the combustor response to a stepwise decrease of fuel flow rate. The curve decays monotonically with time after the peak, the decay rate is basically inversely proportional to the response time as discussed in the ignition transient study. For slower transient input (smaller β), the peak is smaller and occurs at a later time which means smaller transient effect but a longer transient duration as shown by the various curves in Fig. 8.

More transient computation is being carried out and will be reported at a later time.

References

1. DeCorso, S.M. and Carl, D.E., "Structural Analysis of a Preliminary Catalytic Ceramic Design," Proceedings: Third Workshop on Catalytic Combustion, EPA-600/7-79-038 (1979).

2. Cerkanowicz, A.E., Cole, R.B. and Stevens, J.G., "Catalytic Combustion Modeling: Comparison with Experimental Data," ASME paper (1977).

3. Kelly, J.T., Kendall, R.M., Chu, E. and Kesselring, J.P., "Development and Application of the PROF-HET Catalytic Combustor Code," paper presented at the 1977 Fall Meeting Western States Section, The Combustion Institute.

4. Kendall, R.M., Kelley, J.T., Chu, E.K. and Kesselring, J.P., "An Analysis of Catalytic Combustion in Monolithic Honeycomb Beds," Proceedings: Third Workshop on Catalytic Combustion, EPA-600/7-79-038 (1979)

5. Ablow, C.M. and Wise, H., "Theoretical Analysis of Temperature and Composition in a Catalytic Monolith Reactor," ibid.

6. Schwartz, A., Holbrook, L.L. and Wise, H., "Catalytic Oxidation Studies with Platinum and Palladium," Journal of Catalysts, 21, 199-207 (1971).

7. Anderson, D.N., "Preliminary Results from Screening Tests of Commercial Catalysts with Potential Use in Gas Turbine Combustors. Part I. Furnace Studies of Catalyst Activity," NASA TMX-73410 (1976).

8. Marteney, P.J., "Determination of the Rate of Heterogeneous Reaction on Catalytic Surfaces," Proceedings: Third Workshop on Catalytic Combustion, EPA-600/7-79-038 (1979).

9. T'ien, J.S., "Catalytic Honeycomb Combustor: "Steady-State Model and Comparison with Experiment," to be presented as Paper No. 80-1289 at the AIAA/ASME/SAE 16th Joint Propulsion Conference, June 30-July 2, 1980, Hartford, Connecticut.

10. Kays, W.M., Convective Heat and Mass Transfer, McGraw-Hill, New York, 1966.

11. Dryer, F.L. and Glassman, I., "High Temperature Oxidation of CO and CH_4," 14th Inter. Symp. on Combustion, The Combustion Institute, Pittsburgh, Pa., 1973.

12. Dryer, F.L. and Glassman, I., "Combustion Chemistry of Chain Hydrocarbons," in Alternative Hydrocarbon Fuels: Combustion and Chemical Kinetics, Vol. 62, Progress in Astronautics and Aeronautics (1978). Also discussion section, p. 295.

13. Kuo, J.C.W. and Morgan, C.R., "Mathematical Models of the Monolith Catalytic Convertor," SAE Transaction, V. 80, 1971, #710289.

14. Anderson, D.N., "Performance and Emissions of a Catalytic Reactor with Propane, Diesel, and Jet A Fuels," NASA TM-73786 (1977).

15. Anderson, D.N., Tacina, R.R. and Mroz, T.S., "Performance of a Catalytic Reactor at Simulated Gas Turbine Combustor Operating Conditions," NASA TM X-71747 (1975).

Table I. Estimate of Transient Time Scales in Catalytic Monolith Combustor

Time	Definition	Estimated Magnitude
Gas residence time in reactor bed	L^*/u^*_{ref}	3 - 15 msec
Gas residence time in after-bed space	L^*_{af}/u^*_{ref}	0 - 15 msec
Heat/mass transfer time between gas and solid surface in channel	$\frac{1}{Nu_\infty}\frac{1}{\pi}\frac{d^{*2}}{4\alpha^*(0,0)}$	.5 - 7.5 msec for $d^* \leq 3.6$ mm
Chemical reaction times (gas-phase and heterogeneous)		Variable depending on the local temperature and reactant's concentrations
Time for temperature wave to reach the substrate center plane	$\frac{d^{*2}_s}{\alpha^*_s}$	0.5 - 25 msec for $d^*_s \leq .2$ mm
Substrate heat-up time	$\frac{1}{Nu_\infty}\frac{1}{\pi}\frac{A^*_s\rho^*_s C^*_s}{k^*(0,0)}$	0.5 sec - 20 sec
Transient input time	$1/\beta$ for exponential input; see Eq. (22)	variable, specified

Table II. Chemical Kinetic Constants

Reaction (A)	Reaction (B)	Reaction (C)	Reaction (D)
$C_1^* = 1.5 \times 10^5$	$C_2^* = 0.71 \times 10^{14}$	$C_3^* = 2.5 \times 10^3$	$C_4^* = 10^5$
$\alpha_1 = 0.3$	$\beta_1 = 0$	$E_3^* = 10$ (kcal/mole)	$E_4^* = 17.8$ (kcal/mole)
$\alpha_2 = 0.5$	$\beta_2 = 1$		
$\alpha_3 = 1$	$\beta_3 = 0.25$		
$\alpha_4 = 1$	$\beta_4 = 0$		
$E_1^* = 24$ (kcal/mole)	$\beta_5 = 0.5$		
	$E_2 = 40$ (kcal/mole)		

Table III. Estimate of Substrate Heat-up Characteristic Time

$$\tau^* \equiv \frac{1}{Nu_\infty} \frac{1}{\pi} \frac{A^*_s \rho^*_s C^*_s}{k^*(0,0)} = \frac{1}{11.498} \frac{A^*_s \rho^*_s C^*_s}{k^*(0,0)}$$

$k^*(0,0)$ cal/cm sec°K	ρ^*_s g/cm^3	C^*_s cal/g°K	d^* mm	A^*/A^*_s	A^*_s cm^2	τ^* sec
.000135	2.5	.23	1.4	2	.0077	2.85
.000135	2.5	.23	1.8	2	.0127	4.7
.000135	2.5	.23	2.4	3.56	.0127	4.7
.000135	2.5	.23	3.0	5.56	.0127	4.7
.000135	2.5	.23	3.6	8	.0127	4.7
.000135	7.1 (Kanthal metal)	.145	1.8	5	.0051	3.38
.000135	2.5	.23	3.6	2	.051	19.0

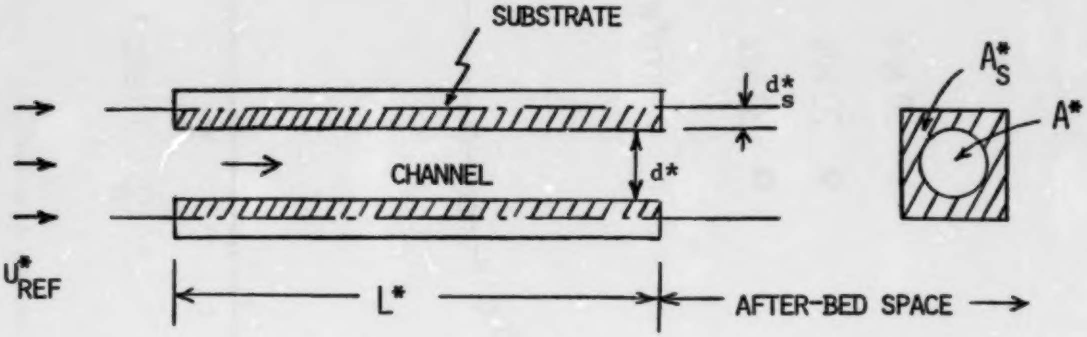
SUBSTRATE
CHANNEL
d_s^*
d^*
A_s^*
A^*
u^*_{REF}
L^*
AFTER-BED SPACE

Figure 1. Schematic Drawing of One Cell Unit

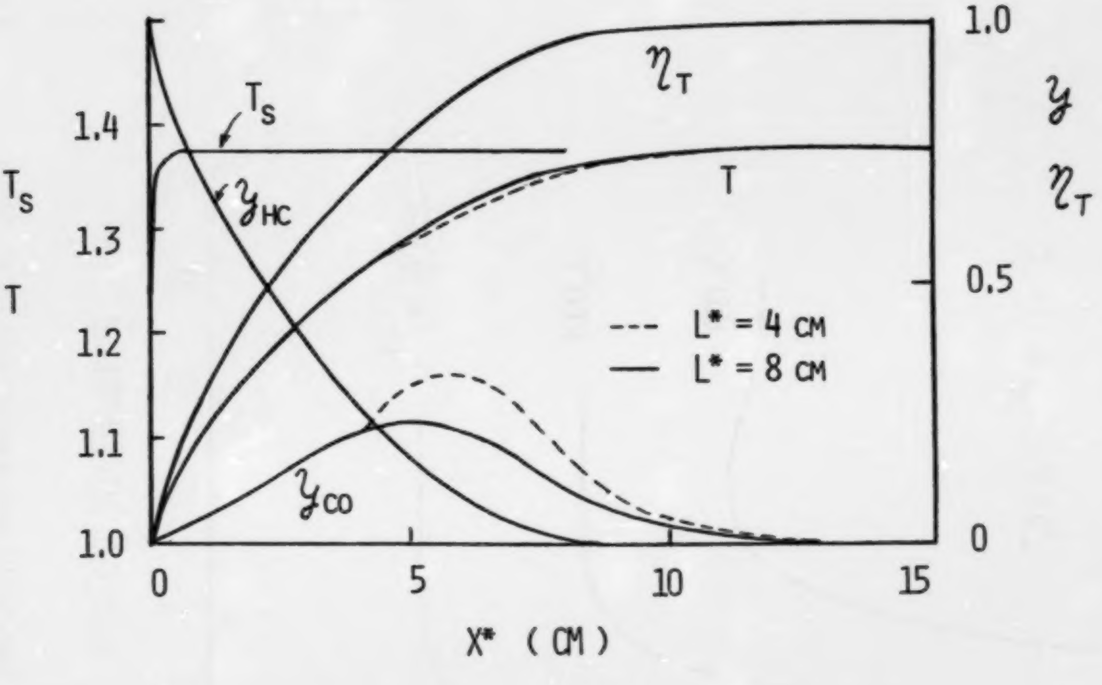

Figure 2. Detailed profiles showing the effect of catalytic bed length. Operating conditions: $p^* = 3$ atm, $T^*_{in} = 1000°K$, $u^*_{ref} = 10$ M/S, $\phi = 0.15$, $d^*_s = 1.8$ mm and $A^*/A^*_s = 2$

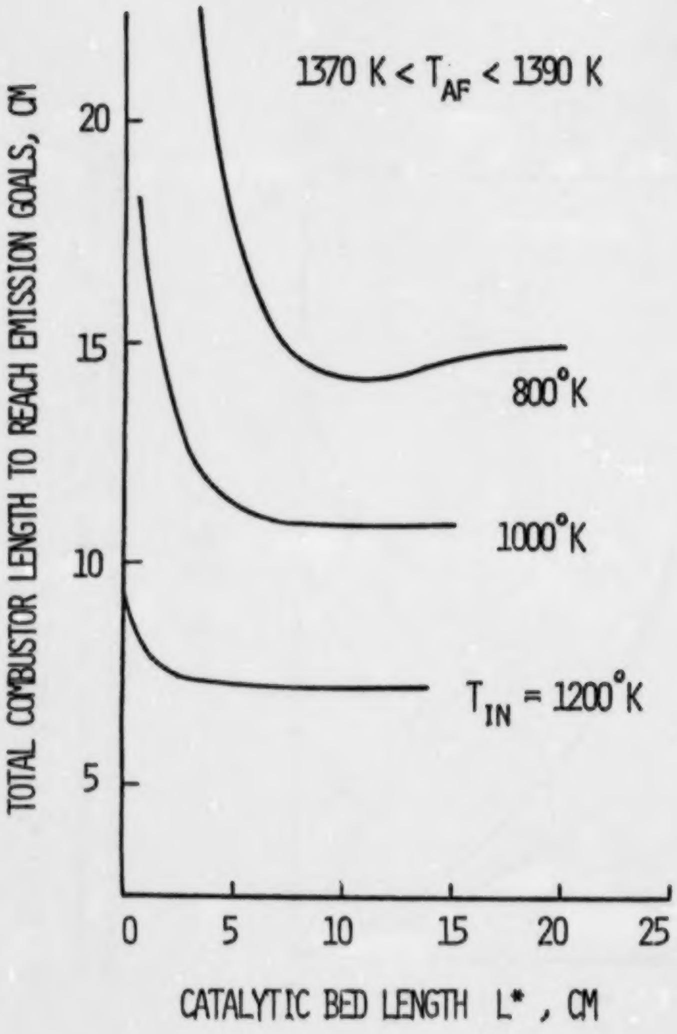

Figure 3. Effect of Catalytic Bed Length and Inlet Temperature on the Total Combustor Length Required to Meet the Emission Goals. $p^* = 3$ atm, $u^*_{ref} = 10$ M/S, $d^*_s = 1.8$ mm and $A^*/A^*_s = 2$

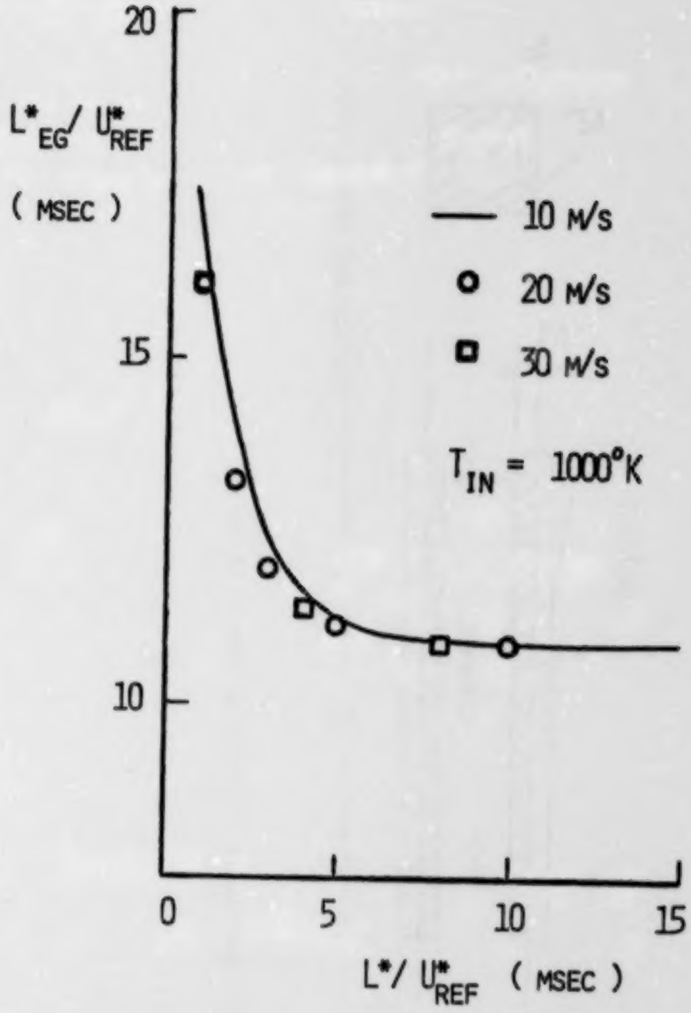

Figure 4. Effect of Computed Approaching Flow Velocities as Correlated by Residence times. Other Operating Conditions Are the Same as in Fig. 3

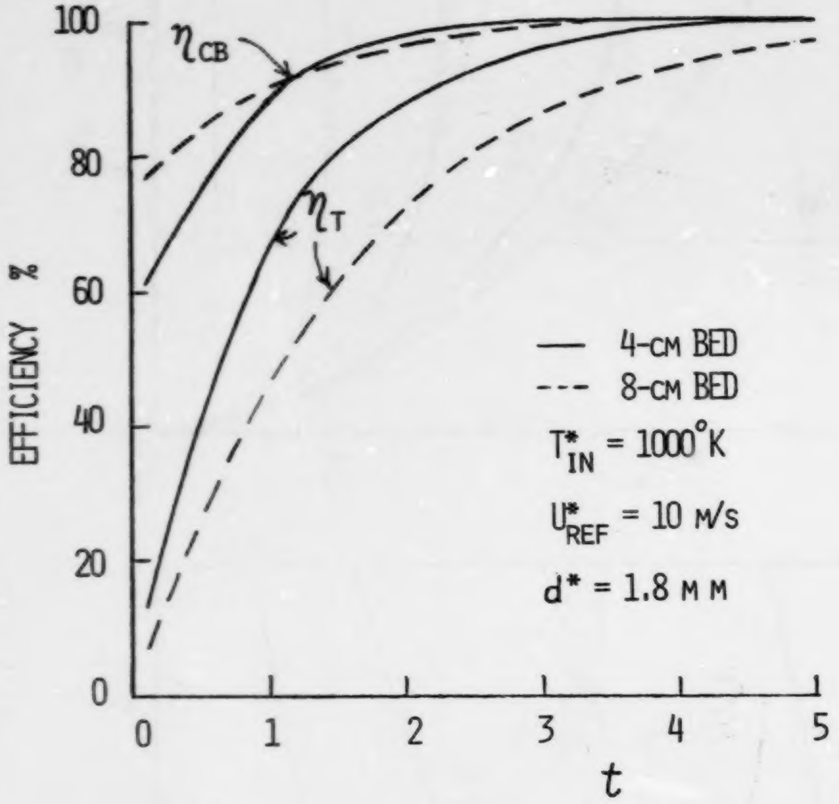

Figure 5. Combustion Efficiencies as a Function of Time during Ignition Transient. $p^* = 3$ atm, $\phi = 0.15$ and $A^*/A^*_s = 2$

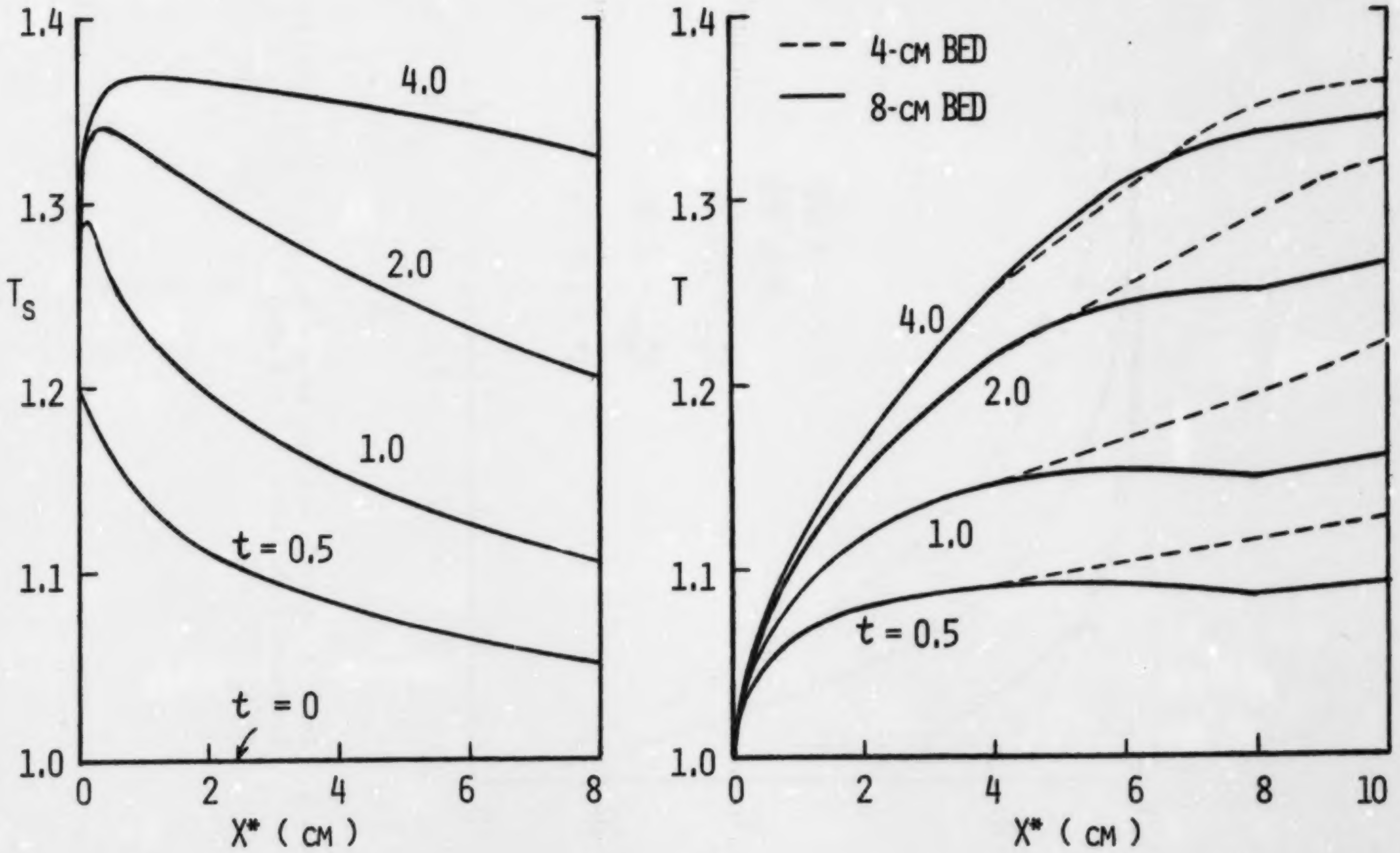

Figure 6. Gas and Substrate Temperature History during Transient Ignition for Two Bed Lengths. Same Operating and Design Parameters as Those in Fig. 5

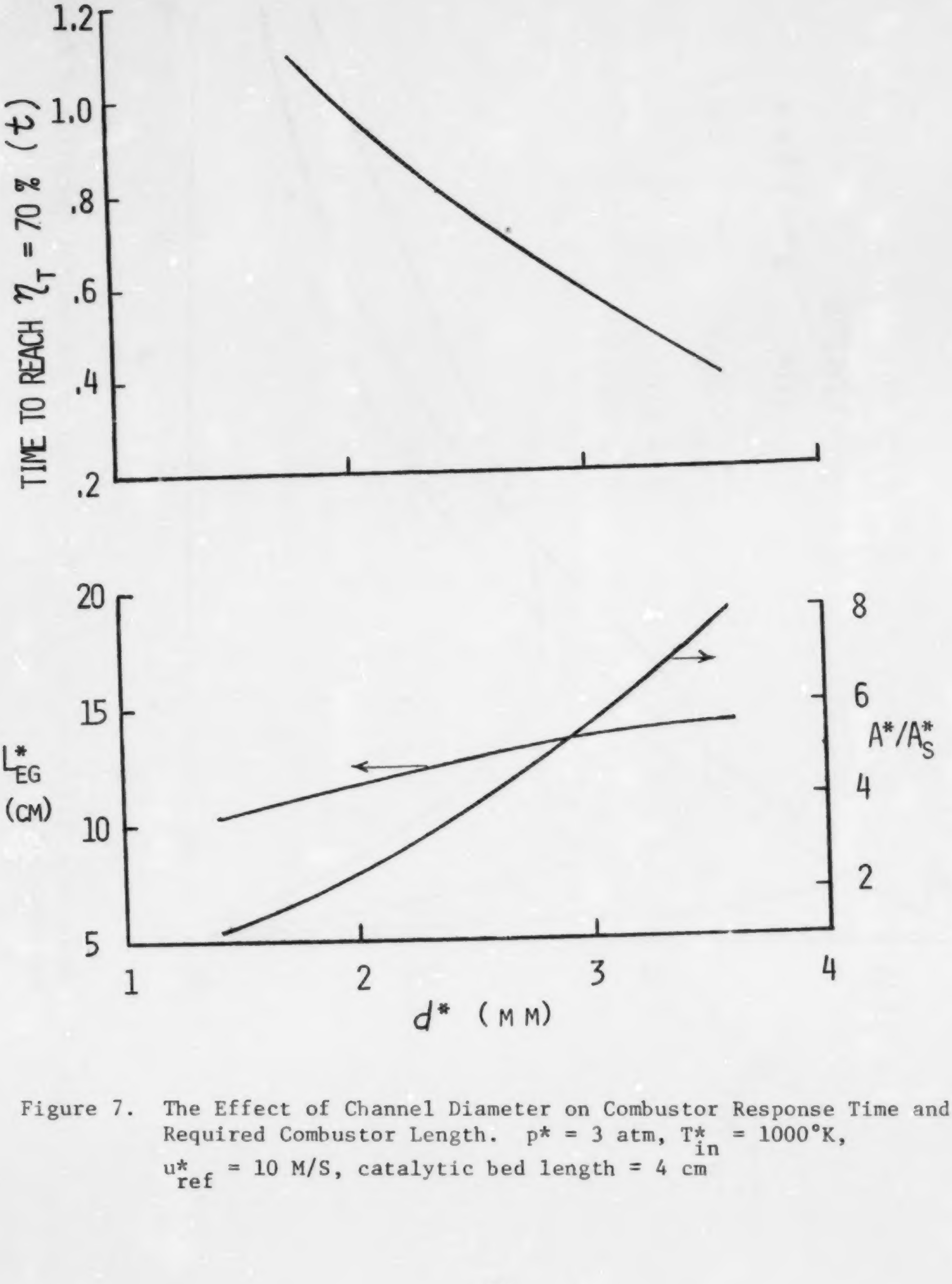

Figure 7. The Effect of Channel Diameter on Combustor Response Time and Required Combustor Length. $p^* = 3$ atm, $T^*_{in} = 1000$°K, $u^*_{ref} = 10$ M/S, catalytic bed length = 4 cm

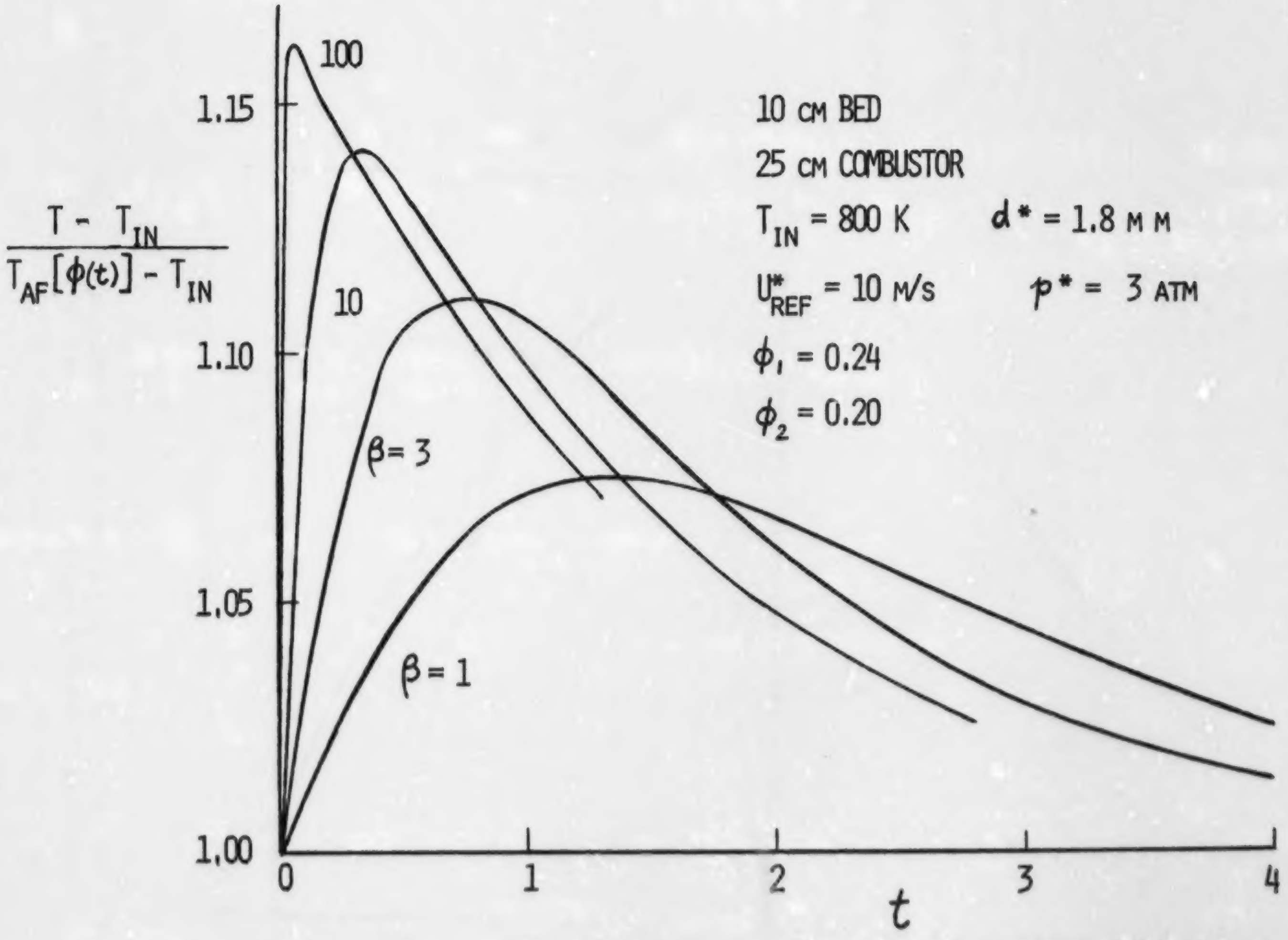

Figure 8. Temperature Difference Ratio vs. Time during an Exponential Reduction of Fuel/Air Equivalence Ratio

THE EFFECT OF CATALYST LENGTH AND DOWNSTREAM REACTION DISTANCE ON CATALYTIC COMBUSTOR PERFORMANCE

By:
David N. Anderson

NASA Lewis Research Center
Cleveland, Ohio 44135

ABSTRACT

A study was made to determine the effects on catalytic combustor performance which resulted from independently varying the length of a catalytic reactor and the length available for gas-phase reactions downstream of the catalyst. Monolithic combustion catalysts from three manufacturers were tested in a combustion test rig with no. 2 diesel fuel at an inlet-air temperature of 1000 K, a pressure of 3×10^5 Pa, reference velocities of 10 and 15 m/s, and adiabatic combustion temperatures of 1200 to 1500 K. Catalytic reactor lengths of 2.5 and 5.4 cm, and downstream gas-phase reaction distances of 7.3, 12.4, 17.5, and 22.5 cm were evaluated. Measurements of carbon monoxide, unburned hydrocarbons, nitrogen oxides, and pressure drop were made.

The catalytic-reactor pressure drop was less than 1 percent of the upstream total pressure for all test configurations and test conditions. Nitrogen oxides and unburned hydrocarbons emissions were less than 0.25 g NO_2/kg fuel and 0.6 g HC/kg fuel, respectively. The minimum operating temperature (defined as the adiabatic combustion temperature required to obtain carbon monoxide emissions below a reference level of 13.6 g CO/kg fuel) ranged from 1230 K to 1500 K for the various conditions and configurations tested. The minimum operating temperature decreased with increasing total (catalytic-reactor-plus-downstream-gas-phase-reaction-zone) residence time but was independent of the relative times spent in each region when the catalytic-reactor residence time was greater than or equal to 1.4 ms.

INTRODUCTION

The study reported here was performed to determine how the emissions and pressure drop of a catalytic combustor are affected by changes in the length of the catalytic reactor and in the length available for gas-phase reactions downstream of the catalytic reactor.

A catalytic combustor contains three major components: (1) the fuel-preparation region, in which fuel is injected and premixed with the inlet airstream; (2) the catalytic reactor, in which both surface and gas-phase combustion reactions are initiated; and (3) the downstream gas-phase reactor in which gas-phase reactions continue after initiation in the catalytic reactor. The importance of gas-phase reactions within the catalytic reactor has been discussed in several reports (ref. 1-6). The study of reference 7 also showed that these reactions can be significant downstream of the catalytic reactor. In that study the emissions levels were strongly dependent on the distance downstream from the catalytic reactor to the gas sampling probe. The observations were based on tests of a single length of catalytic reactor at an inlet-air temperature of 800 K. The present paper reports the effects of changing both the catalytic and the gas-phase reactor lengths at an inlet-air temperature of 1000 K.

The work presented here was performed as support for the Department of Energy's Gas Turbine Highway Vehicle Systems Project. Test conditions simulated the combustor conditions in a regenerative automotive gas turbine engine. The inlet-air temperature was 950 - 1000 K, inlet pressure, 3×10^5 Pa, reference velocity, 10 and 15 m/s, and the combustor exit temperature was varied from 1200 to 1500 K. Catalysts from three manufacturers were tested in a 12-cm-diameter test duct with catalytic-reactor lengths of 2.5 and 5.4 cm. The effect of gas-phase reactor length was determined by varying the axial location of an exhaust-gas sampling probe from 7.3 to 22.5 cm downstream of the catalyst exit plane. Emissions of CO, CO_2, UHC, and NO_x were measured as well as the catalytic-reactor pressure drop.

APPARATUS

TEST RIG

The test rig is illustrated in figure 1. It was fabricated from 15.2-cm (6-in nominal) diameter stainless-steel pipe. Carborundum T30R Fiberfrax tube insulation with a 12-cm inside diameter was inserted inside the pipe. The use of internal insulation served to maintain the inlet-air temperature near the preheater discharge value and to reduce the heat loss from the test section. Test-section metal temperatures were calculated to be less than 600 K.

The inlet air was indirectly preheated to approximately 1000 K for all tests. This temperature was measured in a plane just upstream of the fuel-injection location with an array of 12 Chromel-Alumel thermocouples mounted in a flange. The thermocouples were positioned in the duct so that each measured the temperature of an equal-area segment of the cross-section. The average inlet temperature was then calculated as the numerical average of these twelve thermocouples.

The test-section pressure was controlled by a back-pressure valve to 3×10^5 Pa for all tests. The test-section-inlet pressure was measured at a tap located in the flange containing the inlet thermocouples. The airflow rate entering the test section was measured by a standard ASME orifice. Fuel flow rate was determined with a Flo-tron linear mass flowmeter. This device employs 4 matched orifices arranged to form a hydraulic Wheatstone Bridge network. A constant-volume pump circulates flow through this network, and the mass flowrate is related to the pressure drop across the network.

FUEL INJECTOR AND PREMIXING ZONE

A multiple-conical-tube fuel injector of the type developed by Tacina (ref. 8, 9) was used; it is pictured in figure 2. Although it was designed with two sets of fuel tubes for use with either gaseous or liquid fuels, only liquid fuel (no.2 diesel) was used. The array of 21 conical tubes distributed the airflow uniformly over the duct cross section. No. 2 diesel fuel was introduced into the upstream end of each of these cones through a 0.5-mm-inside-diameter fuel tube. The 21 fuel tubes were all the same length (25 cm) to insure that equal fuel flow rates discharged into each of the air cones.

Because of the good initial dispersion of fuel across the duct, excellent fuel-air ratio uniformity is achieved with this type of injector. Tacina (ref. 8) has reported that 23 cm downstream of the fuel-injector inlet the fuel-air ratio profile was uniform to within ± 10 percent of the mean. The injector tested in reference 8 was designed with 75-percent blockage to the airstream while the injector used in the present study had 87-percent blockage; thus, the performance of the injector used here can be expected to be at least equal to that of reference 8. In the present experiments, the mixing distance from the point of fuel injection to the inlet plane of the catalytic reactor varied from 27.5 cm to 32.5 cm depending on which catalytic reactor was tested. Because the fuel-air ratio profile should already be nearly uniform for even the shortest of the mixing lengths, additional length will have little effect on the fuel-air distribution at the catalytic-reactor inlet and, therefore, little effect on combustion performance.

The pressure drop across the fuel injector was measured with a differential pressure transducer connected between the inlet-pressure tap and one located at the premixing-region thermocouple station.

A single Chromel-Alumel thermocouple was inserted to a depth of about 1 cm into the flow in the premixing zone downstream of the fuel injector. If burning had occurred in the premixing zone, this thermocouple would have triggered a relay to shut off the test-section fuel supply. No burning in the premixer was observed during these tests.

CATALYTIC REACTORS

Catalytic reactors were prepared using catalyst elements from 3 manufacturers: Matthey Bishop, Inc. (MBI), Oxy-Catalyst, Inc. (OCI), and UOP, Inc. (UOP). Reactors were either 2.5- or 5.4-cm long depending on whether one or two catalyst elements were used. Figure 1 was drawn with a two-element reactor in the test section. The two elements were each 2.5-cm long and were separated by a 0.31-cm gap. The 2.5-cm-long reactors were made by removing the upstream element from the two-element reactors.

The removal of an upstream element produced a slightly longer premixing-zone length. For the MBI and OCI reactor tests, premixing-zone lengths of 27.5 and 30.3 cm were used with two-element and one-element reactors, respectively. These lengths are shown in figure 1. Tests with the UOP catalysts were made with premixing-zone lengths of 32.5 and 35.3 cm for the two-element and one-element reactors, respectively.

Table I provides a description of the catalytic reactors tested. The MBI reactors used metal substrates. They were made by Matthey Bishop from Fecralloy foil which was corrugated and wound into a cylinder. The resulting cells had a sine-wave shape, a cell density of 62 per cm^2, and an open area of 93 percent of the duct cross-sectional area. The MBI-2.5 reactor was a single element of this substrate with a palladium catalyst. The MBI-5.4 reactor had a second, platinum-catalyst element placed in front of the palladium-catalyst element. Both elements were previously unused.

The two Oxy-Catalyst elements were identical: both used a palladium catalyst on a Corning cordierite square-cell substrate. The open area was 63 percent of the duct cross-sectional area and the cell density was 47 per cm^2. The OCI-2.5 reactor used one of these elements and the OCI-5.4 used two. These elements had also been unused before this testing.

The UOP elements also used the Corning cordierite square-cell substrate. Both elements were identical with a proprietary noble-metal catalyst. These elements had been furnace aged a total of 300 hours at a temperature of 1400 K prior to testing.

Single platinum-vs-platinum-13-percent-rhodium thermocouples measured the centerline gas temperature upstream of the reactor and in the gap between the elements. The catalytic reactors were held in place by an array of 12 platinum-vs-platinum-13-percent-rhodium thermocouples at the downstream plane.

The pressure drop across the catalytic reactor was measured with a differential pressure transducer connected between the premixing-zone pressure tap and one located 7.3 cm downstream of the catalytic reactor as shown in figure 1.

GAS-PHASE REACTOR

Downstream of the catalytic reactor the combustion products were sampled with a single-point water-cooled probe at the duct centerline. The length of the gas-phase reactor was determined by the axial position of the probe. Data were obtained with the probe at each of four locations: 7.3, 12.4, 17.5 and 22.5 cm downstream of the catalytic reactor. The probe is shown in the 22.5-cm location in figure 1.

The gas-sampling probe was constructed with a single 0.6-cm-inside-diameter sampling passage. The sample line was electrically heated to maintain a temperature of 410-450 K, and it was 18-m long and 0.5 cm in diameter. The continuous-flow samples were analyzed to determine the concentration of nitrogen oxides using a chemiluminescent analyzer, unburned hydrocarbons using a flame-ionization detector, and carbon monoxide and carbon dioxide using nondispersive infrared analyzers.

Temperatures were measured in the gas-phase reactor with platinum-vs-platinum-13-percent-rhodium thermoccuples in each of the 4 gas-sampling planes.

COMPUTATIONS

REFERENCE VELOCITY

The reference velocity was computed from the measured mass flow rate, the average inlet-air temperature, the duct cross-sectional area ($113\ \mathrm{cm}^2$) and the test-section-inlet pressure (3×10^5 Pa).

EMISSION INDEX

The emissions were measured as concentrations in ppm by volume which were converted to emission indexes using the expression

$$(E.I.)_x = C_x \times 10^{-3} \left(\frac{1 + f}{f}\right) \left(\frac{M_x}{M_p}\right)$$

where

$(E.I.)_x$	emission index of specie x, g_x/kg_{fuel}
C_x	concentration of specie x, ppm V
f	fuel-air weight ratio, $(kg/s)_{fuel}/(kg/s)_{air}$
M_x	molecular weight of specie x, $g_x/mole_x$
M_p	molecular weight of combustion products, $g_{products}/mole_{products}$

COMBUSTION EFFICIENCY

The difference between the measured and equilibrium emissions of carbon monoxide and unburned hydrocarbons represents available chemical energy which has not been released in the combustion process. For the conditions of this study, the equilibrium emission indexes of unburned hydrocarbons and carbon monoxide are negligible. Futhermore, measured unburned hydrocarbons emissions resulted in emission indexes less than 0.6 g HC/kg fuel and, therefore, contributed little to inefficiency. Combustion efficiency was consequently determined from the carbon monoxide emissions alone:

$$EFF = 100 - 0.1 \left(\frac{(HV)_{CO}}{(HV)_{fuel}}\right)(E.I.)_{CO}$$

$$= 100 - 0.0235\ (E.I.)_{CO}$$

where

EFF	combustion efficiency, percent
$(HV)_{CO}$	lower heating value of CO, 1.01×10^7 J/kg
$(HV)_{fuel}$	lower heating value of no. 2 diesel, 4.30×10^7 J/kg

FUEL-AIR RATIO

The fuel-air ratio was determined both from the metered fuel flow and airflow rates and by making a carbon balance from the measured concentrations of CO, CO_2, and unburned hydrocarbons. The carbon-balance fuel-air ratio had the advantage that it was the local fuel-air ratio at which the emissions data were obtained.

ADIABATIC COMBUSTION TEMPERATURE

The adiabatic combustion temperature was calculated from the carbon-balance fuel-air ratio using the equilibrium computer program of reference 10.

RESULTS AND DISCUSSION

The carbon-balance fuel-air ratios were typically about 95 percent of those determined from the metered fuel flow and airflow rates. This difference probably results from the use of a single gas-sampling probe at the duct centerline, and it indicates that fuel-air premixing, although good, did not result in a perfectly uniform fuel-air ratio over the entire cross section. It also indicates that plug flow continued downstream of the catalytic reactor so that there was little mixing across the duct. Thus, the emissions measured by the probe were determined by local, rather than average, conditions. The local adiabatic combustion temperature is that calculated from the carbon-balance fuel-air ratio, and it will be used in the presentation of results.

No measurable temperature rise along the length of the gas-phase reactor occurred, and the uncorrected catalytic-reactor exit temperatures measured at the centerline were typically only about 25 K less than the adiabatic combustion temperatures. The performance of the various lengths of catalytic and gas-phase reactors will be compared on the basis of the measured emissions and pressure drop.

EMISSIONS

Allowable emissions from passenger cars have been established by the 1970 Clean-Air Act Ammendments which specifies ultimate emissions standards of 0.25 g NO_x/km, 2.1 g CO/km, and 0.25 g HC/km. Emissions levels are determined by collecting an exhaust sample during a standard metropolitan driving cycle which simulates various transient operating conditions and includes few periods of steady-speed motoring. Thus, there is no simple relationship between the automotive emissions standards and the emissions measured during steady-state tests, such as the ones performed in this study. However, the emissions standards can be transformed into steady-state reference emission indexes by multiplying the standards (in g/km) by an average cycle fuel economy (in km/kg). For this study it was assumed that (1) a gas-turbine powered vehicle could achieve a fuel economy of 9.35×10^3 km/m^3 (22 miles/gallon), (2) no. 2 diesel fuel density was 720 kg/m^3, and (3) the reference values should be based on only half the emissions permitted by the standards. The third assumption provides some margin for unknown transient and durability effects. The reference emission indexes were thus calculated to be 1.6 g NO_2/kg fuel, 13.6 g CO/kg fuel, and 1.6 g HC/kg fuel. The CO reference value represents about 0.32-percent loss in combustion efficiency, and the HC level would result in an additional 0.16-percent loss. The NO_x emissions in this study were never more than 0.25 g NO_x/kg fuel, and unburned hydrocarbons were below 0.6 g HC/kg fuel. Therefore, only the carbon monoxide emissions will be examined in detail.

The carbon monoxide emission indexes for each of the six catalytic reactors are plotted in figure 3(a) - (f) as a function of the adiabatic combustion temperature. The results for the four different gas-phase reaction distances are given in each figure for reference velocities of 10 m/s (solid curves) and 15 m/s (dashed curves). The combustion efficiency which corresponds with each CO emission index is shown as a second ordinate.

Results for the MBI-2.5 reactor are given in figure 3(a). Carbon monoxide levels decreased nearly two orders of magnitude when the adiabatic combustion temperature was increased by 150 - 200 K for all conditions. For both 10- and 15-m/s reference velocities, an increase in the gas-phase-reactor length from 7.3 to 22.5 cm also produced approximately a two-orders-of-magnitude reduction in CO at a fixed adiabatic combustion temperature. Emissions were below the 13.6-g-CO/kg-fuel reference for adiabatic combustion temperatures greater than 1265 K for the 22.5-cm-long gas-phase reactor at a reference velocity of 10 m/s. When the velocity was increased to 15 m/s, the same 22.5-cm-long gas-phase reactor required temperatures of at least 1340 K to achieve the reference level. For the 7.3-cm-long gas-phase reactor at 15 m/s, a temperature of nearly 1500 K was required.

When the catalytic-reactor length was increased to 5.4 cm, the CO emissions, shown in figure 3(b), were lower than those of the 2.5-cm-long catalytic reactor at any given condition. For a 7.3-cm-long gas-phase reactor and a reference velocity of 15 m/s, the adiabatic combustion temperature required to achieve the reference CO level was reduced from nearly 1500 K for the MBI-2.5 catalytic reactor (fig. 3(a)) to 1400 K for the MBI-5.4 reactor (fig. 3(b)). For the same 7.3-cm gas-phase reactor length at 10 m/s the

MBI-2.5 reactor (fig. 3(a)) required an adiabatic combustion temperature of 1365 K to reach the reference level of CO emissions, while the MBI-5.4 reactor (fig. 3(b)) required only 1345 K.

The same general trends were observed for the OCI-2.5 and OCI-5.4 catalytic reactors as shown in figure 3(c) and 3(d), respectively, and for the UOP-2.5 and UOP-5.4 catalytic reactors as shown in figure 3(e) and 3 (f).

MINIMUM OPERATING TEMPERATURE

The minimum operating temperaure is defined as the adiabatic combustion temperature at which all the emissions goals are met. As noted previously, in this study the minimum operating temperature could be determined solely from the CO emissions since unburned hydrocarbons were always well below the reference level. The minimum operating temperature was determined for all of the test configurations by noting the adiabatic combustion temperature at which each of the CO curves of figure 3 crossed the reference emission index level.

The effect of the total catalytic-plus-gas-phase-reactor length on the minimum operating temperature for all six catalytic reactors can be seen in figure 4. The open symbols and solid lines represent the minimum operating temperatures of the 2.5-cm-long catalytic reactors, while the solid symbols and dashed lines are for the 5.4-cm-long catalytic reactors. Results are given at reference velocities of 10 m/s and 15 m/s for each catalytic-reactor length.

From figure 4 it can be seen that within the experimental accuracy there was no difference between the results for the MBI, OCI, and UOP reactors of the same length. The fact that the UOP reactors, after having been aged for 300 hours at 1400 K, performed as well as the unaged catalytsts suggests a potential for a long lifetime. The duration of these tests (typically 5-6 hours per reactor) was insufficient to determine if the MBI and OCI catalysts would also be durable for long periods.

Figure 4 also shows that for each reference velocity and catalytic-reactor length, an increase in the total catalytic-plus-gas-phase-reactor length resulted in a lower value for the minimum operating temperature. For example, for single-element reactors tested at a reference velocity of 10 m/s (solid curve with open circles), an increase in total length from 10 cm to 13 cm reduced the minimum operating temperature from 1375 K to 1335 K. Similar reductions were also observed with the 5.4-cm-long catalytic reactors (dashed line, solid symbols) and at 15 m/s reference velocity (square symbols).

The reduction of 40 K in minimum operating temperature in the above example was achieved by increasing the gas-phase-reactor length with a constant catalytic-reactor length. If the total length had been increased from 10 cm to 13 cm by increasing the catalytic-reactor length from 2.5 cm to 5.4 cm with a constant gas-phase-reactor length, the minimum operating temperature for a reference velocity of 10 m/s would have decreased by 50 K (from 1375 K to 1325 K). Thus, the catalytic-length effect was slightly greater than the gas-phase-length effect at a velocity of 10 m/s.

At a reference velocity of 15 m/s the catalytic-length effect on minimum operating temperature was much greater than the gas-phase-length effect. The increase in total length from 10 cm to 13 cm which was achieved by increasing the gas-phase-reactor length while maintaining catalytic-reactor length constant at 2.5 cm can be seen from figure 4 (solid curve, open squares) to have reduced the minimum operating temperature by 50 K (from 1490 K to 1440 K). When the same increase in total length was obtained by increasing the catalytic-reactor length from 2.5 cm to 5.4 cm while maintaining a constant gas-phase-reactor length, the minimum operating temperature was decreased by 100 K (from 1490 K to 1390 K). At a velocity of 15 m/s, then, there was a clear advantage, in terms of minimum operating temperature, to the use of a longer catalytic reactor as opposed to the use of a longer gas-phase reactor.

Because residence time is a fundamental variable which includes both length and velocity, it is of interest to analyze these results again on the basis of changes in residence time. The minimum operating temperatures have been plotted again in figure 5 to show the effect of the total combustion residence time. The residence time was calculated from the total catalytic-plus-gas-phase-reactor length by assuming that (1) the combustion temperature increased linearly within the catalytic reactor so that the adiabatic combustion temperature was reached at the exit of the first element for either one- or two-element reactors, (2) the gas temperature throughout the rest of the system was constant and equal to the adiabatic combustion temperature, (3) the pressure was constant, and (4) the open area of the catalytic-reactor channels was 93 percent of the duct cross-sectional area for the MBI reactors and 63 percent for OCI and UOP reactors. The residence times of the flow through the various catalytic reactors at each of the two reference velocities have also been indicated in figure 5 to assist in determining the effects of catalytic-reactor residence time. The accuracy of the calculated residence times was dependent on experimental measuring error as well as the validity of these assumptions, and the values shown in figure 5 were estimated to be accurate to within ± 5 percent.

Figure 5 shows that the minimum operating temperature could be decreased by providing more total combustion residence time. In addition to this general trend, the results were segregated according to the catalytic-reactor residence time into two curves. Catalytic-reactor residence times ranged from 0.9 ms to 4.1 ms for this experiment. The configurations which had the lowest catalyst residence times (0.9 to 1.3 ms) also had the highest minimum operating temperatures. When the catalytic-reactor residence time was greater than 1.4 ms, minimum operating temperatures were about 50 K lower than those for catalytst residence times of 0.9 to 1.3 ms. However, no further decrease in minimum operating temperature was obtained when catalytic-reactor residence times were increased to values as high as 4.1 ms at a constant total combustion residence time. Thus, for these experimental conditions, gas-phase residence time was as effective as catalytic residence time in determining minimum operating temperature if the catalytic-reactor residence time was at least 1.4 ms. By this time, apparently, gas-phase reactions were sufficiently established within the catalytic reactor channels that additional catalyst was unnecessary.

PRESSURE DROP

In addition to low-emissions capability, it is necessary for gas-turbine combustors to operate with minimal pressure loss. The pressure-drop measurements made in the present study do not necessarily provide values which would be the same as those of a practical catalytic combustor; however, they do indicate what contribution can be expected from the catalytic components. The pressure drop as a percentage of the total upstream pressure is shown as a function of the adiabatic combustion temperature for the MBI reactors in figure 6(a), for the OCI reactors in figure 6(b), and for the UOP reactors in figure 6(c).

The measured pressure loss increased gradually with increasing adiabatic combustion temperature. The two-element MBI and OCI reactors had pressure losses which varied from 0.7 to 0.95 percent at 15-m/s reference velocity and 0.3 to 0.6 percent at 10 m/s. The UOP reactor produced lower values. The losses measured across one-element reactors were typically about half the values for two-element reactors. The flow in the catalyst channels was laminar for all conditions studied and the measured effect of velocity on pressure drop was consistent with a laminar-flow friction-loss mechanism dominating over entry and exit losses. The pressure drop in the gas-phase reactor was calculated to be less than 2×10^{-3} percent for the test conditions of this study.

The pressure drop across the multiple-conical-tube fuel injector was typically about 1 percent at a reference velocity of 10 m/s and 2 percent at 15 m/s. These losses are higher than would be acceptable for many practical applications; however, the fuel-injector blockage (87 percent) was greater than was necessary. Tacina (ref. 8) achieved an excellent fuel-air ratio profile from another injector of the same type which was designed with less blockage (75 percent). He reported pressure losses to be only 0.25 percent at a velocity of 10 m/s and 1 percent at 20 m/s.

For a low-blockage multiple-conical-tube fuel injector and a two-element catalytic reactor, the combined pressure drop can be predicted to be about 0.75 percent at a reference velocity of 10 m/s and about 2 percent at 20 m/s. Even at the higher velocity, this loss is acceptable for practial combustor applications.

CONCLUDING REMARKS

This study demonstrated that a 2.5-cm length of catalytic reactor followed by a 7.3-cm length of gas-phase reaction distance is adequate to achieve acceptable emissions at the following conditions: an inlet-air temperature of 1000 K, a pressure of 3×10^5 Pa, a reference velocity of 10 m/s, and an adiabatic combustion temperature of 1400 K. Acceptable emissions could also be obtained at adiabatic combustion temperatures lower than this by increasing either the catalytic-reactor length or the gas-phase reaction distance downstream of the catalytic reactor. In other words, the minimum operating temperature (defined as the lowest adiabatic combustion temperature at which the emissions are within acceptable levels) decreased with increasing total combustion (catalytic-plus-gas-phase-reactor) residence time.

The relative time spent by the combustion gases in the catalytic and in the gas-phase reactors was shown to affect the minimum operating temperature only if the catalytic-reactor residence time was less than 1.4 ms. For catalyst residence times greater than 1.4 ms, apparently, gas-phase reactions were well established within the catalytic-reactor channels, and there was no further contribution of surface reactions. Thus, a catalytic combustor designed to operate at the conditions of this study would need to incorporate no more catalytic-reactor length than was necessary to provide a 1.4-ms catalyst residence time. Advanced automotive gas turbine engines may have combustor inlet temperatures as high as 1340 K. For these inlet-air temperatures, even less catalytic-reactor residence time may be required, and therefore, it may be possible to increase reference velocities or reduce catalytic-reactor length without penalizing emissions performance. Alternatively, lower catalyst loadings or substrate cell densities below the 47-62 cells/cm^2 used in this study may be possible. Furthe evaluation is required to establish the effect of higher inlet-air temperatures on the required catalytic-reactor residence time.

The data reported were obtained at only one pressure, 3×10^5 Pa. While this value is representative of part of the automotive-gas-turbine range (1.5×10^5 to 5×10^5 Pa), data are also needed at higher and lower pressures before general conclusions can be drawn about required lengths of catalytic reactors, catalyst loadings, or substrate geometries.

Operation of catalysts at high temperaures for extended periods of time will, of course, result in a loss of catalyst activity. Although one catalyst included in these tests had received a 300-hour furnace aging at 1400 K and showed no disadvantage relative to unaged catalysts, longer combustion aging at higher temperatures will be experienced by catalysts used in catalytic combustors. The subsequent loss of catalyst activity, the changes it will produce in the performance of the catalytic reactor, and its effect on the conclusions of this study cannot be predicted. As catalyst development continues to produce catalysts capable of higher and higher maximum operating temperatures, it is possible that little effect of aging would be seen during the typical lifetime of an automobile. On the other hand, it may be necessary to overdesign the catalytic reactor by making it longer than the initial catalytic activity would necessitate.

Additional work is clearly required to complete the process of establishing design information for automotive gas-turbine catalytic combustors.

REFERENCES

1. Pfefferle, W. C., R. V. Carrubba, R. M. Heck, and G. W. Roberts. Catathermal Combustion: A New Process for Low-Emissions Fuel Conversion. ASME Paper 75-WA/Fu-1, 1975. 13 pp.

2. Wampler, F. B., D. W. Clark and F. A. Gaines. Catalytic Combustion of C_3H_8 on Pt Coated Monolith. Combustion Science and Technology, 14:25-31, 1976.

3. Cerkanowicz, A. E., R. B. Cole and J. G. Stevens. Catalytic Combustion Modeling; Comparisons with Experimental Data. ASME Paper 77-GT-85, 1977. 8 pp.

4. DeCorso, S. M., S. Mumford, R. Carrubba, and R. Heck. Catalysts for Gas Turbine Combustors - Experimental Test Results. J. of Engineering for Power, 99 (2): 159-167, 1977.

5. Pfefierle, W. C. The Catalytic Combustor: An Approach to Cleaner Combustion. J. Energy, 2(3): 142 - 146, 1978.

6. Ablow, C. S., S. Schechter, H. Wise, and B. J. Wood. Contribution of Surface Catalysis and Gas Phase Reaction to Catalytic Combustor Performance. SRI International Corp., Menlo Park, California, 1979. 81 pp. Also AFOSR-79-1146TR, Air Force Office of Scientific Research, AD-A078465.

7. T'ien, J. S. and D. N. Anderson. Gas Phase Oxidation Downstream of a Catalytic Combustor. Paper presented at the American Chemical Society Thirteenth Middle Atlantic Regional Meeting, West Long Branch, New Jersey, March 20-23, 1979.

8. Tacina, R. R. Experimental Evaluation of Fuel Preparation Systems for an Automotive Gas Turbine Catalytic Combustor. NASA TM-78856, 1977. 22 pp.

9. Tacina, R. R. Degree of Vaporization Using an Air-Blast Type Injector for a Premixed - Prevaporized Combustor. NASA TM-78836, 1978. 12 pp.

10. Gordon, S. and B. J. McBride. Computer Program for Calculation of Complex Chemical Equilibrium Compositions, Rocket Performance, Incident and Reflected Shocks, and Chapman-Jouguet Detonations. NASA SP-273, Rev. 1976. 145 pp.

TABLE I . DESCRIPTION OF CATALYTIC REACTORS

Reactor	No. of Elements	Reactor Length, cm	Upstream Element Catalyst Material	Upstream Element Catalyst Loading, kg/m^3	Upstream Element Substrate (see Table Ia)	Downstream Element Catalyst Material	Downstream Element Catalyst Loading, kg/m^3	Downstream Element Substrate (see below)	Manufacturer
MBI-2.5	1	2.5	-	-	-	Palladium	7.1	1	Matthey Bishop
MBI-5.4	2	5.4	Platinum	5.3	1	Palladium	7.1	1	Matthey Bishop
OCI-2.5	1	2.5	-	-	-	Palladium	3.6	2	Oxy-Catalyst
OCI-5.4	2	5.4	Palladium	3.6	2	Palladium	3.6	2	Oxy-Catalyst
UOP-2.5	1	2.5	-	-	-	Noble Metal	*	2	UOP
UOP-5.4	2	5.4	Noble Metal	*	2	Noble Metal	*	2	UOP

The MBI and OCI reactors were unaged.
The UOP elements had been exposed to 1400K air in a furnace for 300 hours.
* Proprietary

TABLE Ia. SUBSTRATE DESCRIPTION

Substrate	Manufacturer	Material	Cell Shape	Cell Density, cells/cm^2	Open Area, percent
1	Matthey Bishop	Fecralloy	Sine wave	62	93
2	Corning	cordierite	square	47	63

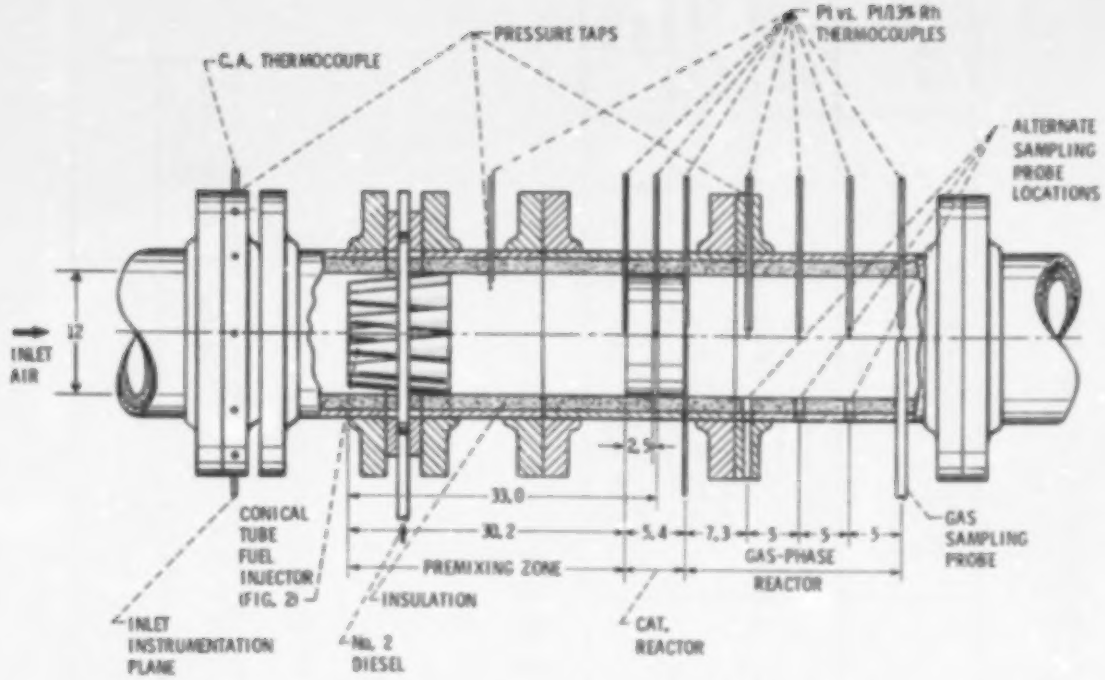
Pt vs. Pt/13% Rh THERMOCOUPLES
PRESSURE TAPS
C.A. THERMOCOUPLE
ALTERNATE SAMPLING PROBE LOCATIONS
INLET AIR
12
2.5
33.0
30.2
5.4
7.3
5
5
5
GAS SAMPLING PROBE
CONICAL TUBE FUEL INJECTOR (FIG. 2)
PREMIXING ZONE
GAS-PHASE REACTOR
INSULATION
INLET INSTRUMENTATION PLANE
No. 2 DIESEL
CAT. REACTOR

Figure 1. - Test section. (Dimensions in cm.) 5.4-cm-long catalytic reactor shown.

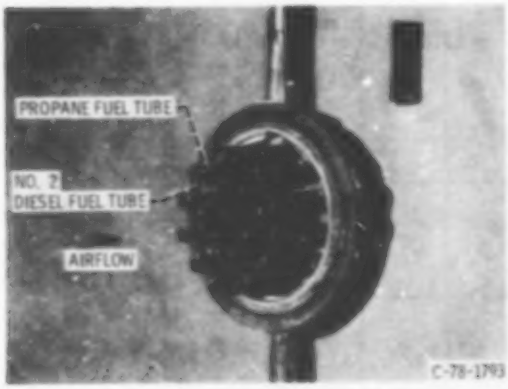
PROPANE FUEL TUBE
NO. 2 DIESEL FUEL TUBE
AIRFLOW
C-78-1793

Figure 2. - Multiple conical tube fuel injector.

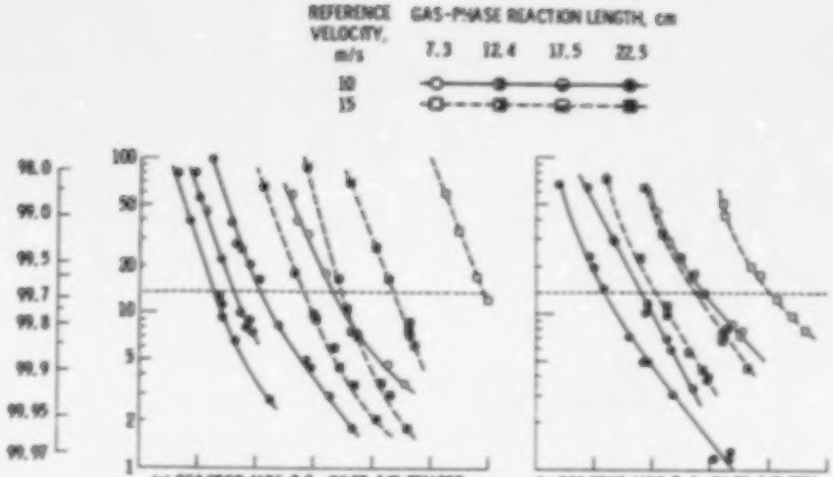

(a) REACTOR MBI-2.5; INLET-AIR TEMPERATURE, 1000 K.

(b) REACTOR MBI-5.4; INLET-AIR TEMPERATURE, 1000 K.

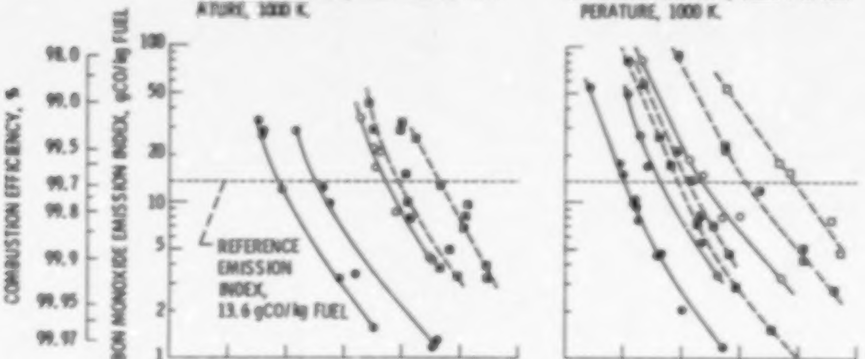

(c) REACTOR OCI-2.5; INLET-AIR TEMPERATURE, 1000 K.

(d) REACTOR OCI-5.4; INLET-AIR TEMPERATURE, 1000 K.

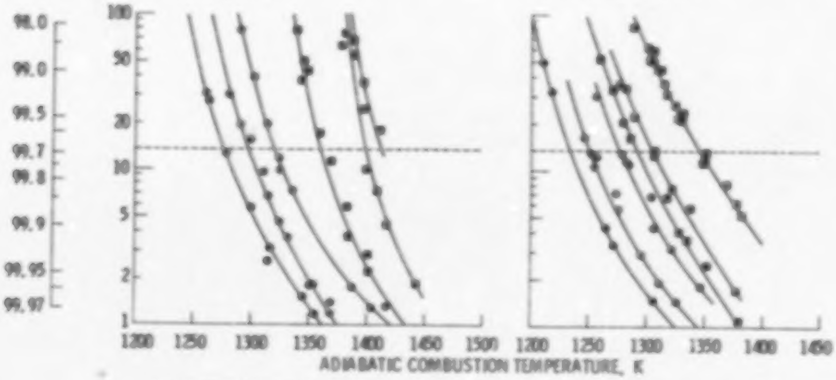

(e) REACTOR UOP-2.5; INLET-AIR TEMPERATURE, 950 K.

(f) REACTOR UOP-5.4; INLET-AIR TEMPERATURE, 950 K.

Figure 3. - Carbon monoxide emissions. Pressure, 3×10^5 Pa.

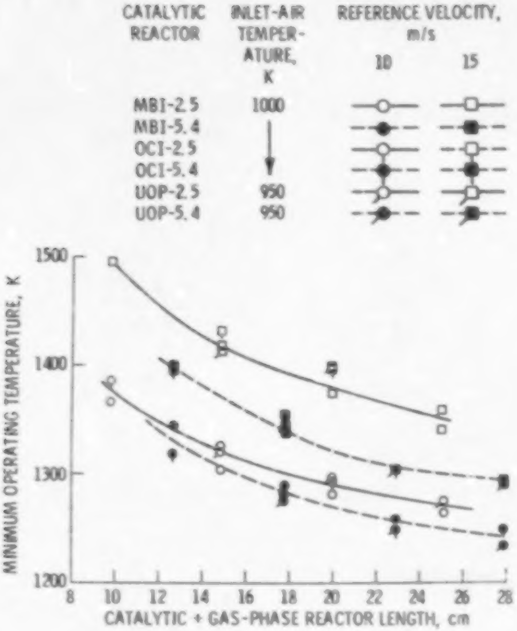

Figure 4. - Effect of combustion length on minimum operating temperature. Pressure, 3×10^5 Pa.

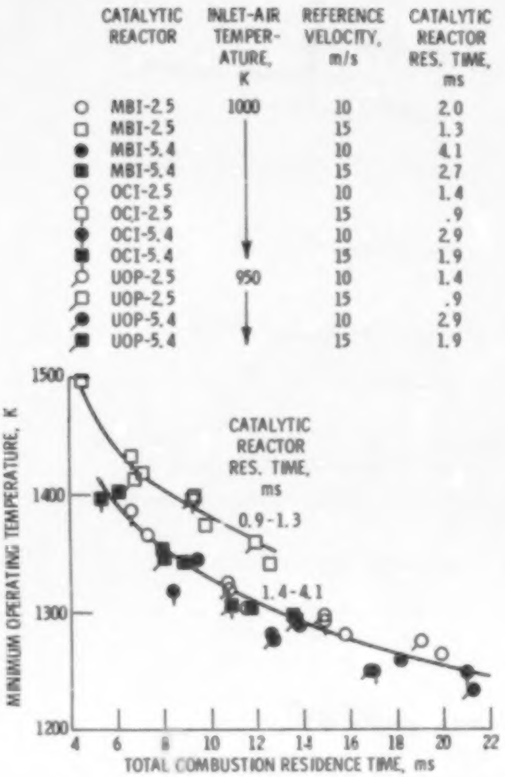

Figure 5. - Effect of residence time on minimum operating temperature. Pressure, $3x10^5$ Pa.

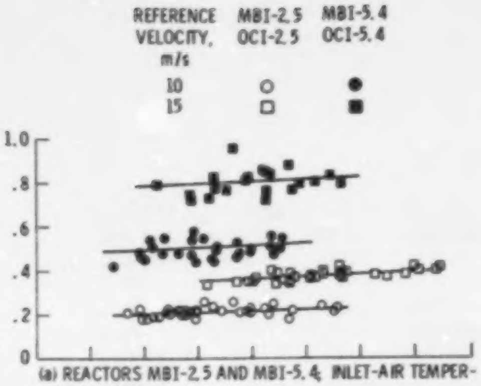

(a) REACTORS MBI-2.5 AND MBI-5.4; INLET-AIR TEMPERATURE, 1000 K.

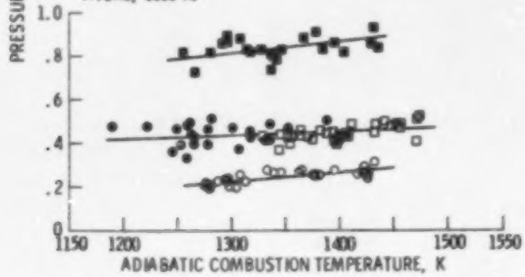

(b) REACTORS OCI-2.5 AND OCI-5.4; INLET-AIR TEMPERATURE, 1000 K.

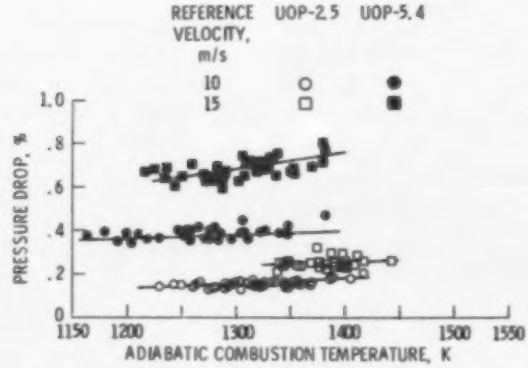

(c) REACTORS UOP-2.5 AND UOP-5.4; INLET-AIR TEMPERATURE, 950 K.

Figure 6. - Catalytic reactor pressure drop. Pressure, $3x10^5$ Pa.

CATCOM* CATALYST 5 ATM 1000 HOUR AGING STUDY

USING #2 FUEL OIL†

By:
I. T. Osgerby
B. A. Olson
H. C. Lee

Engelhard Industries Division
Engelhard Minerals and Chemicals Corporation
Menlo Park, Edison, New Jersey 08817

† Program supported by NASA-Lewis
under Contract NAS 3-19416
R. Priem, Contract Manager

ABSTRACT

Previous publications have described the combustion process designated catalytically supported thermal combustion, which combines the features of catalytic combustion with those of thermal or homogeneous combustion. The process, characterized by extremely low pollutant emissions, in particular NO_x emissions, has been demonstrated over a wide range of operating conditions of pressure, temperature, reference velocity and fuel types of interest to commercial applications ranging from process heat generation to gas turbines.

The durability of a proprietary Engelhard combustor catalyst has been recently demonstrated, under a NASA contract, at five atmosphere pressure, complementing a previous 1000 hour durability study at one atmosphere. Both of these studies were conducted at about 640°K air preheat temperature at a reference velocity of about 14 m/sec^{-1}. The adiabatic flame temperature of the fuel/air mixture was about 1530°K. Performance of the catalyst was determined by monitoring emissions, thermocouple temperatures and catalyst pressure losses, and by examining the physical condition of the catalyst core at the conclusion of the test. Parametric studies were carried out at the beginning and end of the durability test and periodic CO activity tests were carried out to monitor catalytic performance.

The catalyst proved to be capable of low emissions operations after 1000 hours diesel fuel aging, however, more severe deactivation occurred in the five atmosphere test. This was attributed to a loss in kinetic (ignition) activity. Reasons for this loss in kinetic activity are suggested and discussed in terms of observed performance relative to one atmosphere test performance.

---

* CATCOM is a trade name of Engelhard Minerals and Chemicals Corporation.

INTRODUCTION

The development of the process by which fuel and air is combusted in a catalyzed monolith to yield ultra low emissions of carbon monoxide (CO), unburned hydrocarbons (UHC) and nitrogen oxides (NO_x) via catalytically supported thermal combustion was pioneered by Engelhard Industries (References 1 through 7). Many short duration tests (1-50 hours) have been carried out using a variety of gaseous (References 9, 10, 12, 13, 15, 17, 18-23, 25-30, 33, 34) and liquid fuels (References 8-11, 13, 15-20, 24, 28, 31, 32, 35, 36, 38) both in Engelhard's R&D laboratories (References 9, 12, 23, 29-36) and prototype systems (References 23, 29, 35, 36) and government (References 8, 10, 11, 15-20, 28) University and industrial (References 13, 24-27, 38) laboratories. The proven feasibility of the process has been enhanced by investigations either carried out or supported by NASA (References 8, 10, 11, 15-20, 28) the Electric Power Research Institute (References 31, 32, 27, 40) and EPA (References 41-43). These test have demonstrated the unique capabilities provided by combustion catalysts (CATCOM*) in providing high efficiency low pressure loss combustion with low emissions of CO, UHC and NO_x, otherwise not generally attainable (Reference 11).

An outstanding requirement for these combustion catalysts is, of course, long term durability. Durability is essential for the CATCOM* catalyst to have commercial value since long periods are desired between maintenance shutdowns of process equipment and ready acceptance of this new technology by certain industries is not yet apparent.

---

*CATCOM is a tradename of Engelhard Minerals and Chemicals Corp.

Engelhard Industries, a division of Engelhard Minerals & Chemicals Corporation, has pioneered the development of durable CATCOM* catalysts. Early investigations (1970-1975) were internally funded, resulting in proven durability of >1000 hours at design operating conditions on propane and #2 distillate fuels on the first generation catalyst: DXA-111. Deficiencies in off-design performance (increased reference velocities (>15 m sec^{-1}), decreased adiabatic flame temperatures (< 2300°F), led to the development of more stable catalyst systems.

In support of the E.R.D.A. highway vehicle gas turbine engine development program, a test program was initiated with Engelhard Industries, to demonstrate the durability of selected CATCOM* catalysts and catalyst supports and to demonstrate the practicality of catalytically supported thermal combustion. The program, funded by E.R.D.A. and managed by NASA-Lewis, was conducted under NASA contract NAS3-19416. Two CATCOM* catalysts (DXB-222 and DXC-532) were successfully tested for over 1000 hours on #2 distillate fuel at one atmosphere as reported in References 21 and 22.

Further refinements were incorporated into new CATCOM* catalysts resulting in a more reproducible system designated DXE-412. This catalyst was proven to have equal or better performance to DXB-222 at one atmosphere and was selected as the catalyst to be tested at five atmospheres in a continuation of NASA contract NAS3-19416. The highlights of the results of this contract investigation are presented in this paper.

---

*CATCOM is a tradename of Engelhard Minerals and Chemicals Corp.

EXPERIMENTAL PROCEDURES AND TEST PROGRAM

The testing program selected in this study was structured to serve the following purposes:

1. Test the long-term durability of catalysts under realistic combustion conditions.

2. Determine an acceptable low emissions operating range for the catalysts.

In addressing these requirements, a test sequence was set up, which focused mainly on the maintenance of low emissions during a 1000 hour life test with #2 diesel. This life test provided a means of measuring either abrupt or long-range changes in a catalyst core's overall performance. To measure more subtle changes in the activity of the catalyst core, periodic activity tests were conducted at 250 hour intervals using carbon monoxide as a fuel.

The acceptable low emissions operating range for a CATCOM* catalyst was determined using #2 diesel over a range of selcted variables. The catalyst core designated as DXE-442 (Table I) was tested in this experimental program. The catalyst was prepared on a monolith support.

The specifics of the overall testing sequence can be represented schematically as follows:

---

*CATCOM is a tradename of Engelhard Minerals and Chemicals Corp.

Virgin Catalyst

24 hour break-in period

Initial CO activity test

Initial set of parametrics to
map performance range

CO Activity Test

1000 hour life test with #2 diesel fuel
and CO activity test every 250 hours

Final set of parametrics to map
performance range changes

The initial 24 hour break-in period (see Table II for conditions) of each catalyst core was required to remove the initially high activity and stabilize the catalyst's activity level. This prevents potential problems with interpretation of experimental results due to an artificially high initial activity.

1. Life Test with #2 Diesel

The main purpose of this study was to evaluate the effect of pressure on the durability of a catalyst core at combustion conditions for extended periods of steady-state operation. The life test conditions were otherwise identical to the steady-state operating conditions of the previous one atmosphere test. The test fuel was #2 diesel. This fuel contains additives and impurities that provide a sound test for determining the effects of potential poisons on the catalyst core. Table III contains the analyses of the fuel used in the life test.

The steady-state conditions for the 1000 hour life test are shown in Table II. These life tests were conducted on a continuous basis when possible. During shutdown, a house air purge was maintained over the test catalyst cores.

The maintenance of low emissions performance during the life test is considered the prime criteria for determining changes in a specific catalyst core's performance. This life test also provides a measure of the physical durability of the catalyst core support material. The results of this test provide information on long term durability of CATCOM* catalyst cores.

2. Carbon Monoxide Activity Test

In conducting the CO activity test, the life test conditions are discontinued and the CO activity test conditions are then established. The catalyst core is not disturbed and remains inside the test rig reactor.

This test consists of measuring the response of CO conversion to increases in the air preheat temperature. The carbon monoxide test gas was purchased from Scientific Gas Products and is rated chemically pure (C.P.) with a 99.7% minimum purity specification. The remaining tests parameters are held constant and are shown in Table IV. Typical responses for this test are shown in Figure 1.

The response curve in Figure 1 provides two important facts about the catalyst cores' activity. The CO ignition temperature, defined as the lowest air preheat temperature required to obtain a measurable temperature rise across the catalyst core, is a measure of intrinsic catalytic activity. Increases in the ignition temperature reflect possible changes in the energy of activation or pre-exponential factor using the Arrhenius rate expression as the typical reaction rate model. The sloping portion of the response curve in Figure 1 indicates that in this temperature range the rate of reaction is kinetically controlled. The region showing a constant conversion level as a function of temperature is considered to be mass transfer controlled. A mass transfer controlled reaction is independent of the catalyst and temperature, and is only a function of the apparent geometric surface area of the catalyst. If the mass transfer conversion declines with catalyst age, then the apparent mass transfer area is decreasing.

---

*CATCOM is a tradename of Engelhard Minerals and Chemicals Corp.

The utility of this CO activity test is that it provides a means to monitor subtle changes in catalyst core activity without disturbing the catalyst test piece in the reactor.

3. Parametric Testing

In order to define the low emissions operating range for test catalysts, a series of parametric studies was carried out over the following operating range:

Variable	Range
Pressure	$1 \times 10^5 - 5 \times 10^5$ N/M^2
Air Preheat Temperature	630 - 810°K
Adiabatic Flame Temperature	1306 - 1533°K
Reference Velocity	14 - 26 M/S

The parametric tests were conducted initially at the start-of-life testing to determine the range of operation of a virgin catalyst, and at the end-of-life testing to determine if changes in activity had occurred after 1000 hours.

TEST RIG MODIFICATIONS

In order to carry out the experimental program the test rig constructed for the one atmosphere life test had to be modified to allow safe, unattended operation at five atmospheres pressure. The test capabilities of the unit previously described in reference 21 had to be broadened. A simplified schematic of the modified NASA test rig is presented in Figure 2.

The equipment modifications can be broken down to three major categories:

A. Safety System
B. Process Control System
C. Fuel Presentation System

Details of the reactor/controls sytem can be obtained from references 21 and 39.

The experimental reactor used in testing the catalyst cores at combustion conditions is constructed of corrosion-resistant heavy-walled Inconel 601 pipe and designed for long term endurance testing at 1533°K and 5×10^5 N/M^2 (5 atm) and short term testing at 1533°K and 10×10^5 N/M^2 (10 atm). The reactor was instrumented for measurement of:

- catalyst core inlet and outlet temperature
- catalyst core pressure drop
- catalyst core inlet pressure
- catalyst core emissions

The pressure drop apparatus consisted of a manometer with pipe tap locations upstream and downstream of the catalyst core in accordance with ASME recommended practice (reference 44).

The range of operating conditions of the test rig is summarized in Table V. Detailed operating procedures used for 5 atmosphere diesel fuel life testing are given in reference 39.

Emission samples were all taken with a 0.00635M (1/4") diameter water-cooled sample probe. The sampling train adhered to SAE Standard ARP-1256. The description of each individual analytical instrument and standard operating procedures are the same as reported in reference 21.

Fuel Presentation System

In the course of carrying out the experimental program using #2 diesel fuel, it was found that high reactor inlet temperature shutdowns occurred repeatedly at 5 atmosphere life test conditions upon extended operation (overnight) with a fuel injection system essentially identical to that used for 1 atmosphere endurance testing. To improve fuel vaporization and mixing. A Delavan air assist siphon fuel nozzle (#30610-2) in the horizontal inlet section of Unit 6 was used to generate 10-40 micron diameter fuel droplets.

Test Performance of the New Fuel Injector

After making the necessary equipment changes, a continuous run of 90 hours (3.8 days) was made with a duplicate catalyst at 5 atmosphere life test conditions. No pre-ignition or any other safety shutdown occurred using the new air-assisted siphon fuel nozzle. To determine the flashback limit, the inlet temperature at 5 atmosphere life test conditions was increased gradually from 633°K by increasing the air preheat furnace temperatures. At approximately 823°K, the inlet temperature started to climb steadily as flashback occurred. The experiment was repeated and the same result was seen again. At the normal operating inlet temperatures, well below 823°K no flashback or preburning was observed with the new fuel injector.

EXPERIMENTAL RESULTS - PERFORMANCE OF CATALYST CORE DXE-442

Life Testing with #2 Diesel Oil

The most useful technique for monitoring performance of a catalyst during life testing is to monitor daily the input variables and output responses from the test. A control plot of the most critical observations then provides a method for detecting trends which may indicate a degradation in the performance of the catalyst or problems in test rig operation.

Control charts were maintained on a daily basis for the following:

- exhaust gas composition (CO, UHC, NO_x, CO_2, O_2)
- pressure drop
- air preheat temperature
- catalyst core outlet temperature

Perhaps the most significant control plot in the present life test is the exhaust gas analysis and, in particular, the emissions of CO, UHC and NO_x (see Figure 3.). The gas compositions are reported as measured in the exhaust, which was nominally 12.5% oxygen. These plots provide a measurement of stable operation during life testing. Major events occurring in the life test are shown in Figure 4. A summary of performance measurements before and after life testing is shown in Table VI.

Carbon Monoxide Emissions

The CO emissions were constant around 30 Vppm for the initial 200 hours on stream and gradually increased during life testing as shown in Figure 3a. Two high CO emissions data points greater than 2000 ppm were measured after 848 hours on stream. However, after the final CO activity test at 1014 hours on stream, the CO emissions were significantly lower (525 Vppm) under life test conditions. The CO emissions approached initial performance levels after the catalyst had been maintained around [illegible]73°K in the presence of air for two days while a thermocouple was repaired. After this, low CO emissions (less than 200 Vppm) were maintained for 22 continuous hours at the end of the life test.

Unburned Hydrocarbon Emissions

The unburned hydrocarbon emissions exhibit the same trend as the CO emissions (shown in Figure 3b).

Nitrogen Oxides Emissions

The NO_x emissions varied from 3.5 Vppm to 6.5 Vppm during life testing as plotted in Figure 3c. Low NO_x emissions were observed (4.8 Vppm) throughout the life test.

Downstream Temperature Profiles

Maximum outlet temperature measured at 0.1080 M downstream of the catalyst core was around 1475°K and this outlet temperature corresponds to 94% adiabaticity.

Diesel Parametric Tests

In order to define the low emissions operating range for the initial and final catalyst performance after 1000 hours on stream, a series of parametric tests were carried. Table VII gives initial and final parametric test results for the comparison runs, and detailed results are given in reference 39.

Comparison plots showing effects of inlet temperature, reference velocity and pressure on combustion efficiency, are presented in Figures 5, 6 and 7, for the initial (after 63 hours on stream) and final (after 1014 hours on stream) parametric tests over the range of adiabatic flame temperature used.

Carbon Monoxide Activity Test

Carbon monoxide activity tests were performed periodically at 24 hours, 206 hours, 507 hours, 729 hours and 1014 hours on stream during life testing. Carbon monoxide conversion was measured under test conditions listed in Table IV. The test procedures are detailed in references 21 and 39. CO conversion data are plotted versus air preheat temperature in Figure 3.

Activity Test Procedure Modification

Since poor results of the previous standard CO activity test were obtained at 729 hours on stream, a different approach was tried to obtain mass transfer limited CO conversion levels by starting the test from a high temperature (turndown) and with CO fuel on continuously.

High CO conversion data denoted by closed symbols in Figure 9 were obtained with fuel on continuously and mass transfer limited CO conversions of approximately 40% were achieved. Standard CO activity test results are shown in Figure 9 for comparison.

DISCUSSION OF TEST RESULTS

The primary criteria for evaluation of catalyst performance consisted of experimentally determining if the range of low emissions operation and physical durability of the catalyst core could be maintained after 1000 hours of aging with #2 diesel fuel at 5 atmospheres pressure. Secondary criteria considered were the maintenance of carbon monoxide activity and range of low emissions performance in diesel parametric tests before and after 1000 hours aging at 5 atmospheres pressure.

Life Test Results

Emissons Performance:

During the 1000 hour durability life test of the catalyst core, DXE-442, at 5 atmospheres pressure, emissions were as follows:

Emissions Measured		Initial after after 63 hours	After 1014 hours	After 1062 hours
UHC (as C_3)	:	0	146	0
CO	:	35	2420	35
NO_x	:	5.7	5.6	4.3

Combustion efficiencies were calculated from carbon balance (Reference 31) in the exhaust gas stream and plotted in Figure 10.

A high combustion efficiency was maintained around 99.95% during the initial 200 hours of the life test and a gradual degradation in the catalyst performance was noted for the remainder of the life test. Combustion efficiency dropped to 95% at 848 and 1014 hours on stream. There is no evidence for abnormal contaminants in #2 diesel fuel which had been used during the particular period. Final emissions levels obtained after 1062 hours on stream suggest that some sort of reversible catalyst deactivation may have occurred during the life test.

Compared to the one atmosphere life test results (references 21, 22) the deactivation of the catalyst was more severe at 5 atmospheres pressure. The test catalyst was subject to five times the total mass throughput, thus any decline in catalyst performance caused by poison contaminants in the fuel or by attrition of active catalytic components would have been accelerated.

At the end of the life test, catalyst performance was partially restored by passing preheated air in-situ over the catalyst at 673°K for a two day period. Thereafter, high combustion efficiencies were observed as shown in Figure 10. This unexpected result may have been caused by partial catalyst regeneration: 1) removal of fuel deposited poisons from the catalyst surface, or 2) alteration of the active catalyst surface by some other mechanism.

NO_x emissions were fairly stable and ranged from 4-5 ppm by volume. Oxides of nitrogen are generated entirely from fuel bound nitrogen. Significant thermal NO_x generation is unlikely at the operating temperatures used in a well mixed CATCOM* system.

---

*CATCOM is a tradename of Engelhard Minerals and Chemicals Corp.

Physical Durability of DXE-442 Catalyst:

Photographs of the inlet and outlet ends of the test catalyst used for life testing are presented in Figure 11a. Physical damage was limited to minor breakage from catalyst handling during removal of the catalyst substrate and reloading it into the test reactor.

A photograph of the catalyst test configuration is shown in Figure 11b. As shown, the two test segments are separated by 1/4" spacers and secured in the catalyst holder using high temperature cement and Fibre Frax packing around the circumference of the substrates.

Carbon Monoxide Activity Testing

The CO activity test is intended to detect differences in effective catalytic surface area by measuring mass transfer limited CO conversion levels at high flow conditions. Stabilized CO conversion of approximately 40% were obtained at 206 and 507 hours on stream.

From the data taken after 729 and 1014 hours on stream, it was apparent that these conversion levels could not be achieved under normal activity test conditions. It was found, however, that 40% CO conversion levels could be reached by starting up at high temperature and leaving feed CO on while decreasing the air preheat temperature. Lower CO conversion levels were measured when the activity test was done by the standard procedure of increasing the air preheat temperature as illustrated in Figure 9.

The observed hysteresis phenomenon has been well described for heterogeneous reaction systems for CO oxidation over various metal component catalysts (reference 45). Although mass transfer limited conversions in the range of 40% could be achieved after 1000 hours on stream, it is apparent that more severe catalyst deactivation had occurred during the 5 atmosphere life test than observed in any 1 atmosphere life test conducted to date, including that carried out using a similar DXE-442 catalyst preparation.

Diesel Parametrics

Effect of Air Preheat Temperature Before and After Life Testing

Effect of air preheat temperature on combustion efficiency is shown in Figure 5, a plot of the negative logarithm of complement combustion efficiency versus adiabatic flame temperature at 633°K and 723°K air preheat temperatures.

Since combustion efficiency obtained with the initial catalyst core was not sensitive to inlet temperature at a low adiabatic flame temperature, there was no apparent kinetic activity limitation in the overall reaction. Above an adiabatic flame temperature of 1450°K, combustion efficiency was not affected by adiabatic flame temperature

However, the performance of the catalyst had changed after 1014 hours on stream as shown in Figure 5. A kinetic effect was noted at low adiabatic flame temperatures and the catalytically supported homogeneous combustion zone was reduced at high adiabatic flame temperatures. This was attributed to partial deactivation. Thus, combustion efficiency is more sensitive to adiabatic flame temperature after 1014 hours on stream, and higher fuel/air ratios are required to maintain efficient, low emissions performance. After 1014 hours on stream, a minimum adiabatic flame temperature to obtain combustion efficiency greater than 99% is interpolated to be 1513°K from Figure 5 at 633°K air preheat temperature and 14 M/S reference velocity.

Effect of Reference Velocity Before and After Life Testing

Combustion efficiency is a strong function of reference velocity as shown in Figure 6, a plot of the negative logarithm of complement combustion efficiency versus adiabatic flame temperature at 14 M/S and 26 M/S reference velocities. Combustion efficiency substantially declined as reference velocity was increased up to 26 M/S for both the initial and final catalyst performance.

Initial combustion efficiencies greater than 99% were achieved over the entire range of adiabatic flame temperatures at 14 M/S reference velocity. An adiabatic flame temperature of 1553°K was required to obtain combustion efficiencies greater than 99% at 26 M/S reference velocity.

After 1014 hours on stream, an adiabatic flame temperature required for 99% combustion efficiency is extrapolated to be 1597°K at 26 M/S reference velocity from Figure 6.

Effect of Pressure Before and After Life Testing

As shown in Figure 7, a plot of the negative logarithm of complement combustion efficiency versus adiabatic flame temperature, at 1×10^5 N/A^2 and 5×10^5 N/M^2 pressures, shows that pressure is the least sensitive variable, although slightly higher combustion efficiencies were obtained at 5×10^5 N/M^2 pressure and the higher adiabatic flame temperatures. The same trend was observed at the beginning and after 1014 hours on stream.

Low Emissions Operating Range

The low emissions operating regions have been defined as those with combustion efficiency performance greater than 99% as shown in Figure 12. The boundary for the required adiabatic flame temperature was formulated for a high combustion efficiency at a given reference velocity by interpolating parametric test results assuming a linear relationship between each data point in the plot of logarithm of complement combustion efficiency versus adiabatic flame temperature (shown in Figures 5 and 6).

As illustrated in Figure 12, the region of low emissions operation has been narrowed after life testing at 5 atmospheres pressures. Inlet temperature in the range of 633°K to 723°K does not affect the initial boundary but is significant after 1014 hours on stream.

CONCLUSIONS AND RECOMMENDATIONS

The following conclusions and recommendations have been made from the experimental test results obtained under this contract:

1. The catalyst core tested, DXE-442, maintained low emissions for 1000 hours of continuous operation at 5 atmospheres with #2 diesel fuel. Initial and final emissions were:

	Initial	After 1014 hours	After 1062 hours
Unburned Hydrocarbons (C_3, Vppm)	0	146	0
Carbon Monoxide (Vppm)	30	2420	35
Nitrogen Oxides (Vppm)	5.7	5.6	4.3

2. The DXE-442 catalyst core tested maintained its physical integrity throughout the 1000 hour, 5 atmosphere life test at operating temperatures characteristic of catalytically-supported thermal combustion operationg temperatures (1533°K) and withstood the thermal shock of numerous intentional and unintentional startups and shutdowns without any evidence of failure.

3. NO_x emissions measured were consistently low throughout endurance and parametric testing and can be maintained at 4-5 Vppm.

4a. It has been experimentally determined that the operating conditions of the 5 atmosphere test were apparently more severe, in terms of maintaining catalyst activity, than those of the previous test conducted at 1 atmosphere pressure.

4b. The modified CO activity test data indicated that adequate mass transfer surface was retained, but kinetic (ignition, light off) activity had been severely deteriorated. This is presumed due to exposing the inlet section of the catalyst to sustained high temperatures (caused by preburning) and the malfunctioning fuel preparation method, prior to the successful modifications.

5. The observation that combustion efficiencies exceeding 99.5% could be achieved at the end of life testing, although levels as low as 95% had been measured, indicates that at least part of the catalyst deactivation was reversible.

6. It is recommended that either the test be repeated with a new catalyst using the successfully modified reactor, or carry out further development work to improve the catalyst high temperature capability (1644-1700°K) and to improve catalyst life.

REFERENCES

1. Pfefferle, W. C., "Two-Stage Combustion Process", U. S. Patent 3,846,979 (11/12/74).

2. Hindin, Saul G., "Method for Catalytically Supported Thermal Combustion", U. S. Patent 3,870,455 (3/11/75).

3. Pfefferle, W. C., "Method and Furnace Apparatus", U. S. Patent 3,914,090 (10/21/75).

4. Pfefferle, W. C., "Catalytically Supported Thermal Combustion", Belgium Pat. 814,752, November 8, 1974 and U. S. Pat. 3,938,961, December 30. 1975.

5. Pfefferle, W. C., "Method of Operating Catalytically Supported Thermal Combustion System", U. S. Patent 3,940,923 (3/2/76).

6. Hindin, Saul G., and Pond, George R., "Method of Combustion Using High Temperature Stable Catalysts", U. S. Patent 3,966,391 (6/29/76).

7. Dettling. J. and Hindin, S. G., U. S. Patent 3,956,188 (1976) and U. S. Patent 3.945,946 (1976), Hindin, S. G. and Pond, G. R., U. S. Patent 3,966,391 (1976).

8. Blazowski, W. S. and Bresowar, G. E., "Preliminary Study of the Catalytic Combustor Concept, As Applied To Aircraft Gas Turbines", AFAPL-TR-74-32, 1974.

9. Pfefferle, W. C., Heck, R. M., Carrubba, R. V. and Roberts, G. W., "CATATHERMAL Combustion: A New Process for Low-Emissions Fuel Conversion", ASME-57-Wa/FU-1, 1975.

10. Anderson, D. N., Tacina, R. R. and Mroz, T. S., "Performance of a Catalytic Reactor at Simulated Gas Turbine Combustor Operating Conditions", NASA-TMX-71747, 1975.

11. Blazowski, W. S. and Walsh, D. E., "Catalytic Combustion: An Important Consideration for Future Application", Comb. Sci, and Tech., Vol. 10, pp 233-244, (1975).

12. Carrubba, R. V., Chang, M., Pfefferle, W. C. and Polinski, L. M., "Catalytically-Supported Thermal Combustion For Emissions Control", Paper presented at the Electrical Power Research Institute NO_x Control Technology Seminar, San Francisco, Calif., Feb. 6, 1976.

13. DeCorso, S. M., Mumford, S., Carrubba, R. V., and Heck, R. M., "Catalysts for Gas Turbine Combustors - Experimental Test Results", Presented at ASME Gas Turbine Division Conference, New Orleans, La., March, 1976.

14. Anderson, D. N., "Preliminary Results from Screening Tests of Commercial Catalysts with Potential Use in Gas Turbine Combustors. Part I: Furnace Studies of Catalyst Activity", NASA TM X-73410, 1976.

15. Anderson, D. N., :Preliminary Results from Screening Tests of Commercial Catalysts with Potential Use in Gas Turbine Combustors. Part II: Combustion Test Rig Evaluation", NASA TM X-73412, 1976.

16. Rosfjord, T. J., "Catalytic Combustors for Gas Turbine Engines", AIAA pages 76-46, Washington, D. C., (Jan. 1976).

17. Anderson, D. N., "Emissions and Performance of Catalysts for Gas Turbine Catalytic Combustors", NASA TM X-73543 (1977).

18. Anderson, D. N., "Effect of Catalysts Reactor Length and Cell Density on Performance", Presented at the 2nd Workshop on Catalytic Combustion, 21-22, June, (1977).

19. Anderson, D. N., "Emissions and Performance of Catalysts for Gas Turbine Catalytic Combustors", ASME Paper No. 77-GT-65, March, 1977.

20. Anderson, D. N., "Performance and Emissions of a Catalytic Reactor With Propane, Diesel and Jet A Fuels", NASA TM-73786, Sept., 1977.

21. Heck, R. M., "Final Report Part I. Durability Testing at 1 atm of Advanced Catalysts and Catalyst Supports for Automotive Gas Turbine Engine Combustors", NASA CR-135132, June, 1977.

22. Heck, R. M., Chang, M. and Hess, H., Mroz, T., "Durability Testing of Advanced Catalysts and Catalyst Supports for Gas Turbine Engine Combustors", AIChE Symposium Series No. 188, Vol. 75, 1979.

23. Flanagan, P., Norster, E. R., Carrubba, R. V. and Heck, R. M. "Method for Effecting Sustained Combustion of Carbonaceous Fuel", U. S. Patent 4,118,171 (10/3/78).

24. Pogson, J., Mansour, M. N., "Catalytic Combustion of No. 6 Fuel Oil", 3rd Workshop on Catalytic Combustion, 3-4 October 1978.

25. Marteney, P. J., "Determination of the Rate of Heterogeneous Reaction on Catalytic Surfaces", loc. cit.

26. Schefer, R. W., Robben, F. S., Cheng, R. K., "Catalyzed Combustion of H_2/Air Mixtures in a Flate Plate Boundary Layer", loc. cit.

27. Walsh, P. M. Santavicca, D. A., Kim, B., Bracco, F. V., "Progress of Reaction in a Honeycomb Catalyst: CO/Air Combustion", loc. cit.

28. Anderson, D. N., "Effect of Inlet Temperature on the Performance of a Catalytic Combustor", NASA TM-78977 (1978).

29. Flanagan, P., Carrubba, R. V. and Norster, E. R., "The Development of a Gas Turbine Combustor Utilizing a Catalysts", Journal of Energy, 1979.

30. Osgerby, I. T., Heck, R. M., Carrubba, R. V., and Bunker, W. W., "Investigation of Process and System Design Variables for CATATHERMAL Combustion of Low BTU Gas", ASME 79-GT-66.

31. Lew, H., Olson, B. A., Dickson, W. H., Heck, R. M., and DeCorso, S. M. "Experimentally Determined Catalytic Reactor Behavior and Analysis for Gas Turbine Combustors", ASME 79-GT-150.

32. Osgerby, I. T., Olsen, B. A., Lew, H. and Cohn, A. "CATCOM Catalyst Axial Temperature Profile Measurements". Presented at 4th Workshop on Catalytic Combustion, May, 1980.

33. Lee, H. and Osgerby, I. T. "Catalytic Combustion Characteristics of Low and Medium BTU Gas Fuels", loc. cit.

34. Osgerby, I. T., Gleason, G. L. and Mularz, E. J. "Combustion Catalyst Studies For Simulated Aircraft Idle Mode Operation", loc. cit.

35. Osgerby, I. T. and Norster, E. R. "Development of a Prototype Industrial CATCOM Burner for Process Heating". To be published.

36. Osgerby, I. T. "Performance Characteristics of a Prototype Industrial CATCOM Burner For Process Heating". To be published.

37. Angello, L. "The EPRI Stationary Gas Turbine Catalytic Combustor Development Program:. 4th Workshop on Catalytic Combustion, May 1980.

38. Carl, D. and Osgerby, I. T. "High Pressure CATCOM Test Results", loc. cit.

39. Olson, B. A., Lee, H. C., Osgerby, I. T., Heck, R. M. and Hess, H. "Durability Testing at 5 atmospheres of Advanced Catalysts And Catalyst Supports for Gas Turbine Engine Combustors" NASA-CR- 1980.

40. Lew, H. G., et al., "Ceramic Turbine Components R&D. Part 3. Ceramic Combustor Design and Analysis Final Report" (EPRI Project 421-1). (March 1979).

41. Kesselring, J. P., Krill, W. V. and Kendall, R. M., "Design Criteria For Stationary Source Catalytic Combustors", Paper No. 77-32, Western States Section, The Combustion Institute, October (1977).

42. Krill, W. V., et. al., "Catalytic Combustion for Gas Turbine Applications", ASME Paper No. 79-GT-188, (1979).

43. Krill, W. V., et al., "Catalytic Combustions for System Applications", ASME Paper No. 79-HT-54 (1979).

44. Bean, H. S. (ed.) "Fluid Meters: Their Theory and Applications", 6th Ed., 1971.

45. Hlavacek, V. and Votruba, J. "Experimental Study of Multiple Steady States in Adiabatic Catalytic Systems", Chemical Reaction Engineering. II, American Chemical Socity, Washington, pp. 545-558, 1974.

TABLE I. PROPERTIES OF TEST CATALYST CORE

Catalyst Identification	DXE-442
Catalyst Components	Palladium
Support	Zircon Composite
Channel Density	
Nominal	256 Channels/in^2
Actual	144-159 Channels/1" Ø core
Hydraulic Diameter	9.754×10^{-4} M
Open Fraction	65.5%
Bulk Surface Area	2683 M^2/M^3
Length	1524 M

TABLE II. LIFE TEST CONDITIONS

Catalyst Core Dimensions	0.0254 M diameter X 0.1524 M length
Fuel Type	#2 Diesel Oil
Air Flow	1.42×10^{-2} Kg/S
Fuel Flow	3.73×10^{-4} Kg/S
Air/Fuel	38/1 (Kg/Kg)
Inlet Temperature	633°K
Adiabatic Flame Temperature	1533°K
Inlet Pressure	5×10^5 N/M^2
Reference Velocity	14 M/S
Space Velocity at NTP	142 M^3/S - M^3 Cat.

TABLE III. ANALYSES[1] OF #2 DIESEL FUELS USED FOR CATALYST LIFE TESTS

Test	Batch #1[2]	Batch #2[3]	Batch #3[4]
Gravity, API @ 60°F (289°K)	33.8	33.9	34.0
Flash Point, °K	351.0	348.8	333.2
Pour Point, °K	261	258	250
Water and Sediment, Vol. %	0.1	-Nil-	< .05
Ash, Wt. %	-Nil-	Trace	.016
Colour, ASTM		L 2.5	-
Distillation Temperature, °K			
Initial	454.3	461.0	440.0
10%	487.6	489.9	483.2
50%	532.1	534.3	531.0
90%	575.4	583.2	577.6
End Point	608.8	613.2	593.2
Recovery, %	99	98	96
Carbon/Hydrogen Atomic Ratio	0.535	0.602	0.529
Heating Value, Joule/Kg (Gross)	4.57×10^7	4.57×10^7	4.55×10^7
Viscosity, SUS at 311°K	34.6	35.0	35.3
Sulfur, Wt%	.03	.11	.13-.14
Nitrogen, ppm	500	< 10	600
Phosphorous, ppm	-	< 1	< 1
Lead, ppm	1	< 1	2.4

[1] Analyses performed by Saybolt and Co.

[2] Batch #1 used between 0 and 206 hours on stream.

[3] Batch #2 used between 206 and 825 hours on stream.

[4] Batch #3 used between 825 and 1065 hours on stream.

TABLE IV. CARBON MONOXIDE ACTIVITY TEST CONDITIONS

Fuel Type	C.P. Grade CO
Air Flow	10.55×10^{-3} Kg/S
Fuel Flow	4.09×10^{-5} Kg/S
Air/Fuel	258/1 Kg/Kg
Inlet Temperature	Varied up to 733°K
Inlet Pressure	1×10^{5} N/M^2
Reference Velocity at 633°K	36 M/S
Space Velocity at NTP	125 M^3/S-M^3 Cat.

TABLE V. OPERATING RANGES FOR UNIT 6

Automatic Control Operation:	
Air Flow	1.85×10^{-3} to 5.9×10^{-3} Kg/S
Air Preheat Temperature	Up to 810°K
Fuel Flow (Liquid)	6.7×10^{-5} to 67×10^{-5} Kg/S
Reactor Pressure	1.0×10^{5} N/M^2 to 5×10^{5} N/M^2
Adiabatic Flame Temperature*	Up to 1533°K
Fuel Type	#2 Diesel
Manual Operation:	
Air Flow	1.85×10^{-3} to 66.7×10^{-3} Kg/S
Air Preheat Temperature	Up to 810°K
Fuel Flow (Gaseous)	1.7×10^{-4} to 17×10^{-4} Kg/S
Reactor Pressure	1.0×10^{5} to 5.0×10^{5} N/M^2
Adiabatic Flame Temperature*	Up to 1533°K
Fuel Type	C.P. Carbon Monoxide, #2 Diesel

*For conditions of 90% reactor adiabaticity, adiabatic flame temperature may be increased to 1570°K without damage to reactor walls.

TABLE VI. COMPARISON OF PERFORMANCE DATA AT START AND END OF LIFE TEST

	Start	End	Results After Final CO Activity Tests at 1062 Hours
Hours on Diesel Fuel	63	1014	1062
Air Flow Rate (Kg/sec)	1.43×10^{-2}	1.43×10^{-2}	1.43×10^{-2}
Fuel/Air Ratio (by weight)	.02647	.02686	.02647
Temperature (^{o}K)			
Preheat Air	533	633	633
Reactor Outlet	1463	1463	1473
Adiabatic Flame	1539	1539	1539
Pressure			
Inlet (N/M^2)	$5.1 * 10^5$	$5.0 * 10^5$	$5.0 * 10^5$
Drop (N/M^2)	6767	9473	9812
Loss (%)	1.31	1.86	1.93
Reference Velocity (M/Sec)	14.0	14.2	14.2
Heat Release Rate (Joules/sec, M^3, N/M^2)	1136	1111	1151
Combustion Efficiency (%)	99.95	94.97	99.94
+Emissions (Vppm)			
CO	30	2420	35
UHC (as C_3)	0	146	0
NO_x	5.7	5.0	4.3

Catalyst Core Dimension, Nominal 0.0254 M (Diameter)

* 0.1524M (Long)

+All emissions measured with water cooled sample probe located at 0.102 M downstream of catalyst core.

TABLE VII. DIESEL PARAMETRIC TEST RESULTS

Run Number	Pressure (Atm)	Air Preheat Temperature (°C)	Adiabatic Flame Temperature (°C)	Fuel/Air Ratio (W./W.)	Reference Velocity (M/Sec)	Emissions + CO (ppm)	Emissions + UHC (ppm)	Emissions + NOx (ppm)	Combustion Efficiency (%) Initial	Combustion Efficiency (%) Final
146-1	5	360	1093	0.0210	14	345 >5000	0 -	3.6 -	99.20	64.6 *
146-2	5	360	1176	0.0236	14	35 3300	5 310	3.5 5.4	99.90	91.58
146-3	5	450	1093	0.0188	14	300 >5000	4 -	3.2 -	99.21	73.1 *
146-4	5	450	1176	0.0213	14	25 2200	0 145	3.7 4.1	99.94	94.19
146-5	5	450	1260	0.0241	14	15 93	0 0	4.3 5.1	99.97	99.82
146-6	5	360	1093	0.0210	26	> 5000 >5000	- -	- -	49.1*	25.5 *
146-7	5	360	1176	0.0236	26	5000 >5000	900 -	4.0 -	84.87	25.4 *
146-8	5	360	1280	0.0270	26	500 1400	0 45	2.8 4.7	99.12	97.33
146-9	1	360	1093	0.0210	22	> 5000 >5000	- -	- -	36.8*	26.2 *
146-10	1	360	1176	0.0236	22	> 5000 >5000	- -	- -	61.3*	23.2 *
146-11	1	360	1280	0.0270	22	700 2800	11 200	5.2 5.3	98.70	94.08
146-12	5	360	1093	0.0210	14	263 >5000	3 -	4.0 -	99.38	32.0 *
146-13	5	360	1176	0.0236	14	38 2900	0 210	3.5 5.8	99.94	92.97

* Estimate based on % Adiabaticity = (Measured temperature rise/Theoretical temperature rise)
+ Large type denotes emissions at end of life test.
Small type denotes emissions at beginning of life test.

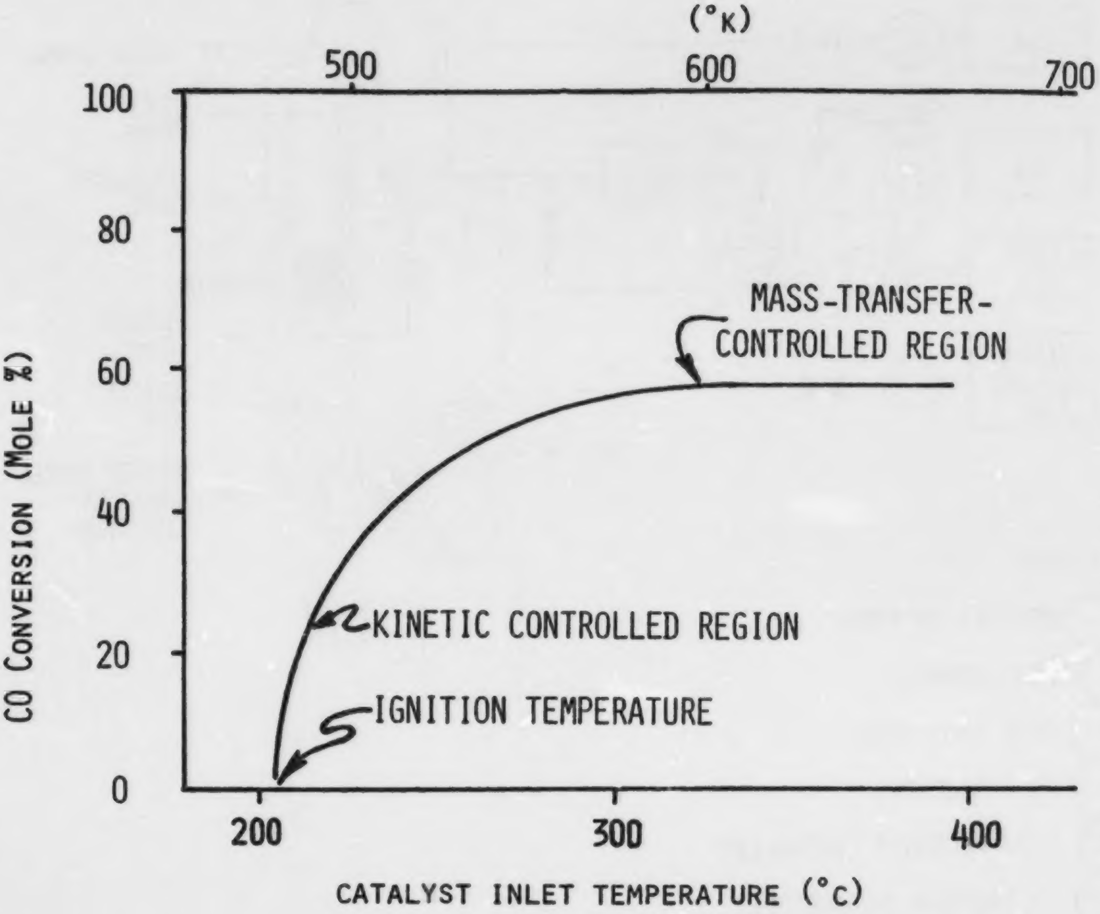

Figure 1. Typical response obtained from carbon monoxide activity test.

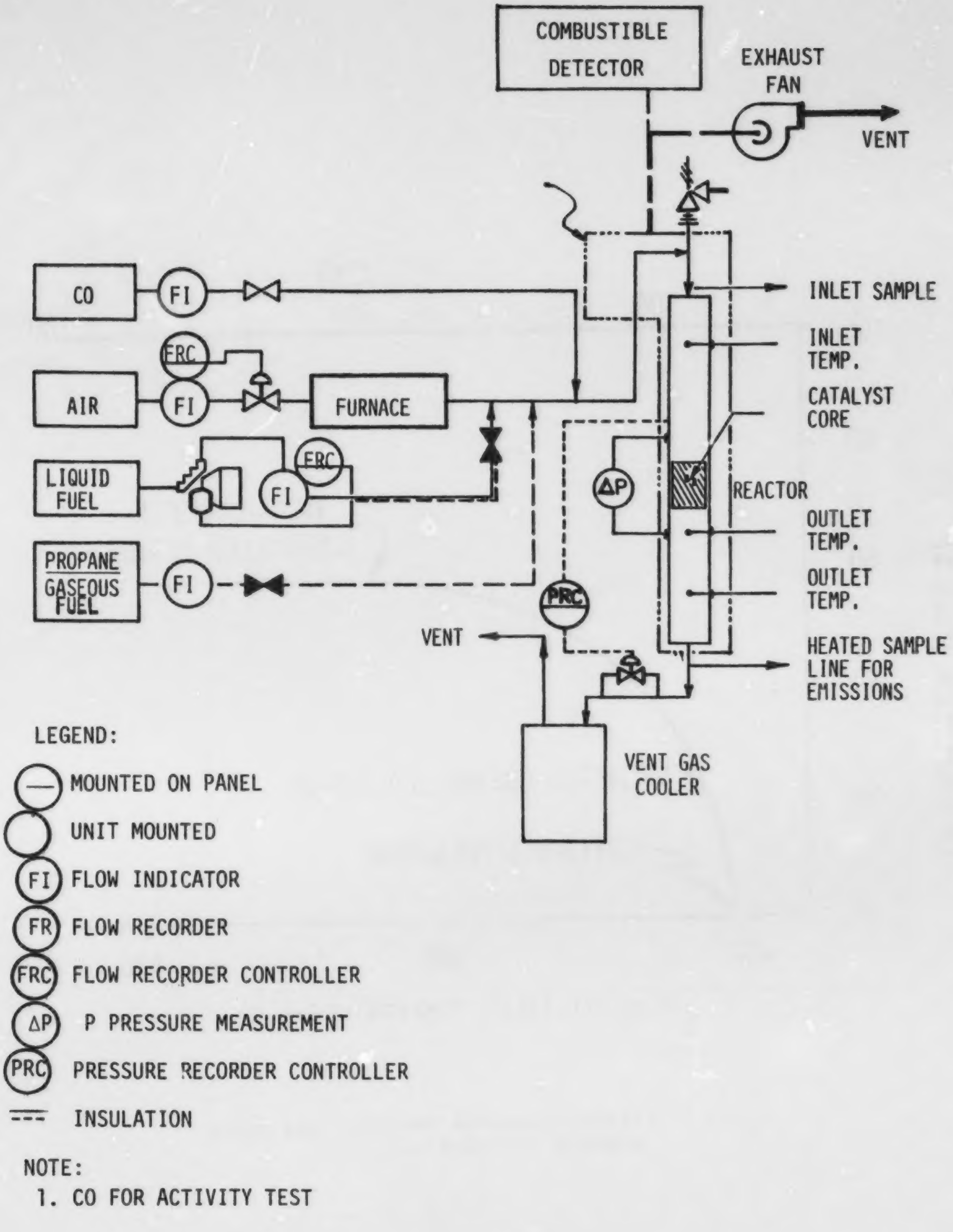
COMBUSTIBLE DETECTOR
EXHAUST FAN
VENT
CO
FI
FRC
AIR
FURNACE
LIQUID FUEL
PROPANE GASEOUS FUEL
INLET SAMPLE
INLET TEMP.
CATALYST CORE
ΔP
REACTOR
OUTLET TEMP.
OUTLET TEMP.
PRC
HEATED SAMPLE LINE FOR EMISSIONS
VENT
VENT GAS COOLER
LEGEND:
MOUNTED ON PANEL
UNIT MOUNTED
FI FLOW INDICATOR
FR FLOW RECORDER
FRC FLOW RECORDER CONTROLLER
ΔP P PRESSURE MEASUREMENT
PRC PRESSURE RECORDER CONTROLLER
INSULATION
NOTE:
1. CO FOR ACTIVITY TEST

Figure 2. Schematic of modified test rig.

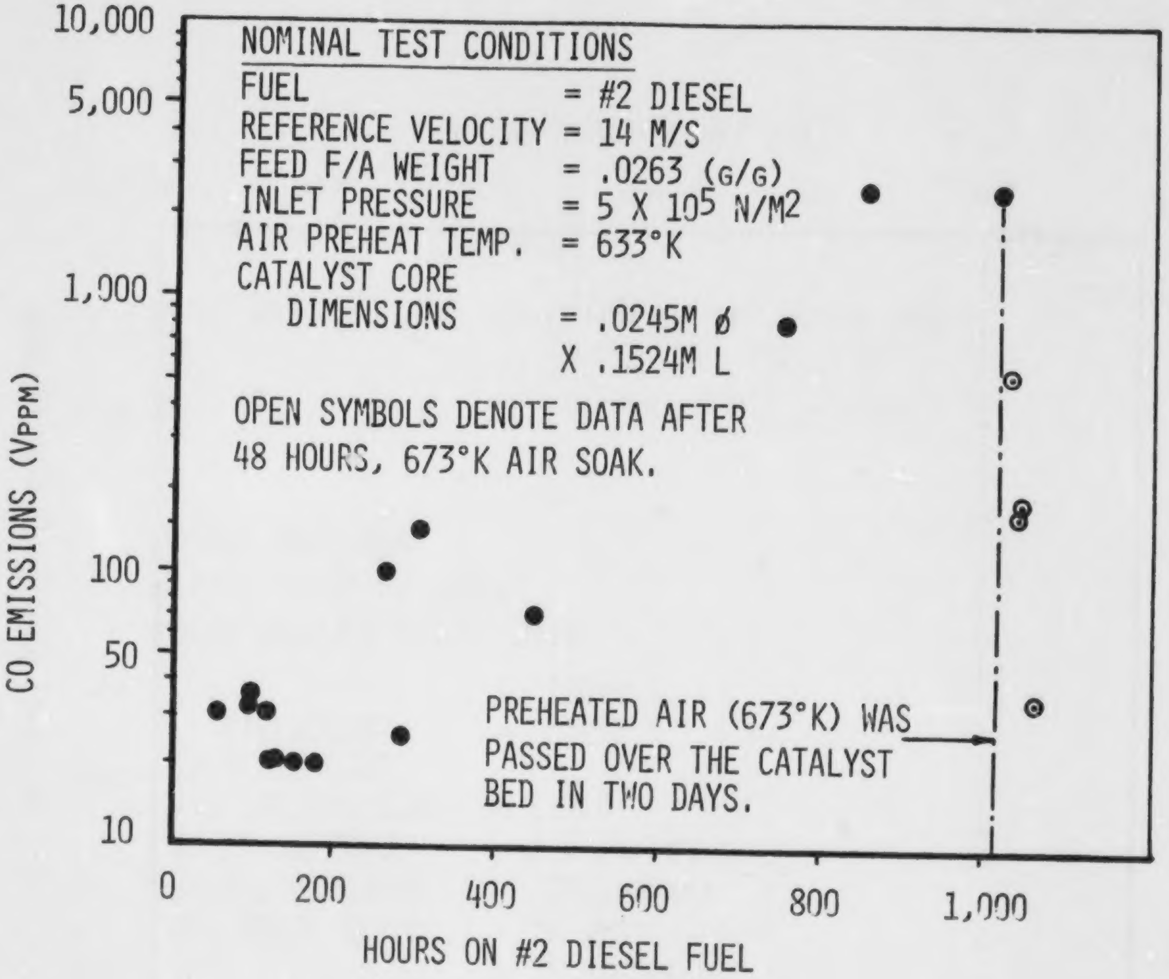

Figure 3a. Carbon monoxide emissions control chart.

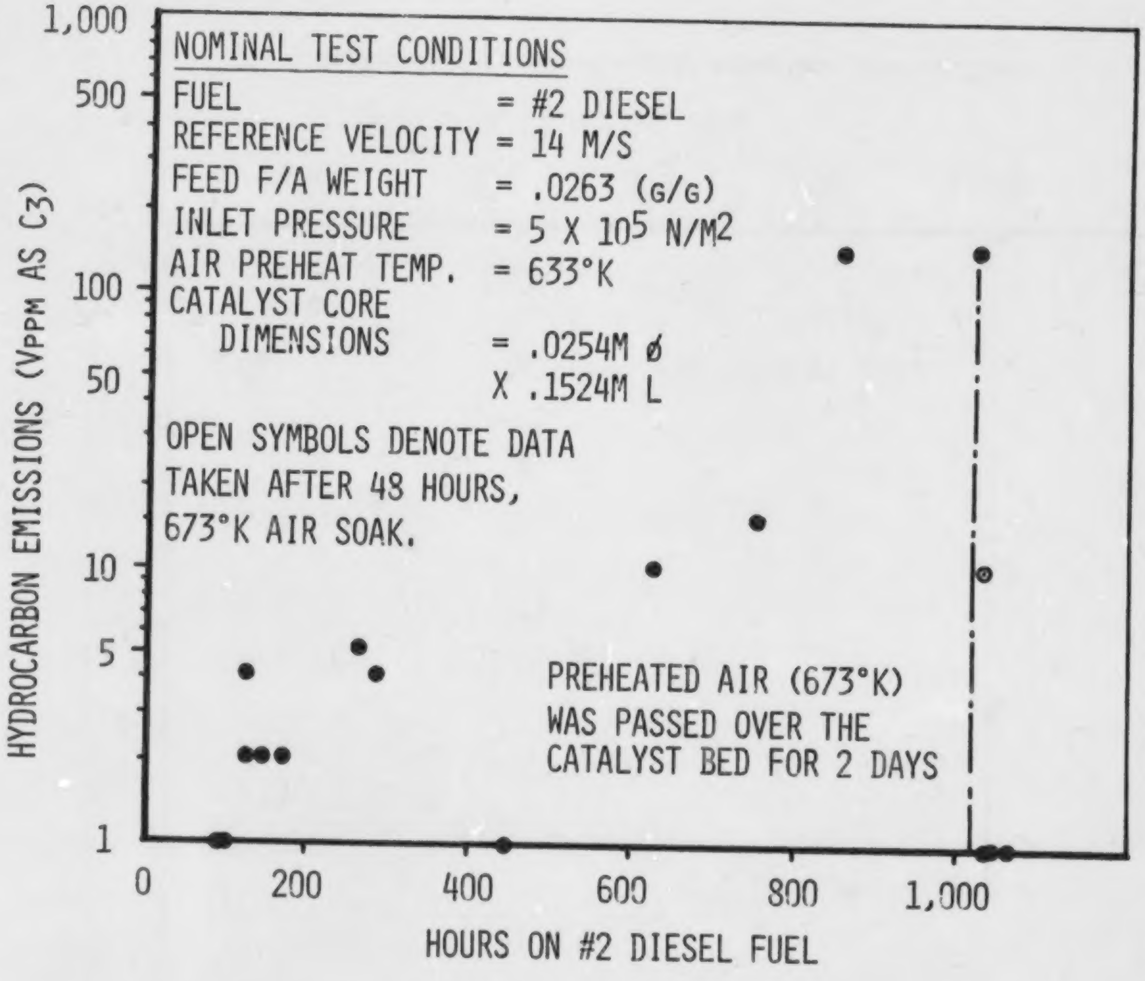

Figure 3b. Hydrocarbon emissions control chart.

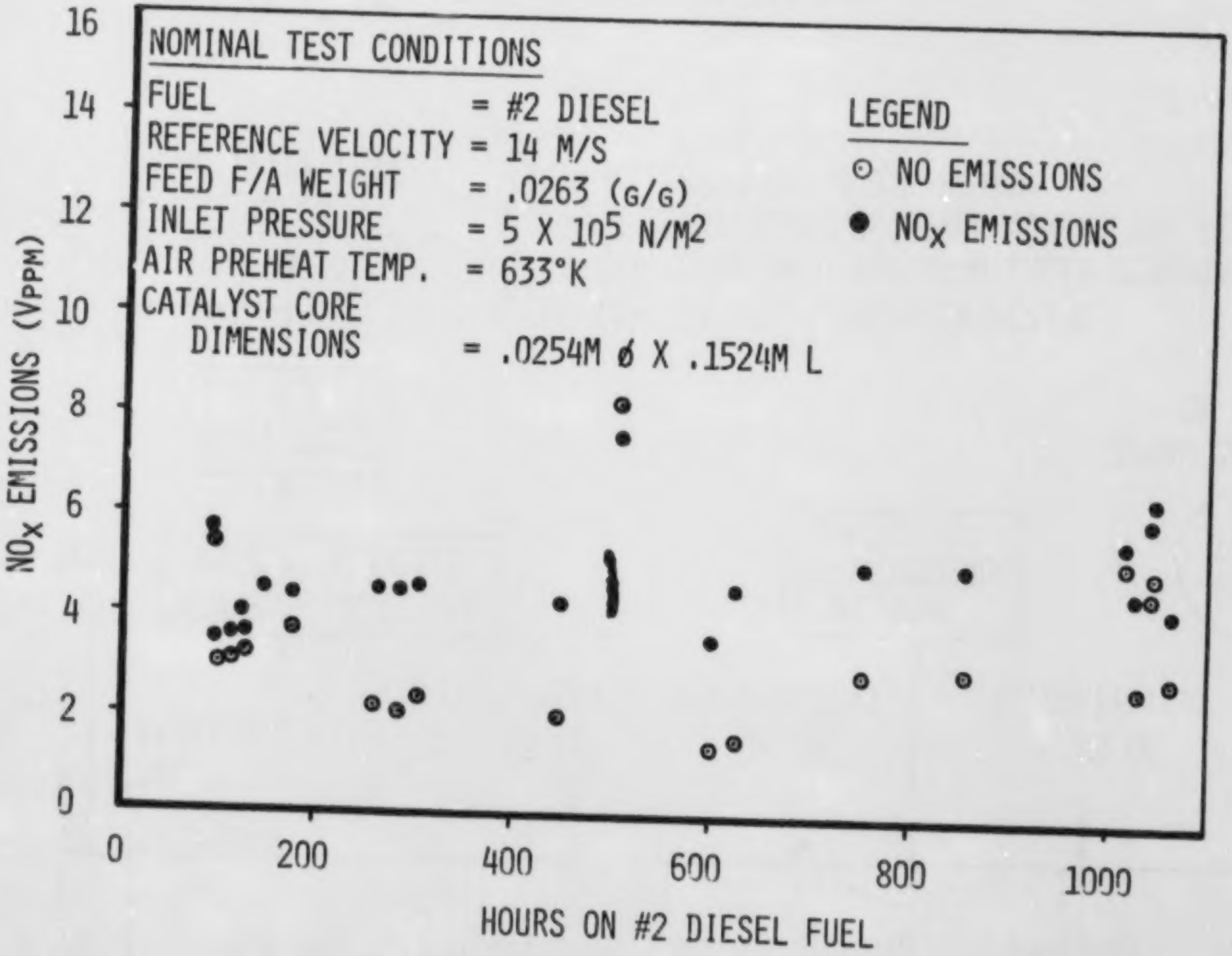

Figure 3c. Nitrogen oxide emissions control chart.

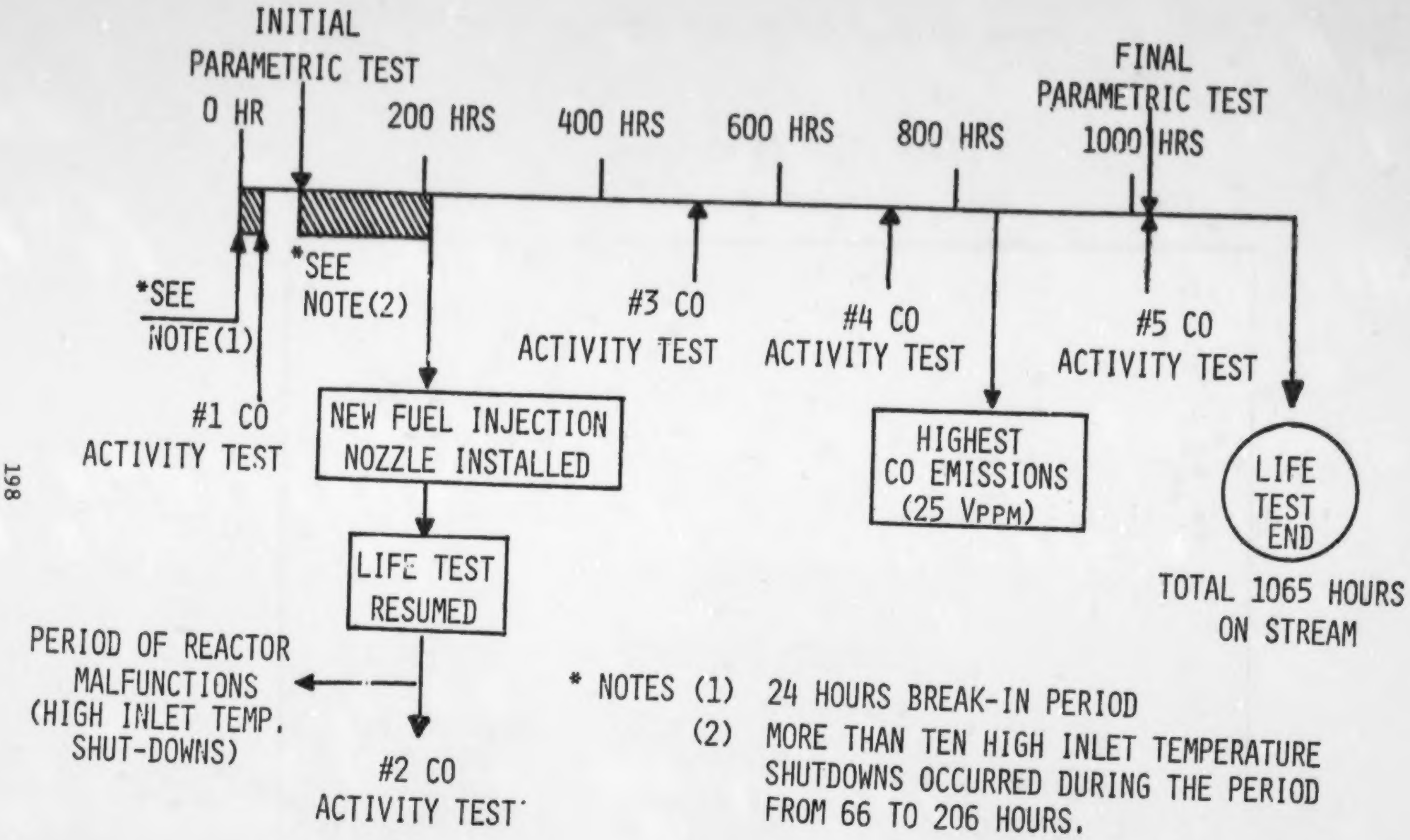
INITIAL
PARAMETRIC TEST
0 HR
200 HRS
400 HRS
600 HRS
800 HRS
FINAL
PARAMETRIC TEST
1000 HRS
*SEE
NOTE(1)
*SEE
NOTE(2)
#1 CO
ACTIVITY TEST
NEW FUEL INJECTION
NOZZLE INSTALLED
LIFE TEST
RESUMED
PERIOD OF REACTOR
MALFUNCTIONS
(HIGH INLET TEMP.
SHUT-DOWNS)
#2 CO
ACTIVITY TEST
#3 CO
ACTIVITY TEST
#4 CO
ACTIVITY TEST
HIGHEST
CO EMISSIONS
(25 VPPM)
#5 CO
ACTIVITY TEST
LIFE
TEST
END
TOTAL 1065 HOURS
ON STREAM
* NOTES (1) 24 HOURS BREAK-IN PERIOD
(2) MORE THAN TEN HIGH INLET TEMPERATURE SHUTDOWNS OCCURRED DURING THE PERIOD FROM 66 TO 206 HOURS.

Figure 4. Event chart for the life test.

Test Conditions

Run No. 146-1 through 5
Fuel : #2 Diesel
Reference Velocity : 14 M/S
Inlet Pressure : 5 X 10^5 N/M^2
Air Preheat Temperature △ : 633°K
⊙ : 723°K

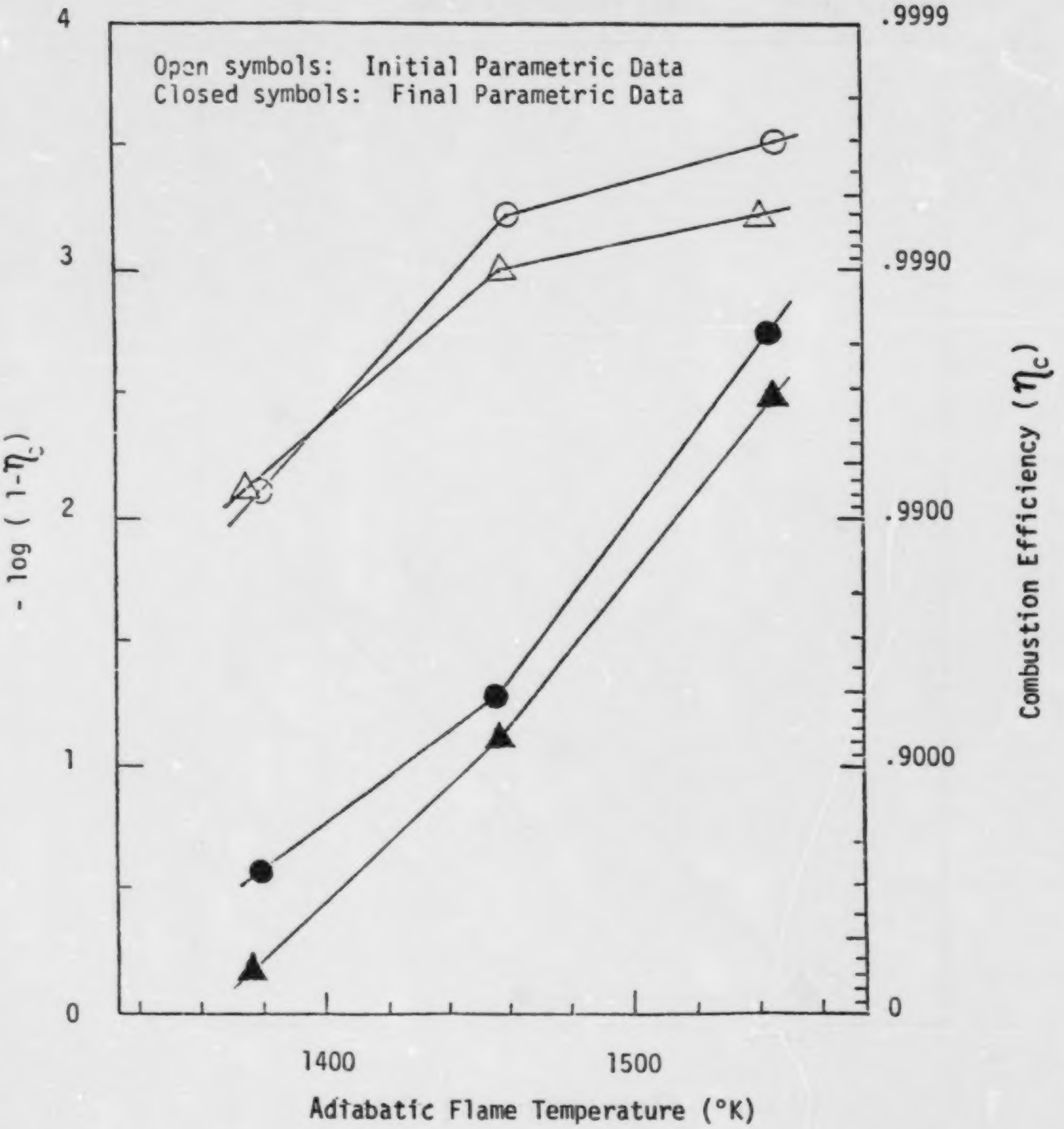

Figure 5. Effect of air preheat temperature on combustion efficiency before and after life testing.

Test Conditions

Run No. 146-1,2,6,7 and 8
Fuel : #2 Diesel
Inlet Pressure : 5×10^5 N/M^2
Air Preheat Temp. : 633°K
Reference Velocity △ : 14 M/S
⊙ : 26 M/S
Open Symbols: Initial Parametric Data
Closed Symbols: Final Parametric Data

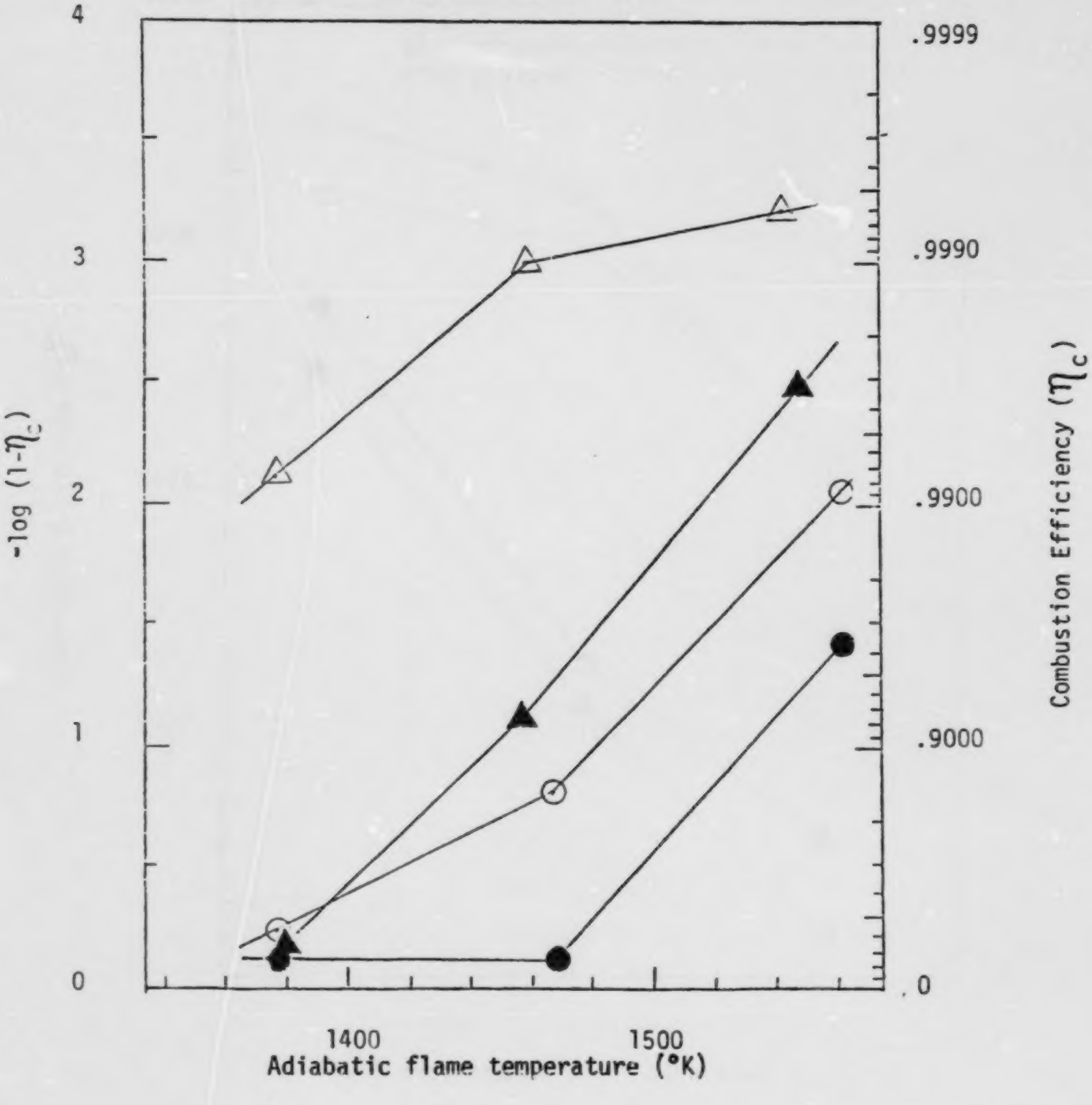

Figure 6. Effect of reference velocity on combustion efficiency before and after life testing.

Test Conditions

Run No. 146-6 through 11
Fuel : #2 Diesel
Reference Velocity : 22-26 M/S
Air Preheat Temperature : 633 ^{o}K
Inlet Pressure ⊙ : 1 X 10^5 N/M^2
△ : 5 X 10^5 N/M^2

Open Symbols: Initial Parametric Data
Closed Symbols: Final Parametric Data

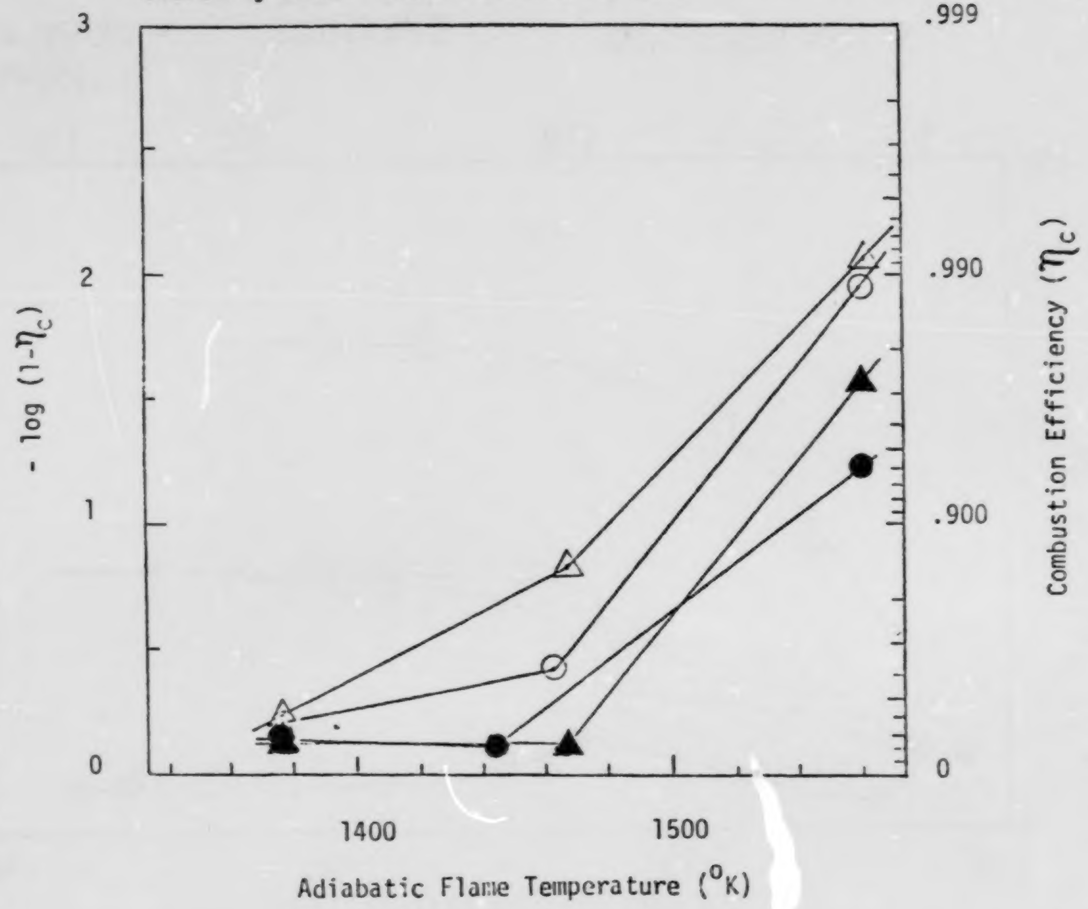

Figure 7. Effect of pressure on combustion efficiency before and after life testing.

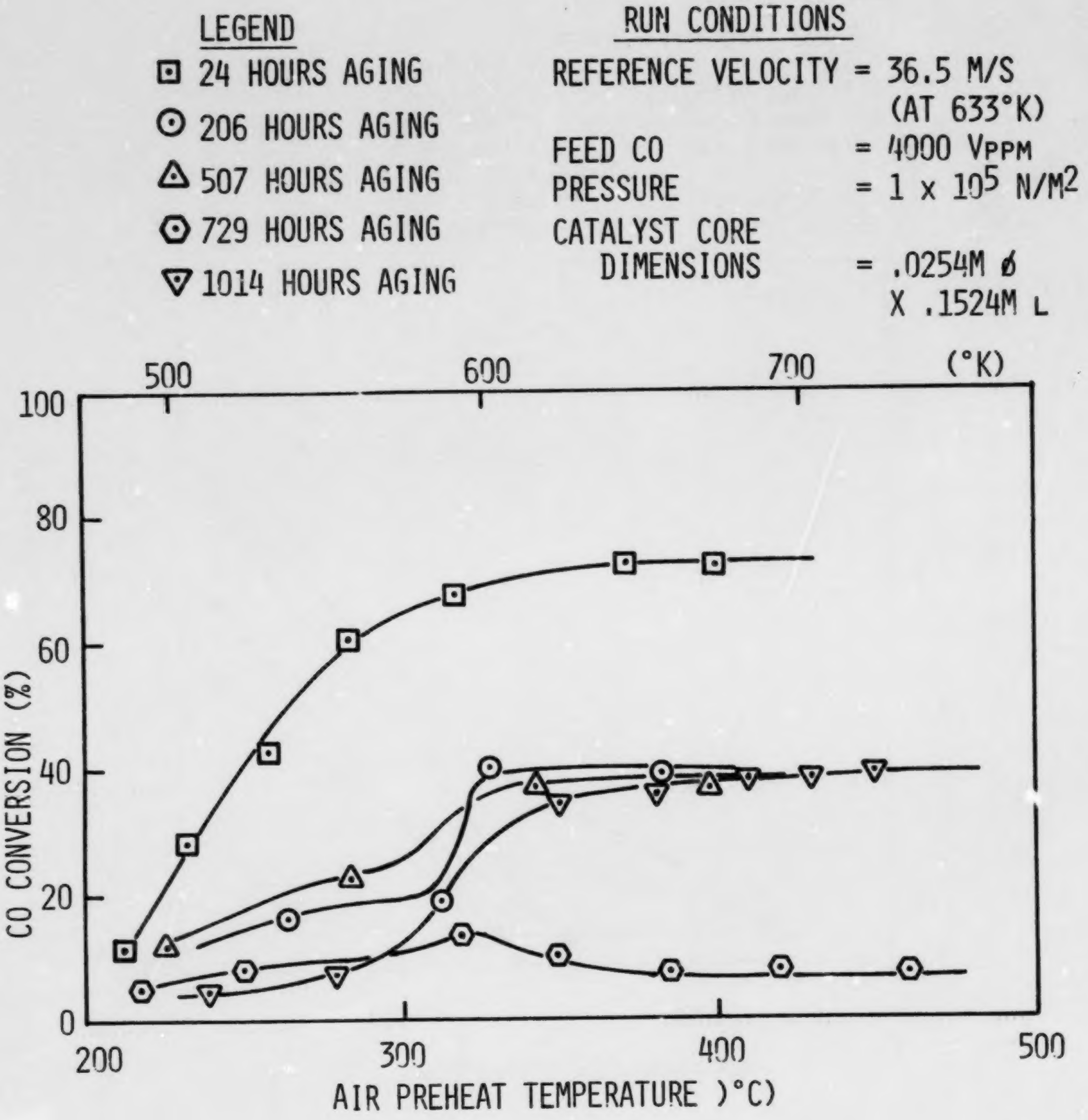

Figure 8. Carbon monoxide activity test response during life test of catalyst core DXE-442.

RUN CONDITIONS

REFERENCE VELOCITY = 36.5 M/S (AT 633°K)
FEED CO = 4000 VPPM
PRESSURE = 1×10^5 N/M^2
CATALYST CORE
DIMENSIONS = 0.254M ø X .1524M L

▽ 1014 HOURS AGING (STANDARD PROCEDURE; TEMPERATURE INCREMENTALLY INCREASED)

▼ 1014 HOURS AGING (MODIFIED PROCEDURE; TEMPERATURE INCREMENTALLY DECREASED)

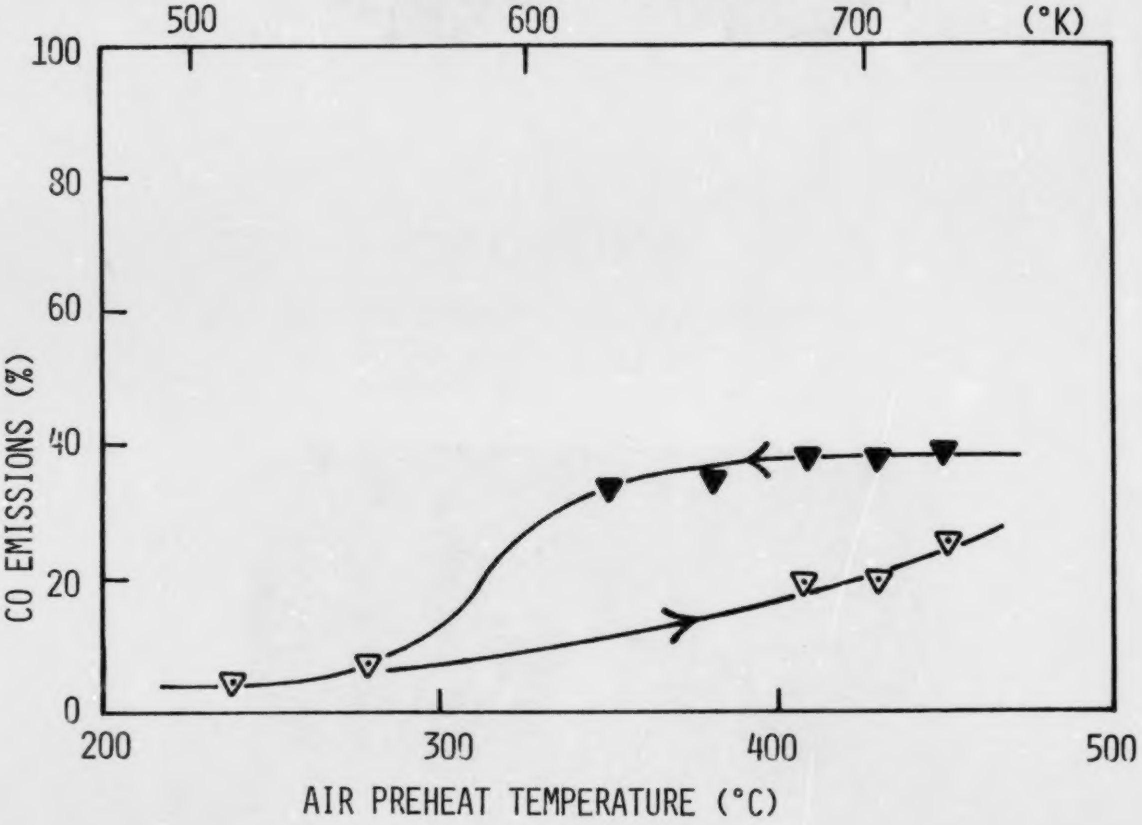

Figure 9. Carbon monoxide activity responses after 1014 hours using catalyst core DXE-442.

INLET ENDS

UPSTREAM
S/N 4070 J-12
DXE-442

DOWNSTREAM
S/N 4070 J-1
DXE-442

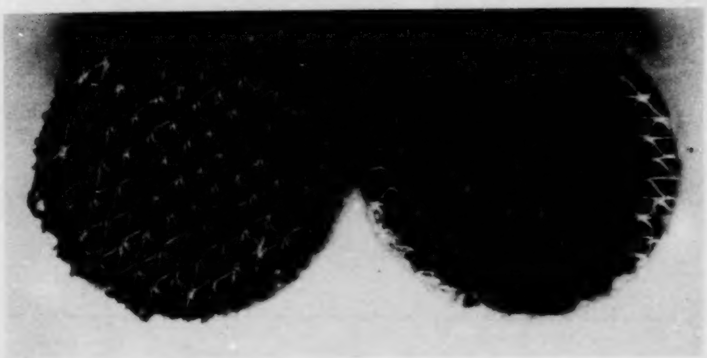

OUTLET ENDS

UPSTREAM
S/N 4070 J-12
DXE-442

DOWNSTREAM
S/N 4070 J-1
DXE-442

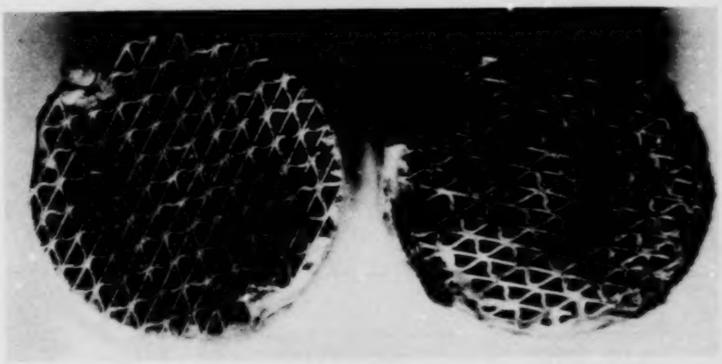

Figure 11a. Photographs of catalyst core DXE-442 after 1000 hours life testing.

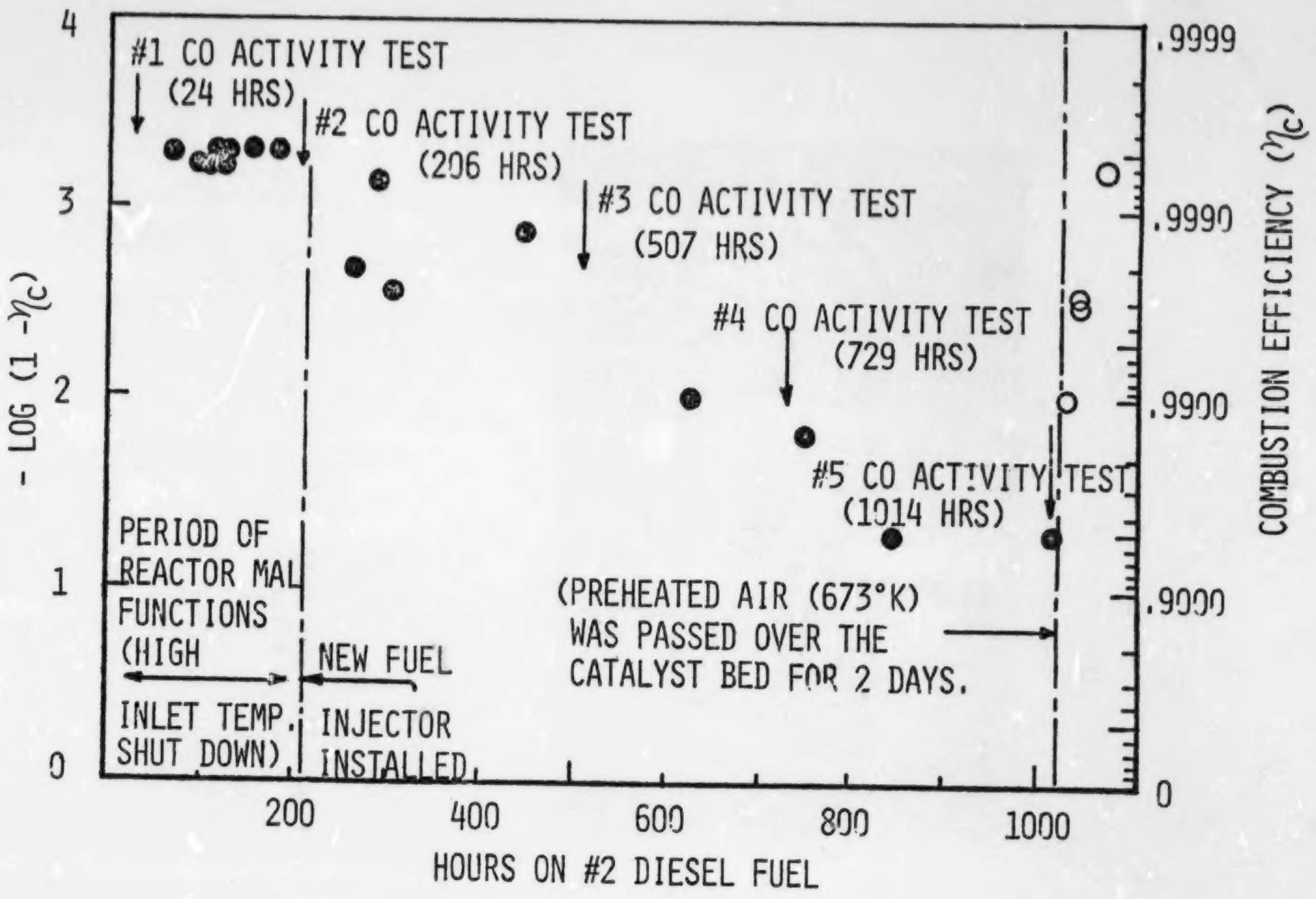

Figure 10. Response of combustion efficiency during five atmospheres life testing.

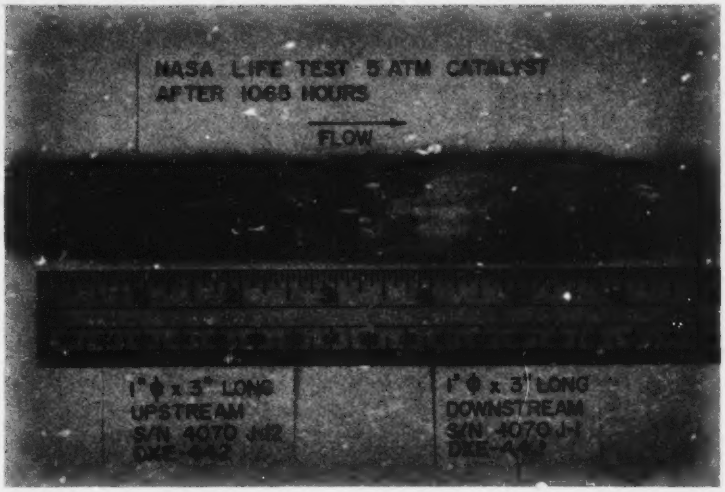
NASA LIFE TEST 5 ATM CATALYST
AFTER 1068 HOURS
FLOW
1" ϕ x 3" LONG
UPSTREAM
S/N 4070 J-2
DXE-442
1" ϕ x 3" LONG
DOWNSTREAM
S/N 4070 J-1
DXE-442

Figure 11b. Photographs of catalyst core DXE-442 after 1000 hours life testing.

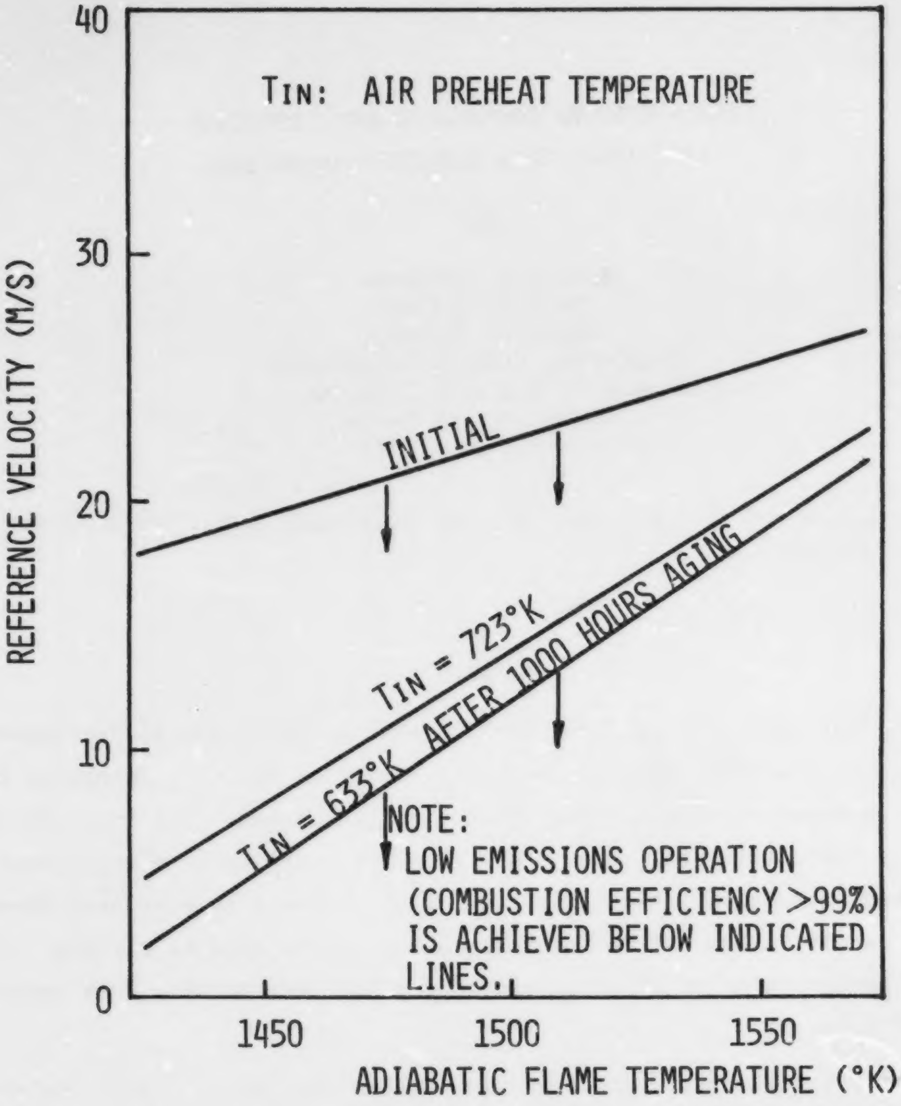

Figure 12. Low emissions operating condition range.

FUEL-NITROGEN CONVERSION AND COMBUSTION EFFICIENCY IN A CATALYTIC COMBUSTOR

By:

Ronald D. Matthews
Mark L. Graham
Jeryl L. Lederman
Combustion Science Laboratory
Department of Mechanical Engineering
University of Texas
Austin, TX 78712

This work supported, in part, by a DOE Institutional Energy Grant to the University of Illinois.

ABSTRACT

This manuscript reports the initial stages of the eventual development of a phenomenological model that can be used to predict fuel-NO_x emissions from catalytic combustion systems. The effects of radial heat loss rate and inlet velocity on combustion efficiency and fuel-NO_x conversion were experimentally investigated. The radial heat loss rate is of interest because envisioned practical catalytic combustors incorporate concentric annular airflow. Because of the different inlet velocities used by various researchers, this parameter is also of interest.

An experimental catalytic combustion system was designed and constructed which allowed the radial heat loss rate to be varied from 0-15% of the energy release rate. The inlet velocity was varied over the range 5-25 cm/s. The equivalence ratio and volumetric energy release (adiabatic flame temperature) were decoupled using argon as a diluent. The equivalence ratio was varied from 0.5 to 1.25 and volumetric energy release cases of 6.2, 8.3, and 10.6 kcal per mole of reactant mixture (T_{AD} = 1400, 1700, 2000K) were used.

It was found that radial heat losses up to 12% of the energy release rate could significantly affect the temperature distributions in the catalytic combustor. This, in turn, can decrease the combustion efficiency and will probably decrease the NO yield (resulting in, presumably, higher unburned fuel-N concentrations in the exhaust). The effect of radial energy loss becomes more pronounced as the mixture gets leaner. Higher inlet velocities also increase the average combustor temperature, resulting in higher combustion efficiencies and NO yields. Increasing the volumetric energy release also increases the combustion efficiency and the NO yield.

This project was supported, in part, by a Department of Energy Institutional Energy Grant to the University of Illinois at Urbana-Champaign. This work was carried out at the Combustion Research Facility, Department of Mechanical Engineering, University of Illinois between May 21, 1978 and December 21, 1979.

ACKNOWLEDGMENTS

The authors would like to thank William F. Hammett who set up the experimental apparatus and obtained the initial data (W. F. Hammett, A. Study of Catalytically Stabilized Combustion at Equivalence Ratios Including Stoichiometric, MS Thesis, University of Illinois, August, 1978). We are also tremendously grateful to Che-Kwan Shum, Ph.D. candidate in Aerospace Engineering at the University of Texas, for developing and running the computer graphics programs.

INTRODUCTION

The use of catalytic combustors in systems that operate with near-stoichiometric mixtures has been the subject of recent research interest (References 1-7). One of the several advantages of catalytic combustors is that they have exhibited a very wide fuel tolerance, being capable of burning fuels as disparate as low-Btu gas (References 5, 6, 8-11), distillate and residual fuel oils (References 7-9, 11), and possibly even pulverized coal (Reference 13). It is probable that those systems that are required to operate near stoichiometric because of system efficiency considerations will also be required to use non-traditional fuels such as these in the future.

Unfortunately these fuels generally contain significant concentrations of bound nitrogen (fuel-N). Investigations of fuel-N in gas phase combustion systems have shown that fuel-bound-nitrogen is oxidized to NO_x (fuel-NO_x) at up to 100% efficiency while molecular nitrogen is oxidized (to thermal-NO_x) at less than 1% efficiency (References 14-16). Most of the combustion modifications that are successful in controlling thermal-NO_x adversely affect fuel-NO_x. Water injection, increased mixing intensity, and inert addition all increase fuel-NO_x (References 17-19). Flue gas recirculation may increase (Reference 20), decrease (Reference 21), or have no effect (Reference 22) on fuel-NO_x. Only staged combustion (References 22, 23) and catalytic combustion (References 1-6) have shown the potential to simultaneously control both thermal-NO_x and fuel-NO_x. In fact, the combination of these two combustion modifications - staged catalytic combustion - appears to be one of the most promising techniques available for decreasing pollutant emissions while maintaining or improving combustion efficiency.

A portion of the results of catalytic combustion fuel-NO_x studies is shown in Figure 1, which exhibits the effect of equivalence ratio on fuel-NO_x yield (the mass ratio of nitrogen in the products as NO_x to fuel-N in the reactants). These results agree qualitatively but the quantitative discrepancies are significant. This paper reports an initial effort to examine the reasons for these discrepancies with an eventual goal in mind of developing a phenomenological model that can be used to predict fuel-NO_x emissions from catalytic combustion systems.

OBJECTIVES

This report is a condensation of the Master's theses of Mr. Graham (Reference 24) and Mr. Lederman (Reference 25). They investigated the effects of radial heat loss and reference (inlet) velocity on combustion efficiency and fuel-N conversion in a catalytic combustor. This was the initial stage of an explanation of the differences in the data of various researchers as depicted in Figure 1. The eventual goal of the project is the development of a phenomenological model that can be used to predict fuel-NO_x emissions from catalytic combustors.

The researchers whose results were used to construct Figure 1 had several experimental conditions in common and several more that were different. All used a ceramic monolith supporting a platinum catalyst. All but Pogson and Monsour (Reference 7) used NH_3 as the model fuel-N compound. (It has been shown that fuel-NO_x conversion is only weakly dependent on fuel-N species in both gas-phase and catalytic combustion systems, (References 1, 3, 14)). Matthews and Sawyer (Reference 1) used fuel-N fractions of 1.75 wt % and 5.0 wt %, Chu and Kesselring (Reference 3) used 2.0 wt %, and Folsum et al (Reference 6) used 0.2 wt % and 1.0 wt %. (The effect of fuel-N fraction is shown in Figure 2. The data of Chu and Kesselring is for different conditions than those discussed here, including a different catalyst). All but Matthews and Sawyer used graded cell catalysts. Matthews and Sawyer did not use air preheat although the other researchers did. Matthews and Sawyer report a maximum bed temperature of 1100K for an adiabatic flame temperature of 2000K while Folsum and coworkers report holding the bed temperature near their adiabatic flame temperature, 1473K. Chu and Kesselring report a bed temperature of 1367K and Pogson and Mansour report the bed temperature ranging from 1340 to 1540K. Matthews and Sawyer decoupled the equivalence ratio and adiabatic flame temperature by using an oxygen/argon mixture as the oxidant. Folsum et al and Chu and Kesselring accomplished this by using an air/nitrogen mixture. Pogson and Mansour did not decouple these parameters but did use argon or nitrogen dilution in some cases to insure that the temperature never exceeded the failure temperature of the quartz housing, 1600K.

The most important differences in the operating conditions used by these researchers are considered to be inlet velocity (and therefore space velocity and energy release rate), radial heat transfer boundary condition, and fuel characteristics. Pogson and Mansour used #6 fuel oil, Folsum and coworkers used a simulated low-Btu gas consisting of CH_4, H_2, and CO, and the other researchers used C_3H_8. The reference velocities used ranged from 5 cm/s by Matthews and Sawyer to 3 m/s by Folsum et al and about 6 m/s by Chu and Kesselring. The velocity in the research of Pogson and Monsour varied from 2.3 to 4.6 m/s. The radial heat transfer boundary condition varied from backheating (heat addition) by Folsum et al to free convection energy loss in the work of Matthews and Sawyer and insulation by the other researchers. This radial boundary condition is of interest because envisioned practical catalytic combustors (References 2, 26-28) have concentric annullar airflow around the catalytic combustor. This, in turn, might affect temperature profiles and combustion efficiency. The purpose of the research reported in this manuscript was to investigate the effects of inlet velocity and radial energy loss on fuel-nitrogen conversion and combustion efficiency. It is believed that these factors are the major parameters of interest in the development of a phenomenological model.

EXPERIMENTAL APPARATUS AND CONDITIONS

The experimental apparatus is similar to that used by Matthews and Sawyer (Reference 1). The flowrates of C_3H_8, O_2, Ar, an Ar/NH_3 mixture, and the coflowing air (used in the radial heat loss cases) were controlled using calibrated rotameters. Unburned hydrocarbons were measured using an FID, NDIR's were used to detect CO and CO_2, and chemiluminescent analysis was used to quantify NO. It was found that the low third body quenching efficiency of Ar offset the high quenching efficiencies of CO_2 and H_2O, yielding a maximum error of 6% due to the relative quenching efficiencies of product third bodies in chemiluminescent analysis (Reference 29).

The combustor was a 51 mm diameter single grade cordierite monolith with an α-alumina washcoat and a 0.187 wt % Pt loading. Upstream from the combustor was a blank ceramic monolith which served as a heat shield to protect glass beads which were used to flatten the velocity profile. The beads, heat shield, and combustor were housed in a stainless steel tube. Outside of this SS housing was either 1) 6 inches of Babcock and Wilcox K30 insulating firebrick with a mean thermal conductivity of 0.288 W/(m-K), or 2) in the radial heat loss cases, a coflowing annular air stream which passed through a conical housing.

Combustion occured at atmospheric pressure and the reactants were not preheated. Inlet velocities of 5, 10, and 25 cm/s were investigated. The O_2/Ar oxidant mixture was used to decouple the equivalence ratio and the equilibrium adiabatic flame temperature (References 1, 24, 25). The equivalence ratios studied ranged from $\phi = 0.5$ (100% excess air) to $\phi = 1.25$ (80% theoretical air). Adiabatic flame temperatures of 1400, 1700, and 2000K (corresponding to volumetric energy release rates of 6.2, 8.3, and 10.6 kcal released per mole of reactant mixture) were studied. Radial heat loss rates were varied from practically zero for the insulated cases up to 15% of the energy release rate.

RESULTS AND DISCUSSION

The effects of radial heat loss and inlet velocity on fuel-N conversion and combustion efficiency were investigated for various equivalence ratios and adiabatic flame temperatures. The combustion efficiency is defined by:

$$\eta_c = \Delta E_{act}/\Delta E_{theo}$$

where ΔE_{act} is the actual energy release rate and is determined from

$$\Delta E_{act} = \Sigma \eta_P h_P - \sum \eta_R h_R$$

where h_P is the enthalpy of each product species at the combustor exit temperature and η_P is the number of moles of each product species formed per mole of fuel burned (obtained from the exhaust gas analysis data, accounting for those species measured on wet and dry bases, and assuming that the total number of moles of products formed per mole of fuel burned, $\Sigma\ \eta_P$, is negligibly different in the actual case than for equilibrium reaction at the combustion temperature). The last term, $\Sigma\ \eta_R h_R$, is the enthalpy of the reactants at room temperature and reduces to the enthalpy of formation of propane. The theoretical energy release is determined from

$$\Delta E_{theo} = \Sigma\ \eta_P' h_P' - \Sigma\ \eta_R h_R$$

where η_P' is the number of moles of each product for equilibrium combustion at the average temperature along the axial centerline for the insulated (no radial energy loss) case corresponding to the particular equivalence ratio, volumetric energy release rate, and inlet velocity of interest. The product enthalpy term, h_P', is determined at 298K. Note that the combustion efficiency is similar to the enthalpy efficiency, η_H, except that the denominator in the definition of η_H is the Lower Heating Value of the fuel. That is, the heat of reaction, ΔH_{R298}, is the denominator of both η_C and η_H, but η_C uses equilibrium products and η_H assumes complete combustion. As expected, it was found that there was no difference in η_C and η_H for lean combustion and only a small difference for rich combustion up to $\phi = 1.25$. The combustion efficiency is presented in this paper because it is the more physically significant of the two.

Figure 3 shows the radial temperature distributions for five axial locations in the combustor. Separate graphs for lean, stoichiometric, and rich operation are presented. The data for Figure 3 was obtained with the combustor insulated. The peak temperature occurs at $\phi = 1.25$, is about 50K lower for the $\phi = 1.0$ and $\phi = 0.75$ cases, and drops an additional 100K for $\phi = 0.5$ even though the equilibrium volumetric energy release (and therefore the adiabatic flame temperature) is constant for all four cases. As expected, the radial temperature profiles are relatively flat. However, the temperature of the upstream face decays rapidly near the edge of the combustor. The temperature differential between the center of the upstream face and the outer edge is not affected by the equivalence ratio but the rate of temperature decay and the portion of the leading edge affected increases as the mixture gets leaner. For $\phi \leq 1.0$, the temperature at $x/L = 0.25$ also decays over the outside 25% of the radius. Therefore, even for an insulated combustor, portions of the temperature distribution appear to be affected by heat transfer losses.

Figure 4 demonstrates the effect of radial heat loss on the temperature distributions for the maximum radial heat loss operating condition. The radial heat loss was obtained by setting the coaxial air flowrate and then varying the mixture ratio in the combustor. Because the combustor temperature was dependent on ϕ (even though ϕ and the volumetric energy release had been decoupled), the radial heat loss rate varied slightly from one equivalence ratio to the next. It is apparent from Figure 4 that radial energy losses significantly affect the axial and radial temperature distributions. In fact, only for rich operation is the peak temperature located at the center of the leading edge of the catalyst. For the $\phi = 0.5$ case, the radial profiles 3/4 up and at the trailing edge are not affected but the temperatures throughout the rest of the catalyst are significantly decreased and show significant radial temperature gradients, especially at the axial plane 1/4 up from the upstream face. With radial heat loss, the upstream face evidences the lowest temperatures, rather than the highest temperatures as was observed for the insulated combustor. For $\phi = 0.75$, the peak temperature is depressed about 200K and there are significant temperature gradients on all axial planes except the downstream face and there is a uniform 50K temperature decrease on this plane. The same general trends are evident for the stoichiometric and rich operating conditions, with lower temperatures throughout the catalyst, especially the upstream face, and steep radial temperature gradients except for the downstream face. The rich data shows the least effect of radial heat loss, with only small differences at $x/L = 0.75$ and $x/L = 1.0$ (downstream plane).

Figure 5 shows the effects of radial heat loss in a slightly different manner. Here the combustion temperature is taken as the average of the five axial temperatures at any given radial location. It is seen that radial heat loss depresses the average temperature throughout the catalyst and increases the average radial temperature gradient. In most cases, the magnitude of radial heat loss is not as significant as the fact that there is heat loss. This is most apparent for the leanest operating condition.

The effect of radial heat loss on combustion efficiency is shown in Figures 6 and 7. Figure 6 shows the characteristic increase in combustion efficiency with increasing equivalence ratio. However, η_c continues to increase past $\phi = 1.0$. This is probably due to the previously noted fact that radial heat loss had the least effect on the fuel rich case. This trend is more visually apparent in Figure 7, which is a graph of relative heat loss rate versus combustion efficiency for the four equivalence ratios studied. For $\phi = 1.25$, increasing heat loss depresses the combustion efficiency only slightly. For stoichiometric and lean mixtures, 3-5% heat loss depresses η_c by 5-20% and approximately doubling the radial heat loss does not result in a further decrease. (In fact, for $\phi = 0.75$, the efficiency appears to increase again. This fact is not readily explainable, but is probably due to a deficiency in the data.) Note that the temperature profiles of Figure 5 also showed the largest change with initial heat loss with generally smaller changes for a further increase in the radial heat loss rate.

The data of Figures 3-6 were obtained with an inlet velocity of 10 cm/s and a volumetric energy release of about 10.6 kcal per mole of reactant mixture (i.e., T_{AD} = 2000K). Figure 8 demonstrates the effect of inlet velocity and volumetric energy release on the average axial centerline temperature and on the combustion efficiency. The data for Figures 7-11 were obtained with an insulated combustor. As evident in Figure 7, the combustion temperature increases significantly with increasing inlet velocity for all cases except for fuel rich combustion at a volumetric energy release of 6.8 kcal/gmole (T_{AD} = 1700K). The combustion efficiency also increases with increasing velocity except for the stoichiometric and fuel rich cases at T_{AD} = 2000K. Attempts to obtain data at 25 cm/s were unsuccessful because of unstable operation.

Figure 9 is a plot of η_c versus ϕ for the two inlet velocities and three volumetric energy release cases studied. It was found that the most stable combustor operation was obtained with the highest volumetric energy release, i.e. T_{AD} = 2000K. The 2000K data shows an increase in η_c with increasing inlet velocity. The 10 cm/s data indicates an increase in η_c with increasing volumetric energy release (T_{AD}).

Figure 10 illustrates the effect of equivalence ratio on the NO yield. The characteristic decrease of NO yield from stoichiometric operation to fuel rich operation was observed (see Figure 1). More importantly, it is seen that increasing the inlet velocity will increase the NO yield for fuel-lean conditions, thereby partially explaining the differences in the results of Matthews and Sawyer and those of Chu and Kesselring. This is probably due, at lease in part, to the higher bed temperatures obtained at higher velocities, as seen in Figure 5. It is also apparent that increasing the volumetric energy release (T_{AD}) increases the NO yield for both lean and rich operation. This is probably also partially due to the higher bed temperatures noted in Figure 5. Although exhause NH_3 was not specifically measured, it is assumed that lower NO yields correspond to higher exhaust NH_3 levels.

Unlike the data presented in Figures 6 and 7, the efficiencies and NO yields presented in Figures 8-10 are not averaged over the cross-sectional exit area of the combustor. This was not thought to be necessary because the radial temperature and species profiles for the insulated combustor were not appreciable. However, as shown in Figure 11, it was determined that radial gradients in the NO yield were apparent for stoichiometric and fuel-rich combustion. This effect would probably be even more pronounced for a combustor with significant radial heat losses.

SUMMARY AND CONCLUSIONS

The effects of radial heat loss and inlet velocity on combustion efficiency and fuel-nitrogen conversion in a catalytic combustor were investigated. Volumetric energy release rates of approximately 6.2, 8.3, and 10.6 kcal/gmole of reactants (T_{AD} = 1400, 1700, and 2000K) were studied and the fuel-air equivalence ratio was varied from 0.5 to 1.25.

Radial heat loss was investigated because envisioned practical catalytic combustors incorporate concentric airflow around the combustor. It was found that radial heat losses up to 12% of the energy release rate can significantly affect the temperature distributions in the combustor. This, in turn, can decrease the combustion efficiency and will probably decrease the NO yield (resulting in, presumably, higher unburned fuel-N concentrations in the exhaust). The effect of radial heat loss on temperature and combustion efficiency becomes more pronounced as the mixture gets leaner.

It was also determined that increasing the inlet velocity will also increase the combustor temperature. This was expected because the energy release rate and inlet velocity are directly coupled. An increase in the combustion efficiency and the NO yield was noted with increasing inlet velocity and increasing volumetric energy release (adiabatic flame temperature).

This manuscript reports the initial stages of the development of a phenomenological model which can be used to predict the fuel-NO_x emissions from a catalytic combustion system. More experimental research is necessary before the model can be formulated. Most notably, it is necessary to: 1) investigate the effect of inlet velocity over a wider range, up to the order of 5 m/s, thereby 2) increasing the bed temperature up to the adiabatic flame temperature. In order to explain Figure 2, it will be necessary to 3) vary the fuel-N concentration for various bed temperatures and equivalence ratios. Other parameters of interest include the 4) catalyst support configuration, 5) catalyst species, and 6) combustor operating pressure.

REFERENCES

1. Matthews, R.D., and R.F. Sawyer. Fuel Nitrogen Conversion and Catalytic Combustion, Paper No. 77-40, Fall Meeting, Western States Section/Combustion Institute, Lawrence Berkeley Laboratory Report LBL-6396, Berkeley, CA, 1977.

2. Krill, W.V., J.P. Kesselring, and E.K. Chu. Catalytic Combustion for Gas Turbine Applications. ASME Paper 79-GT-188, presented at the ASME Gas Turbine Conference, San Diego, CA, March 12-15, 1979.

3. Chu, E.K., and J.P. Kesselring. Fuel-NO_x Control in Catalytic Combustion. In: Proceedings - Third Workshop on Catalytic Combustion. Environmental Protection Agency Publication EPA-600/7-79-038, 1979. pp. 291-330.

4. Krill, W.V., and J.P. Kesselring. The Development of Catalytic Combustors for Stationary Source Applications. In: Proceedings - Third Workshop on Catalytic Combustion, Environmental Protection Agency Publication EPA-600/7-79-038, 1979. pp. 259-290.

5. Folsum, B.A., C.W. Courtney, and M.P. Heap. The Effects of LBG Composition and Combustor Characteristics on Fuel NO_x Formation. ASME Paper 79-GT-185, presented at the ASME Gas Turbine Conference, San Diego, CA, March 12-15, 1979.

6. Folsum, B.A., C.W. Courtney, and M.P. Heap. Environmental Aspects of Low Btu Gas-Fired Catalytic Combustion. In: Proceedings - Third Workshop on Catalytic Combustion. Environmental Protection Agency Publication EPA-600/7-79-038, 1979. pp. 345-384.

7. Pogson, J., and M.N. Monsour. Catalytic Combustion of No. 6 Fuel Oil. In: Proceedings - Third Workshop on Catalytic Combustion. Environmental Protection Agency Publication EPA-600/7-79-038, 1979. pp 111-138.

8. Pfefferle, W.C., R.M. Heck, R.V. Carrubba, and G.W. Roberts. Catathermal Combustion: A New Process for Low Emission Fuel Conversion. ASME Paper 75-WA/Fu-1, 1975.

9. DeCorso, S.M., S. Mumford, R.V. Carrubba, and R.M. Heck. Catalysts for Gas Turbine Combustors - Experimental Test Results. ASME Paper 76-GT-4, 1976.

10. Carrubba, R.V., and I.T. Ogersby. Catalyst Design Studies in Low Btu Gas Combustion. Presented at the Third Workshop on Catalytic Combustion, Asheville, NC, October 3-4, 1978.

11. Osgerby, I.T., R.V. Carrubba, R.M. Heck, and W.W. Bunker. Investigation of Process and System Design Variables for Catathermal Combustion of Low Btu Gas. ASME Paper 79-GT-66, presented at the ASME Gas Turbine Conference, San Diego, CA, March 12-15, 1979.

12. Anderson, D.N. Performance and Emissions of a Catalytic Reactor with Propane, Diesel, and Jet A Fuels. Presented at the Fall Meeting, Western States Section, the Combustion Institute. Palo Alto, CA, 1977.

13. Pfefferle, W.C. Liquid Droplet Heating and Vaporization in the Catalytic Combustor. ASME Paper 79-HT-52, presented at the ASME/AIChE 18th National Heat Transfer Conference, San Diego, CA, August 6-8, 1979.

14. Sarofim, A.F., and R.C. Flagan. NO_x Control for Stationary Combustion Sources. Progress in Energy and Combustion Science, 2: 1-25, 1976.

15. Sawyer, R.F., N.J. Brown, R.D. Matthews, M.C. Branch, and S.M. Banna. The Formation of Nitrogen Oxides from Fuel Nitrogen. Electric Power Research Institute Publication EPRI 223-1, 1976.

16. Matthews, R.D. The Nature and Formation of Nitrogenous Air Pollutant Emissions from Combustion Systems. Lawrence Berkeley Laboratory Report LBL-6850, 1977.

17. Wilkes, C., and R.H. Johnson. TIS Report 74-GTD-75, Technical Information Service, General Electric, 1974.

18. Fenimore, C.P. Effects of Diluents and Mixing on Nitric Oxide From Fuel-Nitrogen Species in Diffusion Flames. Sixteenth Symposium (International) on Combustion, the Combustion Institute, Pittsburgh,

1065-1071, 1977.

19. Appleton, J.P., and J.B. Heywood. The Effects of Imperfect Fuel-Air Mixing in a Burner on NO Formation from Nitrogen in the Air and in the Fuel. Fourteenth Symposium (International) in Combustion, the Combustion Institute, Pittsburgh, 777-786, 1973.

20. Brown, T.D., E.R. Mitchell, and G.K. Lee. Low NO_x Combustion: The Effect of External Flue Gas Recirculation on the Emissions from Liquid Fuel Combustion. Combustion Institute European Symposium. Academic Press, New York, 487-492, 1973.

21. Martin. G.B., and E.E. Berkaü. An Investigation of the Conversion of Various Fuel Nitrogen Compounds to NO_x in Oil Combustion. Presented at the AIChE National Meeting, Atlantic City, NJ, August, 1971

22. Turner, D.W., R.L. Andrews, and C.W. Siegmund. Influence of Combustion Modification and Fuel Nitrogen Content on Nitrogen Oxides Emissions from Fuel Oil Combustion. Combustion: 21-30, 1972.

23. Gibbs, B.M., F.J. Periera, and J.M. Beer. The Influence of Air Staging on the NO Emissions from a Fluidized Bed Coal Combustor. Sixteenth Symposuim (International) on Combustion, the Combustion Institute, Pittsburgh, 461-474, 1977.

24. Graham, M.L. Effect of Radial Heat Loss on Efficiency of a Catalytic Combustor. MS Thesis, University of Illinois, Urbana, IL, 1980.

25. Lederman, J.L. An Investigation of Parameters Affecting Fuel-NO_x Emissions from Catalytic Combustion Systems. MS Thesis, University of Illinois, Urbana, IL. 1979.

26. Flanagan, P., E.R. Norster, and R.J. Carrubba. Development of a Gas Turbine Combustor Utilizing a Catalyst. J. Energy, 3(2): 75-81, 1979.

27. Anderson, D.N., R.R. Tacina, and T.S. Mroz. Catalytic Combustion for the Automotive Gas Turbine. NASA TM X-73589, presented at the Fourth International Symposium on Automotive Propulsion Systems, Washington, D.C., April 17-22, 1977.

28. Enga, G.E. Catalytic Combustion in Actual Engines: A Summary of Engine and Rig Tests. In: Proceedings - Third Workshop on Catalytic Combustion. Environmental Protection Agency Publication EPA-600/7-79-038, 1979. pp. 491-512.

29. Matthews, R.D., R.F. Sawyer, and R.W. Schefer. Interferences in the Chemiluminescent Measurement of NO and NO_2 Emissions from Combustion Systems. Environmental Science and Technology, 11(12): 1092-1096, 1977.

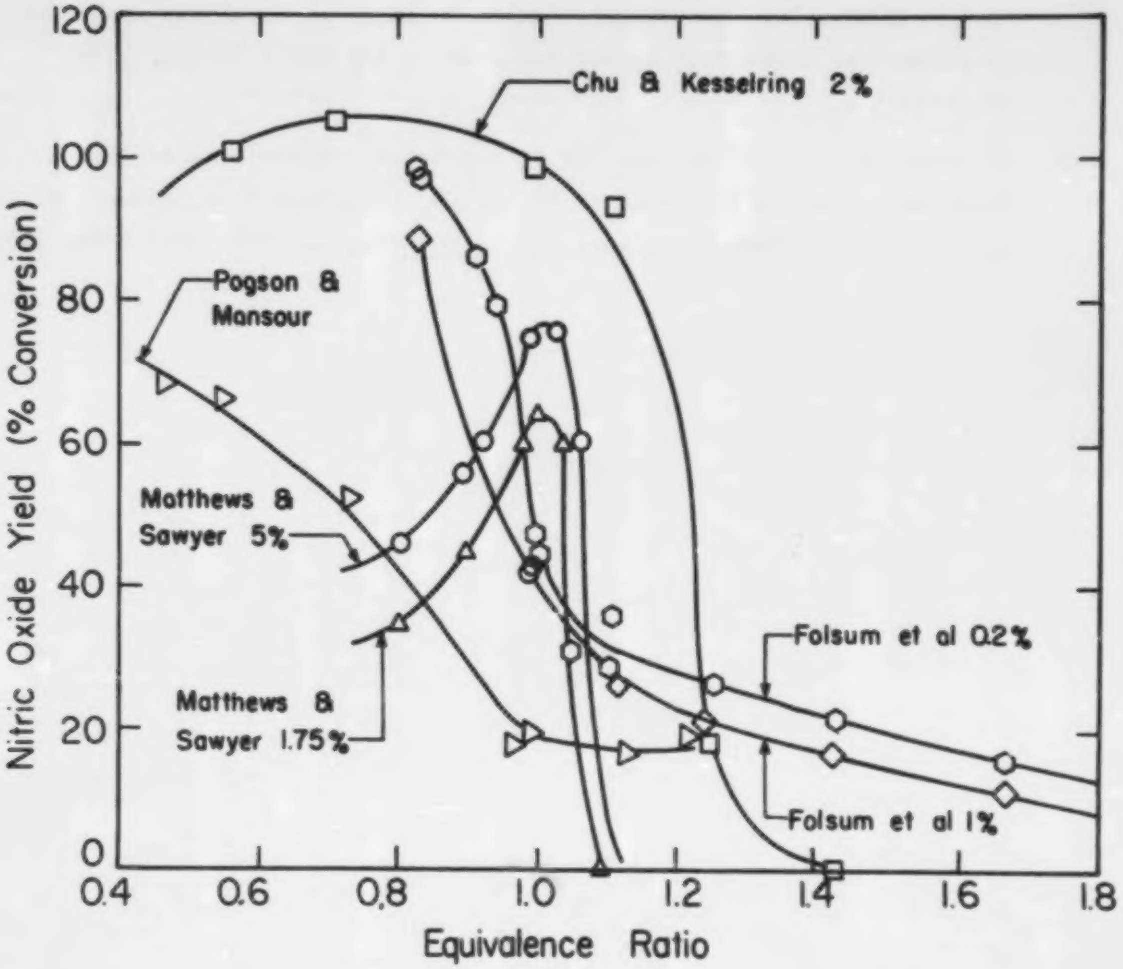

FIGURE 1. Experimental results from fuel-NO_x studies using catalytic combustion systems.

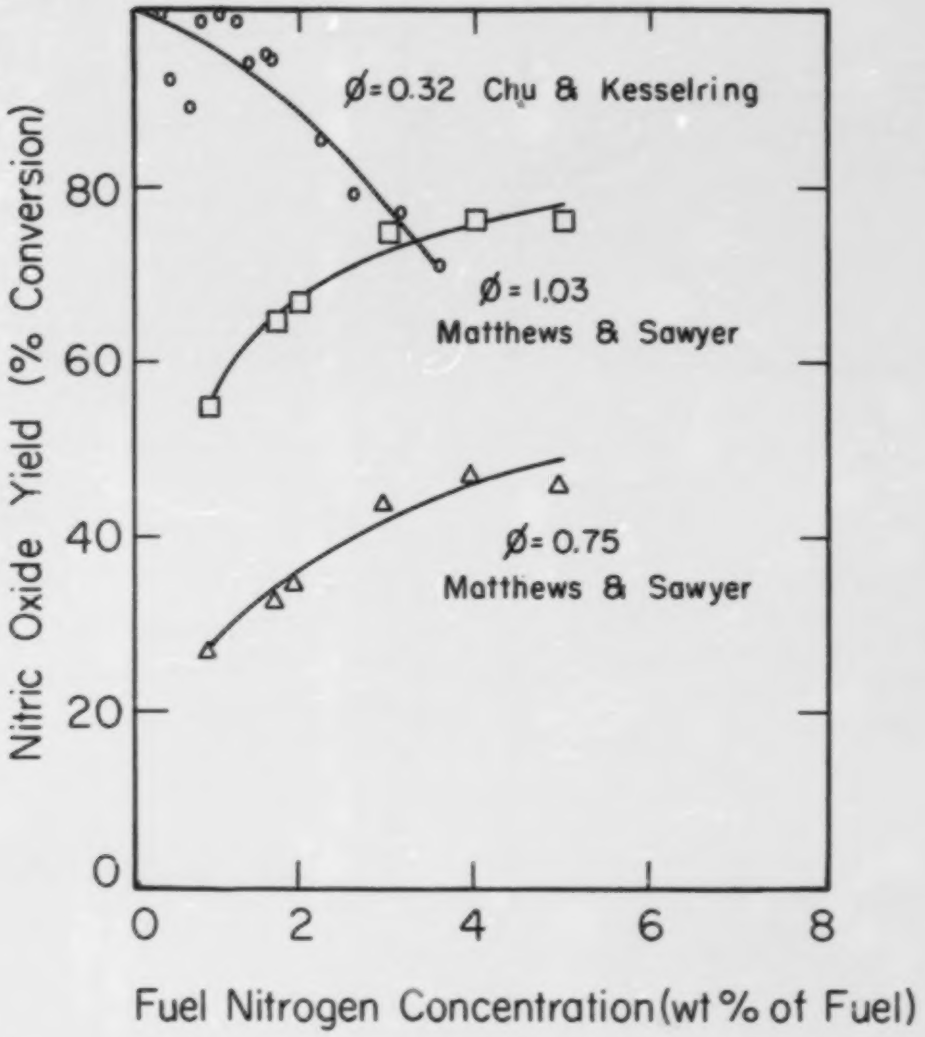

FIGURE 2. Effect of fuel-N concentration on fuel-NO_x production. The data of Chu and Kesselring is for different conditions than those of Figure 1 as discussed in the manuscript. Specific differences include a 1478K bed temperature, use of a proprietary UOP catalyst, and 3.1 m/s inlet velocity

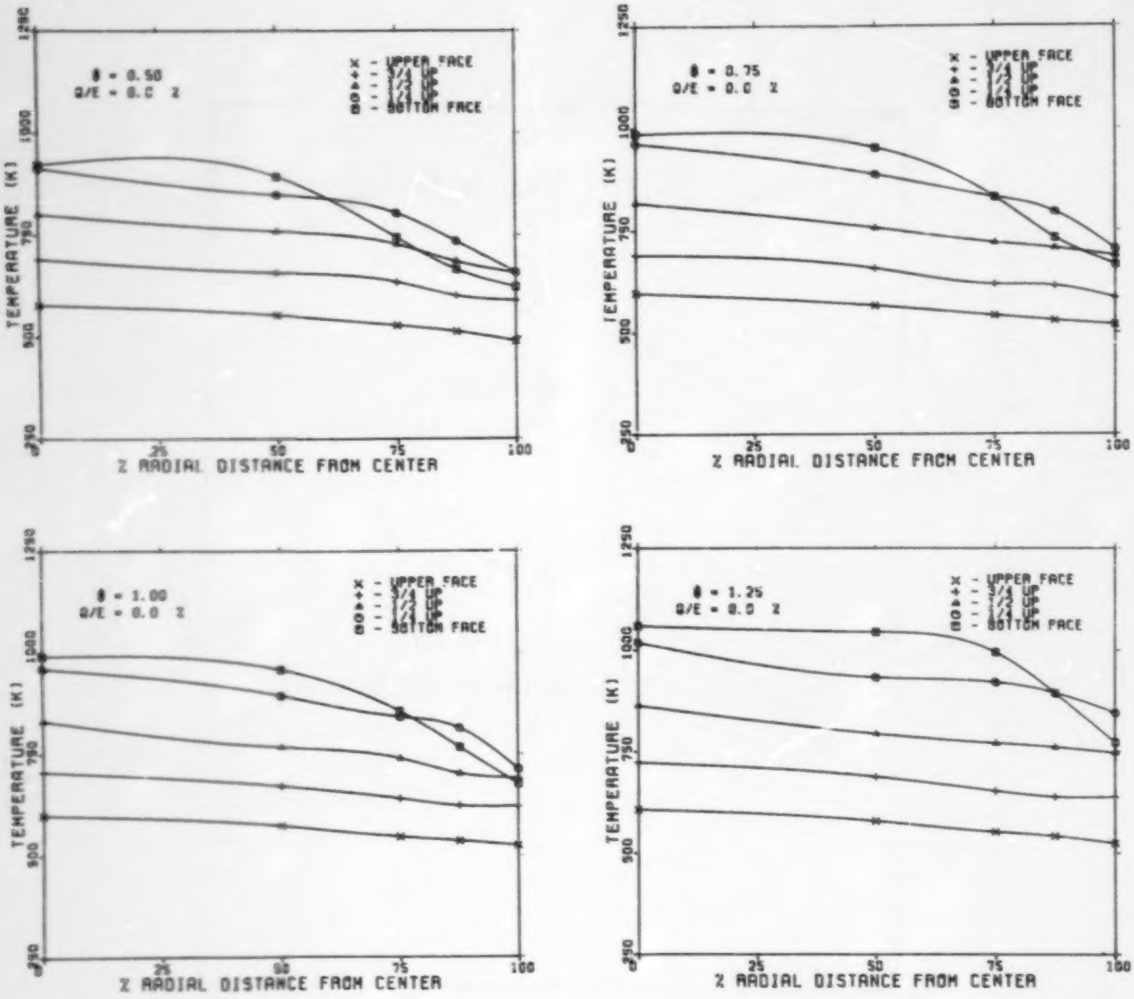

FIGURE 3. Radial temperature distributions at five axial locations for an insulated combustor. Bottom face = downstream plane of combustor. V_{IN} = 100 cm/s, T_{AD} = 2000K, 0% fuel-N.

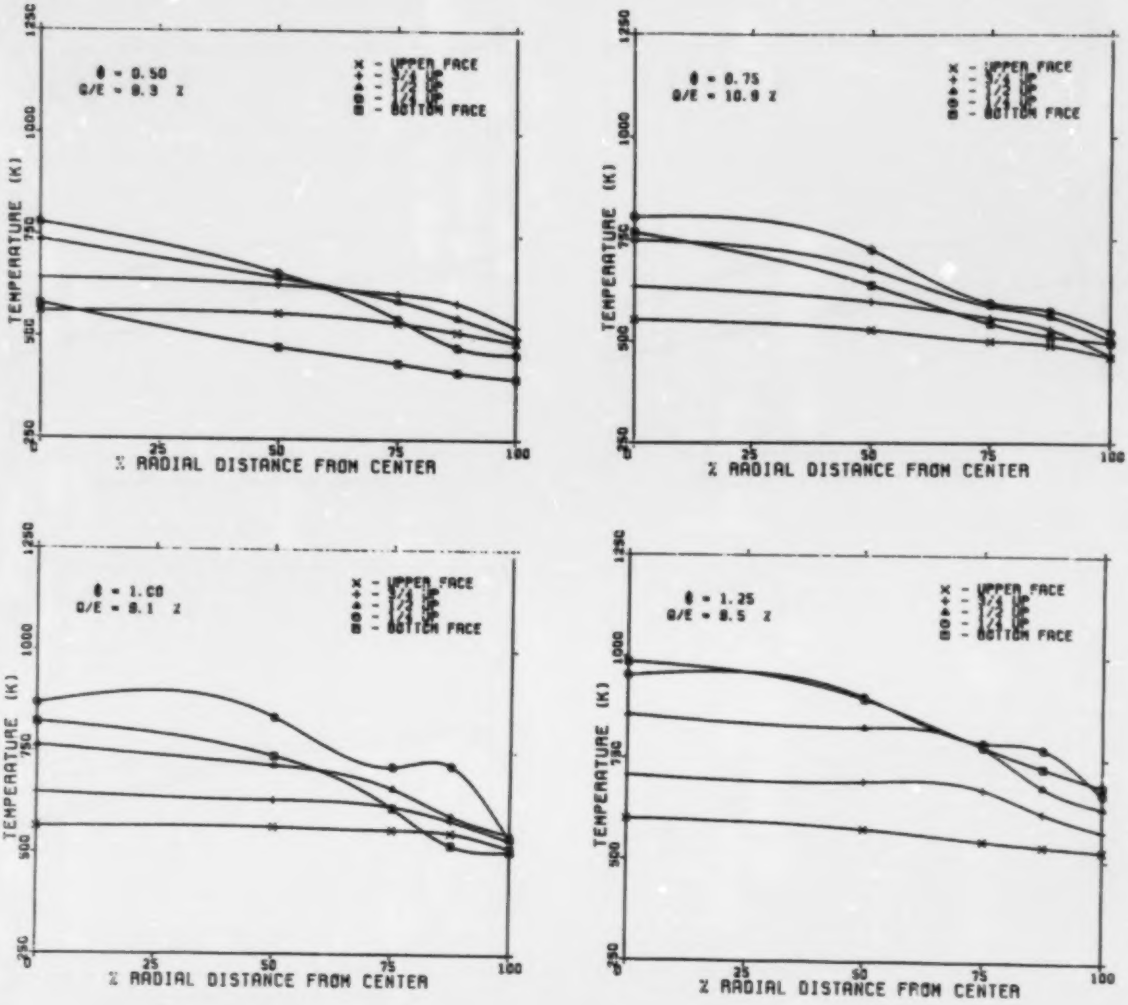

FIGURE 4. Radial temperature distributions at five axial locations with approximately 10% radial heat loss. Upper face = upstream plane of combustor. V_{IN} = 10 cm/s, T_{AD} = 2000K, 0% fuel-N.

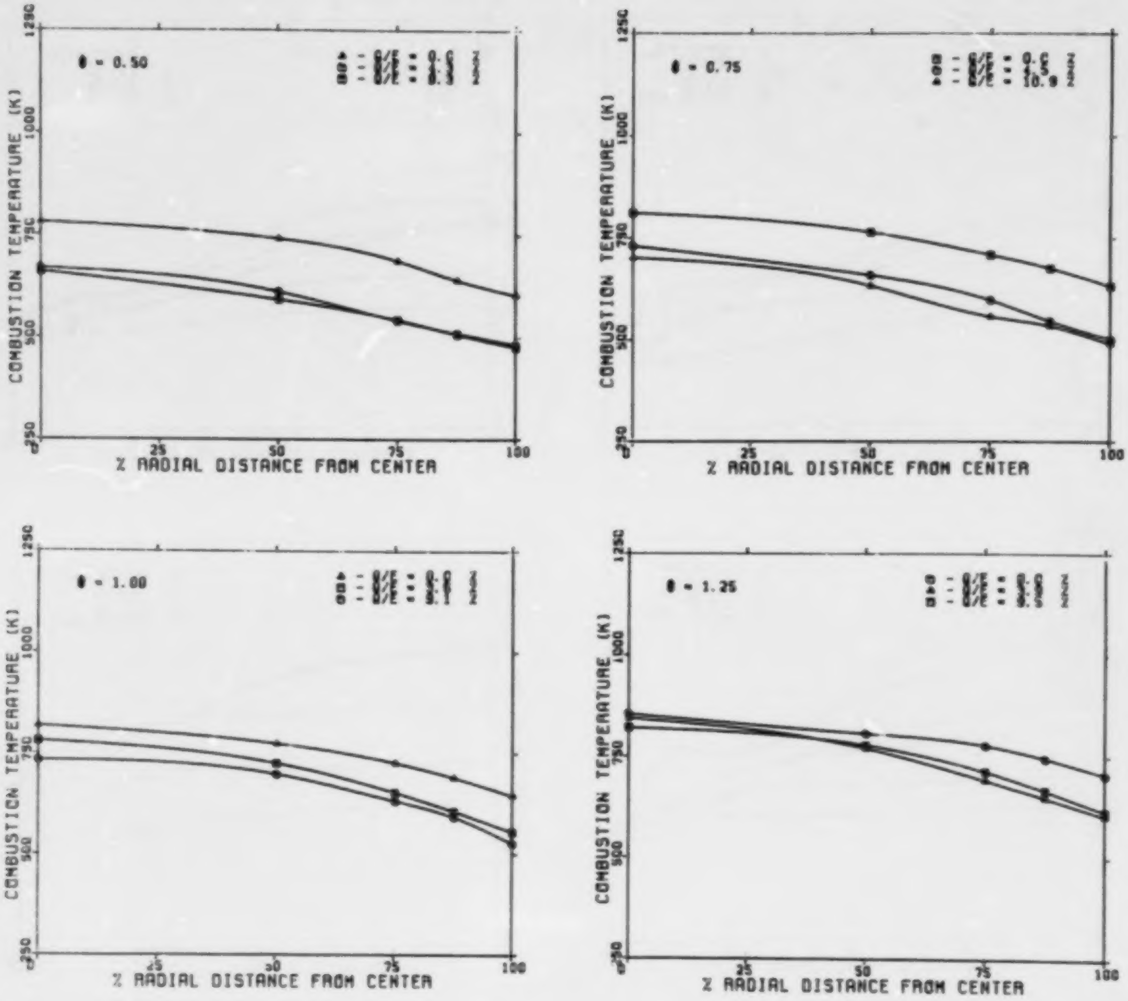

FIGURE 5. Radial temperature distributions of the average axial temperature for three radial heat loss operating conditions, V_{IN} = 10 cm/s, T_{AD} = 2000K, 0% fuel-N.

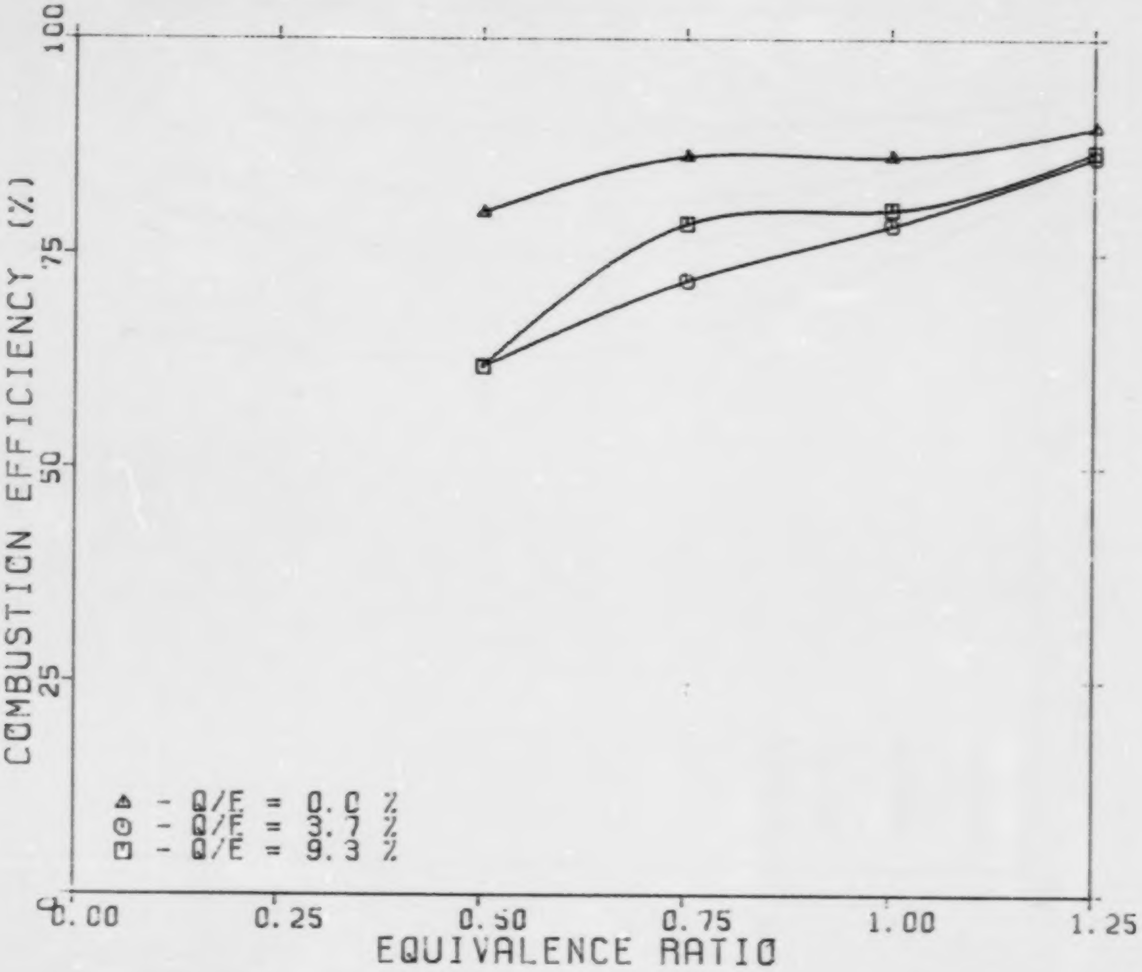

FIGURE 6. Effect of equivalence ratio on radially averaged combustion efficiencies for three different radial heat loss modes. V_{IN} = 10 cm/s, T_{AD} = 2000K, 0% fuel-N.

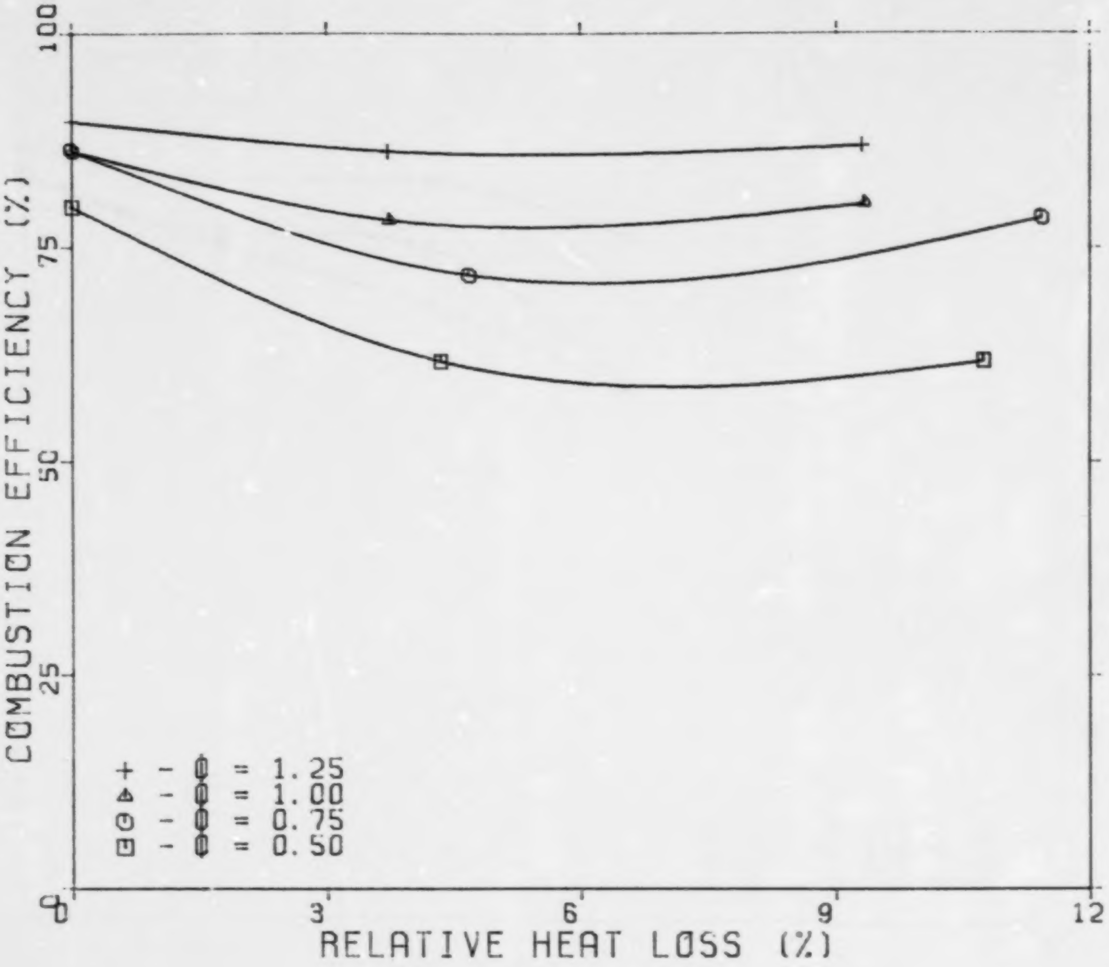

FIGURE 7. Effect of radial heat loss on radially averaged combustion efficiencies as a function of equivalence ratio. V_{IN} = 10 cm/s, T_{AD} = 2000K, 0% fuel-N.

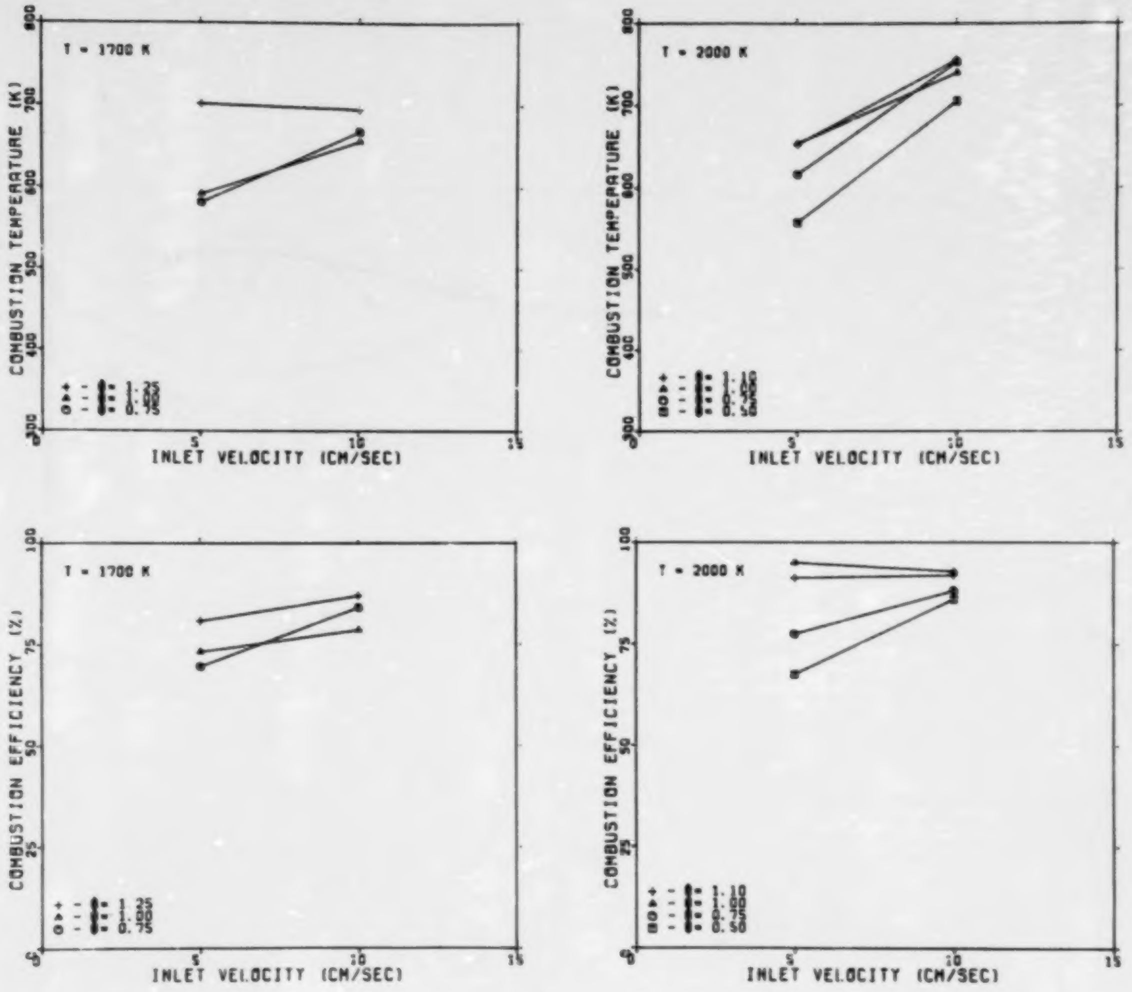

FIGURE 8. Effect of inlet velocity on the average axial centerline temperature and the axial centerline combustion efficiency for an insulated combustor and a mixture containing 2% fuel-N.

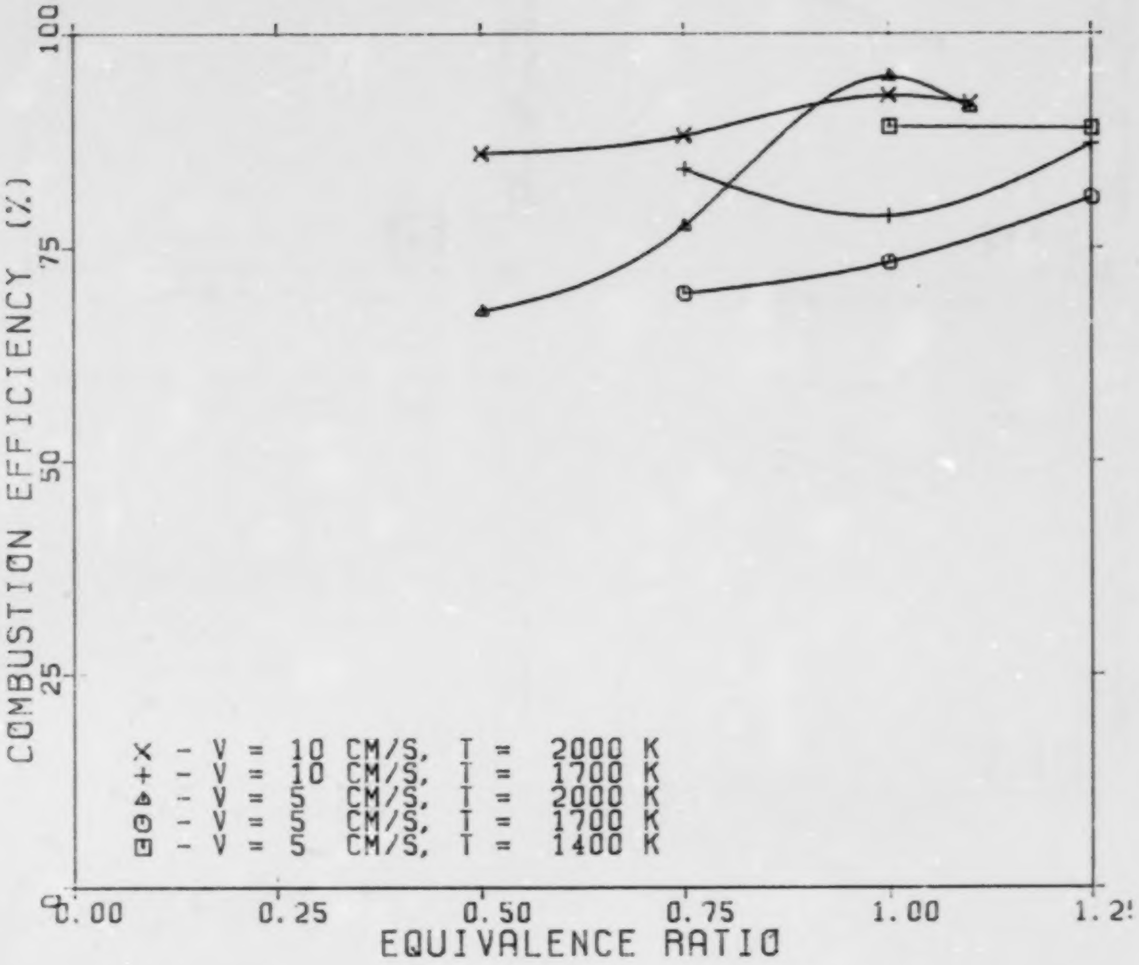

FIGURE 9. Effect of fuel/oxidant equivalence ratio on the axial centerline combustion efficiency as a function of inlet velocity and volumetric energy release for an insulated combustor and a mixture containing 2% fuel-N.

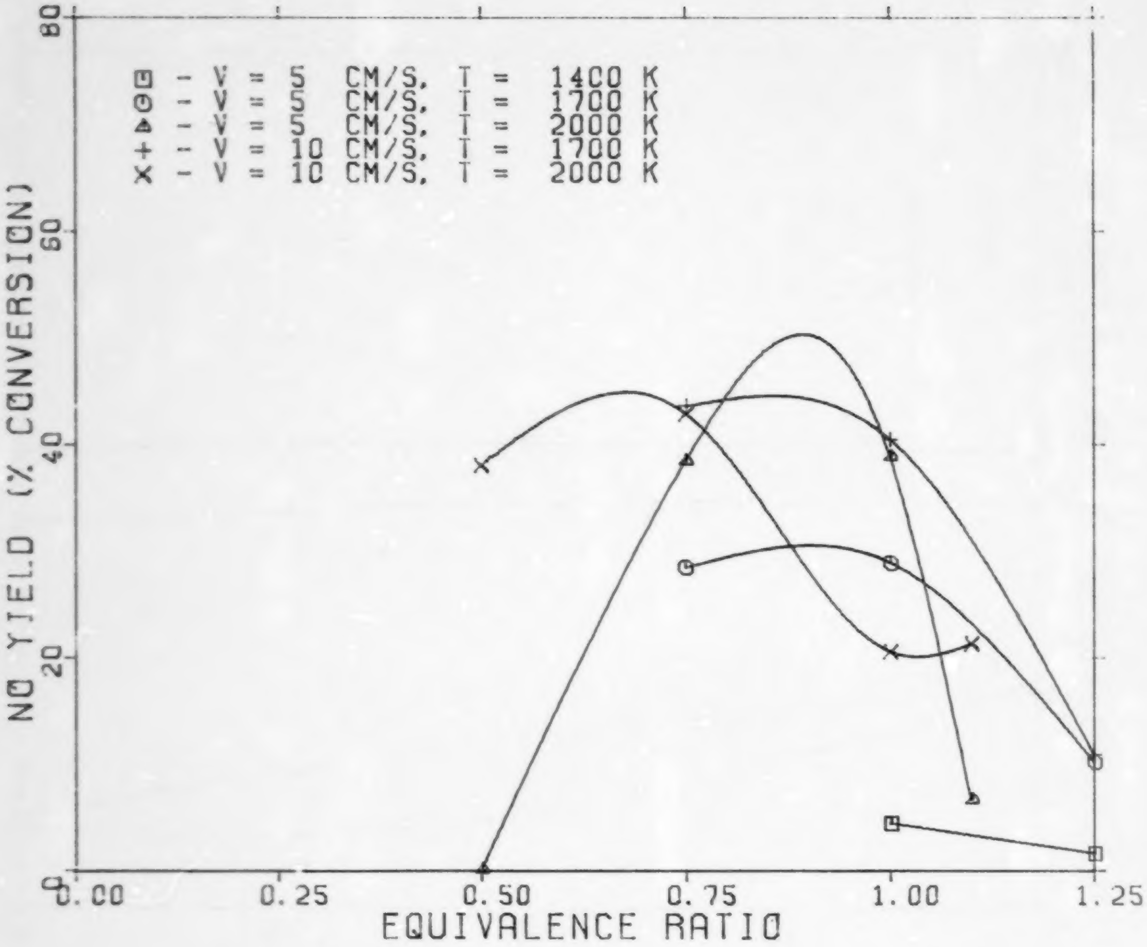

FIGURE 10. Effect of equivalence ratio on conversion of 2% fuel-N to NO for various operating conditions of an insulated combustor.

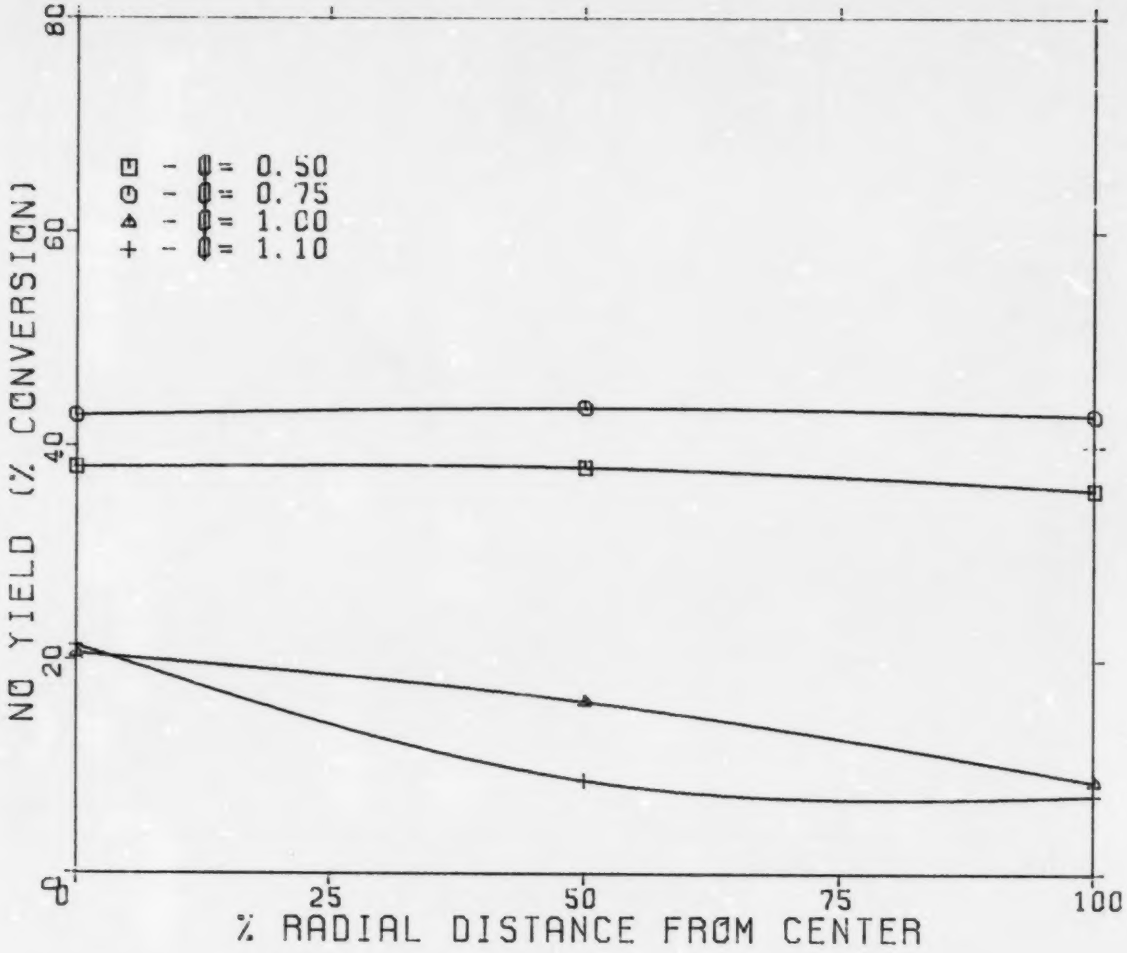

FIGURE 11. Radial gradients in the NO yield for an insulated combustor. V_{IN} = 10 cm/s, T_{AD} = 2000K, 2% fuel-N.

CATCOM* CATALYST AXIAL TEMPERATURE PROFILE MEASUREMENTS

By:

I. T. Osgerby
B. A. Olson
H. Lew
A. Cohn, Electric Power Research Institute

Engelhard Industries Division
Engelhard Minerals and Chemicals Corporation
Menlo Park, Edison, New Jersey 08817

ABSTRACT

Studies have been conducted by Engelhard under a Westinghouse subcontract (No. 51-9-644006) funded by EPRI (Contract No. RP421) to experimentally determine the performance characteristics of CATCOM* catalysts under simulated gas turbine combustion conditions using #2 diesel fuel. A series of axial catalyst monolith temperature profile measurements were made for two lengths of catalyst using small diameter, high temperature, sliding thermocouples positioned in sealed monolith channels. Process variable effects of air preheat temperature, adiabatic flame temperature (based on fuel/air ratios), catalyst inlet reference velocity, and catalyst length were determined. Combustion efficiencies greater than 99% were achieved at adiabatic flame temperature of 2150°F (1176°C) or greater and NO_x emissions averaged less than 3 ppm by volume. Catalyst durability for short time periods was demonstrated up to operating temperatures of 2600°F (1427°C) and at intentional upset conditions of fuel nozzle failure and partial blockage of the catalyst inlet face.

---

*CATCOM and CATATHERMAL are tradenames of Engelhard Minerals and Chemicals Corporation.

DEVELOPMENT OF IMPROVED CATALYST SYSTEMS

By:

J. P. Kesselring, W. V. Krill, M. J. Angwin,
and H. L. Atkins
Acurex Corporation/Energy & Environmental Division
485 Clyde Avenue
Mountain View, California 94042

ABSTRACT

The performance of a graded cell catalyst and a single cell catalyst of identical composition has been compared. The graded cell system achieved nearly three times the maximum throughput prior to surface blowout, and also showed significantly improved axial temperature uniformity. The development of catalytically active monolithic substrates was initiated with tests of five special formulations and three commercially available monoliths. All showed good combustion performance, but thermostructural weakness at high temperatures remains as a problem needing further investigation,

Work supported by U.S. Environmental Protection Agency Contract 68-02-3122.

INTRODUCTION

Limited fossil fuel supplies and environmental constraints make low emissions and high thermal efficiency necessities for combustion systems. Catalytic combustion is actively being investigated as a means of achieving these goals. Nearly all steady-state combustion systems -- including commercial and industrial boilers and furnaces, home heaters, and gas turbines -- can be modified or redesigned to incorporate catalytic combustors.

Catalytic combustors typically use ceramic or metallic honeycomb monolithic supports with many small diameter cells. As shown in Figure 1, premixed fuel and air flow through the cells, where a catalyst coating on the interior surface promotes conversion of fuel and air to combustion products. Near the cell entrance, where most of the gas is at low temperature, gas-phase chemical reactions are unimportant. In this region, catalytic wall chemical reactions control heat release. Further down the channel, where wall reactions have preheated the gas to high temperature, gas-phase reactions become active. In this region fuel is rapidly consumed by a "flame type" phenomenon which controls the amount of unburned hydrocarbon emissions that escape from the system.

Under normal operating conditions, wall and gas-phase reactions are active, and very little unburned hydrocarbon escapes the bed for lean and stoichiometric initial mixture ratios. However, experimental observations have shown that above a certain mass flow limit, small increases in flowrate cause an abrupt rise in unburned hydrocarbon emissions. The abruptness of the increase indicates that a "flame type" phenomenon has been extinguished. This condition, called breakthrough, represents an upper mass throughput for low unburned hydrocarbon emissions.

Increasing the mass throughput in a catalytic bed to levels much above the breakthrough point can cause the front of the bed to become cool. It has been experimentally found that small increases in mass throughput, once the front end of the bed has become cool, can cause the cool region to spread downstream. At this point, all wall reactions are extinguished and the entire bed becomes cold. This condition, called blowout, represents the maximum mass throughput for heterogeneous combustion.

Blowout and breakthrough for catalytic combustors depend on a number of parameters, including initial fuel/air ratio and temperature, honeycomb configuration and dimensions (cell diameter, void fraction, bed overall diameter), length of monolith, and bed and catalyst materials. As described in Reference 1, the use of a catalytic combustor system which has high mass throughput (high blowout limit) and low emissions (no breakthrough) can be constructed by joining two or more bed segments in series. The first segment has cells large enough to prevent blowout but small enough to convert sufficient fuel to meet the preheat/blowout requirement of the second bed segment. The second segment has smaller diameter cells to convert more of the fuel and further heat the bulk gases. The last segment has very small diameter cells and the entering gas preheat is sufficient to light off the homogeneous reactions. This system, called the graded cell catalyst, is depicted in Figure 2.

While the graded cell catalyst system is capable of achieving high throughput with low emissions, the question of catalyst life remains. Experimental results (Reference 2) have shown that maintaining a finely dispersed catalyst coating on substrate materials at high temperatures is difficult, and that the interaction between metal oxide catalysts and substrate materials at high temperatures can result in severe thermostructural weakening of the substrate. Therefore, the desirability of fabricating substrates directly from materials which include active oxides and which have adequate thermostructural strength is apparent. These systems, called active monoliths, are postulated to have improved life while operating at combustor temperatures.

The remainder of this paper describes graded cell and single cell catalyst comparative testing and formulation and testing of active monolith systems.

GRADED CELL AND SINGLE CELL CATALYST TEST RESULTS

The high throughput performance of graded cell catalysts had previously been documented (Reference 3), but a direct comparison between identical graded cell and single cell catalyst configurations had not been conducted. In order to compare the performance of the two systems, a series of comparative tests were run. Two catalyst configurations were supplied by UOP, Inc. on DuPont Torvex alumina honeycomb substrates. The graded cell system consisted of three 2.54-cm segments with cell sizes of 6.4 mm, 4.8 mm, and 3.2 mm. The single cell system used three 2.54-cm segments with a 3.2-mm cell size. Both systems were washcoated and catalyzed by UOP with a proprietary catalyst.

Pretest analysis of the single cell model indicated a surface area and dispersion of 4.88 m^2/g and 1.22 μmoles H_2/g, respectively, while the graded cell indicated 5.36 m^2/g and 17.63 μmoles/g catalyst. Although initially the graded cell had a much higher dispersion than the single cell, following 5 hours of aging, dispersion for both configurations should be essentially the same. This was verified by post-test analyses which indicated greatly reduced dispersions of 0.39 and 1.3 for the single and graded cell monoliths, respectively.

A comparison of the graded cell and single cell catalyst configurations, characterizations, and combustion performance on natural gas fuel is given in Table I. Both systems were operated in an identical manner during testing, which included 5 hours of steady-state operation under lean conditions at 1560K temperature, followed by maximum throughput tests. As a result of this testing, the following was noted:

- At a standard heat release rate of 105.5 MJ/hr, emissions from the graded cell and the single cell monoliths were approximately the same.
- Volumetric heat release at maximum throughput for the graded cell was almost three times higher than for the single cell system (7.4×10^6 J/hr-Pa-m^3 versus 2.6×10^6 J/hr-Pa-m^3).
- Under fuel-rich conditions, both reactor types maintained combustion at preheat temperatures as low as 320K. However, hydrocarbon emissions from the single cell configuration were an order of magnitude higher than for the graded cell catalyst, as shown in Figure 3.

- At the standard heat release rate of 105.5 MJ/hr, the graded catalyst had a much more uniform axial temperature profile than the single cell system

The HET code (Reference 1) was used to predict surface temperature profiles in the graded cell and single cell reactors, and the results are shown in Figure 4. Excellent agreement between code prediction and surface temperature as measured by in-depth thermocouples is noted. The more uniform temperature profile for the graded cell system is important, since in order to avoid poisoning effects, the catalyst should operate at as high a temperature as possible over its entire length. As shown in Figure 4, the single cell reactor runs a significant risk of being poisoned, while the graded cell reactor has a high, relatively uniform temperature profile. In addition to running the risk of poisoning, the single cell reactor is also operating in an unstable mode. A slight change in inlet conditions could move the reaction zone downstream in the combustor, eventually resulting in blowout.

These comparative tests verify that combustors with high volumetric heat release rates can best be achieved with catalysts in the graded cell configuration with no penalties in combustible or NO_x emissions. In addition, the high uniform temperature of the catalyst walls throughout the length of the graded cell model may have important implications in avoiding catalyst poisoning or liquid fuel deposition on the walls.

ACTIVE MONOLITH CATALYSTS

High temperature combustion catalysts have many requirements placed on their performance. They must be active in promoting the oxidation of hydrocarbons and carbon monoxide, be capable of high temperature use without melting or losing activity, maintain structural integrity in combustion conditions, and have good thermal shock resistance to withstand repeated thermal cycling. Currently available materials have difficulty in meeting all these requirements.

Since no ideal high temperature catalysts are available, choosing a material for high temperature catalytic use requires a series of assumptions and approximations. The first step is to test materials which are active at low temperatures and seem capable of tolerating high temperatures. Some of these materials have been tested under combustion conditions, and include:

- Platinum and other noble metals applied to high temperature substrates, such as alumina or zirconia
- Base metal oxides applied to high temperature substrates

Both types of catalysts showed good initial high temperature activity, but lost activity and structural stability after prolonged high temperature combustion. The noble metals tend to agglomerate or volatilize, while the base metals tend to interact with the substrate, destroying its structural stability.

To solve these problems, the active monolith concept was developed. In this type of catalyst, an active metal oxide or mixed metal oxide is incorporated into the structure of the monolith when the monolith is formed. This type of catalyst solves the problems inherent in the previously tested types of catalysts. It depends on base metals, thus eliminating the problem of noble metal agglomeration or volatilization. By incorporating the base metal directly into the monolith, interactions are controlled during the formulation steps and further interaction (destruction) should not occur during test conditions.

Active monoliths will have metal ions that can move readily between valence states; therefore, they are nonstoichiometric or defect structures. It is therefore reasonable to choose an active monolith where the defect structure is incorporated into a well-known refractory structure. One example of this type of system is $MgAl_2O_4 \cdot NiAl_2O_4$, where nickel is incorporated into the spinel structure. It is also important to use phase diagrams to choose high temperature ceramic formulations which will not melt at the intended use temperature, and which will have reduced volatility of the active metal oxide, thereby extending the lifetime.

Based on these configurations, five active "monoliths" were prepared by Trans-Tech, Inc. to Acurex specifications. Three were prepared by pressing and sintering oxide powders into disks approximately 5.7 cm in diameter and 3.2 cm long and drilling 18 to 30 0.64 cm holes axially. The other two were bundled sets of hollow tubes. The surface areas of these dense materials were assumed to be negligible. Table II lists the active monolith materials tested.

ACTIVE MONOLITH TEST RESULTS

Although all the active monoliths were produced with a single cell size and were limited in length and surface area, they showed good catalytic activity. Test results are summarized and compared in Table III.

For the three monolith disks, bed temperatures were undoubtedly higher than those recorded as the catalyst face was visibly cooler around the holes which had been plugged with ceramic cement to secure the bed thermocouples. The flow of mainstream air and fuel was also blocked on the monoliths at the bed perimeter, since there were no holes closer than 0.5 cm from the edge.

Model EPA-041 was a $MgAl_2O_4 \cdot NiAl_2O_4$ composition. Combustion was stable with natural gas under fuel-lean conditions down to a minimum preheat of 436K. Blowout of the catalyst bed did not occur at the highest throughput attained, 849,000 hr^{-1} space velocity. Combustion was relatively unstable with natural gas under fuel-rich conditions, operating only between preheat temperatures of 546K (523°F) and 621K (658°F). On diesel fuel, lean, EPA-041 sustained combustion to a minimum preheat of 587K. During maximum throughput, the bed was not blown out even at a space velocity of 1,152,000 hr^{-1}. Throughout the testing, CO emissions were below 50 ppm, and NO ranged from 1 to 30 ppm. After 10 hours, the center of the bed had cracked, and the thick outer ring had fractured cleanly into a few large chunks. The original blue color and smooth surface appearance were unchanged.

Model EPA-042 was a $LaAlO_3 \cdot LaCrO_3$ composition. This catalyst performed well on natural gas (rich and lean) and diesel (lean) fuels. Emissions of NO did not exceed 20 ppm. On natural gas, the minimum preheat was 464K, both lean and rich. At a throughput of 874,000 hr^{-1} space velocity, the bed was not blown out. Operating lean on diesel fuel, the minimum preheat was 589K, nearly the same as for EPA-041. Blowout occurred at a space velocity of 1,124,000 hr^{-1}. Post-test, the monolith retained its original red-brown color and chalky surface texture. As with EPA-041, structural breakdown occurred with moderate fracturing of the thicker outer section and greater fracturing of the thinner center sections.

EPA-045, the third Trans-Tech monolith model, was a $MgAl_2O_4 \cdot Fe_3O_4$ composition. Operating on natural gas, lean, the minimum preheat for this catalyst was 533K and the maximum space velocity was 874,000 hr^{-1} (without experiencing blowout). Minimum preheat on diesel, lean, was 397K. This was considerably lower than the minimum preheat temperatures for diesel fuel from earlier tests, where the required preheat temperature was at least 550K. NO emissions during this test increased slightly in the low preheat range, 533K to 397K, but did not exceed 30 ppm. EPA-045 was the least durable of the three Trans-Tech monoliths tested, cracking more severely during testing. The color changed from a dark brown with light brown patches to light brown on the exposed surfaces. This indicates the probable change in iron oxidation state to the catalytically active $MgFe_3O_4$.

The first set of tubes fabricated by Trans-Tech was a $MgAl_2O_4 \cdot MgCr_2O_4$ composition, Model EPA-046. This lavender-colored material was formed into 5.1 cm long tubes having nominal dimensions of 0.64 cm OD and 0.32 cm ID. Forty-four tubes, bundled and wrapped in Fiberfrax insulation, were supported vertically within a holder tube on a disk of alumina Torvex 2.5 cm long by 5.0 cm diameter, honeycombed with 0.48 cm diameter cells. Three tubes in the center of the bed were cemented together to form a cavity for the bed thermocouple.

Performance of EPA-046 on natural gas, lean, was good. CO and NO emissions were at or below 18 and 10 ppm, respectively, from preheat temperatures of 658K to ambient. There was no blowout of the bed up to a throughput of 8.8×10^6 J/hr-Pa-m^3. However, on natural gas, rich, and on diesel fuel, bed uniformity could not be maintained. From initial temperatures of 1644K to 1700K, the bed would cool and extinguish rapidly, beginning at the front face. There was no loss in catalytic activity after 5 hours of testing. Twelve of the tubes were broken; the rest were recovered undamaged.

The second set of Trans-Tech tubes (EPA-048) was of $MgAl_2O_2 \cdot Fe_3O_4$ in a 3:1 mole ratio with 40 percent Cr as a cermet. The tubes were 0.95 cm OD by 0.32 cm ID and were instrumented and supported in the same manner as EPA-046. On natural gas, the surface temperature was maintained below 1589K. Minimum preheat temperatures were 367K, lean, and 583K, rich. Blowout occurred at 8.8×10^6 J/hr-Pa-m^3. Also on natural gas, the minimum operating temperature was investigated by increasing theoretical air at a fixed preheat of 533K.

Stability became marginal below 1256K (1800^oF) as partial darkening occurred on the front face of the tubes.

To maintain combustion on diesel fuel, the surface temperature was raised to 1644K. Minimum preheat temperature observed was 683K. Operation was relatively poor, and due to difficulties in relighting the catalyst, diesel testing was terminated. During the 5-hour test period, combustion efficiency was good and NO emissions were less than 10 ppm. After testing, all the catalyst tubes were fractured. The tube ends of the front face of the bed had light brown streaks while the rest of the catalyst remained the original dark brown. As noted with EPA-045 (Trans-Tech $MgAl_2O_4 \cdot Fe_3O_4$ in 9:1 mole ratio), the color change indicates a probable change in oxidation state of the iron present.

Several of the Trans-Tech active monoliths were subjected to SEM and X-ray analysis. On model EPA-041 ($MgAl_2O_4 \cdot NiAl_2O_4$), a comparison between pretest and combustion-tested models showed significant grain size growth. The pretest surface is shown in Figure 5 and the combustion surface is shown in Figure 6. Comparison of the three elemental analyses in these figures shows all active elements to be present in the same relative quantities. No significant depletion of nickel has occurred as with coated nickel catalysts, and the composition is an excellent candidate for long life applications.

The $LaAlO_3 \cdot LaCrO_3$ catalyst (EPA-042) was tested for 8 hours with six combustion cycles. A comparison of the pretest surface and X-ray analysis of Figure 7 with the post-test combustion surface and analysis of Figure 8 shows the surface has remained planar, and the elemental composition is relatively unchanged.

On EPA-045, the pretest $MgAl_2O_4 \cdot Fe_3O_4$ showed some initial lighter "rusty" areas, which were tentatively identified as $MgFe_2O_4$. After combustion testing, the dark $MgAl_2O_4 \cdot Fe_3O_4$ turned considerably lighter. Post-test scanning electron micrographs and elemental analysis showed that the post-test combustion sample resembled the rusty pretest samples. A change of valence of the iron apparently took place during combustion. The iron changed from a mixture of +2 to +3 valence (Fe_3O_4) to all +3 valence ($MgFe_2O_4$). This change can easily take place in the high temperature oxidizing conditions that occur during combustion.

The pretest analyses of the two surface oxidation states are shown in Figure 9. The pretest rusty area showed a somewhat smaller granularity. The post-test combustion sample closely resembles this rusty area in surface appearance (Figure 10). The composition also resembles that of the rusty pretest sample, appearing somewhat depleted in iron. It appears that a valence change in the iron takes place under combustion conditions.

The final model, EPA-048, was also analyzed pre- and post-combustion. Of all models tested, it showed the least physical or compositional change. The original structure of the surface is maintained (Figure 11 compared to Figure 12), and the active elements are all present in the same relative amounts.

These analyses of active monolith surface composition show the enhanced material stability that can be achieved over that of coated catalysts. In general, the surfaces may sinter, but none of the active elements are lost. All of the materials analyzed are fully suitable for further development from the material stability standpoint. Differences in activity and structural characteristics were apparent, however, that make certain compositions appear more attractive.

All of the Trans-Tech fabricated models showed good catalytic activity as evidenced by the ability to run at low surface temperatures and with typical variations in preheat and mass throughput when compared to coated catalysts. As with other oxide catalysts tested, a higher level of preheat energy is required for ignition, but combustion efficiency was high at steady state operating conditions. NO_x levels were low for all five models tested.

Thermostructurally, the material formulations appear promising. The crude, drilled monoliths fractured most readily at the thickest sections, but not as badly as with many commercial monoliths tested under this program. It might be expected that fabrication of these new Trans-Tech materials in monolithic form would have better structural characteristics due to the more uniform web thicknesses and lower material densities that could be achieved.

BARE MONOLITH TEST RESULTS

Due to the success of the Trans-Tech active monolith models and the noted continued activity of several coated catalysts that appeared to have no active catalyst remaining on the surface, it was suspected that several commercial substrate materials may have limited activity of their own. The three substrates tested in graded cell sets were:

- Corning yttria stabilized zirconia (MCB-10), model EPA-035
- Corning zirconia spinel (MCB-12), model EPA-043
- DuPont alumina Torvex, model EPA-047

All have essentially no surface area but were found to be catalytically active to some degree. A summary of test results of the three models is given in Table IV.

The Corning model EPA-035 had a pretest surface area measured as 0 m^2/g as expected. No additional pre- or post-test measurements were made on the three substrate materials. Since no active coating was applied to the substrates and surface degradation of the monolith was not expected to be significant, combustion aging was omitted.

Shortly after lightoff of EPA-035, it was observed that nearly all of the cell walls in the front of the bed had cracked. Also, the monolith had moved downstream within the combustor tube until it rested on the downstream thermocouple. Since the bed was badly fractured, it was not repositioned. The structure did remain intact for the duration of the testing. Later, the thermocouple in the rear of the bed ceased functioning.

Throughout the first 5 hours of testing on natural gas, EPA-035 was uniform and NO_x emissions were low. Maximum CO under lean conditions was 26 ppm with negligible unburned hydrocarbons. Minimum preheat was 478K rich and 372K lean. The blowout point was beyond the capacity of the facility at a volumetric heat release rate of 3.86×10^6 J/hr-Pa-m^3. All natural gas data were taken at a bed temperature near 1561K. The catalyst was also tested on diesel fuel. Stable combustion under lean conditions required an observed minimum preheat of 550K and a bed temperature of 1644K. At the minimum preheat value of 550K, the bed apparently went out due to insufficient prevaporization of the fuel.

Test model EPA-035 exhibited excellent combustion characteristics in the mid-temperature range. Similar results are expected at high temperatures, since the substrate is rated at a use temperature above 2144K. The thermostructural characteristics of the material are extremely poor, however. Early fracturing did not affect testing since the catalyst was held sufficiently to prevent shifting of the pieces, but total fracturing occurred when the bed was removed from the facility.

EPA-043, Corning MCB-12, was described as zirconia spinel. It was catalytically active at bed temperatures of 1556K to 1700K. NO emissions were low, below 10 ppm, except during the maximum throughput test with diesel fuel. CO emissions were ≤ 30 ppm. Minimum preheats required for combustion on natural gas were 399K lean and 537K rich. The maximum throughput attained with natural gas was dictated by facility flowrate limitations. On diesel fuel, lean, the minimum preheat was 603K, and blowout occurred at a throughput of 5.3×10^6 J/hr-Pa-m^3. Following testing, the front (large cell) section was moderately fractured, and the middle section very mildly fractured. The rear segment was undamaged. The substrate had also changed to a somewhat whiter appearance, similar to that noted for post-test MCB-10.

Test model EPA-047 consisted of uncoated DuPont alumina Torvex. With natural gas, lean, combustion was stable and efficient at bed temperatures of 1533K to 1822K. Minimum preheat temperatures were 394K, lean, and 567K, rich. At the facility maximum volumetric heat release rate of 5.9×10^6 J/hr-Pa-m^3 blowout did not occur. The minimum preheat on diesel fuel, lean, was 682K. Blowout on diesel fuel occurred at the facility throughput limit of 7.5×10^6 J/hr-Pa-m^3 volumetric heat release rate. Three and one-half hours of combustion testing resulted in delamination of the Torvex cell walls.

Each of the uncoated substrates exhibited some catalytic activity when operated in the medium temperature range (1478K to 1756K). The activity appeared to be somewhat less than that of the Trans-Tech produced materials as evidenced by minimum required operating temperatures and relatively little flexibility in preheat temperatures for the bare substrates. All models produced low NO_x emissions and were quite combustion-efficient at the velocities tested. Therefore, applications may be possible in systems where sufficient preheat can be provided during ignition to initiate reactions.

Clearly, however, all three monoliths have structural limitations. Cracking of the Corning MCB-10 was severe, and the material is judged to be unacceptable. Similarly, delamination of the DuPont alumina would be unacceptable in application. The Corning MCB-12 exhibited mild fracturing and may have potential for material improvement. Resolution of the structural problems for any of these substrates could lead to potential applications as active monolith catalysts.

CONCLUSIONS

Based upon the comparative testing of the graded cell and single cell catalyst systems, the graded cell catalyst has shown significant improvements in both maximum throughput capability and temperature uniformity within the bed. While excellent performance of graded cell catalyst systems (both noble metal and oxide) have been achieved, the problems of thermostructural degradation and chemical interaction have led to the concept of an active monolith catalyst, in which the active element is an integral part of the substrate. Testing of early prototype active monoliths, including bare monoliths of commercially available materials with no special active elements, have shown good activity and combustion performance. Improvements in manufacturing techniques and material formulations are required, however, to further develop adequate structural life of these systems.

REFERENCES

1. Kendall, R. M., et al. An Analysis of Catalytic Combustion in Monolithic Honeycomb Bed. Proceedings: Third Workshop on Catalytic Combustion, EPA-600/7-79-038, February 1979, pp. 197-238.

2. Kesselring, J. P., et al. Design Criteria for Stationary Source Catalytic Combustion Systems. EPA-600/7-79-181, August 1979.

3. Krill, W. V. and Kesselring, J. P. The Development of Catalytic Combustors for Stationary Source Applications. Proceedings: Third Workshop on Catalytic Combustion, EPA-600/7-79-038, February 1979, pp. 239-268.

TABLE I. COMPARISON OF SINGLE CELL AND GRADED CELL CATALYST PERFORMANCE

Parameter	Graded Cell Catalyst	Single Cell Catalyst
Catalyst manufacturer	UOP	UOP
Cell geometry	(3) 25.4-mm long segments of 6.4, 4.8, and 3.2-mm cell size	(3) 25.4-mm long segments of 3.2-mm cell size
Substrate	DuPont alumina	DuPont alumina
Surface area (m^2/g)		
Pre-test	5.36	4.88
Post-test	0.986	0.05
Dispersion (moles H_2/g)		
Pre-test	17.63	1.22
Post-test	1.30	0.39
Operating temperature (K)	1561	1561
Maximum heat release rate ($J/hr\text{-}Pa\text{-}m^3$)	7.4×10^6	2.6×10^6
Typical emissions (ppm)		
NO_x	1	2
CO	30	60
HC	12	35

TABLE II. ACTIVE MONOLITH TEST CONFIGURATION

Composition	Configuration
$MgAl_2O_4 \cdot NiAl_2O_4$	Cylinder, drilled holes axially
$LaAlO_3 \cdot LaCrO_3$	│
$MgAl_2O_4 \cdot Fe_3O_4$	│
$MgAl_2O_4 \cdot MgCr_2O_4$	Bundled hollow tubes
$MgAl_2O_4 \cdot Fe_3O_4$ with 40% Cr (cermet)	│

TABLE III. COMBUSTION PERFORMANCE OF ACTIVE MONOLITHS

Test Model	Composition	Test Hours	Measured** Bed Temperature	Lean Minimum Preheat Temperature K (°F)		Maximum Volumetric Heat Release Rate MJ/hr-Pa-m³ (MBtu/hr-atm-ft³)	
				Natural Gas	Diesel Fuel	Natural Gas	Diesel Fuel
EPA-041	$MgAl_2O_4 \cdot NiAl_2O_4$	10	1367-1561 (2000-2350)	436 (325)	587 (596)	12 (33)*	22 (59)*
EPA-042	$LaAlO_3 \cdot LaCrO_3$	8	1367-1500 (2000-2240)	464 (375)	589 (600)	14 (39)*	21 (56)
EPA-045	$MgAl_2O_4 \cdot Fe_3O_4$	10.5	1506-1561 (2250-2350)	533 (500)	397 (255)	13 (34)*	18 (48)
EPA-046	$MgAl_2O_4 \cdot MgCr_2O_4$	5	1617-1711 (2450-2620)	354 (178) (ambient)	---	8.8 (24)*	---
EPA-048	$MgAl_2O_4 \cdot Fe_3O_4 \cdot 40\%$ Cr	5	1033-1644 (1400-2500)	367 (200)	---	8.8 (24)	---

*Below blowout point

**Actual temperatures somewhat higher than those measured

TABLE IV. COMBUSTION PERFORMANCE OF BARE MONOLITHS

Test Model	Test Hours	Bed Temperature K (°F)	Lean Minimum Preheat Temperature K (°F)		Maximum Volumetric Heat Release Rate MJ/hr-Pa-m^3 (MBtu/hr-atm-ft^3)		Post-Test Condition
			Natural Gas	Diesel Fuel	Natural Gas	Diesel Fuel	
EPA-035 (MCB-10)	7.5	1506-1867 (2250-2900)	372 (210)	550 (530)	3.86 (10.5)*	--	Poor
EPA-043 (MCB-12)	5.5	1556-1700 (2340-2600)	399 (258)	603 (625)	3.68 (10.0)*	5.34 (14.5)	Fair
EPA-047 (Torvex)	3.5	1533-1822 (2300-2820)	394 (250)	682 (768)	5.89 (16.0)*	7.73 (21.0)	Poor

*Below the blowout point

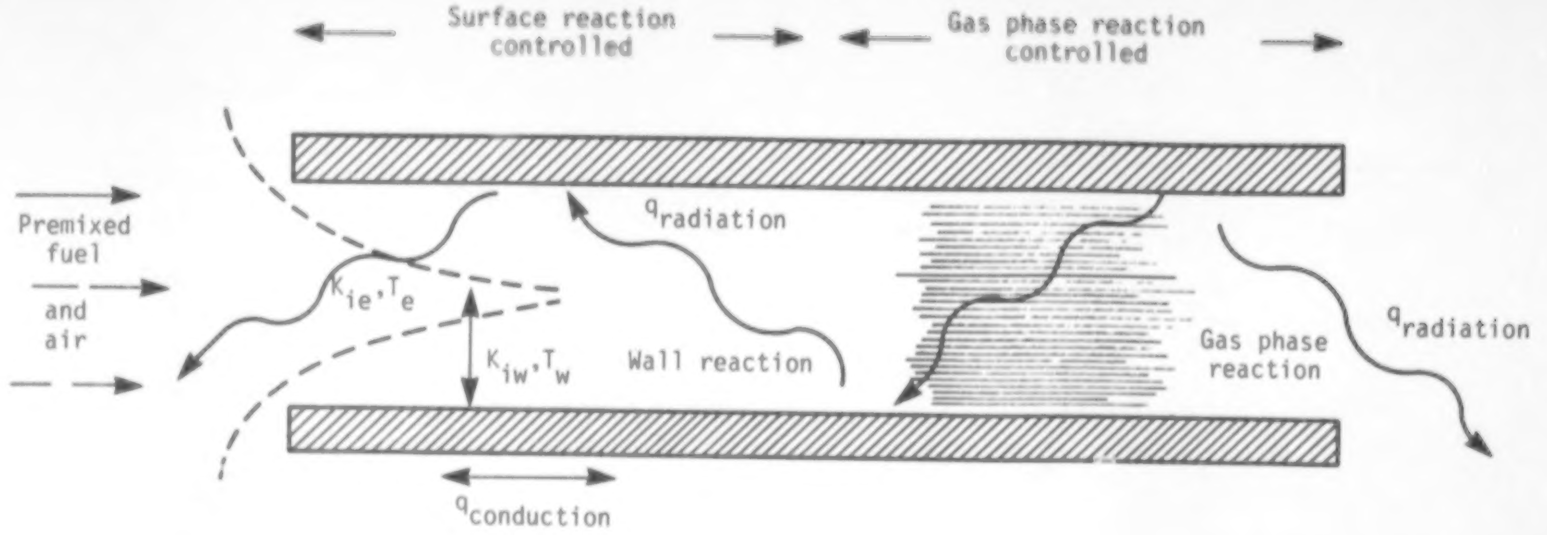
Surface reaction controlled
Gas phase reaction controlled
Premixed fuel and air
K_{ie}, T_e
K_{iw}, T_w
$q_{radiation}$
Wall reaction
Gas phase reaction
$q_{radiation}$
$q_{conduction}$

Figure 1. Physical events occurring in one cell of a honeycomb monolith catalytic combustor.

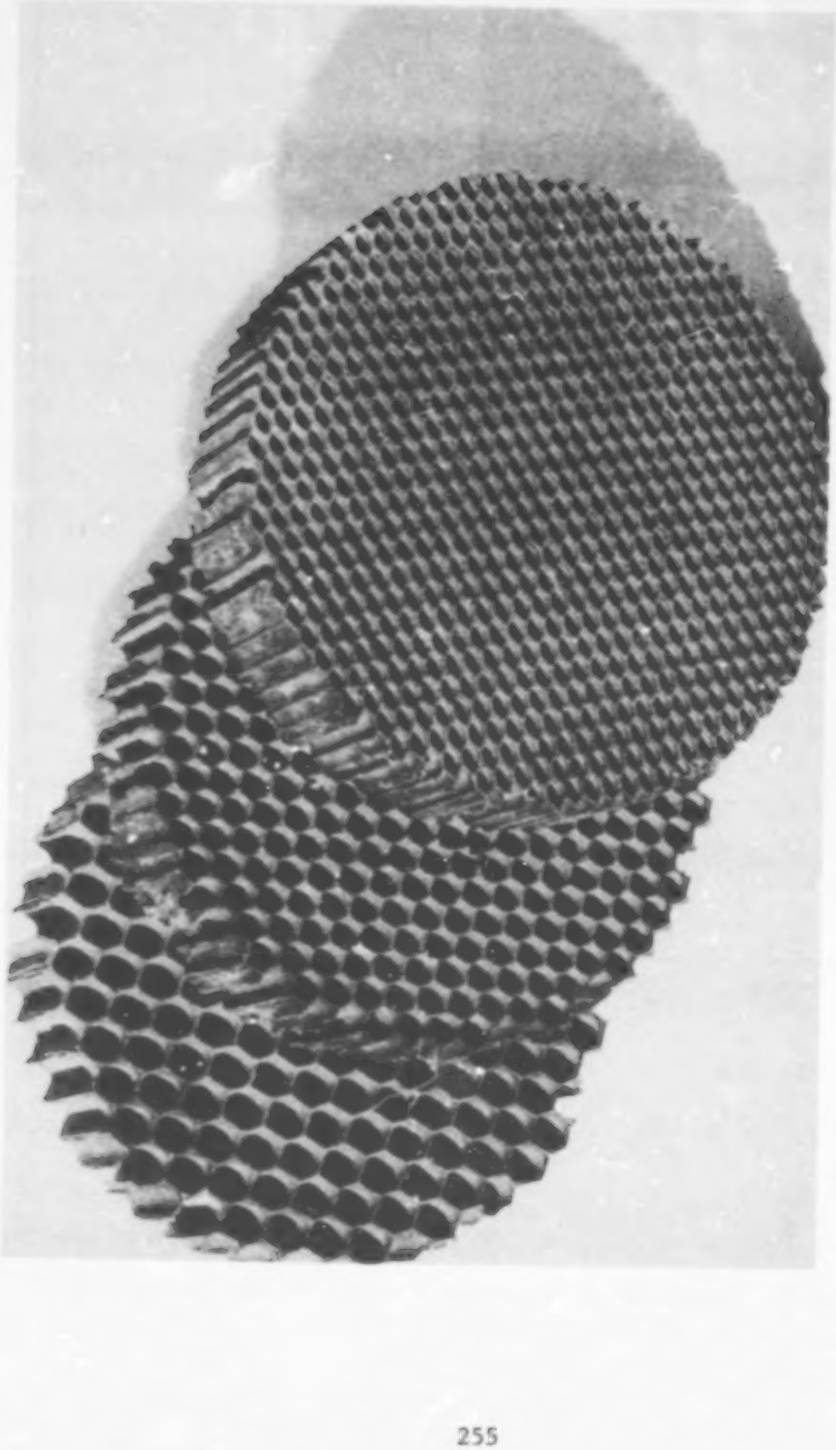

Figure 2. Graded cell catalyst segments. The large cell piece is placed at the bed inlet, and the small cell piece at the bed exit.

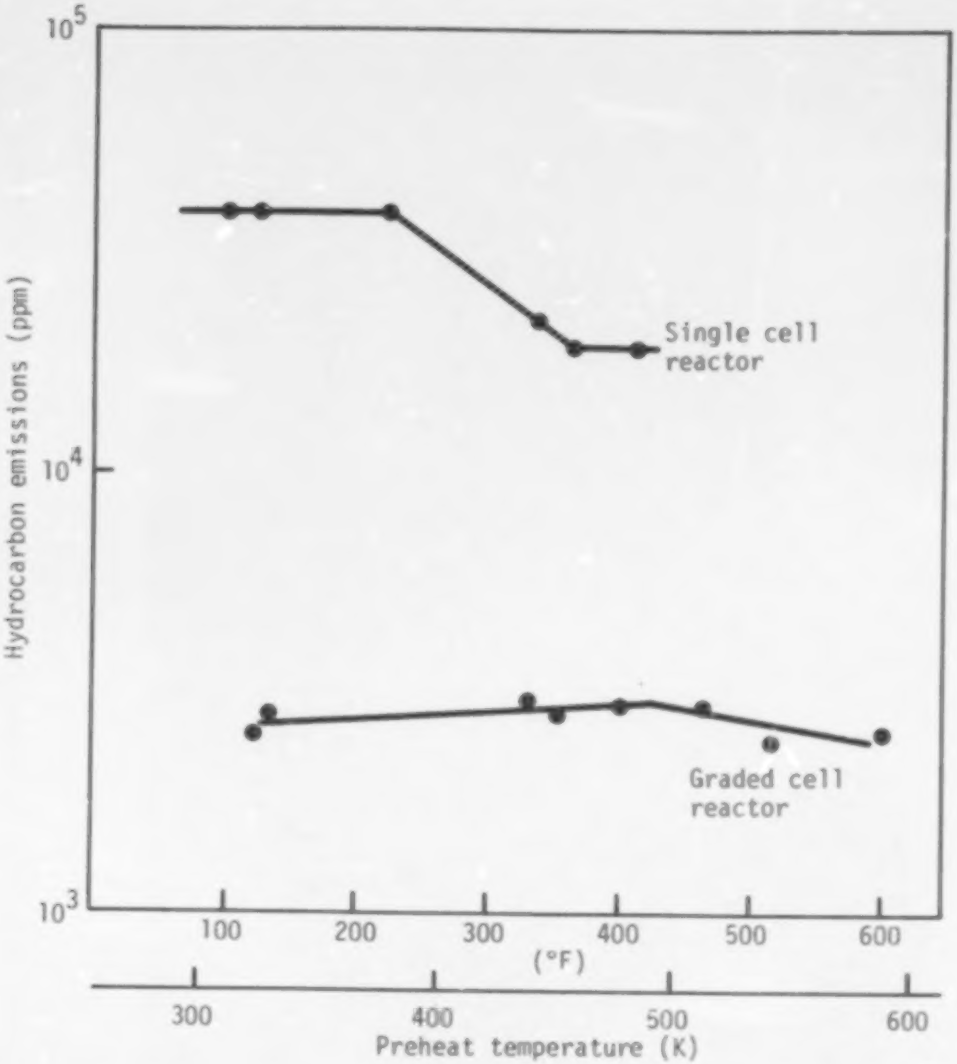

Figure 3. Hydrocarbon emissions comparison for two catalyst geometries at rich conditions.

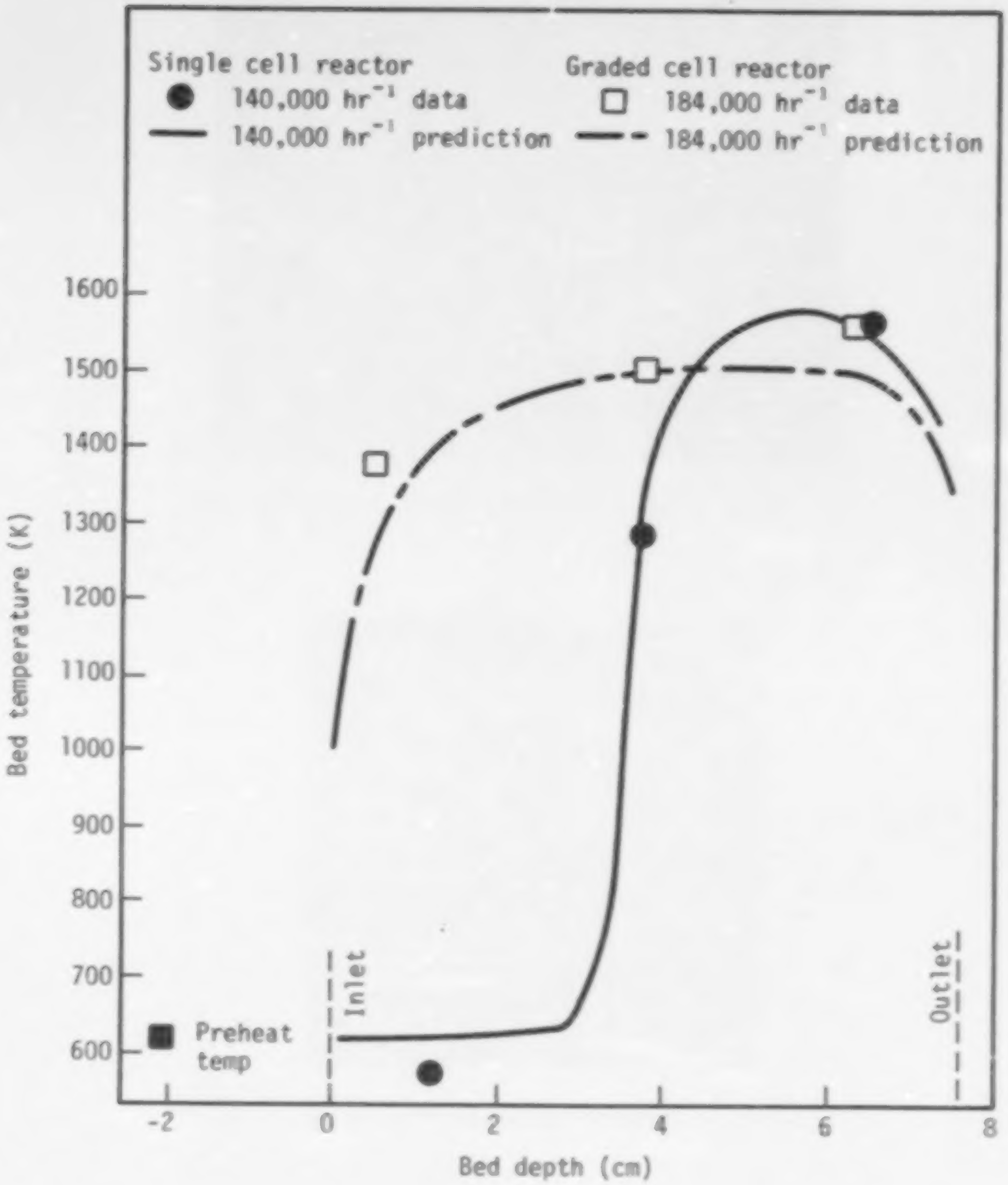

Figure 4. Comparison of graded cell and single cell reactor temperature profiles with HET code predictions.

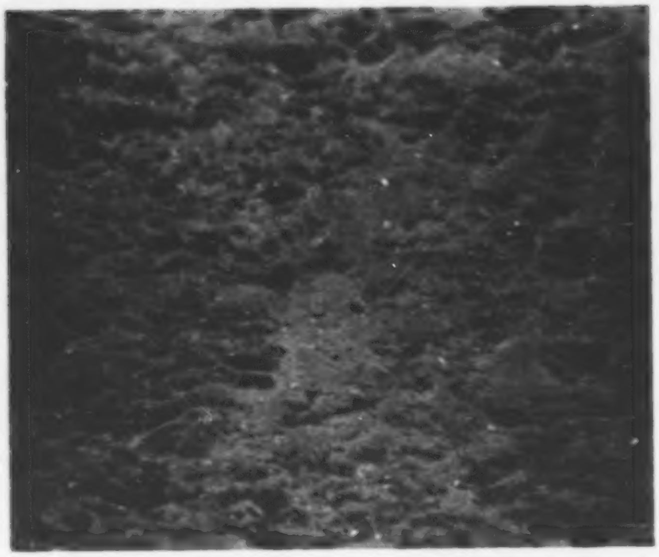

a. Surface appearance at 1000 X magnification

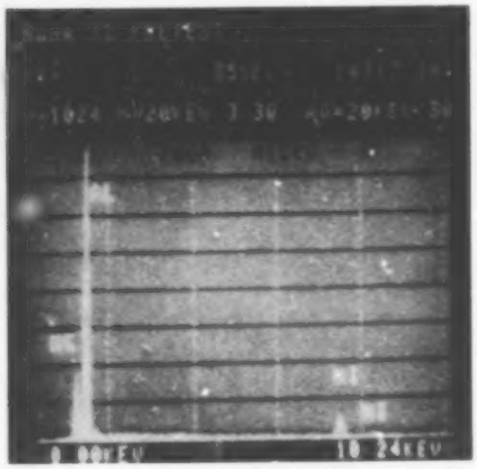

b. Elemental analysis of area a

Figure 5. $MgAl_2O_4 \cdot NiAl_2O_4$ pretest surface analysis.

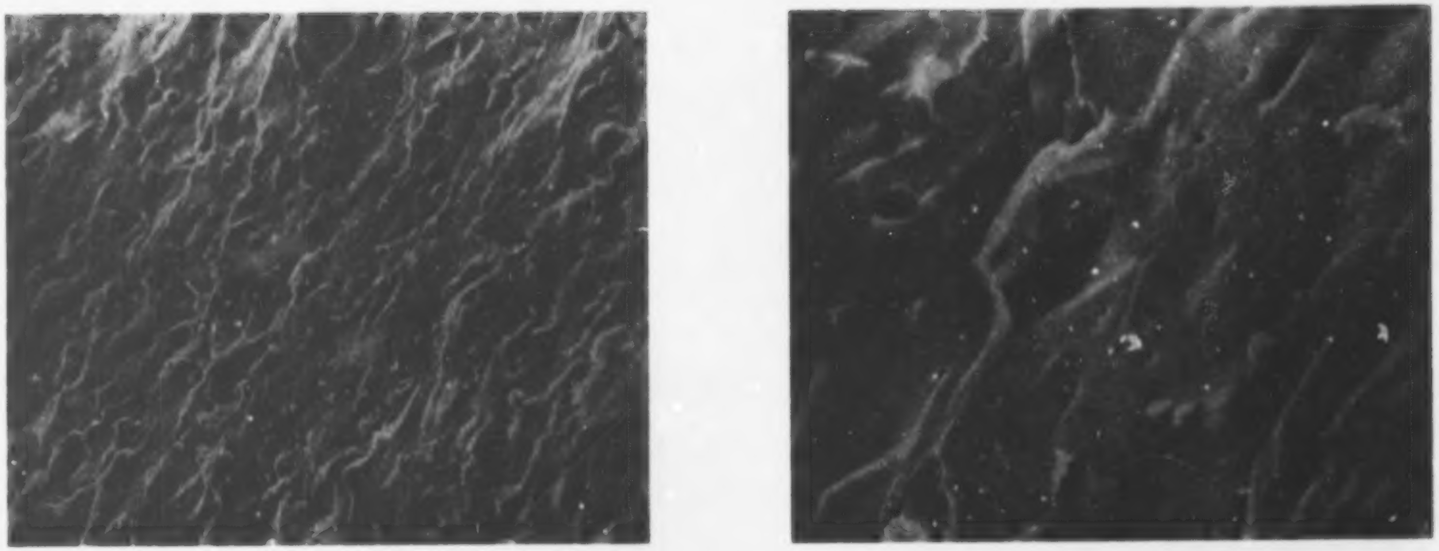

a. Surface appearance at 500X magnification

b. Surface appearance at 2000X magnification

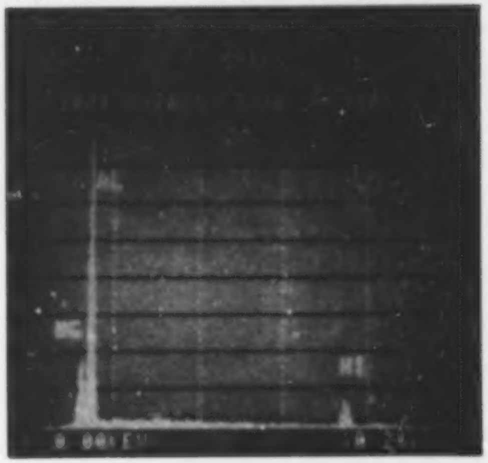

c. Elemental analysis of above area

Figure 6. (above left, above right, and opposite)

$MgAl_2O_4 \cdot NiAl_2O_4$ post-test combustion analysis.

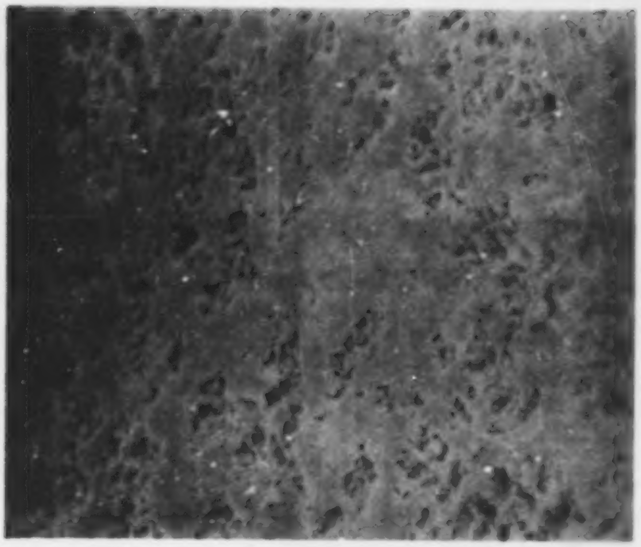

a. Surface appearance at 1000X magnification

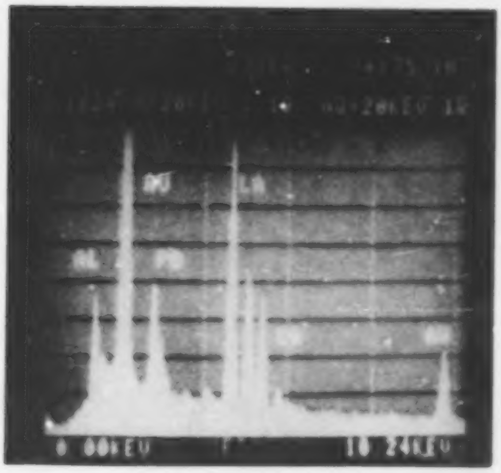

b. Elemental analysis of area a

Figure 7. $LaAlO_3 \cdot LaCrO_3$ pretest surface analysis.

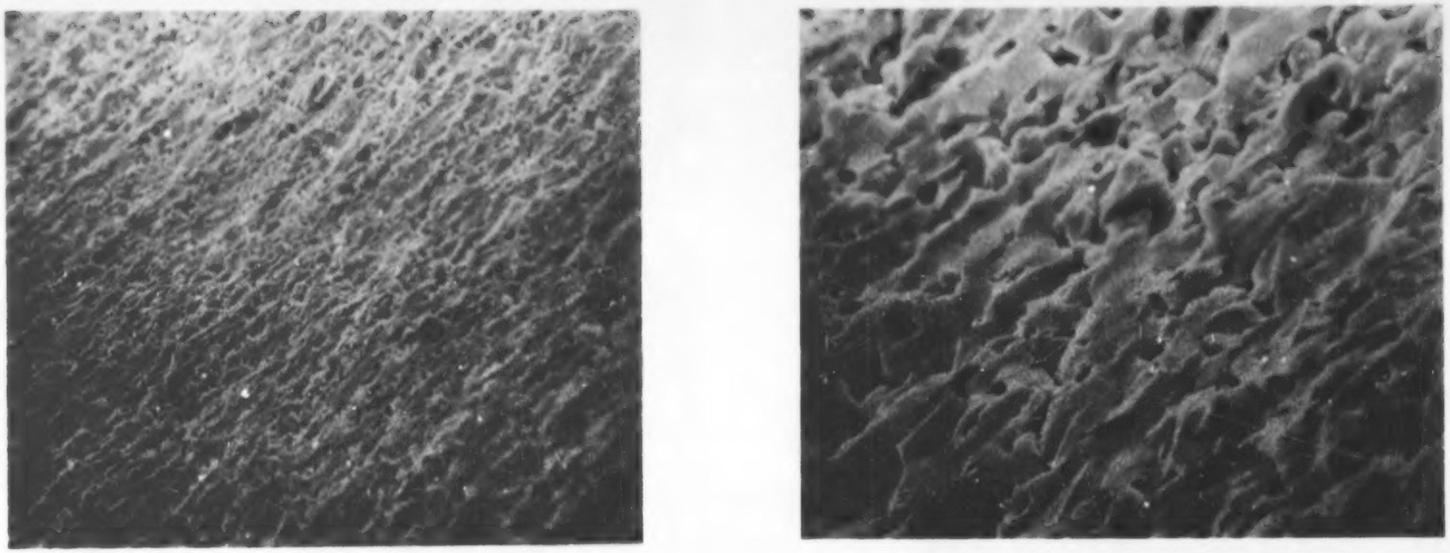

a. Surface appearance at 500X magnification

b. Surface appearance at 2000X magnification

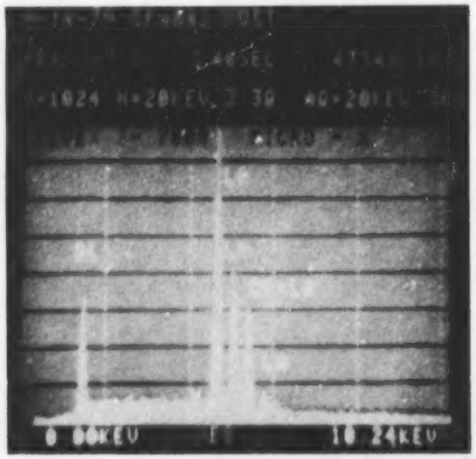

c. Elemental analysis of above area

Figure 8. (above left, above right, and opposite)

$LaAlO_3 \cdot LaCrO_3$ post-test combustion analysis.

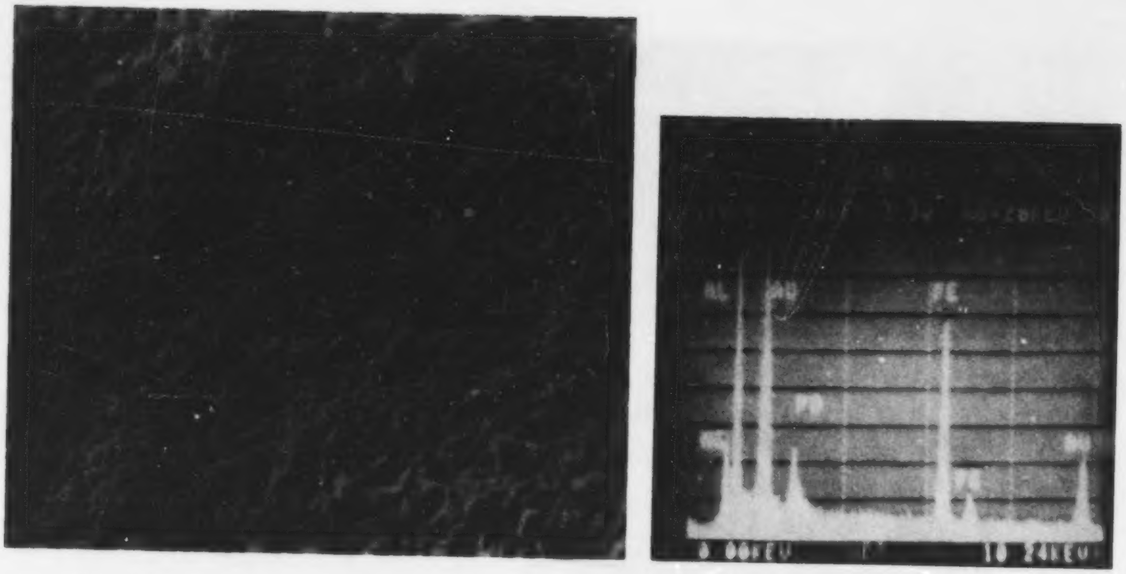
AL
AU
FE
PD
AU
0.00KEV
10.24KEV

a. Normal surface appearance at 1000X magnification

b. Elemental analysis of area a

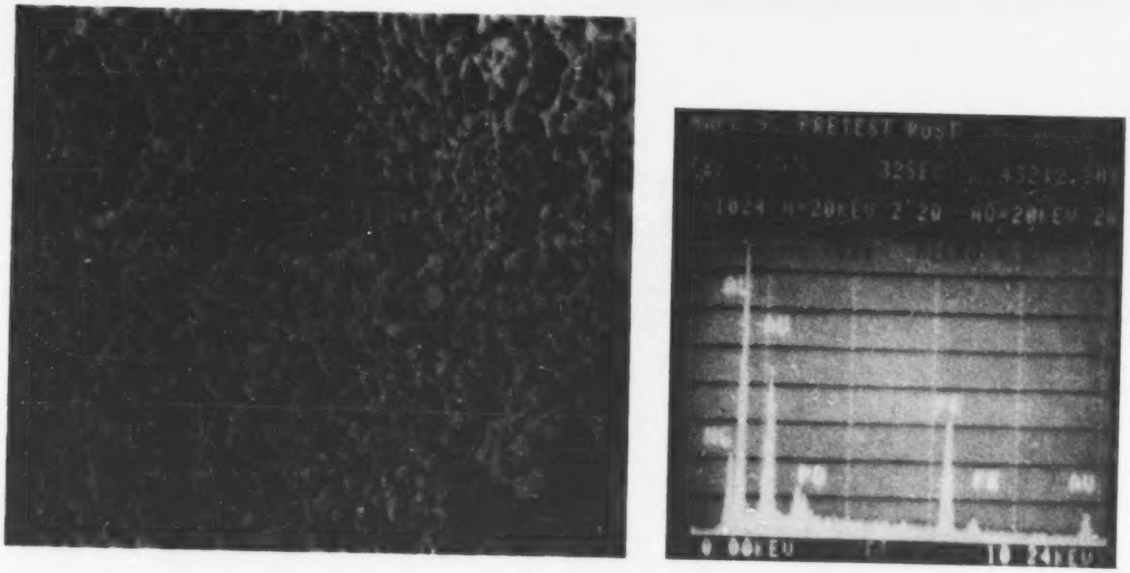
PRETEST RUST
32SEC
AL
AU
MG
PD
FE
AU
0.00KEV
10.24KEV

c. Rusty surface appearance at 1000X magnification

d. Elemental analysis of area c

Figure 9. $MgAl_2O_4 \cdot Fe_3O_4$ pretest surface analysis.

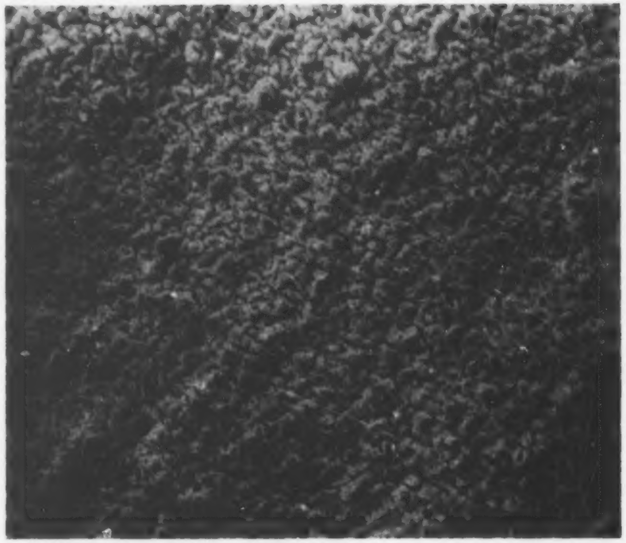

a. Surface appearance at 500X magnification

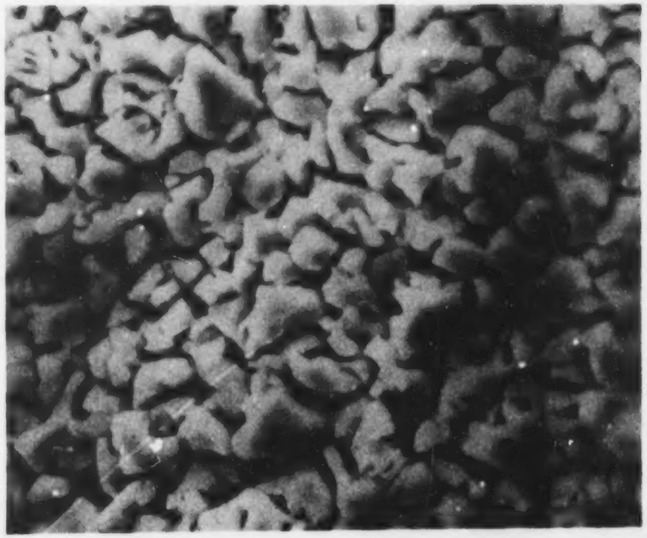

b. Surface appearance at 2000X magnification

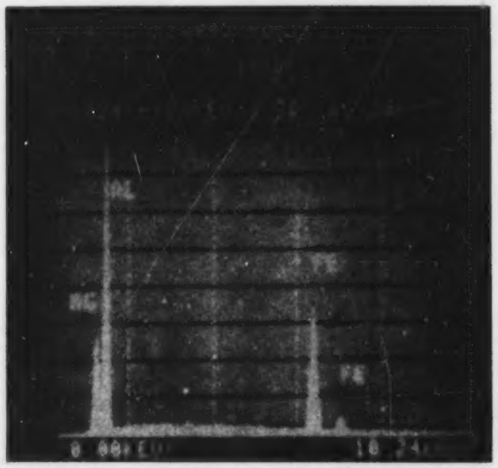

c. Elemental analysis of above area

Figure 10. (above left, above right,
and opposite)

$MgAl_2O_4 \cdot Fe_3O_4$ **post**-test combustion analysis

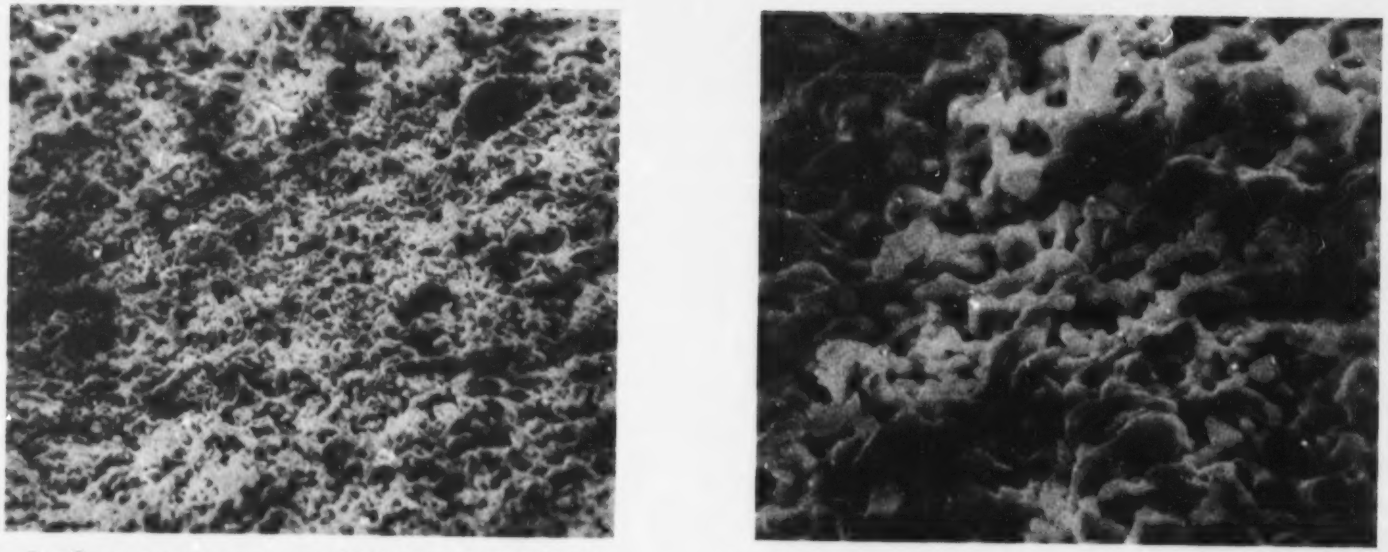

a. Surface appearance at 500X magnification

b. Surface appearance at 2000X magnification

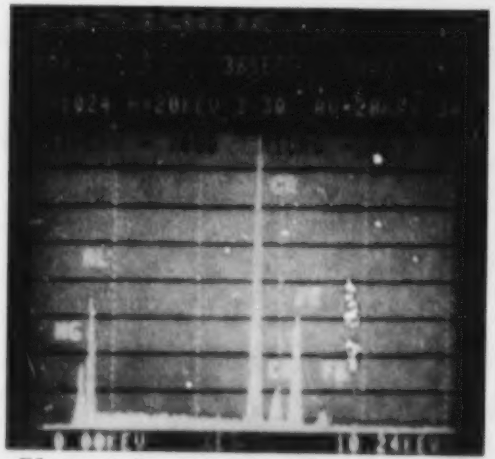

c. Elemental analysis of above area

Figure 11. (above left, above right, and opposite)

$MgAl_2O_4 \cdot Fe_3O_4 \cdot 40\%$ Cr pretest analysis.

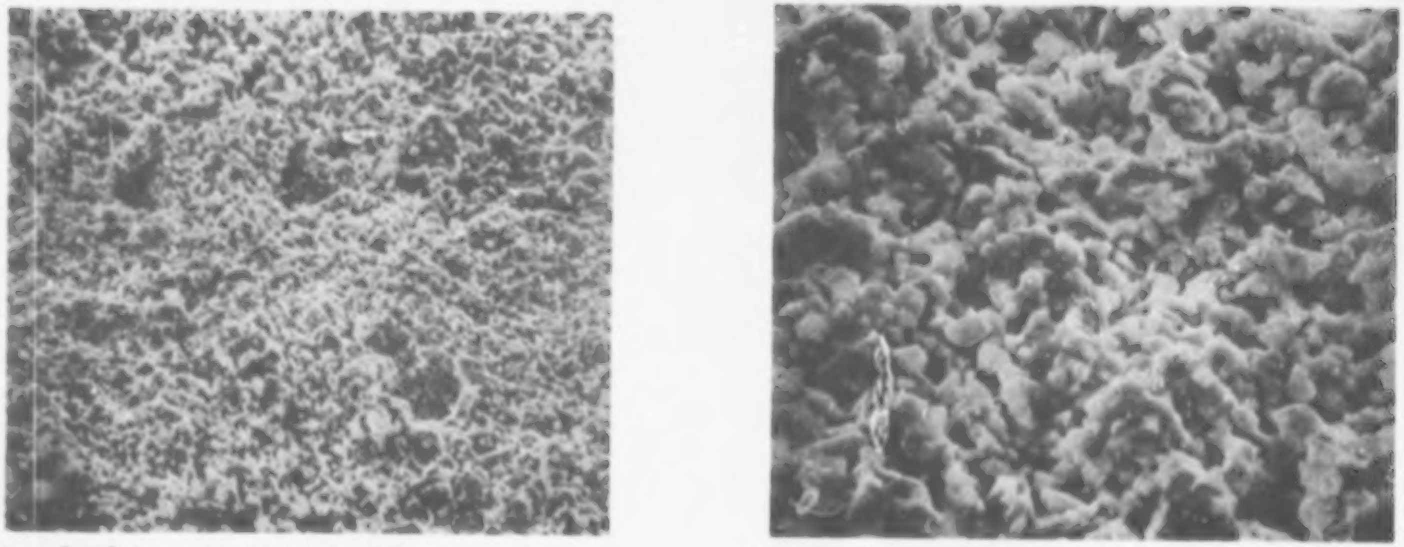

a. Surface appearance at 500X magnification

b. Surface appearance at 2000X magnification

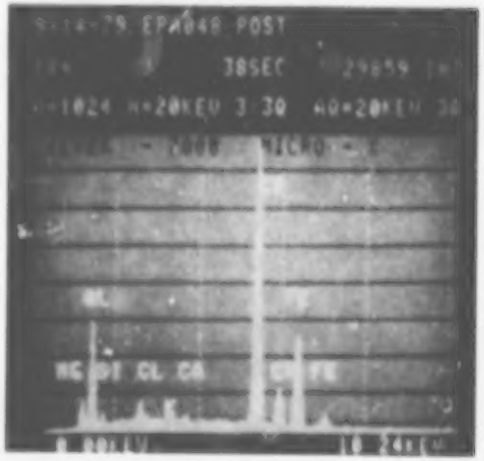

c. Elemental analysis of above area

Figure 12. (above left, above right, and opposite)

$MgAl_2O_4 \cdot Fe_3O_4 \cdot 40\%$ Cr post-combustion test analysis

CATALYZED COMBUSTION
OF LEAN FUEL/AIR MIXTURES

By

R. W. Schefer and F. Robben
Lawrence Berkeley Laboratory
Berkeley, CA 94720

ABSTRACT

A study has been made of the combustion characteristics of lean fuel/air mixtures flowing over heated catalytic and non-catalytic surfaces. The objective of the investigation was to develop a better understanding of the effect of a catalyst on the combustion process as the lean flammability limit of various fuels is approached. The fuels studied were H_2, C_2H_6, and C_3H_8. Gas phase combustion ignition temperatures were determined over a range of equivalence ratios from boundary layer density profiles obtained using Rayleigh scattering. Surface reaction ignition temperatures and surface heat rates were also determined for the above fuels. A comparison of the results for a vacuum deposited platinum surface with results for a relatively "non-catalytic" quartz surface showed that the gas phase ignition temperature is a function of catalyst surface reactivity. At lower temperatures the quartz surface was essentially noncatalytic and resulted in gas phase ignition temperatures up to 100 K lower than with the platinum surface. At increased surface temperatures the catalytic activity of the quartz surface approached that of the platinum and gas phase ignition temperatures were identical for both surfaces. A detailed study of C_3H_8 oxidation on a platinum surface showed that for temperatures less than 670 K, CO is the primary oxidation product and for temperatures greater than 870 K, complete oxidation to CO_2 occurs.

This research was supported by the U. S. Department of Energy, Division of Transportation Energy Conservation under Contract W-7405-ENG-48.

SECTION 1

INTRODUCTION

Lean combustion shows considerable promise as a means of reducing pollutant formation in combustion systems (1). However, the extent to which this concept can be effectively utilized is limited by the combustion characteristics of a particular fuel as its lean flammability limit is approached. Catalyzed combustion has been demonstrated to be effective in extending the stable burning region well below conventional lean gas phase flammability limits while at the same time providing low levels of unburned hydrocarbons and CO (2, 3). While preliminary tests have been quite promising, a number of aspects of catalyzed combustion are either not well understood or the necessary data are lacking. In the development of an optimum catalyst design for lean combustion applications it will be necessary to 1) develop a greater understanding of the role of the catalyst in the combustion process and 2) to determine high temperature catalytic surface reaction mechanisms and reaction rate data. It is the goal of this investigation to provide some of this necessary data for future catalytic combustion design development.

In the present study the surface ignition and gas phase ignition characteristics under conditions approaching the lean flammability limits of several fuel/air mixtures were investigated for boundary layer flow over a heated surface. The fuels used in the study were H_2, C_2H_6, and C_3H_8. To better determine the effect of the catalyst on the combustion process both a catalytic platinum surface and a relatively noncatalytic quartz surface were utilized in the study. Results are also presented on a detailed study of lean C_3H_8 oxidation over a platinum surface.

SECTION 2

EXPERIMENTAL PROCEDURE

Details of the experimental system used in the present investigation have been described in References 4 and 5. Briefly, the configuration consists of a quartz plate with vacuum deposited platinum heating strips mounted as one wall of a 5 cm square, open, atmospheric jet of premixed fuel and air. The gas flow is parallel to the plate surface and results in the formation of a velocity and thermal boundary layer in the region near the wall surface. Control of the surface temperature is provided by five platinum heating strips which have been vacuum deposited on the quartz plate and can be electrically heated to temperatures approaching 1400 K. The heating strips are oriented perpendicular to the flow and are of varying widths to improve temperature control near the plate leading edge. The extent to which gas phase combustion and surface reaction occurs can thus be controlled through variations in plate surface temperature and fuel/air mixture ratio.

Surface temperatures greater than 1000 K were measured using a disappearing filament type optical pyrometer and an emissivity of 0.65 for the platinum surface. Surface temperatures below 1000 K were determined from the measured resistivity of the platinum strips and, independently, with a laboratory built infrared detector. Using this technique plate surface temperatures could be measured to an estimated accuracy of ± 15 K.

In the present investigation the platinum catalytic surface was provided by orienting the quartz plate so that the side with the platinum heating strips was directed toward the flow. To obtain a "noncatalytic" surface the plate was reversed so that the uncoated quartz surface was directed toward the flow.

The presence of gas phase combustion in the boundary layer was determined from total gas density profiles measured using Rayleigh scattering. As discussed in Reference (5), the boundary layer density profiles are self similar along the plate when no gas phase combustion is present. However, heat release due to gas phase combustion results in density profiles characterized by a more positive curvature in the high temperature region near the plate surface and an increase in thermal boundary layer thickness. To determine the gas phase ignition temperature the equivalence ratio was fixed at a desired value and the plate surface temperature was increased in steps of 25 K. After each increase in surface temperature the system was allowed to come to steady state and the boundary layer was traversed using Rayleigh scattering to measure the resulting gas density profile. A comparison of these profiles with profiles for no fuel added at the same surface temperature then made it possible to determine that temperature, defined as the gas phase ignition temperature, at which heat release due to gas phase combustion resulted in a detectable departure from self-similar behavior. The results presented in this paper were based on an analysis of density profiles at a distance of 50 mm from the heated wall leading edge since at distances greater than this, fluctuations in the jet mixing layer become a significant source of disturbance to the boundary layer flow.

To determine steady state surface energy release rates the plate temperature was initially adjusted to the desired value with no fuel present in the flow. This was done by varying the power input to the individual heating strips. Typically strips 1 and 2 required greater power inputs for a constant plate temperature due to the higher heat transfer coefficient near the heated wall leading edge. Fuel was then added to the flow, which increased the surface temperatures to some higher nonuniform value due to surface energy release. The power inputs to the individual strips were then decreased until the desired temperature was again reached. The resulting difference in power input to each strip, with and without fuel addition, is equal to the average heat release due to surface chemical reaction for that particular strip provided heat losses due to other sources remain constant. For a given plate temperature radiative losses are constant. Experimental measurements and numerical calculations have also shown that the boundary layer temperature profiles are self-similar when no gas phase combustion is present, thus losses due to convection and conduction will remain constant for a given free stream velocity at temperatures lower than the gas phase ignition temperatures.

In the present investigation the surface reaction ignition temperature was defined as the surface temperature at which, for a given equivalence ratio, measurable heat release due to surface reaction was present. All results presented in the following sections were taken at a constant free stream velocity of 1.5 m/s under laminar flow conditions.

SECTION 3

RESULTS AND DISCUSSION

Surface Ignition

The dependence of surface ignition temperature on stoichiometry is shown in Fig. 1 for C_3H_8/air and C_2H_6/air mixtures flowing over a platinum surface. In both cases the surface ignition temperature was found to be only a weak function of equivalence ratio over the range of conditions investigated. That is, a small decrease in ignition temperature was observed as the equivalence ratio was increased toward stoichiometric conditions. The minimum ignition temperatures measured for C_3H_8 were approximately 470 K and, for C_2H_6, somewhat higher at 700 K. These results agree well with the data of Hiam, et al. (6), who investigated the catalytic oxidation of C_3H_8 and C_2H_6 on a platinum filament. It should be noted that the corresponding ignition temperatures for gas phase reaction are significantly higher than those shown in Fig. 1 and therefore the observed increase in surface temperature is due to surface reaction only.

Gas Phase Ignition

Gas phase ignition temperatures for H_2, C_3H_8, and C_2H_6 on both platinum and quartz surfaces are shown in Figs. 2 through 4 as a function of equivalence ratio. In all cases at higher equivalence ratios a relatively weak depe dence of ignition temperature on equivalence ratio was observed. However, as the equivalence ratio was reduced a much stronger dependence is noted. In the case of H_2 (Fig. 2) on a platinum surface minimum gas phase ignition temperatures of approximately 1000 K were observed at an equivalence ratio of 0.3. At lower equivalence ratios the ignition temperature rapidly increased to a value of 1220 K at $\phi = 0.1$. This behavior was characteristic of all fuels investigated, that is a weak dependence of ignition temperature on equivalence ratio at higher equivalence ratios and a rapid increase in ignition temperature as the equivalence ratio was reduced.

With the quartz surface at lower surface temperatures, ignition occurs at approximately 100 K lower than with the platinum. The differences in ignition temperature decreases as the equivalence ratio is reduced until at an equivalence ratio of 0.1 identical ignition temperatures of 1220 K are achieved with both surfaces. Similar results were obtained with C_3H_8 and C_2H_6. In both cases at an equivalence ratio of 0.9 ignition with the platinum surface occurred at approximately 1170 K and with the quartz surface it occurred at surface temperatures approximately 100 K lower. At an equivalence ratio of 0.5, where the ignition temperature was 1220 K for both fuels with a platinum surface, a difference in ignition temperature of only 25 K was observed in comparing the quartz and platinum surfaces.

This behavior is consistent with an increase in catalytic activity of the quartz surface at higher temperatures. Numerical calculations for H_2/air mixtures flowing over a catalytic surface (7) have shown that catalytic reactions at the plate surface, particularly surface oxidation of the fuel and radical recombination, result in a surpression of gas phase reactions in the boundary. Thus, the increase in gas phase ignition temperature with respect to the platinum surface at higher surface temperatures would seem to imply an increase in catalytic activity which, at a temperature of 1220 K, equals that of the platinum in the case of H_2. To verify this, surface heat release rates were measured for H_2/air at an equivalence ratio of 0.2 flowing over a quartz surface. Assuming a one step model for surface reaction in which H_2 and O_2 react to from H_2O as a product ($\Delta H_R = 2.38 \times 10^8$ J/kg-mole) values for the surface reaction were calculated. Those results are shown as a function of surface temperature in Fig. 5. Note that the surface reaction rate for quartz has been normalized by the reaction rate for H_2/air mixtures on a platinum surface obtained previously (8). At temperatures less than 870 K no surface reactivity was measured for the quartz surface. However, as the surface temperature was increased above 870 K, a gradual increase in surface reactivity relative to platinum was observed, followed by a rapid increase at temperatures greater than 1170 K. At a surface temperature of 1220 K the catalytic activity of the quartz surface was equal to that of the platinum. Thus, it appears that the observed behavior in gas phase ignition characteristics for the platinum and quartz surfaces is due to the increased activity of the quartz surface at higher temperatures.

Propane Surface Oxidation Studies

Typical experimentally measured surface energy release rates for C_3H_8/air are shown in Figs. 6 and 7 for plate temperatures of 670 K and 870 K and an equivalence ratio of 0.2. The free stream velocity was 1.5 m/s. As mentioned previously, the data points represent average values of the energy release rate over the individual heating strips and not local values. It can be seen that the maximum heat release rates occur at the plate leading edge and then rapidly decrease as one moves downstream. As discussed by Rosner (9), this behavior indicates that mass transfer effects are important under the above conditions. For viscous flow over a flat plate with reactions occurring at the surface, the transport of reactant species from the free stream to the plate surface varies with streamwise distance from the plate leading edge. Near the leading edge where the boundary layer is thin, convective and diffusive transport rates to the surface are rapid and the surface reaction rate approaches its kinetically limited value. Farther downstream the boundary layer becomes considerably thicker and transport rates to the surface are insufficient to prevent local reactant depletion near the surface. Under these conditions the surface reaction rate is limited by the maximum rate at which reactants can be transported to the surface.

Also shown are predicted local surface heat release rates calculated using a computational scheme developed previously (7). Briefly, the program uses a finite difference approach to solve the two dimensional boundary layer equations for flow over a flat plate surface with simultaneous gas phase and surface reactions. In the present application, no gas phase reactions are assumed to occur and the program is used to describe the convective/diffusive transport of reactant and product species through the boundary layer to and from the plate surface. Surface reactions are included in the calculations in the form of a species boundary condition at the surface in which the rate of diffusion of a particular specie to the surface is equal to the surface reaction rate. The rate expression used to describe C_3H_8 oxidation at the plate surface is based on the work of Hiam, et al. (6) and is given by

$$R_S = 1.1 \times 10^7 \, [H_2] \exp(-17000/RT) \, \frac{\text{kg moles}}{m^2 s} \qquad (1)$$

where $[H_2]$ is the concentration of H_2 at the surface (kg moles/m^3). Initial modelling calculations were based on the assumption of a one step reaction in which C_3H_8 and O_2 react at the surface to form CO_2 as the product. These results are indicated by the solid lines in Figs. 6 and 7. As can be seen in Fig. 7, the predicted and experimental results agree well at temperatures greater than 870 K. However, at 670 K it was found that the predicted heat release ratios were approximately a factor of 2 higher than those measured experimentally. If it is assumed that only partial oxidation of C_3H_8 to CO occurs at the surface at lower temperatures then, as shown by the dashed line in Fig. 6, good agreement is obtained with experimental results. These results agree qualitatively with the measurements of Marteney and Kesten (7) in which it was found that the ratio of CO_2 to CO in the product species from a catalytic reactor (utilizing a Matthey Bishop manufactured catalyst material) increased with increasing exhaust temperature.

An Arrhenius plot of experimentally measured average surface energy release rates for C_3H_8 as a function of inverse surface temperature for heating strips 1 and 2 is shown in Fig. 8. Predicted average surface heat release rates for strips 1 and 2 assuming CO_2 (solid line) and CO (dashed line) as the product species are also shown. Once again the transition from CO_2 to CO as the product of surface oxidation is apparent as the surface temperature is decreased from 870 K to 670 K. The effect of diffusion limited behavior on apparent activation energy is also shown. The slope of each curve at a given temperature is equal to E_A/R, where E_A is the apparent activation energy for surface oxidation of C_3H_8 and R is the gas constant. At higher surface temperatures the apparent activation energy is significantly less than the true activation energy. As the surface temperature is reduced the apparent activation energy approaches the true activation energy as the surface reaction rate becomes kinetically limited.

SECTION 4

SUMMARY

The effect of catalytic surface activity on gas phase and surface reaction ignition temperatures was studied for H_2-, C_3H_8-, and C_2H_6-air mixtures flowing over a platinum and a quartz surface. It was found that the gas phase ignition temperature is a function of catalyst surface reactivity. That is at lower temperatures the quartz surface was essentially non-catalytic and resulted in gas phase ignition temperatures up to 100 K lower than with the platinum surface. At increased surface temperatures the catalytic activity of the quartz surface approached that of the platinum and gas phase ignition temperatures were identical for both surfaces. A detailed study of C_3H_3 oxidation on a platinum surface showed that for temperatures less than 670 K, CO is the primary oxidation product and for temperatures greater than 870 K, complete oxidation to CO_2 occurs.

REFERENCES

1. Sawyer, R. F. and Blazowski, W. S. Propulsion Effluents in the Stratosphere, CIAP Monograph 2, Chapter 3. Department of Transportation Report DOT-TST-75-52 (1975).

2. Pfefferle, W. C. The Catalytic Combustor: An Approach to Cleaner Combustion. J. Energy 2, 3, 142 (1978).

3. Blazowski, W. S. and Walsh, D. F., Comb. Sci. Technonl. 10, p. 233 (1975).

4. Schefer, R. W., Robben, F., and Cheng, R. K. Catalyzed Combustion of H_2/Air Mixtures in a Flat Plate Boundary Layer. Proceedings of the Catalytic Combustion Workshop, Ashville, North Carolina (Oct. 1978).

5. Schefer, R. W. Catalyzed Combustion of H_2/Air Mixtures in a Flat Plate Boundary Layer. I. Experimental Results. To be published in Comb. and Flame (1980).

6. Hiam, L., Wise, H., and Chaikin, S. Catalytic Oxidation of Hydrocarbons on Platinum. J. Catal. 10, 272 (1968).

7. Schefer, R. W. Catalyzed Combustion in a Flat Plate Boundary Layer. II. Numerical Calculations. Western States Section/The Combustion Institute, Stanford, CA (1977).

8. Schefer, R., Cheng, R., Robben, F., and Brown, N. Catalyzed Combustion of H_2/Air Mixtures on a Heated Platinum Plate. Western States Section/ The Combustion Institute, Boulder, CO (1978).

9. Rosner, D. E., Convective Diffusion as an Intruder in Kinetic Studies of Surface Catalyzed Reactions, A.I.A.A.J. 2, 593 (1964).

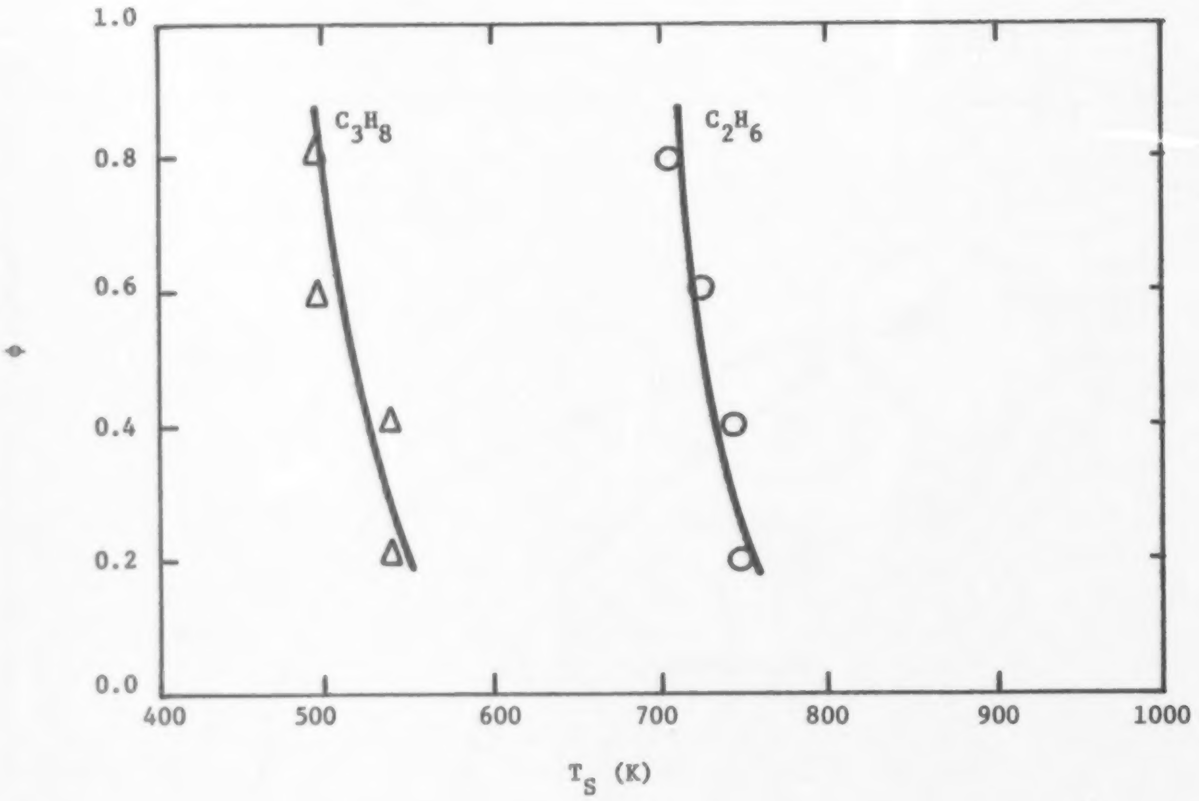

Figure 1. Surface reaction ignition temperatures for C_3H_8 and C_2H_6 on a platinum surface. $U_\infty = 1.5$ m/s.

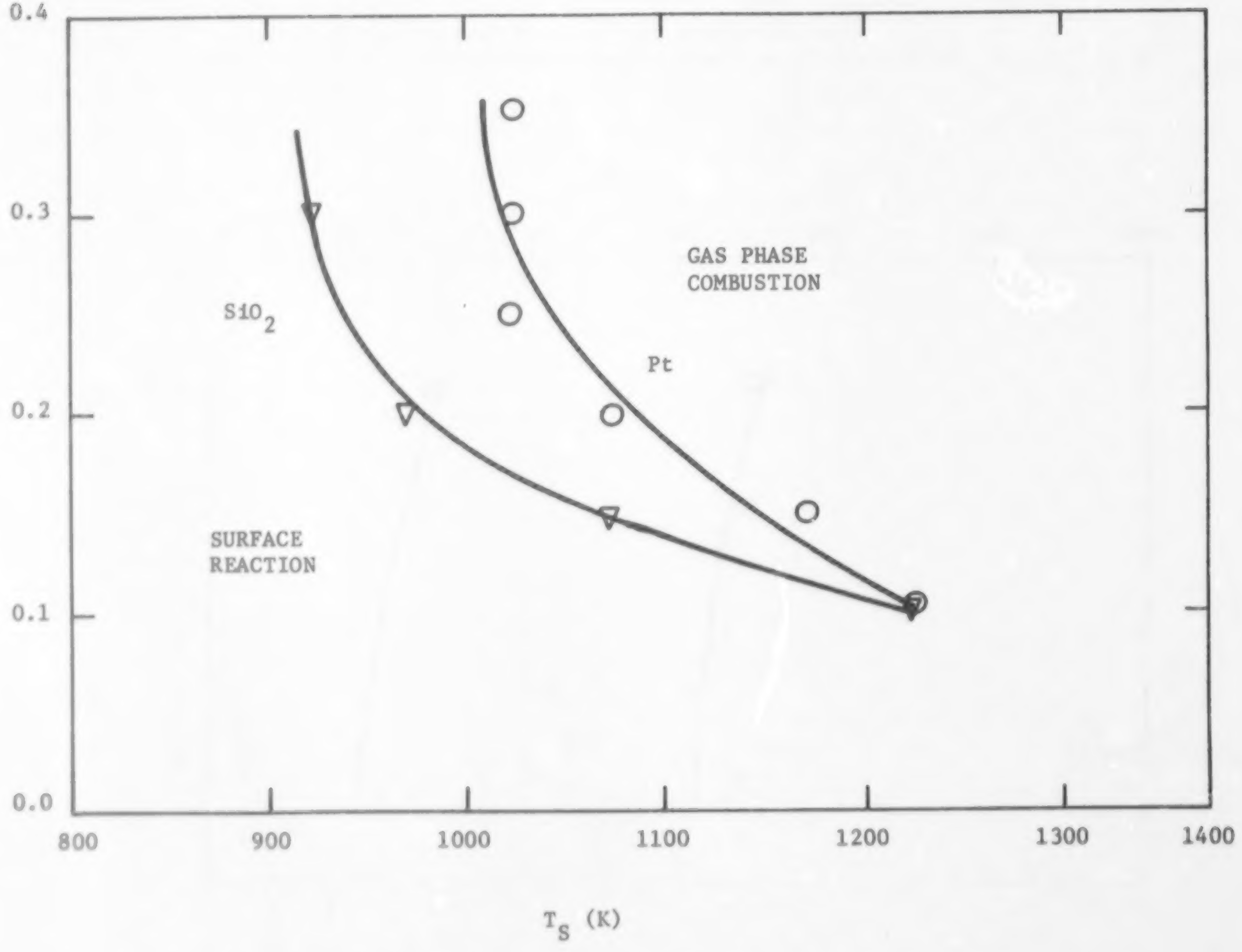

Figure 2. Gas phase ignition temperatures for H_2/air combustion. U_∞ = 1.5 m/s.

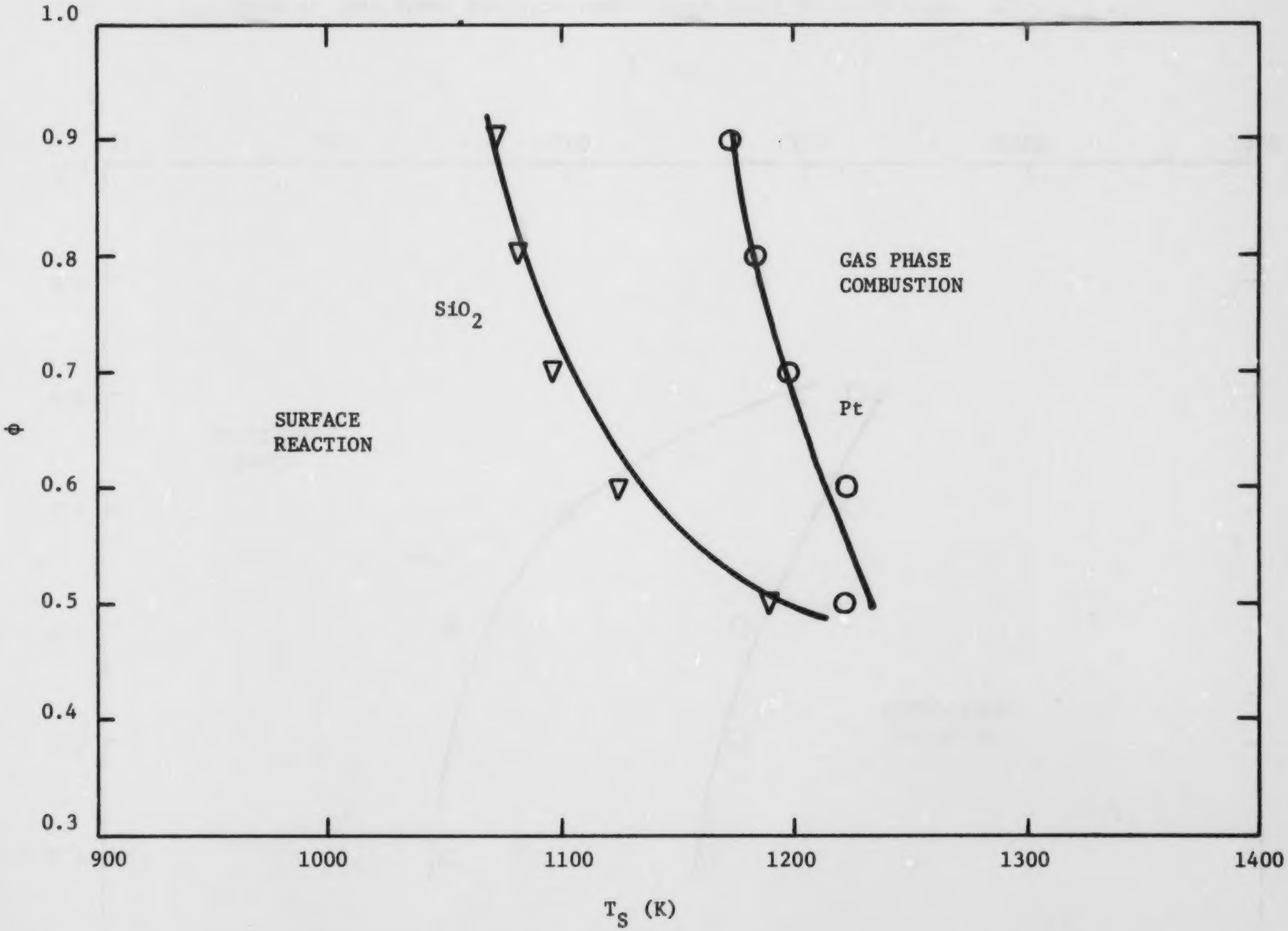

Figure 3. Gas phase ignition temperatures for C_3H_8 combustion. $U_\infty = 1.5$ m/s.

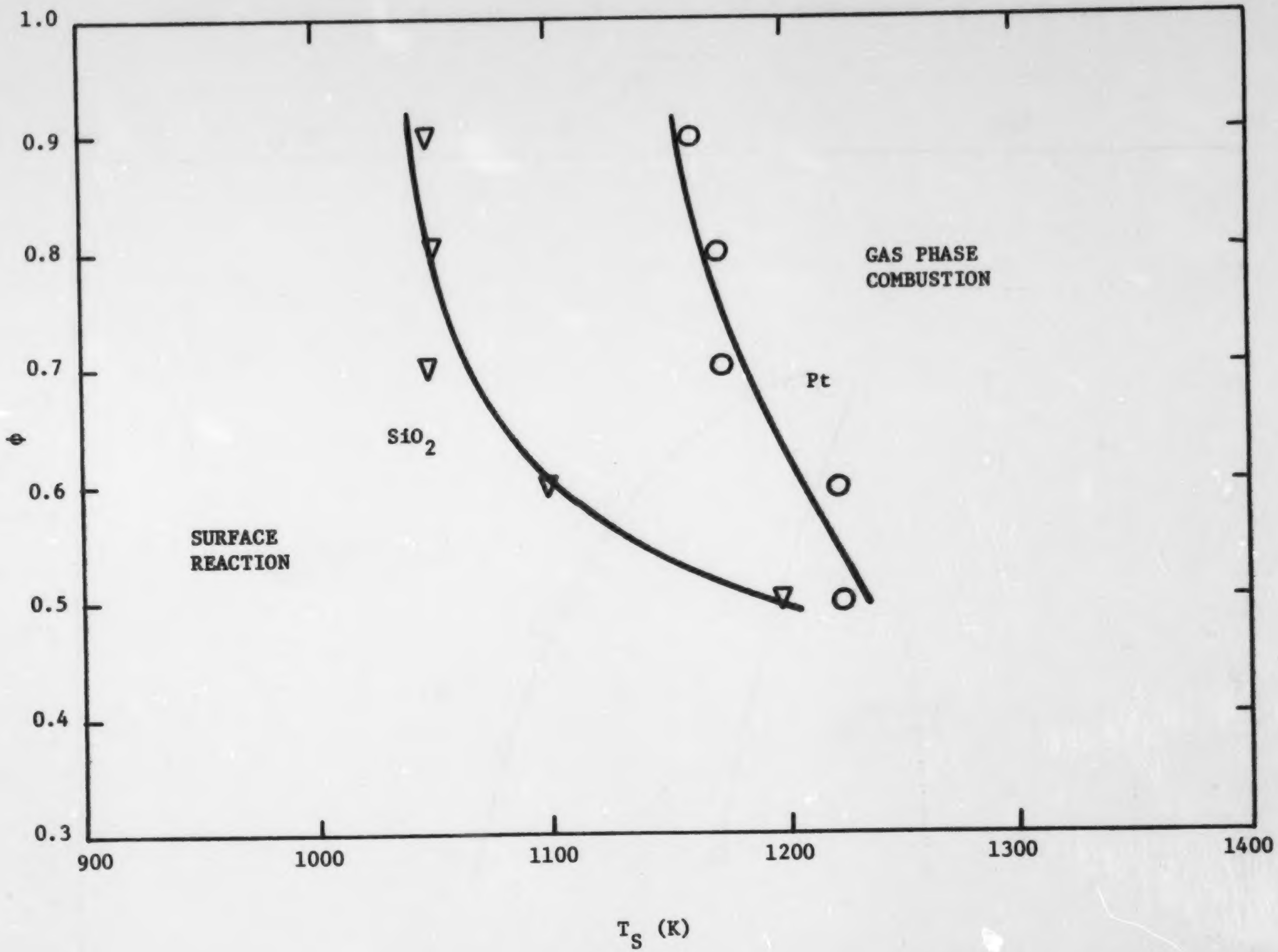

Figure 4. Gas phase ignition temperature for C_2H_6 combustion. $U_\infty = 1.5$ m/s.

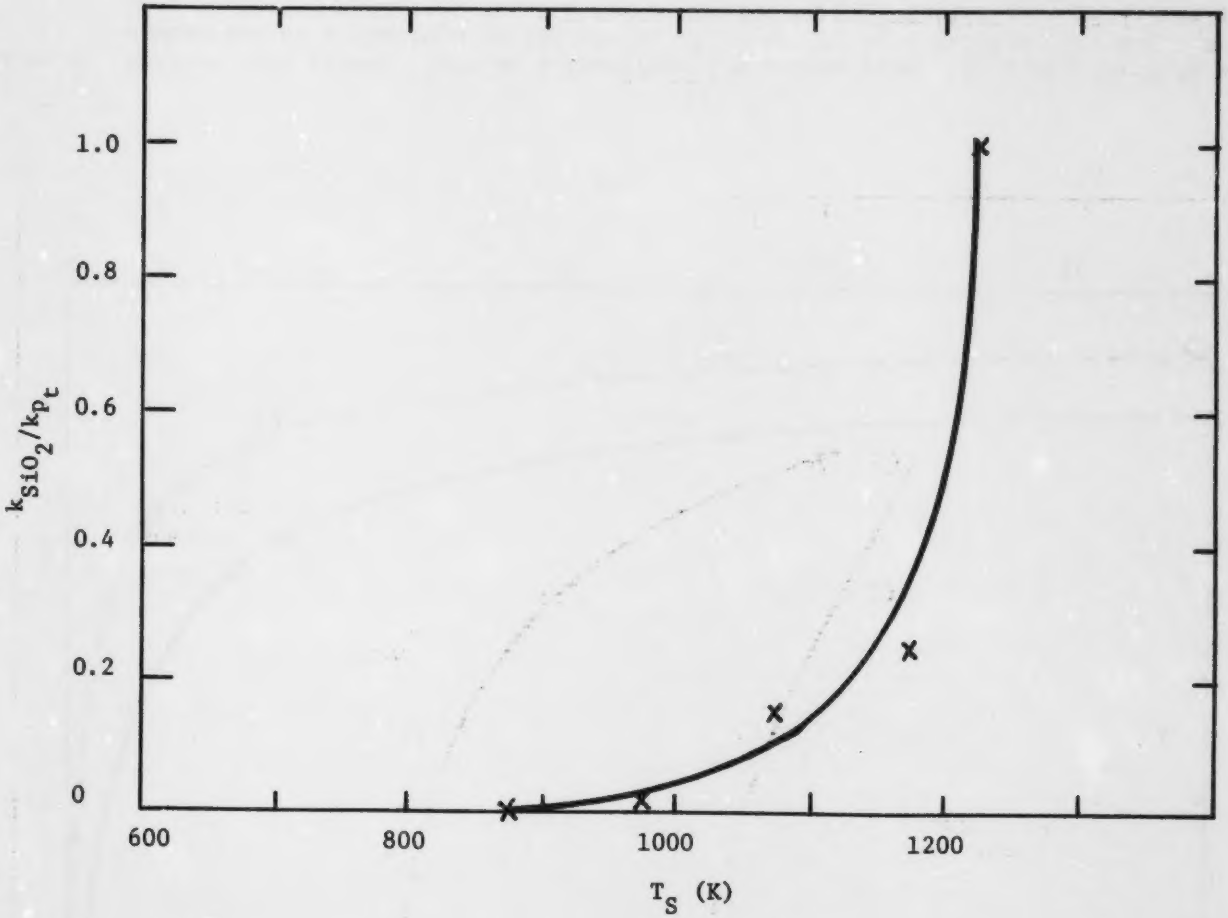

Figure 5. Nondimensionalized surface reaction rate constant as a function of surface temperature for H_2 oxidation on a quartz surface. $\phi = 0.2$, $U_\infty = 1.5$ m/s.

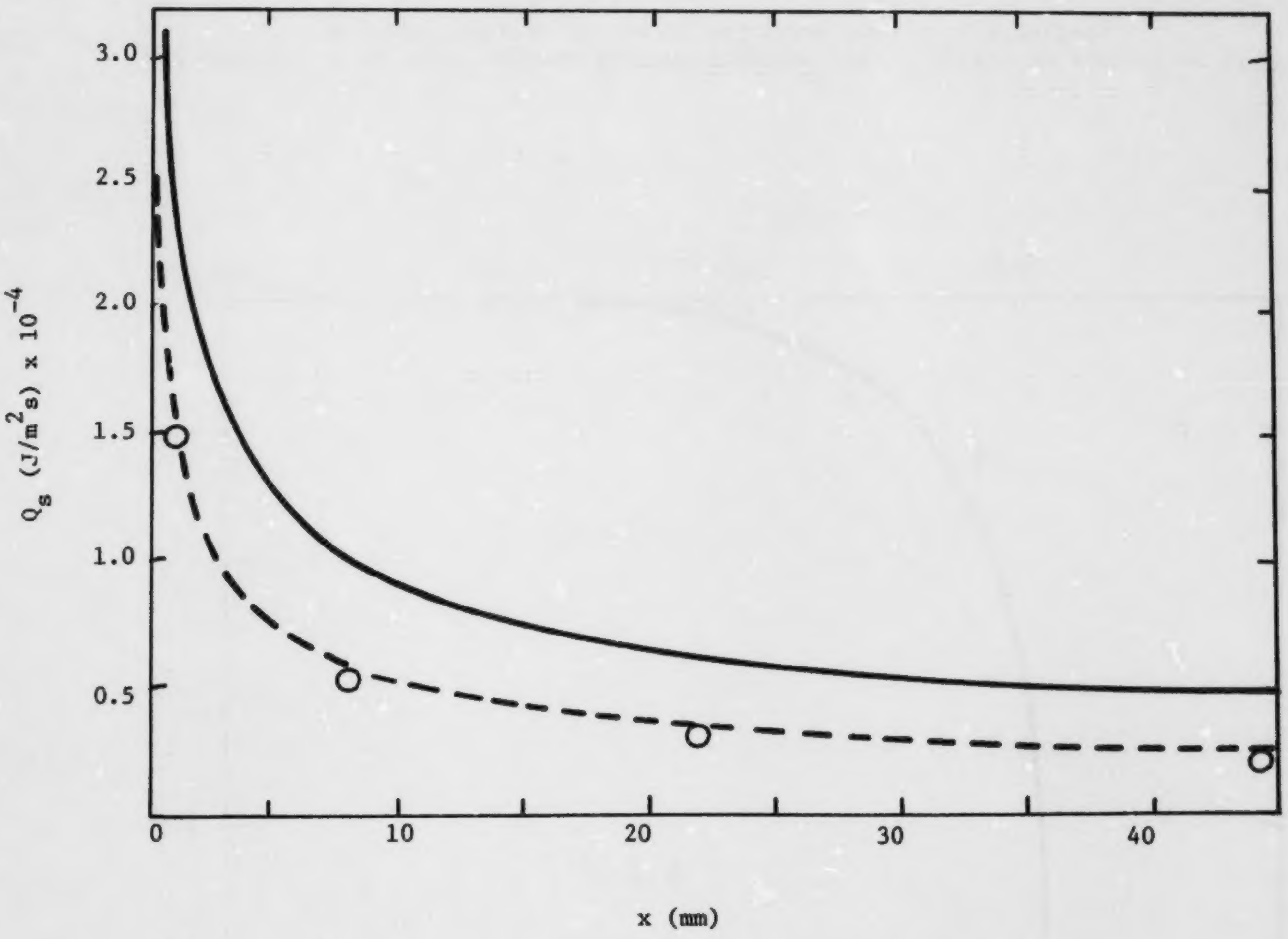

Figure 6. Surface heat release rate as a function of distance along the plate for C_3H_8/air combustion on a platinum coated plate. T_S = 670 K, U_∞ = 1.5 m/s, ϕ = 0.2. Solid line indicates numerical results for oxidation to CO_2; dashed line indicates results for oxidation to CO.

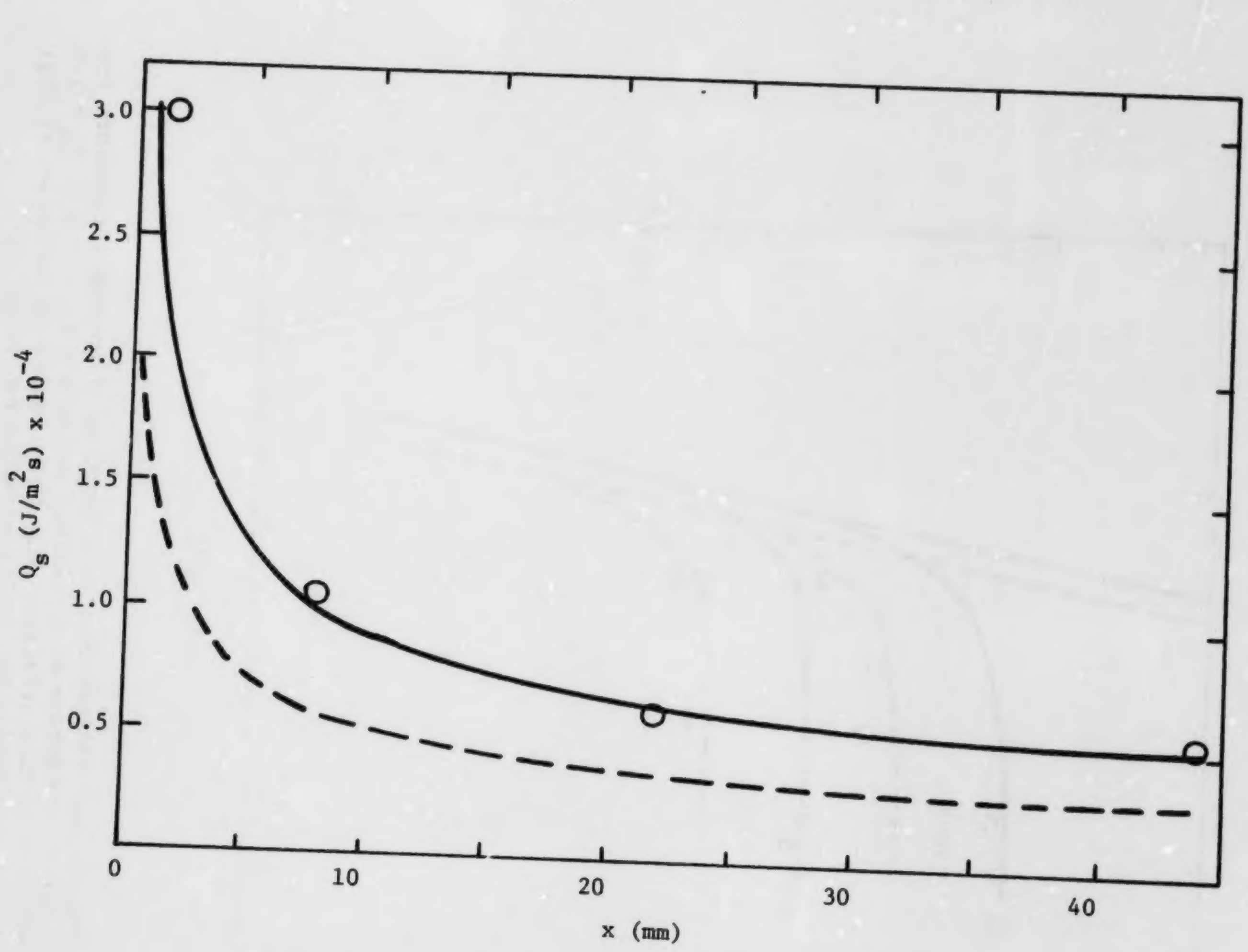

Figure 7. Surface heat release rate as a function of distance along the plate for C_3H_8/air combustion on a platinum coated plate. $T_S = 870$ K, $U_\infty = 1.5$ m/s, $\phi = 0.2$. Solid line indicates numerical results for oxidation to CO_2; dashed line indicates results for oxidation to CO.

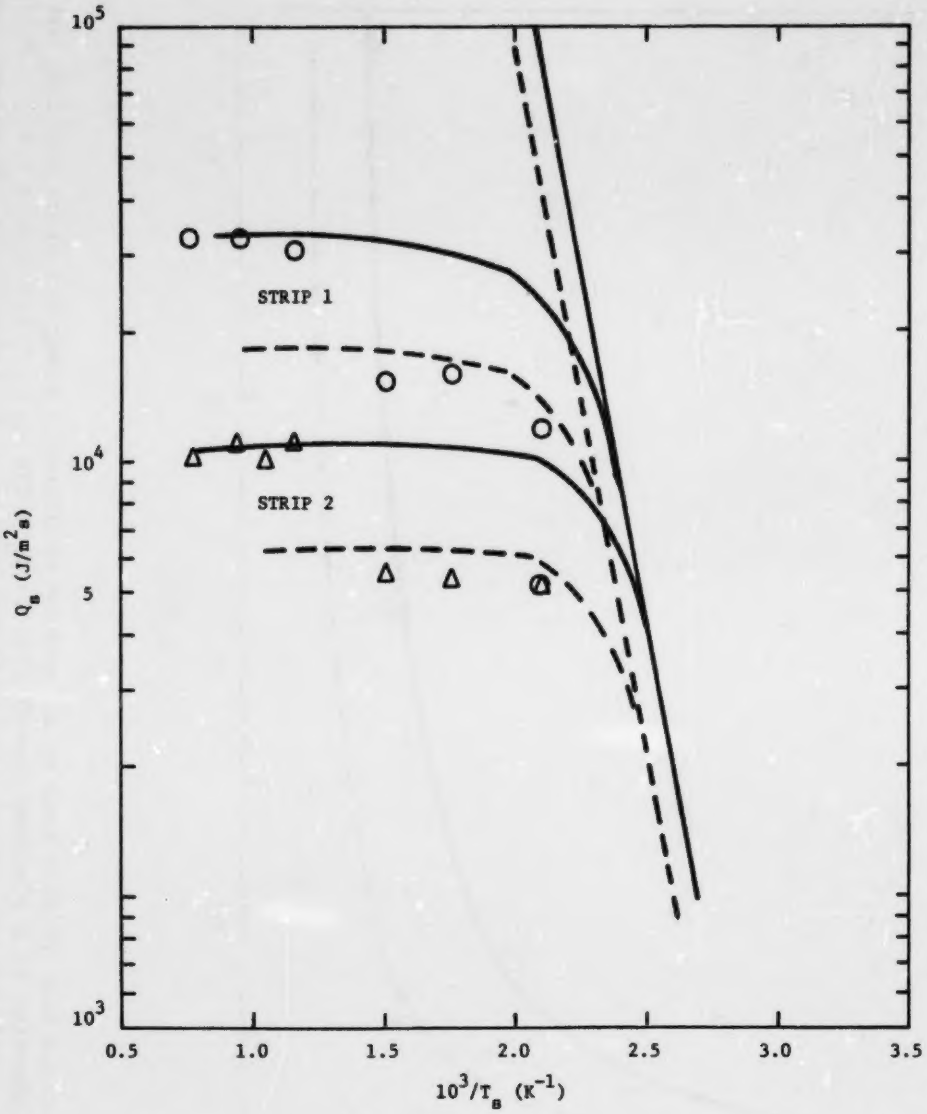

Figure 8. Surface heat release rate as a function of inverse temperature for C_3H_8/air combustion on a platinum coated plate. $\phi = 0.2$, $U_\infty = 1.5$ m/s. Solid line indicates numerical results for oxidation to CO_2; dashed line indicates results of oxidation to CO.

EXAMINATION OF THE NICKEL CATALYST ROLE IN RICH COMBUSTION

by

Gerald E. Voecks
Jet Propulsion Laboratory
California Institute of Technology
4800 Oak Grove Drive
Pasadena, California 91103

and

George Gavalas
Charunya Phichitkul
California Institute of Technology
Pasadena, California 91103

EXAMINATION OF THE NICKEL CATALYST ROLE IN RICH COMBUSTION

Rich combustion has been shown to be maintained successfully with a nickel catalyst in various experiments conducted at JPL. However, the activity of these alumina supported catalysts was found to degrade slowly but consistently with time and reduce the performance in extent of conversion and maximum throughput. To better understand how to maintain catalyst activity and reduce the severity of catalyst degradation, we have begun to study the rich combustion of methane by nickel on alumina. Based on thermodynamic equilibrium and experimental evidence, a mixture of methane and air containing 30% of theoretical stoichiometric air will produce the maximum amount of hydrogen and carbon monoxide without carbon formation and at a temperature near 1000°F.

Since the reaction conditions were to be carefully controlled to permit kinetic studies, an alumina reactor tube 61cm long with a 0.5cm I.D. was used and coupled with a traversing thermocouple located at the centerline. This reactor was mounted inside an insulated furnace to allow isothermal operation. Methane, oxygen and nitrogen were independently controlled to alter the air/fuel ratio and throughput (space velocity) over a range of constant catalyst bed temperatures.

Initial tests were conducted with the Girdler Catalyst Company catalyst G-56B. The catalyst was ground and sieved to a 60-80 mesh and a catalyst bed was packed to a length of 2cm in the center of the reactor. These tests were designed to determine the temperatures at which controlled conversion could be maintained for kinetic measurements at air/fuel ratios near 6.0. The "light-off" temperature at which high methane conversion took place was found to be at approximately 650°C (Figure 1). Once high conversion was achieved, its extinction temperature limit where methane conversion ceased extended far below the light-off temperature. More importantly, however, it was found that two reactions were taking place at temperatures below where light-off had occurred. Of the methane which reacted initially at the "pre-light off" condition (i.e., below 650°C), partial oxidation to carbon monoxide was not observed, but rather, complete oxidation to carbon dioxide took place (Figure 2). Following "light-off", carbon monoxide was the predominant carbon oxide product with some carbon dioxide also formed (approximately 80/20 CO/CO_2). This compares favorably to the thermodynamic equilibrium ratio of 86/14. During the subsequent reduction in operating temperature from 710°C to 500°C, it was found that the methane oxidation reaction continued below the light-off temperature to a greater extent than initial pre-light off. The rates of the two competing reactions (or series of reactions) to form carbon monoxide or carbon dioxide changed, reaching a crossover point at approximately 550°C. A similar phenomenon has been observed during tests in a full sized catalytic rich combustor (methane flows of up to 5 lbs/hr through a catalyst bed 3" long x 3.6" diameter). It appears that the catalyst surface is altered during the reaction sequence. Although this phenomenon is not clearly understood and will be studied later in more detail, the primary direction at this time was to examine more closely the catalyst activity and its degradation in the kinetics controlled regime, i.e., pre-light off temperatures, where no carbon monoxide is formed and only partial methane conversion occurs.

Because the G-56B catalyst (25 wt.% Ni) was too active to control the reaction at temperatures higher than 650°C, in-house catalysts were prepared. Nickel was impregnated into a low surface area alpha alumina support in order to minimize the activity degradation due to spinel (nickel aluminate) formation. The catalyst preparation procedure consistently followed involved the time controlled soaking of the alumina particles in a nickel nitrate solution, filtering, drying at 120°C and finally calcination. The same operating procedure of mixing oxygen, methane and nitrogen independently was used. Examination of the catalyst during deactivation was pursued further because of a similar occurrence which had been observed when commercial nickel on alumina catalysts were used as the catalyst in the larger unit described above.

The effect of catalyst calcining was the first parameter examined. As shown in Figure 3 the relative difference in initial activity between 850°C calcination in air for three hours and 400°C for one hour prior to reaction is nearly an order of magnitude. After a period of five hours continuous operation, the difference in activity had been reduced to half the difference observed at one hour of operation. To explain the relatively stable but less active character of the calcined catalyst which had undergone the high temperature treatment, the catalyst was reduced prior to operating under rich combustion conditions. Figure 4 shows that the relatively stable activity is altered and, further, that it also decreases in activity with time of operation and with increasing temperature of operation. The fact that the stable activity which the calcined catalyst initially possessed could be enhanced by reduction indicated that the catalyst activity responsible for producing the same products, CO_2 rather than CO, may be due to two different catalyst features. In observing the effect of cycling the catalysts, shown in Figure 5, it can be seen that an irreversible process is taking place each time because the same level of activity cannot be regained. In an attempt to understand why this is the case, the effects of reduction time and temperature and also of oxygen were examined. It was anticipated that perhaps crystallite growth could explain part of the irreversible decline in activity. It appears that if crystallite growth is taking place, it continues even in the presence of hydrogen because, as seen in Figure 6, a longer reduction time results in approximately the same loss in activity as if the catalyst was converting methane. Reduction at higher temperature (Figure 7) had no beneficial effect on changing the irreversibility of the catalyst activity decline. A 110 degree Centigrade increase in reduction temperature produced only about the expected activity recovery from the consistantly used 705°C reduction temperature. A change in the oxygen concentration during reaction while maintaining isothermal reaction conditions did not affect the rate of activity decline (Figure 8).

A closer examination of the surface species was expected to lend better insight into the catalyst alteration taking place. Nickel spinel does not form to any appreciable extent from nickel on alumina below 600°C according to various authors. Since the methane oxidation reactions being examined here are taking place at temperatures about 600°C, it is anticipated that this mode of deactivation is possible. However, two interesting points in this work are notable. First, use of alpha alumina as a support should reduce the rate of nickel oxide-alumina reaction to form spinel. Second, the relative ease of reducibility of the surface active catalyst species indicates that spinel is not responsible for the majority of the activity observed. This can be seen in Figure 9 where a prepared nickel spinel was found to have a specific activity two orders of magnitude lower than the nickel/alumina catalysts. It did, however, possess the same property of increasing activity following reduction. Further, from X-ray diffraction data, the active calcined catalyst was found to contain no spinel but simply nickel oxide and alpha alumina. It is expected that the activity associated with the calcined nickel/alumina catalyst is due to nickel-nickel oxide and that the slow loss in activity is due more to the crystallite growth of nickel oxide than to spinel formation at these temperatures.

In order to discount any major role of nickel spinel activity in methane oxidation at "pre-light-off" temperatures, a series of nickel spinels were formed. The ratio of the tetrahedral and octahedral crystal structures were changed to determine if one may possibly have been responsible for enhanced activity. Table 1 shows the comparison of the spinels prepared and Figure 10 illustrates the relative activities of each. In can be seen that the effects of crystal structure of nickel spinel has little to do with the initial activity observed in the nickel alumina catalysts.

In summary, the selective inactivity of nickel supported on alpha alumina to maintain partial oxidation of methane to carbon monoxide at temperatures below "light-off" has been demonstrated. Examination of this type catalyst under various pretreatment conditions seems to indicate that the surface nickel-nickel oxide species is undergoing a loss in activity probably due to crystallite growth. The possibility of nickel spinel being an active catalytic species is nil, regardless of the crystal form in which it may be. Further work is being conducted on improving the understanding of the catalysts involved, the deactivation process and the kinetics of reaction.

TABLE 1. EFFECT OF CALCINATION ON SPINEL PHYSICAL PROPERTIES

CATALYST	SUPPORT	CALCINATION IN AIR	XRD	PERCENTAGE Ni^{++} (tet) IN SPINEL	SPINEL CRYSTAL SIZE (Å)	BET AREA (m^2/g)
T-375 $\alpha\text{-A}\ell_2\text{O}_3$	–	–	$\alpha\text{-A}\ell_2\text{O}_3$	–	–	3.88
SP1	T-375	950^0 C, 8 hours	SPINEL + $\text{A}\ell_2\text{O}_3$	12	250	3.00
SP2	T-375	1200^0 C, 50 hours	SPINEL + $\text{A}\ell_2\text{O}_3$	24	360	2.98
SP3	T-375	1370^0 C, 50 hours	SPINEL + $\text{A}\ell_2\text{O}_3$	29	630	2.37
SP4	T-375	1550^0 C, 50 hours	SPINEL + $\text{A}\ell_2\text{O}_3$	35	630	0.39

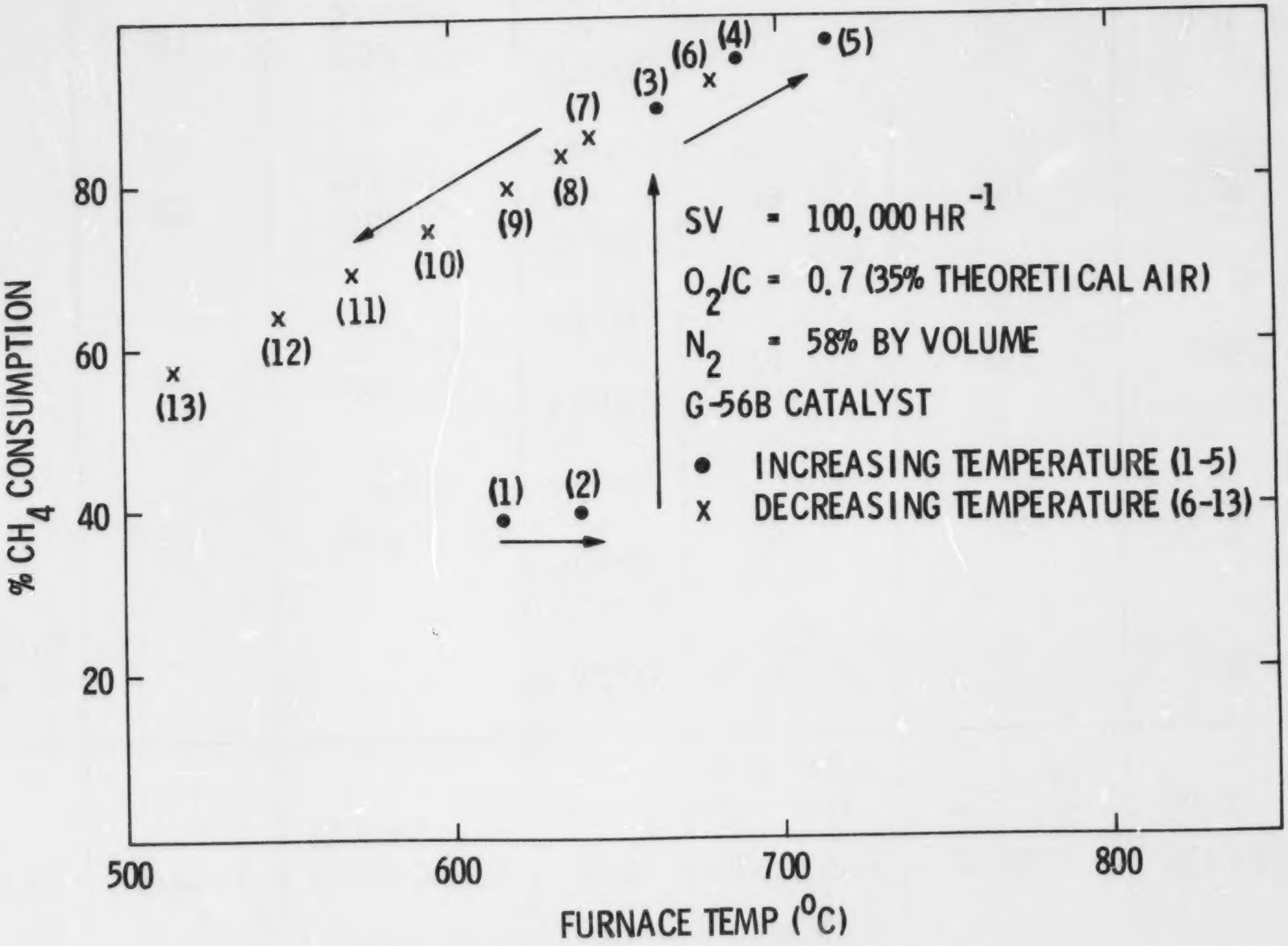

Figure 1. Multiple steady state of rich methane oxidation.

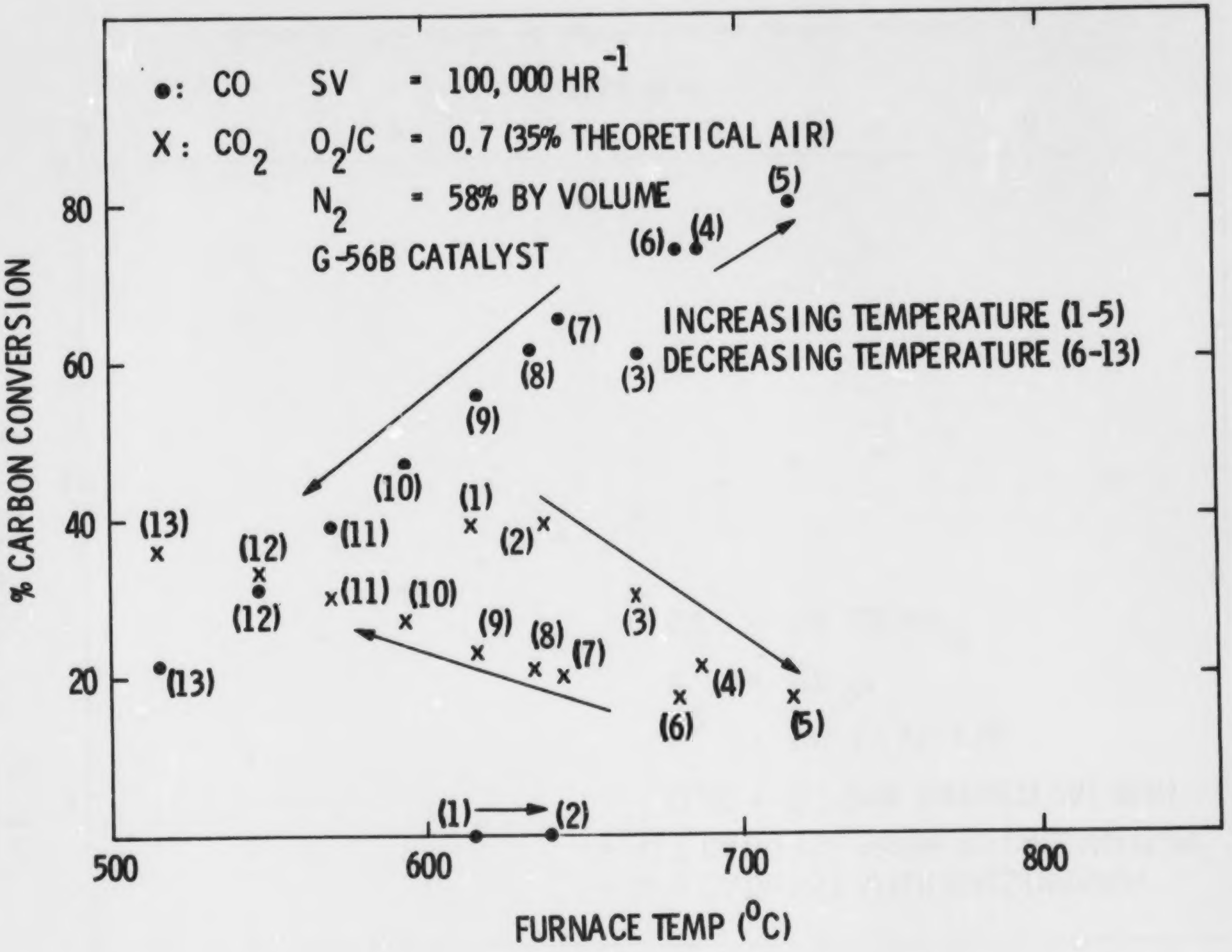

Figure 2. Oxygenated carbon product distribution.

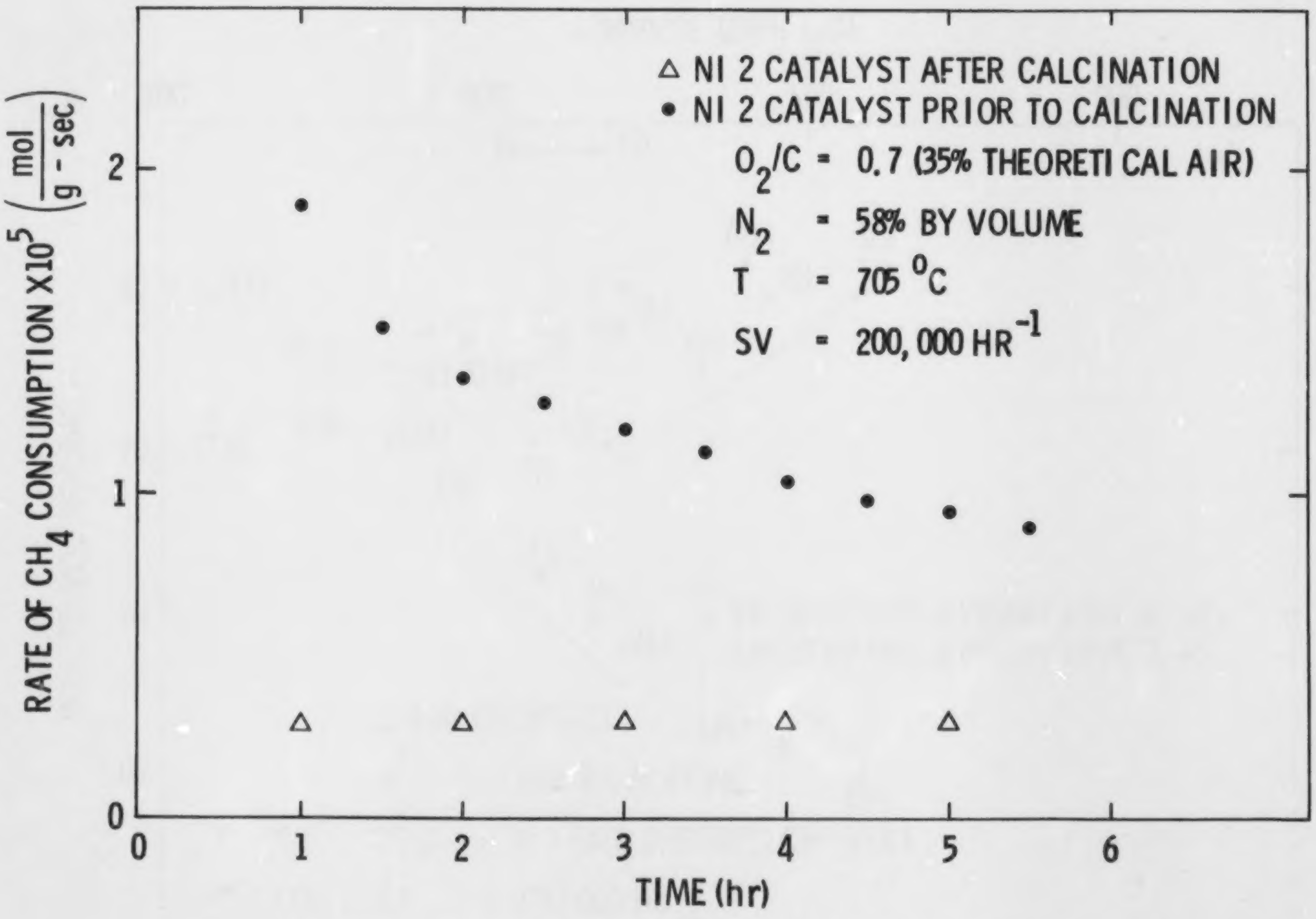

Figure 3. The effect of calcination on catalyst activity.

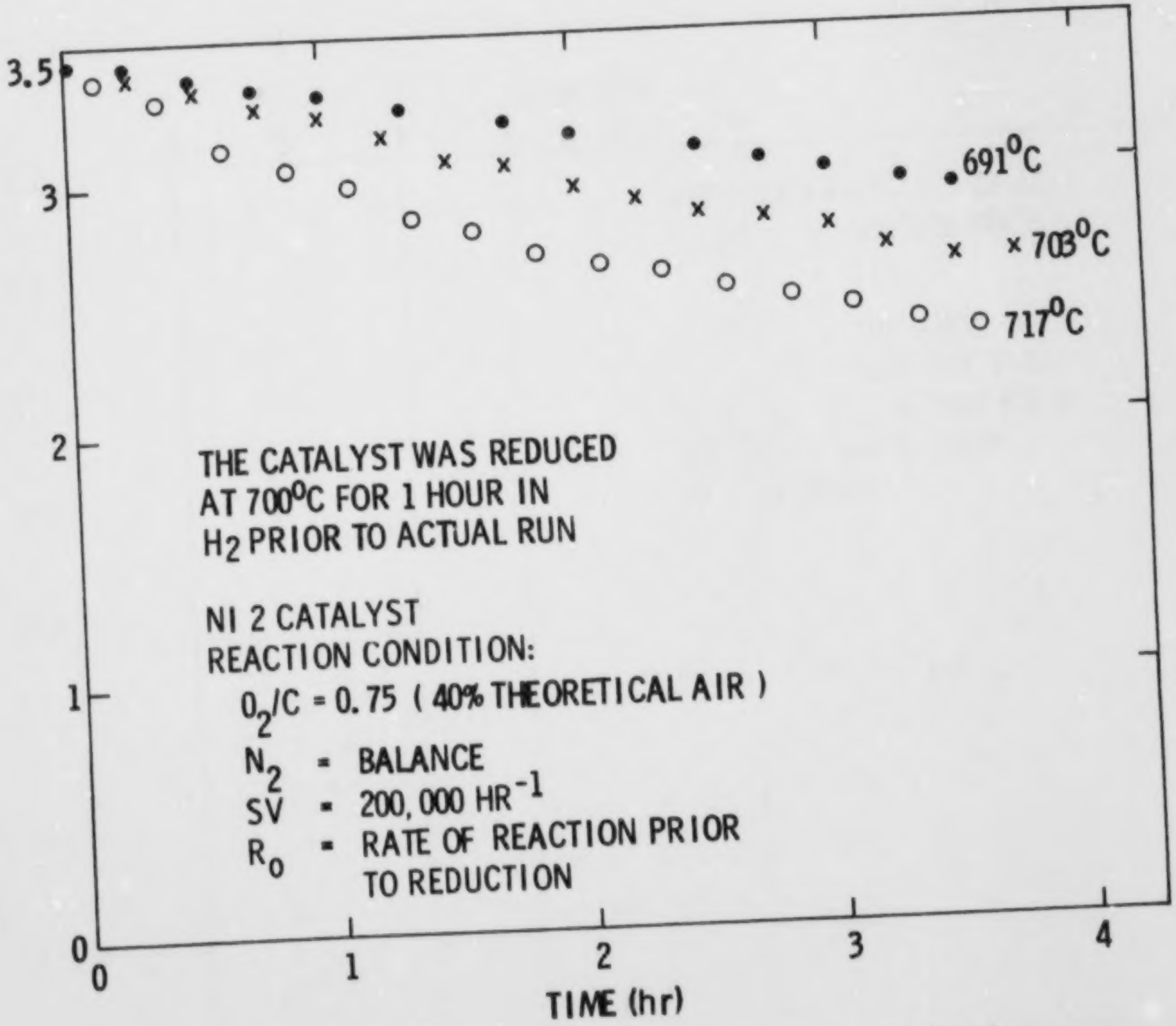

Figure 4. Effect of temperature on deactivation

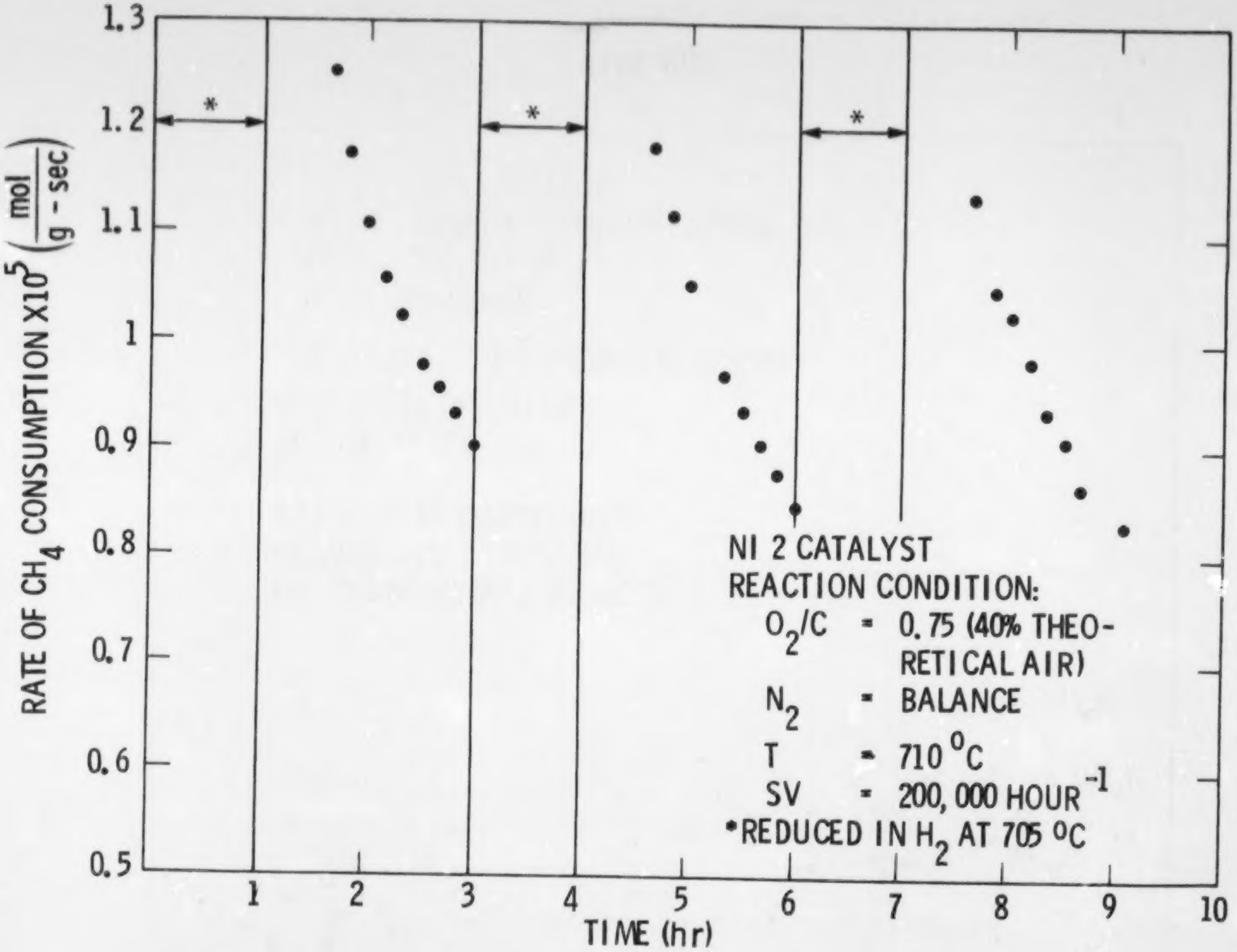

Figure 5. The effect of alternating reduction and oxidation on catalyst activity.

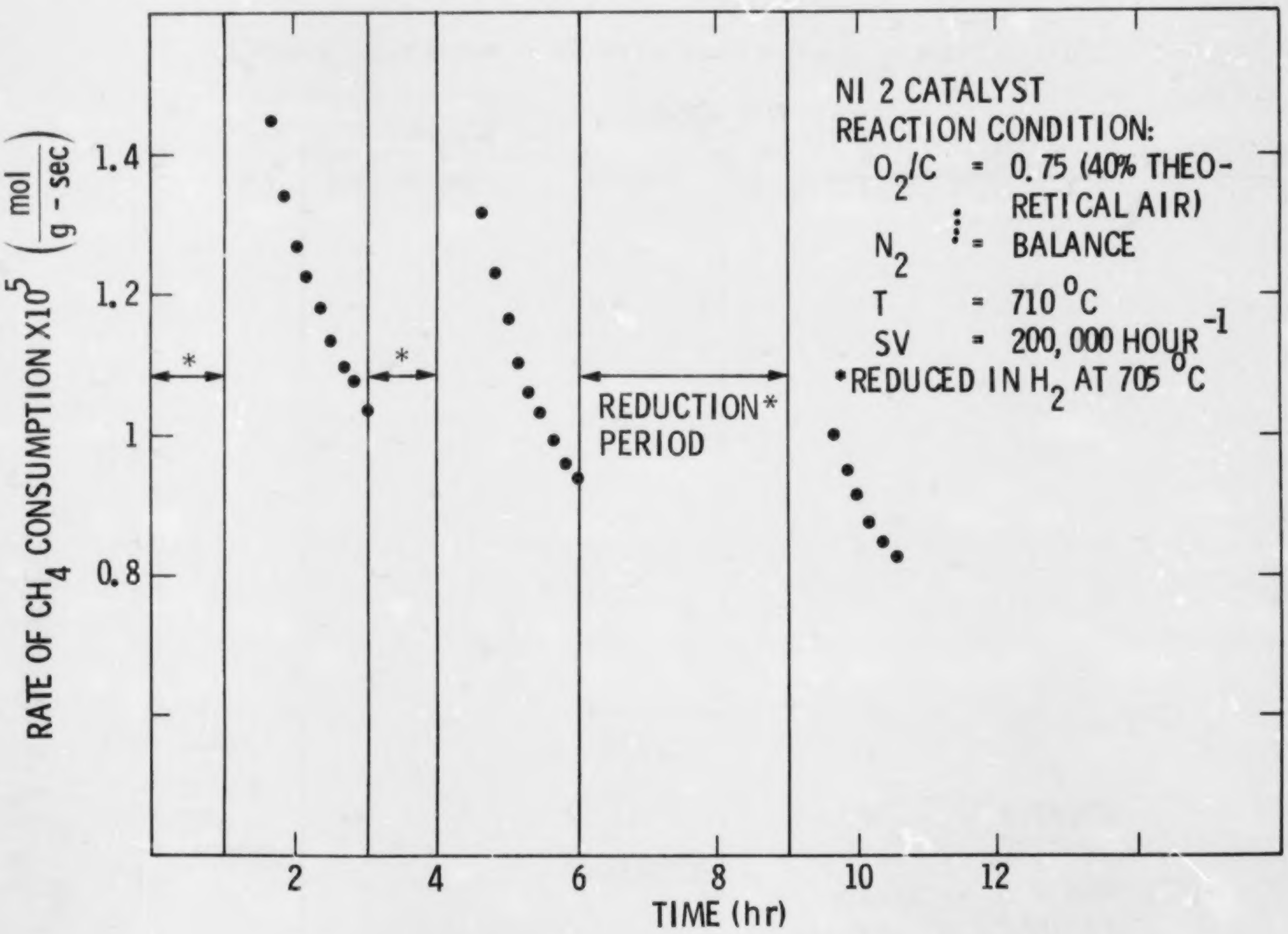

Figure 6. The effect of reduction time on cayalyst activity.

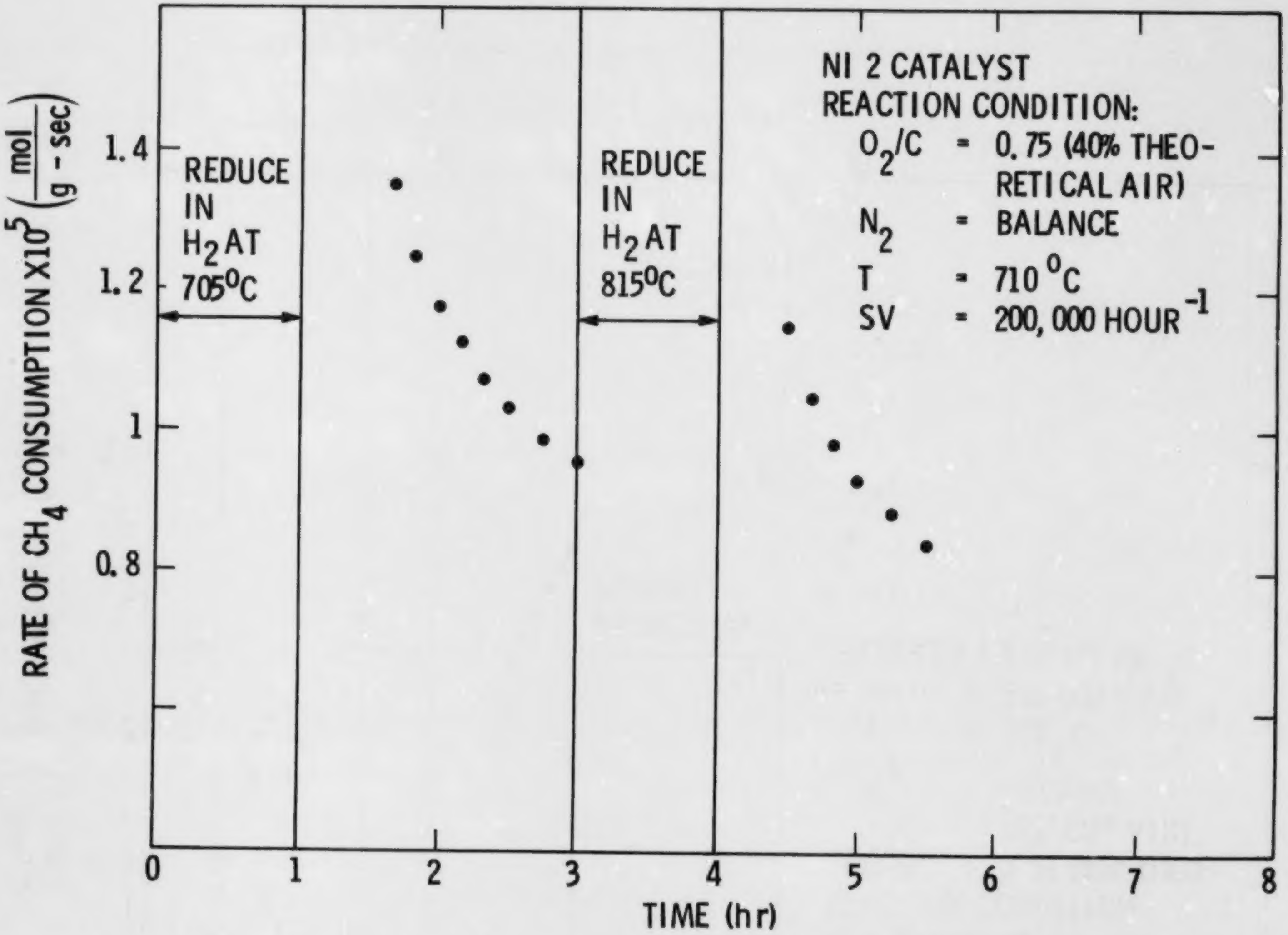

Figure 7. The effect of reduction temperature on catalyst activity

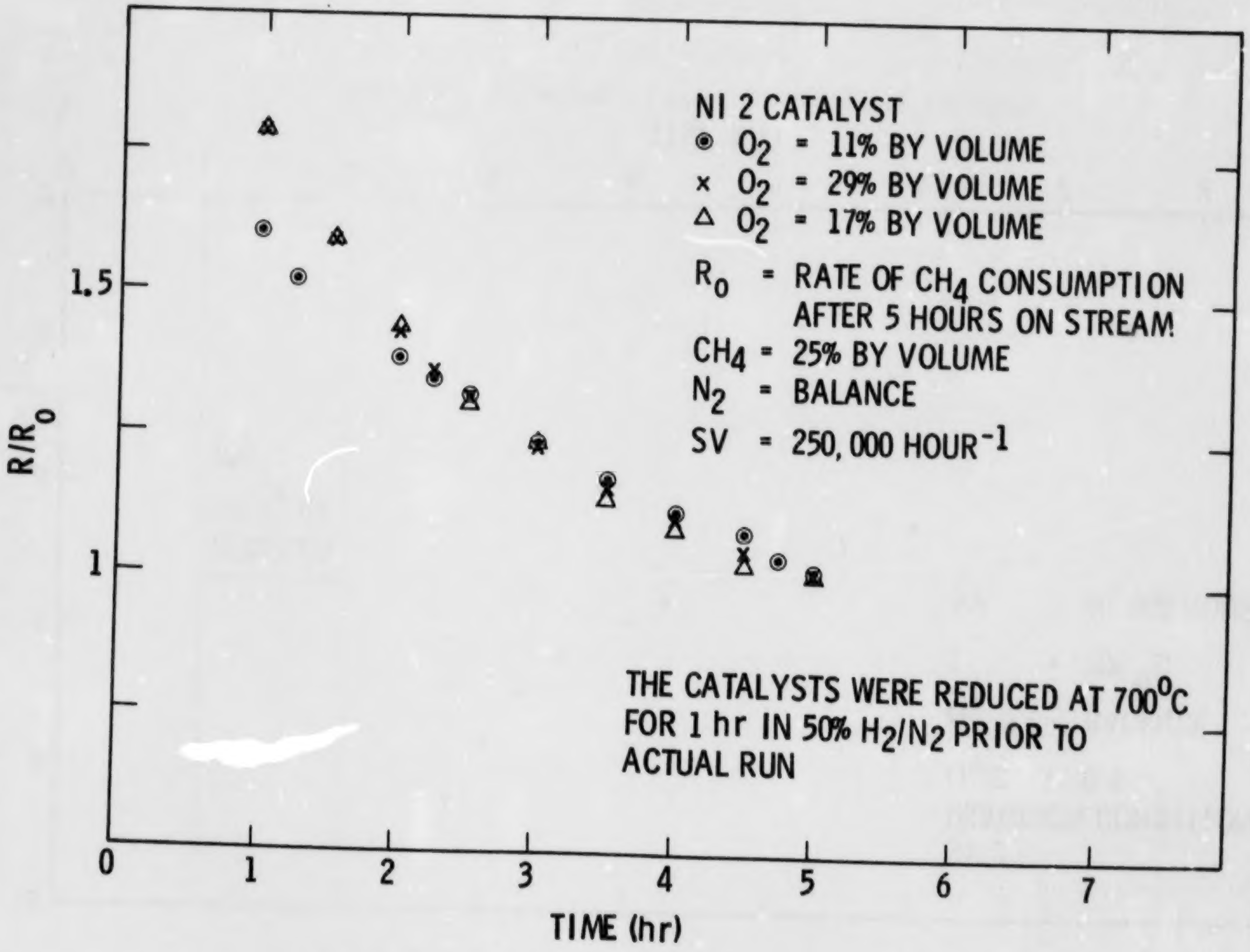

Figure 8. The effect of oxygen on deactivation

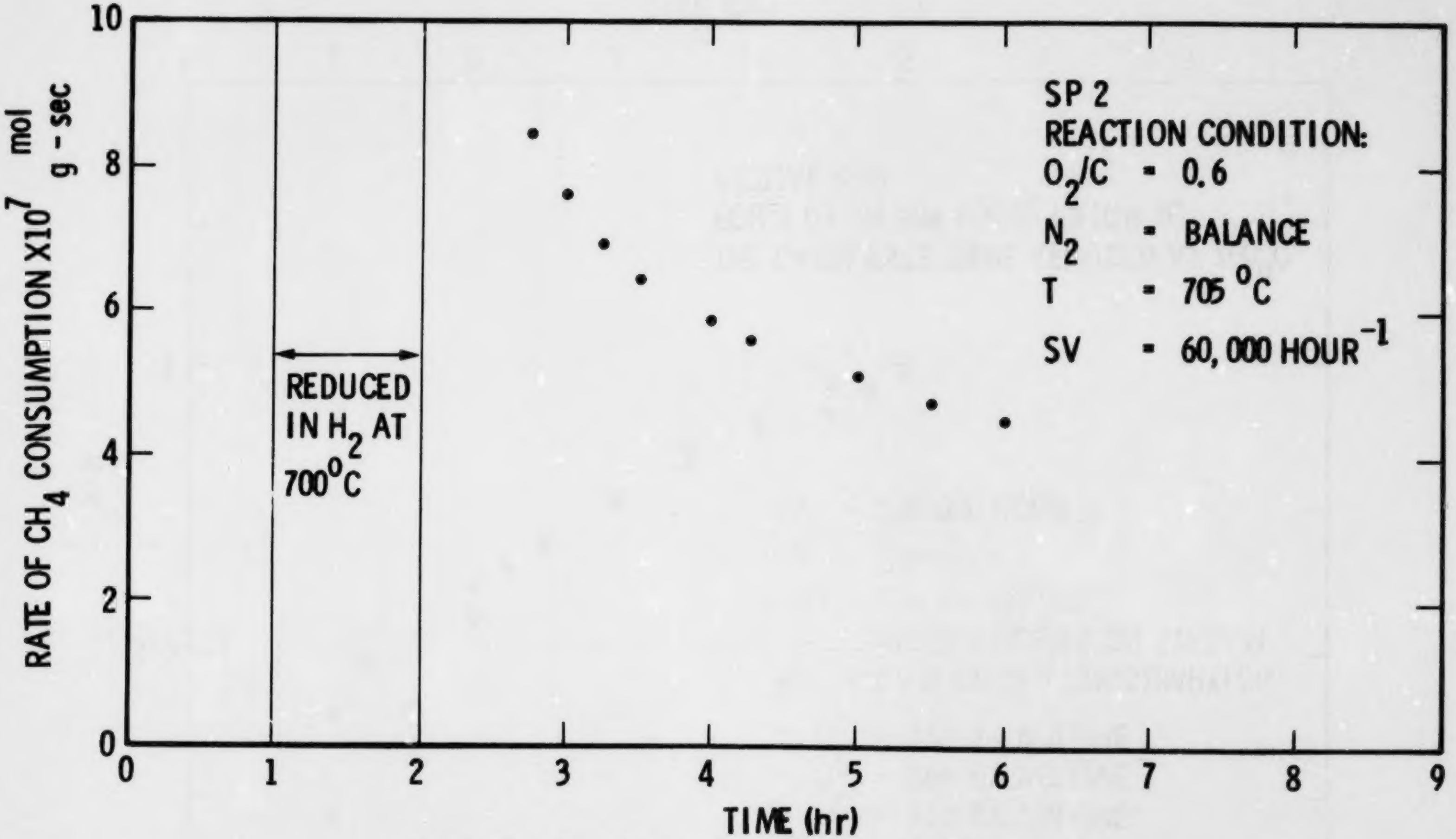

Figure 9. The effect of reduction on spinel activity.

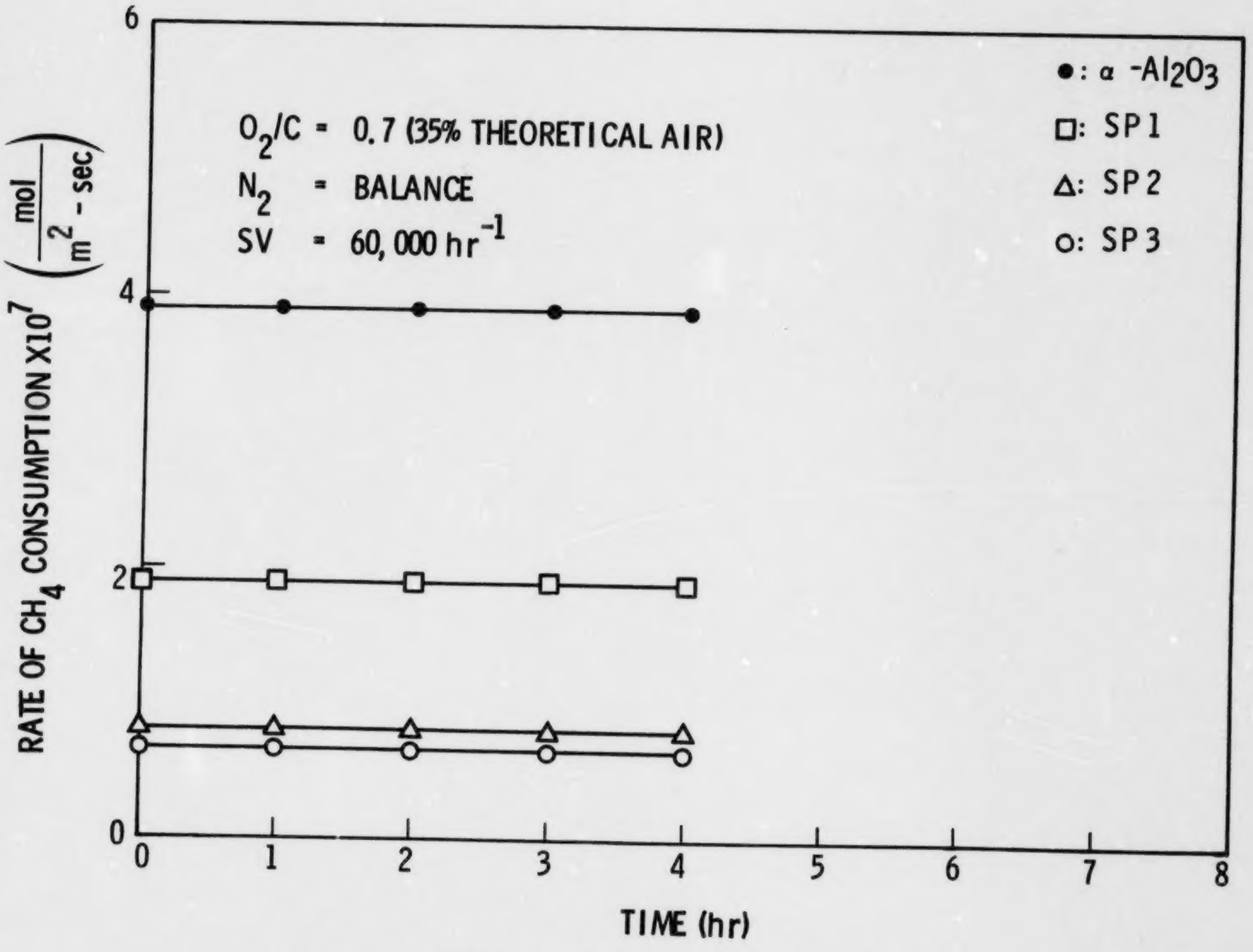

Figure 10. Relative activities of spinel and -Al_2O_3

SESSION III

APPLICATIONS OF CATALYTIC COMBUSTION

PROTOTYPE CATALYTIC SYSTEMS

By:

W. V. Krill, J. P. Kesselring, and S. J. Anderson
Acurex Corporation/Energy & Environmental Division
485 Clyde Avenue
Mountain View, California 94042

ABSTRACT

The development of catalytic combustion systems is continuing toward the prototype demonstration phase. Three combustor concepts have been developed to the system integration stage: (1) a small gas turbine combustor, (2) a watertube boiler concept, and (3) a firetube boiler burner. The results of concept testing are reported.

The model gas turbine combustor shows continued promise for low NO_x emissions with gaseous and distillate fuels. Greatest development difficulties are associated with introduction of the premixed fuel/air mixture and its interaction with catalyst lightoff systems. An integrated system has been developed, including a multiple nozzle, atomizing injector and an opposed jet lightoff burner. Testing of the concept is nearing completion to show its transient and steady state capablities.

The watertube boiler concept uses direct radiative transfer to watertubes in the combustion region. Structural problems of the radiative zone are currently being addressed, and final integration of the concept will follow. Thermal NO_x emissions are typically less than 2 ppm.

The firetube boiler burner also utilizes radiative heat transfer from a fiber matrix burner to the wall of the firetube. The matrix burner operates at a surface temperature below 1644K at low excess air levels to control the formation of thermal NO_x. Pad material screening tests have been conducted, and a mockup burner test is in preparation. Continuing program work will focus on prototype development of the watertube and firetube boiler concepts.

Work supported by the U.S. Environmental Protection Agency Contract 68-02-3122

INTRODUCTION

The advancement of catalytic combustor concepts toward the system demonstration phase is continuing. Through a series of contracts with the Environmental Protection Agency, Acurex Corporation has continued the development of several system concepts. These concepts are being further developed under the current EPA contract 68-02-3122: (1) a model gas turbine combustor, (2) a watertube boiler system, and (3) a firetube boiler burner. This paper presents a brief history of each concept and progress since the Third Workshop on Catalytic Combustion in October 1978.

The development of each of the three combustor types has been supported by other activities of the program. Catalyst development has continued to improve performance and operability of each of the combustors. The separate development of auxiliary systems has allowed fuel injection, lightoff, and temperature measurement problems to be solved. Data analysis and fundamental studies have provided greater ability to predict reactor performance. Finally, technology transfer through report publication, technical panel meetings, and workshops has allowed valuable interchange with the user industries. This multi-level approach is continuing, focusing on the prototype demonstration of watertube and firetube boiler systems.

MODEL GAS TURBINE COMBUSTOR

The demand for low NO_x gas turbine combustors is increasing. Potential applications include utility power systems, pipeline pumping, transportation vehicles, and future combined cycle processes. As a result, government and private development activities have greatly increased. Among selective catalytic reduction, thermal $DeNO_x$, and NO_x scrubbing, catalytic combustion may prove to be the most cost effective NO_x control technique.

COMBUSTOR DESIGN

Under early work with fuel-lean combustors, Acurex developed a model gas turbine can combustor (Reference 1). The combustor consisted of a stainless steel can, multiple cone fuel injector (based on a concept developed at NASA, Reference 2), and the catalyst element. The concept was tested under steady state operating conditions in both Acurex and Pratt and Whitney test facilities. Fuels used were natural gas, propane, and No. 2 oil at test pressures from 0.101 to 0.808 MPa (1 to 8 atmospheres). Very low thermal NO_x emissions (less than 5 ppm) were achieved throughout the test series. The combustor was also tested with nitrogen-doped fuels to investigate fuel nitrogen conversion to NO_x. Lean conversion rates were generally high (greater than 50 percent) at all test conditions.

The greatest system operational problem was injection of fuel to obtain a well-mixed, prevaporized reactant stream at the catalyst. The injector design resulted in flameholding under some operating conditions that would be encountered in machine applications. Therefore, the range of operability required improvement.

A second distillate fuel injector was designed and constructed. The injector incorporated three air-assist atomizing spray nozzles spraying through a perforated air distribution plate. The combustor injector assembly is shown in Figure 1. Cold flow and combustion tests were run on the configuration to verify the injector performance. Flameholding caused by the fuel introduction to the air stream was alleviated following optimization of the spray pattern into the combustor.

To further advance the combustor design, a lightoff system was incorporated to simulate typical turbine ignition and startup requirements. The advanced concept is shown in Figure 2. The system consists of an opposed jet burner, initiated by a spark plug. The opposed jet contains premixed gaseous fuel and air delivered counterflow to the main stream of reactants through a small tube. In application, the jet would be ignited during low air flow conditions and produce energy to accelerate the machine and preheat the catalyst to its lightoff temperature. As the machine approaches a loaded condition, the jet is extinguished by depletion of its flow, and combustion occurs totally in the catalyst. To date, the overall concept has been tested to simulate startup without the catalyst element to investigate operating characteristics of the fuel injector and opposed jet.

TEST RESULTS

Tests were conducted with premixed air and natural gas in the opposed jet and atomized diesel fuel in the mainstream air. The lightoff temperature that could be achieved was determined by varying the amount of diesel flow and hence the mixture adiabatic flame temperature. Tests were run at atmospheric pressure with a mainstream reference velocity of 4.6 m/sec (15 ft/sec) and a preheat temperature of 547K (525°F).

The test data is shown in Figure 3. As the mixture stoichiometry (including jet and mainstream fuels) is decreased toward stoichiometric, the lightoff temperature increases. The increasing adiabatic flame temperature of the mixture is shown for comparison. The actual temperature achieved at a given stoichiometry is dependent on the degree of mainstream fuel consumed. Less fuel is consumed near stoichiometric conditions due to increasing difficulty of burning liquid fuel droplets at 547K preheat. Increasing the preheat would result in greater fuel consumption and higher lightoff temperatures at a given mixture stoichiometry.

At 400 percent theoretical air, the combustor is operating with only jet fuel at a temperature of 1005K (1350°F). Above 400 percent, flame cannot be stabilized in the combustor. At 100 to 150 percent theoretical air, the majority of the fuel is diesel. Below 150 percent theoretical air at the preheat and velocity conditions described, the stabilizied flame could not be extinguished upon depletion of the jet flow.

The wide range of jet operability should allow smooth turbine startup in applications. At low air flow, the jet fuel would be introduced and ignited. During acceleration (and increasing compressor discharge temperature), mainstream fuel would be increased to the catalyst lightoff temperature and the jet extinguished. Final acceleration and loading could then be achieved catalytically by further fuel increases. Testing of the startup and steady state operation of the combustor with a catalyst is in progress.

WATERTUBE BOILER SYSTEM

The effect of NO_x control on boiler systems is even more significant than for gas turbines. Whereas stationary gas turbine combustors contribute approximately 3 percent of the total U.S. NO_x inventory, packaged and utility boilers are estimated to contribute 20 percent and 48 percent, respectively (Reference 3). Clearly, controls developed for watertube and firetube boilers are an important factor in reducing this country's NO_x emissions.

SYSTEM DESCRIPTION AND EARLY RESULTS

A catalytic watertube boiler system has been devised and extensively tested. Combustion occurs on the exterior surface of catalyzed cylinders in crossflow to the premixed reactant stream. Energy is transferred to watertubes by radiation from the combustion surfaces.

The concept is shown in Figure 4. A stoichiometric fuel/air mixture is fed to the radiative section which contains a close-packed array of catalyst elements and watertubes. The mixture is partially combusted by the catalyst which is kept at a low surface temperature by radiation heat loss to the watertubes. The combustion products and remaining unburned fuel and air are then passed to a downstream catalytic adiabatic combustor to complete combustion reactions. A final convective section extracts energy from the fully combusted gases. Both catalyst sections operate well below the maximum use temperature of the catalyst supports -- the radiative section by radiative cooling and the adiabatic section by dilution of the fuel/air mixture with exhaust products from the radiative section.

The radiative section has been constructed and tested independently of the downstream adiabatic combustor and convective sections. In early testing, the staggered tube arrangement (separate catalyst tubes and watertubes) was used. Later tests were conducted with a concentric tube design. The results for the staggered tube configuration were reported in Reference 4. The radiative section was run with natural gas at varying stoichiometry (40 to 220 percent theoretical air) heat release rate (1.09×10^8 to 3.44×10^8 J/hr), and preheat to establish its combustion efficiency, thermal and fuel NO_x emissions, and heat transfer characteristics at varying conditions. The catalyst was a platinum preparation on alumina tubes

At stoichiometric conditions, the combustion efficiency of the staggered tube combustor was approximately 37 percent. This result was slightly lower than the anticipated level of 50 percent necessary to avoid flame temperatures above the temperature capability of the adiabatic section. The thermal NO_x emissions were very low, however, never exceeding 2 ppm at these conditions. To evaluate the conversion of fuel nitrogen to NO_x, natural gas was doped with ammonia (NH_3). A minimum conversion level of 20 percent was measured at approximately 55 to 60 percent theoretical air.

These early combustion test results suggested several design modifications for improvement of the radiative section. Closer spacing of the catalyst tubes would improve the combustion efficiency. It would also be desirable to isolate the cold surfaces of the watertubes from the combustion zone to avoid fouling when firing with fuel oils. To meet these requirements, a concentric tube design was completed where the catalyst tube surrounds the watertube with an air gap between the two. Therefore, combustion energy generated on the catalyst tube outside surface would be transferred by conduction to its inner surface and by radiation across the air gap to the watertube.

CONCENTRIC DESIGN TEST RESULTS

The concentric configuration was first tested under conditions similar to those for the staggered arrangement with a platinum catalyst on alumina tubes. Combustion efficiency was markedly improved, reaching a high of 93 percent fuel conversion at stoichiometric conditions as shown in Figure 5. Thermal NO_x emissions were again less than 2 ppm, and fuel nitrogen conversion was below 30 percent under fuel-rich conditions. Tests were not performed with fuel oil to verify that capability, however.

Despite the improved combustion performance of the concentric watertube design, structural problems were encountered. The configuration develops a substantial temperature gradient across the walls of the ceramic tubes. The temperature difference results in nonuniform radial expansion and, ultimately, fracturing of the material. The stresses that would be encountered in application were calculated as 198 x 10^6 Pa (28,700 psia) to 257 x 10^6 Pa (37,300 psia), clearly greater than the 190 x 10^6 tensile strength of alumina tubes at 1367K (2000°F).

Only one other ceramic can be made with adequate strength and is appropriate for combustion applications. Silicon carbide not only has a high strength of over 400 x 10^6 Pa at the above conditions, but it has a higher thermal conductivity than alumina and therefore results in lower temperature gradients and developed stresses. As a result, tubes of silicon carbide were purchased from the Norton Company in the proper dimensions and coated with a chromia (Cr_2O_3) and platinum catalyst preparation for an additional test series. Testing of the concept is in progress.

FIRETUBE BOILER BURNER

A large percentage (approximately 50 to 65 percent) of the commercial size boiler market is composed of firetube boilers. These smaller units account for over 30,000 gas-fired boilers and an equal number of distillate oil-fired boilers in the 3.2 x 10^9 J/hr (3 x 10^6 Btu/hr) size alone (Reference 5). In fact, of all commercial and industrial size boilers in the field, the majority are firetubes. These applications are principally gas- and distillate oil-fired.

Thus, firetube boilers represent another area for significant NO_x reduction. A catalytic burner would be especially attractive if it were retrofitable into the large number of boilers already installed or at least presented only minor changes to current designs.

BURNER DESIGN CONCEPTS

A number of catalytic burner designs were conceptualized and reviewed with major firetube boiler manufacturers. The simplest and most acceptable to the manufacturing community utilizes a fiber matrix material that is molded into a cylindrical surface burner for insertion into the firetube.

The burner concept is shown schematically in Figure 6. A fuel/air mixture is passed into the central region of the cylindrical fiber matrix.

The cylinder construction is best described by Figure 7. The matrix material is approximately 2.5 cm (1 inch) in thickness, is closed with similar material at the downstream flow end, and is sealed at the upstream end by a combustion chamber flange. The matrix material is rigid, is supported at the upstream end, and has internal flow passages as shown in Figure 7, maintaining concentricity with the boiler firetube.

In the described configuration, premixed fuel and air are forced to flow into an annulus between the fiber matrix and an internal cylinder. The fuel may be gaseous or vaporized liquid. The mixture then flows through the matrix and is ignited at the outer cylinder surface to start the burner. A heterogeneous surface reaction zone is established on the cylinder outer surface, within a depth of only a few millimeters of the matrix thickness. The majority of the matrix thickness remains at the temperature of the incoming reactants and promotes no additional reaction.

Heat is transferred directly from the matrix outer surface to the firetube as shown in Figure 6. The transfer is primarily radiative although convective transfer also contribues. This heat transfer limits the matrix surface temperature to less than 1644K (2500°F), the temperature limitation of the material, although the adiabatic flame temperature of the reactive mixture exceeds 2200K. The heat is transferred through the metal firetube wall to the boiler water to heat the water or raise steam. Flue gases are forced to the end of the firetube and out to the additional firetube passes.

FIBER MATRIX EXPLORATORY TESTS

Catalytic fiber matrix materials have demonstrated low NO_x emissions and high combustion efficiency with gaseous fuels (Reference 6). However, the optimum matrix material, appropriate heat transfer configuration, and ability to operate on distillate fuel required additional study. A series of tests on fiber matrix disks was conducted to evaluate these parameters.

Figure 8 shows the matrix surface temperature of the combustion zone as a function of theoretical air for three values of face velocity. Lower face velocities result in lower surface temperatures at low excess air levels (100 to 130 percent theoretical air) where firetube boilers normally operate. This low surface temperature is advantageous in reducing NO_x emissions as shown in Figure 9. Emissions of less than 10 ppm at 115 percent theoretical air are possible. Tests also indicate high combustion efficiency (low CO and HC) can be achieved simultaneously with low NO_x emissions.

The low surface temperatures of Figure 8 also demonstrate the effective radiative heat transfer away from the combustion zone. The indicated temperatures of 1478K to 1644K (2200°F to 2500°F) at 100 percent theoretical air are within the use temperature capabilities of the alumina silicate fibers and far below the adiabatic flame temperature of 2228K. From these tests, the optimum flow velocity for the selected matrix material appears to be 10 to 15 cm/sec (1/3 to 1/2 ft/sec).

The catalytic burner was also operated on diesel fuel To achieve stable combustion with similar results to natural gas, it was necessary to partially vaporize the oil. This was accomplished by preheating the air stream to 492K (425°F) prior to admitting the fuel. Current firetube boiler designs operate without air preheating systems. Therefore, operation of the matrix burner with fuel oil in a firetube boiler will require additional development of an air preheating technique.

These flat disk burner tests identified the operating requirements of the matrix material. To further develop the concept, a cylindrical burner as in Figure 7 was constructed for testing in a simulated firetube. Results of the tests are pending. The fiber matrix burner does appear attractive for further development and should be applicable to many firetube designs with only minor modifications.

CONCLUSIONS

The development of catalytic gas turbine, watertube boiler, and firetube boiler combustors is rapidly progressing. The potential for near-term reduction of thermal NO_x emissions with clean fuels is promising.

An integrated model gas turbine combustor has been tested to simulate both startup and steady state operating conditions, following refinement of fuel injection and lightoff techniques. Only further refinement of the concept is required for small machine applications. The concept may also be scalable to larger combustor sizes.

The watertube boiler concept shows promise for further development despite being a radically different design from present systems. Production units would probably differ further from those tested. Stress analyses on the catalyst supports determine silicon carbide as the most appropriate ceramic in the preferred concentric tube design. Ongoing testing will verify the material recommendations and lead to testing of the integrated system concept.

The firetube boiler burner is a retrofitable design for gas fired units. For distillate fired firetubes, the fiber matrix concept requires preheated air for acceptable operation. Detailed tests on fiber materials have shown low NO_x emissions due to surface cooling with concurrent low CO and hydrocarbon emissions. A cylindrical burner of the most acceptable material is being fabricated for testing.

The development of burners for these three classes of equipment addresses a large portion of the NO_x emissions in this country. Further EPA program development will focus on prototype demonstration of catalytic boiler systems.

REFERENCES

1. Kesselring, J. P., et al. Design Criteria for Stationary Source Catalytic Combustion Systems. EPA-600/7-79-181, August 1979.

2. Tacina, Robert R. Degree of Vaporization Using an Airblast Type Injector for a Premixed-Prevaporized Combustor. NASA TM-7883b, August 1978.

3. Mason, H. B. and Waterland, L. R. Environmental Assessment of Stationary Source NO_x Combustion Modification Technqiues. Proceedings of the Second Stationary Source Combustion Symposium. EPA-600/7-77-073a, July 1977.

4. Krill, W. V. and Kesselring, J. P. The Development of Catalytic Combustors for Stationary Source Applications. Proceedings: Third Workshop on Catalytic Combustion. EPA-600/7-79-038, October 1978.

5. Evaluation of National Boiler Inventory. EPA-600/2-75-067, 1975.

6. Blair, Martin G. Prototype Surface Combustion Furnace Evaluation. EPA-600/7-79-038, October 1978.

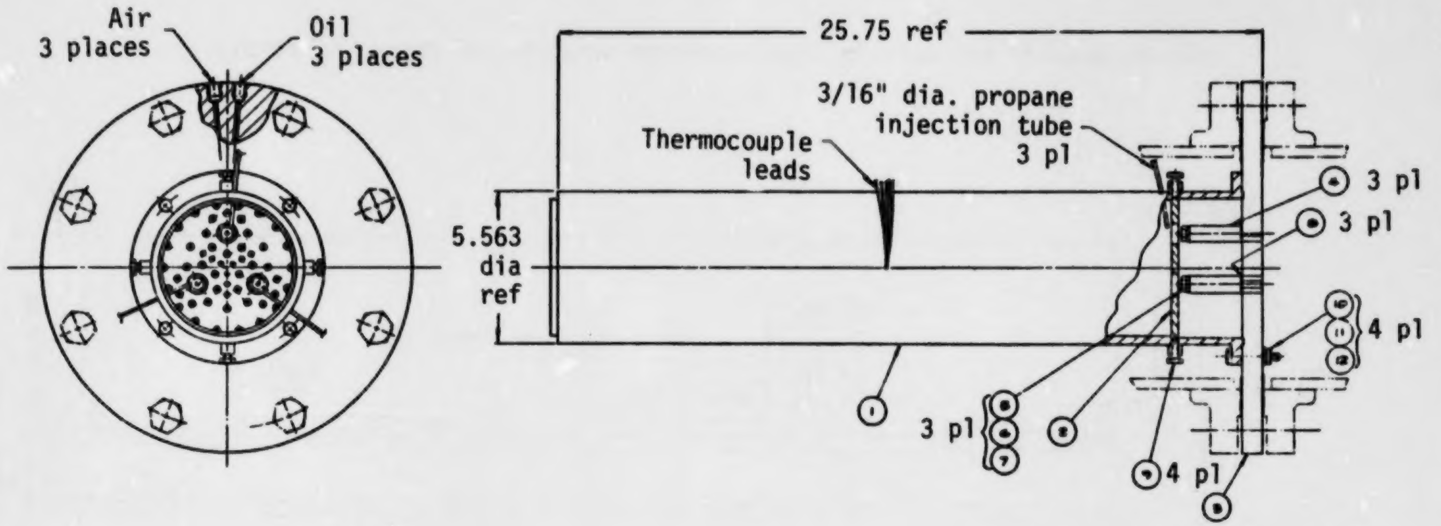
Air
3 places
Oil
3 places
25.75 ref
3/16" dia. propane
injection tube
3 pl
Thermocouple
leads
5.563
dia
ref
1
3 pl
3 pl
4 pl
3 pl
4 pl

-42	-41	ITEM NO	CODE IDENT	PART NO	DESCRIPTION	
	4	12			NUT, HEX - 1/4-20UNC	SST
	4	11			WASHER, SPLITLOCK - 1/4 NOM	SST
	4	10			BOLT, HEX HD - 1/4-20UNC × 1 3/8 LG	SST
	4	9			BOLT, HEX HD - 1/4-20UNC × 5/8 LG	SST
	3	8		B7474-031	GASKET .03 THK	
	3	7		1.	WASHER	SPRAYING SYSTEMS CO
	3	6		NO. 2588 303 SST	RETAINER RING	SPRAYING SYSTEMS CO.
	3	5		NO J 6 303 SST	SPRAY SET-UP	SPRAYING SYSTEMS CO.
	3	4		C7474-029	NOZZLE ADAPTER	
	1	3		D7474-028	FUEL INJECTION PLATE	
	1	2		D7474-027	DIFFUSION PLATE	
	1	1		D7474-026	TUBE, CATALYST SUPPORT	

QTY REQD — LIST OF MATERIALS

NOTES:

1. METALLIC WASHER CAPABLE OF WITHSTANDING 1000° TEMPERATURE REQUIRED.

Figure 1. Model gas turbine combustor assembly.

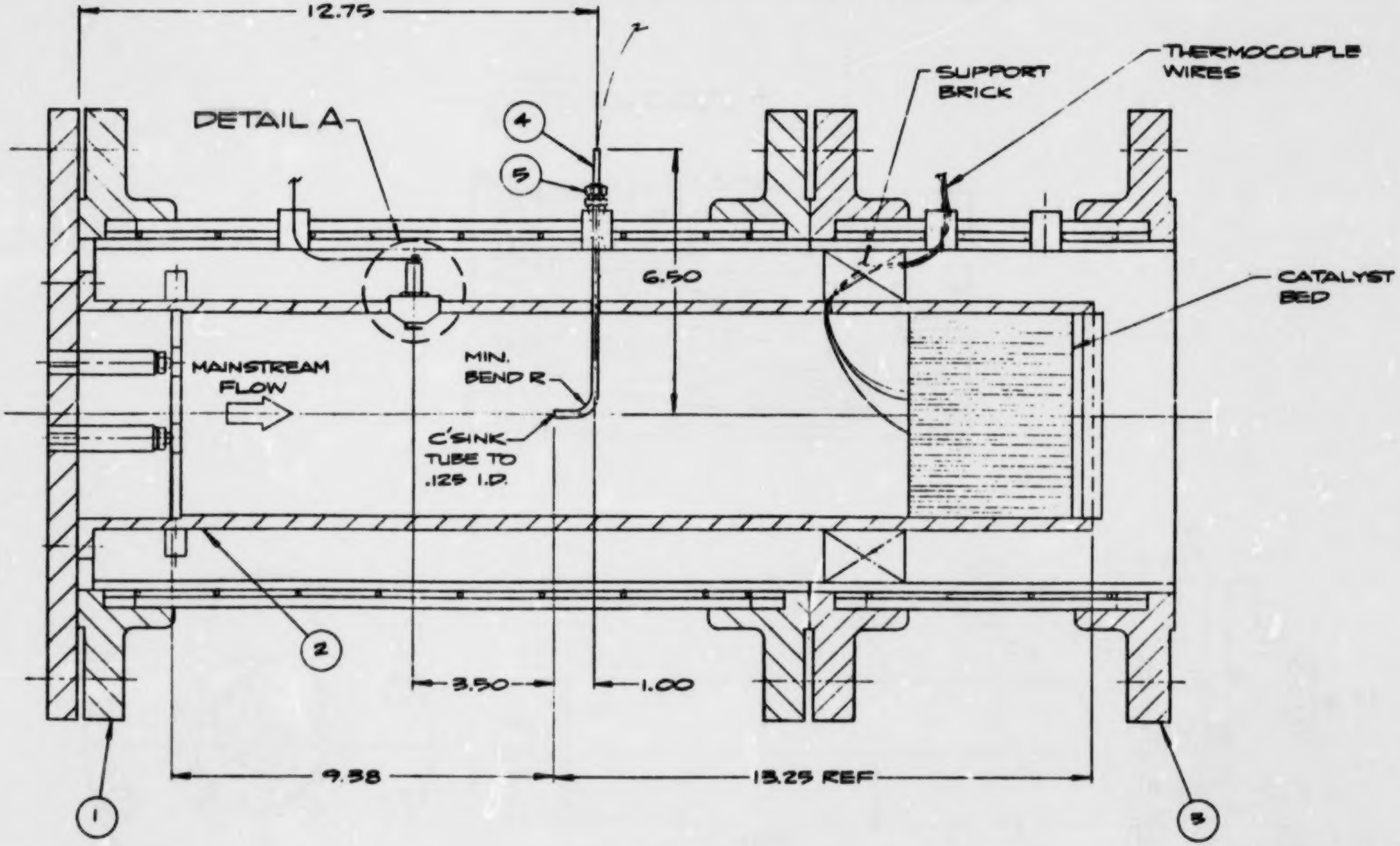
12.75
DETAIL A
4
5
6.50
SUPPORT BRICK
THERMOCOUPLE WIRES
CATALYST BED
MAINSTREAM FLOW
MIN. BEND R
C'SINK TUBE TO .125 I.D.
2
3.50
1.00
1
9.38
13.25 REF
3

Figure 2. Model gas turbine combustor with opposed jet startup system.

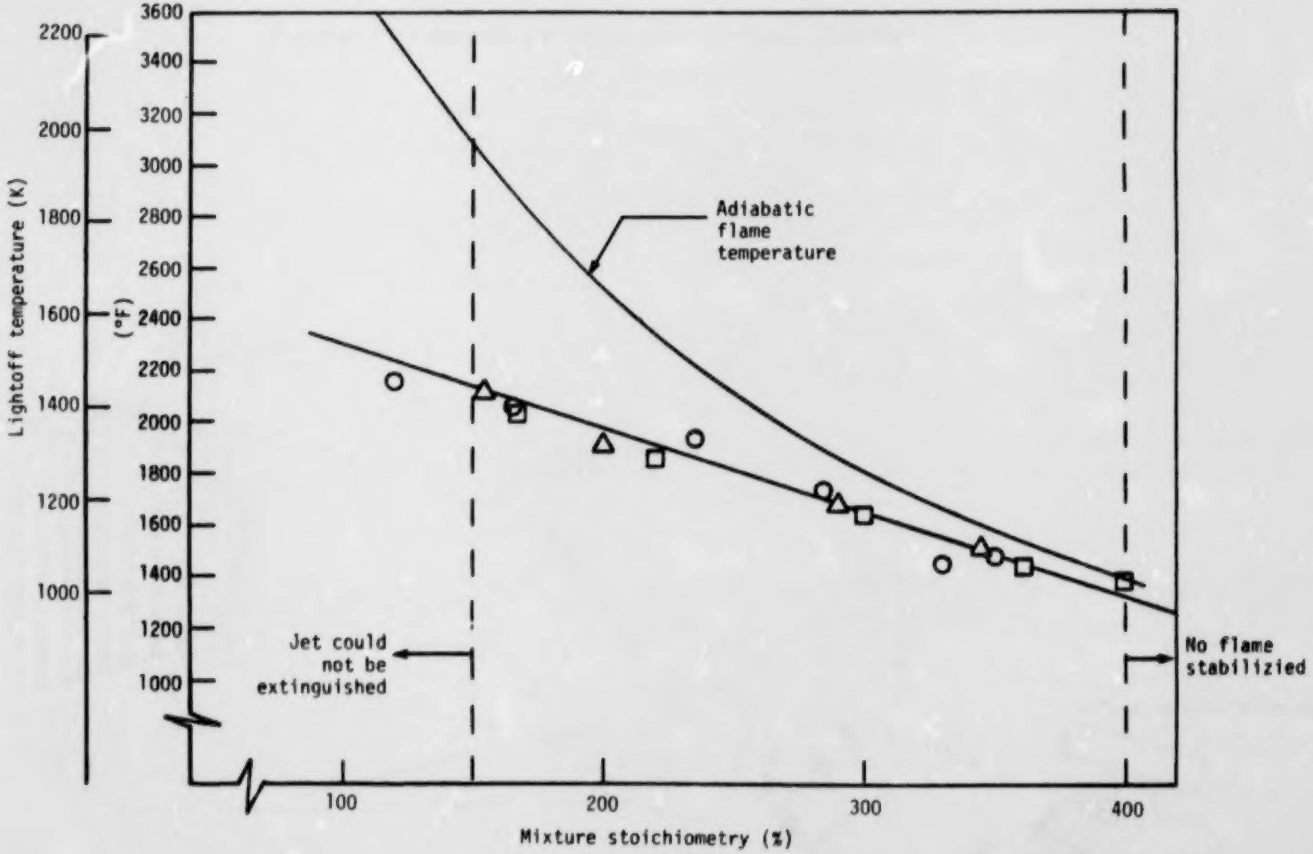

Figure 3. Gas turbine opposed jet results.

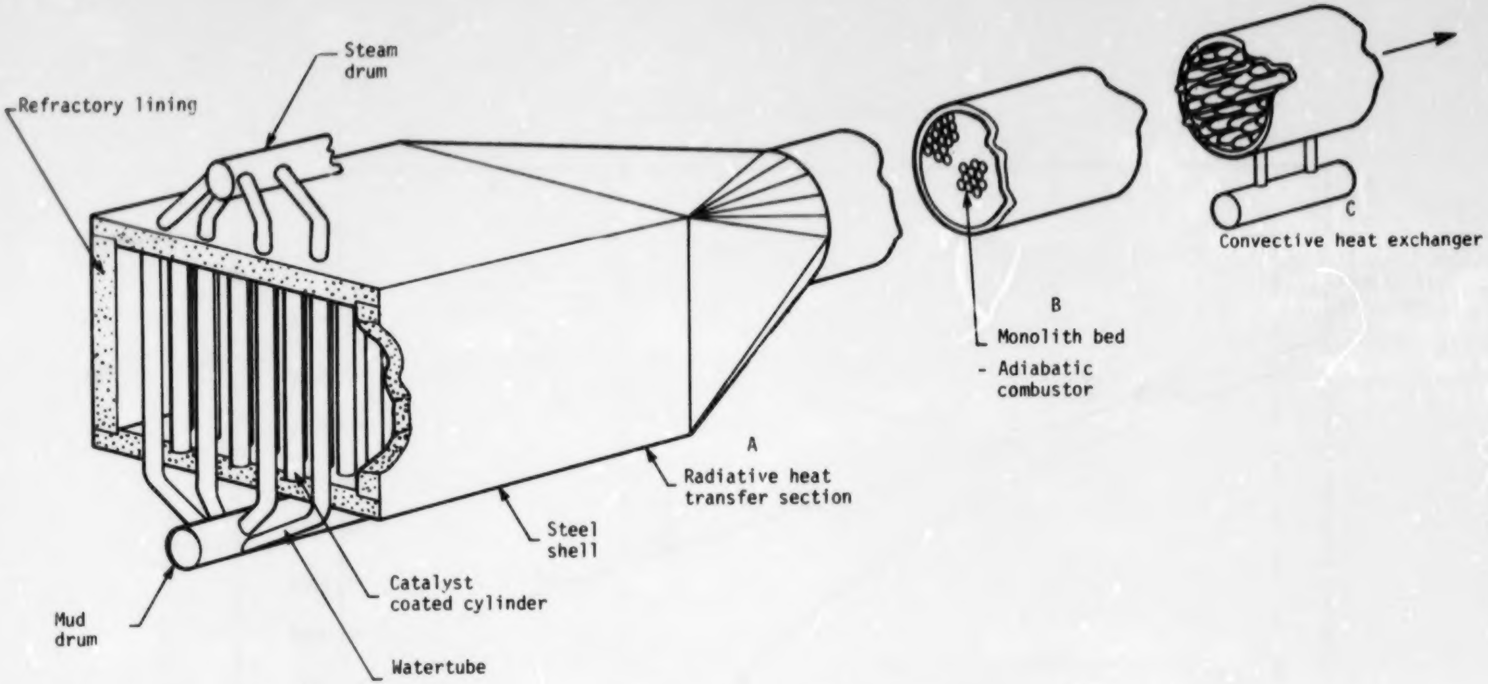
Steam drum
Refractory lining
Mud drum
Catalyst coated cylinder
Watertube
Steel shell
A
Radiative heat transfer section
B
Monolith bed
- Adiabatic combustor
C
Convective heat exchanger

Figure 4. Radiative watertube boiler concept.

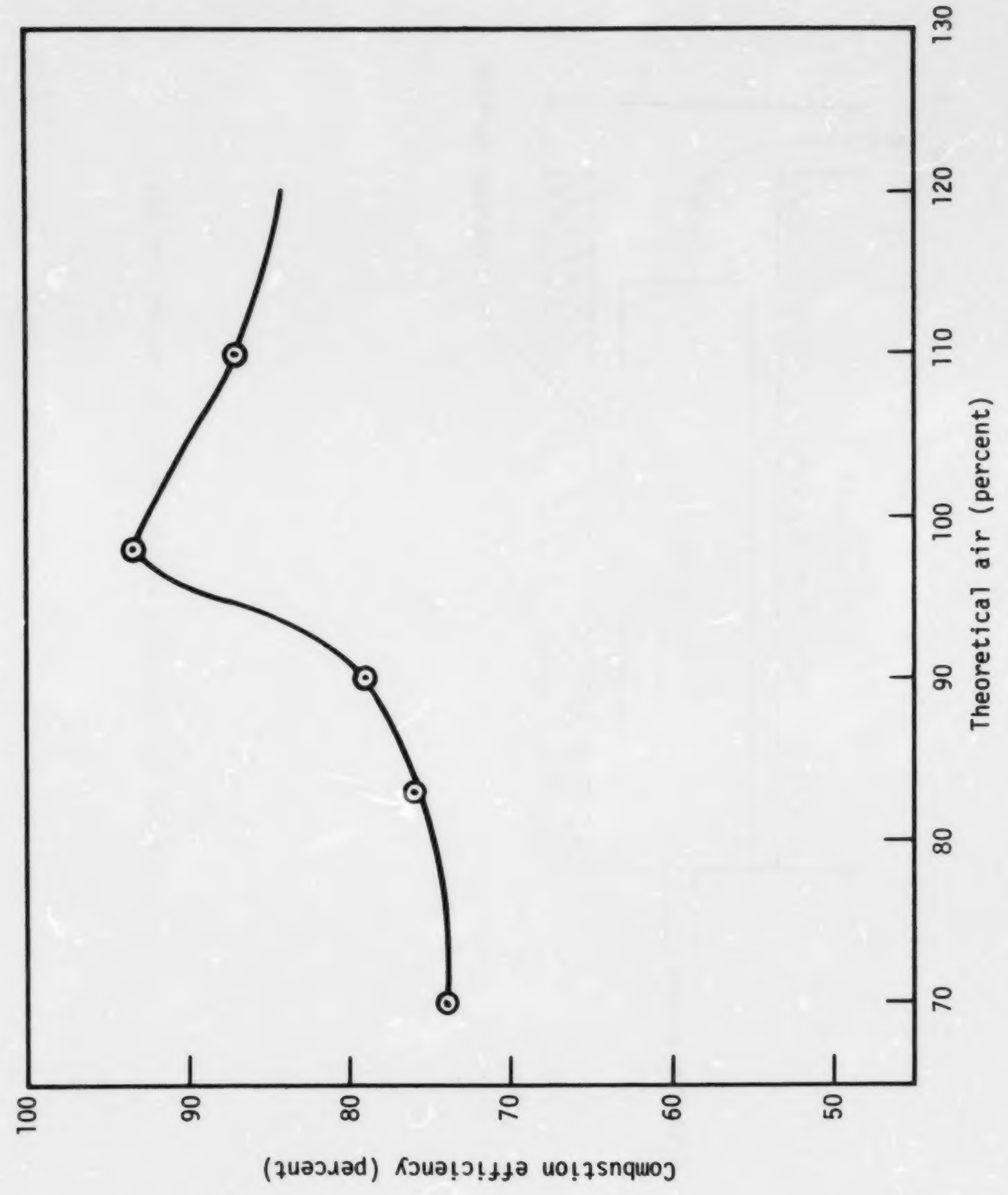

Figure 5. Concentric watertube boiler combustion efficiency.

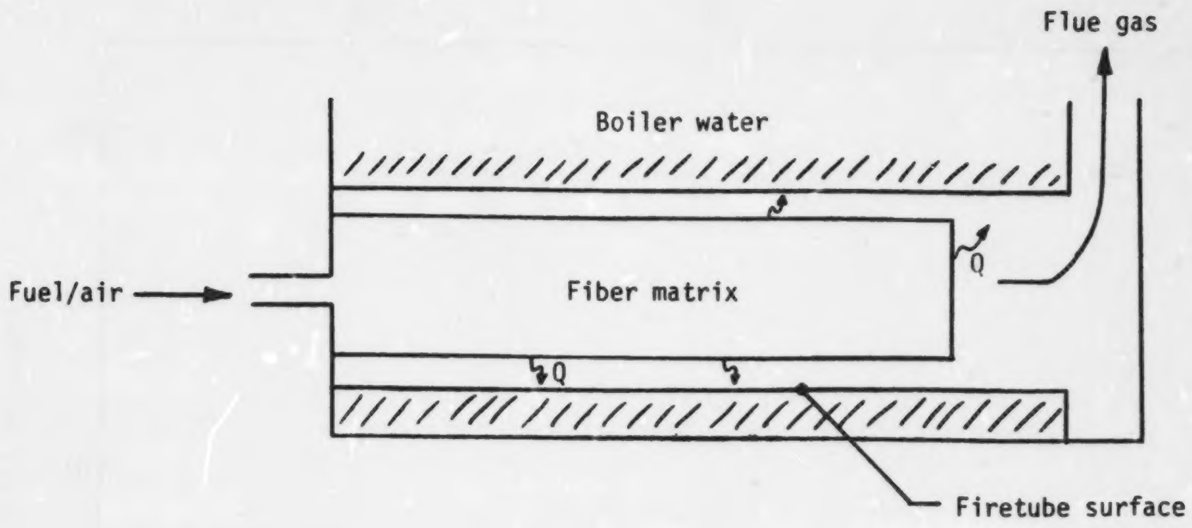
Flue gas
Boiler water
Fuel/air
Fiber matrix
Q
Q
Firetube surface

Figure 6. Firetube boiler catalytic burner concept.

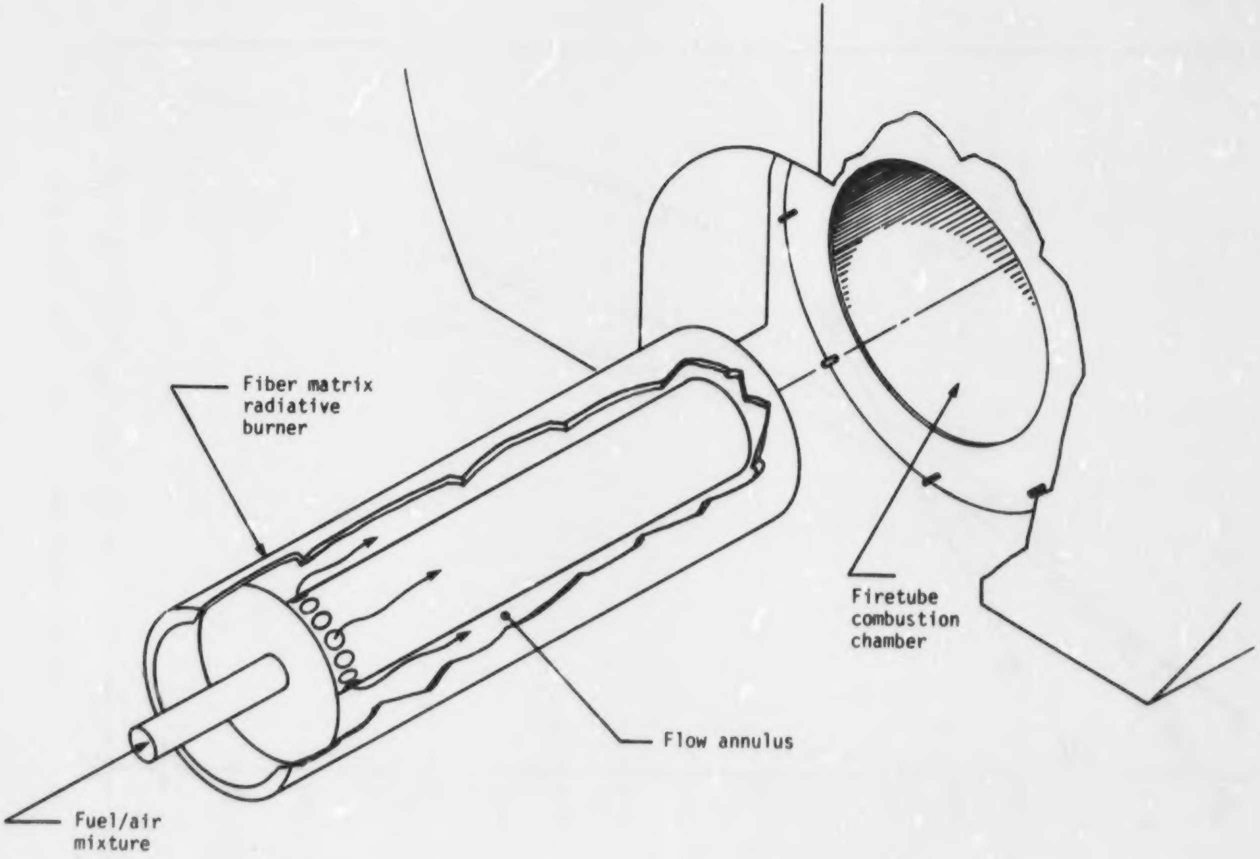
Fiber matrix radiative burner
Firetube combustion chamber
Flow annulus
Fuel/air mixture

Figure 7. Catalytic firetube boiler burner.

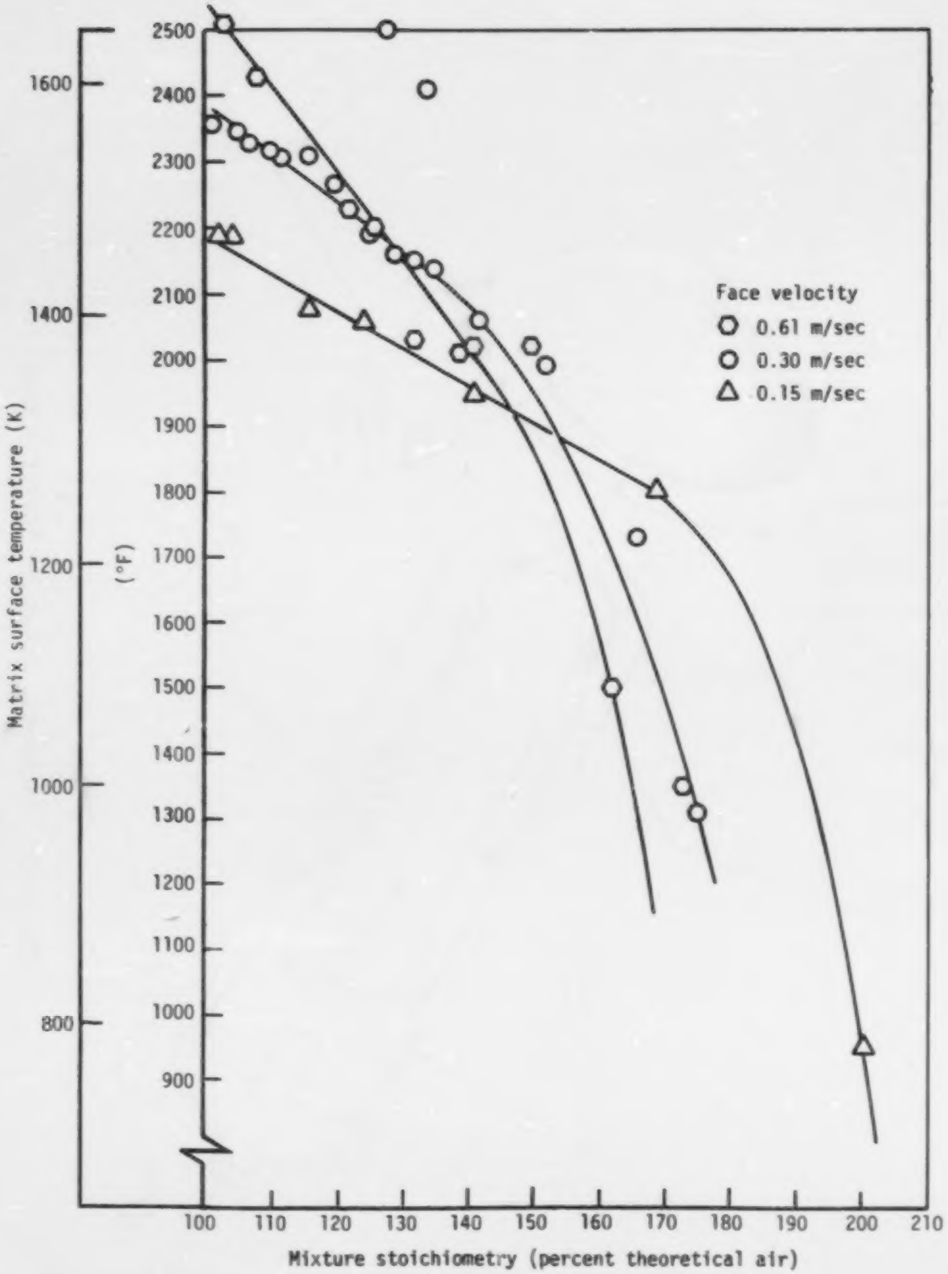

Figure 8. Fiber matrix operating temperature.

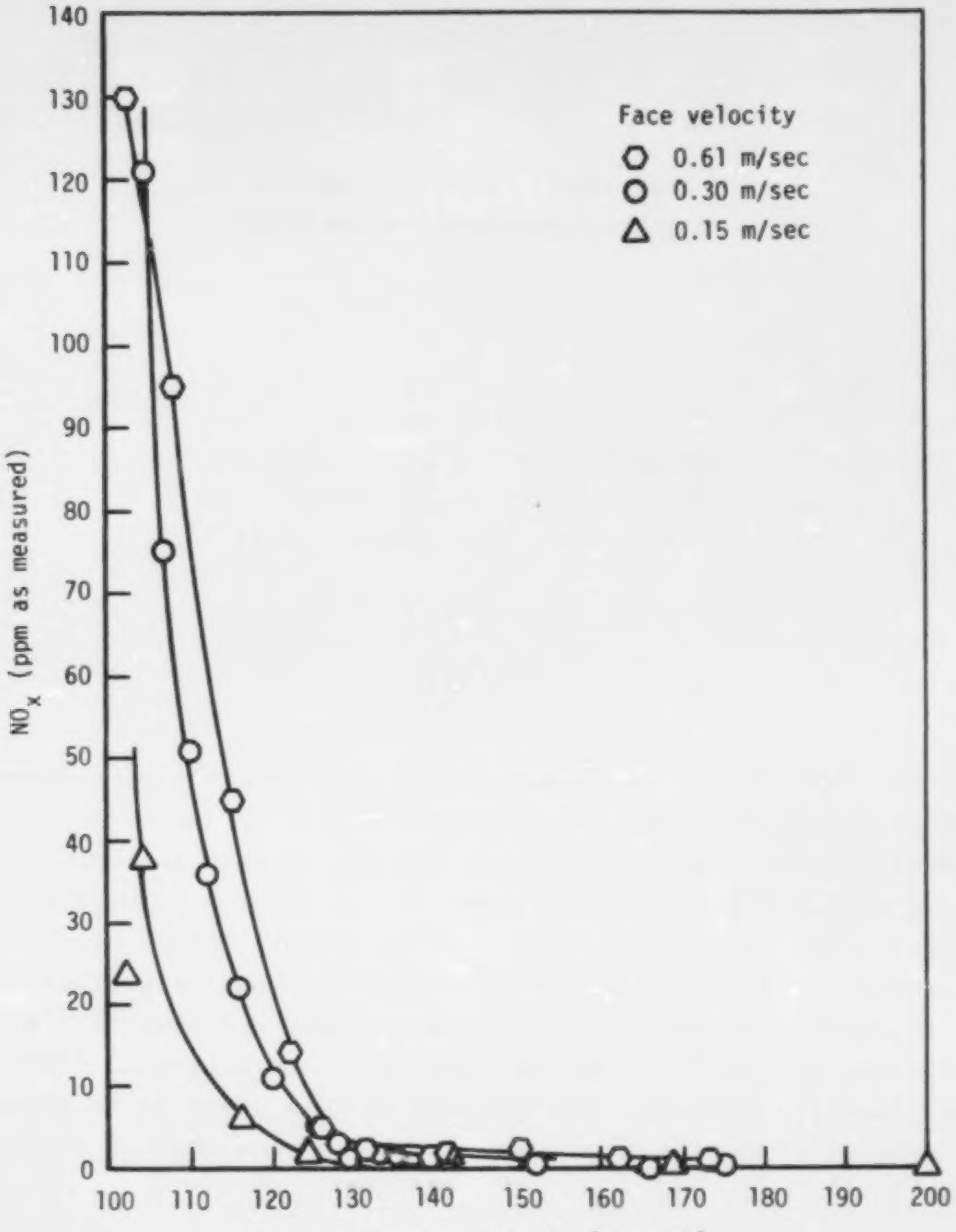

Figure 9. Fiber matrix NO_x emissions.

EPRI STATIONARY GAS TURBINE
CATALYTIC COMBUSTOR DEVELOPMENT PROGRAM

By

LEONARD C. ANGELLO
ADVANCED POWER SYSTEMS DIVISION
ELECTRIC POWER RESEARCH INSTITUTE
PALO ALTO, CALIFORNIA 94303

ABSTRACT

The EPRI Stationary Gas Turbine Catalytic Combustor Development Program is a multi-year, multi-phase major contract effort. The primary program objectives are to design, develop and demonstrate a full-scale, field tested stationary gas turbine combustor, employing catalytic combustion technology for reduced NO_x emissions. The program focus is the development of a practical and reliable catalytic combustor for current and near-future stationary gas turbine designs fired with low nitrogen (>500 ppmw) distillate fuels. The purpose of this paper is to present the overall program approach and details of the Phase I program plan.

INTRODUCTION

The control of nitrogen oxide (NO_x) and unburned hydrocarbon (UH) emissions from stationary gas turbines is of major concern to California utilities. Projections based on current California NO_x emission standards for utility boilers (Rules 67, 475 and 475.1) indicate that in the future even more stringent NO_x control may be required for stationary gas turbines. Although intensive efforts have already been made by utility gas turbine manufacturers to reduce NO_x emissions, current approaches show limitations in meeting projected California emission standards.

The catalytic combustor represents a potentially attractive approach for meeting future emission standards due to its ability to operate at high thermal efficiencies with very low levels of pollutants (NO_x, UH, CO, and smoke). Typical NO_x emission for current stationary gas turbines burning petroleum distillate fuels are about 200 ppmv at base load operation. Initial laboratory studies (References 1 and 2) have shown that the catalytic combustor operating on similar fuels could achieve NO_x emissions of less than 20 ppmv at the same steady-state operating condition.

The above studies, as well as others reported in the literature, have recognized the potential of the catalytic combustor for achieving substantial reductions in NO_x emissions. However, before the emission advantage of the catalytic combustor can be realized in commercial stationary gas turbines engines, it must be demonstrated that a practical and reliable catalytic combustor design is possible.

Although the scope of the current program is restricted to analytical and experimental work with low nitrogen distillate fuels (<500 ppmw), it is recognized that catalytic combustion offers the potential for improved combustor performance on low or medium Btu gas derived from coal gasification. For medium Btu gas, NO_x emissions could be markedly reduced and with low Btu gas, additional stability and improved part load performance could result. It is possible that if work under the current program is successful, further work on coal derived medium and low Btu gases may be appropriate.

PROGRAM DESCRIPTION

The catalytic combustor development program described below has been formulated with primary consideration for the development of a practical and reliable catalytic combustor design. During this program a practical, full-scale, field tested, catalytic combustor capable of extremely low NO_x emissions will be designed, developed and demonstrated. The catalytic combustor developed under this program will be designed for commercial stationary gas turbine engines fired with low nitrogen (<500 ppmw) distillate fuels. The full-scale demonstration of the operational and performance capability of a practical and reliable catalytic combustor design over the entire range of stationary gas turbine operating conditions is the ultimate goal of this effort. This effort is planned to be conducted in three phases:

Phase I - Preliminary Design and Development

Phase I of the overall development plan involves the preliminary design, development, and demonstration of a full-scale, single can, catalytic combustor. Based on a thorough review of current catalytic design information, a single catalytic combustor design concept having the highest practical design potential for full-scale development will be determined. Detailed analytical and experimental evaluation of the selected design concept over a specified stationary gas turbine operating cycle will be performed. Special instrumentation will be used to measure combustor efficiency, pressure losses, temperature distribution, and emissions.

Initial testing will provide the data base for design improvements. Revised designs will be further evaluated as part of the development process for refining the initial catalytic combustor design. This experimental program is expected to provide the design data base for specification of a pre-production prototype catalytic combustor to be evaluated in Phase II.

Phase II - Prototype Design and Evaluation

Phase II of the overall program address the bill of material design, fabrication, and long-term endurance evaluation of a single can, catalytic combustor. Sufficient full-scale rig testing will be performed to adequately assess major durability and performance characteistics of the pre-production prototype design. Special emphasis will be placed on evaluating and optimizing emissions and performance characteristics, durability, engine compatibility, and complexity. Improvements based on these evaluations will be incorporated into the final prototype design. This experimental effort will provide the necessary data base and technology acquisition for specification to be used in the Phase III engine demonstration and field test.

Phase III - Final Design and Field Test

The objective of the Phase III effort will be the verification of the final prototype combustor design in an integrated stationary gas turbine for further refinement toward commercial acceptability. A full set of prototype combustors will be fabricated and installed on a commercial engine. Demonstration testing will be performed to verify the performance, operating, and durability characteristics obtained in Phases I and II. Successful completion of the Phase III effort will demonstrate that development of the catalytic combustor is complete and ready for commercial application.

Program Schedule

The overall planned program schedule is shown in Figure I. The Phase I effort was initiated on June 25, 1980, with issuance of EPRI RFP 1657. Contract initiation was accomplished on March 24, 1980, with completion of Phase I scheduled to occur within 24 months of contract signing. Implementation of Phases II and III will be determined at a future date. For planning purposes, it is expected that Phase II and III will each be approximately 18 months in duration and that the entire development program (Phases I, II, and III) will be completed within five years of the Phase I program initiation.

PROGRAM OBJECTIVES AND GOALS

The Phase I technical effort will employ existing catalyst/support technology to design, develop and demonstrate a practical, full-scale, single can, catalytic combustor capable of estremely low NO_x emissions. The catalytic combustor developed under this effort will be sized for existing or near future stationary gas turbines in the 30 to 100 MW power range. Design goals for this effort include the following:

- NO_x <20 ppmv corrected to 15% O_2 at Base Load
- Smoke < SAE Number 2 at Base Load
- Combustion Efficiency

  Eta > 99.9 at Base Load

  Eta > 99.5 at Spinning Idle

  Eta > 99.1 at all other operating conditions

- Combustion total pressure losses ($^{\Delta P}/_{P}\%$) <5% over all operating conditions

- Combustor life > 2000 hours (Peaking Application)

Combustor designs developed under this program will be based on burning low nitrogen (<500 ppmw) distillate fuels and may employ full utilization (all fuel passed through the catalyst) or partial utilization catalytic devices. Designs may employ pilot burners, fuel staging or variable geometry technology. Design emphasis will be on system integrity, reliability, and ease of maintenance. Methods of determining catalyst flame detection and failure detection will also be addressed.

CATALYTIC COMBUSTOR DESIGN CONSIDERATIONS

Over the past five years, a growing body of technical literature has developed, describing low emission catalytic combustion programs carried out by a number of government agencies and industrial gas turbine manufacturers. These tests have confirmed the potential for achieving extremely low levels of nitrogen oxide emissions and have affirmed the feasibility of the catalytic combustor concept for gas turbine application. From a develoopment point of view, however, the concept is in its infancy.

In previous investigations pipe flow rigs have been used to explore catalyst steady-state performance at or close to a hypothetical full power design point condition. Furthermore, for reasons of experimental control, preheated air streams and an extended mixing length were used. In contrast, a practical stationary gas turbine combustor must start cold and operate over a wide range of fuel/air ratios, inlet temperatures and pressure conditions. Furthermore, stable gas turbine operation is required at high combustion efficiencies over a wide range of fuel turndown conditions. Finally, a practical combustor must be of realistic size and geometry to meet design requirements and of sufficient durability to meet warranty requirements.

From the preceding, it is evident that translation of the exceptional catalytic combustion performance obtained for premixed fuel/air mixtures in steady-state test rigs into practical system hardware operating over the entire range of required stationary gas turbine conditions is a formidable task. Such a task shall require technical innovation based on the comprehensive understanding of both catalyst and combustor design constraints and capabilities. The following discussion is provided as a brief summary of the principle design problems which must be resolved prior to the demonstration of a practical catalytic combustion system.

The Startup and Loading Sequence of a Catalytic Combustion System

Although catalytic combustion has excellent thermal and emissions performance at the design point (full load) condition, at off-design point conditions, the reaction temperature may be too low to sustain stable combustion. This is because the fuel/air ratio turndown is limited to 1.5:1 when diluent gas is not used. To alleviate this problem, modifications to the gas turbine are necesary.

According to conventional combustor design, the percent of air distribution within the combustor is kept constant at all times. When the fuel flowrate (or load) varies, the location of the primary combustion zone inside the combustor also varies. Hence, the only control parameter during the entire sequence is the fuel flowrate.

On the other hand, if a catalytic combustor were implemented, the combustion zone is fixed by the physical location of the catalyst. In order for the system to operate over the entire startup and loading sequence, the catalytic combustor must be designed to sustain combustion over the required fuel/air ratio turndown, or the fuel/air ratio iin the catalytic combustor must be maintained constant by redistributing the air or fuel flow during the sequence. Alternatively, a conventional combustor may be used ahead of a catalytic element.

Catalytic Combustor Durability

For practical purposes, a minimum requirement for catalyst life is 2000 hours for peakload units and 8000 hours for baseload units. However, existing life test data are not sufficient to make a realistic assessment on practical catalytic combustor life. Hence, there is a need for more experimentation in this area.

Another area of concern is the integrity of ceramic monolith support materials may fracture for the following reasons:

- Thermal shock as a result of cyclic operation

- Material fatigue as a result of mechanical vibrations

The failure of the monolith support material will not only shorten the combustor life, but pieces may also damage the turbine blades, and allow the combustion process to move into the turbine area causing blade failure,etc.

The catalyst performance may be degraded for the following reasons:

- Long operaing hours

- Cyclic operation

- Catalyst poisoning

The first effect has been investigated in a preliminary manner by work sponsored by the NASA Lewis Research Center (Reference 3). However, further testing which simulates the gas turbine operating mode is required.

Catalyst Lightoff System

Catalytic combustor ignition systems differ from those of conventional combustors. Catalytic lightoff with air preheat is possible, but the compressor outlet temperature at startup does not meet the 600°F to 1000°F requirements for lightoff. The spark ignition system currently employed by most gas turbines may overheat the catalyst during abrupt lightoff of the fuel/air mixture. The catalyst requires a more gradual lightoff sequence. A pilot flame might provide such a lightoff technique.

The pilot would ideally be a long, internally spark-ignited pilot burner. Upon ignition, it would produce a long and wide flame directly across the incoming fuel and air mixture. This would act as an aerodynamic flame-holder and as an ignitor, the fuel/air mixture would be at least partially combusted, thereby raising the bulk flow temperature. The reactive mixture would then complete the combustion in the catalyst as a result of its increased temperature.

Probable Damage to Turbine by Catalyst Substrate Failures

During cyclic operations, ceramic catalyst substrates may fracture due to thermal stresses. If such an incident occurred, part or all of the combustion process would move to the turbine section, thereby overheating the turbine components. Furthermore, the substrate fragments could be dragged by the high velocity air and impinge on the turbine blades. Depending on the velicity and the size of the fragments, severe turbine blade damage could occur.

In the design of a catalytic combustor, provision should be included for fuel shutoff in case of catalytic substrate failures. This will prevent combustion occurring in the turbine section. Also, the potential for damage to the turbine as a result of fragment impingement should also be estimated prior to the application of catalytic combustors to the gas turbine.

Fuel/Air Preparation for Catalytic Combustors

The use of monolithic substrates as catalyst supports necessitates nearly complete premixing prior to entry of the fuel and air into the catalyst channels. Little can be done to correct a fuel-air maldistribution once inside the catalyst. Since for adiabaic systems the operating temperatures of the catalyst approximates the adiabatic flame temperature of the mixture, it is important that the combination of inlet temperature and fuel concentration profile is more or less uniform. Maldistribution of fuel will cause excessive emissions due to lean fuel mixtures in some portions of the combustor cross section, while in those regions where high fuel concentration leads to high adiabatic flame temperature, catalyst damage can occur. Uniform premixing of the fuel and air prior to entry into the catalyst eliminates these potential problems, while yielding a combustor temperature pattern that, with minor adjustments, is ideal for gas turbine engines.

The question of auto-ignition must also be addressed. Since a uniform mixture is desired from the catalyst performance standpoint, it is important that sufficient residence time upstream of the catalyst is provided consistent with gas turbine shaft length constraints. However, it must be realized that as mixture pressure and temperature are increased, the auto-ignition delay time decreases. At high temperatures the ignition delay time may be reduced sufficiently to approach the time necessary for premixing and vaporization; under such conditions preignition may occur. For conventional distillate fuels, the ignition delay time at 700°F (a reasonable catalyst inlet temperature) ranges from approximately 3 seconds at 2 atmospheres to 500 msec at 10 atmospheres pressure. These times are generally ample for premixing, provided the premixing gas is without stagnant regions. At higher pressures, the margin between preignition and premixing times is less and it is necessary to design for minimum mixing time. In this connection it should be noted that rapid mixing may be obtained through the provisions of pressure loss and of the optimum number and distribution of fuel injectors. The vaporization time for liquid fuels may be comparable with mixing time, if sufficiently small droplets are produced. In addition it should be noted that preignition is not necessarily catastrophic, provided local temperatures do not become excessive. The occurrence of preignition as described would cause a significant loss of machine power due to an increase in catalyst pressure drop.

Combustor Pressure Losses

Finally the question of overall pressure loss must be addressed. Combustor pressure loss will derive from fuel-air premixing and catalyst pressure loss. Both premixing and catalyst pressure loss may be decreased by reducing the inlet velocity to the lowest acceptable value. Combustor design optimization involves minimizing pressure loss consistent with two compensating factors:

- The residence time for feed preparation and presentation to the catalyst must be less than the ignition delay time.

- Low velocities lead to undesirable large combustor cross sectional areas.

In conventional combustors the trend towards lower velocities and higher surface areas cause cooling problems. With the catalyst system the decrease in peak operating temperature results in less cooling problems than is the case with conventional combustors.

PHASE I TECHNICAL EFFORT

The Phase I technical effort consists of eight tasks covering (1) Conceptual Design, (2) Definition of Design Criteria, (3) Design Analysis, (4) Preliminary Design, (5) Design Optimization Plan, (6) Fundamental Studies for Design Verification, (7) Full-Scale Combustor Evaluations, and (8) Prototype Design Specification. The planned Phase I program schedule is shown in Figure 2 and the overall Phase I work flow diagram is contained in Figure 3. The complete Phase I work breakdown structure is shown in Figure 4. Descriptions of the individual Phase I tasks are given below:

Task 1 - Conceptual Design

During this task, a specific stationary gas turbine engine design and operating cycle will be identified as a basis for a conceptual catalytic combustor design. The selected engine design will be representative of a current or near future stationary gas turbine in the 30 to 100 MW power range.

A thorough review of all available information on catalytic combustor design will be conducted. This review will be the basis for establishment of the various critical design requirements including minimum catalyst preheat temperature, maximum catalyst bed temperature, range of allowable reference velocities, pressure drop characteristics, catalytic bed length, startup requirements, and dilution air requirements.

Based on the above review, a catalytic combustion design concept or concepts will be identified for further development. Layout drawings of the identified design concepts(s) will be prepared. These drawings will define the entire combustor system in sufficient detail to define all major assemblies, including fuel injectors and cooling liners and the dimensions of all passages and chambers. The catalytic element or elements of the design shall be characterized as the size, shape, and major constituent. The intent shall be to define the combustor design in sufficient detail to conduct the analyses and evaluations specified in the following section.

Task 2 - Definition of Design Criteria

The conceptual catalytic combustor design(s) previously identified will be analyzed to assess (1) potential for meeting the prescribed emission and performance goals, (2) durability and time-between-overhaul predictions, (3) combustor performance and degradation potentials, (4) system costs, (5) system retrofitability, (6) system safety, and (7) system operating environment.

Task 3 - Design Analysis

The conceptual catalytic combustor design(s) previously identified will be analyzed to assess (1) potential for meeting the prescribed emission and performance goals and (2) feasibility for meeting engine installation and operating goals. In these studies, the identified catalytic combustor concept(s) will be defined and analyzed in detail. Aerothermodynamic analyses will be evaluated to calculate the detailed pressure/velocity and flow distributions throughout the combustor. Heat transfer analyses will be conducted to determine cooling liner flow distributions and metal temperatures. Vibrational analyses will be conducted to determine the effect of gas turbine vibrational amplitudes and frequencies on catalytic combustor hardware durability and reliability. Mechanical analyses will be conducted to define fabrication/assembly details, structural stresses, weights, and estimated life. In addition, relevant design considerations regarding start capability, turndown capability, reliability, and maintainability will be qualitatively evaluated as part of the design analyses performed under this task.

Task 4 - Preliminary Design

Upon completion of conceptual design analysis, a detailed preliminary catalytic combustor design will be prepared. This design will include (1) detailed layout drawing of the refined catalytic combustor design with enough auxiliary views to show all major dimensions, location and size of combustor air dilution holes and how all the parts are assembled, and (2) a design summary which describes the features, intended operating mode, results of design calculations for sizing the flow elements and predicted emission/performance characteristics. Mechanical layout studies will also be conducted to define the combustor fabrication assembly and mounting arrangements for the end application engine design.

Task 5 Design Optimization Plan

Based on the selected preliminary design, a detailed design optimization test plan will be prepared. This plan will describe the critical path development needed to translate the prepared preliminary combustor design into practical system hardware. Areas where additional experimental data are needed to obtain a fundamental understanding of pertinent design principles will be identified and specific experiments to gain this information shall be described. In particular, the optimization plan will define a catalyst/support program to evaluate catalytic combustor failure modes with respect to catalyst poisoning effects, monolith durability and turbine damage potential. The EPRI Project Manager will review and approve the final version of the Design Optimization Plan prior to initiation of Task VI, Task VII, and/or Task VIII.

Task 6 - Fundamental Development Testing for Design Verification

Under this task, fundamental/empirical development experiments will be conducted to provide the required design data identified in the Task V optimization plan. Experiments performed under this task will be at full pressure and may involve both full-scale and subscale evaluations.

Experiments conducted under this task will be closely coordinated with those performed under Task VII, Full-Scale Combustor Evaluation. The primary objective of these fundamental/empirical studies is to guide the full-scale catalytic combustor hardware development. In each of the tests conducted under this task, individual elements of the combustor will be evaluated to answer specific questions with regard to design feasibility. Based on those tests, preferred designs may be substantiated, modified or eliminated as technically unfeasible.

Areas of design anticipated to require fundamental/empirical development under this task include the following:

1. Fuel/Air Preparation System Design - Initial emphasis will be placed on determining the degree of vaporization and premixing required for the catalytic design selected. Based on this data, fuel injectors will be designed, fabricated, and evaluated on their ability to provide the required fuel/air distribution.

2. Ignition/Control System Design - Fundamental data will be obtained to allow design and development of an ignition/control system capable of meeting the startup and loading sequence normally required of generation equipment used by the electric utility industry.

3. Liner Cooling Development - Fundamental data will be acquired to evaluate the effect of steady-state and transient response

on liner cooling schemes. Based on this data required liner cooling schemes will be fabricated and evaluated.

4. Catalyst Packaging Design - Data will be obtained to ensure the adequacy of the catalyst encapulation design. Fabrication of the final encapsulation design will be prepared and used in subsequent material durability evaluations.

5. Material Durability Evaluations - Based on existing catalyst technology, a single catalyst/substate design will be selected for long-term durability evaluation. A cyclic durability evaluation will be performed on the selected catalyst/substrate design at full pressure. Each cycle will be of suitable duration to establish steady state operation at each of the following test conditions: cold start, spinning idle, 50% base load, 70% base load, base load, and peak load. The total number of test cycles shall be sufficient to simulate 2000 hours of engine life (peaking application).

   In addition, a mechanical vibration test will be performed. In these tests catalytic combustors fabricated of the selected substate material will be evaluated at vibration amplitudes and frequencies equivalent to those of an actual gas turbine operation. This test shall be performed at full pressure and shall be made to simulate 2000 hours of actual engine life (peaking application). The intent of this test shall be to demonstrate the mechanical integrity and inherent attrition resistance of the selected substate material over the expected life of the combustor.

Task 7 - Full-Scale Combustor Evaluation

Based on the preliminary design and the results of the fundamental development work performed, one or more full-scale catalytic combustors will be fabricated for test and evaluation. All evaluation and demonstration testing will be conducted in full pressure, reverse flow test rigs capable of handling max peak operating conditions of temperature, pressure, and mass flow. All testing will be performed with non-vitiated air.

Test conditions will include, but not be limited to, the following:

- Average concentration of oxygen (O_2) in the exhaust gas (% O_2, dry basis)
- Average concentration of carbon monoxide (CO) in the exhaust gas (ppmv CO, dry basis)
- Average concentration of unburned hydrocarbons (UHC) in the exhaust gas (ppmv UHC, wet basis)
- Average concentration of carbon dioxide in the exhaust gas (% CO_2, dry basis)
- Average concentration of nitrogen oxides NO_x in the exhaust gas (ppmv NO_x, dry basis)
- Average SAE smoke number
- Total pressure loss over the combustor (strain gage transducers)
- Air flow rate (ASME sharp-edged orifice)
- Average inlet total temperature (thermocouple)
- Average inlet total and static pressure (strain gage transducers)
- Inlet air humidity (LiCl type meter)

- Fuel injector pressure drop (presure transducer)
- Combustor exit temperature (thermocouple)
- Fuel flow rate (turbine flow meter)
- Combustion wall temperatures (thermocouple)
- Catalyst bed temperature (thermocouple)

Based on the above data, the following combustor performance characteristics will be determined:

- Ignition and load acceleration characteristics
- Fuel/air ratio over the operating range (fuel and air flow measurement basis and emission measurement basis)
- Combustion efficiency (enthalpy and emissions basis)
- Exit pattern factor
- Combustor Pressure loss

The above data will be analysed and recommendations prepared for future design improvements. These analyses and recommendations will be reviewed with the EPRI Project Manager for redesign approval. Based on the EPRI Project Manager's approval, the recommended design modification will be made and the retesting of the improved combustor design will be initiated. No more than five combustor redesigns will be allowed under this program.

Task 8 - Prototype Design Specification

Upon successful demonstration of the optimized full-scale catalytic combustor, a final bill-of-materials combustor design specification will be prepared. This specification will include a detailed prototype layout drawing, a detailed design summary and the full identification of all fabricated materials.

A detailed Phase II test plan will also be prepared under this task. Requirements for the Phase II test plan will include definition of the following parameters:

- Test Schedule
- Data Requirements
- Location of Measurement Instrumentation
- Data Analysis Procedures

CONCLUDING REMARKS

Phase I of the EPRI Stationary Gas Turbine Catalytic Combustor Development Program is now in progress. The Phase I contract was awarded to the Westinghouse Electric Corporation in March of 1980. As of the date of this publication, work has begun on Tasks 1 and 2 of the Work Breakdown Structure shown in Figure 4.

Progress to date under Task 1 has identified the Westinghouse Model 501D as the engine/combustor design envelope to be used for the conceptual design studies. Figure 5 is a cut-away view of the Westinghouse Model 501 gas turbine. The Model 501 turbine is a 12:1 compression ratio engine with a 2100°F turbine inlet temperature. It consists of 17 stages axial compressor, 16 can-type combustors and a 4 stage turbine. Each combustor can is approximately 20 inches in diameter. The baseload power output of the Model 501 is 94 MW at a heat rate of 10,660 Btu,kWh.

Figure 6 depicts a conceptual design arrangement of a catalytic combustor for the Model 501 turbine. The principal design features of this arrangement includes 1) a conventional fuel nozzle preburner, 2) multiple secondary fuel injection, and 3) a downstream catalytic element. The purpose of the preburner is to provide for catalyst lite-off and load range capability. The multiple fuel injection allows rapid fuel vaporization and mixing in the fuel preparation zone upstream of the combustion catalyst. The monolithic ceramic element provides minimum pressure loss through the catalyst.

In conclusion, the EPRI Stationary Gas Turbine Catalytic Combustor Development program represents a comprehensive development program to demonstrate catalytic combustion technology for reducing NO_x emission levels in current-design utility gas turbines. The program will examine the durability and reliability of this technology and its successful completion will lead to the eventual commercialization of catalytic combustion technology for utility gas turbine systems.

REFERENCES

1. Blazowski, W. S. and Bresowar, G. E., "Preliminary Study of the Catalytic Combustor Concept as Applied to Aircraft Gas Turbines," AFAPL-TR-74-32, June 1974.

2. Decorso, S. M., Mumford, S., Carubba, R. V., and Heck, R. M., "Catalysts for Gas Turbine Combustor--Experimental Test Results," Journal of Engineering for Power, Vol. 99, No. 2, April, 1977.

3. Heck, R. M., Chang, M., Hess, H., and Carrubba, R. V., "Durability Testing at One Atmosphere of Advanced Catalysts and Catalyst Supports for Automotive Gas Turbine Engine Combustors," Part I, NASA CR-135132, June, 1977.

EPRI Stationary Gas Turbine Catalytic Combustor Development Program
Overall Program Schedule

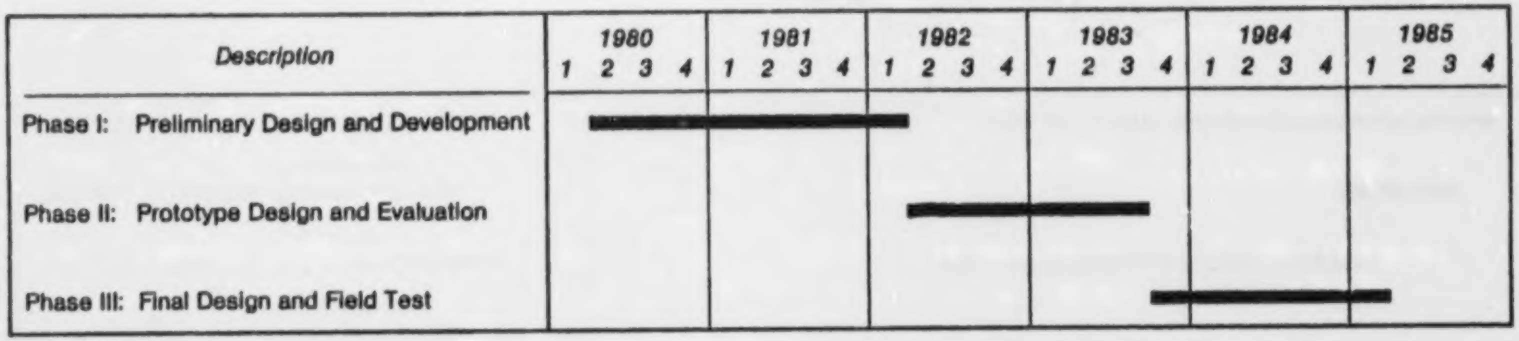

FIGURE 1

EPRI Stationary Gas Turbine Catyalytic Combustor Devlopment Program
Major Milestone Chart

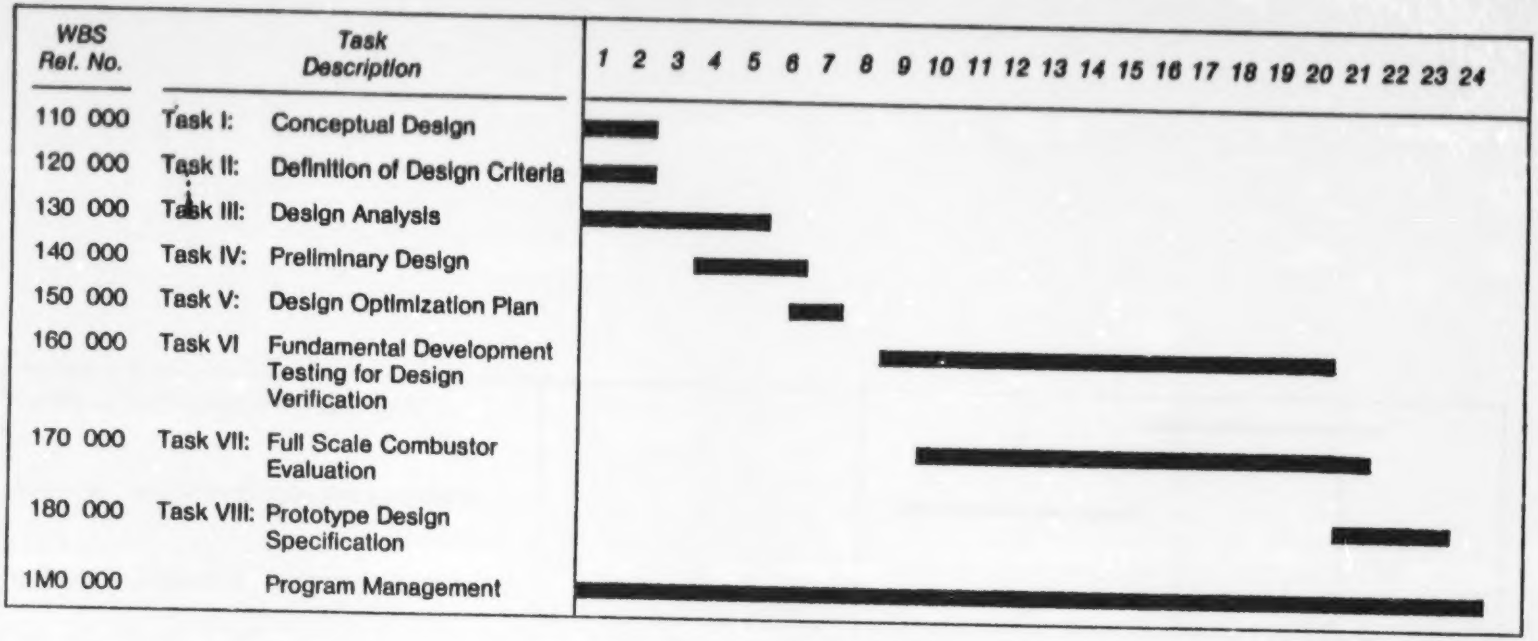

FIGURE 2

EPRI Stationary Gas Turbine Catalytic Combustor Development Program
Phase I Work Flow Logic Diagram

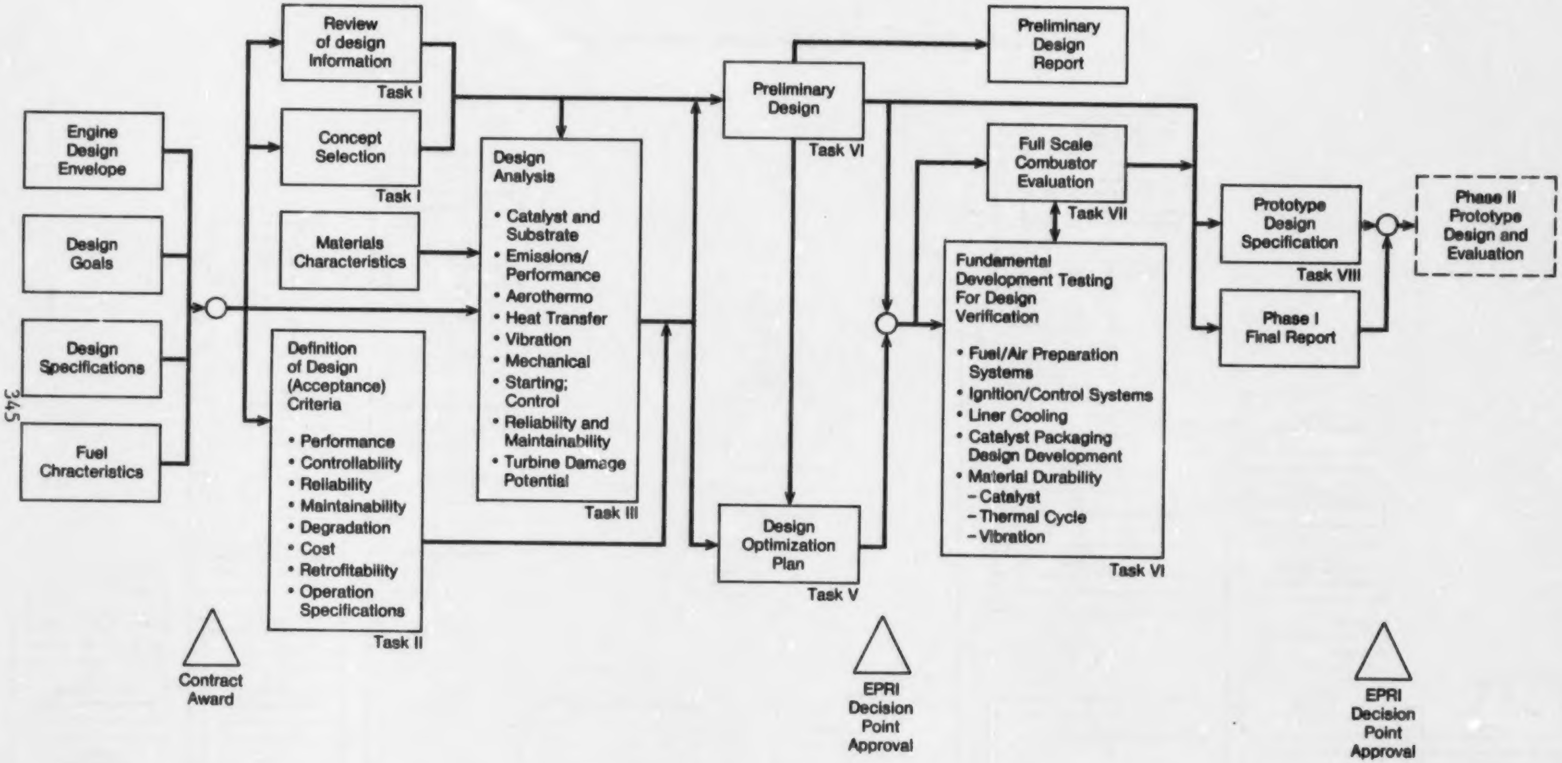
Engine Design Envelope
Design Goals
Design Specifications
Fuel Chracteristics
Contract Award
Review of design Information
Task I
Concept Selection
Task I
Materials Characteristics
Definition of Design (Acceptance) Criteria
• Performance
• Controllability
• Reliability
• Maintainability
• Degradation
• Cost
• Retrofitability
• Operation Specifications
Task II
Design Analysis
• Catalyst and Substrate
• Emissions/ Performance
• Aerothermo
• Heat Transfer
• Vibration
• Mechanical
• Starting; Control
• Reliability and Maintainability
• Turbine Damage Potential
Task III
Preliminary Design
Task VI
Preliminary Design Report
Design Optimization Plan
Task V
EPRI Decision Point Approval
Full Scale Combustor Evaluation
Task VII
Fundamental Development Testing For Design Verification
• Fuel/Air Preparation Systems
• Ignition/Control Systems
• Liner Cooling
• Catalyst Packaging Design Development
• Material Durability
– Catalyst
– Thermal Cycle
– Vibration
Task VI
Prototype Design Specification
Task VIII
Phase I Final Report
Phase II Prototype Design and Evaluation
EPRI Decision Point Approval

FIGURE 3

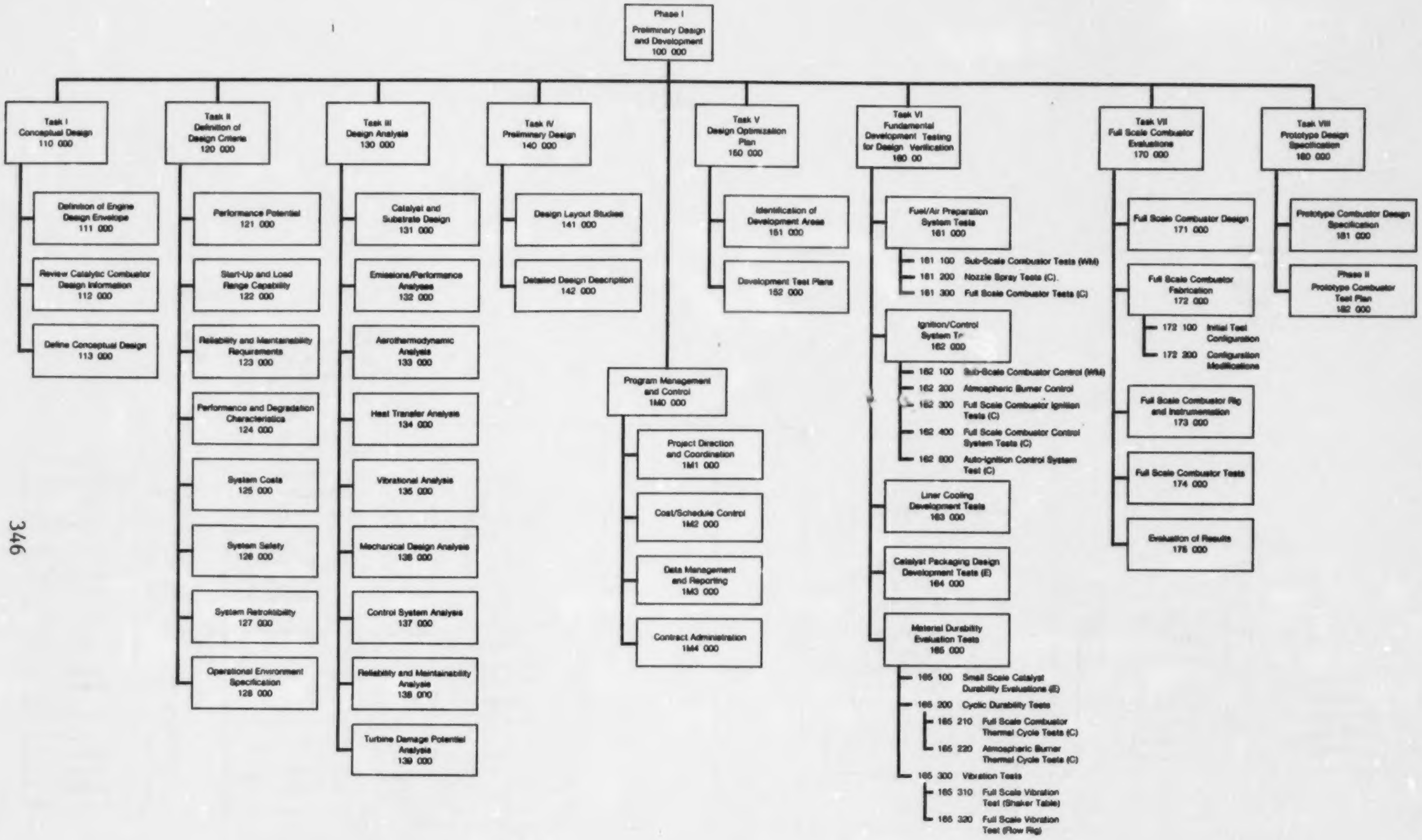
Phase I
Preliminary Design and Development
100 000
Task I
Conceptual Design
110 000
Definition of Engine Design Envelope
111 000
Review Catalytic Combustor Design Information
112 000
Define Conceptual Design
113 000
Task II
Definition of Design Criteria
120 000
Performance Potential
121 000
Start-Up and Load Range Capability
122 000
Reliability and Maintainability Requirements
123 000
Performance and Degradation Characteristics
124 000
System Costs
125 000
System Safety
126 000
System Retrofitability
127 000
Operational Environment Specification
128 000
Task III
Design Analysis
130 000
Catalyst and Substrate Design
131 000
Emissions/Performance Analyses
132 000
Aerothermodynamic Analysis
133 000
Heat Transfer Analysis
134 000
Vibrational Analysis
135 000
Mechanical Design Analysis
136 000
Control System Analysis
137 000
Reliability and Maintainability Analysis
138 010
Turbine Damage Potential Analysis
139 000
Task IV
Preliminary Design
140 000
Design Layout Studies
141 000
Detailed Design Description
142 000
Program Management and Control
1M0 000
Project Direction and Coordination
1M1 000
Cost/Schedule Control
1M2 000
Data Management and Reporting
1M3 000
Contract Administration
1M4 000
Task V
Design Optimization Plan
150 000
Identification of Development Areas
151 000
Development Test Plans
152 000
Task VI
Fundamental Development Testing for Design Verification
160 00
Fuel/Air Preparation System Tests
161 000
161 100 Sub-Scale Combustor Tests (WM)
161 200 Nozzle Spray Tests (C).
161 300 Full Scale Combustor Tests (C)
Ignition/Control System Tr
162 000
162 100 Sub-Scale Combustor Control (WM)
162 200 Atmospheric Burner Control
162 300 Full Scale Combustor Ignition Tests (C)
162 400 Full Scale Combustor Control System Tests (C)
162 800 Auto-ignition Control System Test (C)
Liner Cooling Development Tests
163 000
Catalyst Packaging Design Development Tests (E)
164 000
Material Durability Evaluation Tests
165 000
165 100 Small Scale Catalyst Durability Evaluations (E)
165 200 Cyclic Durability Tests
165 210 Full Scale Combustor Thermal Cycle Tests (C)
165 220 Atmospheric Burner Thermal Cycle Tests (C)
165 300 Vibration Tests
165 310 Full Scale Vibration Test (Shaker Table)
165 320 Full Scale Vibration Test (Flow Rig)
Task VII
Full Scale Combustor Evaluations
170 000
Full Scale Combustor Design
171 000
Full Scale Combustor Fabrication
172 000
172 100 Initial Test Configuration
172 200 Configuration Modifications
Full Scale Combustor Rig and Instrumentation
173 000
Full Scale Combustor Tests
174 000
Evaluation of Results
175 000
Task VIII
Prototype Design Specification
180 000
Prototype Combustor Design Specification
181 000
Phase II
Prototype Combustor Test Plan
182 000

EPRI Stationary Gas Turbine Catalytic Combustor Development Program

FIGURE 4

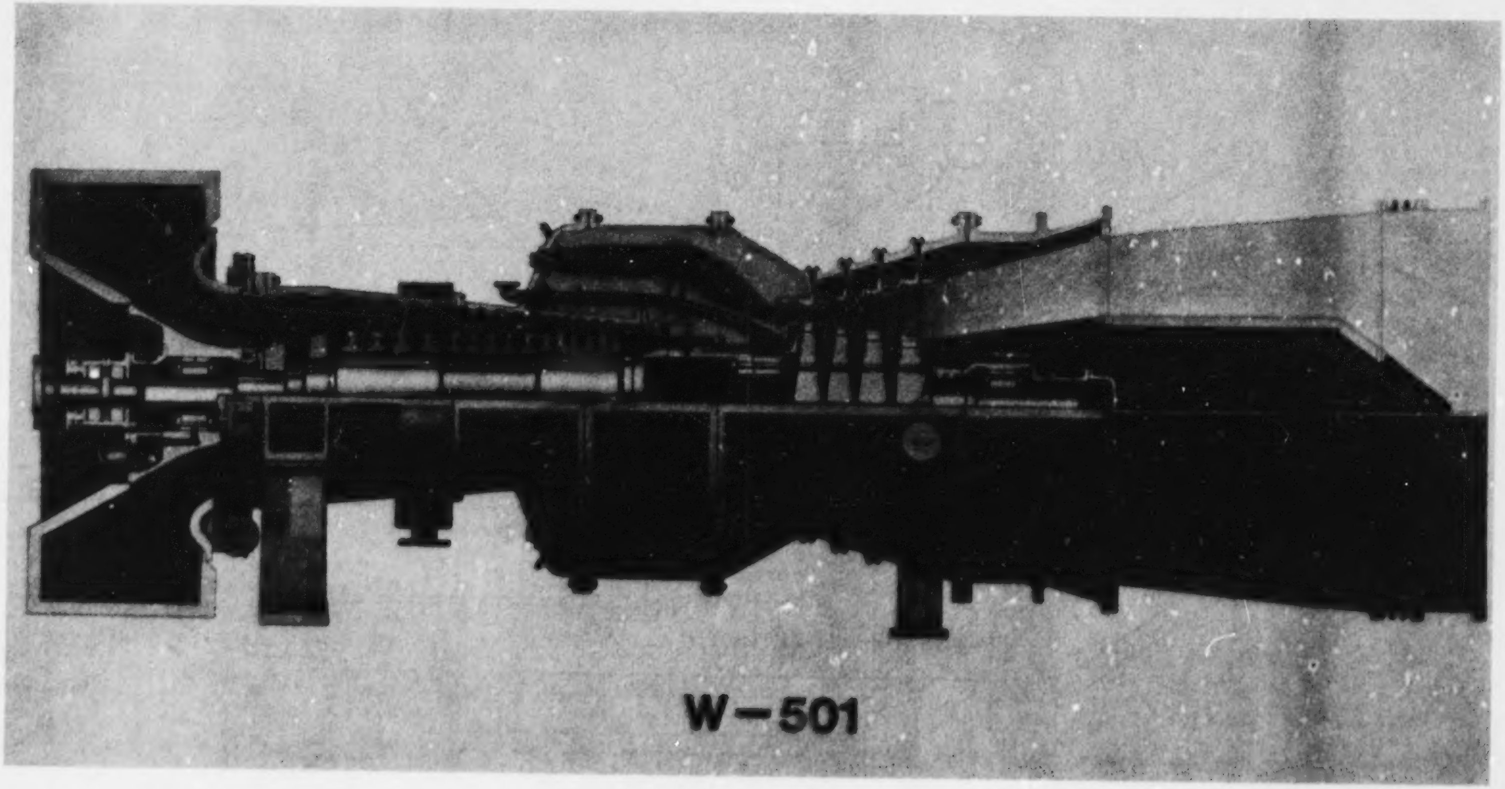

FIGURE 5

A Conceptual Design Arrangement of a Catalytic Ceramic Element in a Stationry Gas Turbine

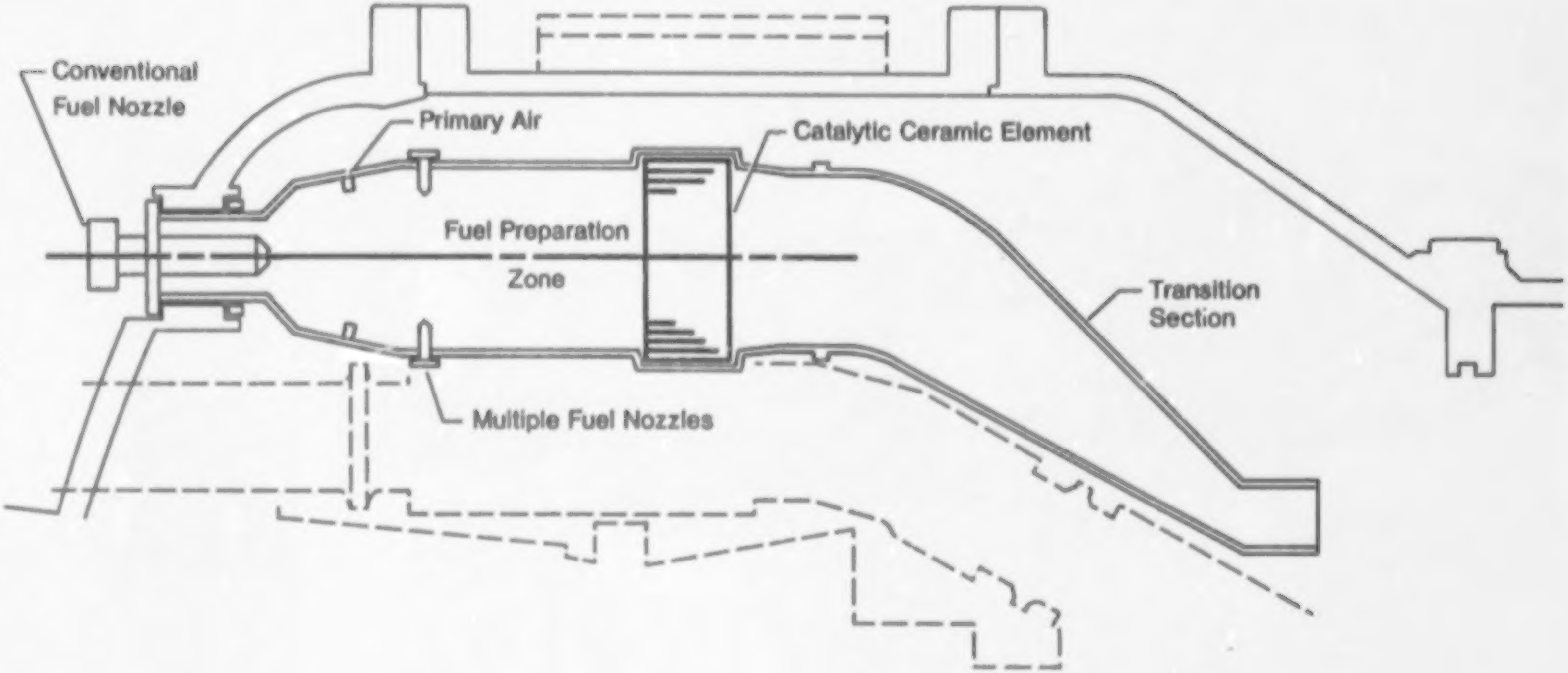
Conventional Fuel Nozzle
Primary Air
Catalytic Ceramic Element
Fuel Preparation Zone
Transition Section
Multiple Fuel Nozzles

FIGURE 6

CATALYTIC COMBUSTION FOR GAS TURBINES

By:

HISASHI FUKUZAWA AND YOSHIMI ISHIHARA
ENERGY AND ENVIRONMENT LABORATORY
CENTRAL RESEARCH INSTITUTE OF ELECTRIC POWER INDUSTRY
KOMAE-SHI, TOKYO, JAPAN

ABSTRACT

A national project for research and development of a high efficiency gas turbine began in Japan in 1978. The objective of the project is to raise the overall thermal efficiency of a combined-cycle power plant system using a high-efficiency gas turbine and a steam turbine. The target efficiency of 55% (LHV) is expected to be reached by 1984.

The CRIEPI research and development program on catalytic combustion for gas turbine combustors includes the development and evaluation of catalysts, determination of optimum operating conditions for combustibility and flue gas composition, and development of a model catalytic combustor. The last stage of the CRIEPI program is to develop a prototype of a low-NOx catalytic combustor for a high-efficiency gas turbine.

A new experimental apparatus for catalyst evaluation at atmospheric pressure was constructed in November 1979, and the characteristics of catalytic combustion were investigated using in-house manufactured catalysts. The results were as follows:

(1) Thermal NOx formation was reduced to as low as below 20 ppm at temperatures up to 1,500° C.

(2) Complete catalytic combustion was achieved at above 1,000° C.

(3) The volumetric heat release rate increased with the temperature and fuel rate, and more than 100×10^6 kcal/h.atm.m^3 was obtained.

INTRODUCTION

A national project for research and development of a high efficiency gas turbine of 100 MW to be operated at 1,500° C under 55 atmospheres was begun in 1978. The objective of the project is to achieve an overall thermal efficiency of 55% (LHV) by a combined-cycle power plant system, shown in Fig. 1.

Heat-resistant materials such as alloys and ceramics, and elements technology for the turbine blade cooling system, compressor, combustion, turbine and controlling system have been investigated according to the R&D schedule shown in Table I.

The design and construction of a 100 MW gas turbine pilot plant to be operated at 1300° C and 55 atmospheres has now been incorporated into this project by the Ministry of International Trade and Industry (MITI).

The CRIEPI R&D program on catalytic combustion was intended to connect with the national project on the development of a high efficiency gas turbine for NOx control. The program includes experiments on pressurized catalytic combustion at 10 atmospheres in 1980 and the development of a model catalytic combustor in 1981. The objective of this program is the application of catalytic combustion technology to a high temperature gas turbine combustor to eliminate NOx formation.

CRIEPI R&D PROGRAM ON CATALYTIC COMBUSTION FOR GAS TURBINES

Promotion of a national project for R&D of a high efficiency gas turbine was begun by the Agency of Industrial Science and Technology of the Ministry of International Trade and Industry in

1978. CRIEPI is participating in this project by conducting some of the research on combined-cycle systems, heat-resistance materials, and cooling systems.

The CRIEPI R&D program on catalytic combustors for gas turbines is being promoted as part of the national project starting in 1980. We are conducting research in the following areas according to the R&D schedule shown in Table II.

1. Development and selection of catalysts
    (1) High operational capability
    (2) Combustion rate of fuels with each catalyst
    (3) Catalyst life at high temperatures
2. Operating conditions and flue gas composition
    (1) Catalytic combustion at atmospheric pressure
    (2) Catalytic combustion at pressurized atmosphere
3. Model catalytic combustor tests for gas turbines
    (1) Development of a model catalytic combustor
    (2) Describing characteristics of a model catalytic combustor
    (3) Design of a full-scale catalytic combustor

Today we are involved in the development and evaluation of catalysts for a catalytic combustor for a high efficiency gas turbine. We are constructing another experimental apparatus for pressurized catalytic combustion at 10 atmospheres.

EXPERIMENTAL CATALYTIC COMBUSTION UNDER ATMOSPHERIC PRESSURE

EXPERIMENTAL APPARATUS

The schematic figure of the experimental apparatus used in this investigation is shown in Fig. 2. The apparatus consisted of an air heater, a catalytic reactor, a gas cooler and analyzers for some contents of flue gases.

LPG was supplied from a cylinder, premixed with preheated air and sent into the reactor at a uniformly controlled velocity. The premixed fuel was oxidized completely on the catalyst surface, settled in the middle of the reactor, and expected temperatures were obtained by controlling fuel/air ratios. Gas temperatures were determined at positions upstream, downstream, and on the surface of the catalyst.

The maximum air flow rate was 120 Nm^3/h and the maximum LPG fuel consumption was 2 Nm^3/h. The inside diameter of the reactor was 9.4 cm and the maximum catalyst size 9.0 cm in diameter and 15.0 cm in length. Flue gas analyses of NOx, THC and CO were made separately by NDIR method analyzers.

Most of the catalysts used in these tests were monoliths 82 mm in diameter and 75 mm in length, including 25 mm long segments. The monoliths consisted of a 2.8 mm square cell mullite or cordierite substrate washcoated with γ-alumina. Thirty kinds of catalysts were loaded on them.

THERMAL NOx FORMATION

The maximum inlet temperature of the gas turbine is expected to be increased to 1,300° C in 1981 and to 1,500°C in 1984 by the national project on high-efficiency gas turbines. Therefore, catalytic NOx reduction FGT equipment will be installed for reducing NOx, assumed to be formed at several hundreds ppm.

With the objective of eliminating the FGT equipment, we have started a R&D program in catalytic combustion technology. In experiments in the first stage of the program, we have confirmed the low thermal NOx emission as described in previous papers.[1]

NOx concentration which corrected to 0% excess air increased while the combustion gas temperature was raised, as shown in Fig. 3. As the figure also shows, NOx concentrations, which varied somewhat with the different catalysts, were as low as 20 ppm at below 1,500° C.

UNBURNED HYDROCARBONS AND CARBON MONOXIDE EMISSION

Small amounts of unburned hydrocarbons (THC), which were analyzed as total hydrocarbons, were emitted in the combustion temperature range from 900 - 1,100° C, but not at above 1,100° C as shown in Fig. 4. Carbon monoxide (CO) was also emitted at 20 ppm or less in the temperature range from 900 - 1,100° C, not at above 1,100° C. But both concentrations of THC and CO increased greatly at temperatures below 900° C.

As a result, a combustion gas temperature of approximately 1,000° C or more was required to effect stable catalytic combustion using LPG fuel. The temperature varied slightly with different catalysts.

COMBUSTION TEMPERATURE

In the catalytic combustor the premixed LPG fuel gas is oxidized on the preheated catalyst surface without an igniter. The preheated temperature required for platinum catalysts was above 330° C.

Combustion temperature was controlled by controlling the preheated air temperature and the fuel/air ratio . The catalyst surface temperature obtained was approximately 50 - 160° C higher than the combustion gas temperature at above 1,200° C, as shown in Fig. 5. Further, the combustion gas temperature agreed with the adiabatic combustion temperature, as shown in Fig. 6.

VOLUMETRIC HEAT RELEASE RATE

The volumetric heat release rate was raised as both the flow rate of premixed fuel and the combustion gas temperature increased.

In catalytic combustion it is possible to burn a large quantity of fuel because the combustion rate is extremely fast. That is, the maximum volumetric heat release rate obtained in these tests was 137×10^6 kcal/h.atm.m^3 at combustion gas temperatures under 1,500° C, 190% of theoretical air, 30.9×10^4 h^{-1} of space velocity. This value indicates the possibility of burning a fuel corresponding to 60 MW of electrical power generation with a thermal efficiency of 40%, that is, about 13 t/h of oil as a fuel.

Figure 7 shows that the volumetric heat release rate will be raised extensively as the premixed fuel gas flow rate increases. The above value of the volumetric heat release rate indicates the catalyst volume is small enough to settle in the combustor designed for high-efficiency gas turbines.

REFERENCES

1. Krill, W.V. and Kesselring, J.P., "The Development of Catalytic Combustors for Stationary Source Applications," Proceedings: Third Workshop on Catalytic Combustion, Asheville, N.C., Oct. 1978, EPA-600/7-79-038 Feb. 1979.

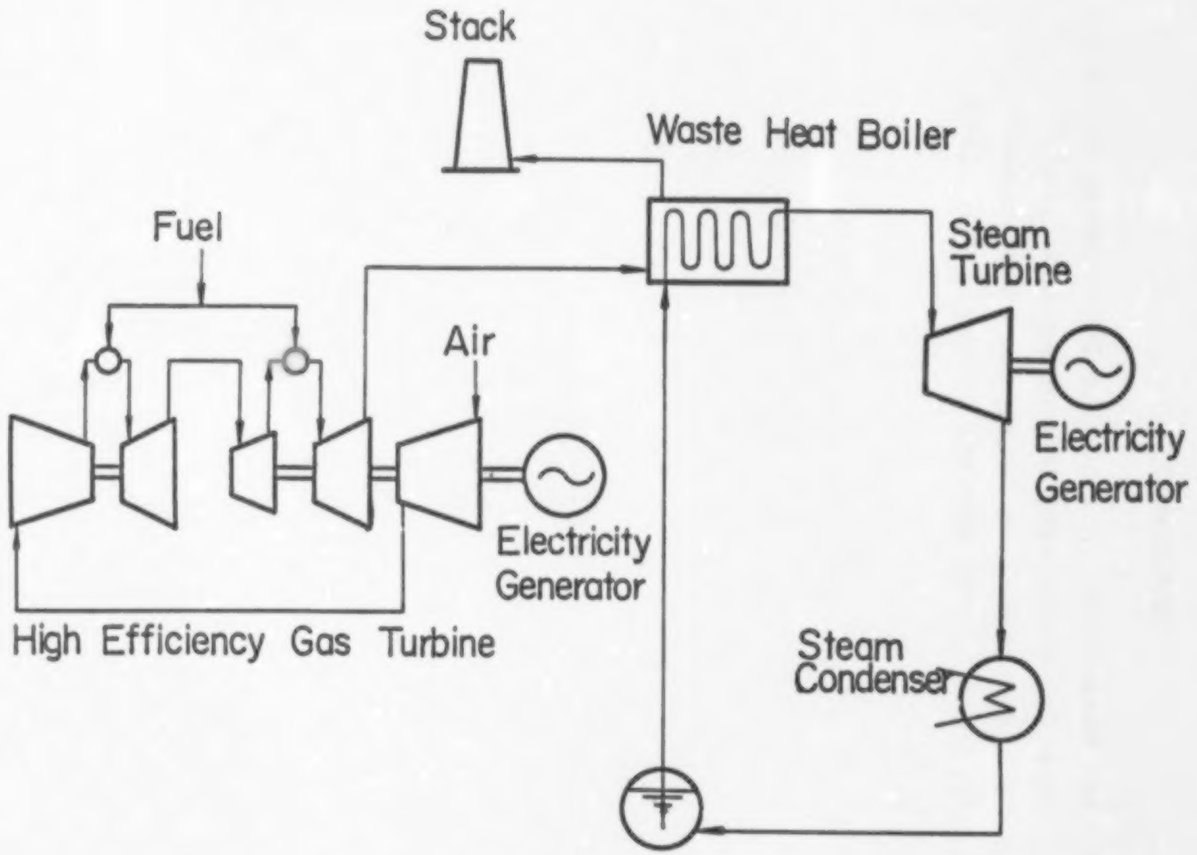
Stack
Waste Heat Boiler
Fuel
Steam
Turbine
Air
Electricity
Generator
Electricity
Generator
High Efficiency Gas Turbine
Steam
Condenser

Figure 1. Schematic Figure Combined-Cycle Power Plant System Having High Efficiency Gas Turbine.

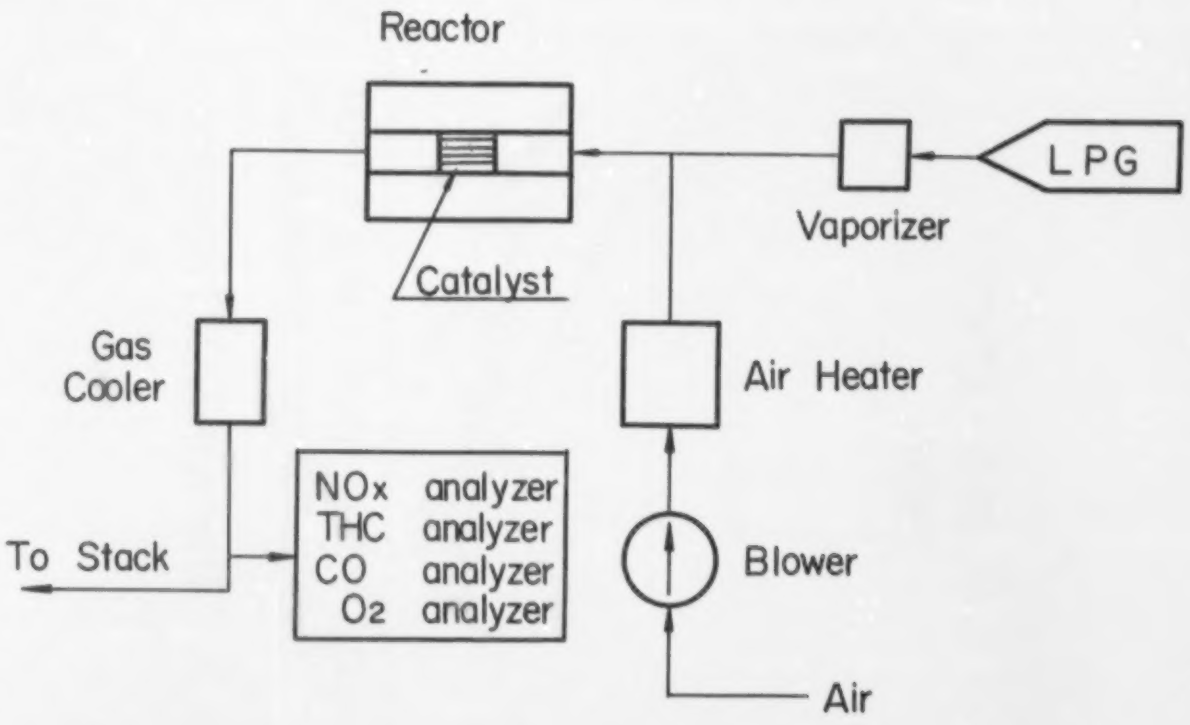
Reactor
LPG
Vaporizer
Catalyst
Gas
Cooler
Air Heater
NOx analyzer
THC analyzer
CO analyzer
O2 analyzer
To Stack
Blower
Air

Figure 2. Schematic Figure of Apparatus for Catalytic Combustion under Atmospheric Pressure.

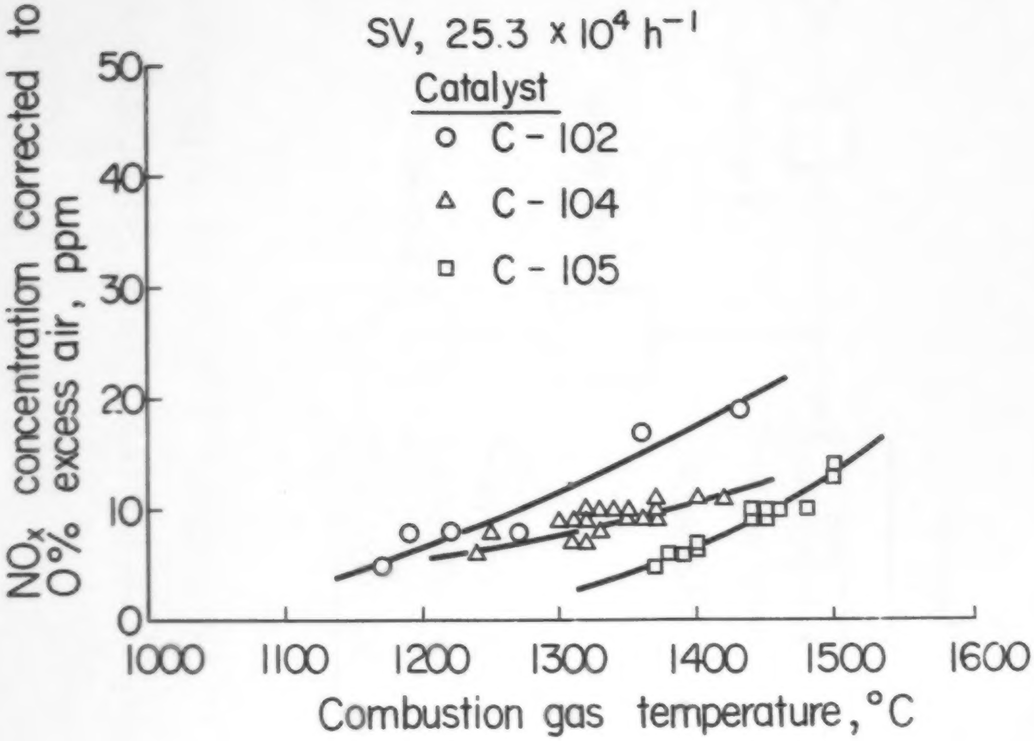

Figure 3. Thermal NO_x Formation

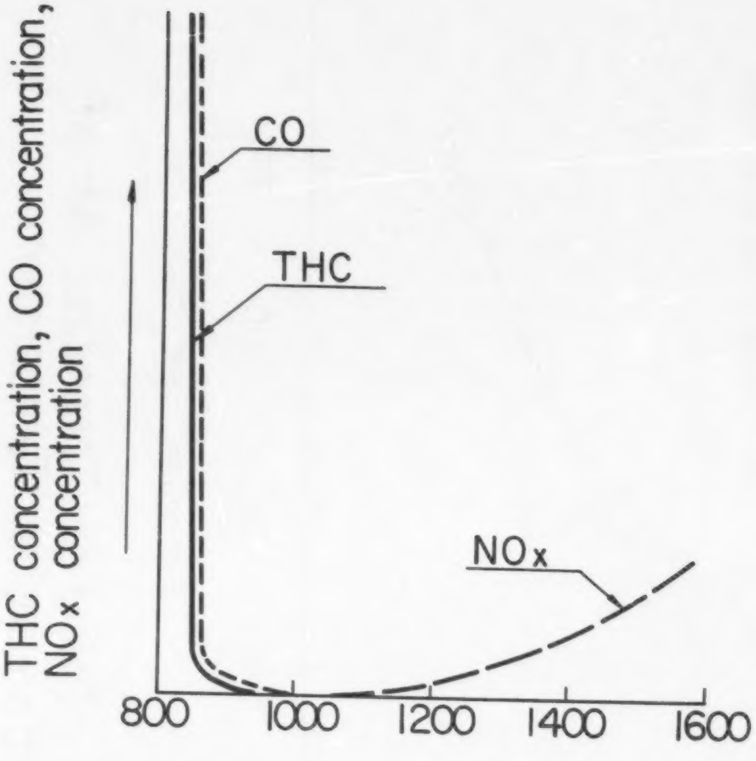

Figure 4. Temperature Zone of Unburned Hydrocarbons and Carbon Monoxide Formation.

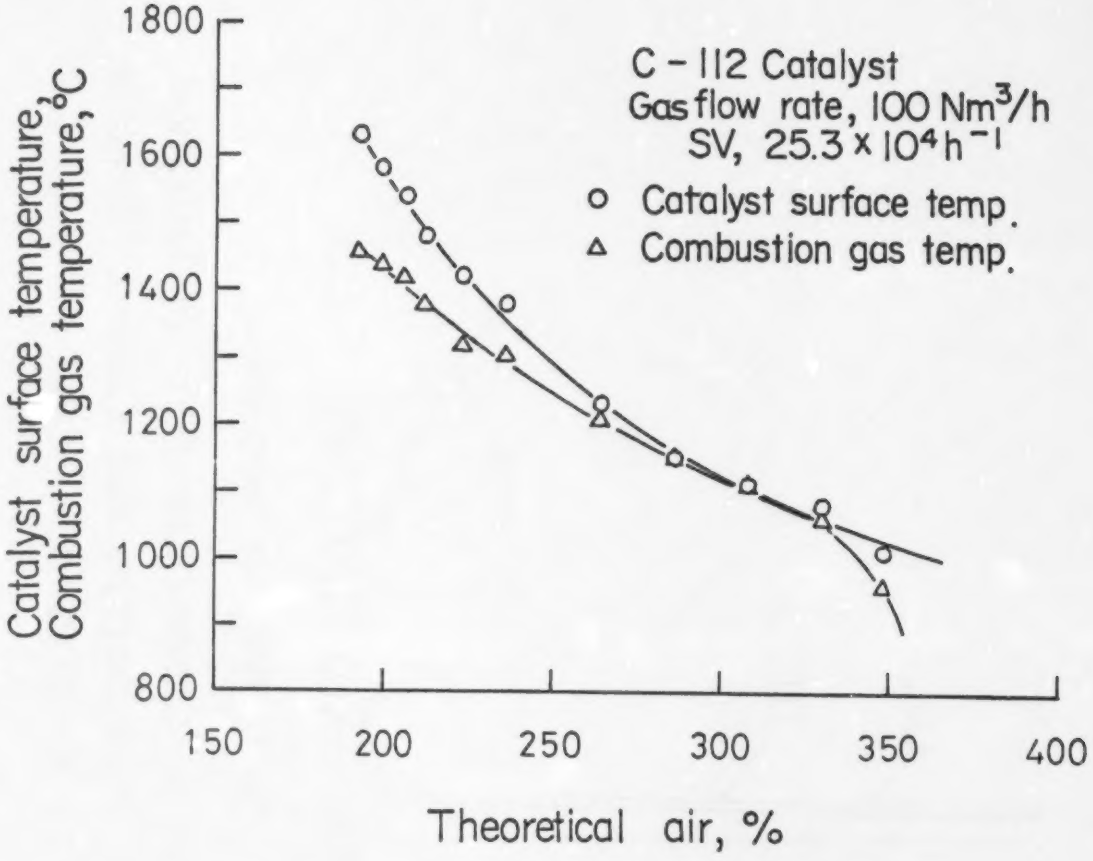

Figure 5. Effect of Theoretical Air on Combustion Temperature.

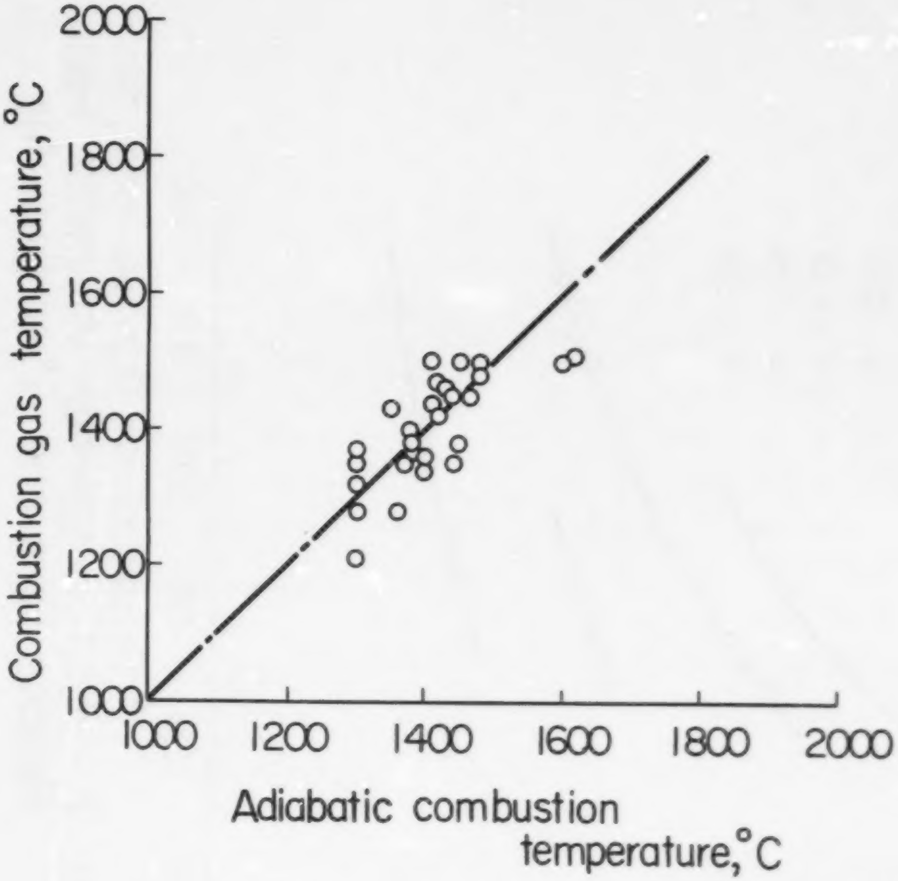

Figure 6. Relation between Combustion Temperature and Adiabatic Combustion Temperature.

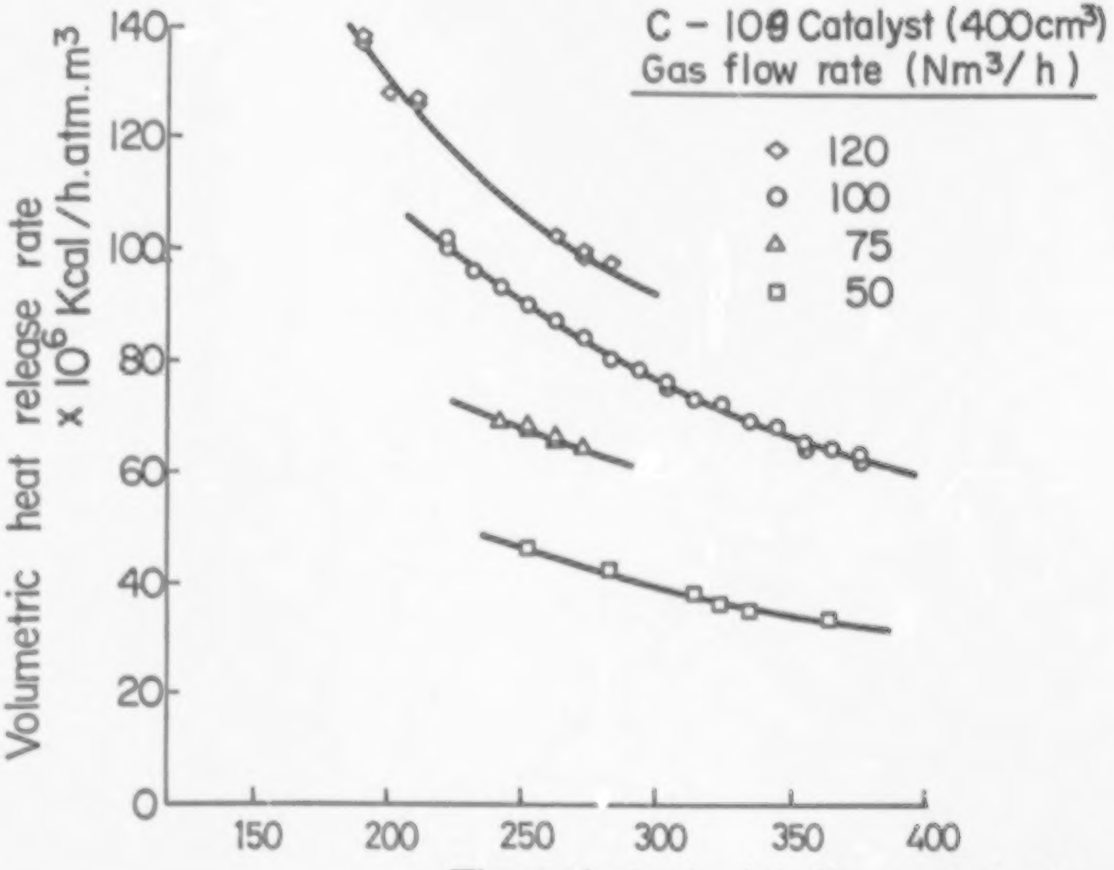

Figure 7. Relation between Volumetric Heat Release Rate and Theortical Air.

Table I. R & D Schedule of Natioal Project for High Efficiency Gas Turbine.

	Calendar Year						
	1978	1979	1980	1981	1982	1983	1984
R & D of heat-resistant materials and elements technology	▨	▨	▨	▨	▨	▨	▨
100 MW Prototype Plant tests					▨ Design	▨ Construction	▨ Operation

Table II. CRIEP Schedule for Low NO_x Emission Catalytic Combustor Program.

	Calendar Year 1979	1980	1981	1982
Development and selection of catalysts	▨	▨	▨	
Operating conditions and flue gas composition	▨	▨	▨	
Development of model catalytic combustor for gas turbine.			▨	▨

SOOT REDUCTION IN DIESEL ENGINES BY CATALYTIC EFFECTS

BY

R. Sapienza, T. Butcher, C. Krishna, J. Gaffney
Brookhaven National Laboratory
Upton, New York 11973

ABSTRACT

Recent tests at Brookhaven National Laboratory indicate that both small additions of alcohols to the fuel and the presence of platinum surfaces in the combustion chamber can reduce soot emissions in a diesel engine. These tests were conducted over a limited range of operation in a single cylinder CFR engine. Most of the testing was done using pure cetane as a fuel at constant speed and load. Possible major features of the reaction mechanisms for both fuel additives and surface catalyst effectiveness are presented.

ACKNOWLEDGEMENT

We are indebted to T. O'Hare, W. Marlow, M. Sansone, J. Barry, J. Hurst, R. Klemm, and C. Waide for their assistance and support. We also wish to thank I. Tang, H. Munkelwitz, F. Salzano, R. Whisker, and A. Berlad for helpful discussions. This research was carried out at Brookhaven National Laboratory under contract with the U. S. Department of Energy.

INTRODUCTION

Diesel car sales are climbing in the United States and some manufacturers are predicting that by 1985 25% of the new cars made in the U.S. may be diesel powered (1). The diesel engine's proven fuel economy and lower emissions of unburned hydrocarbons and carbon monoxide makes it a viable alternative to a gasoline automotive plant, but the inherent production of particulate matter (soot) threatens the expanded use of the diesel engine.

Current diesel cars emit about 13 lbs. of particulate matter for every 10,000 miles - 50 times the gasoline auto. High concentrations of these emissions may have a synergistic effect when combined with other carcinogens in the urban environment (2) and this problem may overshadow the diesel's fuel savings.

A variety of methods have been proposed over the years for reducing soot emissions (3). These methods include engine modifications such as fuel injection optimization, combustion chamber shapes and turbocharging; fuel modifications such as the use of water injection, fuel additives, and fuel fumigation; and more recent suggestions which stress exhaust treatments including "trap oxidizers" similar to catalytic converters and various types of replaceable filters. Fuel blending such as methanol-diesel emulsions, as well as separate introduction of methanol, have also been tried.

In the diesel engine the air charge is compressed to a high temperature and pressure, preceeding fuel injection and combustion begins spontaneously shortly after. The rate of burning and heat release is controlled by the rate of fuel air mixing. This mixing-limited operation leads to not only many of the diesel's desirable characteristics but also to hot, fuel rich zones despite the air charge being in excess of the stoichiometric requirements. Cracking occurs, leading to soot formation in these fuel rich zones. This can be perceived as an autothermal cracking process in which heat, from combustion of the fuel, serves to crack the remainder endothermally (similar to the manufacture of ethylene and acetylene via the pyrolysis of hydrocarbons (4)).

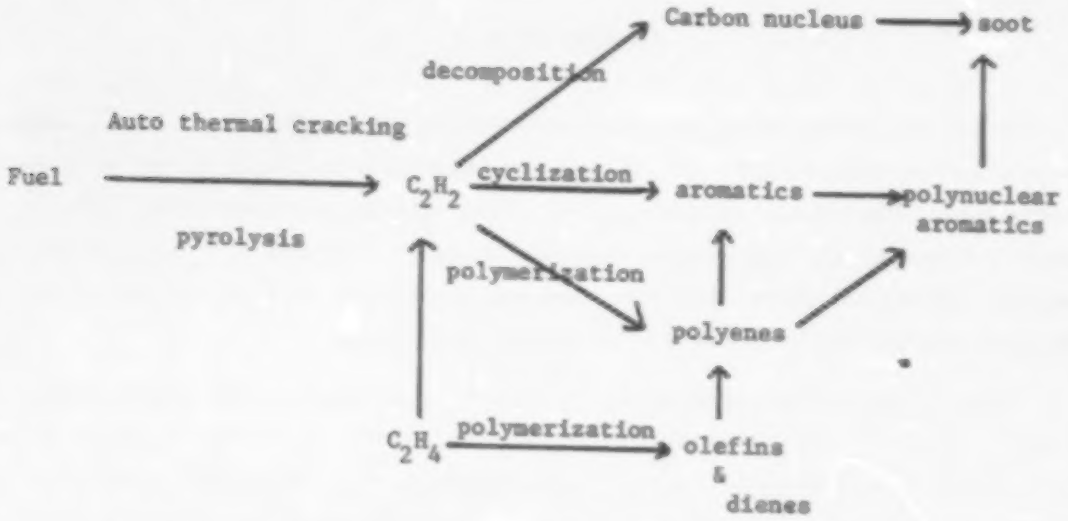
Carbon nucleus
soot
decomposition
Auto thermal cracking
Fuel
pyrolysis
C_2H_2
cyclization
aromatics
polynuclear aromatics
polymerization
polyenes
C_2H_4
polymerization
olefins & dienes

All of the soot formed is not emitted as some of it is combusted in later parts of the engine cycle. It has long been recognized that the engine maximum load is limited by excessive smoking at overall air fuel ratios still well above stoichiometric.

Since a precise mechanism of soot formation during combustion in a diesel engine is not completely defined, a tentative approach was formulated relating the partial combustion of liquid hydrocarbons to the initiation of soot formation in the diesel combustion process. There is ample evidence that soot formed in combustion processes consists of a mixture of surface and gas formed carbons (5), therefore, the influence of both homogeneous and wall reactions in the combustion chamber were considered in order to define the fuel and engine properties which contribute to the formation of particulate matter.

EXPERIMENTAL

Complete combustion must be attained if soot is to be avoided and the introduction of either oxygen carriers or catalytic surfaces, which would increase the probability of contact between fuel and oxygen could influence the formation of soot in the combustion chamber. The addition of hydroxyl (OH) carriers to the fuel was felt to be a direct way to verify or illustrate the proposed chemistry. The possible catalytic influence of wall and valve materials to promote the surface ignition of carbon and soot precursor was also investigated.

EXPERIMENTAL DETAILS

A standard Waukeska CFR engine coupled to a D.C. dynomometer was used in the tests. Cetane was used instead of diesel oil as fuel for obvious chemical reasons and n-butanol was used as the fuel additive. The engine was operated at the ASTM Cetane number test conditions making a concerted effort to keep the engine operating variables constant. Typical engine operating conditions were: speed, 900 rpm; fuel flow, 13 ml/min., compression ratio, 19:10, (see table for each test).

Sampling of the engine's particulate effluent was done by drawing 15.6 l. p.m. through a 47mm Millipore FA filter directly from the exhaust flow, (see Figure 1). This procedure minimized distortion of the sample and maintained the integrity of the structurally-weak filter with no particulate break-off. The filters were equilibrated at constant humidity and weighed to determine the soot by difference. Duplicate samples were reproducible to better than 10% and at least two samples were taken to each data point.

After the cetane/n-butanol mixtures were studied, the engine was dismantled and platinum was deposited onto the piston crown and valve faces by vacuum sputtering to a thickness of approximately 6,000 Å with an MRC model SEM-8620 RF Bias sputter-etch module. Prior to insertion in the chamber the components were cleaned mechanically in a glassblaster and washed with acetone and alcohol as a final step. Sputter etching was not possible.

RESULTS AND DISCUSSION

Use of Alchols

The technology of alcohol fuels utilization in diesel engines is not nearly as advanced as that for spark ignition engines. Since our tentative approach to homogeneous soot formation may be conveniently formulated in terms of the free radical theory of the cracking of hydrocarbons (6), alcohol could suppress the formation of soot by providing species which remove or retard radical fuel pyrolysis intermediates.

Alcohols Action

1. Radical Retardation

    a. Transfer agent

    $P\bullet + RCH_2OH \longrightarrow PH + R^{\bullet}CHOH$

    $P\bullet + R^{\bullet}CHOH \longrightarrow PH + RCHO$

    $P\bullet + RCHO \longrightarrow RCO + PH$

    b. Copolymerization agent

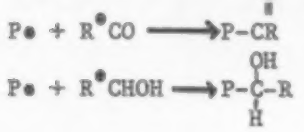

    $P\bullet + R^{\bullet}CO \longrightarrow P\text{-}\overset{\bullet}{C}R$

    $P\bullet + R^{\bullet}CHOH \longrightarrow P\text{-}\overset{OH}{\underset{H}{C}}\text{-}R$

2. Precursor Trap

    a. reaction with acetylene

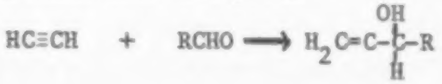

    $HC{\equiv}CH + RCHO \longrightarrow H_2C{=}C\text{-}\overset{OH}{\underset{H}{C}}\text{-}R$

    b. inhibits diene cyclization reactions

    c. reaction with aromatic radicals

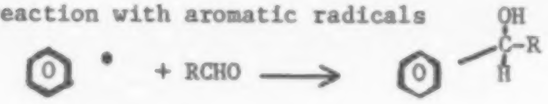

The observed data as presented in Figure 2, reveal a rapid and then gradual decrease in soot with n-butanol addition with an optimum 30-40% reduction at ∿ 7% n-butanol addition. Similar results were observed when using conventional diesel fuel and ethanol mixtures (Figure 3).

Although recent tests using methanol and ethanol/diesel emulsions have shown particule reduction (7,8), to our knowledge this represents the first systematic investigation of specific alcohol addition versus reduction of soot particulates in a diesel engine. These results seem to support our concept of controlling the gas-phase mechanism of soot formation utilizing the radical retarding effect of alcohols.

Use of Metals

Catalytic combustion can promote the oxidation of long chain hydrocarbons and soot precursors minimizing polymerization reactions which result in soot formation.

The mechanism by which metal containing fuel additives reduce smoke is obscure (9), but British Petroleum tests suggest that successful soot suppressants lower the soot ignition temperature while other ineffective additives yield little change in this temperature (10).

Alkaline-earth metal fuel additives such as barium salts affect homogeneous soot formation in a manner similar to that proposed for alcohols. These metals which reduce soot in all oxygen-fuel ratios, act by the gas-phase catalysis of the decomposition of hydrogen or water vapor to yield hydroxyl radicals (11).

Other effective metal fuel additives such as molybdemum, tungsten and chromium perform only at high oxygen-fuel ratios, (>.9) suggesting a different mechanism for their action (11). It is our contention that these metals act as surface catalysts in the combustion process.

Early exploratory work on surface combustion has shown that hot surfaces have the capability of accelerating combustion at the boundary region between gaseous and solid phases (12). Considering that the nature of the reactor wall has a significant effect on the rate of carbon formation and, the composition of the exit gas in a cracking reactor (13), the oxidation properties of the combustion chamber surface could determine the quantity and quality of the particulate emissions in a diesel engine.

Since an oxidation catalyst serves as the source of oxygen transferred to the reactant molecule, the most important property generally ascribed to a combustion catalyst is its ability to dissociate oxygen molecules into adsorbed oxygen atoms. If the formed oxide can be reduced by the hydrocarbon to a lower oxide or the metallic state, the metal will function as an active catalyst.

We wish to propose a novel yet simple mechanism which would provide a unified picture capable of explaining or predicting catalyst behavior. The basis for this hypothesis was generated from various studies in slow combustion, which neglected wall effects in elucidating the mechanism and understanding the chemistry of combustion (14).

This proposal starts with the assumption that oxygen must become activated upon a surface, M (step A). This may be the metal in catalyzed combustion or even the walls of the reaction vessel. It has been found that reaction initiation in the absences of walls may be severe (15) and most radical mechanisms use the walls to convert intermediates to products (6).

The carbonaceous material (e.g., ethylene in diagram) reacts with the surface oxygen forming a saturated intermediate (B) which undergoes carbon-carbon bond cleavage to give the oxymethylene species, (C). This would be associated with the induction period of combustion, and would be an exothermic reaction. This species would explain why formaldehyde, which would chemisorb on a surface in this manner, is responsible for branching (F) in the combustion of many simple fuels (16). Similarly, saturated hydrocarbons could form acetaldehyde as an intermediate (I). The addition of formaldehyde or acetaldehyde to a hydrocarbon combustion reaction should eliminate the induction period and indeed this is the case in the oxidation of ethane (17). The possible reaction paths of the oxymethlyene intermediate result in the various products observed in the slow combustion of ethylene (16).

Carbon dioxide arises from the reaction of the oxygen coordinated carbon monoxide with surface oxide (G). This step is consistent with the mechanism of carbon monoxide oxidation (18). Carbide or soot formation occurs (H) when the adjacent surface oxide is not present (e.g., thru reduction). If the oxide site were available soot formation would be reduced.

An interesting feature of this scheme is that it is closely related to the recently proposed oxide Fischer-Tropsch (F-T) mechanism (19). Since both proposals assume similar reaction intermediates correlations of metal catalysts should be noted. Indeed, metals that form strong oxides are not good F-T catalysts and will inhibit the oxidation of carbon. This relationship is particularly attractive in the examination of controlled combustion for chemical conversion.

In view of the well known combustion catalytic effects of platinum (20) the coating of the combustion chamber surfaces with platinum was tried.

The platinum coated combustion surface produced ∿ 40% reduction in soot with no alcohol addition. Addition of alcohol to the platinized reactor was found to further reduce soot with reduction up to ∿ 80% being measured (see Figure 4).

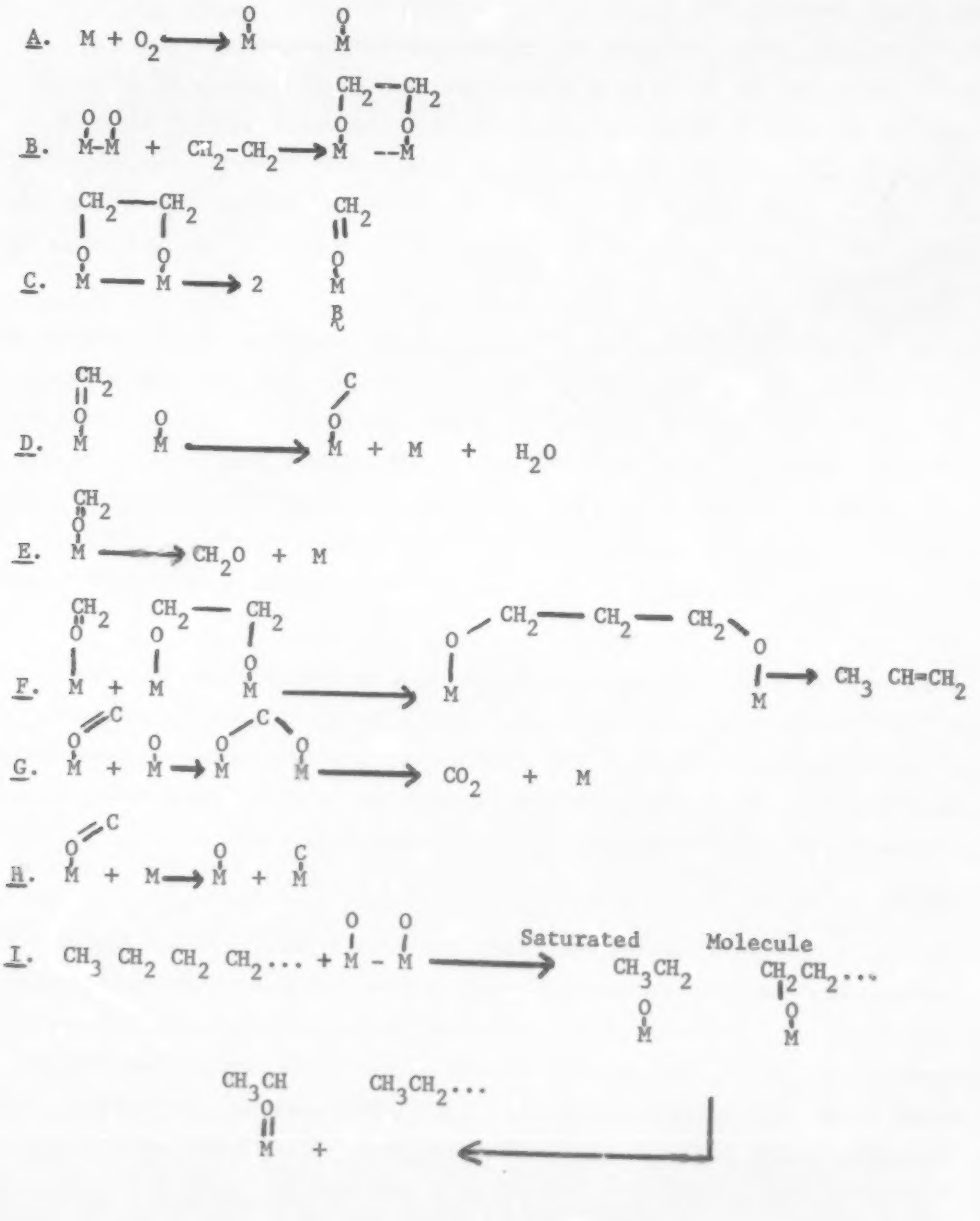

A. M + O2 → M(O) M(O)
B. M(O)–M(O) + CH2–CH2 → M(O)–CH2–CH2–(O)M
C. → 2 M(O)=CH2
D. → M–O–C + M + H2O
E. → CH2O + M
F. → CH3 CH=CH2
G. → CO2 + M
H.
I. CH3 CH2 CH2 CH2... + M(O) – M(O) →
Saturated Molecule
CH3CH2
CH2CH2...
CH3CH
CH3CH2...

The cyclic oxygen transfer mechanism appears to offer reasonable explanations of these results since the free energy decrease on reduction of iron oxides with carbon (or hydrocarbons) is less than that for the reduction of platinum oxide. Because platinum will markedly lower the ignition temperature of carbon (21) and promote ultralean combustion of hydrocarbons, (20) soot and unburned fuel reaching the platinized combustion chamber surface could be partially or completely oxidized leading to reduced particulate emissions. Heterogeneous reactions of this sort will be limited by the amount of carbon reaching the surface by molecular and turbulent transport but may produce products which also affect the homogeneous chemistry. That is, reaction intermediates initially formed at the surface, breakoff to take part in homogeneous reactions. This chemistry would be similar to the action of alcohol described earlier.

After eight hours of continuous operation the platinum coated surface was lost, and the observed soot emission found to be identical with the original iron surfaced piston and valves. Although the precise mechanism by which the platinum was removed is unknown, we believe that surface impurities such as, iron carbon and oxide may have caused problems in the platinum adhesion since no stringent cleaning of the piston crown was performed prior to coating. Thermal expansion differences or excessive vibration would also have deleterious effects (22).

The short service life may also be ascribed to penetration by poisons or oxygen through the catalytic lining with resulting pitting or corroding of the iron alloy composing the piston. To overcome this a hard, smooth, non-catalytic and non-absorbtive cap of low corroding properties (e.g., chrome-iron) should be interposed between the catalyst and the coated body (23).

CONCLUSION

This work towards reducing soot emission from diesel engines suggests that both homogeneous and heterogeneous approaches are feasible. The homogeneous approach consisted in mixing small quantities of alcohol with the fuel and the heterogeneous approach consisted of coating parts of the combustion chamber (bounding) surface with an oxidation catalyst like platinum. Both approaches produced significant reductions in soot emissions. These tests were conducted over a small range of operation in a single cylinder engine (a CFR type), with most of the testing done using pure cetane as fuel at constant speed, and load. Although the engine and test conditions are not representative of an automotive diesel engine, the results may be useful to assess the feasibility of soot reduction in automotive and truck diesel engines, using these methods.

The major features of the reaction mechanisms proposed for both fuel additive and surface catalyst effectiveness could be applied to various combustion problems.

REFERENCES

1. Goen, R. L. and Ivory, M. E. Diesel Cars in the United States. TID-28735, 1978.

2. French, C., Monaghan, M., Fresse, P. G. A Study of the Diesel as a Light-Duty Power Plant, EPA-PB 236-896 (NTIS), 1974.

3. Chalmers, J. F., Fullenwider, E. D., Minton, M. G., and Tomlinson, J. C. Review of the Research Status on Diesel Exhaust Emissions. ATR-78(7716)-3, The Aerospace Corporation, 1978.

4. Kamptner, H. K., Krause, W. R., and Schilken, H. P. High Temperature Cracking. Chemical Engineering, 73:93-98, 1966.

5. Palmer, H. B. J. Chem. Phys., 87, April 1969.

6. Rice, F. O. The Thermal Decomposition of Organic Compounds from the Standpoint of Free Radical, I. Saturated Hydrocarbons, J. Amer. Chem. Soc., 53:1959-1972, 1931.

7. Havemann, H. A., Rao, M. R. K., Natarajan, A., and Narasimhan, T. L. Alcohol with Normal Diesel Fuels. Gas and Oil Power, 50:15-19, 1955.

8. Lawson, A. and Last, A. J. Development of an On-Board Mechanical Fuel Emulsifier for Utilization of Diesel/Methanol and Methanol/Gasoline Fuel Emulsions in Transportation. Proceedings of the Third International Symposium in Alcohol Fuels Technology, Asilomar, California, 1979.

9. Lahaye, J. and Prado, G. Mechanisms of Carbon Black Formation. Chemistry and Physics of Carbon, P. L. Walker, Jr. and P. A. Thrower, eds., Marcel Dekker, Inc., New York, 1978 pp.167-294.

10. McConnell, G. and Howells, H. E. Diesel Fuel Properties and Exhaust Gas - Distant Relations. SAE 670091, 1967.

11. Cotton, D. H., Friswell, N. J., and Jenkins, D. R. The Suppression of Soot Emission from Flames by Metal Additives, Comb. Flame, 17:87-98, 1971.

12. Bone, W. A. Surface Combustion with Specific Reference to Recent Development. Gas Journal, p.423, 1923.

13. Trimm, D. L. The Formation and Removal of Coke from Nickel Catalyst. Cat. Rev. Sc. Eng., 16:155, 1977.

14. Bone, W. A. and Townend, D. T. A. Flame and Combustion in Gases. Longmans Green, London, 1927.

15. Boudart, M. Chemical Kinetics and Combustion. Proceedings of the Eight Symposium (International) on Combustion, The Wilkams and Wilkins Co., Baltimore, Maryland, 1962, pp.43-50.

16. Minkoff, G. J. and Tipper, C. R. H. Chemistry of Combustion Reactions. Butterworths, London, 1962.

17. Lewis, B. and VonElbe, G. Combustion, Flames, and Explosions in Gases. Academic Press, New York, 1951.

18. Happel, J., Kiang, S., Spencer, J. L., Oki, S., and Knatow, M. A. Transient Rate Tracer Studies in Heterogeneous Catalysis: Oxidation of Carbon Monoxide, J. Catalysis, 50:429-440, 1977.

19. Sapienza, R. S., Sansone, M. J., Spaulding, L. D., and Lynch, J. F. Novel Interpretation of Carbon Oxide Reductions. Fundamental Research in Heterogeneous Catalysis, 3:179, 1979.

20. Pfefferle, W. C. The Catalytic Combustor: An Approach to Cleaner Combustion. J. Energy, 2:142-146, 1978.

21. Robell, A. J., Ballou, E. V., and Boudart, M. Surface Diffusion of Hydrogen on Carbon, J. Phys. Chem., 68:2748-2753, 1964.

22. Roessler, W. U., Weinberg, E. K., Drake, J. A., White, H. M., and Iuara, T. Investigation of Surface Combustion Concepts for NO_x Control. EPA 650/2-73-014, U. S. Environmental Protection Agency, Research Triangle Park, North Carolina, 1973.

23. Prentice, J. U.S. Patent 1,869,0771, 1932.

TABLE I

SOOT EMISSION MEASUREMENTS AS A FUNCTION OF ADDITION OF N-BUTANOL TO A CONVENTIONAL (IRON) CFR ENGINE

PERCENT ALCOHOL ADDITION	SOOT (mg)[a]	ENGINE OPERATING CONDITIONS			
		HP	RPM	INJECTION[b] ADVANCE	IGNITION[b] DELAY
0	1.15	2.8	890	8.4	5.2
1	1.00	3.0	895	8.7	4.7
2	.94	2.9	925	8.8	4.7
5	.86	2.9	880	7.8	4.6
8	.77	2.7	880	7.5	4.7
10	.76	2.6	890	8.2	4.7
20	.70	2.4	900	7.4	5.3

[a] Soot samples taken for 30 seconds (see experimental section for details).

[b] In degrees.

TABLE II

SOOT EMISSION MEASUREMENTS AS A FUNCTION OF ADDITION OF N-BUTANOL TO CFR ENGINE WITH PLATINUM COATED PISTON CROWN AND VALVE FACES

PERCENT ALCOHOL ADDITION	SOOT (mg)[a]	ENGINE OPERATING CONDITIONS			
		HP	RPM	INJECTION[b] ADVANCE	IGNITION[b] DELAY
0	.66	2.8	930	9.2	4.7
1	.62	2.7	890	8.3	4.7
5	.57	2.6	890	8.2	4.9
10	.55	2.5	920	8.3	5.2
20	.31	2.1	885	7.4	5.2
50	.28	1.9	930	7.2	5.7
0[c]	1.13	2.5	915	8.2	4.5
2[c]	.96	2.6	910	7.9	5.0
15[c]	.76	2.3	885	7.5	5.2

[a] Soot samples taken for 30 seconds (see experimental section for details).

[b] In degrees.

[c] Platinum coating lost from surfaces.

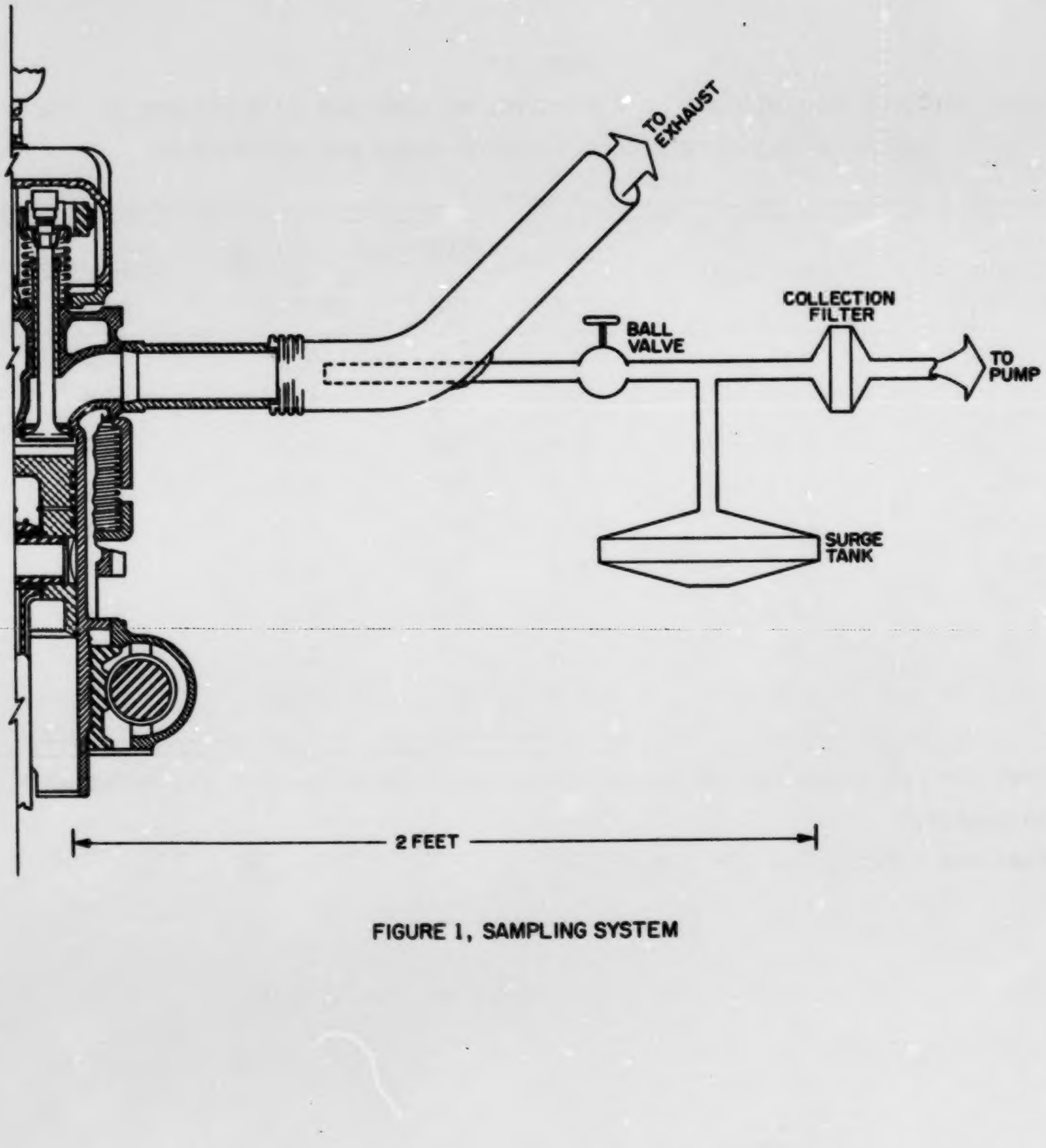
TO EXHAUST
BALL VALVE
COLLECTION FILTER
TO PUMP
SURGE TANK
2 FEET

FIGURE 1, SAMPLING SYSTEM

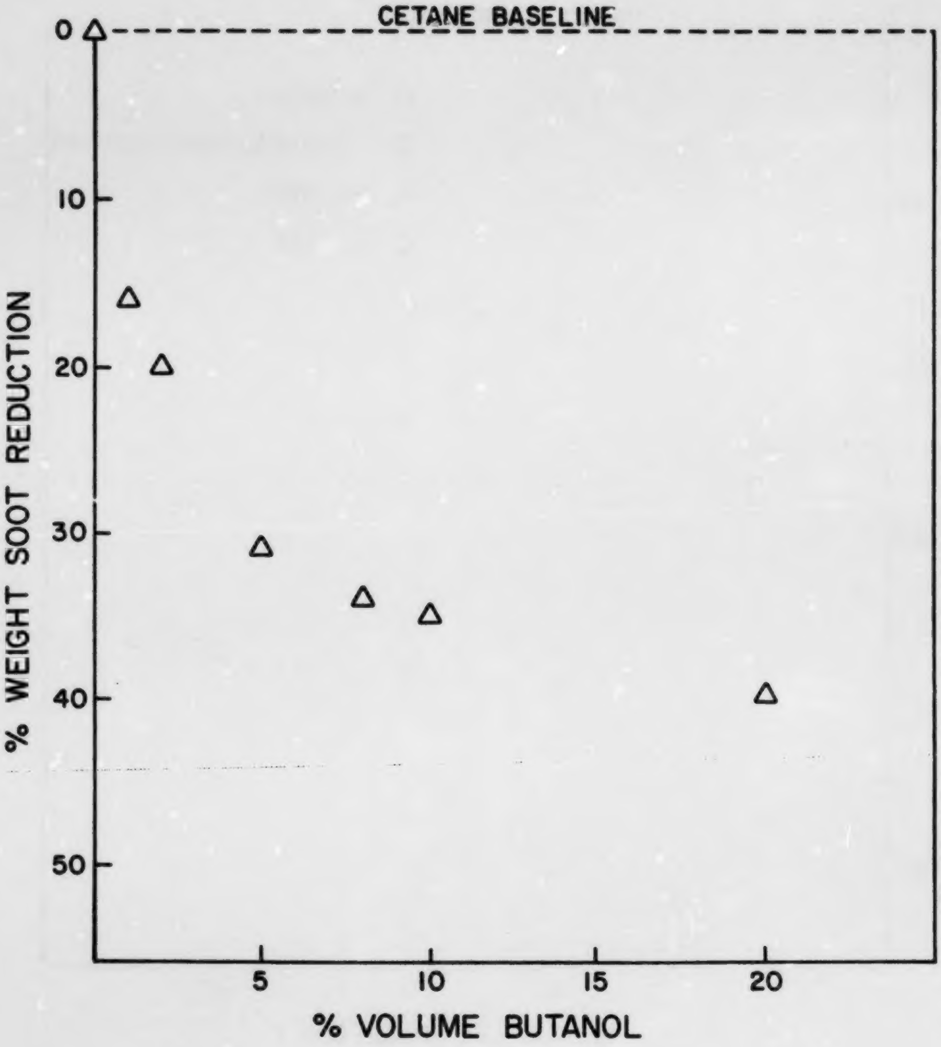

FIGURE 2. BUTANOL ADDITION TO CETANE

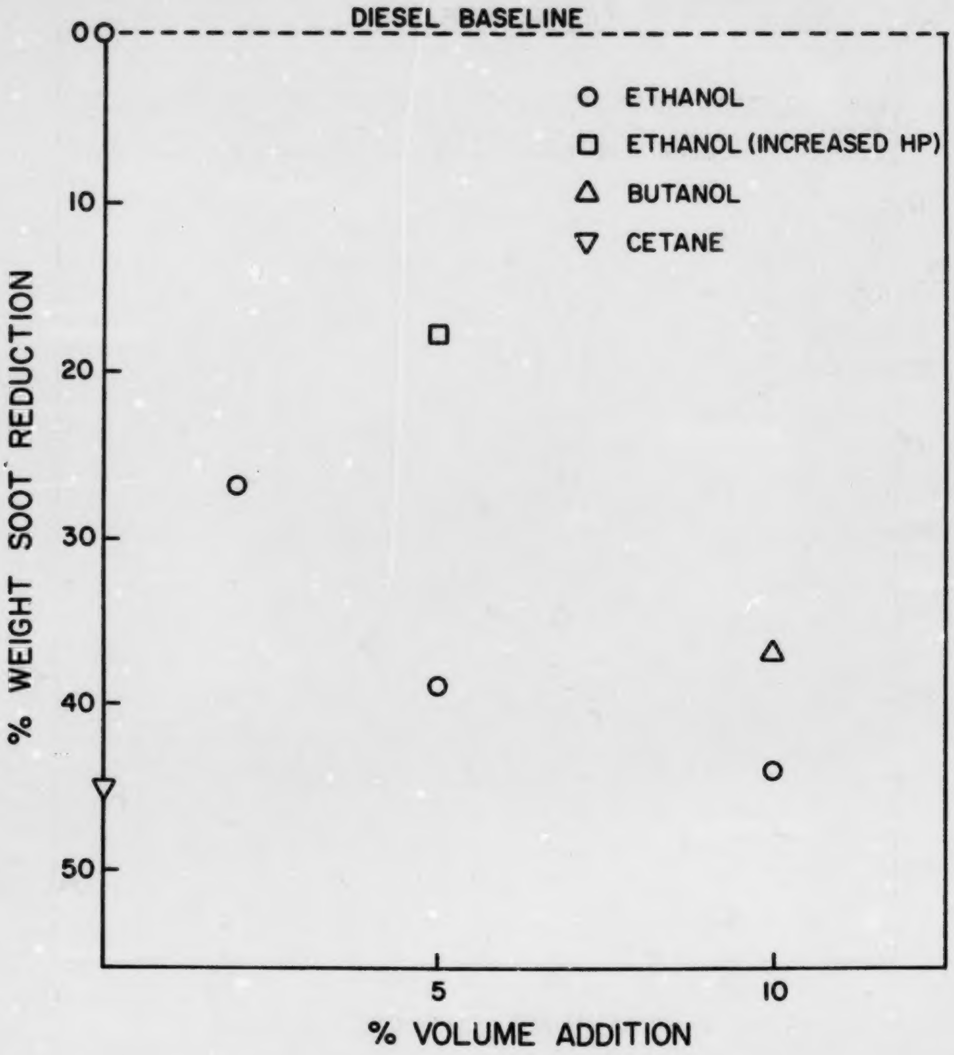

FIGURE 3. DIESEL FUEL DATA

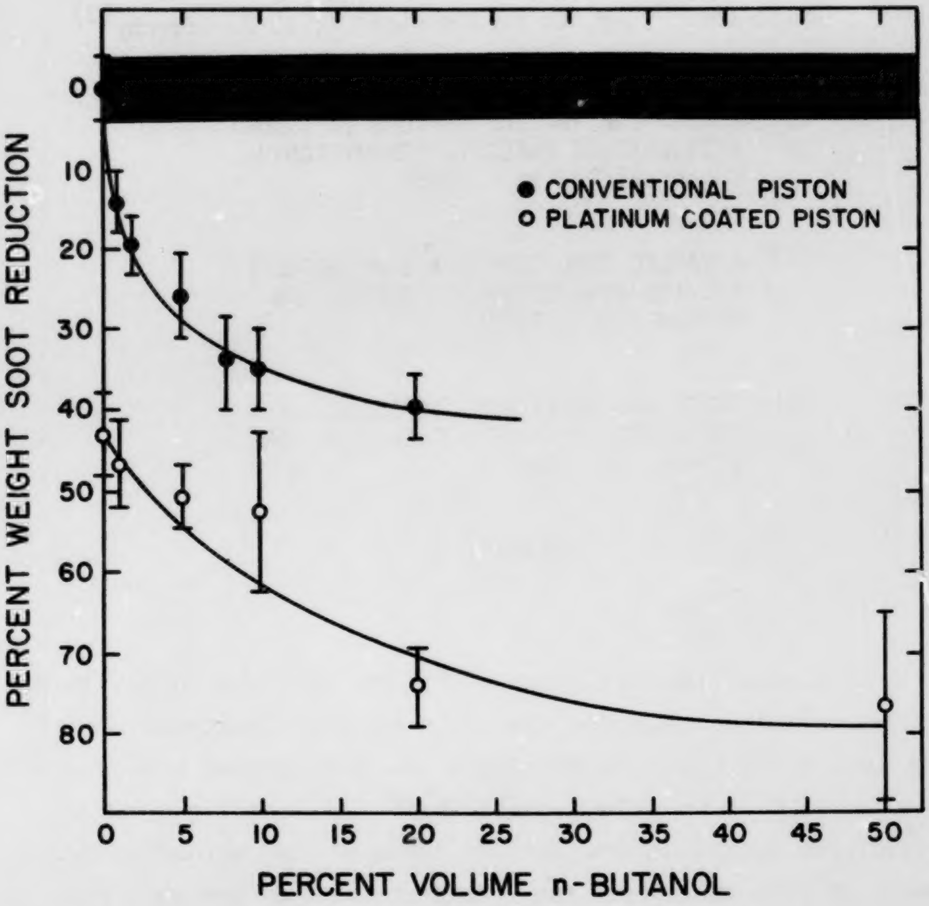

FIGURE 4. EFFECT OF CATALYST (PLATINUM)

HIGH PRESSURE TEST RESULTS

By

D. E. Carl(1), M. C. Krepinevich(2), I. T. Osgerby(3)

(1) COMBUSTION TURBINE SYSTEMS DIVISION
WESTINGHOUSE ELECTRIC CORPORATION
Concordville, PA 19331

(2) ADVANCED COAL CONVERSION DEPARTMENT
WESTINGHOUSE ELECTRIC CORPORATION
Madison, PA 15025

(3) ENGELHARD INDUSTRIES DIVISION
ENGELHARD MINERALS & CHEMICALS CORP.
Edison, NJ 08817

ABSTRACT

The Westinghouse/Engelhard program with the objective of developing a full scale prototype catalytic combustor requires judicious use of sub-scale test facilities. On this basis the Westinghouse test program at the Waltz Mill facility was established. The specific areas of effort involving design information are those of the evaluation and development of both conceptual fuel preparation zones and catalysts. Selected accomplishment thus far have been the following:

- Advanced catalytic combustor test technology to 15 atmospheres. This has included extensive rig and instrumentation development spanning a period of approximately 18 months.

- Recorded excellent emission of 12 ppmv CO and 1 ppm NO_x at 190 psig, 2200°F outlet temperature (CATATHERMAL operation).

HIGH PRESSURE TEST RESULTS

INTRODUCTION

Monolithic catalysts have been successfully tested at high pressure in the newest of the Westinghouse combustion facilities--the Advanced Coal Conversion Department (ACCD) Test and Development Center. The principal accomplishments thus far have been the following:

- Observed CATATHERMAL operation at pressures up to 190 psig in four inch diameter on distillate oil fuel.
- Advanced catalytic combustor test technology to 15 atmospheres. Whereas earlier successful testing at 3 atmospheres was carried out with relative ease, high pressure testing has required extensive rig and instrumentation development.
- Recorded excellent emissions of 12 ppmv CO and 1 ppmv NO_x at 190 psig, 2200°F outlet temperature (CATATHERMAL operation).
- Demonstrated adequate fuel preparation zone (FPZ) performance for research purposes with the multiple-conical (NASA-type) fuel-injector.
- Observed no apparent catalyst deterioration following liquid impingement during startup or during brief episodes of premature ignition in the FPZ.

FACILITY DESCRIPTION

The Test and Development Center, operated by the Westinghouse Advanced Coal Conversion Department, is located at the Corporation's Waltz Mill Site in Madison, Pennsylvania. It was designed and constructed between 1975 and 1978 to provide flexible, modern facilities for conducting development tests on gas turbine combustors, as well as life tests on turbine blade materials and coatings, and for determining the corrosion/erosion/deposition characteristics of fuels and cooled-airfoil surfaces.

The Waltz Mill test complex is shown on Figure 1. The 600-square-foot main laboratory contains a 33 foot high- bay at the north end, and two stories of laboratories and offices in the south half. The experimental area is monitored from a second floor control room that overlooks the high bay. A near-by Compressor Building houses a centrifugal and a reciprocating compressor; a fuels blending facility with day tanks for testing fuel oils and pumps for the cooling water systems; and a Fuel Storage Area containing underground storage tanks.

The schematic in Figure 2 shows the installed facilities and the connections required to serve the test passage.

Non-Vitiating Air Preheaters

Two dual-fuel fired heat exchangers heat the air from the process air compressors before it enters the test passages. The air side operates at full process pressure. The complete unit can raise 7.5 lb/sec from 200 to 1200°F or the entire 12.5 lbm/sec to a lower temperature. The heaters are fired by natural gas or No. 2 fuel oil.

Fuel System

No. 2 fuel oil and clean coal liquids are stored underground in two 10,000 gallon tanks and in one 5,000-gallon tank. The fuel can be transferred from these tanks to five 500 gallon day tanks located in the Fuels Blending Building. These day tanks are connected to the Process Laboratory combustion passage test area.

On-Line Gas Analysis Facility

On-line continuous monitoring of combustion rig emissions is accomplished with a Beckman-designed gas analysis system. The system includes a heated sample line, a smoke meter with detached densitometer, and the instruments listed below:

Analyzer	Method	Type
NO/NO_x	Chemiluminescence	Beckman 951 H
CO	Infrared	Beckman 865
CO_2	Infrared	Beckman 865
H_2O	Infrared	Beckman 865
O_2	Magnetic susceptibility	Beckman
Hydrocarbons	Flame ionization	Beckman 402
Smoke	SAE	Beckman

The gas analysis includes provisions for continuous recording of all parameters except smoke. Sample flow to any instrument can be interrupted for on-line calibration check. General operating practices include calibration prior to and following each test period.

DATA ACQUISITION SYSTEM

All sensors provided in the combustion laboratory at Waltz Mill are electronic, and the site is equipped with a PDP-11/34 computer. A Digital Equipment Co. data acquisition system serves as interface between sensors and computer. A similar computer has served the Coal Gasification Process Development Unit at the same site for four years.

CATALYTIC COMBUSTOR TEST RIG AND INSTRUMENTATION

The catalytic combustion test passage (Figure 3) is constructed of 8 in. O.D. Sch 80 stainless steel pipe with a 5 in. I.D. combustor section. This internal dimension allows for cooling air and insulation around the combustor internals. The 8 in. pipe is the pressure boundary and is rated at 300 psig at 1000°F. The test passage consists of four sections:

- Air preparation
- Fuel vaporization
- Combustion
- Cooling

The air preparation section takes the preheated process air and directs it to the vaporization section. The process air must have an even distribution for good catalytic combustion, which is accomplished with an appropriate device upstream of the fuel injector.

The fuel vaporization section consists of a NASA-type fuel nozzle with 24 injection tubes. The vaporization section is designed to mix the fuel with preheated air to yield a homogeneous fuel/air mixture.

The combustion section contains the catalyst where oxidation of the fuel/air mixture takes place. The inside liner of the combustion section has cooling fins and cooling air flow on the outside wall. This cooling air mixes with the combustion air at the exit of the combustion section.

The cooling section is the place where the hot combustion gases are cooled by a high pressure water spray and exhausted to the muffler house.

Test data are recorded by the data acquisition system (DAS), for subsequent retrieval and analysis. These data include the following:

- Air mass flow
- Oil flow
- Preheat temperature
- Test passage pressure
- Catalyst pressure drop
- Catalyst outlet temperature profile
- Combustion gas temperature
- Exhaust gas analysis.

The DAS has the capability of collecting all required data at the rate of one set every ten seconds. This data rate is ideal for steady-state operation, yet is sufficient for characterization of start-up conditions because the start-up transient takes several minutes.

Process air mass flow rate is measured by the pressure drop of a Venturi and is compensated by pressure and temperature corrections. The mass flow-rate computed from the Venturi Δp, pressure, and temperature is fed back to the process air controller. The oil flow is measured by a full flow turbine meter. Test rig temperatures are measured by either type K or type S thermocouples. The gage pressure and differential pressures of the test rig are measured by transmitters. The combustion gas products are sampled and analyzed for the following contents:

- Unburned hydrocarbons
- Nitric oxide
- Nitrogen dioxide
- Oxygen
- Carbon monoxide
- Water vapor
- SAE smoke number

These data are continuously recorded so that combustion efficiency and catalyst performance can be evaluated. The specific emissions analysis instrument action available at Waltz Mill was described earlier.

For this test, Engelhard provided a catalyst designated as DXE-442, which uses palladium as the principal precious metal component supported by a stabilized alumina washcoat. The monolithic support is a zircon composite having a cell density of 256 channels per square inch. The catalyst configuration consist of two 3.8 inch diameter catalysts, each 2 inches long, with a 0.25 inch space between the two segments as shown in Figure 4.

RESULTS

The test procedure for the subject catalyst included operation in the CATATHERMAL Mode at 110, 150, and 190 psig. At each pressure, air flows were varied so that the CATATHERMAL reaction was extinguished and re-established. The results at each pressure are shown in Figures 5, 6 and 7. The results show that the catalyst pressure drop was never greater than 4.02 percent.

The flat temperature profiles verify the adequacy of the fuel preparation zone. The predicted temperature, based on measured fuel and air flow rates is shown on each figure. The temperature measured by means of exhaust gas analysis at the centerline is in agreement with the other temperatures.

There appears to be a slight pattern factor developing in the catalyst exit temperature profile at the higher pressures. This occurence is still being investigated, but the most likely explanation is that it is due to a change in the FPZ.

CONCLUSION

The catalyst has been shown to operate as well or better at 190 psig as it does at lower pressures. Catalyst transition from non-CATATHERMAL to CATATHERMAL operation at pressures up to 190 psig has been demonstrated through testing so far.

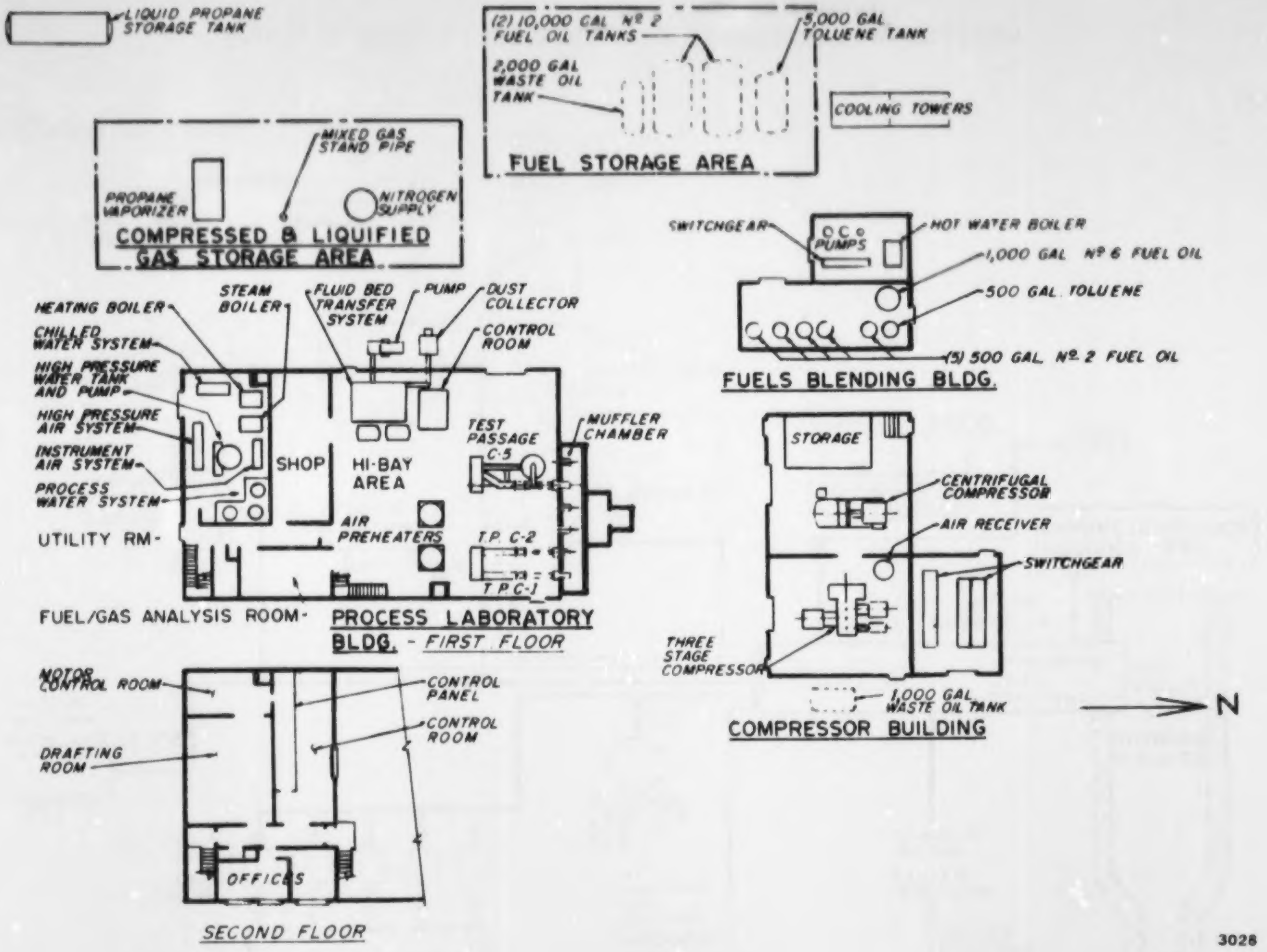
LIQUID PROPANE STORAGE TANK
(2) 10,000 GAL Nº 2 FUEL OIL TANKS
5,000 GAL TOLUENE TANK
2,000 GAL WASTE OIL TANK
COOLING TOWERS
FUEL STORAGE AREA
MIXED GAS STAND PIPE
PROPANE VAPORIZER
NITROGEN SUPPLY
COMPRESSED & LIQUIFIED GAS STORAGE AREA
SWITCHGEAR
PUMPS
HOT WATER BOILER
1,000 GAL Nº 6 FUEL OIL
500 GAL. TOLUENE
(5) 500 GAL. Nº 2 FUEL OIL
FUELS BLENDING BLDG.
HEATING BOILER
CHILLED WATER SYSTEM
HIGH PRESSURE WATER TANK AND PUMP
HIGH PRESSURE AIR SYSTEM
INSTRUMENT AIR SYSTEM
PROCESS WATER SYSTEM
UTILITY RM
STEAM BOILER
FLUID BED TRANSFER SYSTEM
PUMP
DUST COLLECTOR
CONTROL ROOM
SHOP
HI-BAY AREA
TEST PASSAGE C-5
AIR PREHEATERS
T.P. C-2
T.P. C-1
MUFFLER CHAMBER
FUEL/GAS ANALYSIS ROOM
PROCESS LABORATORY BLDG. - FIRST FLOOR
STORAGE
CENTRIFUGAL COMPRESSOR
AIR RECEIVER
SWITCHGEAR
THREE STAGE COMPRESSOR
1,000 GAL WASTE OIL TANK
COMPRESSOR BUILDING
N
MOTOR CONTROL ROOM
CONTROL PANEL
CONTROL ROOM
DRAFTING ROOM
OFFICES
SECOND FLOOR
3028

FIGURE 1. WESTINGHOUSE WALTZ MILL COMBUSTION/PROCESS LABORATORY

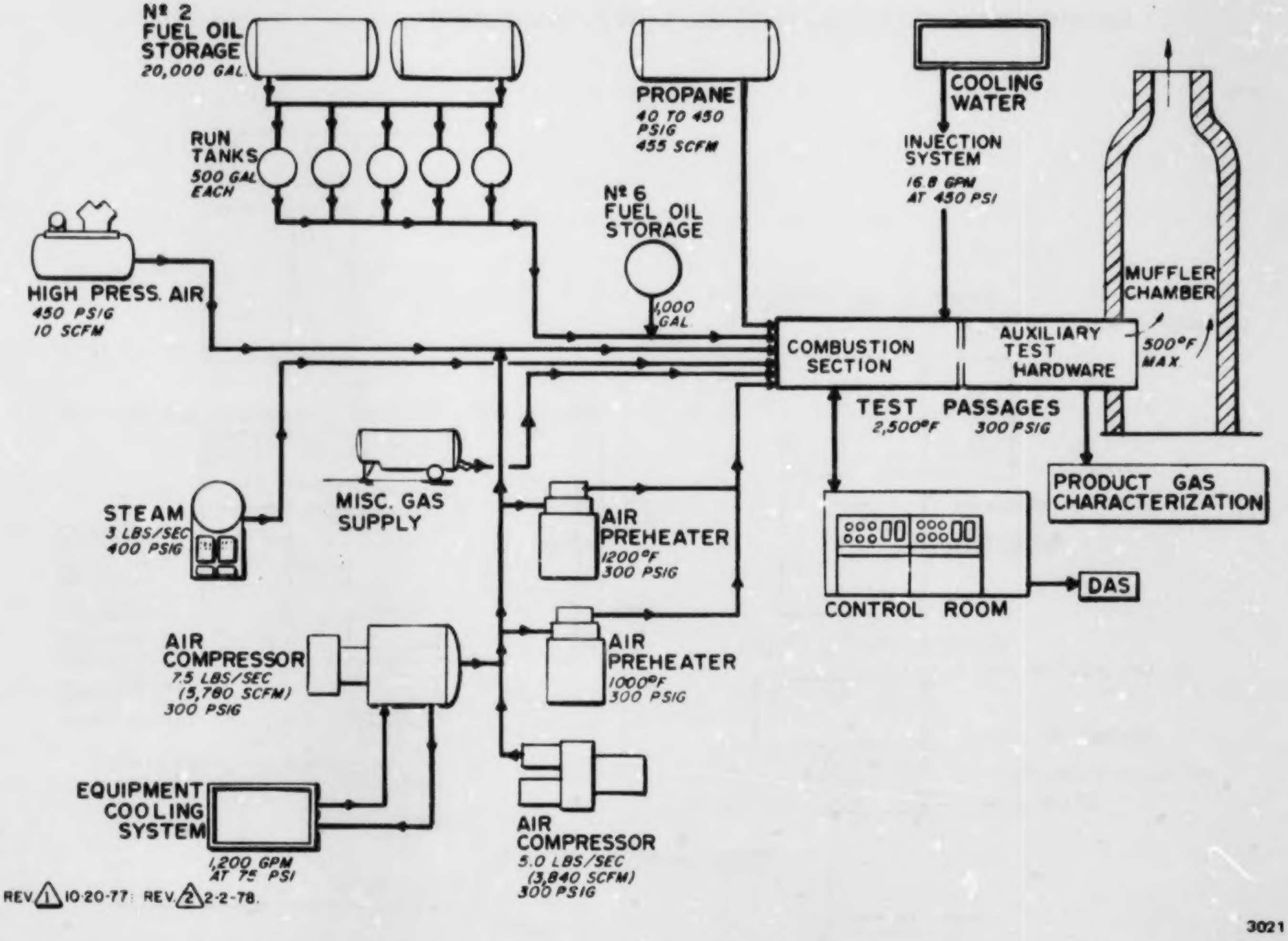
Nº 2 FUEL OIL STORAGE 20,000 GAL.
RUN TANKS 500 GAL EACH
PROPANE 40 TO 450 PSIG 455 SCFM
COOLING WATER
INJECTION SYSTEM 16.8 GPM AT 450 PSI
MUFFLER CHAMBER
500°F MAX
HIGH PRESS. AIR 450 PSIG 10 SCFM
Nº 6 FUEL OIL STORAGE
1,000 GAL
COMBUSTION SECTION
AUXILIARY TEST HARDWARE
TEST PASSAGES 2,500°F 300 PSIG
PRODUCT GAS CHARACTERIZATION
MISC. GAS SUPPLY
STEAM 3 LBS/SEC 400 PSIG
AIR PREHEATER 1200°F 300 PSIG
CONTROL ROOM
DAS
AIR COMPRESSOR 7.5 LBS/SEC (5,780 SCFM) 300 PSIG
AIR PREHEATER 1000°F 300 PSIG
EQUIPMENT COOLING SYSTEM 1,200 GPM AT 75 PSI
AIR COMPRESSOR 5.0 LBS/SEC (3,840 SCFM) 300 PSIG
REV. 1 10-20-77: REV. 2 2-2-78.
3021

FIGURE 2. OVERALL FLOW DIAGRAM FOR PROCESS LABORATORY

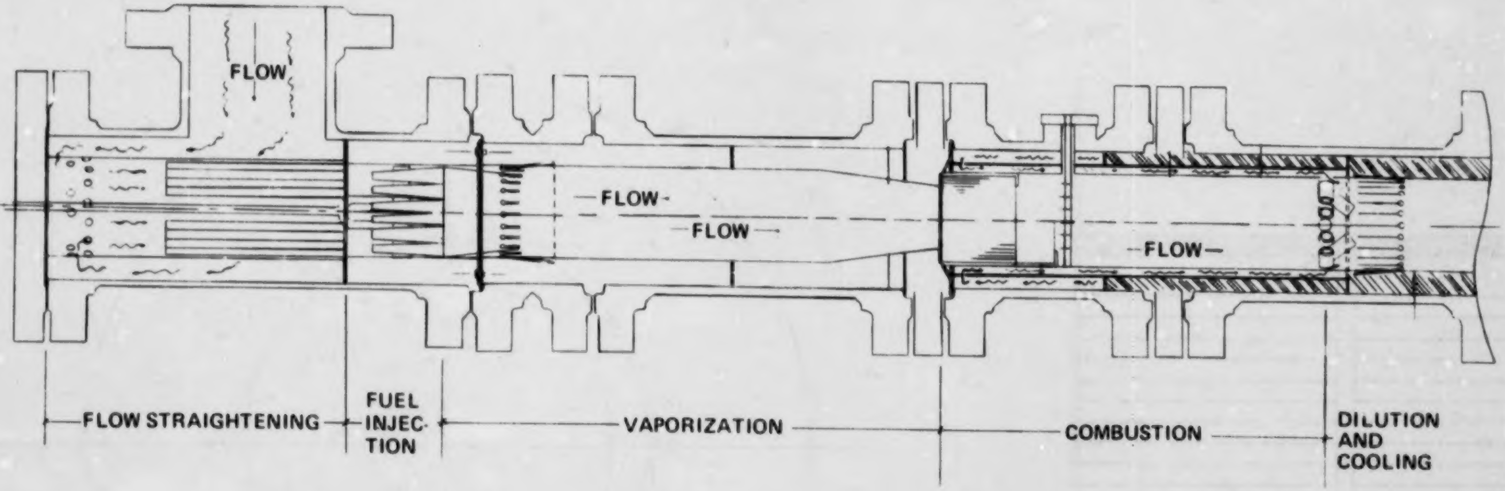
FLOW
FLOW
FLOW
FLOW
FLOW STRAIGHTENING
FUEL INJECTION
VAPORIZATION
COMBUSTION
DILUTION AND COOLING

FIGURE 3. CATALYTIC COMBUSTION TEST PASSAGE

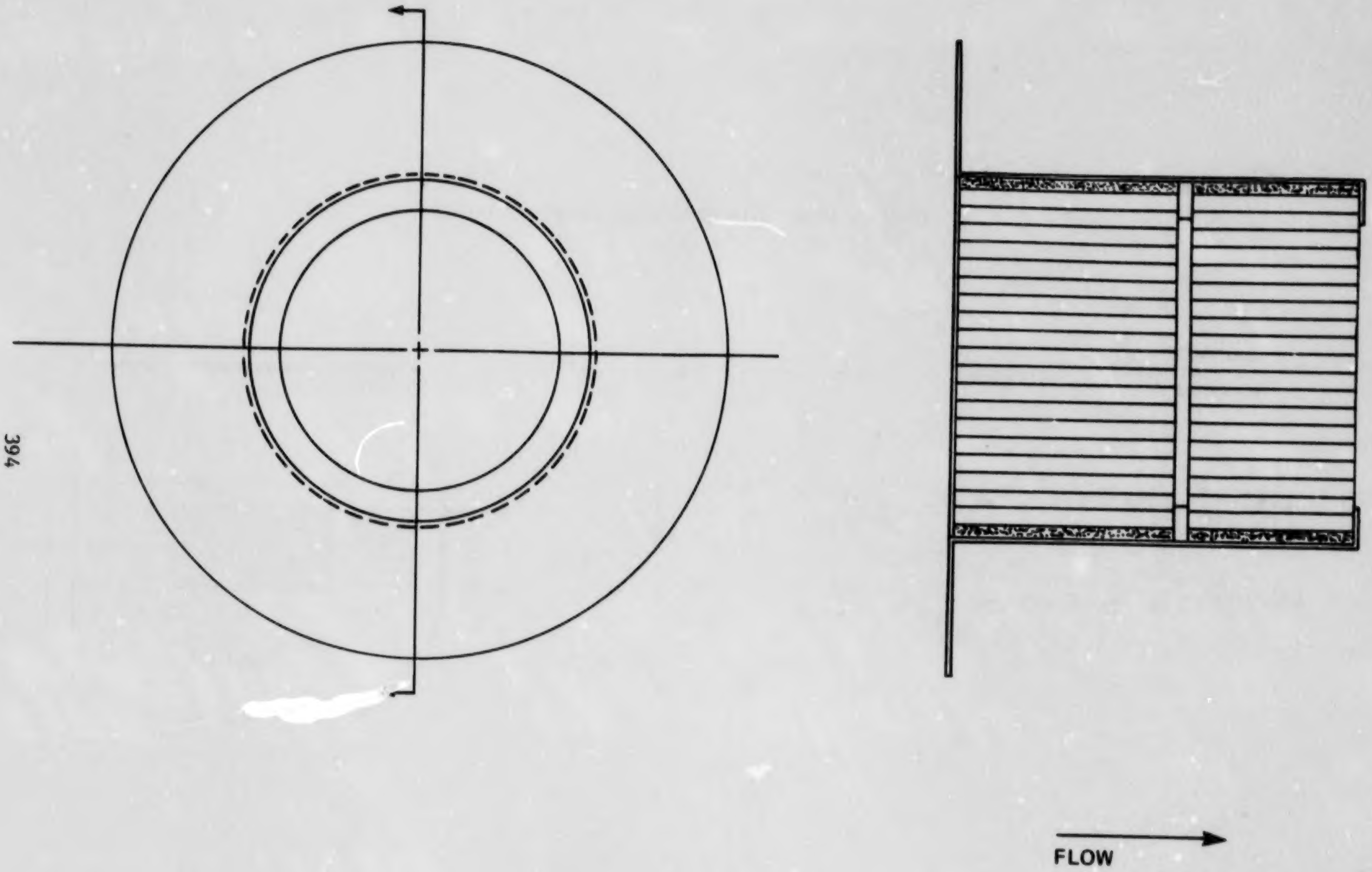

FIGURE 4. CATALYST IN HOLDER

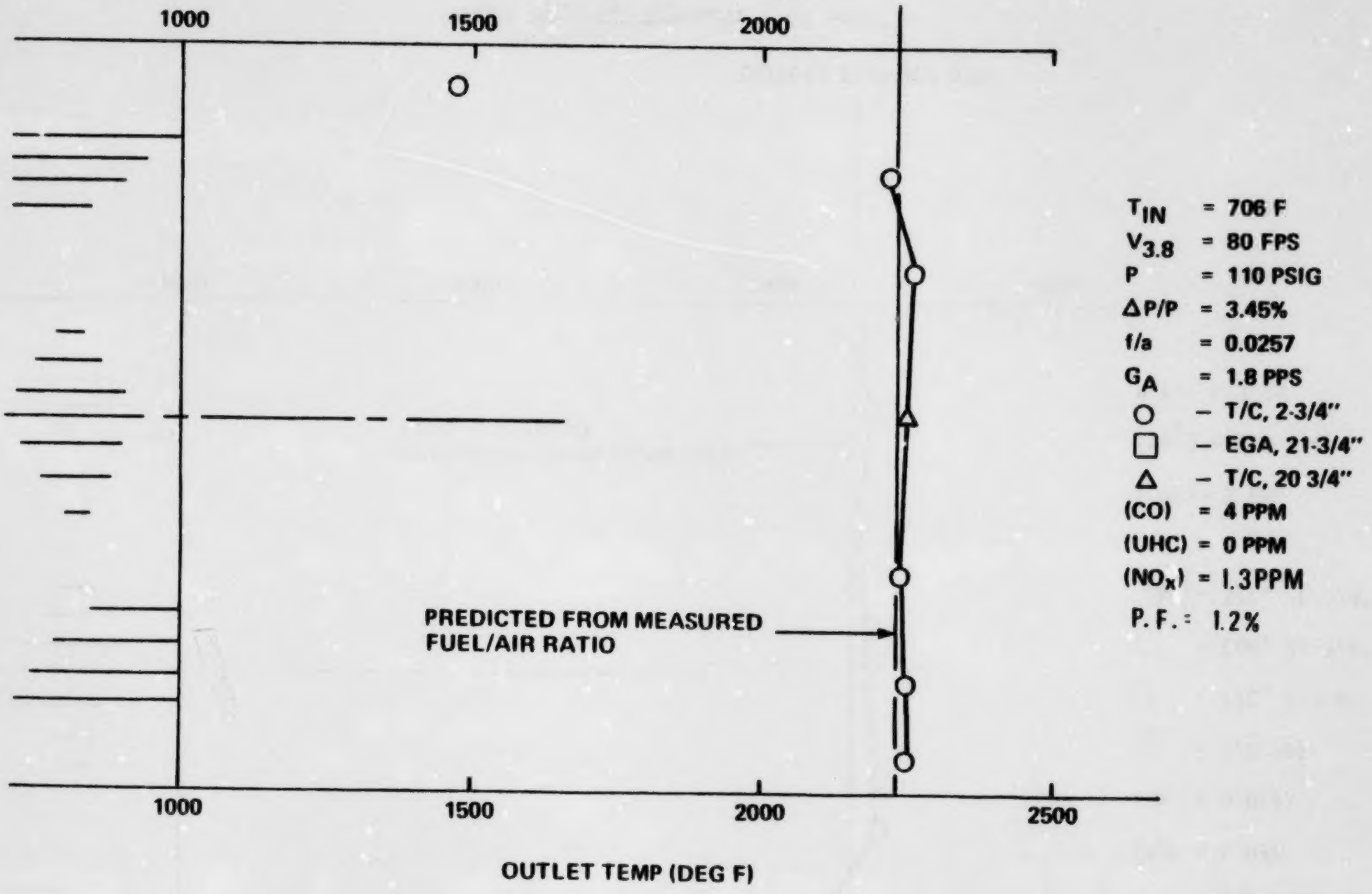

FIGURE 5. TEST RESULTS: 110 psig

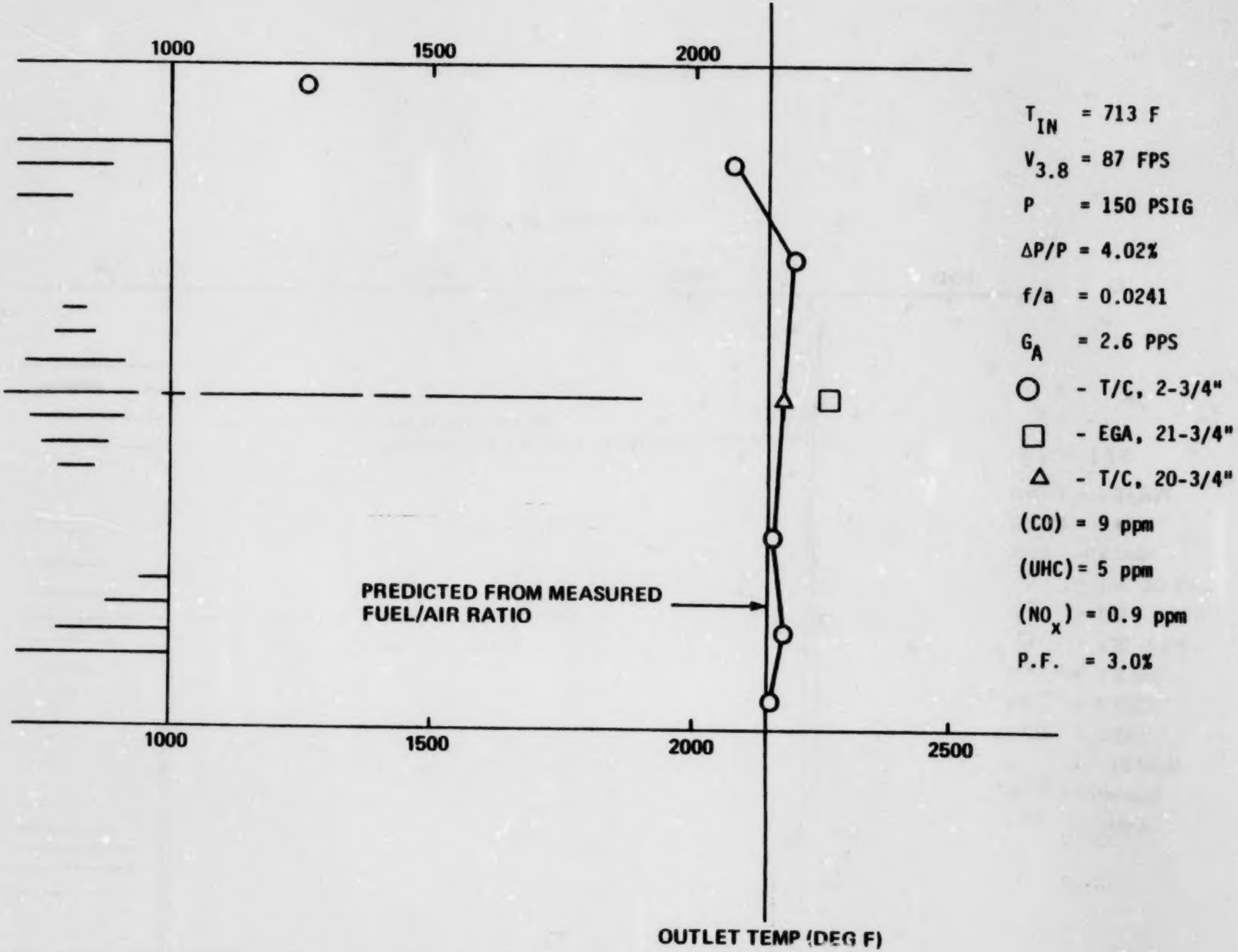

FIGURE 6. TEST RESULTS: 150 psig

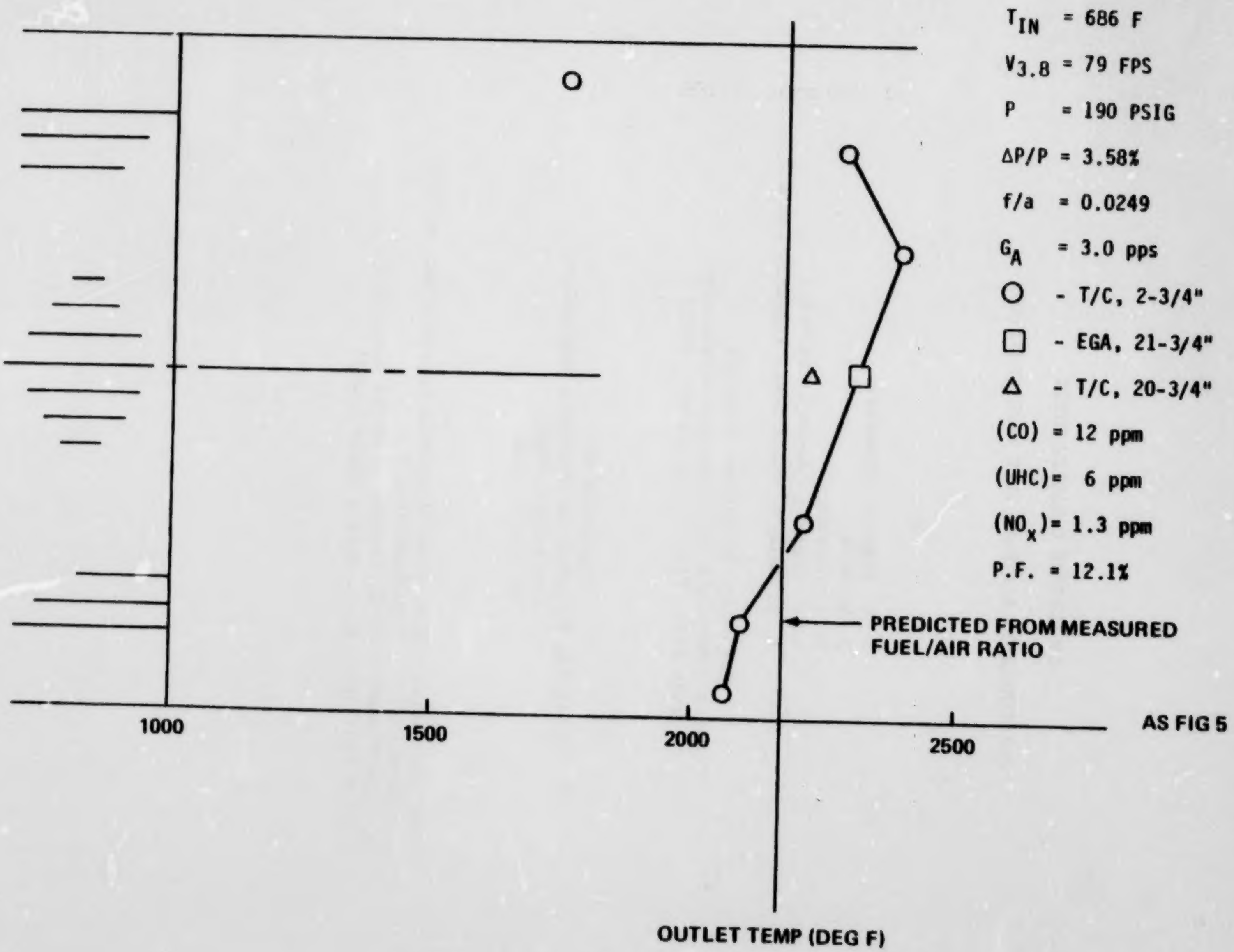

FIGURE 7. TEST RESULTS: 190 psig

COMBUSTION CATALYST STUDY
FOR SIMULATED AIRCRAFT IDLE MODE OPERATION

By:

I. T. Osgerby (Speaker)
R. M. Heck
R. V. Carrubba
C. C. Gleason (General Electric)
E. J. Mularz (NASA-Lewis Research Center)

Engelhard Industries Division
Engelhard Minerals and Chemicals Corporation
Menlo Park, Edison, New Jersey 08817

Presented at
Fourth EPA Workshop on Catalytic Combustion
Cincinnati, Ohio
May 14-15, 1980

Prime Contractor:	G.E. from NASA-Lewis Contract NAS 3-20580
Subcontractor:	Engelhard from G.E.
Contract Manager:	C. C. Gleason (General Electric)
Program Monitor:	E. J. Mularz (NASA-Lewis)

ABSTRACT

One of the advanced combustor design concepts under investigation involves the use of a catalytic reactor downstream of a conventional gas turbine combustor to reduce CO and unburned hydrocarbon emissions at engine idle conditions. Laboratory screening tests were conducted to evaluate the effect of catalyst cell geometry on clean-up performance for CO and propane fuels.

The gas feed to the catalyst configurations tested simulated combustion gases from a conventional combustor. Analysis of the screening test results provided performance and design criteria for assessing clean-up conversion and pressure losses over a wide range of operating conditions. A preferred catalyst configuration was selected from this study based on the design goals of:

Catalyst Pressure Loss $\frac{\Delta P}{P} < 3.\%$

Emissions Index CO $\leqslant$ 10 g/Kg fuel

UHC $\leqslant$ 1. g/Kg fuel

NO_x emissions for this design approach would be determined by the flame preburner, and were essentially zero in all laboratory simulation tests. (Preburner was simulated with a CATCOM* catalyst used to completely combust the Jet A fuel.)

Parametric studies were conducted to measure the benefits of a homogeneous reaction contribution at the higher catalyst operating temperatures typical of the intended application. These results showed that at operating temperatures of 960°C the CO emission requirements were attained, but the UHC emissions were borderline. At operating conditions above 960°C, it is anticipated that the emission requirement will be met.

---

* CATCOM is a trade name of Engelhard Minerals and Chemicals Corporation.

NOMENCLATURE

a	Geometric total surface to volume ratio
D_H	Hydraulic diameter
$D_{f\text{-}air}$	Diffusivity of species in air
η	Combustion efficiency
F^*	Apparent friction factor
L	Catalyst channel length
N_{Re_c}	Reynolds' number in catalyst channels
N_{S_h}	Sherwood number (dimensionless mass transfer parameter)
N_{S_c}	Schmidt number (dimensionless mass transfer parameter)
P	Pressure
Δ	Pressure drop
ρ	Density
σ	Percent open area of honeycomb support
T	Temperature
V	Catalyst face velocity
X	Mole fraction of seed fuel
χ	Conversion

I. INTRODUCTION

Exploratory investigations of the application of catalytically supported combustion to gas turbine combustor design (References 1, 2, 3) have previously confirmed the potential for achieving ultra-low emissions under controlled, high power conditions. These studies further identified engine idle conditions as a potential problem area, since low compressor discharge and operating temperatures lead to high hydrocarbon emissions.

One design concept proposed to achieve low emissions at engine idle is to employ a preburner and to utilize the catalyst in the "clean-up" mode to reduce preburner hydrocarbon emissions. Conceptually, at higher power the preburner operation is terminated, and the catalyst operated under catalytically supported combustion conditions, to maintain ultra-low emissions.

An experimental program was carried out to determine whether acceptable hydrocarbon and CO conversion levels could be achieved with a combustion catalyst operated as a catalytic converter at simulated aircraft idle mode conditions. Correlations obtained in this study were utilized to design a clean-up catalyst for testing in combustor sector hardware as reported separately (Reference 4).

The performance goals for the catalytic converter were as follows:

A. Clean-up capability to maintain combustor emissions less than 10 g/Kg fuel of CO and 1 g/Kg fuel UHC.

B. Converter pressure losses of $\leqslant$ 3%.

An additional constraint was imposed by the hardware design in that the space available for catalyst was restricted to a maximum length of 9.5 cm.

Combustor Design Concepts

One catalytic convertor design approach is illustrated in Figure 1A in which the catalyst is placed downstream of a conventional combustor with the total combustion mass flow passing through the catalyst for emission reduction. Preliminary calculations indicated that severe pressure losses would be incurred and low conversion levels obtained at the operation conditions listed in Table I (Mode A-1). Reducing the catalyst mass flow by bypassing combustor air round the catalyst, and mixing the bypass air with the catalyst exhaust products, reduces the pressure losses and increases anticipated catalytic conversion performance. Additional calculations indicated that using a configuration with 50 percent bypass air (Figure 1B) provides a broad range of combustor operation with pressure losses < 3%, while maintaining peak catalyst inlet temperatures under 1260°C. Catalytic convertor inlet conditions for 50 percent bypass air are listed in Table I under Mode A-2.

Combustor A-2 is assumed to be operated as a conventional gas turbine combustor primary zone with the balance of the combustor catalyst air introduced between the primary zone and catalyst to mix with and cool the primary zone products. It was assumed that at least 98% combustion efficiency is maintained in the primary zone. This corresponds to an emissions level at the catalyst inlet of approximately 600 Vppm to 1200 Vppm as carbon over the operational range of (overall) fuel/air ratios 0.008 to 0.0155. Catalytic conversion of 95% of the remaining hydrocarbons and 80% of the carbon monoxide would then yield the required emissions goals. Thus, the catalyst will be operated in a "clean-up" mode in which emissions conversion will be predominantly catalytic with any contribution due to homogeneous reaction dependent on the operating temperature.

The initial phase of the laboratory test program was designed to allow evaluation of purely catalytic performance of various CATCOM* catalysts (described in Table II and shown in Figure 2) by selecting test conditions which precluded homogeneous combustion. The basis for evaluating catalyst performance was the trade-off between catalyst conversion-length requirements and pressure loss-length restrictions. The catalyst configuration chosen for this test series were all essentially identical Engelhard proprietary preparations of palladium on zircon composite monolithic catalyst and differed only in cell density of the honeycomb support. These were 6, 14 and 39 holes per square cm (see Table II). Catalyzed honeycomb lengths were selected based on equal geometric surface area, with one additional length of catalyst tested to provide additional information for prediction of catalyst conversion. These screening test conditions (listed in Table III) were sufficiently comprehensive to allow comparative emissions performance and pressure drop criteria to be established and to allow a preferred catalyst-length configuration to be selected.

---

* CATCOM is a trade name of Engelhard Minerals and Chemicals Corporation.

An additional series of tests was carried out with the preferred catalyst configuration to determine the enhancement in emissions clean-up capability with simultaneous catalytic and homogeneous combustion contribution.

II. APPARATUS AND PROCEDURES

Configuration A-2 was simulated using a two-stage catalytic reactor as shown in Figure 3. This reactor is a 2.54 cm Inconel 601 pipe and contains the following sections:

A. A primary stage in which preheated air and Jet A fuel are combusted using a catalyst operated adiabatically under catalytically supported thermal combustion conditions to provide hot, vitiated air with negligible emissions.

B. A mixing section (2.54 cm diameter, 2.54 cm long) in which additional preheated air is added to obtain a desired total mass flow and mixture temperature. Seed fuels CO and C_3H_6, premixed with this additional (secondary) air, are added to simulate incomplete combustion in the primary zone of the combustor.

C. A secondary stage containing the test catalysts for which emissions clean-up capability is to be determined.

The primary flows to the reactor were metered using a calibrated rotameter for the air and a calibrated Crane double-acting piston pump for the fuel. The primary and secondary air were separately preheated using two electric furnaces. The secondary flows (air, CO and C_3H_6) were metered using calibrated rotameters. Mixing of all feed gases was accomplished by passing each feed through three stages of static mixers. The actual concentration of the seed gases (CO and C_3H_6) in the secondary feed was also monitored by passing samples through the carbon monoxide and hydrocarbon analyzers.

The catalysts (primary and secondary) were mounted in thin-walled Inconel 601 holders which were inserted into the vertical tubular reactor. The reactor was operated downflow.

Thermocouple arrays and pressure taps were located upstream of the primary catalyst, in the mixing section and downstream of the test (secondary) catalyst. Pressure tap installations conformed to ASME codes. A 0.64 cm diameter water-cooled sampling probe was mounted 10.1 cm downstream of the test catalyst. Probe placement was set at this distance to prevent severe cooling of the test catalyst.

The instrumentation system used for emissions measurement included a Beckman Model 402 heated oven flame ionization detector (F.I.D.) for measurement of unburned hydrocarbons (UHC), a Beckman Model 315 BL non-dispersive infrared analyzer for measurement of carbon monoxide (CO) and a Beckman Model 951 chemi-luminescence analyzer for measurement of nitrogen oxides (NO/NO_x).

Preliminary Checkout Tests

A. Pressure Losses

Pressure losses were measured via the static taps and manometers. Preliminary tests were carried out which confirmed that pressure drop measurements accurately reflected test catalyst performance and were not affected by the method of secondary feed addition.

B. Mixing Tests

Tests were also carried out which confirmed that the secondary air and seed fuel mixtures were well mixed with the hot, vitiated exhaust from the primary stage. In these tests a blank (uncatalyzed) honeycomb test piece was installed in the secondary catalyst holder to form the downstream boundary of the mixing region, and the unreacted species downstream of the blank were sampled. Test measurements were uniform and non-fluctuating.

C. Preburning Tests

Preliminary tests were carried out which defined operating mixture temperature limits below which no homogeneous combustion occurred in the mixing section or secondary (test) catalyst section. These tests were carried out with the honeycomb blank in the secondary catalyst holder. Up to 930°C, no homogeneous reaction was observed.

III. RESULTS AND DISCUSSION

The objective of this experimental program was to obtain pressure loss and emissions clean-up performance data on the alternative test catalysts configurations, and provide a basis for determining the preferred catalyst design. The selection of a preferred catalyst configuration involves determining the trade-off between having sufficient catalyst length for emission clean-up, and yet not exceeding the allowable pressure loss limits. Because of the very broad range of operating temperatures of the clean-up catalysts (700-1300°C), it was anticipated that catalytic reactions would predominate at the lower temperatures, while gas phase homogeneous reactions would be significant at the higher temperature. In order to uncouple these two effects and evaluate the catalytic clean-up performance of each configuration, a two part experimental program was devised.

A. A screening test program conducted with the four catalyst configurations over a sufficiently broad range of operating conditions to allow correlations to be developed to predict both catalytic clean-up performance and pressure losses as a function of catalyst length. The operating temperatures and seed gas concentrations for these runs were selected to minimize the contribution of homogeneous gas phase reactions.

B. A brief parametric study conducted with the preferred catalyst configuration, selected from the performance correlations derived from the screen test program, at higher operating temperatures (see Table V) to measure the effects (and benefits) of homogeneous gas phase reaction on emissions clean-up.

Screen test data are shown in Tables V through VIII.

Catalytic Clean-Up

Previously reported results (Reference 3) have indicated that at the operating temperature range of the screening test program (540-760°C), it is highly probable that the catalytic oxidation reaction rate is mass transfer controlled. Dimensionless mass transfer numbers were derived from the screen test data on CO and C_3H_6 conversion to test this hypotheses and derive design correlations.

Since the temperature rise across the catalyst configurations is negligible for these conditions, a simplistic mass transfer model was derived.

$$\text{Conversion } (X) = 1. - X_{f,out}/X_{f,in} \qquad (1)$$

$$= 1. - \exp\left[\frac{N_{Sh} D_{f-air} aL}{V\ D_H}\right] \qquad (2)$$

where X_f is the seed fuel concentration and subscripts in and out denote catalyst inlet and exit. All other terms are defined in the nomenclature section.

Physical properties are evaluated at the average temperature in the catalyst. Diffusivities of CO and C_3H_6 were estimated using standard formulas (Reference 5).

Calculated values of the dimensionless mass transfer and flow parameters can be used to develop a plot of

$$\mathrm{Log}\left[\frac{N_{Sh}}{N_{Sc}{}^{.56}}\right] \text{ vs. } \log\left[N_{Re}\frac{D_H}{L}\right]$$

where N_{Sc} is the dimensionless Schmidt number, and
N_{Re} is the dimensionless Reynold's number.

This correlating technique was developed by Votruba (Reference 6) for mass transfer in honeycomb catalysts. Data that is in the kinetically controlled regime will not be correlated by this technique because of the strong effect of operating temperature in the Arrhenius rate expression. Figure 4 shows the experimental results that gave a linear correlation on a log-log plot. Additional proof of mass transfer control is the excellent agreement on this plot for all four different catalyzed honeycombs.

Mass transfer control performance allows extrapolation to other configurations using the following mass transfer scaling criteria derived from Equation 2:

$$\frac{L_1}{L_2} = \frac{\ln (1 - X_1) V_1 (N_{Sh} D_{f-air})_2}{\ln (1 - X_2) V_2 (N_{Sh} D_{f-air})_1} \qquad (3)$$

Pressure Drop

Since the tests were essentially isothermal, the pressure losses (ΔP) at each test condition were reduced to dimensionless isothermal (apparent) friction factors following standard friction factor correlation procedures. The free stream face velocity is utilized to calculate the channel velocity from $V_{ch} \cdot (\sigma) = V$, and therefore

$$F^* = \frac{1}{2}\frac{\Delta P}{\rho V_{ch}^2}\frac{D_H}{L} = \left(\frac{\sigma^2}{2}\right)\left(\frac{\Delta P}{\rho V^2}\right)\frac{(D_H)}{L} \qquad (4)$$

where ρ is the density and σ is the percent open area of the test catalyst. The apparent friction factor includes entrance and exit flow momentum losses, as well as frictional losses, for both developing and fully developed flow, and hence is higher than the conventional pipe flow friction factor. The data for the four catalysts are plotted in Figure 5, with the pipe flow equation provided for reference.

Note that the friction factor for the 6 holes/cm^2 catalyst C is far in excess of the reference value. The explanation for this anamolous value has not been resolved.

Catalyst Comparison

The pressure drop and mass transfer correlations provided as Figures 4 and 5 were utilized to estimate the performance of the catalyst configurations at the idle mode design condition of

$T = 890°C$

$P = 300$ kPa

$V = 35$ m/sec

The additional constraint of a maximum length of 9.5 cm narrowed the choice to the selection of the channel size that most closely achieved the pressure drop and conversion requirements.

The result of this analysis is shown as Figure 6, where for 9.5 cm of each catalyst, the pressure drop and mass transfer conversion are calculated. These curves indicate that at 35. m/sec catalyst A (the 39 hole/cm^2 monolith) will yield

CO = 80% conversion

UHC = 72% conversion

%ΔP/P = 3.4% conversion

Thus, at this or lower flow velocities, the catalyst only slightly exceeds pressure drop constraints. CO emissions goals can be met, but UHC objectives cannot be attained by mass transfer reaction alone. Since the design temperature is close to a level where thermal reactions become significant, gas phase reactions are anticipated to increase hydrocarbon conversion to the design objective.

Lower cell density catalysts were well within the pressure drop constraint but did not approach the mass transfer conversion goals for the program. Based on these results, the 39 hole/cm^2 catalyst cell density was selected.

Design Point Tests

A series of runs was carried out with the selected catalyst design at conditions simulating the idle mode design point. Note that the operating pressure was reduced from 300 kPa to 200 kPa due to rig limitations. Test results are given in Table IX. Conversion performance with two seed fuel concentration levels, 600 Vppm and 1200 Vppm carbon, were measured at each test condition.

CO The data indicate that the CO performance goal was achieved at 910°C and higher. Comparison with calculations indicates little or no gas phase reaction contribution.

C_3H_6 The performance goal of 95% conversion was approached at a temperature of 910°C. Comparison with calculations shows that homogeneous reaction provided a significant contribution to the conversion at 910°C. Some conversion to CO was observed, attributable to the gas phase reactions.

% Pressure Drop

Measured values were slightly above predicted values, due perhaps to the lower operating pressure in the laboratory runs.

Further runs made in the test series evidenced a falling off in catalyst activity. Subsequent examination indicates that some catalyst damage had incurred, attributed to an overtemperature of the primary stage catalyst during fuel/air ratio adjustment. Inspection of Table IX indicates the malfunction occurred during run 5. The conclusions listed are primarily drawn based on the screen test results and the first four runs.

IV. CONCLUSIONS

Laboratory tests were carried out in simulation of the use of a catalyst reactor for jet engine emissions clean-up at idle mode conditions. This design concept implies the use of a flame preburner, with 50% air bypass around the catalyst. The test series was carried out with three different honeycomb supports having 6, 14 and 39 holes per square cm and an identical catalyst preparation. The tests were performed to develop design criteria for use of a combustion catalyst in the "clean-up" mode. The following summarizes the test results:

- The preferred catalyzed honeycomb configuration is 39 holes per cm^2 in the configuration 5.08 cm + .64 cm space + 3.8 cm of Engelhard DXD-222, to be installed downstream of a 98% efficient preburner.

- CO emissions were below the emission index design goal of 10 g/Kg fuel at temperatures above 910°C in parametric tests with the preferred catalyst.

- C_3H_6 emissions approached the emissions index design goal of 1 g/Kg fuel at a temperature of 910°C in parametric tests with the preferred catalyst configuration.

- Estimated pressure losses are 3% at 30.5 m/sec at the design point pressure of 3 atmospheres and 890°C temperature: design goal was 35 m/sec.

- Homogeneous reaction contribution is necessary to meet C_3H_6 emissions goal.

- Yield of CO from homogeneous combustion of C_3H_6 was significant and may affect emissions performance if C_3H_6 is truly representative of UHC clean-up.

V. ACKNOWLEDGEMENT

This program was performed at Engelhard Industries R&D under NASA Contract NAS3-20580 and subcontract to the General Electric Aircraft Engine Group.

VI. REFERENCES

1. Pfefferle, W. C., et al. "CATATHERMAL Combustion: A New Process for Low-Emissions Fuel Conversion", ASME Paper Number 75-WA/FU-1, Nov. 1975.

2. Anderson, D. N., Tacina, R. R. and Mroz, T. S., "Performance of a Catalytic Reactor at Simulated Gas Turbine Operating Conditions", NASA-Lewis Research Center Technical Memorandum NASA TMX-71747 (June 1975).

3. Blazowski, W. S. and Walsh, D. E., "Catalytic Combustion: An Important Consideration for Future Applications", Combustion Science and Technology, 10, pp. 233-244 (1975).

4. Mularz, E. J., Gleason, C. C. and Dodds, W. J., "Combustor Concepts for Aircraft Gas Turbine Low-Power Emissions Reduction", Fourteenth Propulsion Conference co-sponsored by the American Institute of Aeronautics and Astronautics and the Society of Automotive Engineers, NASA TM-78875, July 1978.

5. Bird, R. B., Stewart, W. E. and Lightfoot, E. N., "Transport Phenomena", John Wiley & Sons, Inc., 1960.

6. Votruba, J., "Heat and Mass Transfer in Honeycomb Catalysts - II", Chem. Eng. Sci., 30, 1974.

7. Hawthorn, R. D., "Afterburner Catalysts - Effects of Heat and Mass Transfer Between Gas and Catalyst Surface". A.I. Chem. E. Dallas Meeting, February 1973.

TABLE I. CLEANUP CATALYST OPERATING CONDITIONS FOR TWO OPERATING MODES

Operating Mode	Operating Range P (kPa)	 V (m/s)	 T (^oC)	Fuel Concentration(1) CO Vppm	 UHC Vppm C
Full Flow Combustor (A-1)	200-400	46-122	430-820	Up to 2000	Up to 1000
50% Bypass Combustor (A-2)	200-400	18-61	700-1290	Up to 1200	Up to 1200

(1) Assumes conventional combustor operating at 98% efficiency upstream of catalytic converter

TABLE II. CATALYST DESCRIPTION

CODE NO.	CELL DENSITY HOLES/cm^2	CELL SHAPE	LENGTH CM	HYDRAULIC DIAMETER CM	PER CENT OPEN AREA
A. DXD-222	39	SINE WAVE	7.62	.0975	.655
B. DXD-221	14	TRAPEZOID	11.43	.1722	.542
C. DXD-225	6	SINE WAVE	15.24	.2997	.733
D. DXD-221	14	TRAPEZOID	15.24	.1722	.542

SUPPORT: ZIRCON COMPOSITE

CATALYST: PALLADIUM ON STABILIZED ALUMINA

TABLE III. SCREENING TESTS FOR SELECTION OF PREFERRED CATALYST CORE: CLEAN-UP MODE

BASIS:
Low pressure drop
High conversion of first stage emissions

TEST CONDITIONS:
Pressure: 200 kPa
Temperature: 540, 760°C
Velocity: 24, 30, 49, 60 m/sec
Fuels added: 200/400 Vppm CO
200/400 Vppm C_3H_6

TABLE IV. PARAMETRIC TESTS

RUN #	PRESSURE kPa	TEMPERATURE °C	VELOCITY m/sec.	SEED 1 Vppm CO	SEED @ Vppm C_3H_6
1	200	980	36.6	600 & 1200	200 & 400
2	"	870	"	"	"
3	"	760	"	"	"

TABLE V. SCREENING TEST RESULTS: CATALYST A

	Conditions			Results		
Run	P atm	T °F	U ft./sec	$\frac{\%\Delta P}{P}$	x_{CO}	x_{UHC}
1	2.	617	53.	1.2	-	-
2	"	1427	89.	2.52	$.75^{(1)}$	$.79^{(1)}$
3	"	"	"	"	$.77^{(2)}$	$.77^{(2)}$
4	"	581	92.	3.1	-	-
5	"	1080	126.	4.24	.19	.56
6	"	"	"	"	.21	.56
7	"	612.	62.	1.61	-	-
8	"	1436.	98.	3.33	.59	-
9	"	"	"	"	.65	-
10	"	581	99	3.67	-	-
11	"	1076	139	5.55	.17	.46
12	"	"	"	"	.22	.51
13	"	619	57.	1.46	-	-
14	"	1414	93.	2.87	.67	.75
15	"	"	"	"	.71	.73

(1) Fuel feed concentration 200 Vppm C

(2) Fuel feed concentration 400 Vppm C

TABLE VI. SCREENING TEST RESULTS: CATALYST B

	Conditions			Results		
Run #	P atm	T °F	U ft./sec	$\frac{\% \Delta P}{P}$	x_{CO}	x_{UHC}
1	2.	635	48.	.95	-	-
2	"	1418	82.	1.82	.66 (1)	.68 (1)
3	"	"	"	"	.72 (2)	.74 (2)
4	"	572	81.	2.28	-	-
5	"	1022	114	3.6	.28	.55
6	"	"	"	"	.31	.53
7	"	637	54.	1.11	-	-
8	"	1436.	93.	2.21	.71	.75
9	"	"	"	"	.75	.77
10	"	572	74	1.92	-	-
11	"	1126.	113.	3.48	.33	.52
12	"	"	"	"	.4	.53

(1) Fuel feed concentration 200 Vppm C

(2) Fuel feed concentration 400 Vppm C

TABLE VII. SCREENING TEST RESULTS: CATALYST C

Run #	Conditions			Results		
	P atm	T °F	U ft./sec	%ΔP/P	x_{CO}	x_{UHC}
1	2.	617.	50	.98	-	-
2	"	1400	85.	2.06	.65 (1)	.67 (1)
3	"	"	"	"	.68 (2)	.66 (2)
4	"	581.	85	2.46	-	-
5	"	1031	119.	3.75	.21	.51
6	"	"	"	"	.24	.51
7	"	635	56.	1.15	-	-
8	"	1418	96.	2.28	.72	.78
9	"	"	"	"	.73	.76
10	"	599	79.	2.06	-	-
11	"	1162	119.	3.5	.43	.48
12	"	"	"	"	.43	.48

(1) Fuel feed concentration 200 Vppm C
(2) Fuel feed concentration 400 Vppm C

TABLE VIII. SCREENING TEST RESULTS: CATALYST D

Run #	Conditions P atm	 T °F	 U ft./sec	Results $\frac{\%\Delta P}{P}$	 x_{CO}	 x_{UHC}
1	2.	626	47	1.16	-	-
2	"	1391	81	2.33	.64 (1)	.69 (1)
3	"	"	"	"	.7 (2)	.69 (2)
4	"	599	84	-	-	-
5	"	1112	120.	4.03	.12	.56
6	"	"	"	"	.21	.54
7	"	626	53.	1.39	-	-
8	"	1396.	89.	2.89	.66	.74
9	"	"	"	"	.74	.73
10	"	617.	76.	2.45	-	-
11	"	1238.	117.	4.31	.36	.5
12	"	"	"	"	.44	.55

(1) Fuel feed concentration 200 Vppm C
(2) Fuel feed concentration 400 Vppm C

TABLE IX. PARAMETRIC TEST RESULTS: 3.5 INCHES OF DXB-222

	Conditions				Results	
Run #	P atm	T °F	U ft./sec.	% $\frac{\Delta P}{P}$	X_{CO}	X_{UHC}
1	2.	1670	112.	4.66	.85(1)	-
2	"	"	"	"	.89(2)	-
3	"	1760	118	3.76	.77	.88(1)
4	"	"	"	"	.88	.95(2)
5	"	1598	120	3.19	.45	.64
6	"	"	"	"	.58	.74
7	"	1463	125	3.13	.31	.48
8	"	"	"	"	.44	.54
9†	"	1603	124	4.56	.47	-
10	"	"	"	"	"	-
11	"	1612	95	2.93	.41	.46
12	"	"	"	"	.49	.56
13	"	1769	89.	2.66	.54	.74
14‡	"	"	"	"	.65	"

† Catalyst repacked due to low % ΔP/P on tests 5 and 7.
‡ Post-test inspection showed catalyst inlet damaged.

(1) Fuel feed concentration 600 Vppm C
(2) " " " 1200 Vppm C

ALTERNATIVE OPERATING MODES

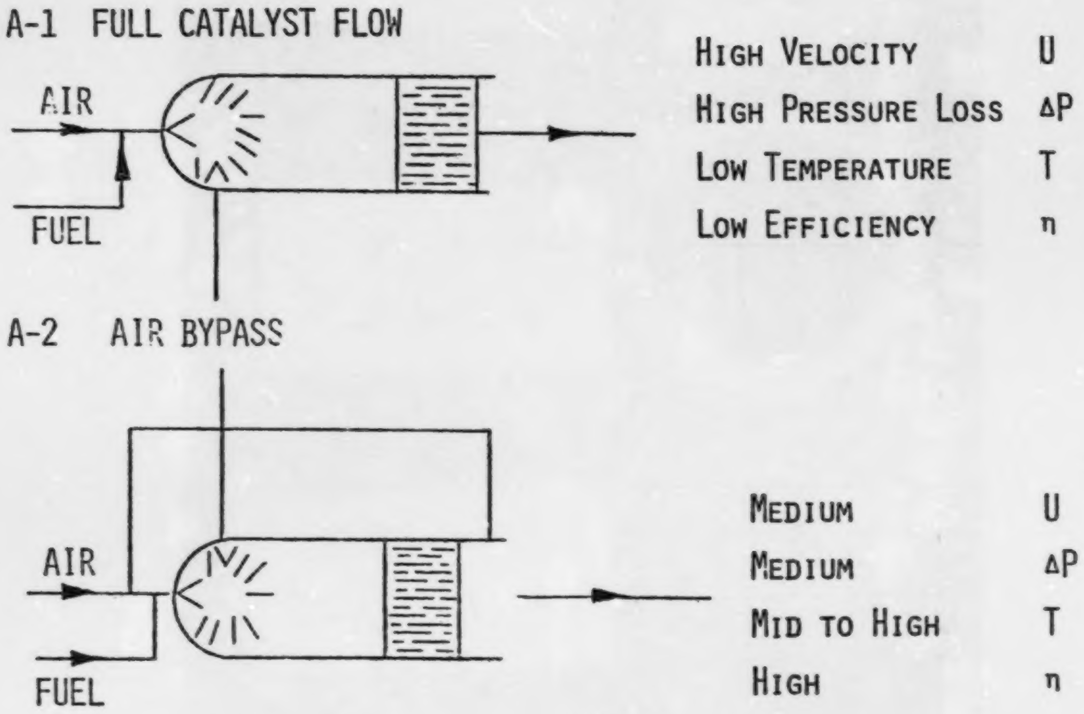
A-1 FULL CATALYST FLOW
AIR
FUEL
HIGH VELOCITY U
HIGH PRESSURE LOSS ΔP
LOW TEMPERATURE T
LOW EFFICIENCY η
A-2 AIR BYPASS
AIR
FUEL
MEDIUM U
MEDIUM ΔP
MID TO HIGH T
HIGH η

Figure 1. Idle Mode Combustor Configurations

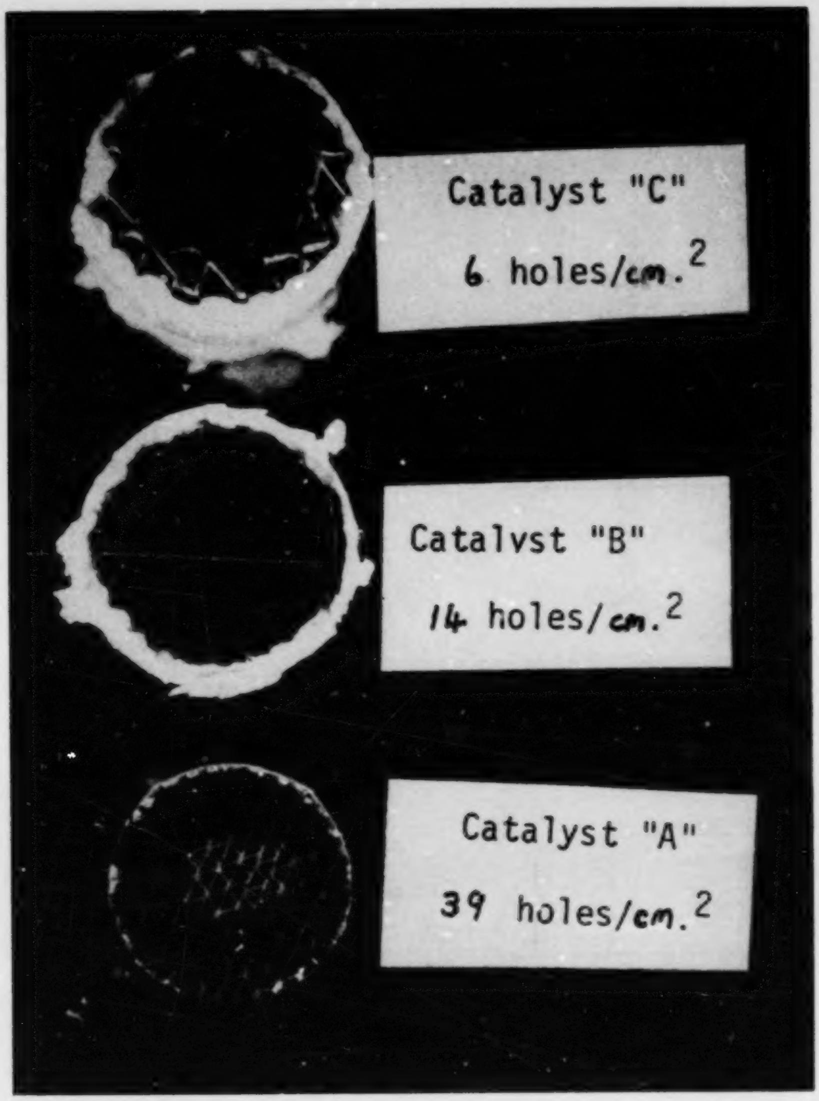
Catalyst "C"
6 holes/cm.^{2}
Catalyst "B"
14 holes/cm.^{2}
Catalyst "A"
39 holes/cm.^{2}

Figure 2. Catalyzed Honeycomb Types Tested

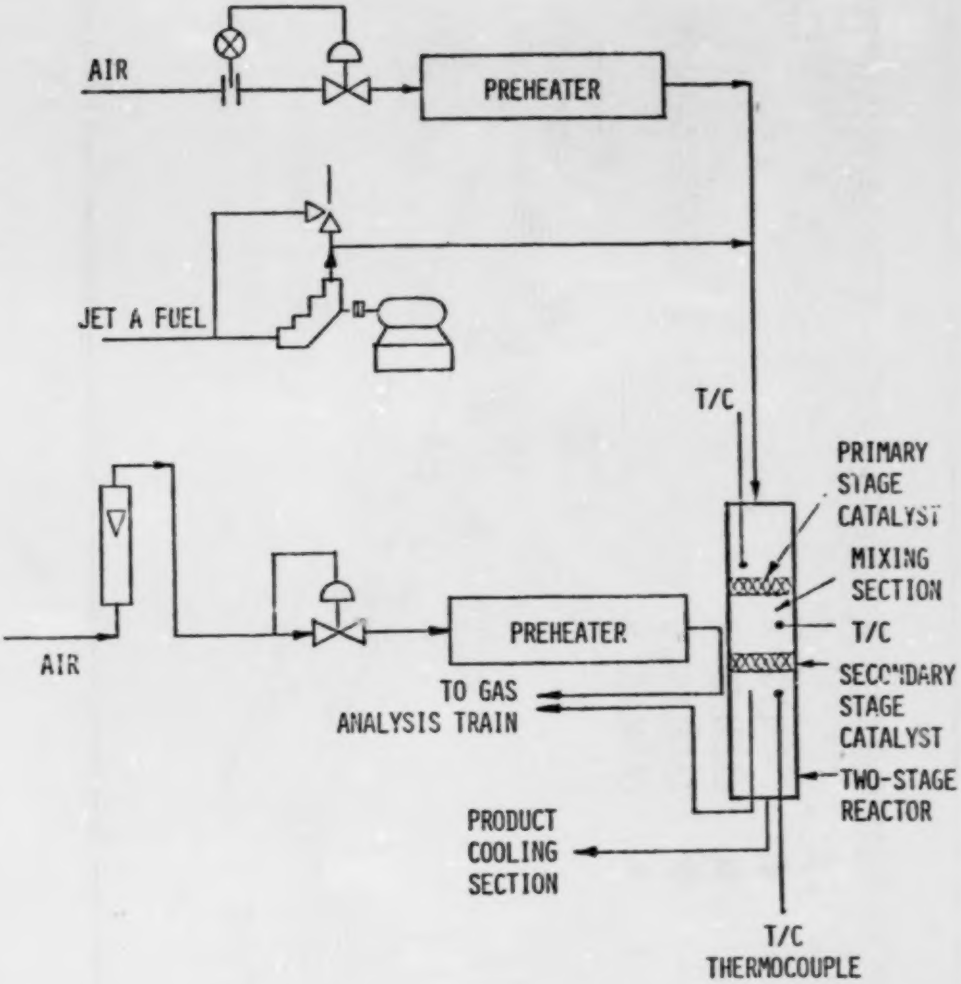
AIR
PREHEATER
JET A FUEL
T/C
PRIMARY STAGE CATALYST
MIXING SECTION
T/C
SECONDARY STAGE CATALYST
TWO-STAGE REACTOR
AIR
PREHEATER
TO GAS ANALYSIS TRAIN
PRODUCT COOLING SECTION
T/C THERMOCOUPLE

Figure 3. High Temperature Two-Stage Reactor

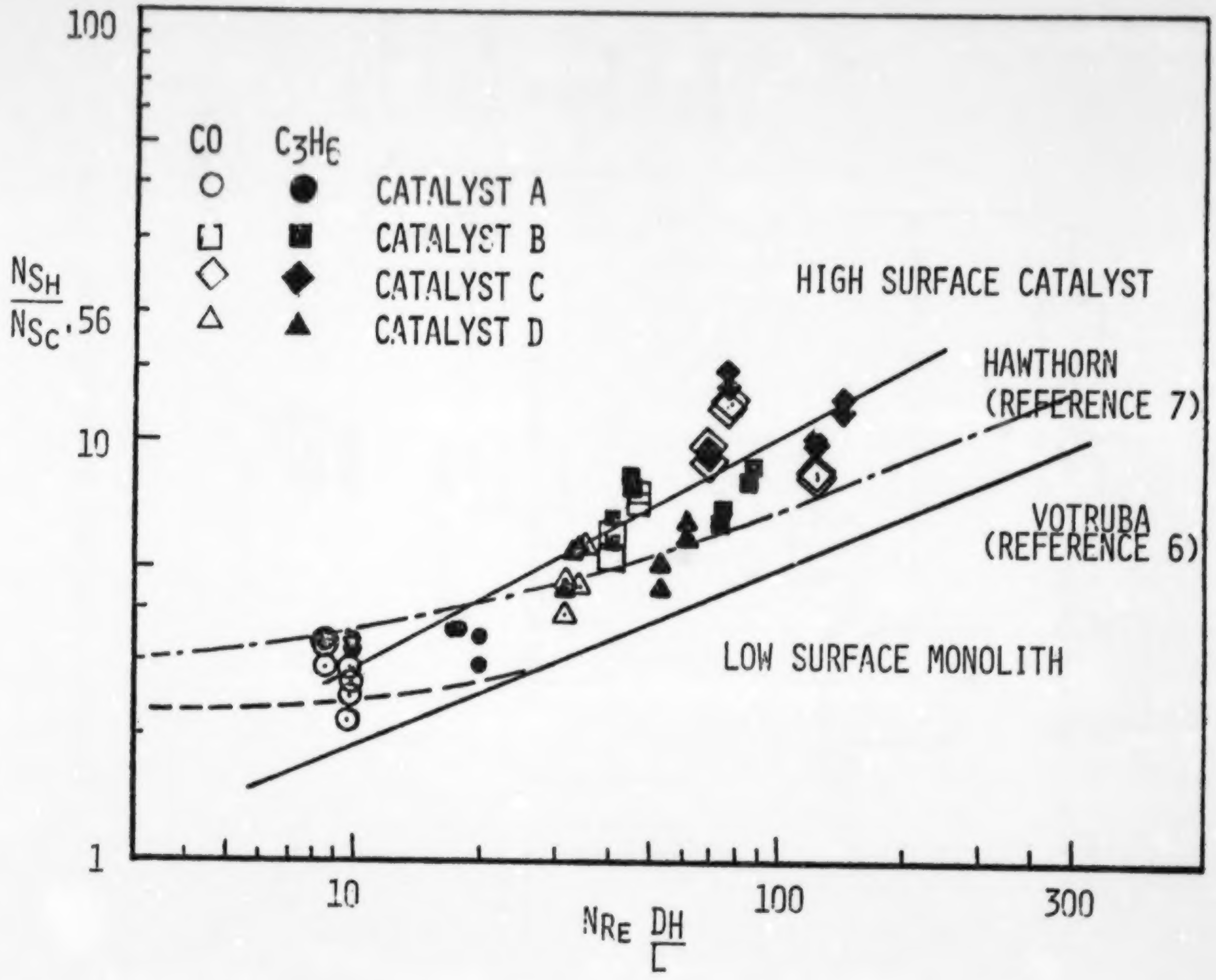

Figure 4. Mass Transfer Conversion vs. Reduced Reynolds' Number

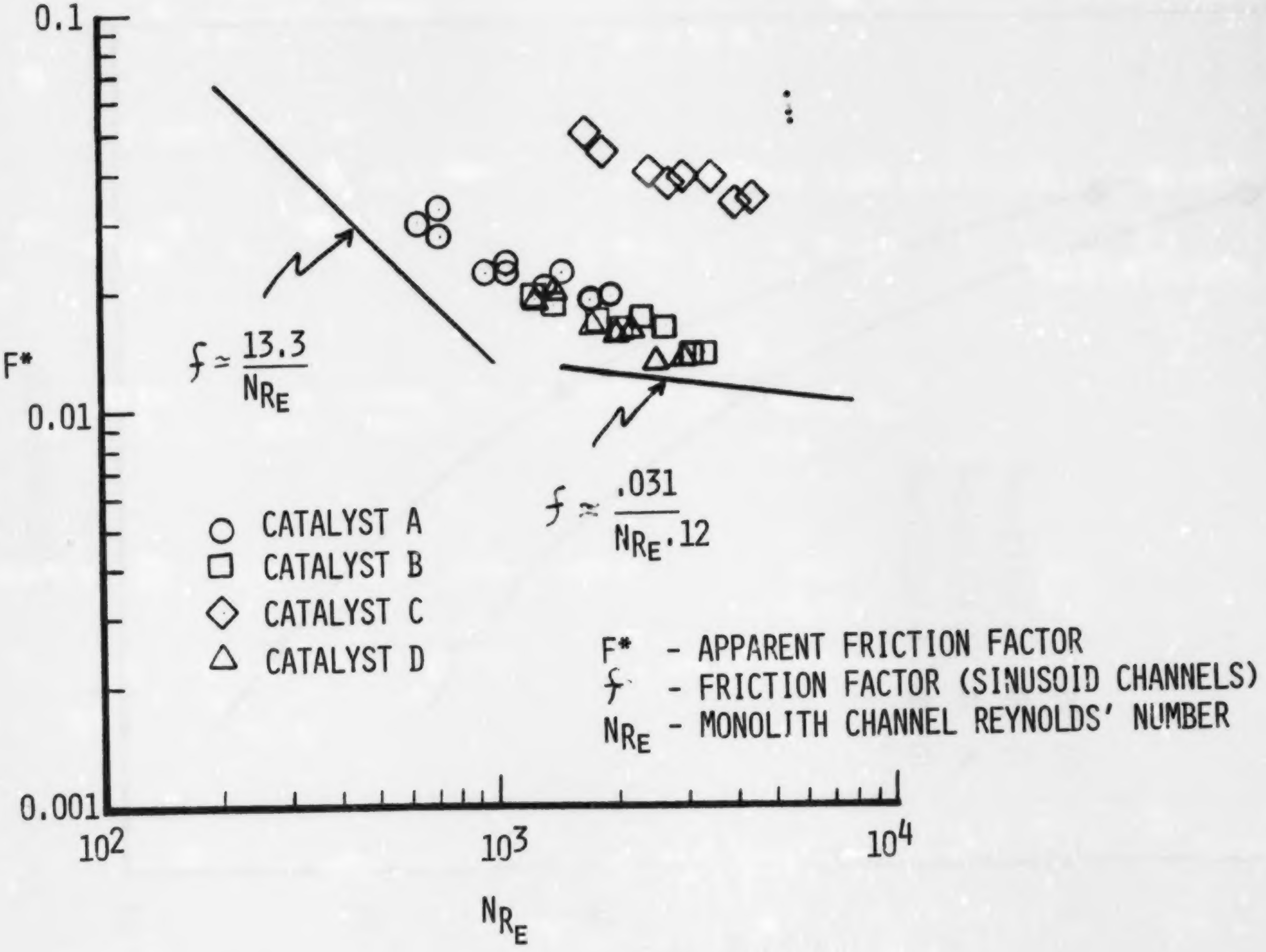

Figure 5. Friction Factor Correlation

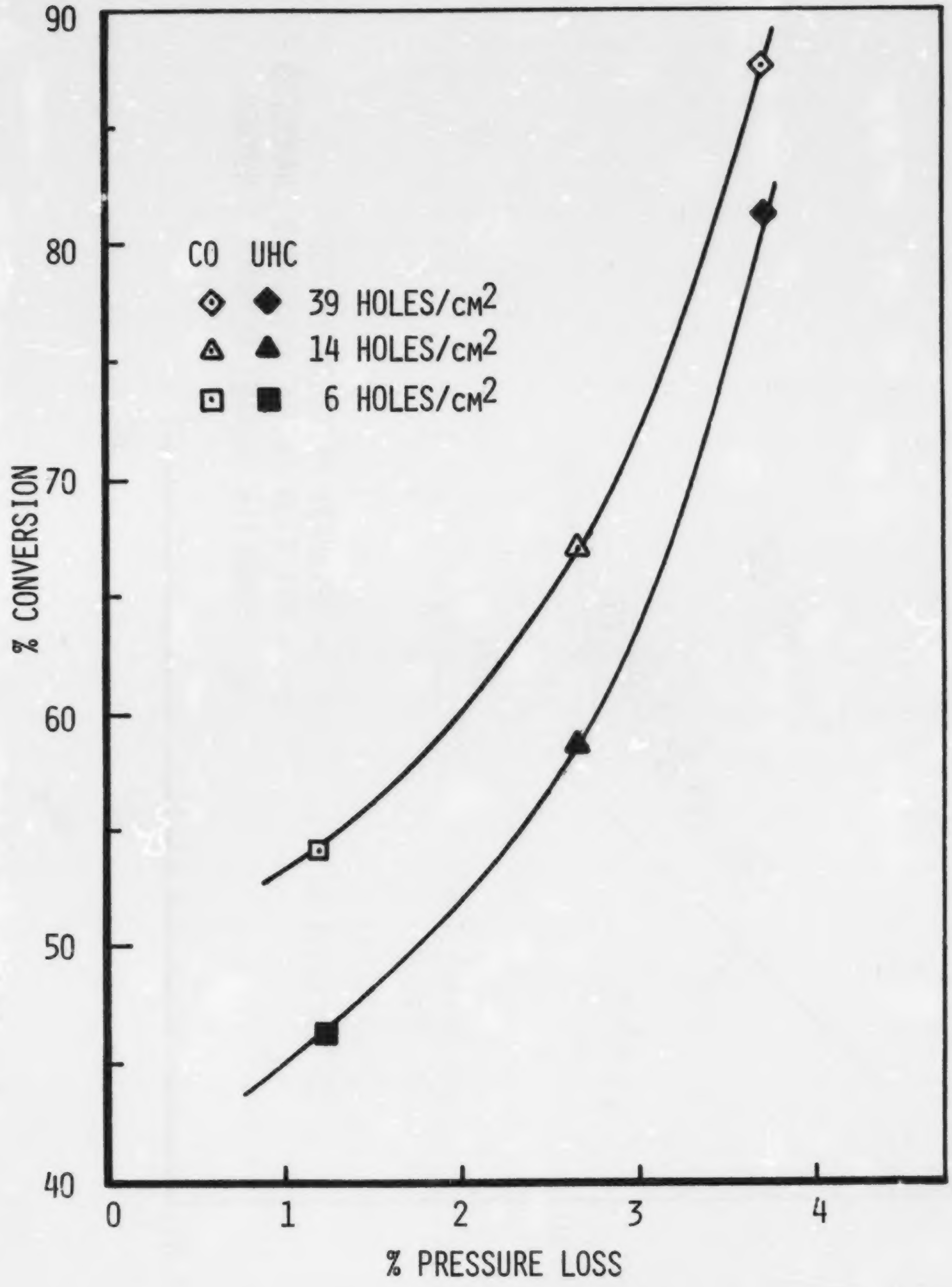

Figure 6. Pressure Drop vs. Mass Transfer Conversion

EXPERIMENTAL EVALUATION OF CATALYTIC COMBUSTION WITH HEAT REMOVAL AT NEAR STOICHIOMETRIC CONDITIONS

By:

Daniel Bulzan
National Aeronautics and Space Administration
Lewis Research Center
Cleveland, Ohio 44135

ABSTRACT

Two concentric tube configurations were tested to evaluate catalytic combustion with heat removal at near stoichiometric conditions. Tests were conducted at one pressure, 1.5×10^5Pa, inlet fuel-air mixture temperatures from 780 to 960K, combustion air flowrates from .78 to 1.5g/sec, equivalence ratios up to .87, and a range of cooling air flowrates. Propane and Propylene fuels were used. Both configurations utilized air flowing through the center tube for cooling and combustion occuring in the annulus on the catalytic surface. One configuration had the catalyst applied to the outside diameter of the inner tube for a length of 56 cm. The outside diameters of the inside and outside tubes were 1.27 and 2.54 cm respectively. At an inlet mixture temperature of 960K, a combustion air flowrate of 1.5 g/sec, and a fuel flowrate of 6.0×10^{-2}g/sec, 34% of the heat available from the propylene fuel was transferred to the cooling air using a Pt catalytic tube. Conversion of the fuel was very low for this configuration. The second configuration had the catalyst applied to the inside diameter of the outer tube for a length of 56 cm. The outside

diameters of the inside and outside tubes were .95 and 1.59 cm respectively. At an inlet mixture temperature of 925K, a combustion airflow of 1.0 g/sec, and a fuel flowrate of 6.0 x 10^{-2}g/sec, 58% of the heat available from the propylene fuel was transferred to the cooling air with a Pt/Rh catalyst. At equivalence ratios as high as .87, NO_x emissions less than .2g NO_x/kg fuel were obtained. Combustion efficiencies greater than 99.5% were measured with this configuration for some operating conditions.

SESSION IV

ALTERNATE FUELS AND THE CATALYTIC COMBUSTOR

FUEL NITROGEN CONVERSION - THE IMPACT OF CATALYST TYPE

By:

B. A. Folsom, W. D. Clark, C. W. Courtney, M. P. Heap, W. R. Seeker
Energy & Environmental Research Corporation
8001 Irvine Blvd., Santa Ana, CA 92705

ABSTRACT

Data has been presented comparing the performance of two bench scale catalytic reactors burning simulated LBG doped with ammonia. The performance criterion of interest was the conversion, or retention of, NH_3 to other nitrogen compounds under both fuel-rich and fuel-lean conditions. The two reactors tested were an alumina-supported platinum catalyst and a zirconia-supported nickel oxide catalyst. The major difference in their performance was the concentration of total fixed nitrogen (TFN equals NH_3 + HCN + NO) measured in fuel-rich products as a function of percent theoretical air.

LIST OF FIGURES

Figure 1 Experimental Apparatus

Figure 2 Catalytic Reactor and Housing

Figure 3 Catalytic Reactor Test Apparatus

Figure 4 NH_3 Processing in LBG Platinum Catalytic Reactor

Figure 5 NH_3 Processing in LBG-Fired Nickel Oxide Catalytic Reactor

Figure 6 Unstaged Nickel Oxide Catalytic Reactor with 500 ppm NH_3

Figure 7 Staged Nickel Oxide Catalytic Reactor with 500 ppm NH_3

Figure 8 Summary: Nickel Oxide Catalytic Reactor with 500 ppm NH_3

Figure 9 Summary: Nickel Oxide Catalytic Reactor with 2400 ppm NH_3

LIST OF TABLES

Table I   Nickel Oxide Catalytic Reactor Constant Test Conditions

ACKNOWLEDGMENT

The investigations described in this paper were carried out under EPA contract 68-02-2196. The authors wish to express their appreciation to Mr. G. B. Martin, the EPA Project Officer, and to Dr. J. Kesselring of the Acurex Corporation for his help in obtaining the catalysts.

SECTION 1

INTRODUCTION

The integrated gasifier LBG - fired gas turbine - steam turbine cycle is one of several advanced coal based power cycles currently being developed. The primary advantage of this cycle is the potential for low emission of sulfur products without the economic and efficiency penalties associated with stack gas sulfur removal. Since the coal gasification process operates fuel-rich, the sulfur in the coal is converted mainly to hydrogen sulfide (H_2S) in the low Btu offgas which can be removed (potentially) more easily than sulfur dioxide (SO_2). During the gasification process, some of the nitrogen in the coal is converted into ammonia (NH_3) in the LBG. Under typical gas turbine combustor operating conditions a large fraction of the NH_3 may be converted to NO resulting in significant emission.

The concentration of NH_3 in the LBG depends upon gasifier design and operating parameters and may be as high as 0.38 percent (1). The gas cleanup system, which functions primarily to remove sulfur products and particulates from the LBG, may remove a portion of NH_3, but the remainder will enter the gas turbine combustor and may be oxidized to nitrogen oxides (NO_x). A concentration of 0.38 percent NH_3 in the LBG would produce approximately 1370 ng/J (3.2 lb $NO_2/10^6$ Btu) if all NH_3 is converted to NO_2. At present there are no New Source Performance Standards (NSPS) for LBG fired combined cycle power systems. However, it is reasonable to expect that when NSPS are promulgated they will be at least as stringent as current NSPS for other power systems such as gas turbines or gas fired steam generators. The current NSPS for gaseous fossil fuel-fired steam generators with greater than 73.3 MW (250×10^6 Btu/hr) heat input is 86 ng/J (0.2 lb $NO_2/10^6$ Btu) (2). For a combined cycle firing an LBG with 0.38 percent NH_3 to meet this emission level, the overall conversion of NH_3 to NO would have to be less than 6.3 percent.

This paper describes some of the work being carried out under EPA Contract 68-02-2196 to develop low NO emission combustor concepts for LBG containing ammonia. Comparative tests have been carried out with two catalysts to assess their suitability for the primary stage of a two stage combustor to minimize fuel nitrogen conversion.

SECTION 2

EXPERIMENTAL SYSTEMS

The experimental systems used in this investigation can be conveniently divided into the following subsystems:

- Reactant Metering and Supply
- Modular Reactors
- Analytical Train

A schematic of the total system is shown in Figure 1. Although several different reactor systems have been tested, only those involving catalyst beds will be described below.

REACTANT METERING AND SUPPLY

The LBG was synthesized by blending together high purity gases from cylinders. All gases were high purity grade (99.97 percent or better) with the exception of CO (99.0 percent). NH_3, NO and HCN were supplied as custom grade mixtures in nitrogen (± 2 percent accuracy) to facilitate metering. The oxidant was dry air. All gases were metered with sapphire jewel orifices operated in the critical flow (sonic) regime. The pressures upstream of the orifices were measured with high accuracy variable capacitance pressure transducers which were calibrated periodically against a laboratory reference. The pressures downstream of the orifices were maintained constant and the flow rate through each orifice was calibrated by filling an evacuated tank. The estimated total inaccuracy in each gas flow rate was 0.5 percent.

Variations in water vapor content of the LBG were achieved by metering distilled water with a calibrated rotameter and prevaporizing before mixing with the other reactant gases. The mixture was maintained well above the dewpoint temperature to prevent subsequent condensation. Other design details of the reactant flow system are discussed in Reference 3.

Catalytic Reactors

Two catalytic reactor systems were used during the investigation. The initial investigations were carried out with the system shown in Figure 2. Later work was carried out with the series staged configuration shown in Figure 4.

The premixed catalytically supported reactor is shown in Figure 2. The two catalysts used in these tests were an alumina-supported platinum and a zirconia-supported nickel oxide catalyst with some platinum on the upstream cells to promote light-off; both were supplied by the Acurex Corporation. The desirable features of the graded cell catalyst have been discussed previously (4). The maximum recommended temperature for this catalyst is 1588 K (2400 F). Type K thermocouples were cemented in two of the cells in the downstream segment to monitor maximum monolith temperature. To minimize heat losses and approximate adiabatic conditions, the catalyst was mounted in a refractory tube and electrically backheated. The reactants passed through a sintered stainless steel disc immediately upstream of the catalyst and combustion products were sampled with a stainless steel water cooled probe. Additional details of this reactor's construction and operation are documented in Reference 5.

The series staged configuration is shown in Figure 3; it is similar to the earlier reactor except that:

- the sintered stainless steel flashback arrestor was moved about two inches upstream,
- a reactant sample tap was installed to permit the NH_3 concentration in the reactants to be measured immediately upstream of the catalyst,
- a small bead ($\sim$0.007 in dia) type K thermocouple was installed immediately upstream of the catalyst to measure reactant preheat and sense flashback,
- a shorter (4.0 in.) refractory-lined tube was used to couple the reactor housing to the mixer,
- a secondary air injection system was added to allow burnout of the rich primary zone products.

Analytical Train

Both fuel-rich and lean products were analyzed for O_2, CO, CO_2, NO, NO_x, NH_3 and HCN. The sample train components were constructed entirely of stainless steel, glass and Teflon. Ammonia and HCN were trapped by bubbling known volumes of combustion products through three water baths in series. The absorbed NH_3 and HCN concentrations were then measured by ion specific electrodes. The other product species were monitored continuously. The sample was dried to a dewpoint of 273 K in a cyclone water trap located close to the sample probe to minimize residence time between probe and trap. Nitric oxide and NO_x were measured with a Thermo Electron Corporation Model 10A chemiluminescent analyzer. NO_x concentrations were measured after the sample had passed through a stainless steel converter operated at 1073 K. This converter could not be operated under oxygen-deficient conditions because of the well-known reduction of NO.

SECTION 3

RESULTS

Previous papers have described the results obtained with the alumina-supported platinum catalyst. Typical results illustrating the following qualitative behavior are presented in Figure 4.

- For fuel-lean conditions the majority of the NH_3 in the reactants was converted to NO.
- For fuel-rich conditions NO, NH_3 and HCN were measured in the combustion products in amounts depending on stoichiometry.
  - NO decreased as the stoichiometry was reduced (more fuel-rich)
  - NH_3 and HCN increased as the stoichiometry was reduced
- A distinct minimum in total bound nitrogen species ($\Sigma XN = NO + NH_3 + HCN$) occurred under fuel-rich conditions.
- For stoichiometries richer than that corresponding to the minimum, ΣXN increased sharply.

Typical results obtained with nickel oxide catalyst are shown in Figure 5. Under fuel-lean conditions the results were similar to those obtained with the platinum catalyst. However, under fuel-rich conditions the concentrations of NO, NH_3 and HCN were much lower than those measured with the platinum catalyst and there was no distinct minimum ΣXN. Under very fuel-rich conditions (44 percent T.A.), the ΣXN for the nickel oxide catalyst was 2.5 percent of the original NH_3 in the reactants, while ΣXN was essentially 100 percent for the platinum catalyst. Tests of the nickel oxide catalyst, over a range of adiabatic flame temperatures (1000-1400°C) and with CH_4 as the fuel yielded similar results.

The performance of the nickel oxide catalyst suggests that a simple staged combustor could be constructed to burn nitrogen containing fuels. However, because such a behavior had not been reported by others, further tests were carried out to verify the repeatability of the results with the nickel oxide catalyst. The series staged reactor was operated under the test conditions listed in Table 1. It was fired with 500 and 2400 ppm of NH_3 in the low Btu gas and operated with and without secondary air injection (staged and unstaged). During all of these tests the combustion products were sampled for O_2, CO and CO_2 to verify operating conditions, and for NO and NO_x or NO, NH_3 and HCN. For most tests the NH_3 concentration in the reactants was also measured.

The test results involving 500 ppm in the low Btu gas are presented in Figures 6, 7 and 8. The unstaged results in Figure 6 are similar to those previously obtained with this catalyst (Figure 4) except that the ΣXN levels under fuel-rich conditions are slightly higher (7 to 18 percent versus 3 to 6 percent). There also appears to be a slight minimum at about 80 percent theoretical air. The staged results are shown in Figure 7 and are consistent with essentially full conversion of the ΣXN in the rich combustion products to NO_x in the lean secondary combustion zone. Figure 8 compares the ΣXN measured in the reactants, and in the unstaged and staged products. The reactant ΣXN was all NH_3 and should have corresponded to 100 percent "conversion." The differences are attributable to inaccuracies in reactant preparation and/or NH_3 concentration measurements. In any case, correction of the results to account for the measured NH_3 concentration in the reactants would only slightly lower the total ΣXN (expressed as a fraction of the reactant NH_3 concentration).

Test results involving 2,400 ppm of NH_3 in the LBG are summarized in Figure 9 and are essentially similar to those obtained at lower ammonia concentrations.

SECTION 4

CONCLUDING REMARKS

Data has been presented comparing the performance of two bench scale catalytic reactors burning simulated LBG doped with ammonia. The performance criterion of interest was the conversion of NH_3 to NO or HCN or the retention of NH_3 under both fuel-rich and fuel-lean conditions. The two reactors tested were an alumina-supported platinum catalyst and a zirconia-supported nickel oxide catalyst. The major difference in their performance was the concentration of total fixed nitrogen (TFN equals NH_3 + HCN + NO) measured in fuel-rich products as a function of percent theoretical air. The platinum-based catalyst gave almost total conversion of NH_3 to XN under fuel-lean conditions. A minimum conversion of 35 percent was achieved at 70 percent theoretical air. The TFN concentration increased as the primary air percentage was decreased further giving almost complete conversion at 40 percent theoretical air. For fuel-lean mixtures, the results with the nickel oxide catalyst were similar to those obtained with the platinum catalyst. However, for fuel-rich mixtures, TFN concentration drops to less than 10 percent conversion of the inlet ammonia as the reactant mixture approaches 80 percent theoretical air. This conversion appears to be independent of the stoichiometry of the primary zone and remains low even for reactant mixtures approaching 40 percent theoretical air. Also, further tests indicate that these conclusions are also valid for reactant mixtures with higher inlet ammonia concentrations.

These preliminary results are particularly significant to the design of staged catalytic combustors for nitrogen-containing fuels. If the primary zone is to be operated fuel-rich, two design objectives must be satisfied:

1) The inlet reactants should have a composition which will minimize the TFN concentration of the first-stage reactants to reduce exhaust NO_x concentrations.

2) The temperature of the first-stage catalyst should be less than the critical level for catalyst degeneration. If the heat-release in the primary zone is too high, the combustor must be designed to allow heat extraction from the primary zone. The need for heat extraction will depend upon the stoichiometry of the primary reactants.

Based upon these investigations, the nickel oxide catalyst would allow the first stage to operate very fuel-rich and therefore without heat extraction, and yet minimize exhaust TFN concentrations. In addition, combustor operation is made easier because there is no need for precise control of the inlet reactant stoichiometry.

A scaled-up two-stage reactor using a nickel-based catalyst is currently being tested at pressures up to ten atmospheres. Additional bench scale tests are planned to investigate the influence of fuel nitrogen speciation.

REFERENCES

1. Robson, F. L., Blecher, W. A. and Giramonti, A. J. Combined-Cycle Power Systems. EPA-600/2-76-149, U. S. Environmental Protection Agency, Washington, D. C., 1976. p. 359

2. Environmental Protection Agency Title 40, Chapter 1, Subcharter C, Part 60-Standards of Performance for New Stationary Sources, Federal Register, Vol. 36, No. 247, December 23, 1971.

3. Folsom, B. A. and Courtney, C. W. Chemiluminescent Measurement of Nitric Oxide in Combustion Products. In Proceedings of the Third Stationary Source Combustion Symposium, March 1977.

4. Kesselring, J. P., Krill, W. V. and Kendall, R. M. Design Criteria for Stationary Source Catalytic Combustors. EPA-600/7-77-073c, U. S. Environmental Protection Agency, Washington, D. C., July 1977. p. 193

5. Folsom, B. A., Courtney, C. W. and Heap, M. P. Environmental Aspects of Low Btu Gas-Fired Catalytic Combustion. Proceedings of the Third Workshop on Catalytic Combustion, October 3-4, 1978.

TABLE I. NICKEL OXIDE CATALYTIC REACTOR CONSTANT TEST CONDITIONS.

LBG Composition (percent by volume)		
H_2	20	
CO	20	
CH_4	5	
N_2	55	
Total Reactant Flow Rate		= 93.5 scfh
Heat Release Rate		= 3730 Btu/hr
Preheat Temperature		= 200°C
Adiabatic Flame Temperature (adjusted by N_2 dilution)		= 1200°C
Measured Reactor Temperatures		≈ 1000-1200°C
Space Velocity		= 1.44×10^5/hr
Actual Reactant Velocity		= 10.0 ft/sec

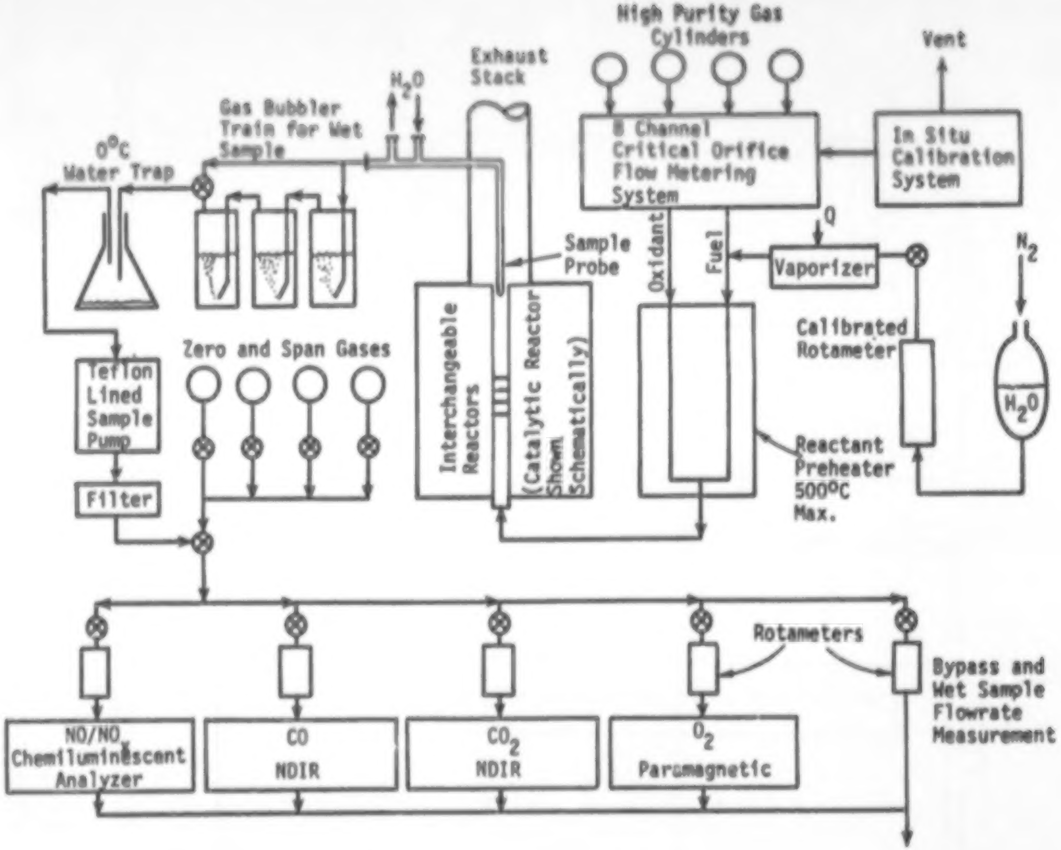
High Purity Gas Cylinders
Vent
In Situ Calibration System
8 Channel Critical Orifice Flow Metering System
Exhaust Stack
H_2O
Gas Bubbler Train for Wet Sample
0°C Water Trap
Sample Probe
Oxidant
Fuel
Q
Vaporizer
N_2
Calibrated Rotameter
H_2O
Interchangeable Reactors
(Catalytic Reactor Shown Schematically)
Reactant Preheater 500°C Max.
Zero and Span Gases
Teflon Lined Sample Pump
Filter
Rotameters
Bypass and Wet Sample Flowrate Measurement
NO/NO_x Chemiluminescent Analyzer
CO NDIR
CO_2 NDIR
O_2 Paramagnetic

Figure 1. Experimental apparatus.

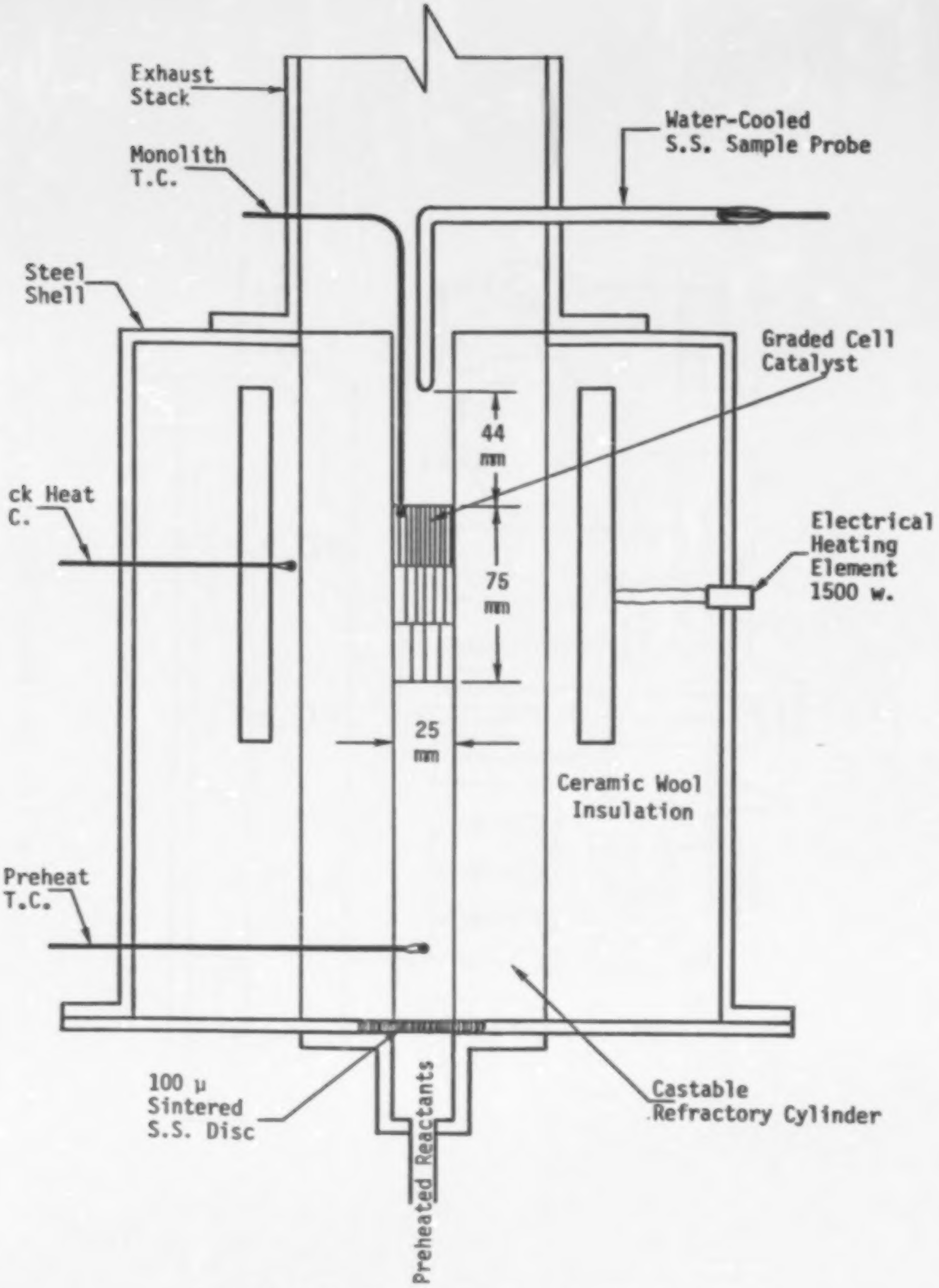
Exhaust Stack
Water-Cooled S.S. Sample Probe
Monolith T.C.
Steel Shell
Graded Cell Catalyst
44 mm
ck Heat C.
Electrical Heating Element 1500 w.
75 mm
25 mm
Ceramic Wool Insulation
Preheat T.C.
100 µ Sintered S.S. Disc
Castable Refractory Cylinder
Preheated Reactants

Figure 2. Catalytic reactor and housing.

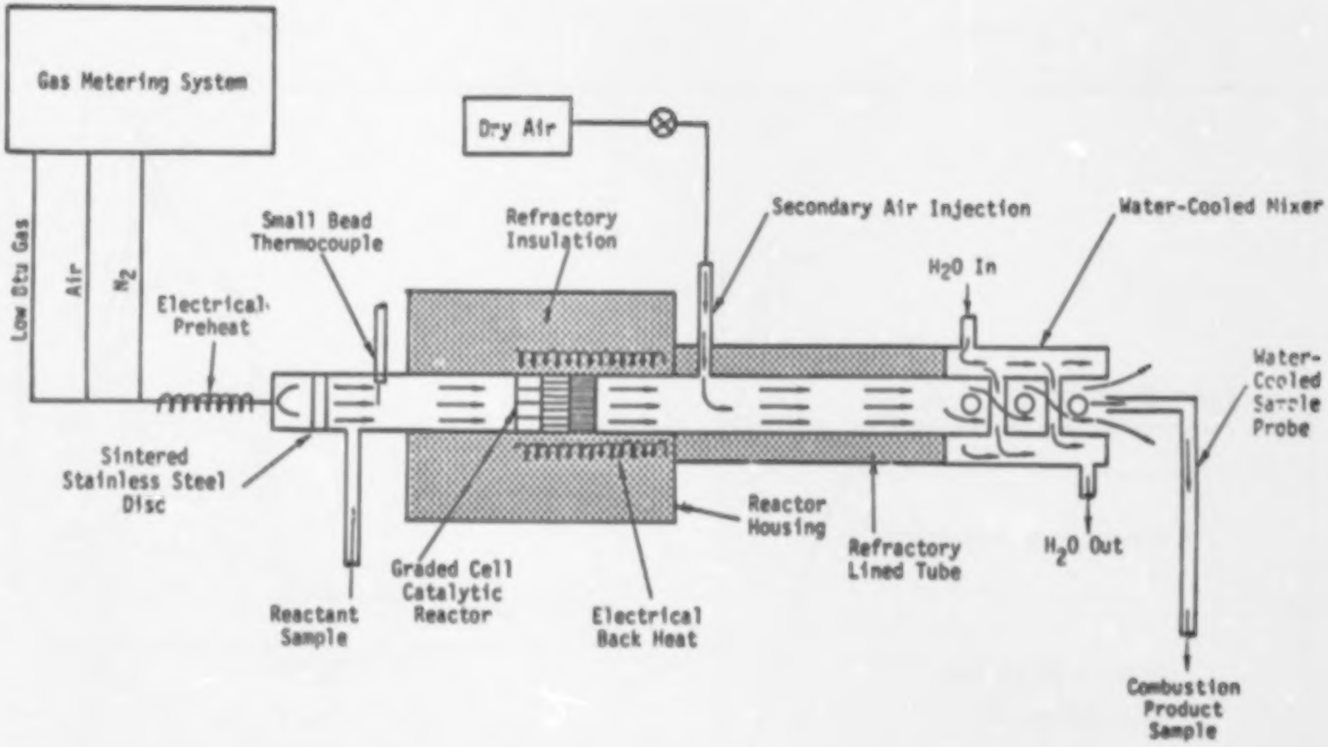
Gas Metering System
Dry Air
Low Btu Gas
Air
N_2
Electrical Preheat
Small Bead Thermocouple
Refractory Insulation
Secondary Air Injection
Water-Cooled Mixer
H_2O In
Water-Cooled Sample Probe
Sintered Stainless Steel Disc
Reactant Sample
Graded Cell Catalytic Reactor
Electrical Back Heat
Reactor Housing
Refractory Lined Tube
H_2O Out
Combustion Product Sample

Figure 3. Catalytic reactor test apparatus.

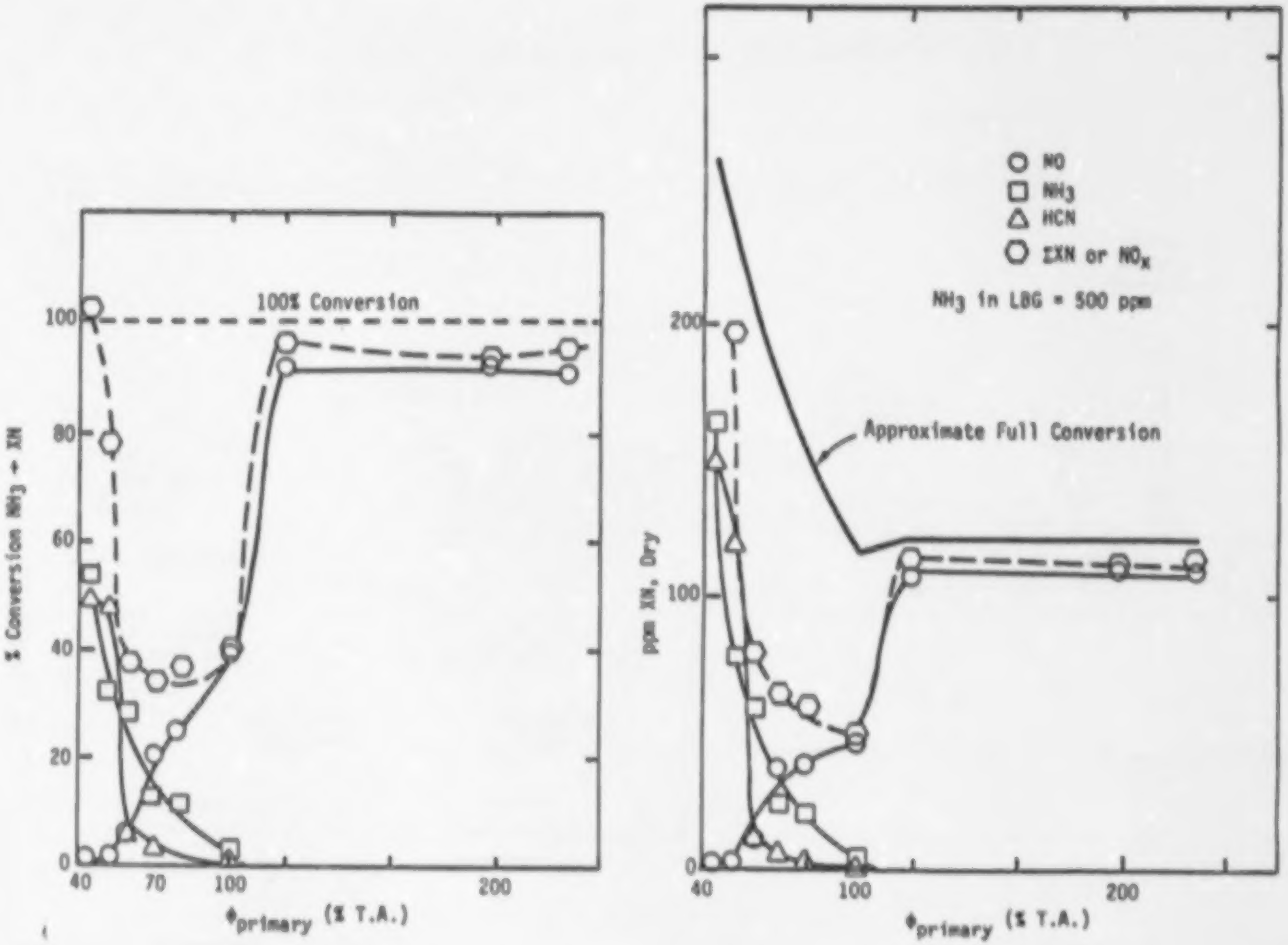

Figure 4. NH_3 processing in LBG platinum catalytic reactor.

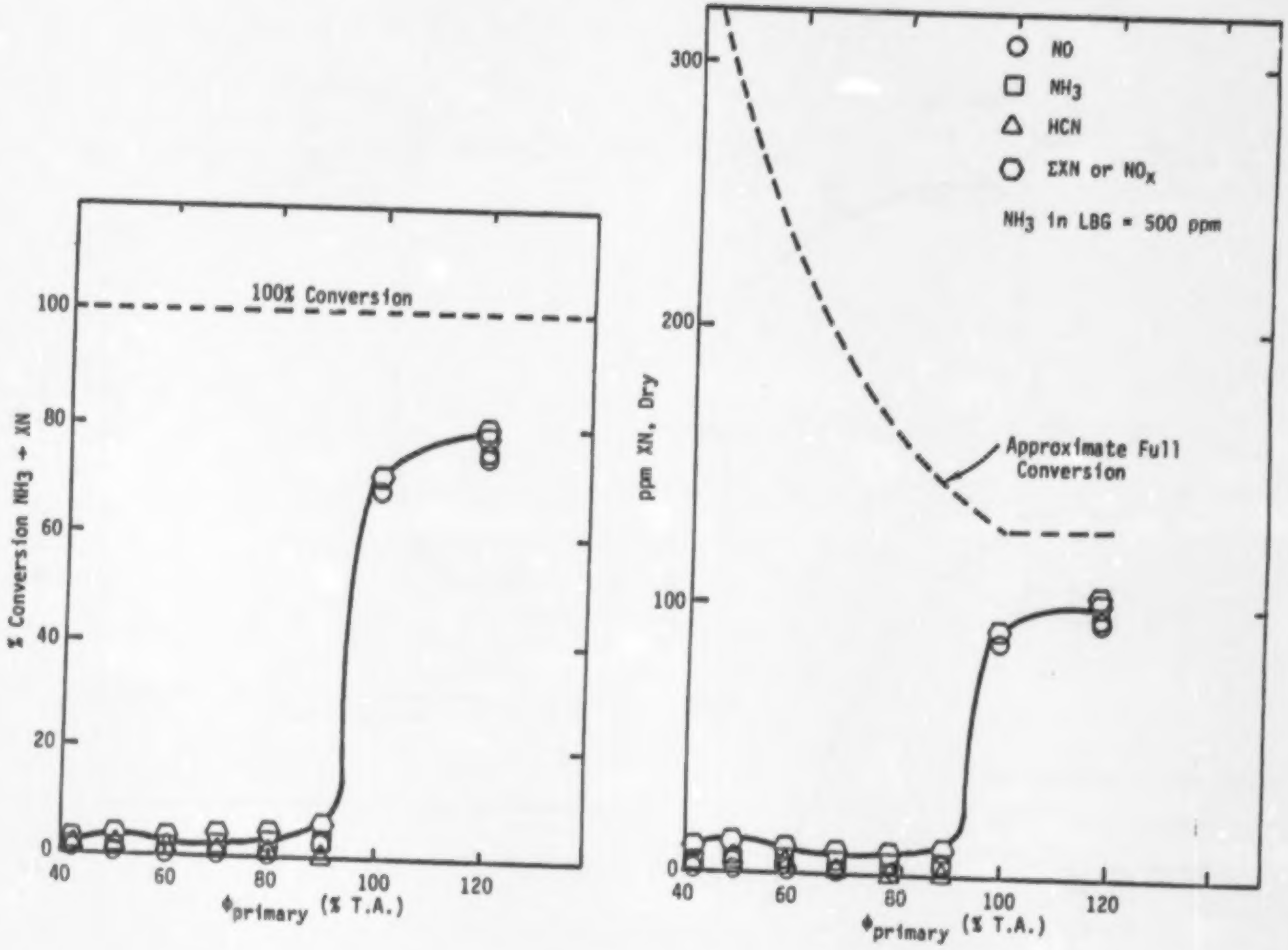

Figure 5. NH_3 processing in LBG-fired nickel oxide catalytic reactor.

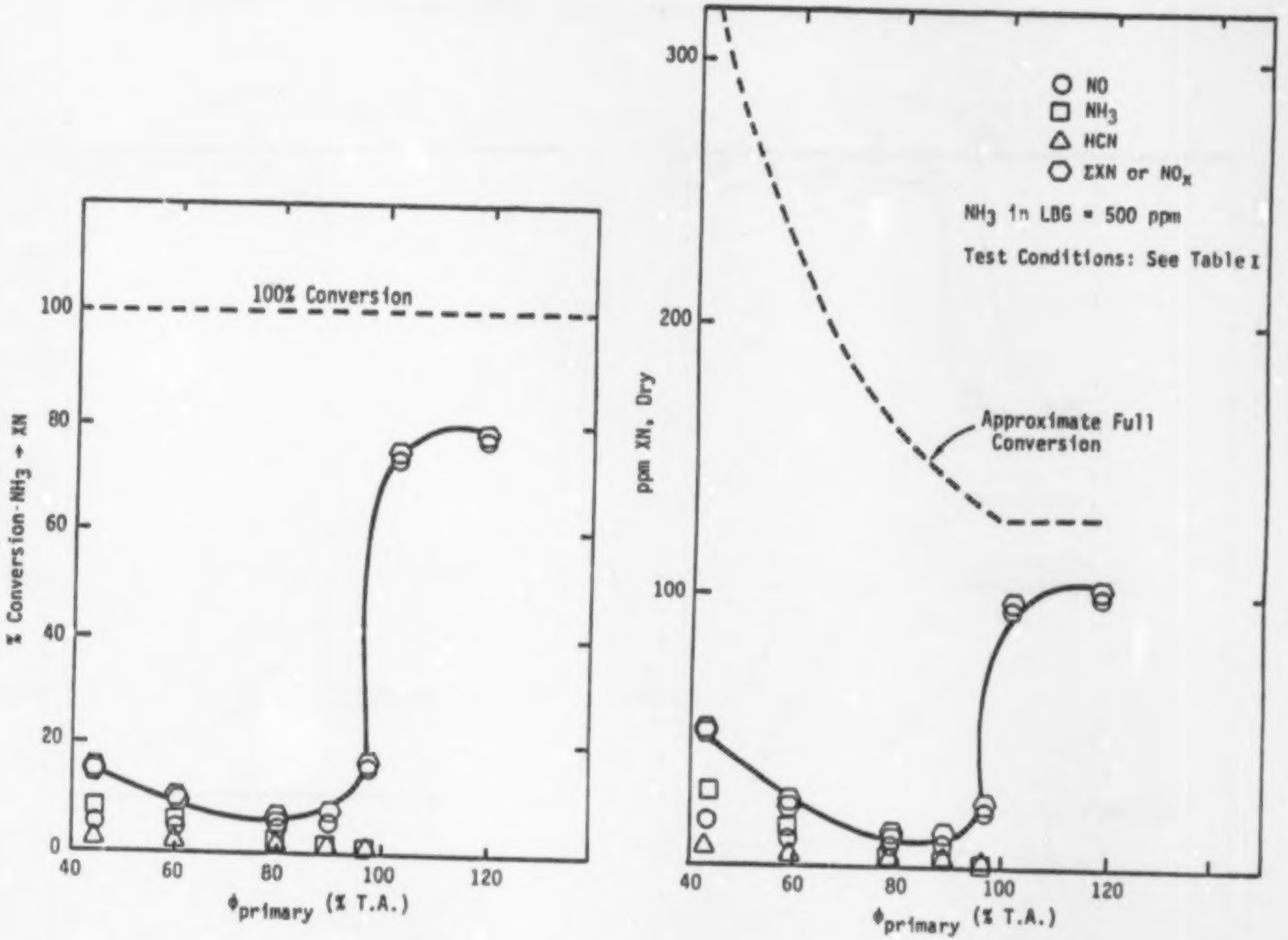

Figure 6. Unstaged nickel oxide catalytic reactor with 500 ppm NH_3.

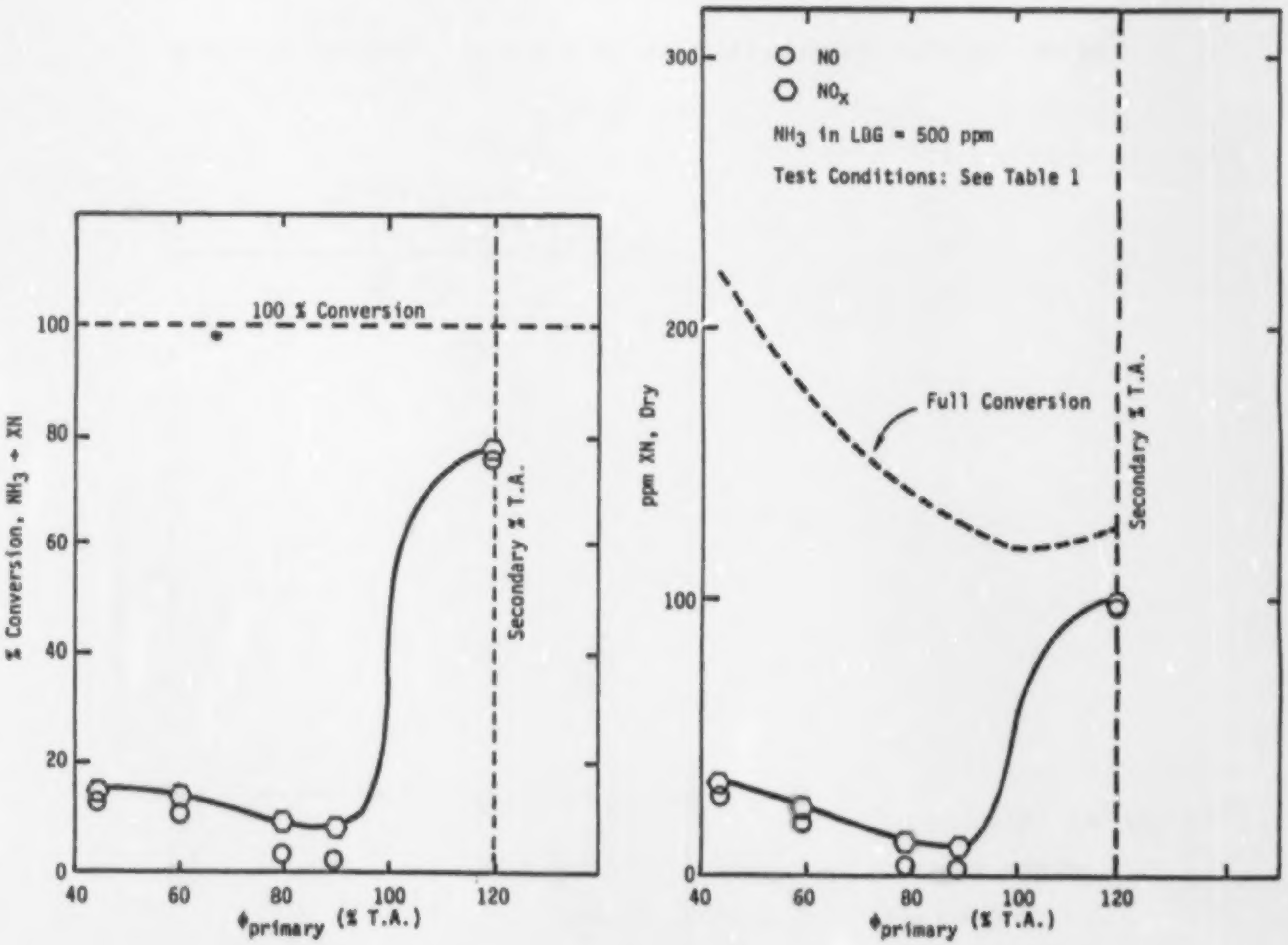

Figure 7. Staged nickel oxide catalytic reactor with 500 ppm NH_3.

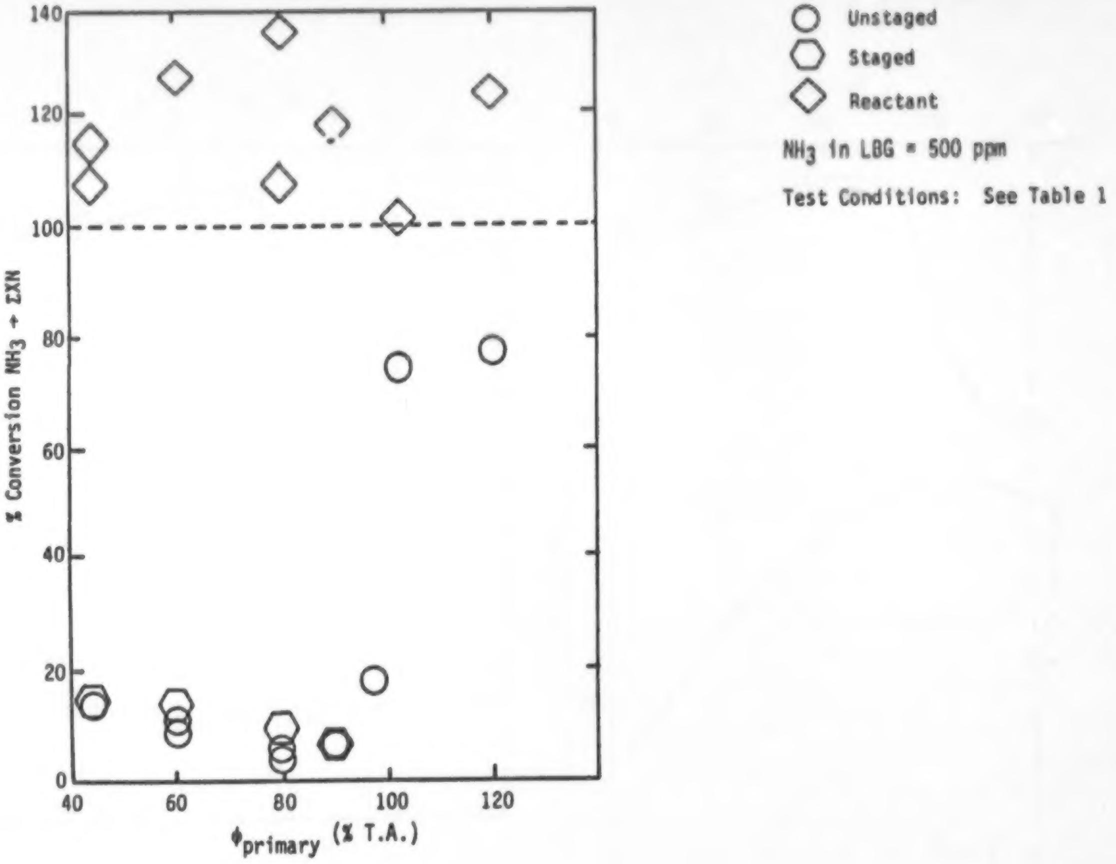

Figure 8. Summary: Nickel oxide catalytic reactor with 500 ppm NH_3.

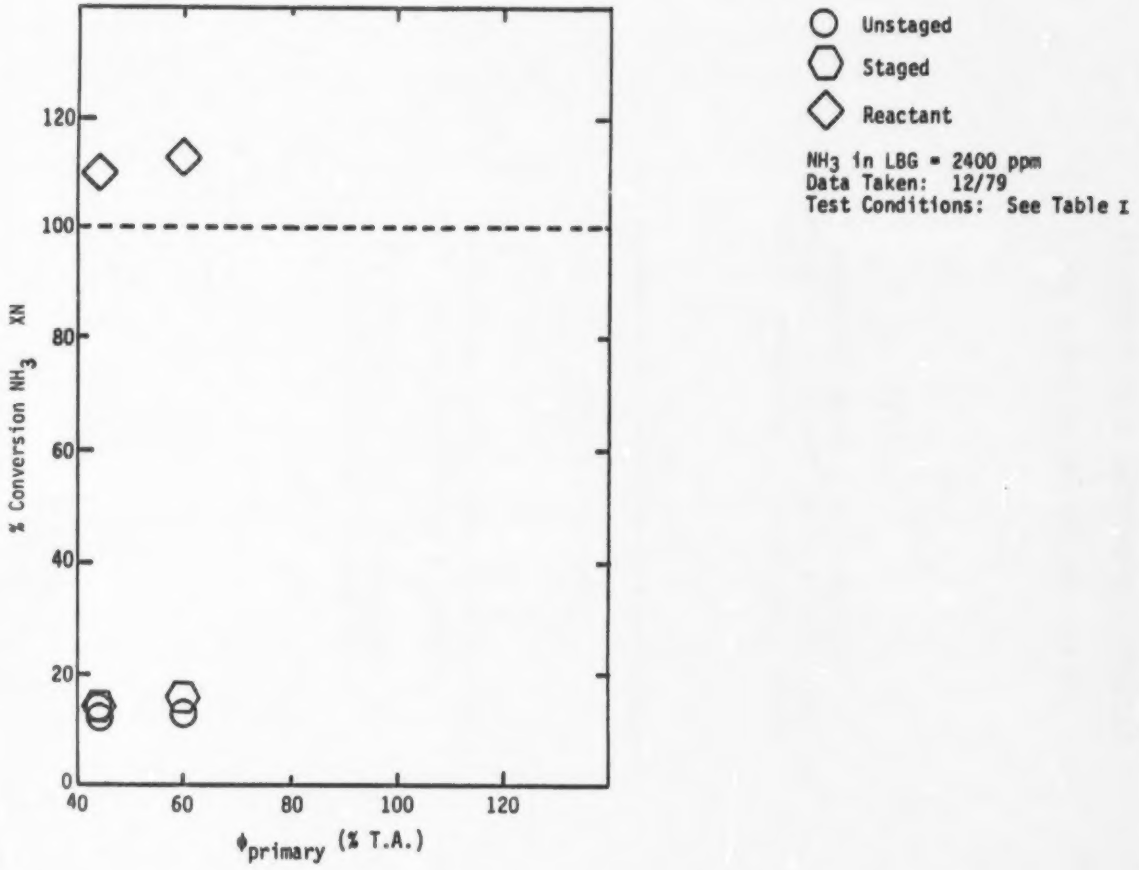

Figure 9. Summary: Nickel oxide catalytic reactor with 2400 ppm NH_3.

CATALYTIC COMBUSTION CHARACTERISTICS OF LOW AND MEDIUM BTU GAS FUELS

By:
H. C. Lee
I. T. Osgerby

Engelhard Industries Division
Engelhard Minerals and Chemicals Corporation
Menlo Park, Edison, New Jersey 08817

Presented at
Fourth EPA Workshop of Catalytic Combustion
Cincinnati, Ohio
May 14-15, 1980

Sponsor: U.S. Department of Energy
Power Systems Department

Contract No. EF-77-C-01-2683
W. W. Bunker, Contract Monitor

ABSTRACT

A test program was carried out to determine the feasibility of catalytically-supported thermal combustion (CATATHERMAL*) of low and medium BTU gas fuels.

Combustion characteristics of CATCOM* catalysts were investigated over the range of heating value 4.5 to 12.0 MJ/m^3 (120 ~ 320 BTU/ft^3), using simulated low and medium BTU gas fuels. The laboratory test results showed that low and medium BTU gas can be catalytically burned to accomplish high efficiency and essentially emissions-free combustion with acceptable pressure losses at 30 m/sec reference velocity and 300°C inlet temperature.

Efficiency for catalytically-supported thermal combustion is significantly affected by operating temperature and reference velocity. The maximum reference velocity for low emissions combustion was halved when the catalyst inlet temperature was decreased to 150°C. The turndown capacity of the catalyst system at 30 m/sec reference velocity and 300°C inlet temperature is estimated to be around 1.4, provided the maximum operating temperature for practical catalyst supports is limited to 1500°C. The effect of pressure on combustion efficiency was negligible over the range (1 to 5 atm) covered in laboratory test. Combustion efficiency was also shown to be a function of the ratio of hydrogen to combustible components in low and medium BTU gas. The higher the proportion of hydrogen, the better the combustion performance regardless of total fuel heating values.

The upper limit of reference velocity in the region of operability for the combustion of low and medium BTU gas was bounded by the pressure loss requirement (< 5 percent) above an inlet temperature of 235°C and by combustion efficiency below 235°C. The low limit boundary of reference velocity was set by the requirement of flashback-free operation.

The catalyst performance at a given pressure loss was also shown to be a function of physical properties of substrates, i.e., open area, hydraulic diameter and cell shape.

---

* CATCOM and CATATHERMAL are tradenames of Engelhard Minerals & Chemicals Corporation.

NOMENCLATURE

a	Numerical constant
DH	Channel hydraulic diameter
f_*	Apparent friction factor
L	Length of catalyst
p	Pressure
Δp	Pressure drop
T	Temperature
U	Velocity
σ	Open fraction of substrate
η_c	Combustion efficiency based on carbon balance

Subscripts

I	Isothermal
in	Inlet
Ref.	Reference (catalyst inlet-face)
T	Combustion

INTRODUCTION

Low and medium BTU gas obtained from gasification of coal is one of the principle new fuel sources being investigated by industry and the U.S. government. The commercial utilization of low and medium BTU gaseous fuels in a combined cycle power plant requires the solution of critical engineering problems in both the gasifier and turbine systems.

The laboratory-scale investigation into the catalytically-supported combustion of low and medium BTU gas was carried out under contract to the Department of Energy (Ref. 1) to evaluate the performance characteristics of this combustion process. Potential applications are to pressurized gasifiers, where advantage may be taken of the excellent combustion stability of this process in the presence of fluctuations in gasifier heating value.

Incentives for utilizing catalytically supported combustion include:

: high combustion efficiency
: excellent combustor stability
: negligible thermal NO_x emissions
: combustion both inside and beyond flammability limits
: uniform temperature profiles

Carrubba et al (Ref. 2) reported the low emissions combustion of $H_2/CO/N_2$ mixtures with heating values from 2 MJ/m^3, well below the conventional flammability limits. Additional confirmation of these performance characteristics was provided by DeCorso et al (Ref. 3). This latter evaluation of catalytic reactor performance utilized a 5 inch diameter pressurized static test rig. Exit gas temperature profiles were measured and reported to be as narrow as ± 30°C at 1300°C catalyst exit temperature.

The present study was directed toward establishing a technical data base with respect to low and medium BTU gas combustion, flashback potential, catalyst design, and low emissions operating ranges. All tests were carried out utilizing proprietary Engelhard precious metal CATCOM† catalysts evaluated in a one inch diameter test rig.

The program was divided into the following steps:

: Select five nominal fuel compositions (Table I) for the test to represent typical low and medium BTU coal gas fuels and define the test conditions to simulate gas turbine combustor operation.

: Determine the boundary of flashback free operation at the maximum preheat levels and select operating conditions without flashback for subsequent tests.

: Evaluate five different configurations varying reference velocity, inlet temperature, pressure and fuel heating value, and determine a preferred catalyst configuration to meet the objectives of >99% combustion efficiency and <5% pressure loss at 30 m/sec reference velocity and 300°C inlet temperature.

: Define the region of operability for constraints of combustion efficiency, pressure loss and flashback-free operation with the preferred configuration, and generate performance data applicable to the design of a prototype combustor for combustion of low and medium BTU gaseous fuels.

---

† Engelhard Minerals and Chemicals Tradename

EXPERIMENTAL FACILITIES

Experimental facilities used in the test program are described in Reference 4, including fuel-air supply system, preheating system, mixing system, reactor system, control instrumentation and analytical system.

Figure 1 gives a schematic drawing of the flashback reactor. A one inch diameter (nominal) test catalyst is loaded into a catalyst holder with a flashback arrestor to prevent fuel-air mixture from preigniting before entering the catalyst. The flashback arrestor consisted of a sintered blank honeycomb and a refractory ceramic liner insert. Partially open channels of catalyst core are completely blocked by high temperature cemment and channeling of the preheated gas in the reactor is prevented by Fiberfrax®† packing around the catalyst core.

Air preheat temperature was maintained by indirect electric preheat furnaces and reactor pressure was adjusted with a pressure regulator on the exhaust line, downstream of a cooling jacket. Throughout the tests, gas samples were taken with a water-cooled probe located 0.1016 m downstream of the catalyst core for measurement of emissions (CO, unburned hydrocarbon, NO/NO_x, O_2 and CO_2 concentrations in the reactor effluent stream). The sample probe location was evaluated during previous tests to keep the distance as close as possible to the catalyst without undesirable cooling effects.

RESULTS AND DISCUSSION

Flashback Tests

Flashback tests were conducted to establish the region of operability without flashback for configuration selection and parametric tests. The flashback arrestor developed for low BTU gaseous fuel (<20% H_2 concentration) did not prevent flashback in fuel/air mixtures containing high hydrogen concentration.

---

† Fiberfrax is a registered trademark of the Carborundum Company.

Accordingly, various types of arrestor were tried with 7.5 MJ/m^3 fuel (containing 40% H_2) at the maximum preheating level of 300°C. As shown in Figure 1, an uncatalyzed honeycomb (0.0127 m long, located 0.00635 m in front of catalyst with 15° slant angle to the flow) together with a refractory ceramic insert (placed just upstream of an arrestor) prevented flashback at the following limiting conditions:

Pressure	< 4 atmospheres
Inlet Temperature	< 300°C
Reference Velocity	> 15 m/sec
Heating Value	= 4.5-12.0 MJ/m^3

Preferred Catalyst Configuration Selection

A series of tests were carried out to select a preferred catalyst configuration which could meet the objectives of low emissions and high combustion efficiency (> 99%) at acceptable pressure losses (< 5%).

Previous tests (Ref. 4) demonstrated that combustion efficiency is strongly affected by reference velocity and inlet temperature, but the effect of pressure on combustion efficiency and pressure loss in turbulent flow is negligible. Thus, configuration selection tests were performed at a constant adiabatic flame temperature of 1260°C and varying reference velocity by changing pressure at a constant mass flow rate. The fuel with a medium BTU heating value of 12.0 MJ/m^3 was selected for the tests due to its lower hydrogen concentration to minimize flashback problems.

Five different catalyst configurations (A.2, C.2, E.2, G.2 and H.2 in Table II) with palladium on stabilized alumina on a Zircon composite support were evaluated, using a test procedure developed in Reference 4.

Test results for combustion efficiency and pressure losses versus reference velocity at 150 and 300°C inlet temperatures are presented in Figures 2 through 4 and summarized in Table III.

Combustion Efficiency

Figure 2 shows a linear relationship of the negative logarithm of complement combustion efficiency vs. reference velocity at 300°C inlet temperature. All catalyst configurations except catalyst A.2 yielded combustion efficiencies greater than 99% at 30 m/s reference velocity. A combustion efficiency >98% was obtained only from catalyst configurations C.2 and E.2 when the inlet temperature was reduced to 150°C as shown in Figure 3. A significant drop in combustion efficiency was noticed especially with catalyst configuration H.2.

Catalyst configurations A.2 and H.2 were expected to have large entrance region effects due to low open area (A.2) and small length to cell size ratio (H.2) in each segment. Poor performances were attributed to high mass transfer rates near the entrance of the catalyst.

Catalyst configurations C and E were selected on the basis of combustion efficiency for low emissions operation over a wide range of velocities and inlet temperatures.

NO_x emissions were less than 2.5ppm for all catalysts tested under all operating conditions.

Pressure Losses

Figure 4 shows isothermal pressure losses for configurations A.2, C.2, E.2, G.2 and H.2, indicating a linear relationship of isothermal pressure loss vs. (U^2Ref/T). The apparent friction factor is essentially a constant in turbulent flow and the isothermal pressure loss is expressed as follows:

$$\frac{(\Delta P_I/P)}{(U^2 Ref/T)} = a \cdot \left(\frac{L}{DH}\right) \cdot \frac{1}{\sigma^2} \cdot f^* \qquad (1)$$

Table III gives the parameters of interest for each configuration, indicating a wider variation of σ^2 than $(\frac{L}{DH})f^*$ for each configuration.

The combustion pressure loss for each configuration is also presented in Table III. Low isothermal pressure losses with a high ratio of combustion to isothermal pressure loss represents good catalyst performance (in a single-segment catalyst configuration) to attain low emissions operation within acceptable pressure loss. Results for configurations C.2 and E.2 show a high ratio of combustion to isothermal pressure loss, however, configuration C.2 does not meet the pressure loss requirement <5%.

Note that the flame arrestor accounted for 20-30% of the total pressure drop.

The superiority of configuration E.2 is apparent over the entire range of operating conditions as shown in Figures 2, 3, and 4. Its superior performance is attributed to an optimum combination of geometric properties, i.e., open area, hydraulic diameter and cell shape.

Configuration E.2 was also selected as the preferred catalyst configuration in combustion of low BTU gaseous fuel (Ref. 4). The preferred configuration, Configuration E.2 consists of:

> 0.1619 m refractory ceramic liner + 0.0127 m uncatalyzed 14 channels/cm^2 honeycomb (flashback arrestor) + 0.00635 m space + 0.0762 m catalyzed 6 channels/cm^2 honeycomb catalyst: palladium on stabilized alumina on zircon composite honeycomb support.

Catalyst Performance Tests

A parametric test program was formulated to determine the region of operability for high combustion efficiency at acceptable pressure losses with the preferred catalyst Configuration E.2.

Emissions and pressure losses were measured, varying reference velocity, inlet temperature and fuel heating value. Total flow rates were set to maintain high Reynolds numbers (> 5000) throughout the characterization tests to preserve scalability to industrial gas turbine operating conditions. A pressure of three atmospheres was selected for the test but some runs were carried out to investigate the effect of pressure on emissions.

Additional tests were carried out to examine effects of adiabatic flame temperature and fuel components on catalyst performance.

Effect of Operational Variables

Reference Velocity: The effect of reference velocity on combustion efficiency is pronounced and the plot of the negative logarithm of the complement combustion efficiency versus reference velocity is linear at high combustion efficiencies >95% over the velocity range 15 to 35 m/s. The linear relationship is invalid at combustion efficiencies <95%, as shown in Figures 5 and 6.

Inlet Temperature: Combustion efficiency was significantly reduced at low inlet temperature, except for combustion of 7.5 MJ/m^3 fuel. Combustion efficiencies >99% at 150°C were obtained for a reference velocity <20 m/s. At inlet temperatures below 150°C, low and medium BTU gas fuels did not light-off near the entrance of the catalyst bed due to low kinetic activity and the selected catalyst length was not sufficient for complete

CATATHERMAL reactions. Minimum inlet temperature to obtain combustion efficiency greater than 99% at a reference velocity of 30 m/sec is interpolated to be 200 and 240°C, in Figures 5 and 6, for combustion of low and medium BTU fuels, respectively.

In order to examine the effect of inlet temperature, combustion efficiency was measured at a constant space velocity - corresponding to a reference velocity of 30 m/s at 150°C - and plotted versus the reciprocal inlet temperature for 7.5 and 12.0 MJ/m^3 fuels in Figure 7.

Combustion efficiency is strongly affected by both inlet temperature and adiabatic flame temperature due to the exponential dependence of the reaction rate constant on temperature. However, a weak temperature dependence was observed with the 7.5 MJ/m^3 heating value fuel as shown in Figure 7.

A mechanism for catalytically supported thermal combustion is postulated to comprise regions of kinetic control, mass transfer control and catalytically-supported thermal reactions, and the temperature dependency for reaction in each zone has a distinct characteristic (Ref. 5) . The activation energy for kinetic control and catalytically-supported thermal reaction regions are greater than 15 Kcal/gmol for H_2 and CO fuels, but the temperature dependency is negligible in the mass transfer region (Ref. 6, 7).

Thus a weak overall temperature dependency for 7.5 MJ/m^3 fuel indicates that kinetic effect is not important for the combustion with 7.5 MJ/m^3 fuel, while a kinetic reaction is controlling for 12.0 MJ/m^3 in a range of 150°C to 300°C inlet temperature. Since the 7.5 MJ/m^3 fuel has a higher ratio of hydrogen to carbon monoxide and the rate constant for hydrogen is 15-20 times higher than for carbon monoxide in the kinetic zone (Ref. 7), the fuel mixture easily lights-off even at 150°C inlet temperature and combustion efficiency is not less than 99.4 percent over the entire range of operating conditions covered in the characterization tests.

Pressure: The effect of pressure on combustion efficiency was not discernible in the pressure range covered in this test program.

Fuel Composition/Heating Value

Hydrogen: Tests were conducted with fuel composition varied at constant heating value (7.5 MJ/m^3) and reference velocity (30 m/s.). Measured combustion efficiencies declined as hydrogen concentration decreases. A high combustion efficiency was obtained with a fuel having a high ratio of hydrogen to mix gas ($CO + CH_4$) as shown in Table IV and Figure 8. Comparing test results obtained with 7.5 and 12.0 MJ/m^3 fuel, no apparent effect of fuel heating value on combustion efficiency was observed. A similar result was obtained with low BTU fuels (Ref. 4).

$CO + CH_4$: From the test results shown in Figure 8, CO and CH_4 concentrations in the fuel appears to have an adverse effect on the catalyst performance.

In order to determine the reactivity of CO and CH_4, the combustion efficiency derived from test data obtained at a low inlet temperature of 150°C was plotted in Figure 9. The combustion efficiency of CH_4 is much higher than CO on the basis of complete combustion of CH_4. This may be due to:

: CO may be more difficult to oxidize due to the strong adsorption of CO on active sites of the catalyst at low temperatures (inlet zone).

: CH_4 is partially converted to CO and hence gives a misleading result.

Non-Combustible Components (CO_2, N_2 and Steam): Additions of nitrogen and steam to the fuel-air mixture resulted in lower combustion efficiencies. No significant difference in effect of nitrogen or steam on combustion efficiency was observed except for lowering the fuel/air ratio (dilution effect). Similar result was observed with low BTU fuels (Ref. 4).

Effect of Adiabatic Flame Temperature

The effect of adiabatic flame temperature on catalyst performance was investigated by changing the fuel/air ratio, to determine the turndown temperature for 99% combustion efficiency. Two series of tests were carried out at inlet temperatures of 250 and 300°C with 12.0 MJ/m^3 fuel. Test results are shown in Figures 10 and 11.

Minimum temperature required for low emissions operation is interpolated to be around 1160°C at 30 m/sec reference velocity and 300°C inlet temperature. This corresponds to a turndown ratio of ≈1.4 provided the maximum operating temperature is limited to 1500°C. The minimum temperature was 1220°C at an inlet temperature of 250°C as shown in Figure 11.

Comparison of Low and Medium BTU Test Results

Performance test results in Figures 5 and 6 indicate that the combustion efficiency with low BTU fuel (4.5 - 6.75 MJ/m^3) is slightly higher than results obtained with medium fuel (12.0 MJ/m^3). An excellent combustion efficiency was always observed with 7.5 MJ/m^3 fuel as shown in Table V-A.

Even though the catalytic combustion of gas fuels are complicated by various fractions of each component in the gas mixture, overall combustion performance is generally affected by the ratio of hydrogen to other combustible components, regardless of fuel heating value(Table V-B). Note that the actual combustion efficiency of coal gas fuel is higher than results reported in this test program on the basis CO and CH_4 as reactants (Hydrogen was not included).

Region of Operability for Low and Medium BTU Fuels

The region of operability was defined for low and medium BTU fuels as shown in Figure 12, considering the constraints of combustion efficiency > 99%, pressure loss < 5% and flashback-free reactor operation. The boundary for combustion efficiency was derived from the extrapolation of parametric test results assuming a linear relationship in the plot of the negative logarithm of the complement combustion efficiency versus reference velocity.

As shown in Figure 12 for low BTU fuel, pressure loss is the limiting factor on allowable reference velocities above 210°C inlet temperature and combustion efficiency controls the region of operability below 210°C.

The transition temperature for pressure loss and combustion efficiency increases to 250°C for medium BTU fuel. Thus, the region of operability for combustion of medium BTU fuel is slightly narrower than the region for low BTU fuel. The low limit boundary of reference velocity is set by the requirement of flashback-free reactor operation, an artifact of the Engelhard reactor, and will be different for a practical combustor.

CONCLUSIONS

From the results of laboratory tests for combustion of low and medium BTU coal gas fuels, the following conclusions have been drawn:

1. Based on the laboratory test results, catalytically supported combustion has been shown to be capable of combusting a wide range of low and medium BTU fuel compositions with high combustion efficiency, low emissions and acceptable pressure drop at conditions simulating gas turbine combuster operation.

2. Combustion efficiency of 99.8 percent and pressure losses below 4.2 percent were achieved with the preferred CATCOM* catalyst. Configuration E, i.e., palladium catalyst on 0.0762 m zircon composite honeycomb, at 30.5 m/sec reference velocity and 300°C inlet temperature. Emissions were:

Carbon Monoxide	80-190 Vppm
Unburned Hydrocarbon (as C_3)	1 Vppm
Nitrogen Oxides	2.3 Vppm

3. NO_x emissions were always < 2.5 Vppm. Thus, NO_x formation from thermal nitrogen fixation is negligible at an adiabatic flame temperature of 1260°C.

4. Catalyst Configuration E.2 with the highest open area was selected as the preferred configuration for high combustion efficiency at acceptable pressure loss in the combustion of low and medium BTU gaseous fuel.

5. Combustion efficiency was affected by reference velocity, inlet temperature and adiabatic flame temperature, but not affected by pressure or heating value.

6. Combustion performance with low BTU fuel (4.5-6.75 MJ/m^3, $H_2/CO = 0.68 - 0.86$) better than results obtained with medium BTU (12.0 MJ/m^3, $H_2/CO = 0.52$) fuel but an excellent combustion efficiency was always obtained with 7.5 MJ/m^3 ($H_2/CO = 1.92$) fuel attributed to the much higher ratio of H_2 to CO in the fuel.

---

* CATCOM is a trade name of Engelhard Minerals & Chemicals Corp.

7. Since combustion efficiency with 7.5 MJ/m^3 fuel containing a high ratio of H_2/CO (1.92) was not sensitive to inlet temperature, the surface reaction rate might not be critical, however, the kinetic rate controlled the overall rate of combustion of low and medium fuels with a low ratio of H_2/CO (<0.86).

8. Pressure losses were correlated with the dynamic momentum divided by the absolute inlet temperature with a slope approximately equal to unity on a logarithmic plot in the range of channel Reynolds number greater than 5000. It indicates that the apparent friction factor is constant in turbulent flow.

9. Flashback was more severe with medium BTU fuel and was attributed to the increase in H_2 concentration.

REFERENCES

1. Catalytically Supported Thermal Combustion of Coal Derived Low BTU Gas -- D.O.E. Contract EF - 77 - C - 10 - 2683.

2. Carrubba, R. V., Chang, M., Pfefferle, W. C. and Polinski, L. M., "Catalytically Supported Thermal Combustion for Emissions Control" - Electric Power Research Institute NO_x Control Seminar, February 6, 1976.

3. Decorso, S. M., Mumford, S., Carrubba, R. V., and Heck, R., "Catalysts for Gas Turbine Combustors -- Experimental Test Results' - ASME gas Turbine Division Conference, New Orleans, LA (March, 1976).

4. Osgerby, I. T., Carrubba, R. V., Heck, R. M., and Bunker, W. W., "Investigation of Process and System Design Variables for CATATHERMAL Combustion of Low BTU Gas", ASME 79-GT-66, presented at the ASME Gas Turbine Conference, San Diego, California, March 12-15, 1979.

5. Pfefferle, W. C., "Catalytically-Supported Thermal Combustion", U.S. Patent 3,928,961 (1975).

6. Hlavacek, V., and Votruba, J., "Experimental Study of Multiple Steady States in Adiabatic Catalytic Systems", Chemical Reaction Engineering II, American Chemical Society, Washington, 545-558 (1974).

7. Hawthorn, R. D., "Afterburner Catalysts-Effects of Heat and Mass Transfer Between Gas and Catalyst Surface". Shell Development Co., Rept. p. 2121, 1972.

TABLE I

SYNTHETIC GAS COMPOSITIONS FOR LOW AND MEDIUM BTU FUELS

	LOW BTU			MEDIUM BTU		
MIX:	I	II	III	IV	V	
CO, % (dry)	15.0	20.5	24.5	18.6	51.5	
H_2	14.4	15.6	18.7	40.0	30.0	
CH_4	1.8	2.4	2.9	2.2	6.1	
CO_2	6.4	8.7	10.4	39.2	12.4	
N_2	62.4	52.8	43.5	-	-	
Heating Value	120	150	180	200	320	($^{\text{BTU/SCF}}_{\text{1 Atm, } 0^\circ\text{C}}$)
	4.5	5.62	6.75	7.5	12.0	MJ/m^3

TABLE II

CATALYST CONFIGURATIONS FOR LOW AND MEDIUM BTU GAS TESTS

		GEOMETRIC PROPERTIES FOR SUBSTRATES			
Catalyst† Configuration	Length (cm)	Channels per cm^2	Hydraulic Diameter (cm)	Open Area(%)	Bulk Surface Area (cm^2/cm^3)
A	7.62	14	0.1722	54.2	12.6
B**	2X5.08	6	0.300	73.3	9.8
C	3.81	40	0.098	65.5	26.8
D	5.08	14	0.1722	54.2	12.6
E	7.62	6	0.300	73.3	9.8
F*	2X5.08	6	0.300	73.3	9.8
G	7.62	17	0.1940	68.8	14.2
H**	3X2.54	9	0.2930	61.0	8.8

* Over-temperature test (Ref. 1)

** Single-Cell multi-segment configuration

† Pd/Al_2O_3 on Zircon Composite Support

TABLE III

CONFIGURATION SELECTION FOR CONFIGURATIONS A, C, E, G, AND H

Configuration	Combustion Efficiency (%)	Pressure Losses			Physical Parameter	
		Isothermal	Combustion		(Eq'n 1)	
		$\frac{\Delta P_I}{P}(\%)^+$	$\frac{\Delta P_T}{P}(\%)$	$\frac{\Delta P_T}{\Delta P_I}^+$	(L/DH)f*	$1/\sigma^2$
		at U_{Ref} = 30m/s and Tin = 300°C				
A.2	97.0	2.5	7.8	1.5	0.64	3.40
C.2	99.6	2.2	6.6	2.1	0.82	2.33
E.2	99.8	1.3	4.2	2.1	0.61	1.86
G.2	99.4	1.4	5.0	1.8	0.57	2.11
H.2	99.5	1.5	5.0	1.5	0.51	2.69

Note (+): Catalyst only (pressure loss through the flashback arrestor is excluded)

TABLE IV

EFFECT OF FUEL COMPOSITION (H_2, CO, CH_4, N_2 and CO_2)

Catalyst	Configuration E.2
Inlet Temperature	225°C
Pressure	200 kPa
Reference Velocity	30 m/sec
Fuel Heating Value	7.5 MJ/m^3

Fuel Composition (%)							
H_2	CO	CH_4	N_2	CO_2	$\frac{\text{Fuel*}}{\text{Air}}$	$\frac{H_2}{CO+CH_4}$	Combustion Efficiency
40.0	18.6	2.2	39.2	-	.2531	1.92	.9971
35.0	21.8	2.6	40.6	-	.2536	1.43	.9959
30.0	25.0	3.0	42.0	-	.2541	1.07	.9896
25.0	28.3	3.3	43.4	-	.2533	0.79	<.9222
40.0	18.6	2.2	-	39.2	.2704	1.92	.9965

* For an adiabatic flame temperature 1260°C

TABLE V

COMPARISON OF LOW AND MEDIUM BTU TEST RESULTS

A. COMBUSTION EFFICIENCY

Fuel Heating Value MJ/m^3	Configuration "A"		Configuration "C"		Configuration "E"	
	Tin=150°C	300°C	Tin=150°C	300°C	Tin=150°C	300°C
6.75 (Low BTU)	<.90	.9967	-	.9947	-	.9964
7.5 (Medium BTU)	.987	.9941	-	-	.9939	.9984
12.0 (Medium BTU)	<.90	.9700	.9720	.9969	.8971	.9974

B. FUEL COMPOSITION

Fuel	Heating Value MJ/m^3	Fuel Fraction (By Volume)		
		$\frac{H_2}{H_2 + CO + CH_4}$	$\frac{CO}{H_2 + CO + CH_4}$	$\frac{H_2}{CO + CH_4}$
1. Low BTU Gas	4.5	0.46	0.48	0.86
	5.62	0.41	0.53	0.68
	6.75	0.41	0.53	0.68
2. Medium BTU Gas	7.5	0.66	0.31	1.92
	12.0	0.34	0.59	0.52

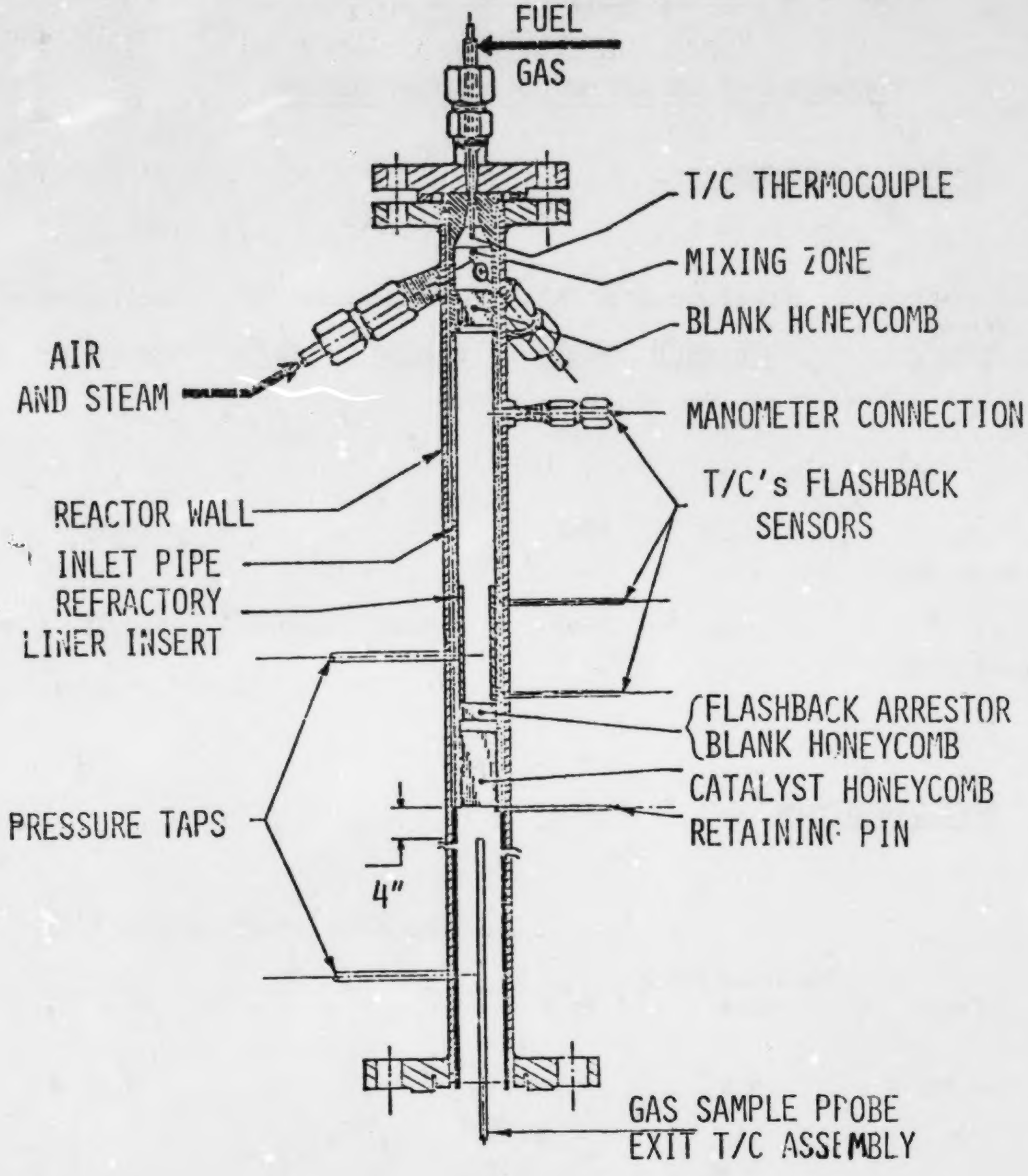
FUEL
GAS
T/C THERMOCOUPLE
MIXING ZONE
BLANK HONEYCOMB
AIR
AND STEAM
MANOMETER CONNECTION
T/C's FLASHBACK
SENSORS
REACTOR WALL
INLET PIPE
REFRACTORY
LINER INSERT
FLASHBACK ARRESTOR
BLANK HONEYCOMB
CATALYST HONEYCOMB
RETAINING PIN
PRESSURE TAPS
4"
GAS SAMPLE PROBE
EXIT T/C ASSEMBLY

FIGURE 1. SCHEMATIC OF FLASHBACK REACTOR

FIGURE 2 PLOT OF COMBUSTION EFFICIENCY VS. REFERENCE VELOCITY AT 300°C INLET TEMPERATURE

TEST CONDITIONS

INLET TEMPERATURE : 300°C
PRESSURE : 100~400 kPa
ADIABATIC FLAME TEMPERATURE: 1260°C
FUEL HEATING VALUE : 12.0 MJ/m^3

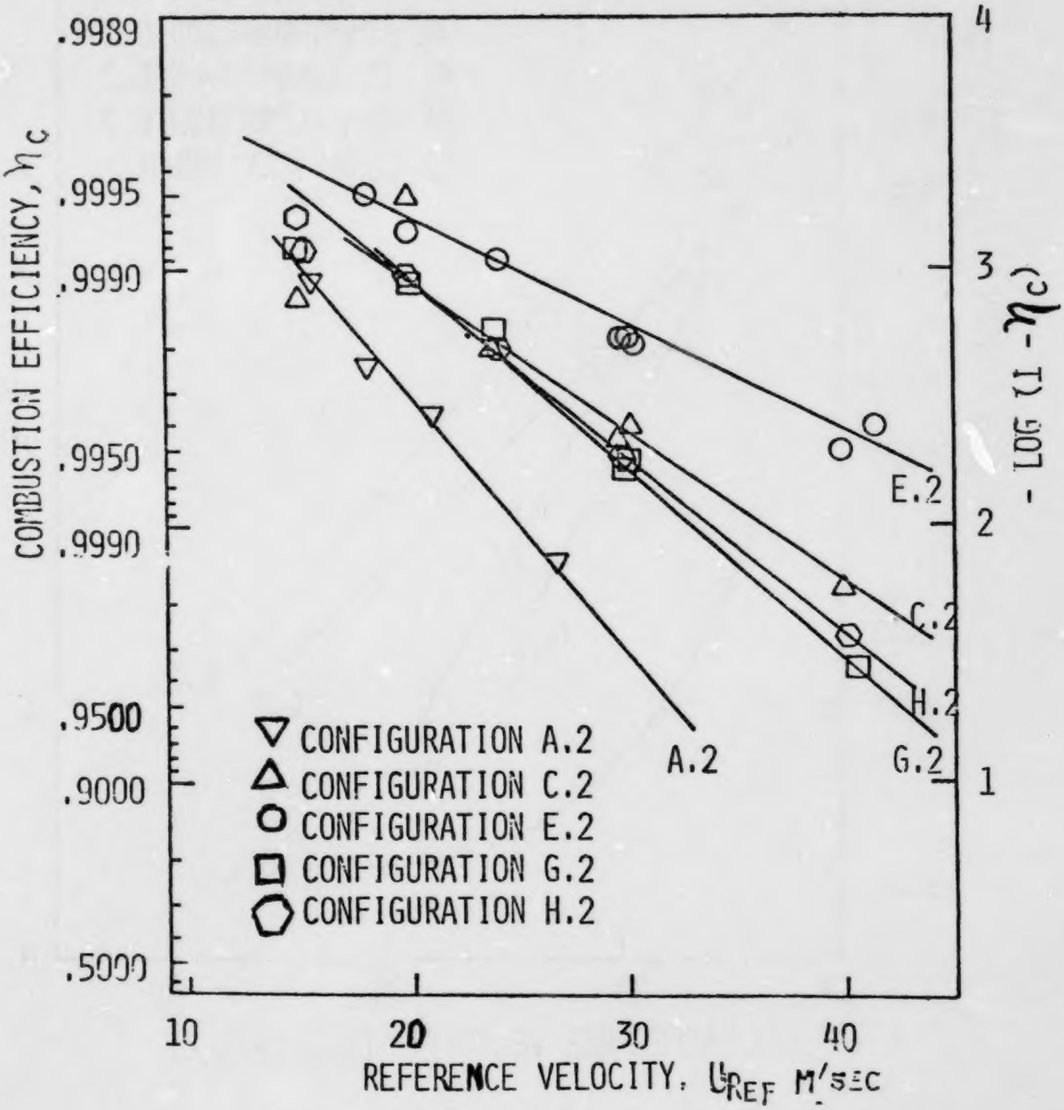

FIGURE 3. PLOT OF COMBUSTION EFFICIENCY vs. REFERENCE VELOCITY AT 150°C INLET TEMPERATURE

TEST CONDITIONS

INLET TEMPERATURE : 300°C
PRESSURE : 100~400 kPa
ADIABATIC FLAME TEMPERATURE: 1260°C
FUEL HEATING VALUE : 12.0 MJ/m^3

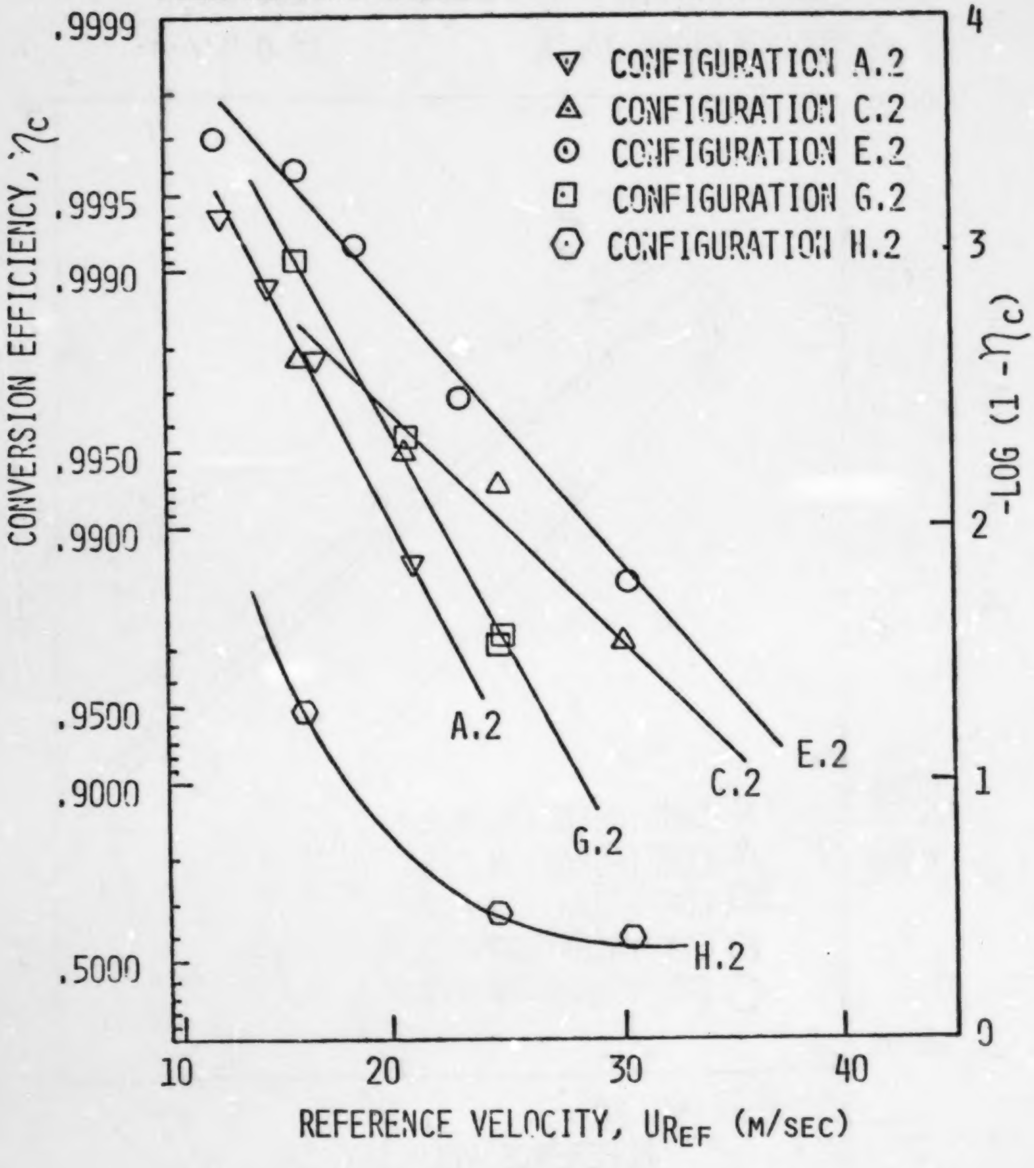

FIGURE 4. COMPARISON OF ISOTHERMAL PRESSURE LOSSES

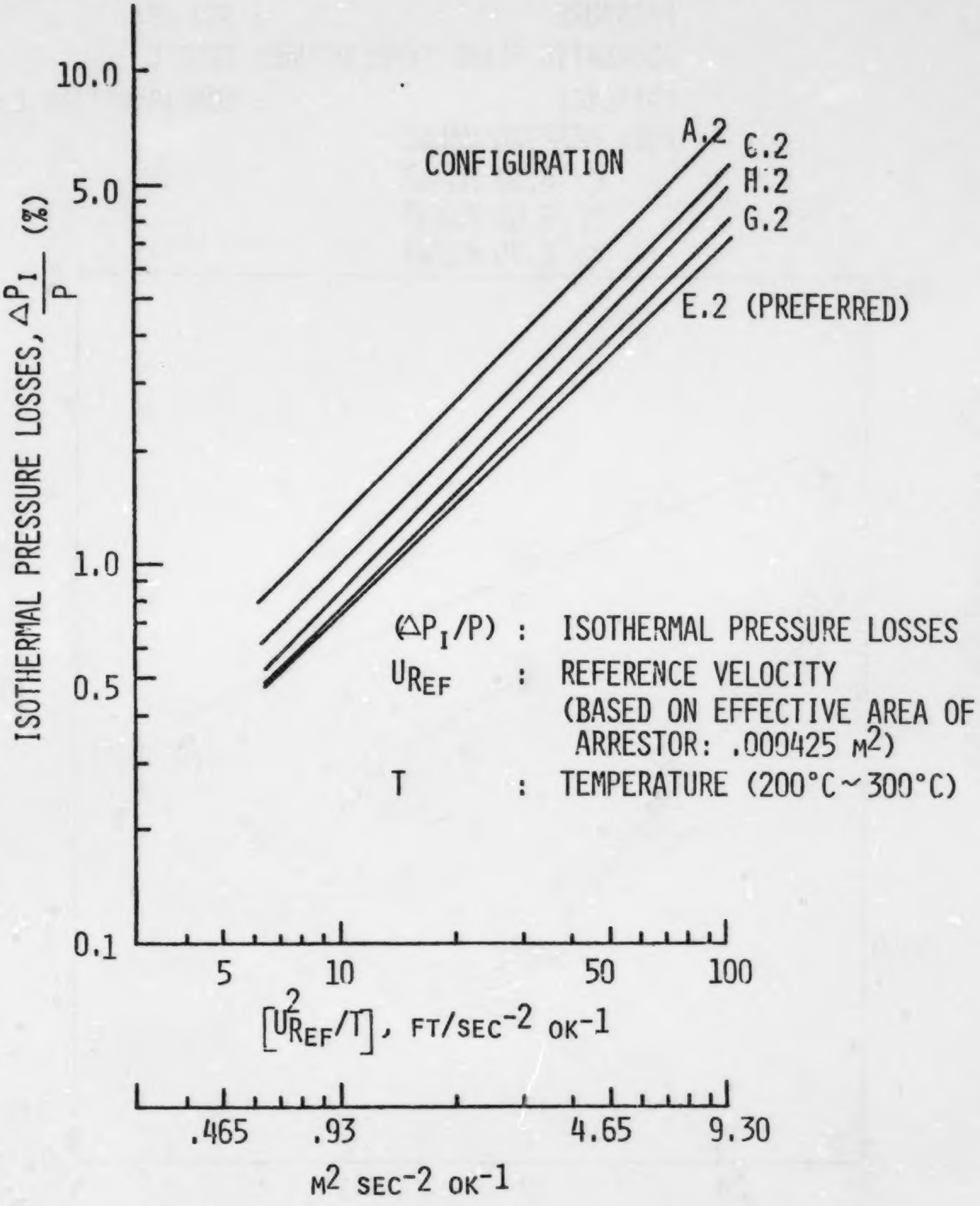

FIGURE 5. PERFORMANCE TEST RESULTS WITH LOW BTU FUEL

TEST CONDITIONS

INLET TEMPERATURE	: 150°C, 200°C, 300°C
PRESSURE	: 300 kPa
ADIABATIC FLAME TEMPERATURE	: 1260°C
CATALYST	: CONFIGURATION E.2

FUEL HEATING VALUE
- ○ 4.50 MJ/m^3
- □ 5.62 MJ/m^3
- ◇ 6.75 MJ/m^3

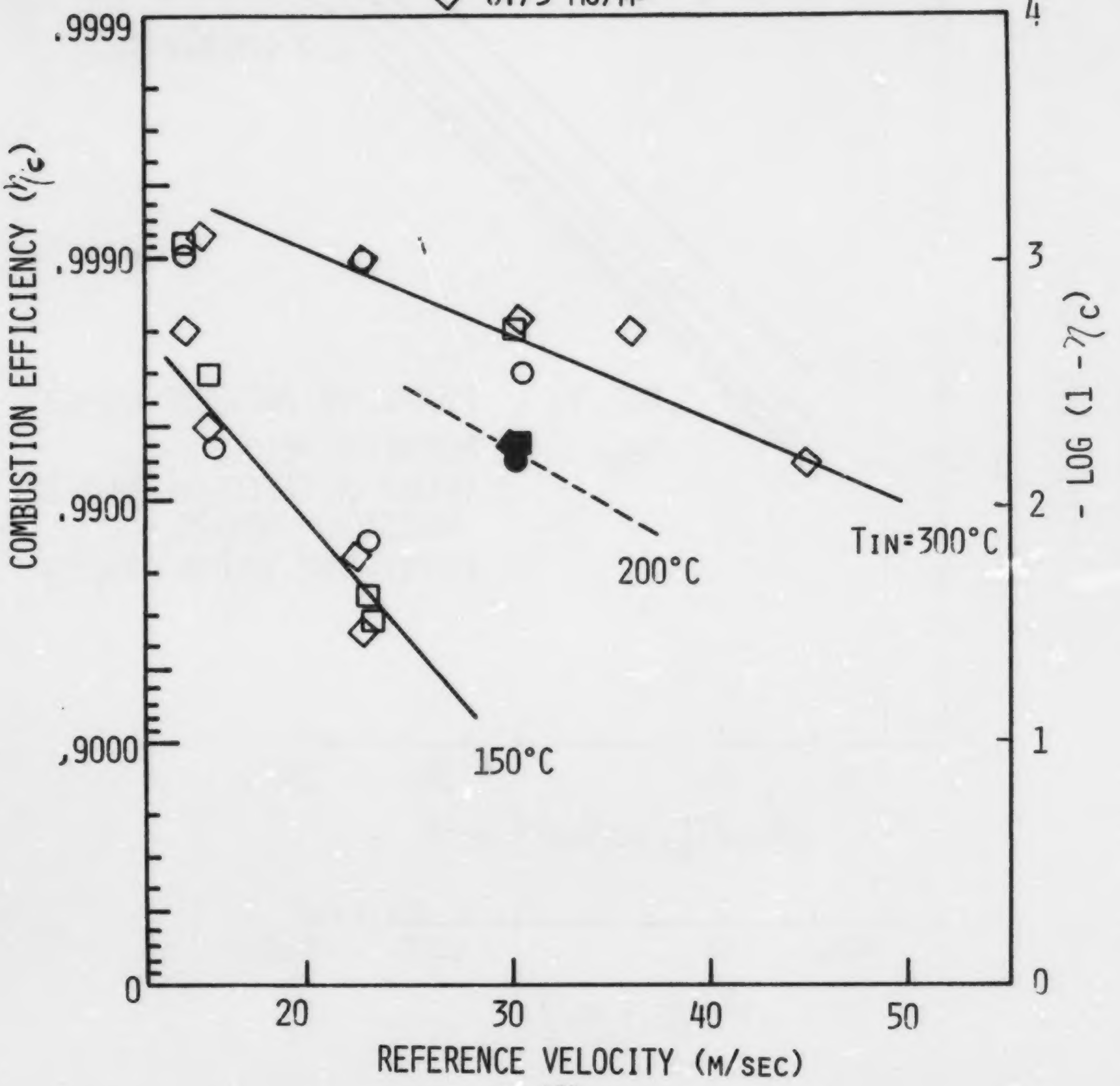

FIGURE 6. PERFORMANCE TEST RESULTS WITH MEDIUM BTU FUEL

PRESSURE : 300° kPa
ADIABATIC FLAME TEMPERATURE : 1260°C
CATALYST : CONFIGURATION E.2 (PREFERRED)
FUEL HEATING VALUE
△ : 7.5 MJ/m^3
○ : 12.0 MJ/m^3

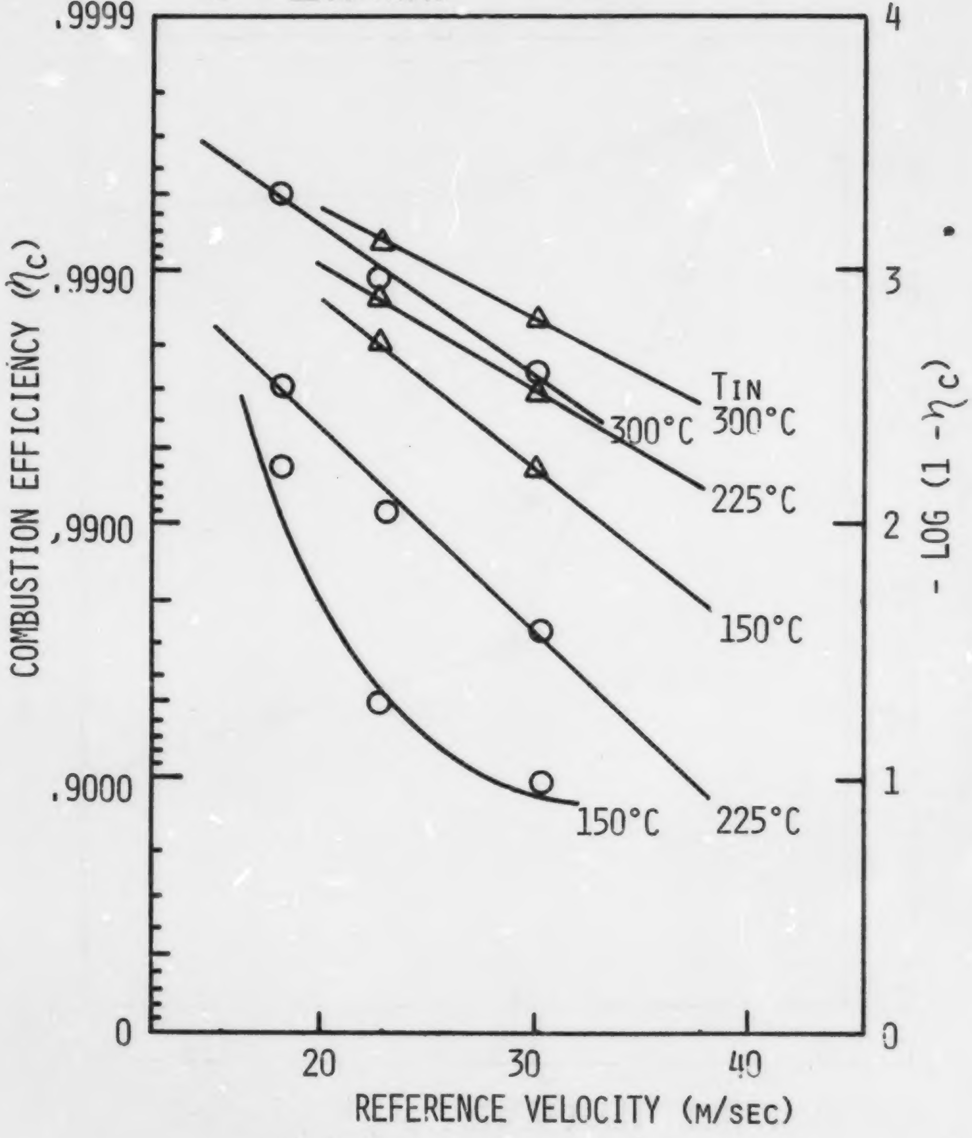

FIGURE 7 EFFECT OF INLET TEMPERATURE ON COMBUSTION EFFICIENCY

TEST CONDITIONS

REFERENCE VELOCITY : 30 M/SEC (@ 150°C)
ADIABATIC FLAME TEMPERATURE: 1260°C
CATALYST : CONFIGURATION E.2 (PREFERRED)
FUEL HEATING VALUE
△ : 7.5 MJ/M^3
○ : 12.0 MJ/M^3

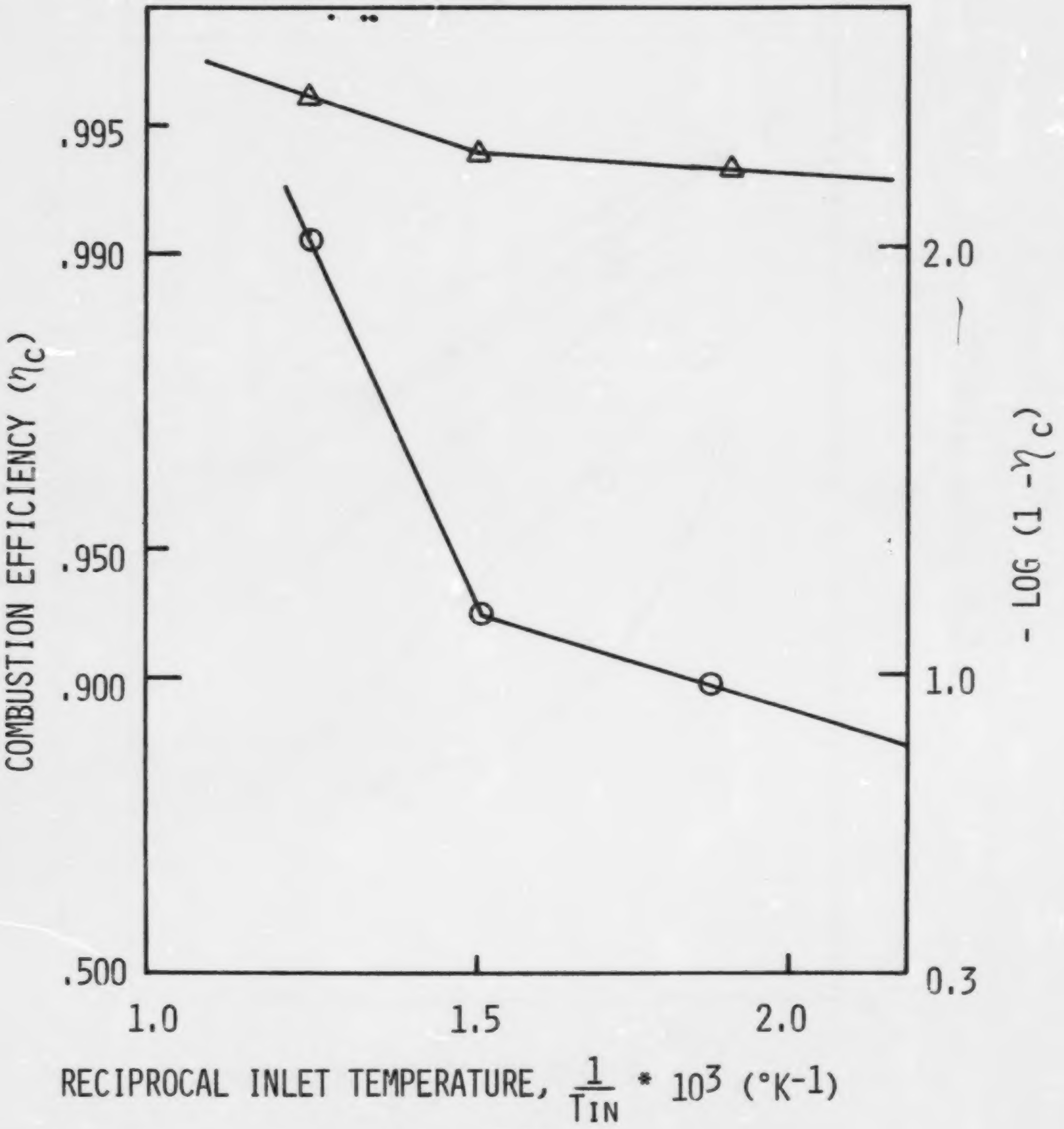

FIGURE 8. EFFECT OF HYDROGEN IN FUEL

TEST CONDITIONS

INLET TEMP. = 225°C
PRESSURE = 200 kPa
REFERENCE VELOCITY = 30.0 m/sec
FUEL HEATING VALUE = 7.5 MJ/m^3
CATALYST = CONFIGURATION E.2 (PREFERRED)

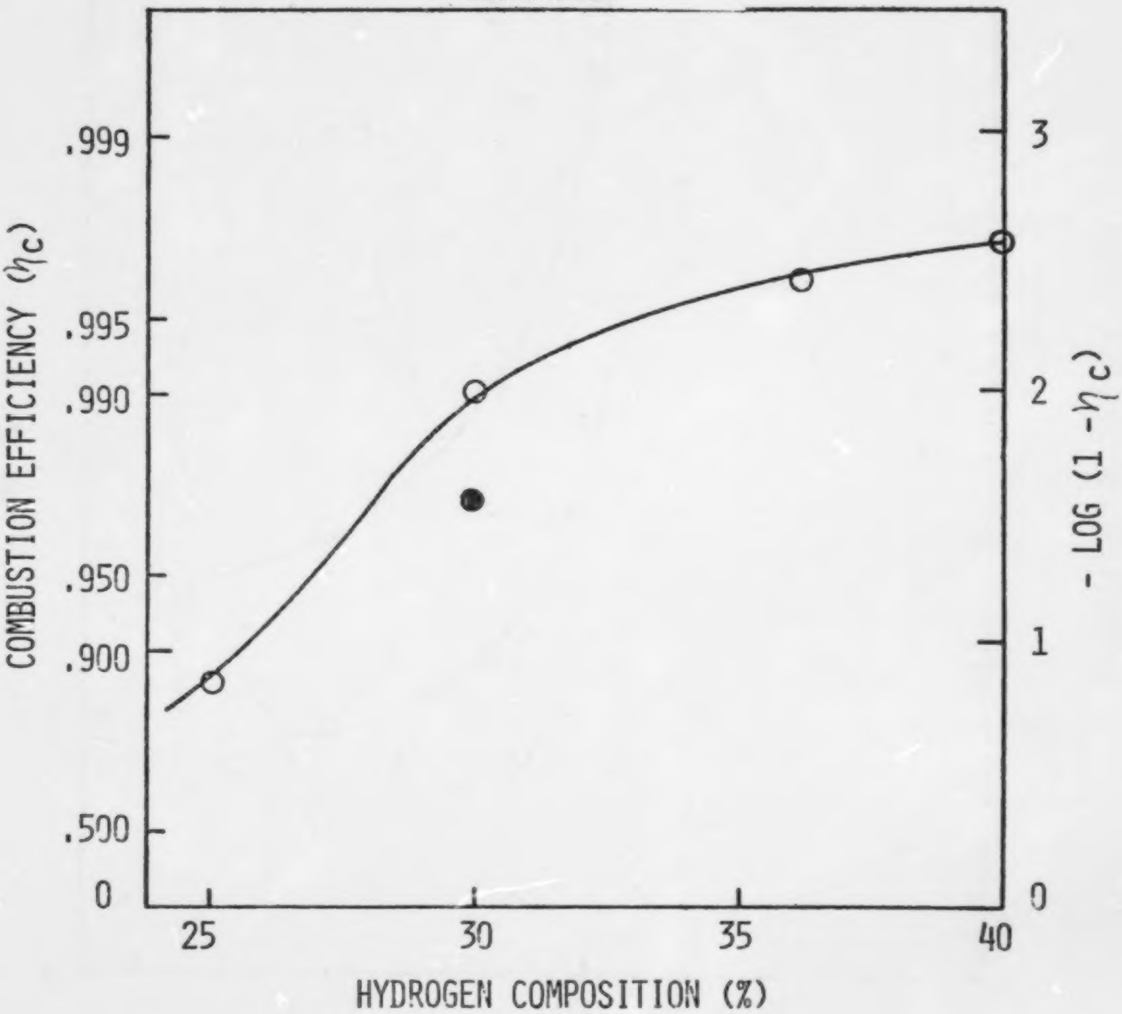

FIGURE 9. COMBUSTION EFFICIENCIES OF CO AND CH_4

TEST CONDITIONS

INLET TEMP.	: 150°C
PRESSURE	: 300 kPa
FUEL HEATING VALUE	: 12.0 MJ/m^3
FUEL/AIR	: 0.266 MOLES/MOLE
CATALYST	: CONFIGURATION E.2 (PREFERRED)

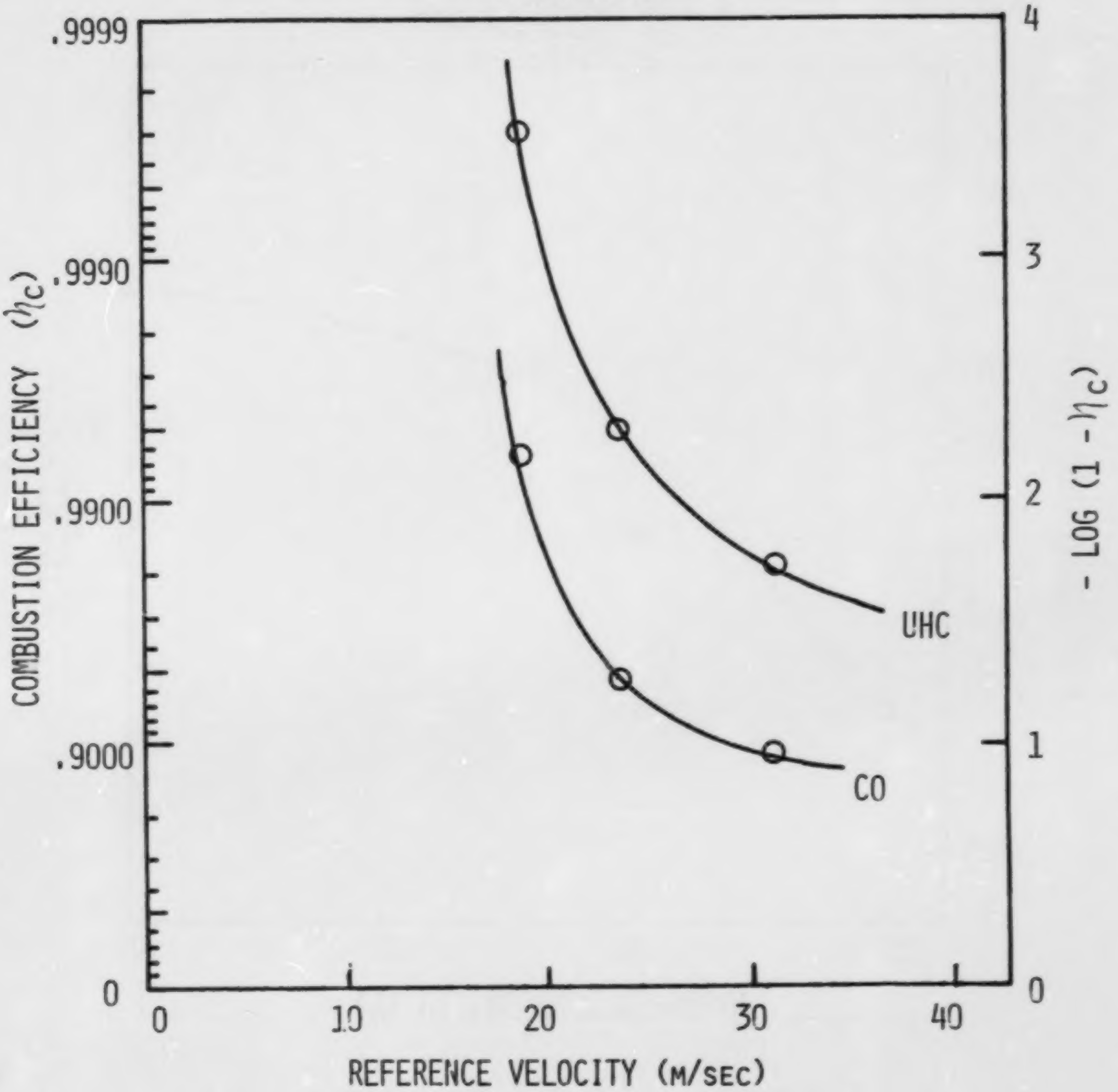

FIGURE 10. EFFECT OF ADIABATIC FLAME TEMPERATURE AT 300°C INLET TEMPERATURE

TEST CONDITIONS

INLET TEMPERATURE : 300°C
REFERENCE VELOCITY : 30 M/SEC
PRESSURE : 300 KPA
FUEL HEATING VALUE : 12.0 MJ/M^3
CATALYST : CONFIGURATION E.2 (PREFERRED)

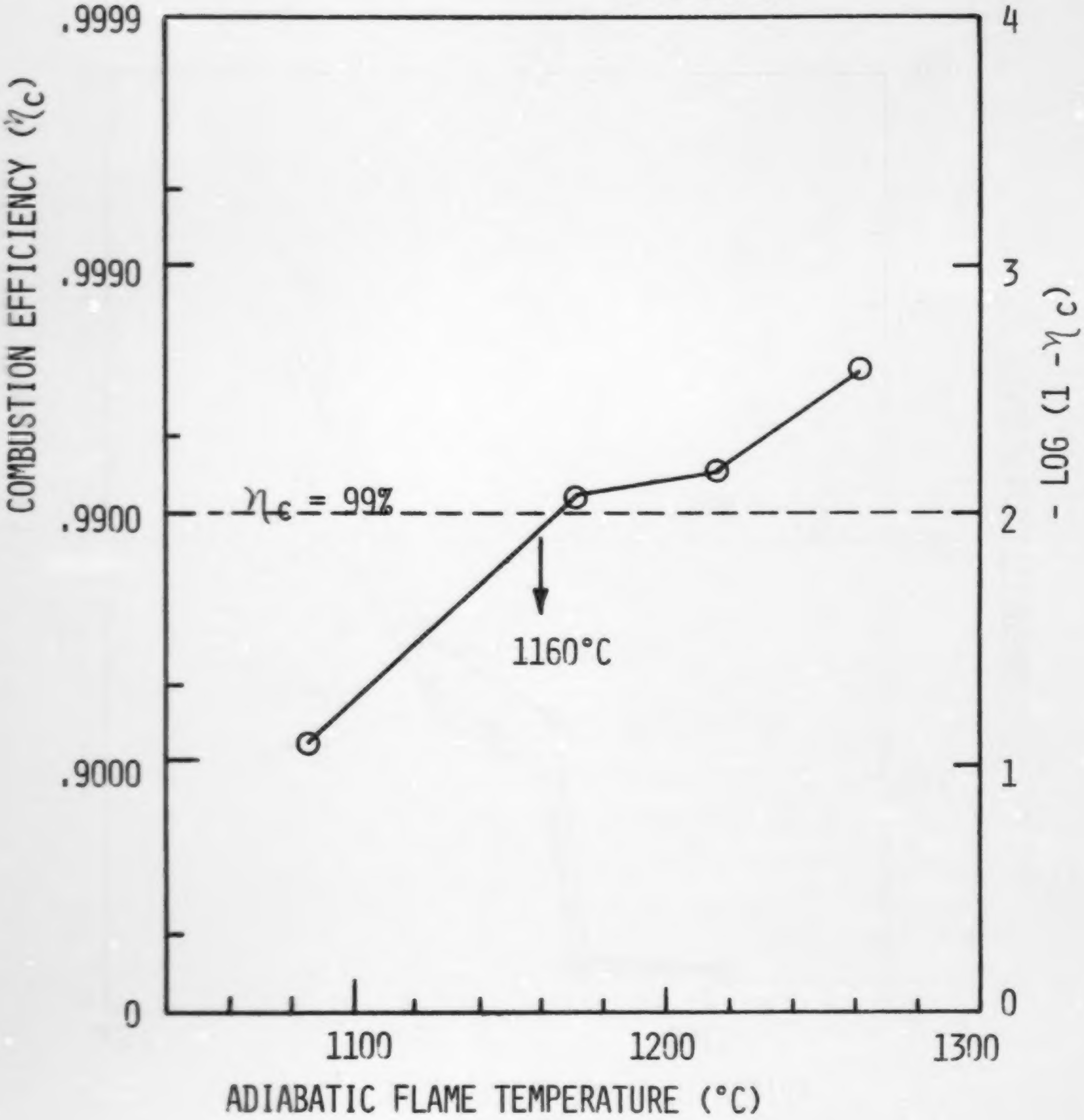

FIGURE 11. EFFECT OF ADIABATIC FLAME TEMPERATURE ON MEDIUM BTU FUEL AT 250°C INLET TEMPERATURE

TEST CONDITIONS

INLET TEMPERATURE : 250°C
PRESSURE : 100~400 kPa
FUEL HEATING VALUE : 12.0 MJ/m^3
CATALYST : CONFIGURATION E.2 (PREFERRED)
REFERENCE VELOCITY
○ 30 m/sec
□ 23 m/sec
△ 18 m/sec

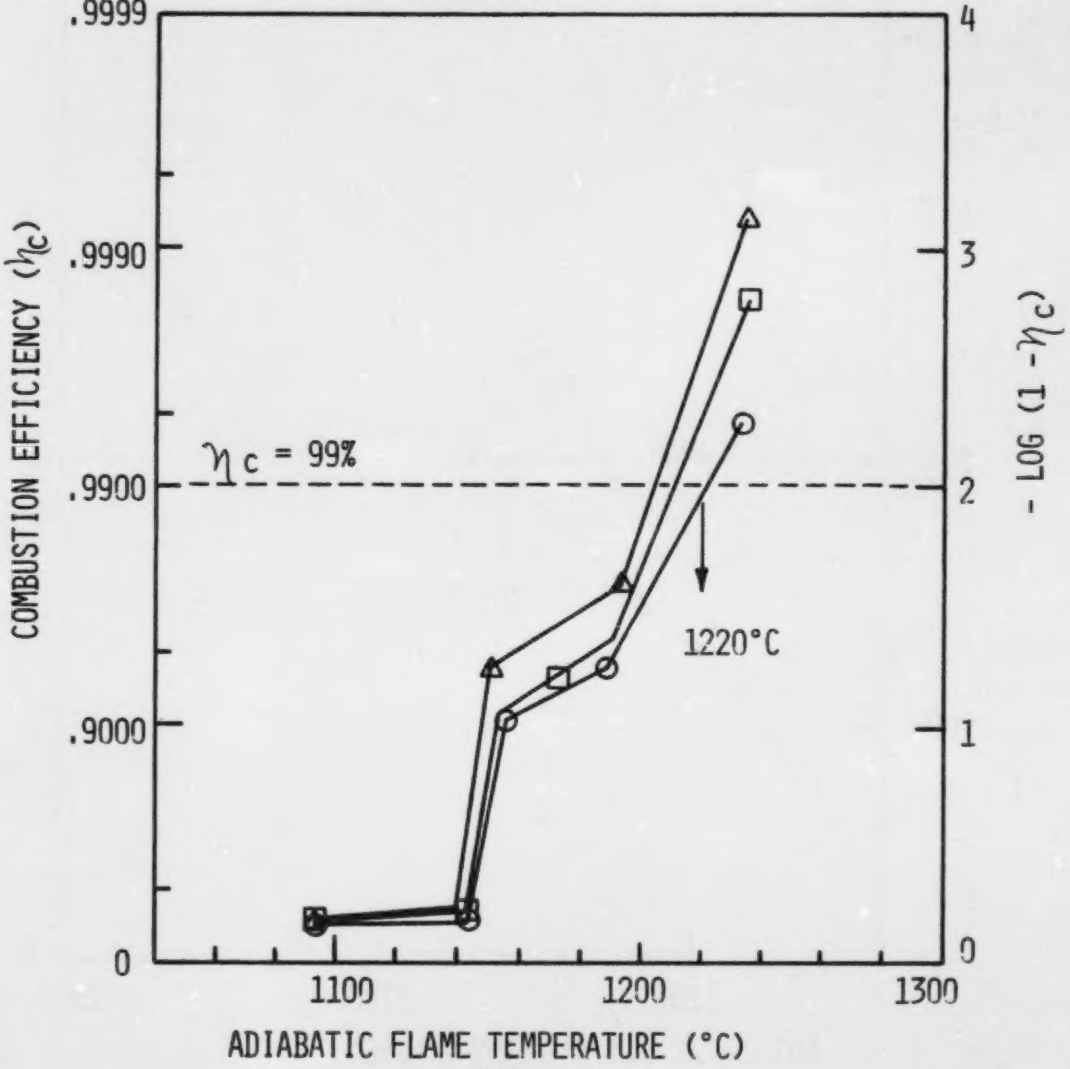

FIGURE 12. REGION OF OPERABILITY FOR LOW AND MEDIUM BTU GAS FUELS

- BOUNDARY FOR LOW BTU GAS : BELOW SOLID LINE
- BOUNDARY FOR MEDIUM BTU GAS: BELOW DOTTED LINE
- LOW BOUNDARY OF REFERENCE VELOCITY WILL BE DETERMINED BY FLASHBACK CRITERIA FOR LOW AND MEDIUM BTU FUELS.

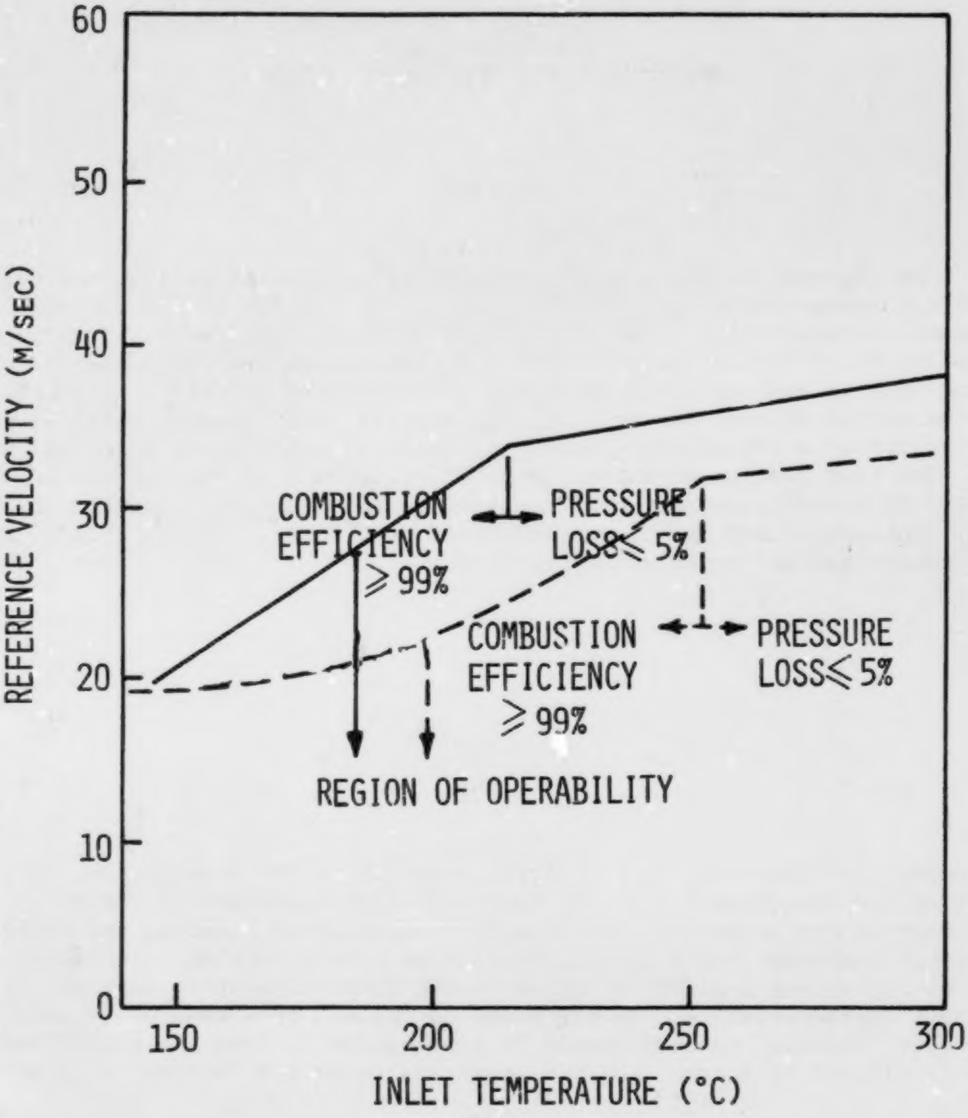

CATALYTIC COMBUSTION OF ALTERNATIVE FUELS

By:

Henry Tong, Edward K. Chu, and Gerry C. Snow
Acurex Corporation/Energy & Environmental Division
485 Clyde Avenue
Mountain View, California 94042

ABSTRACT

In the past 2 years, Acurex has conducted several programs on the catalytic combustion of alternative fuels. The results from three of these programs are described. The first program used a simulated LBtu gas to define the problems of burning gasifier fuels at low combustion temperatures. The second program evaluated the performance of different catalytic reactors for the combustion of coal derived liquids, and the third program examined the feasibility of a radiatively cooled catalytic flameholder of heavy No. 6 fuel oil. The test results show that these alternative fuels can be burned efficiently with catalytic reactors; however, problems unique to combinations of fuel, application and operating conditions need to be resolved before significant commercialization of catalytic combustors.

Note:

The purpose of this note is to correct an error in the presentation of this paper by the senior author at the Fourth Catalytic Combustion Workshop. In the study on the catalytic combustion of coal-derived liquids, the third catalytic combustor was a reactor fabricated from a Corning proprietary monolith with platinum applied by Acurex to the first element to improve the lightoff characteristics. In the paper to follow, this reactor is referred to as the "Corning" reactor simply to distinguish it from the second reactor, also fabricated by Acurex, which is referred to as the "Acurex" reactor.

INTRODUCTION

In the next 10 years we expect to see significant changes in power generation equipment. This will be a consequence of efforts to minimize our dependence on foreign oil, increasingly stringent emissions requirements and an increasing awareness to be energy efficient. For gas turbine engines, this has resulted in many programs to develop efficient, low emissions combustor concepts that can handle high nitrogen and/or low energy content fuels. Some of the combustor concepts that show significant benefits use catalytic combustion and much of the past research and development contributions have come from Engelhard and Westinghouse. More recently, many more groups have joined in the development of catalytic combustion as reflected in the agenda of this and past catalytic workshops.

In much of the current combustor research, especially as it relates to gas turbines, catalytic combustion is compared with lean premixed prevaporized (LPP) combustion systems. Although one can easily evoke a significant debate on the relative benefits of catalytic and LPP combustion, the authors feel that catalytic combustion is really a special LPP combustor in which the flame is initiated and stabilized by a catalytic surface. Except for some studies on the catalytic combustion of partially vaporized liquid droplets, most catalytic combustion concepts have a fuel preparation section to mix and vaporize (in the case of liquid fuels) the fuel/air mixture to present a nearly homogeneous gaseous mixture to the catalyst.

With regard to the viewpoint that catalytic combustion is a special case of LPP, the concept may be applied to extend the flammability limits to very lean conditions as well as the blowout limits. Several small gas turbine power systems are designed around combustor temperature rises of a few hundred degrees. Mixtures this lean would be difficult if not impossible to burn (at least as premixed fuel and air). Thus catalytic combustion may allow greater flexibility in the design of gas turbine cycles.

More advanced fuel delivery systems or combustor sectoring concepts for both LPP and catalytic combustors may be necessary to obtain the full range of turndown required for most gas turbine applications. System complexity must therefore increase if these combustors are used to control emissions. Additional research work will be required to minimize these complexities to achieve an acceptable level of system reliability.

In the past two years we have completed several research and development programs to attain a better understanding of catalytic combustion characteristics with the hope of applying this knowledge to design and demonstrate low emissions, high efficiency gas turbine combustors. The objectives of these studies were to examine the feasibility of catalytic combustion concepts, evaluate catalyst stability and lifetime, evaluate fuel nitrogen conversion and the generation of other pollutants and to measure combustion efficiency.

In this paper we will summarize the results of the following studies:

- Catalytic combustion of simulated low Btu gas (internal R&D)
- Catalytic combustion of coal derived liquid fuels (funded by EPRI)
- Rich flameholder for heavy fuels (funded by UTRC)

CATALYTIC COMBUSTION OF SIMULATED LOW BTU GAS

The objective of this experimental program was to determine some of the combustion characteristics of low Btu gases from typical state-of-the-art coal gasifiers. For these evaluations it was not practical to use a "real" gasifier product so a premixed synthetic gas was used to simulate the products from a Wellman-Galusha gasifier. The molar composition of this test gas was 29.4% CO, 15.4% H_2, 2.8% CH_4, 3.4% CO_2, and 49.0% N_2. The heating value of this gas was about 170 Btu/ft^3. The stoichiometric air/fuel ratio was about 1.3 by volume.

Since a small amount of sulfur will be present in typical gasifier products (even after a water wash), the target turbine inlet temperature was selected to be less than 1600°F to minimize sulfur corrosion. This temperature is also representative of turbine inlet temperatures for many small gas turbine engines.

The catalytic reactor was a two-size graded cell configuration as shown in Figure 1. However, since the test gas contained a modest amount of hydrogen, grading was probably not necessary and similar results are likely with a catalyst of only fine cells. Past experience with similar materials as in this reactor has shown that about 3 inches of total length was sufficient for complete combustion of methane or propane at temperatures greater than 2100°F. However, a longer configuration was selected for these tests because of the low design combustion temperature which may limit the occurrence of the gas phase combustion, especially CO and methane.

Data was obtained for stoichiometries ranging between 260 and 762 percent theoretical air and for air preheat temperatures between 200 and 850°F. Because there was no model fuel bound nitrogen compounds and the combustion temperatures were low (1000 to 1900°F), NO_x emissions were too small to be of interest. Unburned hydrocarbons and CO emissions are shown in Figures 2 and 3. Also shown in Figure 2 are the lines of constant bed temperature. As might be expected, CO and hydrocarbons increase as the bed temperature decreases; however, the CO concentrations are significantly below theoretical if none of the initial CO was oxidized. This would imply that the governing factor for efficient combustion of this synthetic fuel is the rate at which CH_4 is oxidized. CO that is in the fuel apparently oxidizes quite rapidly, perhaps due to catalytic combustion and the presence of water vapor. This is probably true even at low combustion temperatures. However, the CH_4 oxidation reactions are much slower than H_2 reactions at low preheat temperatures and therefore take place further into the reactor bed when the bulk gas temperature is sufficiently heated as a result of H_2 and CO combustion. CO formed here apparently has insufficient residence time to oxidize. Interestingly, at low preheat and high theoretical air (low bed temperatures) the sum of CO and hydrocarbons is the same magnitude as the input concentration of CH_4 (~12,000 ppm). These emissions could probably be reduced by higher reactor temperatures, longer catalyst beds, finer monolith cells, or lower frontal velocities.

CATALYTIC COMBUSTION OF COAL DERIVED LIQUID FUELS

The objective of this study was to determine the effect of coal derived liquid (CDL) fuels on catalytic reactors. The basic scenerio of interest was to assume that petroleum distillate fueled catalytic combustors will be used in future utility gas turbines. In the event of a shortage of these fuels, the utilities may elect to use CDL fuels temporarily. If this were the case, it would be important to know if the catalyst would be poisoned or deactivated by the CDL, or whether the catalyst would suffer any permanent change in performance characteristics when the utility returns to distillate fuels. A longer term interest was to understand the mechanisms which lead to catalyst deactivation, especially with CDL fuels, and possibly identify ways to improve catalytic reactors.

CDL fuels, in many respects, are much different from petroleum distillates. For example, the carbon/hydrogen ratios of most CDLs are larger than those for petroleum fuels. The heteroatom concentrations such as nitrogen and oxygen are also larger. These differences and the metallic contaminants in CDL fuels may lead to deactivation of catalytic reactors.

In this experimental program, two CDL fuels, SRC II (350^{o}F-850^{o}F distillation range) and H-coal distillate (300^{o}F-500^{o}F distillation range) were used. The SRC II was obtained from the pilot plant in Tacoma, Washington, and is a 5:1 blend of middle and heavy distillates. The H-coal was obtained from Hydrocarbon Research, Inc. of New Jersey and was produced from the distillation of atmosphere overhead products. Chemical analyses for these fuels are shown in Table 1. Also shown in this table is the chemical analysis for a diesel fuel that was used as a baseline fuel. The carbon contents of these fuels are almost identical; however, the hydrogen content for SRC II is lower than that for H-coal which in turn is lower than for diesel. Typical physical properties for all three fuels are shown in Table 2.

The above fuels were tested on three reactor systems. The first reactor was a proprietary noble metal (UOP) catalyst on a washcoated zirconia spinel. This was a high activity reactor. The second reactor was an Acurex reactor with a 2 weight percent platinum loading on a Torvex alumina substrate. No washcoat was used. The third reactor was a Corning proprietary monolith with 2 weight percent platinum (applied by Acurex) to the first element. Each reactor was a graded cell configuration composed of five 1-inch thick elements to form a reactor 5 inches long and 2-1/2 inches in diameter.

Combustion data were obtained under fuel-rich and fuel-lean conditions, as shown in Table 3, for a combustion pressure of 1 atm. Additional combustion data were also obtained at 3 atm for fuel-lean conditions using H-coal and the UOP reactor; however, this data will not be presented.

Both lean and rich combustion tests were started by first passing 30 to 40 ft/sec preheated air through the reactor bed until the bed reached a steady state temperature of about 700°F. Initial lightoff was achieved with propane and used to stabilize the reactor at a nominally fuel-lean stoichiometry. The system was then transitioned over to a liquid fuel test condition. This lightoff procedure was generally completed in about 20 minutes. Rich combustion conditions were achieved following a lean lightoff by rapidly decreasing the combustion air flowrate while maintaining a fixed fuel flowrate. This procedure was complete quickly enough so that the system thermal inertia prevented reactor overheating as the equivalence ratio passed momentarily through unity. Since the combustion temperature at the desired fuel-rich condition was greater than maximum allowable reactor temperatures, nitrogen diluent was mixed and preheated with the combustion air.

The fuel-lean combustion efficiencies at 1 atm pressure are shown in Figures 4, 5, and 6 for each of the reactor systems. Except for the Corning reactor where diesel baseline data were not run, it can be seen that the combustion efficiencies for H-coal and diesel are essentially 100 percent for face velocities between 40 and 85 ft/sec. (This upper velocity is the maximum flowrate capability of the test facility.) For H-coal at the higher velocities, a very slight decrease in combustion efficiency was observed for the Corning reactor. Also shown on these figures are the combustion efficiencies for SRC II. Generally this combustion efficiency is a few tenths of a percentage point lower than that for H-coal or diesel. Except perhaps for the Corning reactor, this reduced efficiency is probably unimportant at low face velocities; however, a rapid decline, indicating breakthrough, is seen at the higher face velocities. Each of the three reactor systems are less active for SRC II than for the other two fuels.

Fuel nitrogen conversion for each reactor with H-coal is shown in Figures 7, 8, and 9 for equivalence ratios between 0.4 and 1.3.* Each reactor was held at constant temperature with nitrogen diluent. The UOP and Corning reactors show nearly 100 percent conversion to NO_x under fuel-lean conditions. The conversion decreased to about 80 percent at $\phi = 1.0$ and continues to decrease as ϕ becomes greater than 1.0. Although there is significant data scatter, the Acurex reactor achieved only 80-90 percent conversion under fuel-lean conditions and increased to about 100 percent at $\phi = 1.0$. The remaining data are not conclusive about the conversion for ϕ greater than 1.0. As has been demonstrated previously with other fuels, catalytic combustion under lean conditions is, unfortunately, very efficient for converting fuel nitrogen to NO_x. Also as expected, rich combustion converts a significantly smaller fraction of fuel nitrogen to NO_x and NH_3 with the lowest values obtained on the UOP reactor.

The conversion of fuel nitrogen in SRC II on the UOP reactor is shown as a function of equivalence ratio in Figure 10. Data for the other reactors were not taken because fuel-rich combustion was unstable and steady conditions could not be achieved. Fuel nitrogen conversion with SRC II shows the same trend as with H-coal except that the fuel-rich percent conversion is lower. However, the fuel nitrogen content of SRC II is about a factor of 3 (by weight) greater than for H-coal.

Reactor degradation (combustion efficiency) is shown as a function of time in Figures 11, 12, and 13 for lean combustion conditions. With H-coal, all reactors performed fairly well even though some gradual degradation was observed. With SRC II, lean stable combustion could not be maintained for the Acurex and Corning reactors so data for these tests are not shown. Although the UOP reactor behaved better, it too would not maintain steady operating conditions. This is exhibited in the combustion efficiencies shown in Figure 12.

Under SRC II fuel-rich conditions, neither the UOP nor the Acurex reactors behaved acceptably. Deactivation of the catalysts was very rapid.

---

*Because the fuel sulfur emissions interfered with the specific ion electrode technique used to measure HCN, only NH_3 and NO_x conversions are shown.

No rich SRC II tests were conducted with the Corning reactor since its deactivation time was already very short, about 20 minutes, for lean SRC II combustion conditions.

With H-coal under fuel-rich conditions, significant deactivation of the Acurex and Corning reactors was observed after less than 1 hour of combustion testing. The UOP reactor was tested for 7 hours of rich H-coal combustion with no significant degradation in performance.

The results of this experimental study show that CDL fuels could be effectively combusted with the right choice of catalyst. However, long term durability data is insufficient to evaluate the potential lifetime of catalytic reactors. Of the two fuels tested, SRC II had a greater detrimental effect on the reactors than H-coal and of the three reactors, the high dispersion noble metal catalyst (UOP) was the least affected. Lean catalytic combustion resulted in essentially 100 percent conversion of fuel nitrogen to NO_x and although unacceptable for normal utility operations, this may be acceptable in emergency situations. Fuel-rich combustion, which in a rich-lean configuration may control fuel nitrogen conversion, was demonstrated only for the UOP catalyst although some degradation and reduced performance was observed with SRC II.

RICH FLAMEHOLDER FOR HEAVY FUELS

The objective of this test was to evaluate the performance of a rich burn catalytic flameholder which could be part of a rich burn quick quench combustor. The intent was to operate the flameholder at the rich stoichiometry which produced minimum NO_x and precursors without diluent gases. This would be achieved with a highly nonadiabatic catalytic reactor with radiation as the principal energy loss mechanism. In addition, data were also obtained over a range of theoretical air between 70 and 170 percent. No. 6 fuel oil, with the properties shown in Table 4, was used in all tests.

Two different catalytic flameholders were tested without noticeable differences in performance. The first was a noble metal on a proprietary Corning monolith and the second was a noble metal on Torvex alumina. In both cases, the monolith was 1 inch long and had a nominal cell size of about 1/4 inch.

Results from this test series are shown in Figure 14. The rich burn minimum was observed to occur between 70 and 80 percent theoretical air. In this range the flameholder temperature was about 2100°F to 2300°F and is a practical temperature for available materials.

A major problem encountered in these tests was a buildup of ash and coke which caused blockage of the flameholder. In most cases under fuel-rich operation, the deposit buildup starts at the outer ceramic wall of the catalyst holder at the front face of the reactor. To minimize these problems, it was necessary not to have any flow discontinuities in the tube walls upstream of the catalyst. However, the flameholder monolith physically obstructs about 15 percent of the cross sectional area, causing a natural adverse gradient and flow interference. Even under the best of conditions some deposition of ash/coke occurred at these leading edges. These small depositions did not cause the termination of any tests.

From these tests we conclude that stable combustion can be achieved at high heat release rates under fuel-rich conditions based on a radiatively cooled catalytic flameholder. In addition, the usual minimum in NO_x conversion was observed under fuel-rich conditions. Fuel-lean conversions were similar to conventional flame values. Ash/coke buildup could lead to catalyst plugging or poisoning. The severity of this problem is related to the stoichiometry, flow patterns, and degree of vaporization.

SUMMARY

In the above discussion, we have presented a brief summary of some studies that we have conducted to evaluate the performance of catalytic combustors with alternative fuels. The results show that various alternative fuels can be efficiently burned with catalytic reactors; however, problems which may be unique to the combination of fuel, application, and operating condition still exist. We believe some of the more significant problems are not conceptual but materials and systems related. It is hoped that enough of these will be overcome in the next few years so that the benefits of catalytic combustion can be applied to gas turbine engines.

TABLE 1. FUEL CHEMICAL PROPERTIES

Analysis Type	Analysis Technique	SRC II	H-Coal	Diesel
Elemental Analysis, wt %				
Carbon	ASTM E191	86.09	86.20	86.62
Hydrogen		9.09	11.19	12.90
Nitrogen	ASTM E258	0.86	0.31	0.035
Sulfur	ASTM D129	0.22	0.094	0.13
Ash	ASTM D482	0.011	0.010	0.003
Oxygen	By difference	3.74	2.08	0.31
Heat of Combustion, Btu/lbm				
Net		16,470	17,640	18,230
Gross		17,300	18,700	19,410
Trace Metals, ppm wt	Wet Chemical/ spectrographic			
Calcium		1.5/1.5	0.31/0.18	0.25/0.55
Iron		13.0/13.0	38.0/52.0	0.70/1.90
Manganese		0.22/0.26	0.07/0.11	<0.05/0.05
Magnesium		0.34/1.40	0.04/0.16	0.08/0.51
Nickel		0.11/0.10	0.08/0.03	<0.05/0.13
Vanadium		<1.0 /0.03	<0.04/0.003	<1.0 /----
Sodium		0.39/<0.10	0.15/----	0.14/0.02
Zinc		----/0.60	----/14.0	----/2.0
Copper		----/0.23	----/2.6	----/0.15
Silicon		----/24.0	----/0.18	----/5.70
Tin		----/1.03	----/0.32	----/0.26
Aluminum		----/13.0	----/0.50	----/1.10
Boron		----/0.31	----/0.06	----/0.03
Lead		----/0.17	----/0.27	----/0.66
Molybdenum		----/0.03	----/0.05	----/----
Titanium		----/0.85	----/0.02	----/0.11
Silver		----/0.002	----/0.001	----/0.007
Cobalt		----/0.02	----/0.005	----/----
Cadmium		----/0.15	----/0.17	----/0.35
Potassium		----/----	----/----	----/----
Phosphorus		----/----	----/----	----/0.26
Chromium		----/1.4	----/----	----/----

TABLE 2. FUEL PHYSICAL PROPERTIES

Physical Properties	SRC II	H-Coal	No. 2 Diesel
Flash point, °F	170	11.0	175
Pour point, °F	-60	-65	-10
Gravity, °API	10.3	29.5	32.0
Boiling range, °F	360-700	260-552	358-672
Kinematic viscosity, CS @ 100°F	4.42	1.17	2.61

TABLE 3. CDL SCREENING TEST MATRIX

Fuel	SRC II		H-Coal		Diesel	
Reactor	Lean	Rich	Lean	Rich	Lean	Rich
UOP	x	x	x	x	x	x
Acurex	x	x	x	x	x	x
Corning Active Monolith	x		x	x		

TABLE 4. CHARACTERISTICS OF #6 FUEL OIL

	#6 Fuel Oil
Gravity, °API	12.3
Moisture and sediment, %	0.005
Gross heat of combustion, Btu/lb	18,325
Viscosity at 100°F, SUS	4,894
Flash point, COC	182
Nitrogen, Dohrmann, ppm	---
Nitrogen, Coleman, %	0.81 0.82
Carbon, hydrogen, % Perkin Elmer	C = 85.57 H = 10.52
Sulfur, XRF, %	0.93
Ash, D 482, %	0.089
Trace elements, %	Al: 0.0012 Ca: 0.0086 Cr: 0.0006 Cu: 0.0002 Fe: 0.0075 Mg: 0.0033 Mn: 0.0004 Ni: 0.0085 Si: 0.0009 Ti: 0.0005 V: 0.0073 Zn: 0.0014 Pb: 0.0002 Ba: 0.0001 Mo: 0.0001

- CATALYST AND WASHCOAT
  - UOP PROPRIETARY
- SUPPORT
  - CORNING MCB-7 ZIRCONIA SPINEL
- GEOMETRY
  - 2" DIAM, 5-1/4" LONG, GRADED CELL

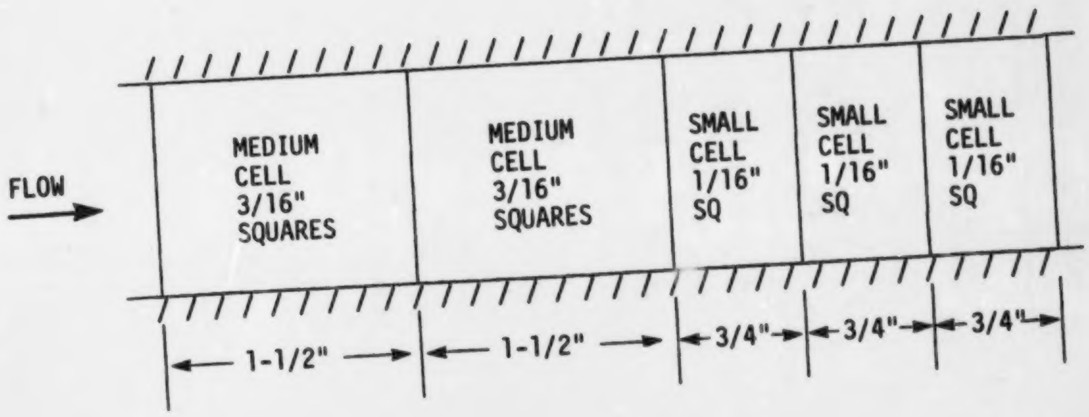
FLOW
MEDIUM CELL 3/16" SQUARES
MEDIUM CELL 3/16" SQUARES
SMALL CELL 1/16" SQ
SMALL CELL 1/16" SQ
SMALL CELL 1/16" SQ
1-1/2"
1-1/2"
3/4"
3/4"
3/4"

Figure 1. Catalytic Reactor for LBtu gas.

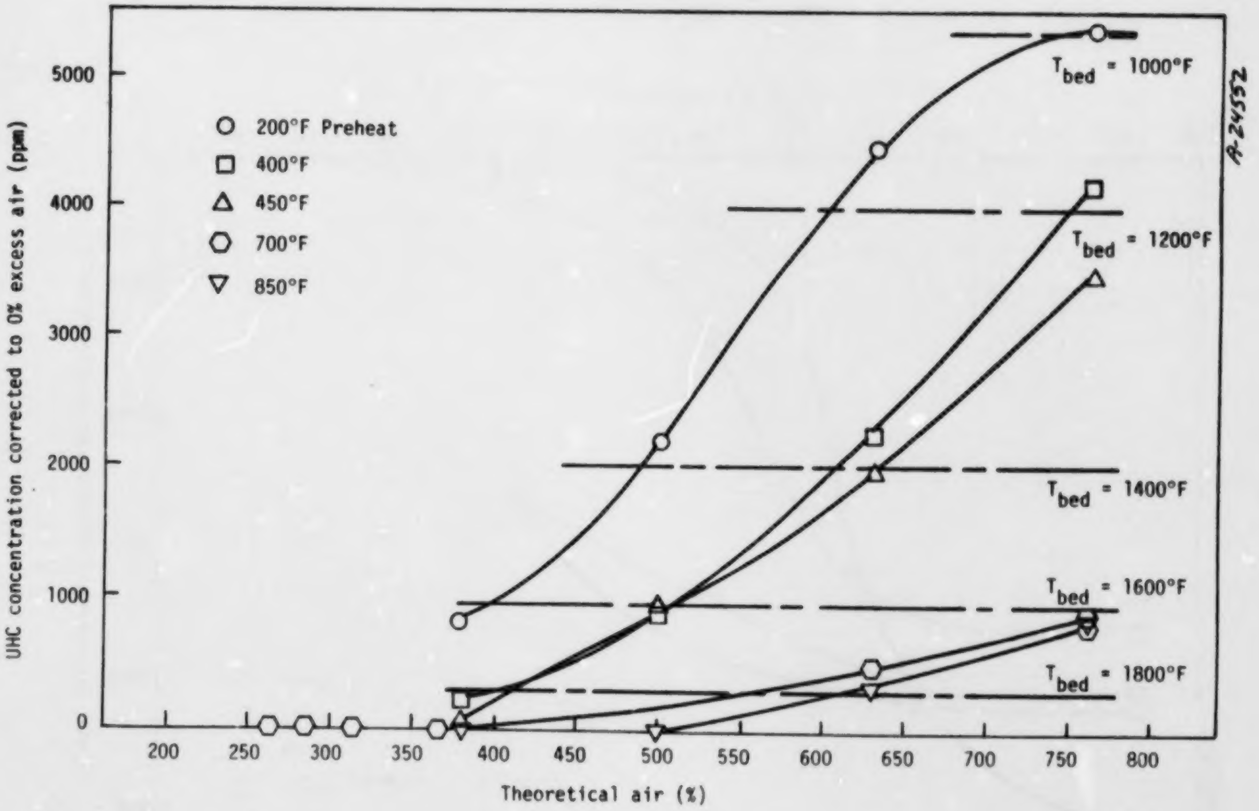

Figure 2. UHC as a function of theoretical air for LBtu gas.

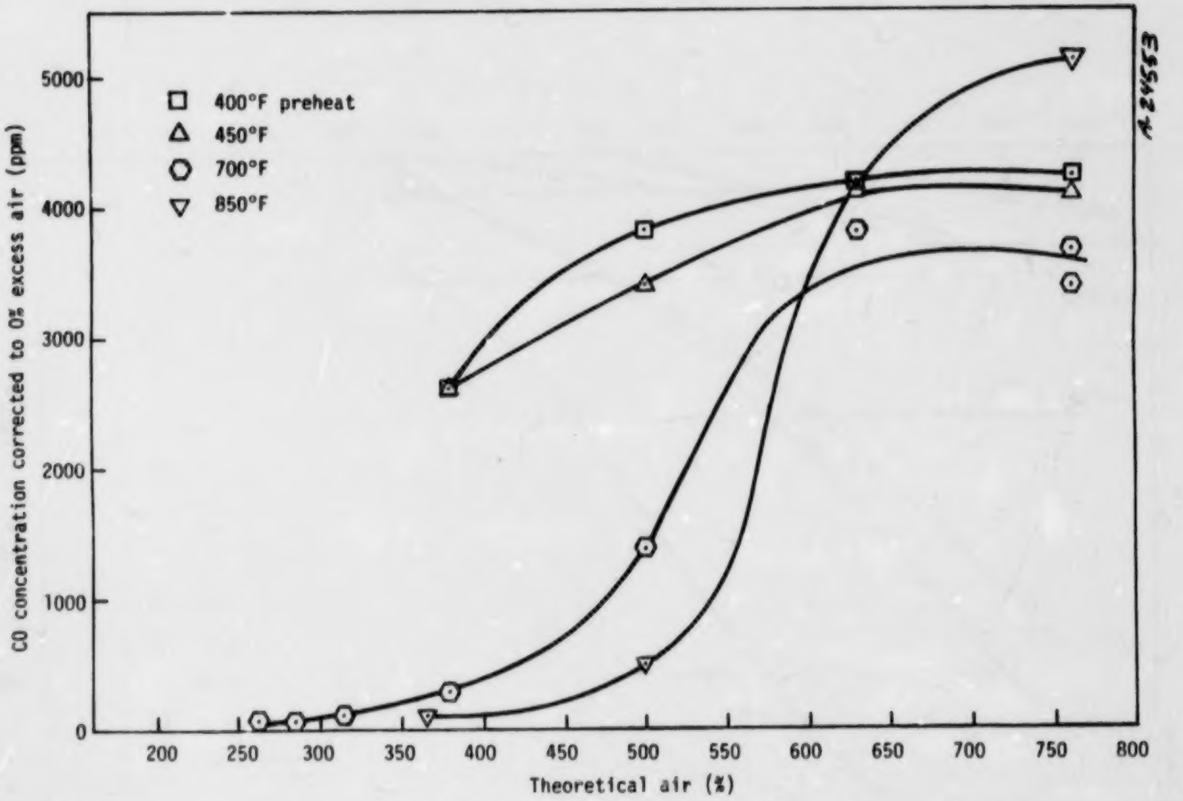

Figure 3. CO as function of theoretical air for LBtu gas.

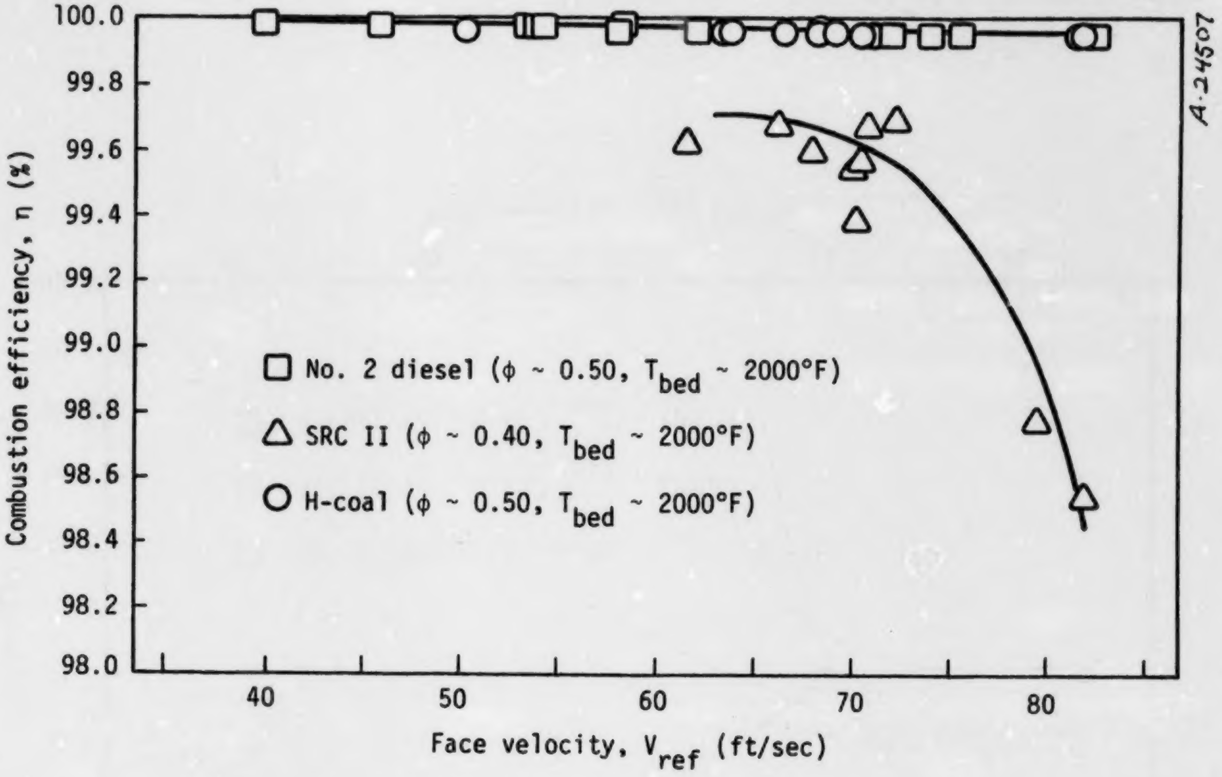

Figure 4. Fuel-lean combustion efficiency versus face velocity, UOP reactor.

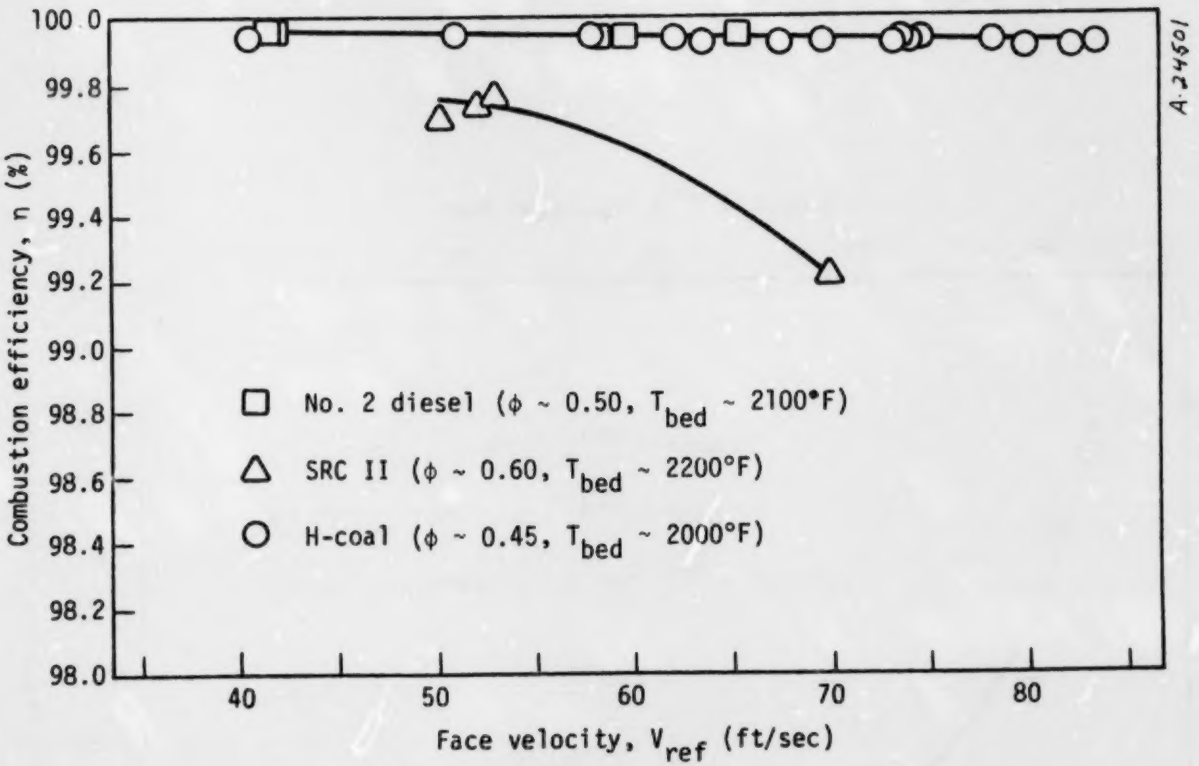

Figure 5. Fuel-lean combustion efficiency versus face velocity, Acurex reactor.

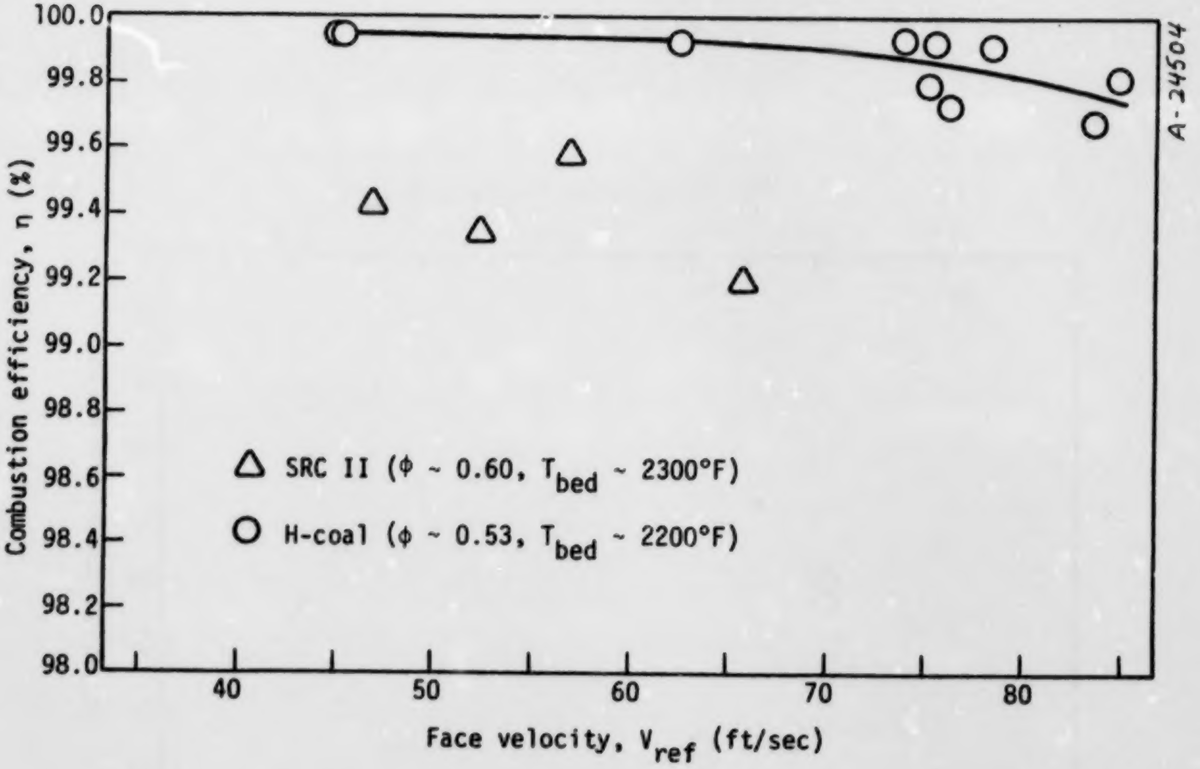

Figure 6. Fuel-lean combustion efficiency versus face velocity, Corning reactor.

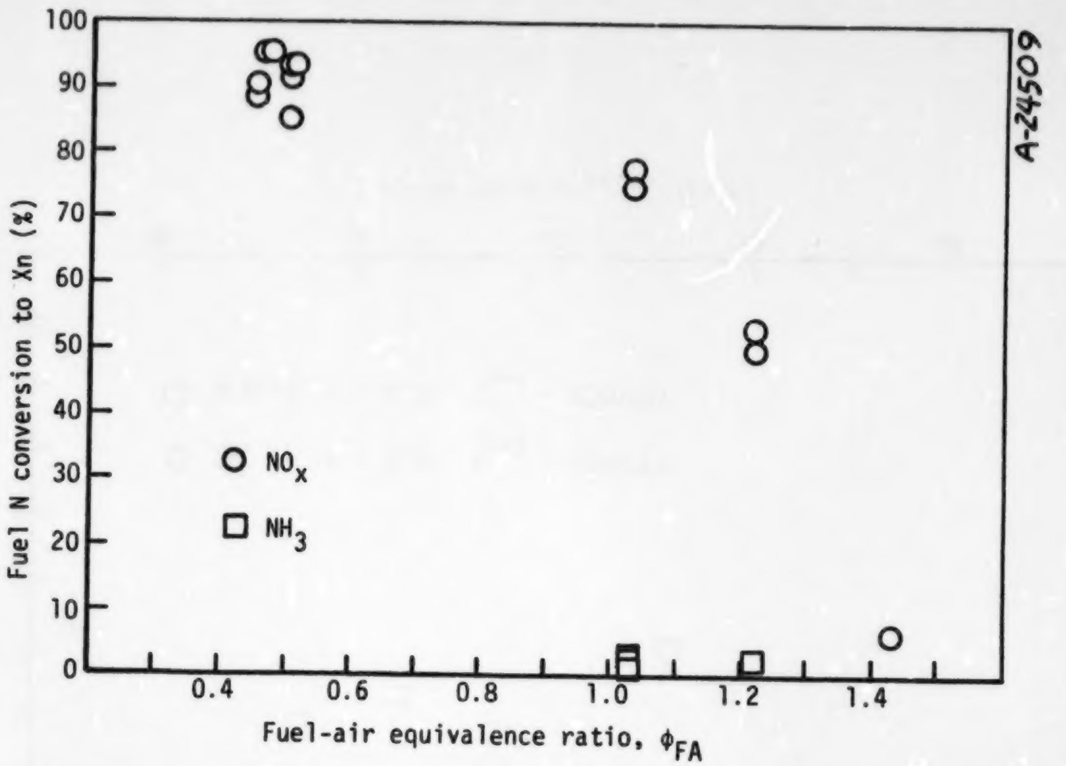

Figure 7. Fuel-N conversion to XN, UOP reactor, H-coal.

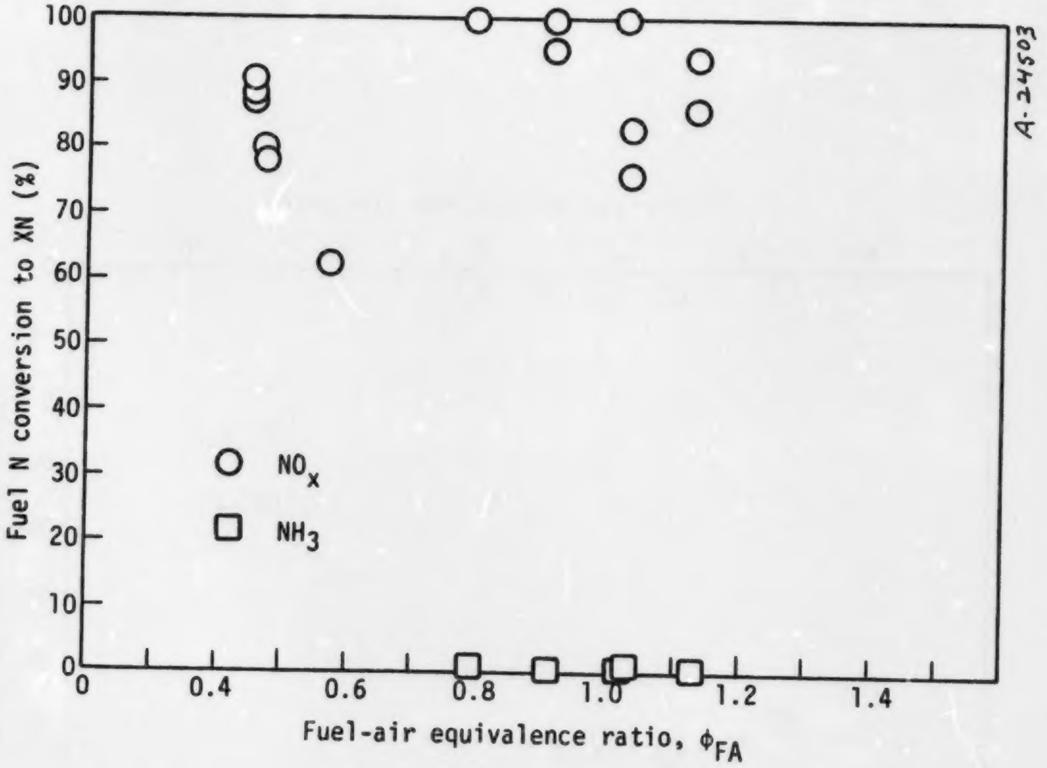

Figure 8. Fuel-N coversion to XN, Acurex reactor, H-coal.

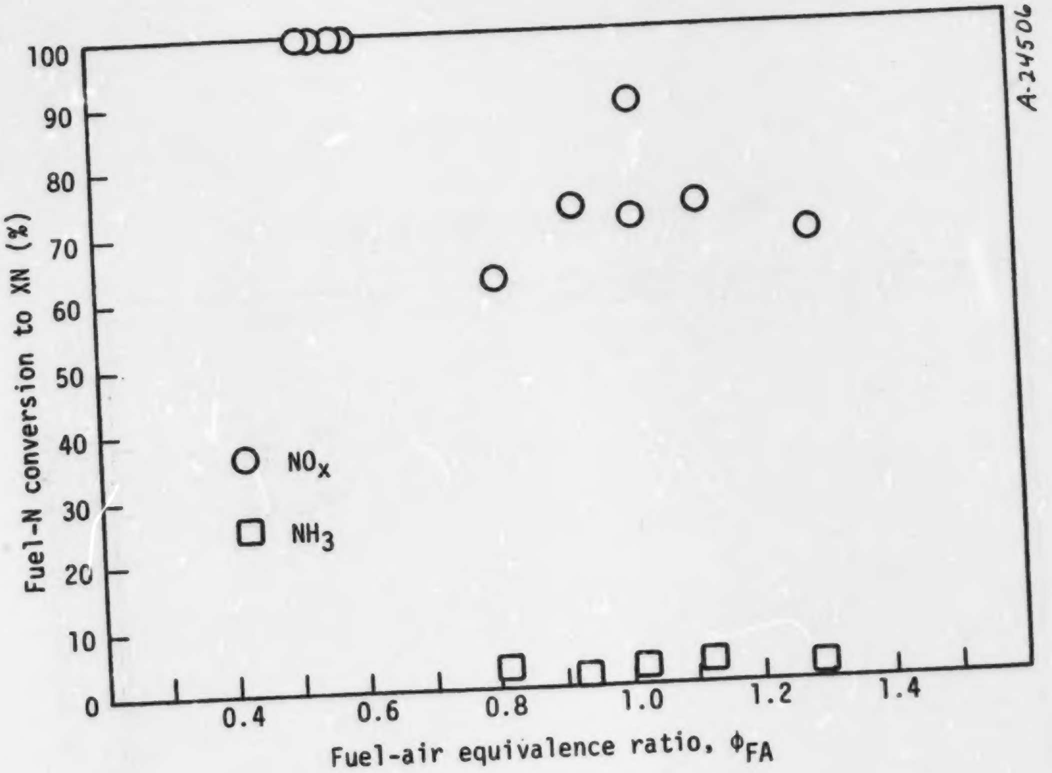

Figure 9. Fuel-N conversion to XN, Corning reactor, H-coal.

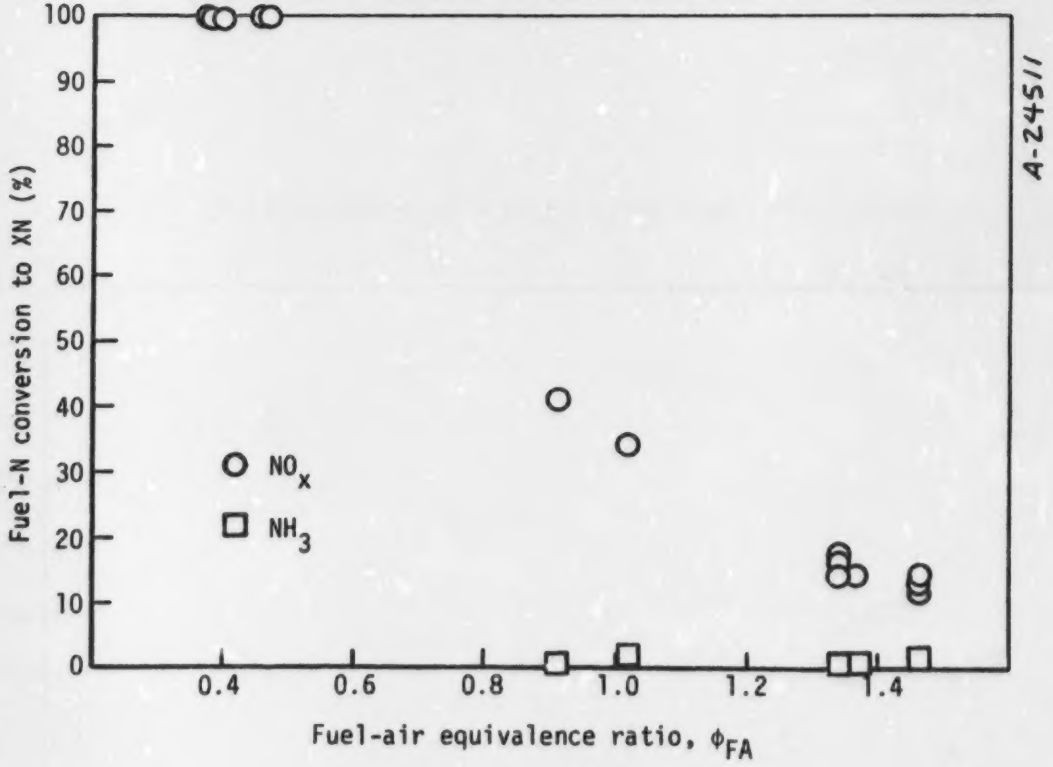

Figure 10. Fuel-N conversion to XN, UOP reactor, SRC II.

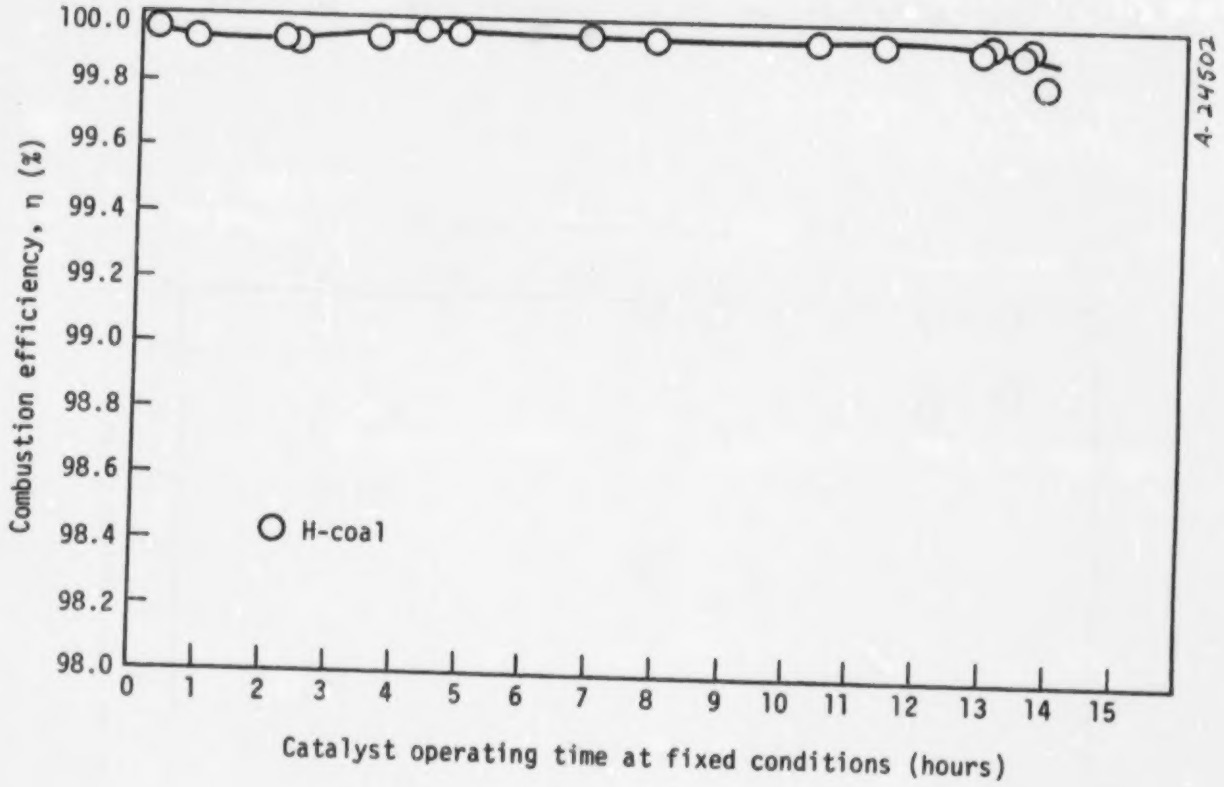

Figure 11. Combustion efficiency versus elapsed time, Acurex reactor.

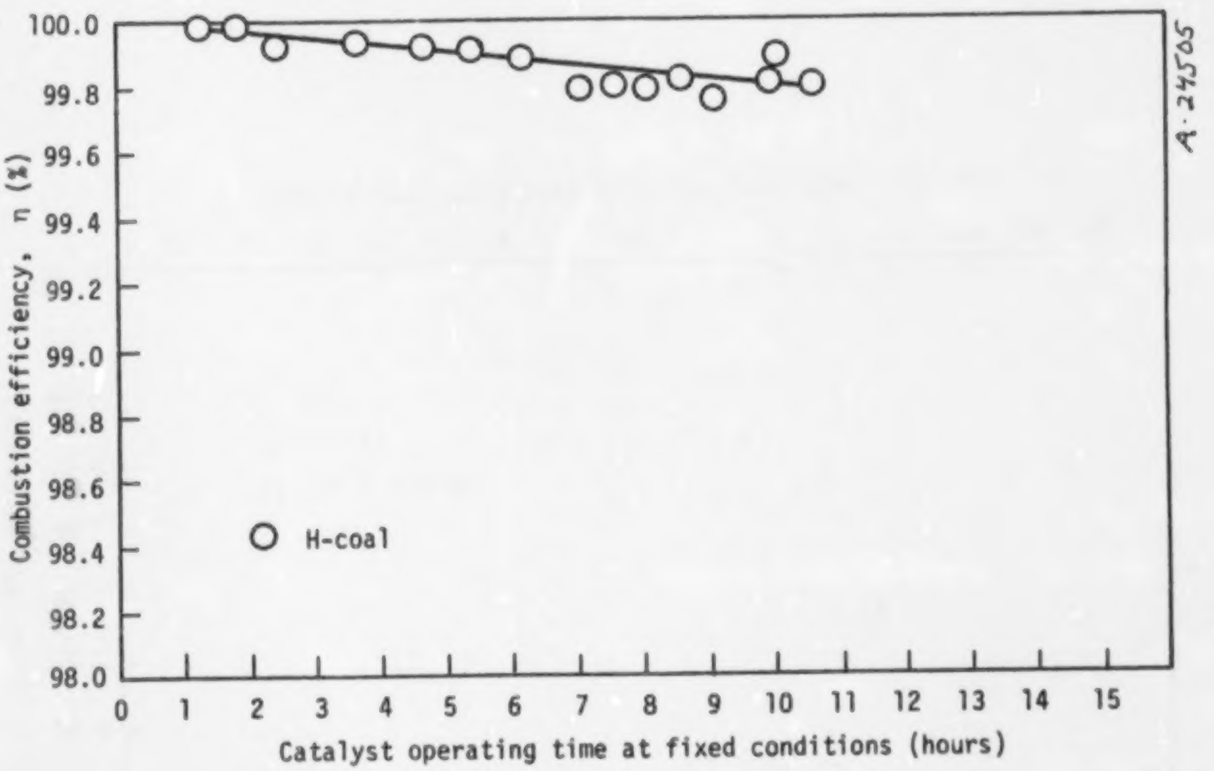

Figure 12. Combustion efficiency versus elapsed time, Corning reactor, fuel-lean combustion.

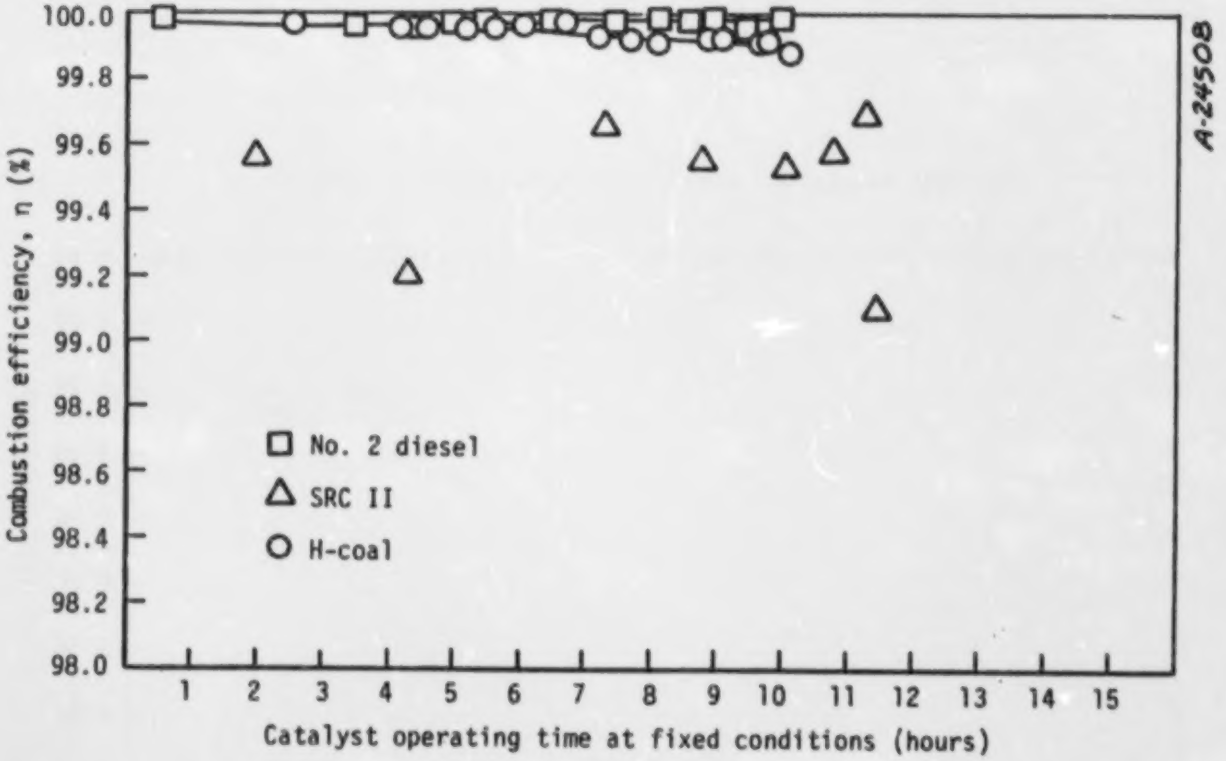

Figure 13. Combustion efficiency versus elapsed time, UOP reactor, fuel-lean.

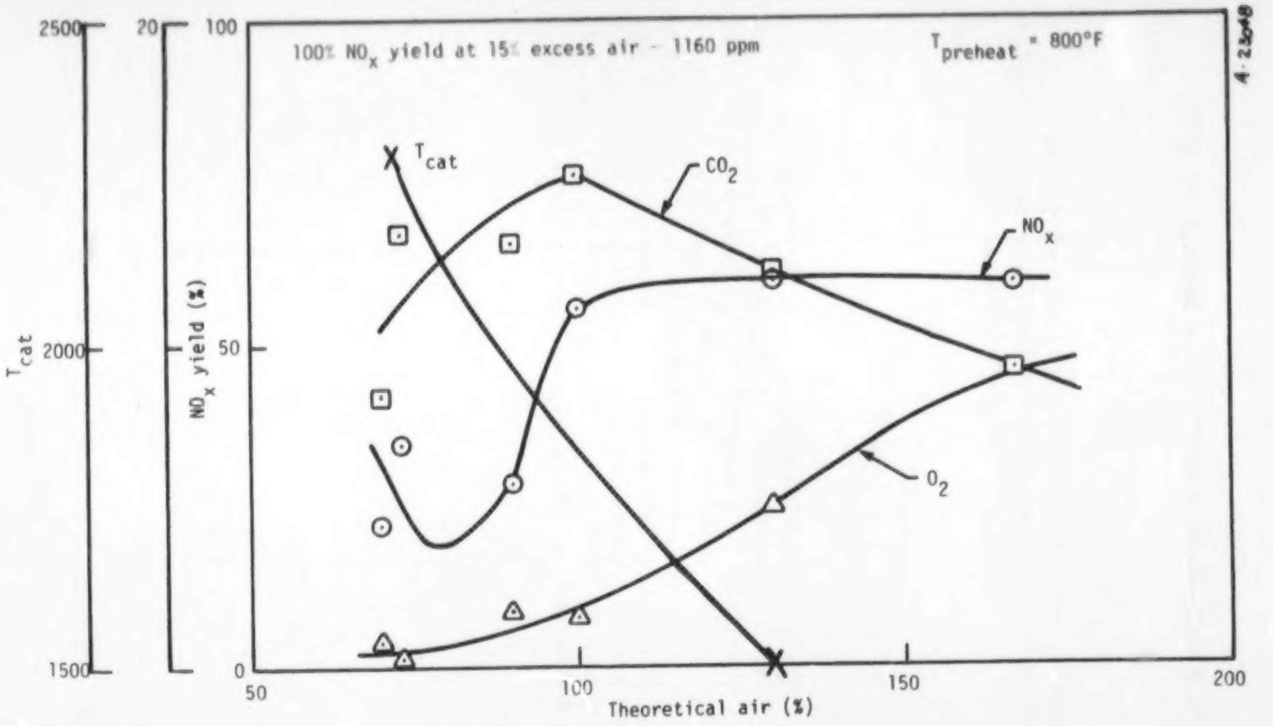

Figure 14. Catalytic flameholder performance.

GASIFICATION OF A HEAVY AND A DISTILLATE FUEL

By:

E. J. Szetela, United Technologies Research Center
R. A. Sederquist, United Technologies Power Systems Division
J. A. TeVelde, United Technologies Research Center

ABSTRACT

A catalytic gasifier which consists of an air-atomizer and a catalytic monolith was tested with a residual oil and a No. 2 oil. Test ranges included equivalence ratios from 6 to 8, reference velocity from 30 to 35 fps, and air temperature upstream of the injector from 740 to 1200 F. During runs of short duration, up to 17 min, catalyst wall temperature, catalyst discharge temperature, and effluent observation indicated that considerable fuel gasification occurred. Moderate wall temperatures were encountered allowing the application of available monolith materials. Further work will be needed to extend gasifier life and demonstrate catalyst and support material durability.

INTRODUCTION

The catalytic gasification of gasoline and other distillate fuels with air has been examined by a number of investigators. At Siemens in Germany (Reference 1), oxidative catalytic reforming in an autothermal catalytic reactor has been carried out at fuel-air equivalence ratios as high as 10 and catalyst temperatures of 1400 to 1600 F without the generation of soot in the product gas. This process, which is carried out at low residence times, produces cracked hydrocarbons, methane, hydrogen, water, and oxides of carbon. At Jet Propulsion Laboratory (Reference 2), distillate fuels have been partially oxidized and reformed over catalyst monoliths at equivalence ratios above 3 and catalyst temperatures above 1800 F without the formation of soot. The addition of small amounts of steam permitted higher equivalence ratio operation. At United Technologies (Reference 3), No. 2 heating oil containing 3300 ppm sulfur has been partially oxidized and steam reformed over a packed bed catalyst at equivalence ratios in excess of 4 without soot formation. This process has also been successfully applied to a number of coal-derived distillates.

These successful programs have led to the consideration of catalytic partial oxidation for the gasification of heavy fuel which cannot be vaporized by conventional methods. A program was initiated at the United Technologies Research Center to determine the feasibility of the catalytic gasification concept. This paper describes the experimental approach that has been taken and the initial results that have been obtained.

OPERATIONAL REQUIREMENTS

The objective of the catalytic gasification of residual fuel is to achieve significant improvement in fuel preparation for combustion in stationary gas turbines or furnaces over the conventional atomization, vaporization, and mixing techniques. The catalytic gasifier must operate without soot formation while being supplied fuel-air mixture in which only a small portion of the fuel is vaporized. The presence of a large fraction of liquid fuel droplets entering the catalyst monolith must not deactivate the catalyst or quench the catalytic combustion process.

Soot or carbon formation is predicted at high temperatures in thermodynamic equilibrium at an atomic oxygen-to-carbon ratio of 1 (which corresponds to an equivalence ratio of 3). Figure 1 shows thermodynamic equilibrium carbon boundaries for the H-C-O system. Under equilibrium conditions, operation above an equivalence ratio of 3 (below an O/C ratio of 1) would produce carbon. It is therefore necessary when operating above an equivalence ratio of 3 that equilibration of the fuel-air mixture by reforming of the fuel be limited such that the product gas atomic oxygen to carbon ratio for the mono-carbon species is held above the critical value of 1 as shown in Equation 1.

$$\frac{Y_{CO} + 2Y_{CO_2} + Y_{H_2O}}{Y_{CO} + Y_{CO_2} + Y_{CH_4}} > 1 \tag{1}$$

where Y is the product gas mole fraction.

In a functioning gasifier, it is probable that all of the oxygen is consumed in the combustion process and the remaining fuel is in the form of cracked or intermediate hydrocarbons. It is necessary to use short residence time in the catalyst monolith and possibly an activity which controls or selectively limits the amount of reforming and prevents formation of carbon. Short residence time can also reduce methane formation and soot production by thermal cracking of the fuel.

The presence of large quantities of unvaporized fuel droplets can present an operational problem. At high equivalence ratios only a small fraction of the fuel is expected to vaporize. Fuel droplets impinging on the catalyst can crack and form coke which can plug and poison the catalyst. Metallic impurities and ash in the fuel may affect long term catalyst activity and operation. For these reasons it is generally concluded that a large catalyst cell size would minimize surface impingement of fuel droplets which can poison the catalyst and quench the reactions by wall cooling.

EXPERIMENTAL APPARATUS AND PROCEDURE

Tests were conducted using the steady flow facility shown in Figure 2. The facility consisted of an electric air heater, a flow straightener, a swirl-type, air-atomizing fuel nozzle, a catalytic reactor section, a liquid separator and an afterburner section. The diameter of the rig was 2.4 in. upstream of the reaction section and 2.0 in. at the catalyst test section. The rig was insulated with fiberglass to minimize heat losses. Calibrated rotameters were used to measure the main airflow rate, atomizing airflow rate, water coolant flow rate and propane flow rate. The fuel flow was measured using a Fluidyne positive displacement flowmeter. The electric heater was capable of preheating the inlet air to a temperaure of 1200 F. The amount of nozzle airflow required to obtain a fine fuel mist was checked by visual observation of the spray into quiescent air.

Thermocouples were used to measure the inlet air temperature, fuel temperature and the fuel-air mixture temperature prior to entering the catalyst reactor. Thermocouples located on the substrate walls and at the exit centerline were used to indicate the performance of the reactor. Indication of carbon or soot formation was monitored by a continuous measurement of the pressure drop across the reactor section. The cyclone separator, used for non-vaporized liquid effluent collection, was rated by the manufacturer to have a collection efficiency of 95 percent for droplets larger than 5.0 microns.

Initiation of a test began with the main airflow rate being established and heated to the prescribed inlet temperature. After a steady state rig temperature was reached, propane and atomizing air were introduced through the fuel nozzle to preheat the catalyst bed to an initial temperature capable of sustaining the chemical reactions (approximately 1200 F). In order to minimize transients during switchover to liquid fuel, the liquid flow rate was preset using a bypass system. Upon reaching the desired catalyst preheat temperature, the propane flow was terminated and liquid flow through the catalyst initiated.

Catalyst performance parameters including temperature and pressure drop measurements were monitored during the test. The test was terminated when appreciable performance deterioration was noted.

FUEL

The majority of the tests have been performed using a residual heating oil with a viscosity which was near the lower level of the residual fuel band. The properties of the fuel are shown in Table I. An additional test was run with No. 2 oil in preparation for combustor tests that will be run in the near future.

TABLE I. FUEL PROPERTIES

Specific gravity	0.90
Hydrogen-carbon ratio	1.77
Percent nitrogen	0.11
Percent sulfur	0.38
Viscosity, CS	122 @ 77 F 16.6 @ 194 F

CATALYST HARDWARE

Three ceramic monoliths were procured by catalyst manufacturers, prepared for the catalyst by applying porous alumina on the substrate surfaces, and catalyzed with noble metals. Catalyst 1 had a zirconia spinel honeycomb substrate with square cells which had 0.10 in. sides. The substrate consisted of a single section having a length of 3 in. The substrate was catalyzed by Oxycatalyst with a 2 Pd:1 Pt coating applied at a loading of 1.4 g/m^2.

Catalyst 2 had a Torvex alumina honeycomb substrate with hexagonal cells which had an 0.17 in. distance between parallel sides. The substrate consisted of two butted sections, each one having a length of 1.5 in. The substrates were catalyzed by Matthey Bishop with a Pd:Pt coating applied at a loading of 4.9 g/cm^2.

Catalyst 3 had a zirconia spinel honeycomb substrate with square cells which had 0.27 in. sides. The substrate consisted of two butted sections, each one with a length of 3 in. The substrates were catalyzed by Oxycatalyst with a 2 Pd:1 Pt coating applied at a loading of 1.7 g/m^2.

Catalyst 4 consisted of a 1.5 in. length of Catalyst 3 followed by a 1.5 in. length of Catalyst 2.

EXPERIMENTAL RESULTS WITH RESIDUAL OIL

The first series of tests were run with Catalyst 1. Three tests were run and although good results were obtained in the first run, it was found that performance deteriorated in subsequent runs as shown in Table II. Reference velocity is based on the flow of air at the inlet temperature immediately upstream of the monolith. After Run 1, the separator exit reservoir contained no fuel. After Run 2, a small amount of fuel was found in the reservoir and a considerable amount of fuel was found after Run 3.

TABLE II. RESULTS WITH CATALYST 1

Run No.	1	2	3
Run Time, Min.	1.4	1.2	5.3
Reference Velocity, FPS	32	35	34
Equivalence Ratio	6.6	8.2	6.8
Air Inlet Temperature, F	1170	1180	1040
Temp. Downstream of Injector, F	610	570	550
Catalyst Wall Temp, F	1110	1020	780
Catalyst Discharge Temp, F	1500	800	620

The second series of tests were run with Catalyst 2. Good results were obtained in the first run and performance deterioration was not as severe as with Catalyst 1. The results with Catalyst 2 are shown in Table 3.

The third series of tests was run with Catalyst 3. Four tests were run and in each test, it was noted that pressure drop across the catalyst increased progressively. However, during shutdown, the obstruction seemed to be removed because the pressure loss at the beginning of any test was the same as the pressure loss at the beginning of the previous test. Initial conditions with Catalyst 3 are shown in Table IV. Performance changes noted during tests with Catalyst 3 are shown in Table V.

TABLE III. RESULTS WITH CATALYST 2

	Beginning	End	Beginning	End
Run No.	1	1	2	2
Run Time, Min.	–	9.0	–	5.0
Reference Velocity, FPS	33	33	32	32
Equivalence Ratio	6.0	6.0	6.0	6.0
Air Inlet Temperature, F	1120	1120	1175	1175
Temp Downstream of Injector, F	590	560	590	590
Catalyst Wall Temperature, F	1140	990	1120	920
Catalyst Discharge Temp, F	1560	1220	1355	1350

TABLE IV. INITIAL RESULTS WITH CATALYST 3

Run No.	1	2	3	4
Reference Velocity, FPS	33	32	31	35
Equivalence Ratio	6.2	6.2	6.2	6.2
Air Inlet Temp, F	1080	1115	1045	1215
Temp Downstream of Injector, F	605	660	590	785
Catalyst Wall Temp, F	1280	1325	1300	1365
Catalyst Discharge Temp, F	1150	1670	1275	1415

TABLE V. PERFORMANCE CHANGES WITH CATALYST 3

Run		Time Min	Catalyst Discharge Temperature, F	Pressure Drop, in. H_2O
1	Beginning	0	1150	2.2
	End	5.8	1300	15.0
2	Beginning	0	1670	2.4
	End	3.0	1650	6.0
3	Beginning	0	1275	2.5
	End	2.5	1040	4.5
4	Beginning	0	1350	2.6
	End	3.5	1250	17.5

EXPERIMENTAL RESULTS WITH NO. 2 OIL

A single test was run using No. 2 oil with Catalyst 4. The inlet air temperature was reduced for this test to duplicate the air temperature planned for the actual combustor test. Although the pressure drop increased at the beginning, it returned to its initial value and the results shown in Table VI were encouraging. Approximately 10 percent of the total fuel flowed during the run with No. 2 oil was found in the liquid reservoir after the test was completed.

TABLE VI. RESULTS WITH NO. 2 OIL AND CATALYST 4

Run Time, Min	0	5	10	17
Reference Velocity, FPS	30	30	30	30
Equivalence Ratio	7.5	7.5	7.5	7.5
Air Inlet Temperature, F	740	740	760	760
Catalyst Wall Temp, F	1530	1570	1460	1410
Catalyst Discharge Temp, F	1035	1035	1055	1100
Pressure Drop, in. H_2O	2.5	4.5	2.9	2.6

CONCLUSIONS

Tests to date indicate the feasibility of the catalytic gasification of residual and alternative fuels as a means of preparing these fuels for subsequent combustion in stationary gas turbines and furnaces. Catalytic gasification at high equivalence ratio results in moderate catalyst temperatures allowing the application of available catalyst monolith materials. Further optimization is required to select the operating conditions, the monolith dimensions, and the catalyst formation that achieves the best level of gasification without forming carbon. Additional work is required to extend gasifier life, determine maximum fuel flow capability, and demonstrate catalyst and support material durability under all operating conditions.

REFERENCES

1. Henzel, H. J., H. Kostka, and A. Michel. Autothermal Gasification of Liquid Hydrocarbons by Partial Oxidation. Paper presented at ERDA meeting on Fuel Processing for Fuel Cell Power Generation, April 13, 1977.

2. Voecks, G. E. and D. J. Cerini. Application of Rich Catalytic Combustion to Aircraft Engines. Presented at Third Catalytic Combustion Workshop, October 4, 1978.

3. Bett, J. A. S., R. R. Lesieur, D. R. McVay, and H. J. Setzer. Adiabatic Reforming of Distillate Fuels. National Fuel Cell Seminar, San Francisco, CA, June 1978.

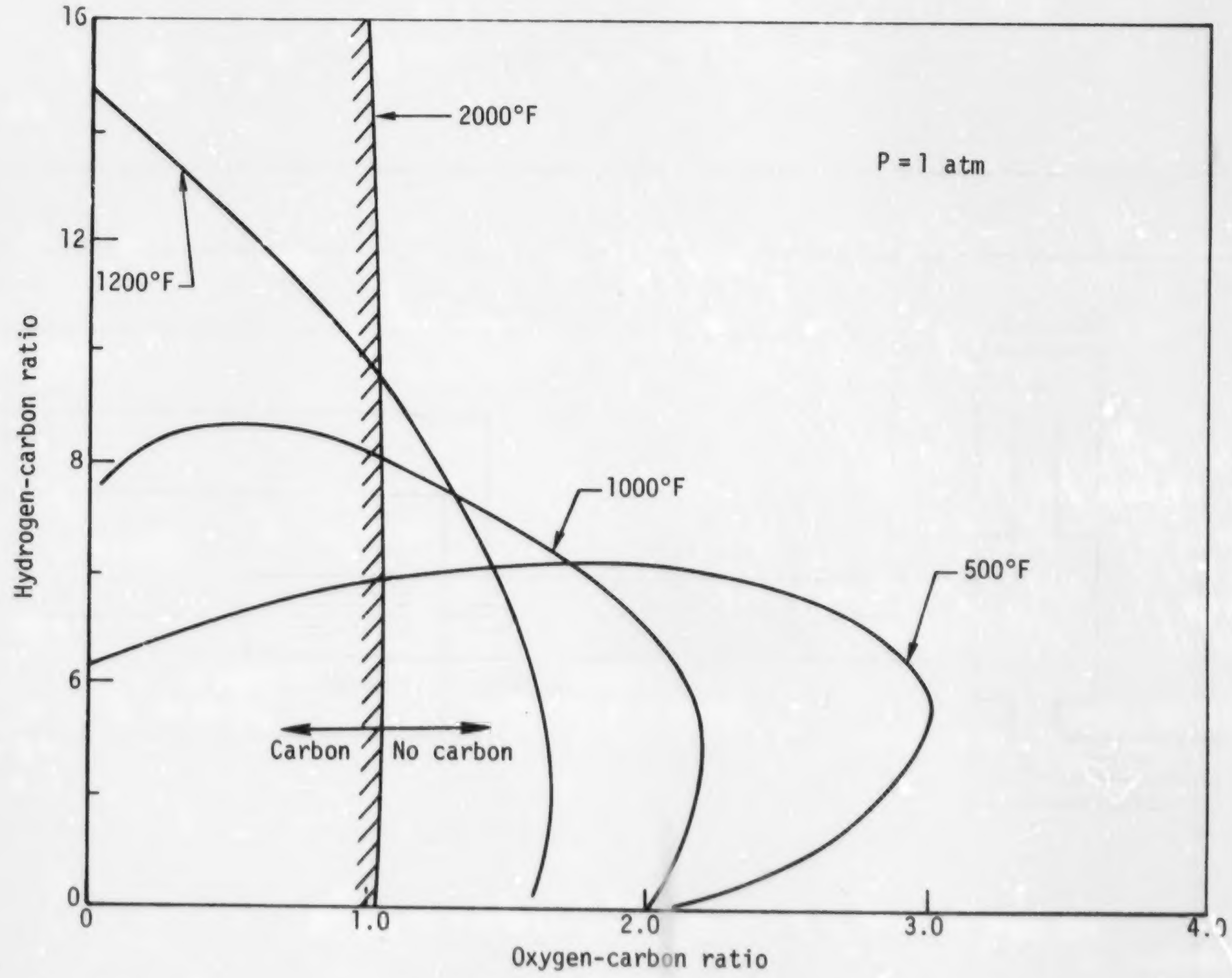

Figure 1. Carbon formation boundaries in the H-C-O system.

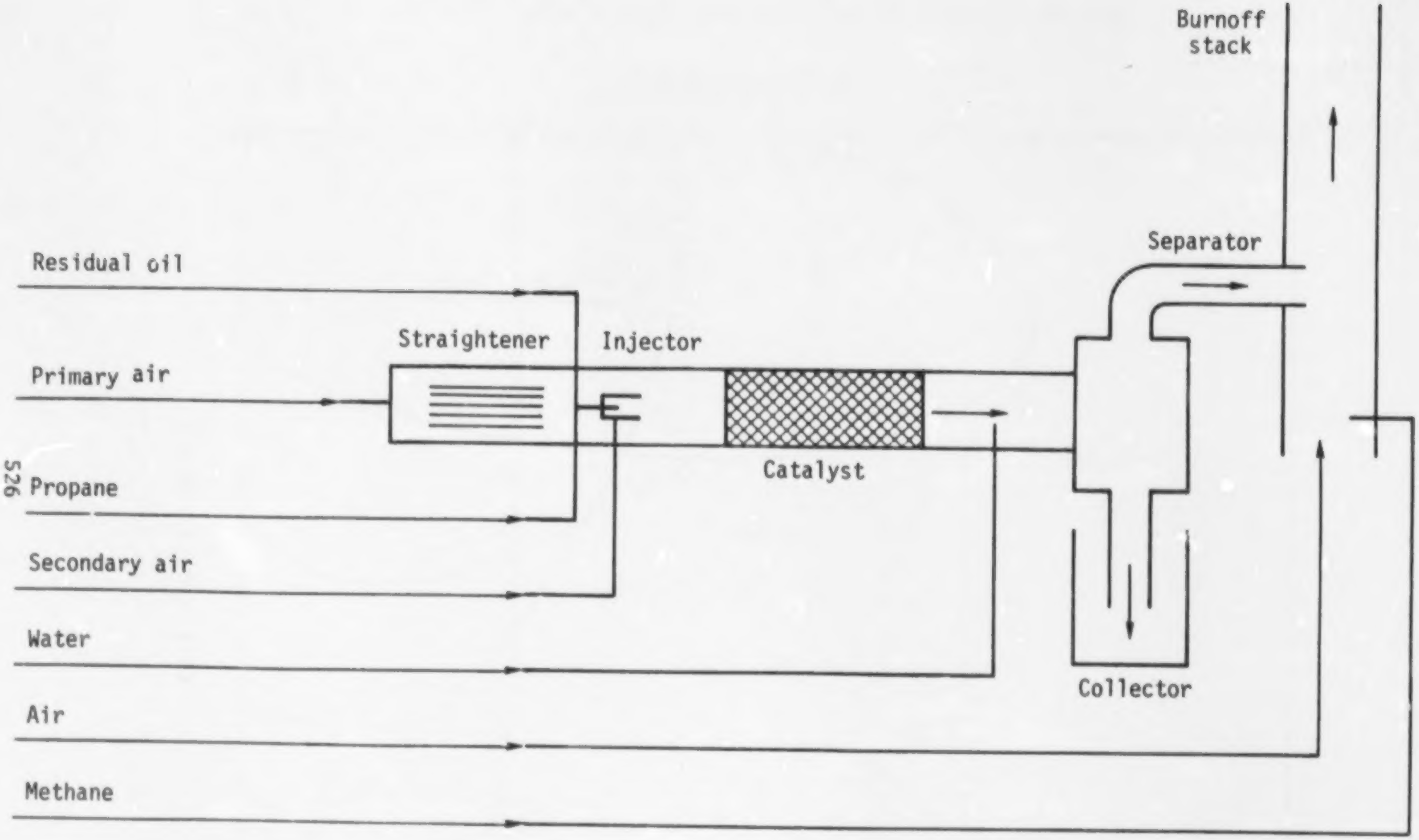

Burnoff
stack
Separator
Residual oil
Straightener
Injector
Primary air
Catalyst
Propane
Secondary air
Water
Collector
Air
Methane

Figure 2. Catalytic gasifier test rig.

CATALYTIC COMBUSTION OF HEAVY PARTIALLY-VAPORIZED FUELS

By:

T. J. Rosfjord
United Technologies Research Center
East Hartford, Connecticut

ABSTRACT

An experimental program to demonstrate efficient catalytic combustion of fuel-lean and fuel-rich mixtures of residual fuel and air, and to assess the influence of incomplete fuel vaporization on the performance of a catalytic reactor is being conducted. A 7.5-cm diameter catalytic reactor was designed and will be tested over a matrix of conditions representative of a gas turbine combustor inlet. For each of three test phases, two series of tests with a uniform but poorly vaporized (less than 50 percent) mixture of No. 6 fuel oil and air will be performed. In the first series, the non-vaporized fuel will be contained in a spray of droplets with a Sauter Mean Diameter (SMD) less than 30 microns. In the second series, the non-vaporized fuel will be characterized by a spray SMD approximately equal to 100 microns. The designs of the fuel injection system and the catalytic reactor are described in this paper.

INTRODUCTION

Current concerns regarding pollutant emissions are occurring at a time when continued development of the gas turbine engine as an industrial prime mover depends in part on the capability to use fuels with far less attractive physical and chemical properties than those of the fuels currently used. Increasingly stringent emission standards prompt even greater emissions reductions, especially of NO_x, than may be attainable with current combustor design technology. Therefore, to increase the options available for low emission, fuel flexible engine designs, novel combustion concepts ought be investigated. Catalytic combustion is a candidate approach in this application. Catalysts have been shown to promote stable, efficient combustion at exceptionally lean fuel-air ratios. However, the preponderance of combustion-related work with catalysts has involved the use of either gaseous or relatively volatile fuels coupled with fuel-air preparation systems configured so that the catalyst was not confronted with a fuel-air mixture in which the majority of the fuel was in the liquid state or in droplets having a large diameter. Thus, with the growing requirement to use low-volatility alternative and residual fuels for stationary gas turbine engines, investigations to elucidate the behavior of catalytic combustion systems using incompletely vaporized heavy fuel are required. Additionally, recognizing the promise of controlling NO_x formed from fuel-bound nitrogen by employing a staged combustion sequence, it is necessary to define the operational characteristics of catalytic reactors for both fuel-rich and fuel-lean mixtures.

United Technologies Research Center, under contract from NASA-Lewis Research Center, is conducting an experimental program directed toward demonstrating efficient catalytic combustion of fuel-lean and fuel-rich mixtures of residual fuel and air, and assessing the influence of incomplete fuel vaporization on the performance of a catalytic reactor. A 7.5-cm diameter catalytic reactor was designed and will be tested over a matrix of conditions representative of a gas turbine combustor inlet. For each of three test phases, two series of tests with a uniform but poorly vaporized (less than 50 percent) mixture of No. 6 fuel oil and air will be performed. In the first series, the non-vaporized fuel will be contained in a spray of droplets with a Sauter Mean Diameter (SMD) less than 30 microns. In the second series, the non-vaporized fuel will be characterized by a spray SMD approximately equal to 100 microns.

UTRC has overall responsibility for the technical program, including the design and fabrication of the test facility and execution of the test program. Acurex Corporation, as a subcontractor to United Technologies, will support UTRC in the design, fabrication and evaluation of the catalytic reactors. Problems in obtaining the desired substrate material have delayed the initiation of the test program. Therefore, this paper describes only the fuel preparation system and the catalytic reactor designed to satisfy the program requirements.

Fuel Preparation System

A fuel injection system was designed to satisfy three operational requirements at the following condition: inlet air temperature = 600 K; pressure = 600 kPa; reference velocity = 20 m/s; fuel-air ratio = 0.020. First, the system must provide distributions of fuel-air ratio and velocity which are uniform to within ± 10 percent of the mean value at the catalytic reactor inlet. Second, the fuel must be less than 50 percent vaporized at the catalytic reactor inlet. Third, the device must be capable of producing sprays characterized by a SMD of either less than 30 microns or in the range of 70-150 microns. These requirements were satisfied by designing a system which employed a multiple venturi fuel injection system followed by a straight mixer/vaporizer duct. The injector contains 19 venturi tubes distributed over a 7.5-cm diameter circular area. The fuel will be injected normal to the airstream through 0.76-mm inside diameter tubes which penetrate thirty percent across each venturi throat (Fig. 1). The injector was fabricated by an electrical discharge machining technique to permit the 7-deg half angle conical diffusers to terminate along the natural cone intersections. This geometry eliminates regions of recirculating base flow which would promote autoignition within the fuel preparation system. A review of correlations developed for the atomization of heavy fuels concluded that an expression developed for an air spray injector by Jasuja (Ref. 1) was applicable for the injector of interest. The correlation developed was:

$$\mathrm{SMD} = 0.19\ \frac{(\sigma_\ell/\rho_\ell)^{0.35}}{u_a\ \rho_a^{0.35}}\left(1 + \frac{1}{\mathrm{AFR}}\right)^{0.25} + 0.127\ \mu_\ell\left(\frac{D}{\rho_\ell\ \sigma_\ell}\right)^{0.50}\left(1 + \frac{1}{\mathrm{AFR}}\right)$$

where: SMD - droplet diameter, m
σ_ℓ - liquid surface tension, N/m
ρ_ℓ - liquid density kg/m^3
μ_ℓ - liquid viscosity, Ns/m^2
ρ_a - air density, kg/m^3
u_a - air velocity, m/s
D - orifice diameter, m
AFR - air to fuel ratio in injector by weight

The correlation is the sum of two terms; the first is dominated by the air velocity while the second is responsive to the liquid (i.e., fuel) viscosity. Proper selection of injector blockage and fuel temperature will produce the desired air velocity and fuel viscosity, respectively, to form droplet sizes which satisfy the requirements of the program. A 0.54-cm venturi throat diameter was specified to produce a velocity of the 245 m/s at the fuel injection site, insuring that the first term will always have a small value. Variation in the second term, and thus the SMD, will be achieved by varying the fuel temperature. Analysis of the fuel for this program indicated that for a fuel temperature of 373 K, a spray characterized by SMD = 25 microns will be obtained, while at a temperature of 329 K an SMD = 100 micron spray will be formed.

The rate of vaporization of the injected fuel was analyzed using the UTRC Spray Vaporization Analysis. The analytical program is a multiple streamtube code which uses a marching finite difference solution procedure to provide a streamwise evolution of the two-phase flow properties. Vaporization calculations were performed using No. 6 fuel oil properties. Fuel droplets with diameters of 30 and 35 microns at an initial temperature of 380 K and of 100 and 125 microns at 330 K were "injected" into air having a velocity of 245 m/s as would exist in the throat of any one of the nineteen fuel injector venturi tubes. The airflow was decelerated in the injector diffuser prior to entering a constant area streamtube representing one-nineteenth of the total flow area. In order to simultaneously limit the vaporization to the 50 percent maximum and achieve a mean droplet diameter of less than 30 microns at the reactor inlet, the maximum allowable spray SMD at the injector was determined to be approximately 35 microns. Therefore, as shown by the calculation results (Fig. 2), the mixer/vaporizer must not be longer than 18 cm. Note that over this length, the larger droplets vaporize to a much lesser extent; after 18 cm, a droplet initially with a diameter of 100 microns will vaporize only 10 percent. The length required by the large droplets to achieve 50 percent vaporization is approximately one meter, an impractical length for either this test program or for a conventional engine configuration. Since the gaseous fuel-air ratio corresponding to 10 percent fuel vaporization is below the minimum at which catalytic combustors have been operated with distillate fuel, there is a concern that the reactors will be ineffective. Two provisions are being considered in this instance. First, a longer mixer/vaporizer could be used to raise the level of vaporization. It is anticipated that this approach would provide minimal benefit however since the increase in extent of vaporization with additional length is small. Second, in an attempt to determine a threshold for efficient reactor operation, tests could be performed with intermediate droplet sizes (produced by raising the fuel temperature) which would provide more favorable levels of vaporization (but still less than 50 percent). This approach is compatible with the fuel injection system and offers the opportunity to define an operational limit.

The mixing of the injected fuel into the airstream was also analyzed using the UTRC Spray Vaporization program. The initial fuel concentration was represented as a "top hat" profile (centered on the longitudinal axis of a venturi) with a width equal to two fuel tube diameters. An eddy diffusivity equal to the value determined by Longwell (Ref. 2) for the turbulent transport of fuel droplets was employed. The results from the calculations indicated that fuel-air mixture uniformity to within approximately ± 5 percent of the mean is achieved 12.7 cm downstream from the fuel tube. The calculations also indicated that a uniform air velocity profile would be realized. Tacina (Ref. 3) obtained uniformity at 17.8 cm downstream from a jet fuel, multiple-venturi injector configured to distribute 21 injection sites over a 12-cm diameter circular area. The injector being fabricated for this program will have 19 injection sites distributed over a 7.5 -cm diameter, providing an injection site density 2.2 times the Tacina design. Assuming a similar mixing rate, the decreased distance between injection sites should result in uniformity at 12 cm downstream from the fuel tube. It is recognized that, because of differences in the fuel spray (fuel properties, droplet sizes) and the precise injector geometry, the consistency of this prediction with the UTRC model calculations does not guarantee the mixer performance. The agreement does, however, establish a level of confidence in the design procedure. Additionally, based upon the vaporization calculations presented above, the mixer/vaporizer length was specified at 18 cm providing even greater distance to achieve uniformity.

Catalytic Reactor

Acurex Corporation, as a subcontractor to UTRC, designed the catalytic reactors for this program (Ref. 4). A 7.5-cm diameter reactor was designed to achieve a 99.5 percent combustion efficiency at the following condition: inlet air temperature = 600 K; pressure = 600 kPa; reference velocity = 20 m/s; adiabatic combustion temperature = 1400 K. The maximum allowable pressure drop through the reactor was specified at 5 percent.

A three-phase design analysis was performed. In the initial phase, it was assumed that the reactor was adiabatic and the fuel droplets did not ignite. The second analysis phase superimposed the droplet ignition phenomena on the initial results by considering the autoignition and combustion time for the droplets within the reactor. The third phase of the analysis considered the non-adiabatic characteristics of the reactor, particularly the de-stabilizing influence of radiation from the upstream face of the bed.

In the initial adiabatic analysis, the governing differential equations for the bulk gas energy and mass balances, droplet energy and mass balances, and surface energy balance were solved using a finite difference procedure. Because of the lack of quantitative data on kinetic rates for residual fuel and air catalytic reactions, it was assumed that the fuel consumption rate was diffusion limited. The initial reactor investigated was a graded-cell device configured to include 5-cm, 2.5-cm, and 15-cm lengths of 0.63-cm, 0.32-cm, and 0.16-cm diameter cell monolithic substrates, respectively. Typical results are shown in Fig. 3

which illustrates the variation in the substrate temperature, bulk gas temperature, droplet radius, local gaseous fuel-air ratio and fuel conversion efficiency with distance along the reactor length for the design condition. As indicated, the events are guided by the droplet evaporation. As the droplet vanishes the wall temperature increases to the adiabatic temperature and the bulk gas temperature and fuel conversion efficiencies begin to increase rapidly. These results indicate that in the absence of homogeneous combustion or droplet ignition the goal of 99.5 percent combustion efficiency will require a reactor length significantly in excess of 25 cm. A benefit of the analysis is that it provided the temperature history required to calculate the autoignition length of the fuel droplets. It was determined that droplet ignition would occur at approximately 21 cm from the inlet face of the reactor, and that complete combustion of the droplet would occur within 1 additional cm. Thus, it appeared that a 25-cm long, graded-cell catalytic reactor can achieve high efficiency at the design condition. The principle non-adiabatic effect analyzed was the heat loss due to thermal radiation upstream from the inlet face of the catalytic reactor. Results indicated that approximately a 100 K depression in the substrate temperature could be experienced on the face; the radiation loss would affect the initial 2-cm length of the catalytic reactor. Surface reactions in this region would be suppressed, decreasing the initial heat release and thus having a de-stabilizing effect on the catalytic reactor operation. Since the length of the largest cells is more than twice the length influenced by upstream radiation it is believed that reactor stability will be preserved.

Based upon analyses of several reactor geometries at the design condition and near-design condition, the final reactor was designed to be a graded-cell device constructed from Corning MCB-12, zirconia-spinel substrate. It would be constructed from 5-cm, 2.5-cm, and 17.5-cm lengths of 0.63-cm, 0.32-cm, and 0.16-cm, diameter cell elements, respectively. The catalyst is a proprietary formulation applied by UOP. Analyses indicate that the device should impose approximately a 4 percent pressure loss. The reactors will be assembled by Acurex and instrumented with high temperature thermocouples embedded in a dedicated substrate channel along the reactor centerline.

Status

The items described in the previous two sections are the primary components of the test rig. The fuel injection system has been fabricated; the catalytic reactors have not been delivered because of problems in substrate availability. It has become clear that the availability of high temperature substrates for catalytic reactors can become the pacing factor in conducting future catalytic combustion programs. The test program will be initiated when the reactors have been obtained. The initial test phase is an evaluation of the catalytic reactor over a range of test parameters including: inlet air temperature -- 600 K, 500 K; test section pressure -- 600 kPa, 900 kPa; reference velocity -- 10 to 30 m/s;

fuel air ratio -- 0.016 to 0.026. The fuel injector will be operated to produce the two ranges of droplet sizes described above over these ranges of conditions. The second test phase is an evaluation of two alternative reactor designs over a subset of the previously described test conditions. The third test phase is an evaluation of the catalytic reactor over a range of rich fuel-air ratios. Test results from these tasks will be presented as available in the oral presentation.

REFERENCES

1. Jasuja, A. K.: Atomization of Crude and Residual Fuel Oils. Journal of Engineering for Power, Vol. 101, pp 250-258, April 1979.

2. Longwell, J. P. and M. A. Weiss: Mixing and Distribution of Liquids in High Velocity Air Streams. Industrial and Chemical Engineering, Vol. 45, 1953.

3. Tacina, R. R.: Experimental Evaluation of Fuel Preparation Systems for an Automotive Gas Turbine Catalytic Combustor, NASA TM-78856, 1977.

4. Chu, E.: Catalytic Reactor Design for Combustion of Partially Vaporized No. 6 Fuel Oil. Acurex Project 7543 Report, 1979.

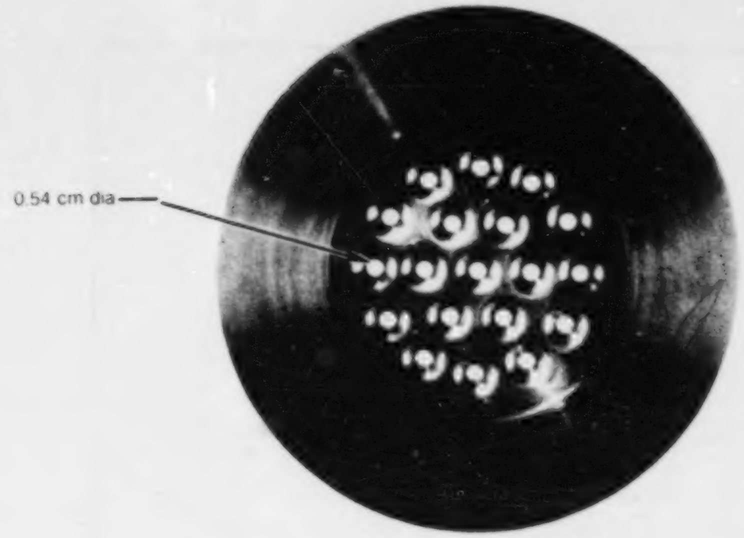

a) VIEW FROM UPSTREAM

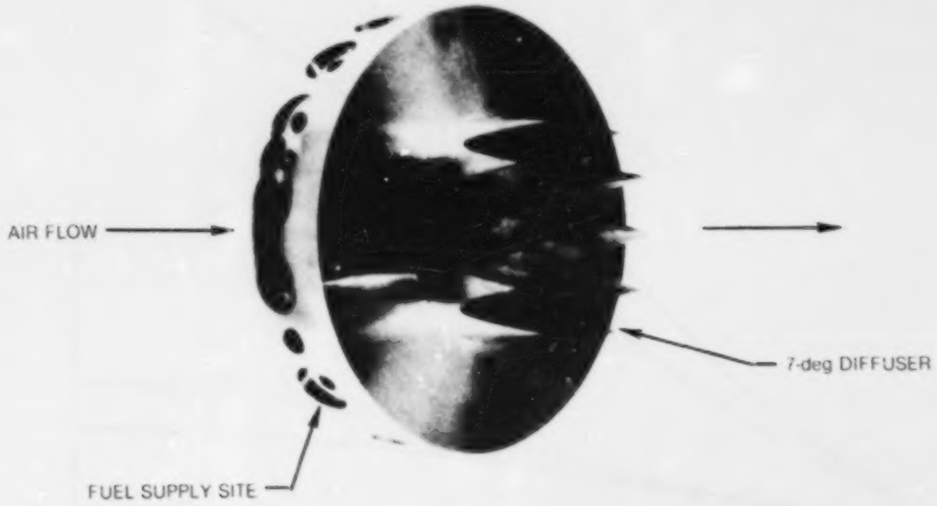
AIR FLOW
7-deg DIFFUSER
FUEL SUPPLY SITE

b) VIEW FROM DOWNSTREAM

Figure 1 Multiple Venturi Fuel Injector

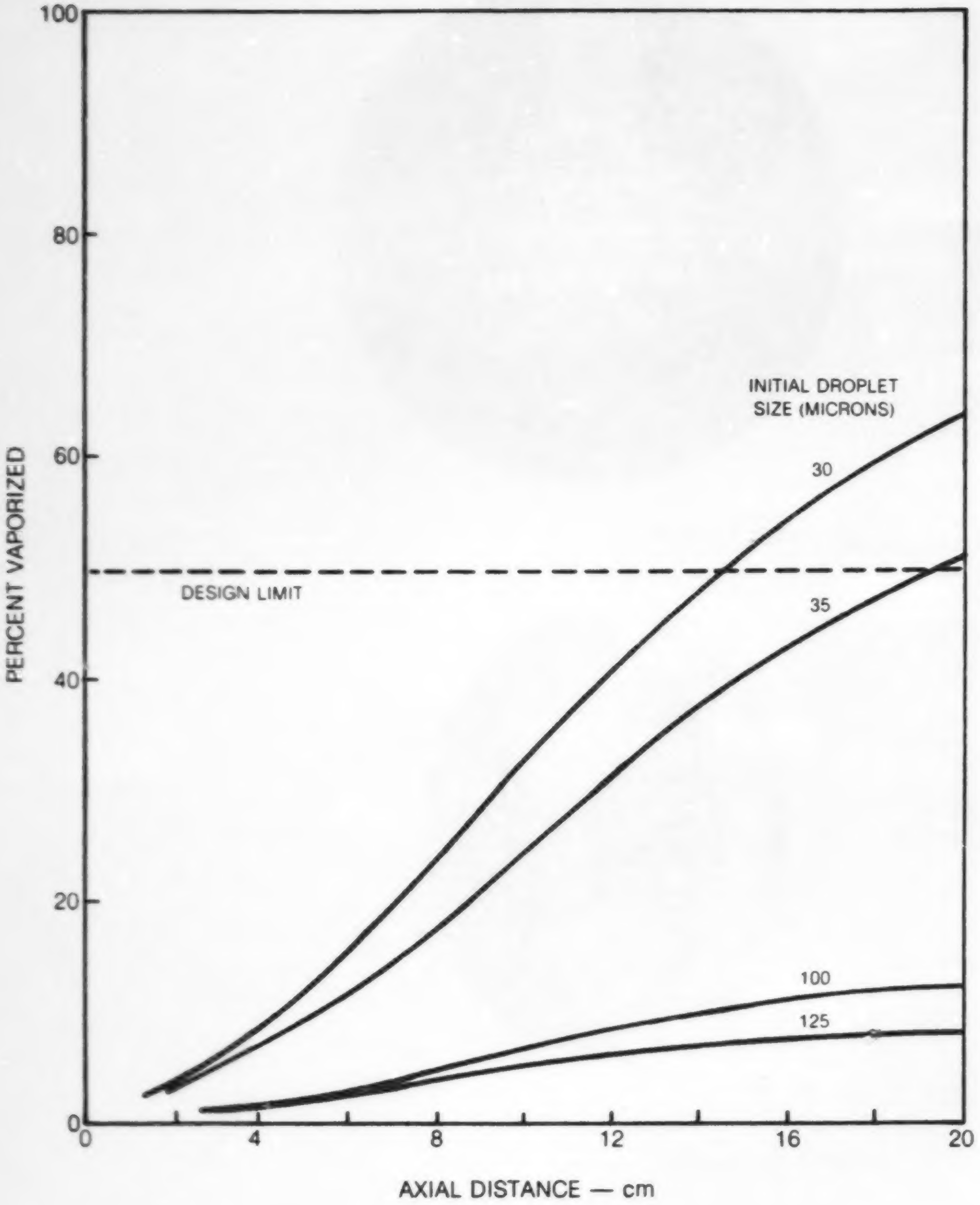

Figure 2 No. 6 Fuel Oil Droplet Evaporation Characteristics

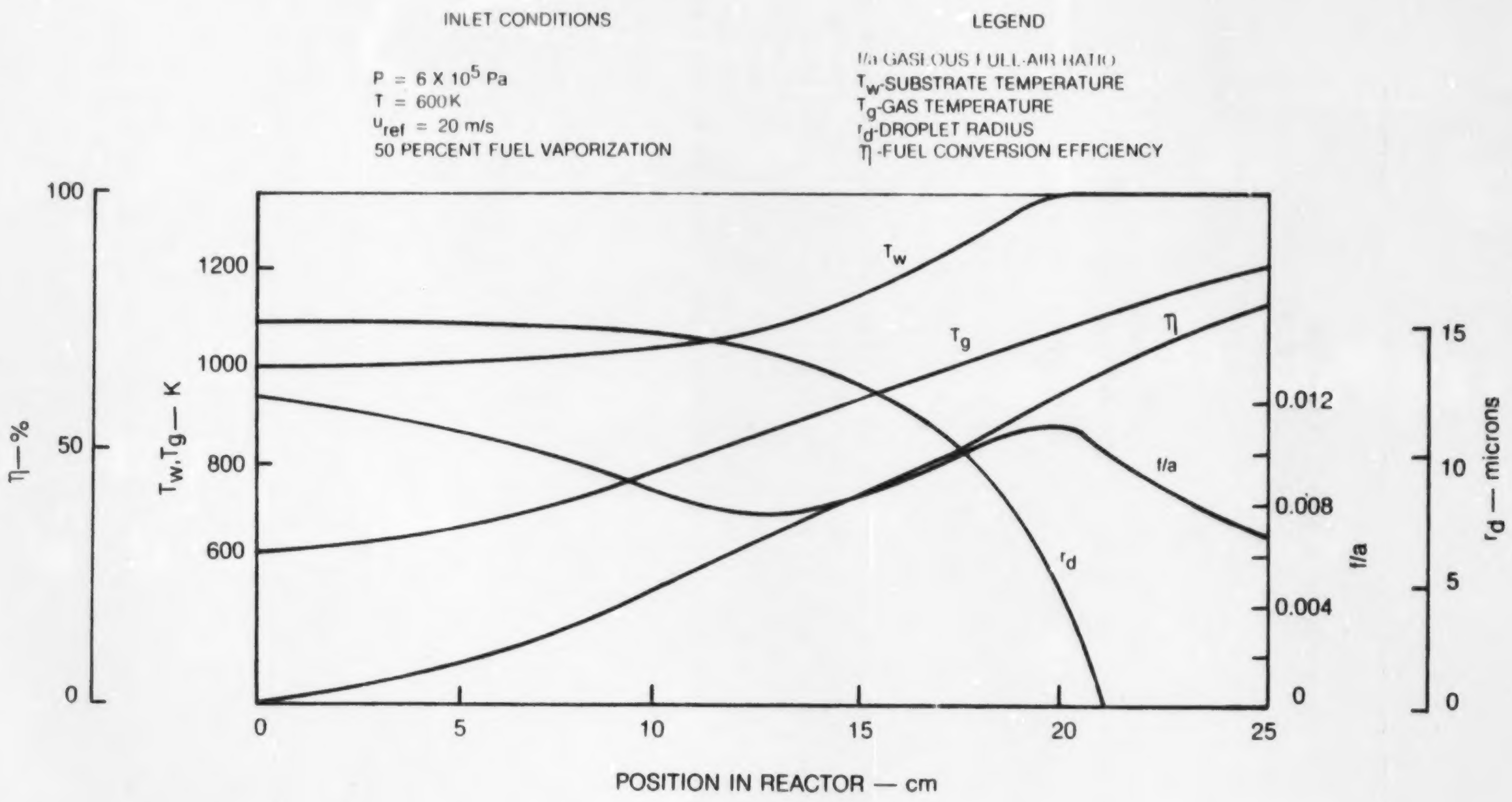

Figure 3 Droplet Burning History in Catalytic Reactor

EVALUATION OF A NOVEL LEAN BURN LOW NO_x CATALYTIC COMBUSTION CONCEPT

By:

E. K. Chu, R. Chang, and H. Tong
Acurex Corporation/Energy & Environmental Division
485 Clyde Avenue
Mountain View, California 94042

ABSTRACT

An experimental program to evaluate the feasibility of a lean burn low NO_x catalytic combustion concept is being conducted. Two catalytic reactor configurations were designed and tested over a matrix of inlet conditions representative of gas turbine operations. The fuel tested was a doped diesel fuel with a nitrogen content of 0.5 weight percent of the fuel. The model fuel nitrogen was pyridine. One of the design configurations was found to have low NO_x emissions. However, CO emissions were also found to be very high.

INTRODUCTION

The objective of the present study is to examine a low NO_x, lean burn, catalytic combustion concept for fuels containing fuel bound nitrogen. Under lean burn conditions, fuel NO_x formation predominates and thermal NO_x is subdued. Suppression of fuel NO_x formation therefore becomes a primary concern.

The present concept is based on findings by various investigators (References 1 and 2) that NO_x in combustion effluents can actually be reduced by the injection of hydrocarbon-oxygen mixtures in one case and NH_3 in another. It seems that the presence of various intermediate species of reaction (CO, CH_x, CN, NH_x) simultaneously with NO_x will sometimes reduce NO_x to N_2 given favorable temperatures and residence times. Further, the presence of a solid surface also tends to enhance such reduction of NO_x as revealed by coal combustion studies (References 3 and 4) and a laboratory scale study by DeSoete (Reference 5). In the present study nitrogen doped fuel is introduced into a first stage catalyst monolith where it is partially converted to intermediate products as well as some NO_x. The catalytic reaction is then temporarily "frozen" by introducing a small gap between the first and second stages. This enables the intermediate products of reaction to interact with the NO_x present, hopefully to reduce the NO_x to N_2. The gap is then followed by a second set of catalyst monoliths where fuel conversion is completed.

Since the concept is highly exploratory, the optimum condition, if any exists, cannot be defined a priori. In the present study, two reactor arrangements were examined for diesel fuel doped with pyridine under various conditions by varying the fuel/air ratio and the approach velocity and monitoring the reactor effluents. If the concept is viable, there should be some combination favoring low NO_x formation.

METHOD OF APPROACH

All tests were performed in the Acurex subscale catalytic combustion test facility shown schematically in Figure 1. The catalyst was mounted in a stainless steel test section lined with a ceramic insulating material. Visual observation of the catalyst reactor was made from the aft end of the test section through a quartz window. Bed temperatures were monitored with thermocouples located at various points in the catalyst bed. Exhaust gas composition was monitored continuously with gas analyzers. In a few studies, measurements of NH_3 and HCN concentrations were also made by absorption in solution and then reading with ion selective electrodes. No. 2 diesel fuel doped with pyridine (0.5 wt % N) was used as the test fuel and was introduced as a fine spray with an air atomized injector into a mixing zone above the combustor.

The test conditions examined were:

Inlet pressure:	1 atm
Inlet temperature:	700°F
Reference velocity:	30-80 ft/s
F/A (fuel/air) ratio:	0.02-0.035 (by weight)

Two catalyst arrangements were examined. The first (Figure 2) consisted of two large cell monoliths (2 inch diameter, 1 inch thick, 9 cells/sq inch) and one medium cell monolith (2 inch diameter, 1 inch thick, 16 cells/sq inch) in series as the front section followed by a rear section made up of two small cell monoliths (2 inch diameter, 1 inch thick, 200 cells/sq inch). A gap of 1-1/2 inches separated the two sections. In the second arrangement (Figure 3), two large cell monoliths (2 inch diameter) made up the front section and two medium cells (2-1/2 inch diameter) and one small cell monolith (2-1/2 inch diameter) the rear section. A gap of 2-1/2 inches separated the two sections.

RESULTS AND DISCUSSION

Results are summarized in Tables 1a, b and 2.

Tables 1a and b summarize results with catalyst arrangement 1. Table 1a is a baseline study using pure No. 2 diesel. As expected, NO_x emissions were low in the absence of fuel nitrogen. Table 1b assesses the same catalyst arrangement with the pyridine doped diesel. The first four points were preliminary studies to assess the general stability of the system. At the fuel/air ratios and approach velocities used, combustion was stable and efficient with low unburned hydrocarbon (UHC) and CO emissions. Fuel NO_x conversion, however, also approached 100 percent.

The next series of points summarizes the effect of changing the approach velocity at more or less constant fuel/air ratios. Again, combustion was complete, but NO_x conversions were high, averaging about 75 percent and remaining rather steady as the velocity changed.

The fuel/air ratio was then changed gradually at constant approach velocity. As the fuel/air mixture got leaner, the NO_x conversion also decreased, but with a corresponding rise in CO and UHC emissions. This indicated that combustion was incomplete. Unfortunately, no measurements were made on the presence of other nitrogen species, in particular ammonia and cyanide. At the temperatures encountered in the combustor, it is expected that all the pyridine would be dissociated.

The second catalyst arrangement was then studied and results summarized in Table 2. The major differences in this arrangement compared to the first are:

- The gap is wider (2-1/2 inches vs. 1-1/2 inches)
- The front section is less reactive (two large cell monoliths vs. two large plus one medium cell monolith)
- The back section is more reactive (larger diameter monoliths)

The results show the same general trend: NO_x emmissions were low at low fuel/air ratios. This time, however, some measurements were also made on NH_3 and HCN. For the points where NO_x emissions were low,

NH_3 and HCN emissions were also low. Since NH_3, HCN, NO_x, and N_2 are the primary nitrogenous species formed in most combustion systems, our findings above are strong indications that the fuel nitrogen has probably been converted to gaseous nitrogen. The combustion in the second arrangement with the wider gap, however, seemed less stable than in the first arrangement. Bed temperatures fluctuated more in this arrangement and it was more difficult to maintain a steady test condition. In fact, we had tried an earlier series of test runs with a catalyst arrangement similar to Figure 2 except with a gap of 5 inches. The combustion was so unstable that we failed to maintain a constant test condition. These results are therefore not reported.

In both arrangements, the systems were not operating adiabatically as evidenced by the low temperatures in the catalyst bed. At a fuel/air ratio of 0.03 and 0.024, adiabatic bed temperatures should approach 2800°F and 2400°F respectively. The gap temperatures (measured in arrangement 1 and estimated in arrangement 2 due to thermocouple breakdown) should be taken as rough estimates only. Radiation from the bed on both sides of the thermocouple may cause higher temperature readings for the gas phase in the gap.

In general, however, a trend seems to be established in the tests run so far. This is summarized in Figure 4. Fuel nitrogen to NO_x decreased with fuel/air ratios. Catalyst arrangement 1 had a higher fuel nitrogen conversion at the same fuel/air ratio compared to arrangement 2 as evidenced by the shift in the curves. This is probably due to the more reactive front section in arrangement 1 (more surface area) indicating that too much fuel conversion in the first section may not be desirable. In fact, to achieve comparable NO_x emissions, arrangement 1 required a higher approach velocity (70 ft/s versus 40 ft/s) which lowers fuel conversion and lower fuel/air ratios which lowers bed temperatures.

The high heat loss in the reactor beds also makes the temperatures in the system generally lower than a comparable adiabatic system. For an adiabatic system, lower front section activity (less surface area or lower catalyst activity) may be more desirable for a given fuel/air to achieve low NO_x emissions. On the other hand, the front section must be sufficiently active to provide some fuel conversion. The interactions of fuel/air ratio, approach velocity, catalyst activity, and bed temperature, however, are difficult to determine from the present data. The effect of gap width cannot be assessed since in both arrangements studied, low NO_x conditions were achieved. Although it may be argued that the second arrangement had lower gap residence time due to lower approach velocities and longer gap distance, the front section catalyst activities were not the same and it is difficult to uncouple all the effects with the current data. The back section of the catalyst bed following the gap is essentially a cleanup section where the fuel and intermediates are fully converted. The high CO and UHC breakthrough seems to indicate that a more reactive second section is required for efficient cleanup under conditions favoring low NO_x.

CONCLUSIONS AND RECOMMENDATIONS

Results from our series of studies indicate that we may indeed have a viable concept for low NO_x production from fuel containing fuel bound nitrogen. However, a large number of parameters affect system performance. The limited amount of data we have at present do not allow us to uncouple all the viable interactions among key variables. To design a full scale system for gas turbine applications, we need to be able to scale up from bench scale results as well as to build in the flexibility of operation required in order to respond to start up, changing loads and shut down. More information will therefore be needed around design conditions to see how various parameters affect the results. It is also imperative that more tests be made to confirm our present findings.

There are a number of variables which will most likely affect our system and need to be considered in greater detail, in particular around design conditions.

- Fuel/air ratios — affects system temperature and reactant concentration

- Approach velocity — affects residence time and therefore conversion as well as temperature
- Gap distance — determines residence time available for gas phase reaction in the absence of catalyst
- Catalyst activity — controls temperature and conversion, particularly important in the front section. A sufficiently active rear section is also needed for efficient cleanup under all conditions
- System heat balance — how well the system approaches adiabatic conditions may determine how the other variables should vary since heat loss affects system temperatures
- Others — pressure, fuel type and nitrogen content may all affect system performance.

Given the large number of parameters that have to be examined, a more comprehensive test program will be required to provide sufficient data for performing a full scale design.

REFERENCES

1. Myerson, A. L., "The Reduction of Nitric Oxide in Simulated Combustion Effluents by Hydrocarbon Oxygen Mixtures," Fifteenth Symposium (International) for Combustion, The Combustion Institute, Pittsburgh, p. 1085, 1974.

2. Banna, S. M. and Branch, M. C., "NH_3-NO Reaction in the Post-Flame Region of a Flat Flame Burner," Paper No. 78-50, Fall Meeting, Western States Section, Combustion Institute, Lagunne Beach, CA, October 1978.

3. Beér, J. M., et al., "NO Reduction by Char in Fluidized Combustion."

4. Kelly, J., Personal communication, Acurex Corporation, April 1980.

5. DeSoete, G. G., "Mechanisms of Nitric Oxide Reduction on Solid Particles," paper presented at the Fifth EPA Fundamental Combustion Research Workshop, Newport Beach, January 1980.

TABLE 1a. COMBUSTION RESULTS ON CATALYST ARRANGEMENT 1 (FIGURE 2), DIESEL

F/A	TA	V	Temperature Distribution*					Emissions						
			Front Section		Gap	Back Section		NO_x (ppm)						
		(ft/s)	T_1	T_2	T_G	T_3	T_4	Theoretical/Actual	% Conversion	NH_3 + HCN (ppm)	UHC (ppm)	CO (ppm)	CO_2 (%)	O_2 (%)
0.034	200	30	1325	1444	1065	1565	2196	N.A.[†]/20	to ∑XN[††]	--	1	50	7	11.8
0.035	200	30	1337	1465	1090	1589	2245	N.A.[†]/20		--	2	50	7	11.6

*See Figure 2 for actual location of temperature measured

[†] N.A. = not applicable

[††] $\sum XN = NO_x + HCN + NH_3$

F/A = fuel ratio, TA = theoretical air, V = approach velocity

TABLE 1b. COMBUSTION RESULTS ON CATALYST ARRANGEMENT 1 (FIGURE 2), DIESEL + PYRIDINE.

F/A	TA	V	Temperature Distribution*					Emissions						
			Front Section		Gap	Back Section		NO_x (ppm)	%	NH_3 + HCN	UHC	CO	CO_2	O_2
	(%)	(ft/s)	T_1	T_2	T_G	T_3	T_4	Theoretical/Actual	Conversion	(ppm)	(ppm)	(ppm)	(%)	(%)
0.029	240	40	--	--	--	--	2266	294/300	102	--	3	50	6.7	12.4
0.029	240	36	1471	1576	(1259)**	1647	2197	294/300	102	--	--	30	6.6	12.5
0.029	240	36	1377	1681	1560	1752	2270	294/300	102	--	6	30	6.8	12.0
0.03	230	53	1404	1786	1831	1838	2227	310/300	97	--	5	40	6.9	12.0
0.034	200	53	1221	1679	1548	1634	2224	350/260	74	--	30	50	7.5	11.0
0.033	210	55	1227	1695	1650	1644	2183	334/250	75	--	20	40	7.4	11.5
0.033	210	63	1243	1744	1769	1691	2220	334/260	78	--	13	50	7.5	11.5
0.034	200	72	1271	1806	1938	1765	2229	350/250	71	--	7	30	7.2	11.5
0.035	200	82	1275	1802	1995	1750	2232	350/250	71	--	7	60	7.2	11.5
0.03	230	67	1284	1827		1867	2393	310/260	84	--	4	50	7.5	10.7
0.025	280	72	1225	1637	1628	1681	2010	252/235	93	--	3	70	6.3	12.3
0.023	300	72	1172	1454	1476	1552	1710	235/190	81	--	31	1540	5.5	13.5
0.021	330	70	1114	1376	1363	1432	1555	215/90	42	--	1500	1030	1.4	18.0
0.024	290	69	1163	1436	1407	1495	1630	244/80	33	--	3000	1510	2.3	17.4

*See Figure 2 for actual location of temperature measured

**No actual gap temperature was measured, average of T_2,T_3 taken

F/A = fuel/air ratio, TA = theoretical air, V = approach velocity

TABLE 2. COMBUSTION RESULTS ON CATALYST ARRANGEMENT 2 (FIGURE 3), DIESEL + PYRIDINE

F/A	TA	V	Temperature Distribution*					Emissions						
			Front Section		Gap	Back Section		NO_x (ppm)						
		(ft/s)	T_1	T_2	T_G^{**}	T_3	T_4	Theoretical/Actual	% Conversion	NH_3 + HCN (ppm)	UHC (ppm)	CO (ppm)	CO_2 (%)	O_2 (%)
0.032	215	37	1374	1475	(1518)	1561	2097	326/300	92	--	5	>1200	7.1	11.5
0.031	222	38	1380	1475	(1517)	1559	2003	320/290	91	--	4	>1200	7.0	11.5
0.027	256	43	1338	1440	(1476)	1513	1860	276/260	96	--	2	510	6.4	12.0
0.026	265	40	1329	1412	(1440)	1469	1781	274/220	80	--	12	--	5.9	13.5
0.024	287	44	1300	1368	(1399)	1430	1687	247/34	14	--	19	~8000	3.5	15.5
0.022	314	46	1314	1392	(1419)	1447	1711	226/44	30	4.2 + 18.7	11	8300		15.2
0.027	256	59	1428	1519	(1554)	1590	1892	276/240	87	--	5	440	6.4	12.6
0.023	300	65	1386	1467	(1491)	1516	1760	236/19	17	2.8 + 18.9	25	~9000	2.7	16.5
0.025	276	61	1410	1504	(1532)	1560	1846	256/145	61	2.6 + 8	3	~4100	5.5	13.5

*See Figure 3 for actual location of temperature measured

**No actual gap temperature was measured, average of T_2,T_3 taken

F/A = fuel/air ratio, TA = theoretical air, V = approach velocity

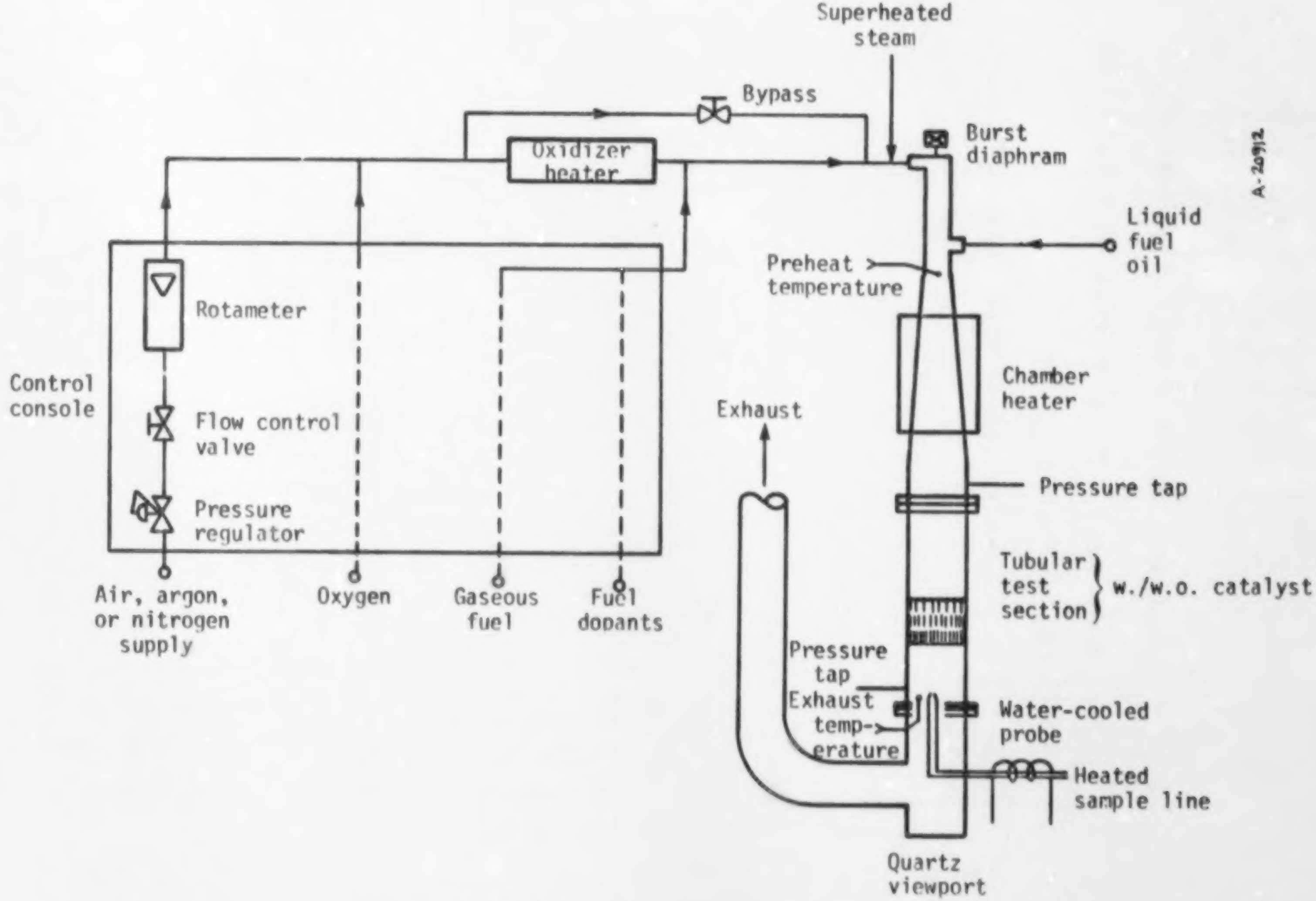
Superheated steam
Bypass
Burst diaphram
A-20912
Oxidizer heater
Liquid fuel oil
Preheat temperature
Rotameter
Control console
Flow control valve
Pressure regulator
Chamber heater
Exhaust
Pressure tap
Tubular test section
w./w.o. catalyst
Air, argon, or nitrogen supply
Oxygen
Gaseous fuel
Fuel dopants
Pressure tap
Exhaust temp-erature
Water-cooled probe
Heated sample line
Quartz viewport

Figure 1. Catalytic combustion test facility.

A-24382

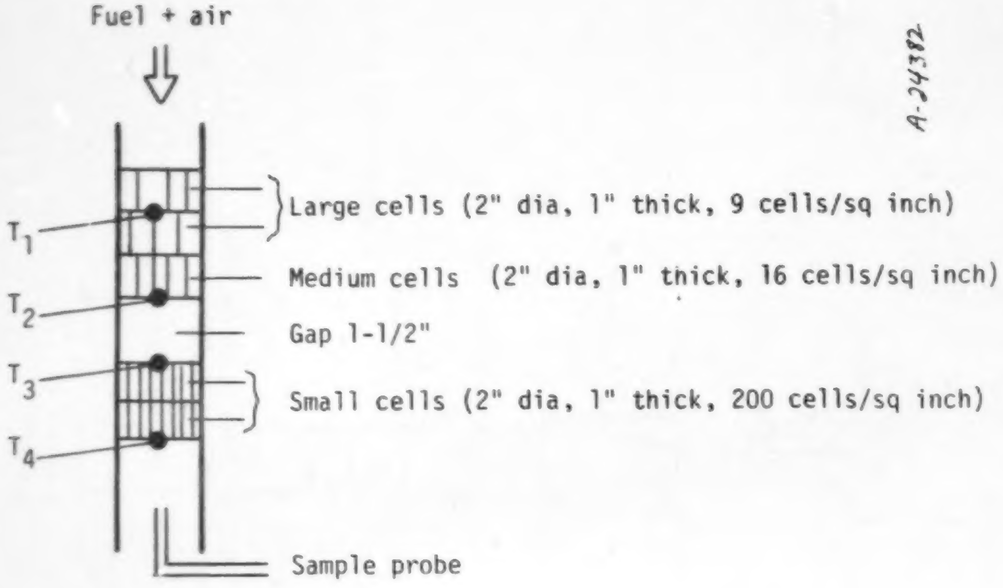
Fuel + air
T_1
T_2
T_3
T_4
Large cells (2" dia, 1" thick, 9 cells/sq inch)
Medium cells (2" dia, 1" thick, 16 cells/sq inch)
Gap 1-1/2"
Small cells (2" dia, 1" thick, 200 cells/sq inch)
Sample probe

Figure 2. Schematic of catalyst monolith arrangement 1.

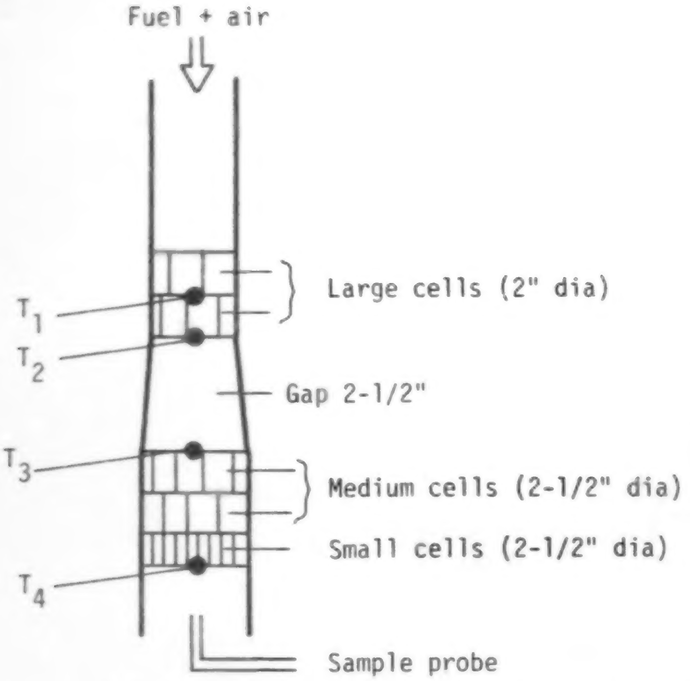
Fuel + air
T_1
T_2
T_3
T_4
Large cells (2" dia)
Gap 2-1/2"
Medium cells (2-1/2" dia)
Small cells (2-1/2" dia)
Sample probe

Figure 3. Schematic of catalyst monolith arrangement 2.

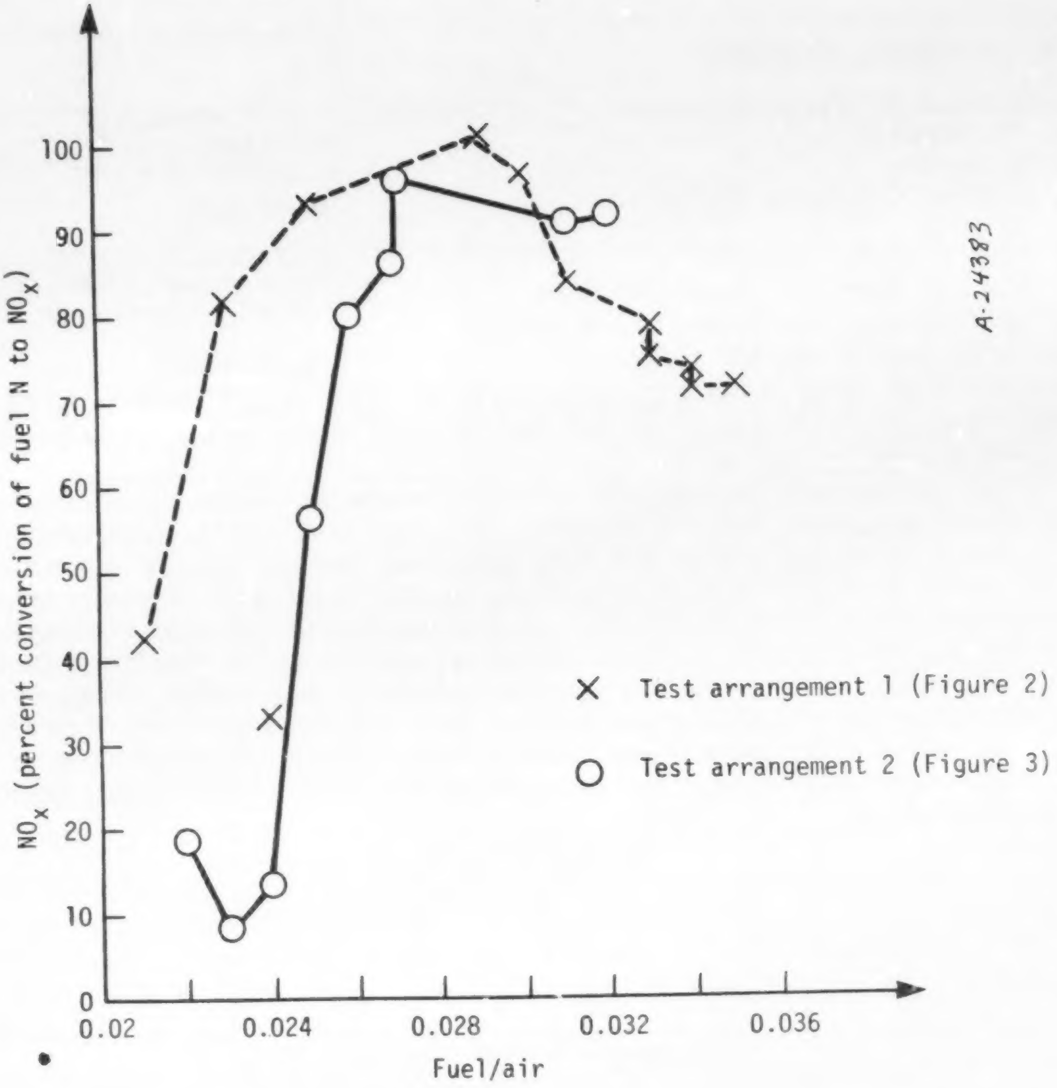

A-24383

Figure 4. Fuel nitrogen conversion to NO_x as a function of fuel/air ratio.